

UNCLASSIFIED

AD NUMBER
AD463601
NEW LIMITATION CHANGE
TO Approved for public release, distribution unlimited
FROM Distribution authorized to U.S. Gov't. agencies and their contractors; Administrative/Operational Use; 1962. Other requests shall be referred to Bureau of Ships, Washington DC.
AUTHORITY
BUSHIPS ltr, 11 Apr 1966

THIS PAGE IS UNCLASSIFIED

UNCLASSIFIED

AD 463601

DEFENSE DOCUMENTATION CENTER

FOR

SCIENTIFIC AND TECHNICAL INFORMATION

CAMERON STATION ALEXANDRIA, VIRGINIA



UNCLASSIFIED

NOTICE: When government or other drawings, specifications or other data are used for any purpose other than in connection with a definitely related government procurement operation, the U. S. Government thereby incurs no responsibility, nor any obligation whatsoever; and the fact that the Government may have formulated, furnished, or in any way supplied the said drawings, specifications, or other data is not to be regarded by implication or otherwise as in any manner licensing the holder or any other person or corporation, or conveying any rights or permission to manufacture, use or sell any patented invention that may in any way be related thereto.

ANALYSIS OF
INDUCTION MOTOR
NOISE AND VIBRATION

BUREAU OF SEDRS
CONTRACT NObs 77171
INDEX NO. NE-713,230

ALLIS-CHALMERS MFG. COMPANY

104459

REFERENCE COPY NO. /
BUSINESS TECHNICAL LIBRARY

ANALYSIS OF INDUCTION MOTOR NOISE AND VIBRATION

BUREAU OF SHIPS

CONTRACT NOs 77171

INDEX NO. NS-713-230

463601

ALLIS-CHALMERS MFG. COMPANY

NORWOOD DEVELOPMENT LABORATORY

NORWOOD OHIO

104459

PREFACE

This report is the result of a study conducted by the Norwood Development Laboratory of Allis-Chalmers Manufacturing Company, Norwood, Ohio for the Bureau of Ships under contract NObs 77171. The purpose of this study was to analyze the factors which produce or amplify vibration and airborne noise of alternating current induction motors, and to determine how this noise and vibration may be eliminated or attenuated. This study is specifically concerned with 60 cycle induction motors and various formulas throughout the report have incorporated this frequency into the equation constants. The theory, however, is more general and may be applied to other input frequencies. Motor vibration was of greater interest than airborne noise in this study.

Study performed under this contract falls into three categories: literature study, theoretical analysis, and test evaluation. Material obtained in the literature study has been incorporated into this report to make it as comprehensive as possible. Both the theoretical work performed under this contract and that reported in the literature was verified by testing of sample motors.

The results of this study are summarized in a list of recommended design criteria for low noise induction motors.

Jon S. Campbell
Jon S. Campbell
Project Engineer

Approved:

W. A. Andersen
W. A. Andersen
Supervisory Engineer

V B Honsinger
V. B. Honsinger
Chief Engineer
Norwood Development Laboratory

CONTENTS

Preface	
Section 1. Introduction	1-1
Section 2. Measurement of Motor Noise	2-1
2.1 Introduction	2-1
2.2 Noise and Vibration Units	2-1
2.2.1 Sound Pressure Levels	2-1
2.2.2 Sound Power Levels	2-1
2.2.3 Vibration Acceleration Levels	2-2
2.3 Frequency Analysis	2-2
2.3.1 Weighting Networks	2-2
2.3.2 Octave Band Analysis	2-3
2.3.3 Narrow Band Analysis	2-3
2.3.4 One-third Octave Band Analysis	2-3
2.4 Instrumentation and Test Conditions	2-4
2.5 Definitions	2-5
Section 3. Magnetic Noise	3-1
3.1 Introduction	3-1
3.2 Fundamental Flux and Flux Force Waves	3-1
3.3 Magnetostriction	3-3
3.4 Comparison of Force Wave and Magnetostrictive Deflections	3-5
3.5 Effect of Flux Harmonics	3-7
3.6 Means of Reducing Magnetic Noise	3-8
3.6.1 Air Gap Flux Density	3-9
3.6.2 Rotor-Stator Slot Combination	3-10
3.6.3 Rotor and Stator Geometry	3-11
3.6.4 Stator Coil Pitch	3-12
3.6.5 Skew of Rotor Bars	3-12
3.6.6 Grain Orientation of Core Steel	3-15
3.6.7 Annealing of Core Steel	3-16
3.7 Conclusion	3-17
Spectrograms	S3-1
Section 4. Bearing Noise	4-1
4.1 Introduction	4-1
4.2 Sleeve Bearings	4-1
4.3 Ball Bearings	4-2
4.4 Relative Advantages of Sleeve and Ball Bearings	4-3
4.5 Means of Reducing Ball Bearing Noise	4-3
4.5.1 Bearing Preload (a)	4-3
(b)	4-4
(c)	4-6
4.5.2 Shaft-Bearing Interference	4-6
4.5.3 Bearing Locknut	4-6
4.5.4 Bearing Lubricant	4-6
4.6 Conclusion	4-8
Spectrograms	S4-1
Section 5. Fan Noise	5-1
5.1 Introduction	5-1
5.2 Turbulence Effect	5-1
5.2.1 Drip-proof Protected Motors	5-1
5.2.2 Totally Enclosed, Fan Cooled Motors	5-3
5.3 Siren Effect	5-4

CONTENTS (Continued)

Section 5. Fan Noise (continued)	
5.4 Whistling Effect	5-4
5.5 Conclusion.....	5-4
Spectrograms.....	S5-1
Section 6. Unbalance Noise.....	6-1
6.1 Introduction.....	6-1
6.2 Cause of Unbalance Noise	6-1
6.3 Relative Effect of Unbalance Noise	6-1
6.4 Reduction of Unbalance Noise.....	6-2
6.5 Conclusion.....	6-3
Spectrograms.....	S6-1
Section 7. Effect of Load.....	7-1
7.1 Introduction.....	7-1
7.2 Test Motors.....	7-1
7.3 Magnetic Noise.....	7-2
7.4 Bearing Noise.....	7-3
7.5 Fan Noise.....	7-5
7.6 Unbalance Noise.....	7-5
7.7 Conclusion.....	7-5
Spectrograms.....	S7-1
Section 8. Miscellaneous Studies.....	8-1
8.1 Introduction.....	8-1
8.2 Tolerances.....	8-1
8.3 Frame Materials and Rigidity.....	8-2
8.4 Damping Compounds.....	8-3
8.5 Encapsulating Compounds.....	8-4
8.6 Internal Isolation	8-4
Spectrograms.....	S8-1
Section 9. Prototype Motors.....	9-1
9.1 Ratings and Purpose	9-1
9.2 Design Data.....	9-1
9.3 Additional Studies	9-2
9.3.1 Tolerances.....	9-2
9.3.2 External Balance Rings.....	9-2
9.3.3 Preload Adjustor.....	9-3
9.4 Noise Analysis of Prototype Motors	9-3
9.4.1 Unbalance Noise.....	9-4
9.4.2 Magnetic Noise	9-4
9.4.3 Bearing Noise	9-5
9.4.4 Fan Noise.....	9-5
9.4.5 Narrow Band Analysis	9-7
9.4.6 Comparison With MIL-E-22843.....	9-7
9.5 General Comments	9-8
Spectrograms.....	S9-1
Section 10. Summary.....	10-1
10.1 Design Criteria.....	10-1
10.2 General Conclusions	10-2

Bibliography

SECTION 1

INTRODUCTION

The study of the sources and elimination of induction motor noise is such a broad field that a few words concerning the organization and format of material are in order.

This study was conducted over a period of a year and a half. During this time a considerable amount of test data was obtained. This material has been thoroughly reviewed and duplicate tests have been reported only where additional information is thereby derived. The noise and vibration testing was conducted using one-third octave analysis. This frequency analysis and other facets of the present state of the art of motor noise measurement are briefly reviewed in Section 2. The test conditions and noise instrumentation utilized in this study are also described in this section.

The analysis of the test data has been accomplished by the use of tabulations of the one-third octave levels. It is realized that these tables are not easily read but the alternative bar graphs very closely duplicate the recorded spectrograms and are only useful for two condition tests. Important levels are printed in bold face to facilitate reading of the tables. The complete frequency spectrograms of all reported tests are furnished at the end of the various sections and often provide a ready visual indication of the change in motor noise.

Insofar as was possible, the material has been classified as to the source of motor noise. Studies of magnetic, bearing, fan, and unbalance noise are treated in Sections 3 through 6 respectively. The term "fan noise" is used to refer to noise generated by the cooling airstream as well as that directly caused by the motor fan. Because of other scheduled work, a comprehensive study of unbalance noise was not made under this contract. A discussion of the causes of unbalance noise and certain preliminary studies are reported in Section 6.

The effect of motor load on the noise production, which affects all four sources of motor noise, is treated separately in Section 7 because of the relative scarcity of information concerning this aspect. Certain miscellaneous studies, many of a transmission or attenuation nature, are treated in Section 8. Section 9 furnished a description and noise analysis of four prototype motors supplied under this contract.

The results of this study, summarized in Section 10, are divided into design criteria and facts of a more general nature.

Wherever the discussion of motor noise is based on or verified by published material, reference is made to the papers or books listed in the bibliography. In compiling this bibliography, only the more important and authoritative sources were selected.

SECTION 2

MEASUREMENT OF MOTOR NOISE

2.1 INTRODUCTION

In this section, the present state of the art of noise and vibration measurement is reviewed. First, the various units used to specify the level of airborne noise and structureborne vibration produced by a noise source are described in the following sections:

- 2.2.1 Sound Pressure Levels
- 2.2.2 Sound Power Levels
- 2.2.3 Vibration Acceleration Levels

Next, the weighting and filtering networks employed in frequency analysis are discussed in sections:

- 2.3.1 Weighting Networks
- 2.3.2 Octave Band Analysis
- 2.3.3 Narrow Band Analysis
- 2.3.4 One-third Octave Band Analysis

The instrumentation used and the test conditions maintained in this study are described. Definitions of the important units and terminology are listed for reference at the end of this section.

2.2 NOISE AND VIBRATION UNITS

2.2.1 Sound Pressure Levels

Airborne sound is a variation in air pressure about the atmospheric pressure as a mean. The extent of variation in pressure is measured in terms of a unit called the microbar, which is a pressure of one dyne per square centimeter or approximately one-millionth of the normal atmospheric pressure. Actually this unit is not often mentioned in noise measurement, but, as will be shown, it is implied when the more common term "decibel" is used.

The loudest sound pressure that a person can hear without experiencing pain is approximately 10 million times the softest sound that is barely discernable under ideal conditions. This ratio (10⁷:1) makes the use of a linear unit for sound pressure extremely impractical and suggests a logarithmic unit. The unit in universal use is the decibel (db). A power ratio expressed in db is numerically equal to ten times the common logarithm of the power ratio.

$$\text{Power ratio in db} = 10 \log_{10} \frac{P_1}{P_2}$$

where P_1/P_2 is the ratio of two powers measured in the same units.

Since sound pressure is proportional to the square root of sound power in a linear system (1), a pressure ratio expressed in db is twenty times the common logarithm of the pressure ratio.

*Numbers in parentheses refer to references listed in the Bibliography.

$$\begin{aligned} \text{Pressure ratio in db} &= 10 \log_{10} \frac{p_1^2}{p_2^2} \\ &= 20 \log_{10} \frac{p_1}{p_2} \end{aligned}$$

where p_1/p_2 is the ratio of two pressures in the same units.

It is more convenient to express a sound pressure as a pressure level with respect to (re) a reference pressure. The standard reference pressure is 0.0002 microbar (dyne/cm²). The definition of sound pressure (L_p) is:

$$L_p \text{ in db re } 0.0002 \text{ dyne/cm}^2 = 20 \log_{10} \left(\frac{\text{Measured pressure}}{0.0002} \right)$$

The measured pressure must now be expressed in microbars (dynes/cm²). This is somewhat of a technicality since sound measuring equipment is almost always calibrated to read sound pressure levels directly in decibels. The reference level of 0.0002 dynes/cm² is implied even if it is not stated.

The decibel is an extremely convenient unit to use. Zero db not only represents the threshold of hearing at 1000 cps, but a difference of one db is approximately the smallest that the average person can notice. If one sound pressure is twice another, the sound pressure level will be very nearly 6 db higher (6.021). If one pressure is 10 times another, the number of decibels is exactly 20; if one pressure is 100 times another, the number is 40.

An idea of the loudness of various common noises in terms of decibels may be gained from the following table. (1,2)

TABLE 2-1

DECIBELS	NOISE SOURCE
140	Threshold of Pain
130	Pneumatic Rock Drill
120	Loud Automobile Horn
110	Punch Press
100	Automatic Lathe
90	Noisy Factory
80	Truck Passing
70	Noisy Office
60	Conversational Speech
50	Private Business Office
40	Average Residence
30	Broadcast Studio
20	Rustle of leaves
15	Average Threshold of Hearing
0	Acute Threshold of Hearing

2.2.2 Sound Power Levels

Although sound pressure levels are very useful in specifying the "noise level" of an area, they are not indicative of the noise produced by a source such as motor. The sound pressure at a given point near a source is dependent on the directivity of the sound radiation, the distance from the source and the acoustical characteristics of the environment. Sound power

measurement is used to determine the total acoustical power radiated from a source.

Since the range of acoustic powers that are of interest is about one billion billion to one ($10^{18} : 1$), the decibel is used to specify sound power levels. Two reference powers are currently used: 10^{-13} watts and 10^{-12} watts. Sound power level referred to 10^{-13} watts is:

$$L_w \text{ in db re } 10^{-13} \text{ watts} = 10 \log_{10} \frac{\text{power (watts)}}{10^{-13} \text{ watts}}$$

Sound power levels re 10^{-12} watts are 10 db lower than equivalent levels re 10^{-13} watts.

Sound power levels cannot be measured directly but are determined from a number of sound pressure measurements in a prescribed environment (3). Sound power levels are essentially independent of the environmental conditions or the distance from the source and can be used to calculate the sound pressure level at any point in the noise field of the source under varying environmental conditions.

2.2.3 Vibration Acceleration Levels

Motor vibration, like any oscillatory motion, may be expressed in terms of displacement, velocity or acceleration. The displacement or distance that the motor moves during vibration is important in designing the foundation or substructure. Balance (or unbalance) is usually measured in terms of displacement of the bearing housing hub. Much test data has been taken in terms of velocity or, more usually, in terms of velocity decibels (Vdb) defined below. It is becoming more standard, however, to measure vibration in terms of acceleration, because according to Newton's second law ($F=ma$), the acceleration is proportional to the force that the vibratory motion transmits to the substructure.

The values of acceleration which are of interest have a range similar to the sound pressure levels described previously. Therefore the basic unit of the decibel has been adapted for vibration measurement. Since power is proportional to the square of acceleration (4), an acceleration measured in terms of decibels is 20 times the logarithm of the ratio of the acceleration to a reference acceleration which has been standardized as $1/1000$ centimeter per second², r.m.s. The term used to describe an acceleration expressed in decibels is vibration acceleration level. It is customary to state these levels in terms of "acceleration decibels" (adb) to avoid confusion with Sound Pressure levels. Thus

$$\text{Vibration acceleration level in adb} = 20 \log_{10} \frac{\text{measured acceleration}}{10^{-3} \text{ cm./sec}^2}$$

The measured acceleration must be in terms of cm/sec² r.m.s. Vibration measuring instruments are usually calibrated to read directly in terms of accel-

eration decibels. A vibration acceleration level can only be stated for motor vibration along a specified axis. The adb readings along mutually perpendicular axes are often quite dissimilar.

It is worthwhile to notice that sound pressure level, sound power level, and vibration acceleration level include the word "level". Whenever "level" is included in the name of a quantity, it can be expected that the value of this level will be given in decibels and that a reference pressure, acceleration, or other quantity is either stated or implied.

2.3 FREQUENCY ANALYSIS

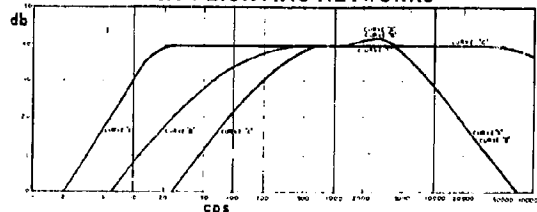
Defining the level of the sound pressure or acceleration, while necessary, is not sufficient. The human ear reacts quite differently to sounds having different frequencies. A certain sound pressure level may be perfectly acceptable at one frequency and unbearable at another. The frequency of vibration is of greater importance in this study because of the attenuation (or amplifications) characteristics of motor components and foundation which vary considerably with frequency. Several methods are used to indicate the frequency composition of motor noise and vibration.

- 1) Weighting Networks (Airborne Sound only)
- 2) Octave Band Analysis
- 3) Narrow Band Analysis
- 4) One-third Octave Analysis

2.3.1 Weighting Networks

Perhaps the best known method of frequency analysis is the use of the weighting networks specified by the American Standards Association. (5) These are applicable only for airborne sound and are an approximation of the varying apparent loudness that the human ear attributes to sound pressures of different frequencies. Figure 2-1 furnishes typical frequency response curves of weighting networks that meet the limits specified in the ASA Curves A, B, and C. Curves A and B are the 40 and 70 db equal loudness contours, respectively. Readings taken with an ASA A or B network are not sound pressure levels due to the weighting and are termed "sound levels". As shown in figure 2-1, the C Curve discriminates against only extremely low and high frequencies and is flat between 20 and 35,000 cps. This flat region is so extensive that the C Curve is not really weighted and is considered to give an overall noise level.

FIGURE 2-1
ASA WEIGHTING NETWORKS



measurement is used to determine the total acoustical power radiated from a source.

Since the range of acoustic powers that are of interest is about one billion billion to one ($10^{18} : 1$), the decibel is used to specify sound power levels. Two reference powers are currently used: 10^{-13} watts and 10^{-12} watts. Sound power level referred to 10^{-13} watts is:

$$L_w \text{ in db re } 10^{-13} \text{ watts} = 10 \log_{10} \frac{\text{power (watts)}}{10^{-13} \text{ watts}}$$

Sound power levels re 10^{-12} watts are 10 db lower than equivalent levels re 10^{-13} watts.

Sound power levels cannot be measured directly but are determined from a number of sound pressure measurements in a prescribed environment (3). Sound power levels are essentially independent of the environmental conditions or the distance from the source and can be used to calculate the sound pressure level at any point in the noise field of the source under varying environmental conditions.

2.2.3 Vibration Acceleration Levels

Motor vibration, like any oscillatory motion, may be expressed in terms of displacement, velocity or acceleration. The displacement or distance that the motor moves during vibration is important in designing the foundation or substructure. Balance (or unbalance) is usually measured in terms of displacement of the bearing housing hub. Much test data has been taken in terms of velocity or, more usually, in terms of velocity decibels (Vdb) defined below. It is becoming more standard, however, to measure vibration in terms of acceleration, because according to Newton's second law ($F=ma$), the acceleration is proportional to the force that the vibratory motion transmits to the substructure.

The values of acceleration which are of interest have a range similar to the sound pressure levels described previously. Therefore the basic unit of the decibel has been adapted for vibration measurement. Since power is proportional to the square of acceleration (4), an acceleration measured in terms of decibels is 20 times the logarithm of the ratio of the acceleration to a reference acceleration which has been standardized as $1/1000$ centimeter per second², rms. The term used to describe an acceleration expressed in decibels is vibration acceleration level. It is customary to state these levels in terms of "acceleration decibels" (adb) to avoid confusion with Sound Pressure levels. Thus

$$\text{Vibration acceleration level in adb} = 20 \log_{10} \frac{\text{measured acceleration}}{10^{-3} \text{ cm/sec}^2}$$

The measured acceleration must be in terms of cm/sec^2 r.m.s. Vibration measuring instruments are usually calibrated to read directly in terms of accel-

eration decibels. A vibration acceleration level can only be stated for motor vibration along a specified axis. The adb readings along mutually perpendicular axes are often quite dissimilar.

It is worthwhile to notice that sound pressure level, sound power level, and vibration acceleration level include the word "level". Whenever "level" is included in the name of a quantity, it can be expected that the value of this level will be given in decibels and that a reference pressure, acceleration, or other quantity is either stated or implied.

2.3 FREQUENCY ANALYSIS

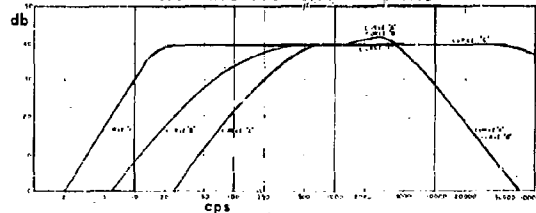
Defining the level of the sound pressure or acceleration, while necessary, is not sufficient. The human ear reacts quite differently to sounds having different frequencies. A certain sound pressure level may be perfectly acceptable at one frequency and unbearable at another. The frequency of vibration is of greater importance in this study because of the attenuation (or amplifications) characteristics of motor components and foundation which vary considerably with frequency. Several methods are used to indicate the frequency composition of motor noise and vibration.

- 1) Weighting Networks (Airborne Sound only)
- 2) Octave Band Analysis
- 3) Narrow Band Analysis
- 4) One-third Octave Analysis

2.3.1 Weighting Networks

Perhaps the best known method of frequency analysis is the use of the weighting networks specified by the American Standards Association. (5) These are applicable only for airborne sound and are an approximation of the varying apparent loudness that the human ear attributes to sound pressures of different frequencies. Figure 2-1 furnishes typical frequency response curves of weighting networks that meet the limits specified in the ASA Curves A, B, and C. Curves A and B are the 40 and 70 db equal loudness contours, respectively. Readings taken with an ASA A or B network are not sound pressure levels due to the weighting and are termed "sound levels". As shown in figure 2-1, the C Curve discriminates against only extremely low and high frequencies and is flat between 20 and 35,000 cps. This flat region is so extensive that the C Curve is not really weighted and is considered to give an overall noise level.

FIGURE 2-1
ASA WEIGHTING NETWORKS



2.3.2 Octave Band Analysis

Another method of frequency analysis divides the frequency spectrum into various octave bands. An octave is the frequency band between any two frequencies having a ratio 2:1. There are two sets of standard octave bands presently used. The first set, specified in American Standard Z24.10-1953 (6), are designated by their limiting frequencies. These standard octaves are 75 - 150, 150 - 300, 300 - 600, 600 - 1200, 1200 - 2400, and 2400 - 4800 cps. Two other bands, 20 - 75 cps and 4800 to 10,000 cps, are usually included. Octave analysis using these frequency bands prevails at the present time.

American Standard S1.6-1960 (7) lists new preferred frequencies for acoustical measurements. In this standard, frequency bands are listed by their center or geometric mean frequency, i.e. the 1000, 2000, and 4000 cps octaves. The geometric mean frequency is the square root of the product of the upper and lower limiting frequencies. The recommended octave bands and their limiting frequencies are listed in Table 2-2. Octave analysis using these bands is not yet common since most measuring apparatus in use was designed to meet the previous standard. However, the new standard provides a guide to future design and construction of noise measuring apparatus. In the future, octave analysis using the bands specified in Table 2-2 will predominate.

TABLE 2-2
STANDARD OCTAVE BANDS
American Standard S1.6-1960

Lower Frequency	Band Center	Upper Frequency
11.2	16	22.4
22.4	31.5	44.7
44.7	63	89.2
89.2	125	178
178	250	355
355	500	709
709	1,000	1,410
1,410	2,000	2,820
2,820	4,000	5,630
5,630	8,000	11,200
11,200	16,000	22,400

Note: Higher and lower preferred frequencies are obtained by successive multiplication and division by 1000.

Octave band analysis is applicable to and used for both airborne and structureborne noise testing. However, induction motors often have sources producing more than one frequency of noise within a particular octave. This fact makes the identification of the source and thus the elimination of the noise difficult. For such complex noise generators, such as a motor, a narrower frequency band is required.

2.3.3 Narrow Band Analysis

Various analyzers are built for noise analysis of

frequency bands considerably smaller than an octave in width. These may have either a constant bandwidth, or more frequently a constant percentage bandwidth. In constant percentage bandwidth analysis, each successive frequency band is larger than the preceding band. The bands have a width which is a specified percentage (such as 5% or 8%) of the geometric mean frequency of the band. Narrow band analysis permits accurate identification of the motor noise sources but the large number of bands usually make any automatic recording of the motor as a spectrogram, physically long. The time analysis of test results are quite time consuming for repetitive tests.

2.3.4 One-Third Octave Analysis

A fourth method of frequency analysis, coming into prominence, is a compromise between the rapid but inadequate octave band analysis and the time consuming but precise narrow band analysis. This method divides the frequency spectrum into one-third octave bands. A one-third octave is a band of frequencies in which the ratio of the extreme frequencies is equal to the cube root of two. Standard bands, which are essentially one-third octaves, have been normalized to provide for repetition of bands by multiples of 10. They are bands having the characteristic $f_u/f_L = 10^{0.1}$.

TABLE 2-3
STANDARD ONE-THIRD OCTAVE BANDS
American Standard S1.6-1960

Lower Freq.	Band Center	Upper Freq.	Lower Freq.	Band Center	Upper Freq.
14.1	16	17.8	563	630	709
17.8	20	22.4	709	800	892
22.4	25	28.2	892	1,000	1,120
28.2	31.5	35.5	1,120	1,250	1,410
35.5	40	44.7	1,410	1,600	1,780
44.7	50	56.3	1,780	2,000	2,240
56.3	63	70.9	2,240	2,500	2,820
70.9	80	89.2	2,820	3,150	3,550
89.2	100	112	3,550	4,000	4,470
112	125	141	4,470	5,000	5,630
141	160	178	5,630	6,300	7,090
178	200	224	7,090	8,000	8,920
224	250	282	8,920	10,000	11,200
282	315	355	11,200	12,500	14,100
355	400	447	14,100	16,000	17,800
447	500	563			

Note: Higher and lower preferred frequencies are obtained by successive multiplication and division by 1000.

One-third octaves are designated by their geometric mean frequencies: a 63, 80, or 100 cps one-third octave. The standard values for geometric mean frequencies are those numbers whose mantissae of their common logarithms are multiples of 0.1. (7). Rounded-off values of the center frequencies and the

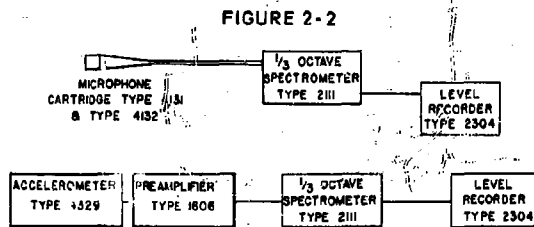
limiting frequencies of the standard one-third octave bands are given in Table 2-3. A comparison of Tables 2-2 and 2-3 reveals that the standard one-third octaves correspond to the new standard octaves rather than those in widespread use. The band width of a one-third octave is 23% of the center frequency, a fact which is useful in correlating data with narrow band analysis.

A one-third octave is sufficiently narrow to permit ready identification of the sources of induction motor noise. Most sources produce noise at some multiple of the rotational frequency. Rarely do two prominent sources produce noise in the same $\frac{1}{3}$ octave. The rapidity and ease of measurement more than make up for the reduced accuracy in pinpointing the exact frequency produced. However, if there is any doubt as to the source of the noise or as to whether there is only one noise source, a narrow band analysis should be taken.

2.4 INSTRUMENTATION AND TEST CONDITIONS

In this study, most analyses were either based upon, or verified by noise measurements on motors. The conclusions are dependent upon the quality of the performed tests. Also, a knowledge of the instrumentation used, as well as certain test conditions, are prerequisites to correct interpretation of the test data. For these reasons, a brief description of the instrumentation used in this study is presented here.

The airborne and structureborne noise metering equipment used in this study was manufactured by Bruel and Kjaer, Copenhagen, Denmark. The majority of the tests were taken with a one-third octave spectrometer. A block diagram of the equipment used for one-third octave analysis is shown in Figure 2-2. The airborne sound measuring equipment consists of a calibrated condenser microphone, a one-third octave analyzer, and a recorder. An accelerometer and a preamplifier were substituted for the condenser microphone for structureborne vibration measurement. The preamplifier contains an integrating network permitting spectrograms of the vibration to be taken either in terms of acceleration, velocity, or displacement.

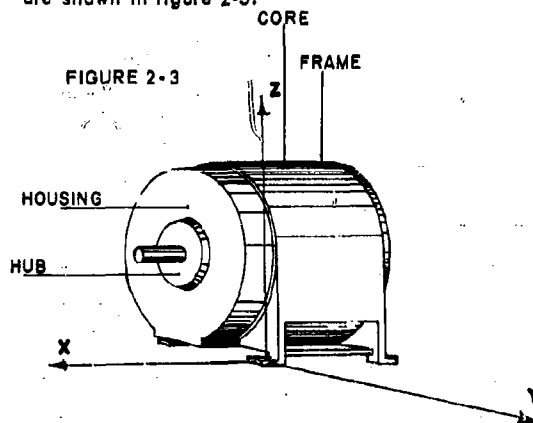


AIRBORNE & STRUCTUREBORNE
NOISE METERING EQUIPMENT
BRUEL & KJAER
COPENHAGEN, DENMARK

These components are electrically coupled to form an integrated unit which automatically records the noise or vibration levels for the standard one-third octaves on preprinted, frequency calibrated paper. After recording the frequency spectrum from 14.1* to 35,500 cycles per second, the levels measured on the ASA weighted networks A, B, and C are recorded. The levels for the ASA A and B networks (an approximation to the hearing response of the human ear) are, although automatically recorded, meaningless for vibration measurements. The C network has a flat response to all frequencies between 20 and 35,000 cps, and records the overall level for both airborne and structureborne noise measurements. Throughout this report the term "overall" refers to levels recorded on the C Scale as shown in Figure 2-1.

The vertical scale of the recording paper has a range of 50 db. Attenuators, built into the analyzer, permit the scale to be positioned wherever desired, i. e., 10-60 db, 20-70 db, etc. For airborne noise measurements, the equipment is calibrated to read in db re 0.0002 dyne/sq cm. Vibration acceleration levels are measured in acceleration decibels (adb) re 10^{-3} cm/sec²; vibration velocity levels may be measured in velocity decibels (vdb) re 10^{-6} cm/sec. Displacement measurements (made only in the unbalance study) were not taken with this equipment.

As indicated previously, vibration acceleration levels, are only meaningful for a specified axis. On almost all tests, readings were taken on three mutually perpendicular axes on the motor feet. The X-Axis is parallel to the rotor shaft; the Y-Axis is horizontal and perpendicular to the shaft; the Z-Axis is vertical. For specific tests, other axes were monitored. Axes parallel to the shaft and on the bearing housing (Hsg) and bearing housing hub (Hub) were used in the bearing study. Readings on vertical axes on both the frame and motor core were taken for magnetic noise studies and for internal isolation tests. These axes are shown in figure 2-3.



*Test data taken prior to 27 November 1959 has a lower frequency cutoff of 35.5 cps.

Unless otherwise specified, the following test conditions were maintained:

- 1) Motors were mounted on resilient mounts which have a vertical resonant frequency of approximately 10 cycles per second under load conditions. At 60 cps or higher, these isolators were attenuating any transmitted vibration a minimum of 20 db.
- 2) In order to segregate noise sources, totally enclosed motors were tested without external fans and fan bowls for other than windage noise studies. Dripproof protected motors were usually tested with rotors cast without rotor fan blades.
- 3) In order to further segregate noise sources (except certain bearing tests), preloaded bearings meeting the Anderson limits of MIL-B 17931A, Amendment 2, dated 16 September 1959, were used to minimize bearing noise.
- 4) During any one test, extreme care was taken to assure that factors, other than those being investigated, did not change. For instance, related tests were taken in brief time succession. Often the initial condition was re-tested to verify that the test conditions had not changed. However, no attempt was made to maintain conditions between different tests. Therefore, comparison of test results furnished in separate tabulations is not recommended.

2.5 DEFINITIONS

The following definitions are summarized here for reference purposes:

1. **Airborne noise:** Airborne noise is undesired sound in air. It is characterized by fluctuations of air pressure about the atmospheric pressure as a mean.
2. **Structureborne noise:** Structureborne noise is undesired vibration in, or of solid bodies, such as machinery or ship structures.
3. **Decibel:** The decibel is a dimensionless unit for expressing the ratio of two values of power. One of these values may be standard of reference. The number of decibels is equal to 10 times the logarithm to the base 10 of the power ratio, i. e.,

$$\text{Power ratio in db} = 10 \log_{10} \frac{P_1}{P_2}$$

Under commonly accepted conditions quantities proportional to power include the square of rms values of either the pressure, velocity or acceleration. For quantities whose square is proportional to power, the decibel is 20 times the logarithm of the ratio.

4. **Sound pressure level:** Sound pressure level is the r.m.s. sound pressure expressed in decibels relative to a standard reference pressure of 0.0002

dyne per square centimeter. (NOTE - 1 dyne per square centimeter is equal to 1 microbar.) Thus:

$$L_p \text{ in db} = 20 \log_{10} \frac{\text{measured pressure (dynes/cm}^2 \text{ r.m.s.)}}{0.0002 \text{ dynes/cm}^2}$$

5. **Sound power level:** Sound level is the sound power emitted by a source expressed in decibels relative to a standard reference power of 10^{-13} watts. Thus:

$$L_w \text{ in db} = 10 \log_{10} \frac{\text{power (watts)}}{10^{-13} \text{ watts}}$$

It is a quantity that may be calculated from sound pressure level measurements in a known acoustic environment.

6. **Vibration acceleration level:** Vibration acceleration level is the r.m.s. vibration acceleration of a body along a specified axis, expressed in decibels relative to a standard reference acceleration of 10^{-3} cm/sec^2 . Thus: Vibration acceleration level in

$$\text{adb} = 20 \log_{10} \frac{\text{measured acceleration (cm/sec}^2 \text{ r.m.s.)}}{10^{-3} \text{ cm/sec}^2}$$

7. **Vibration velocity level:** Vibration velocity level is the r.m.s. vibration velocity of a body along a specified axis, expressed in decibels relative to a standard reference velocity of 10^{-8} cm/sec . Thus: Vibration velocity level in

$$\text{vdb} = 20 \log_{10} \frac{\text{measured velocity (cm/sec r.m.s.)}}{10^{-8} \text{ cm/sec}}$$

Vibration acceleration level in adb may be converted to velocity level in vdb at any given frequency by the equation:

$$\text{vdb} = (\text{adb} + 44) - 20 \log_{10} f$$

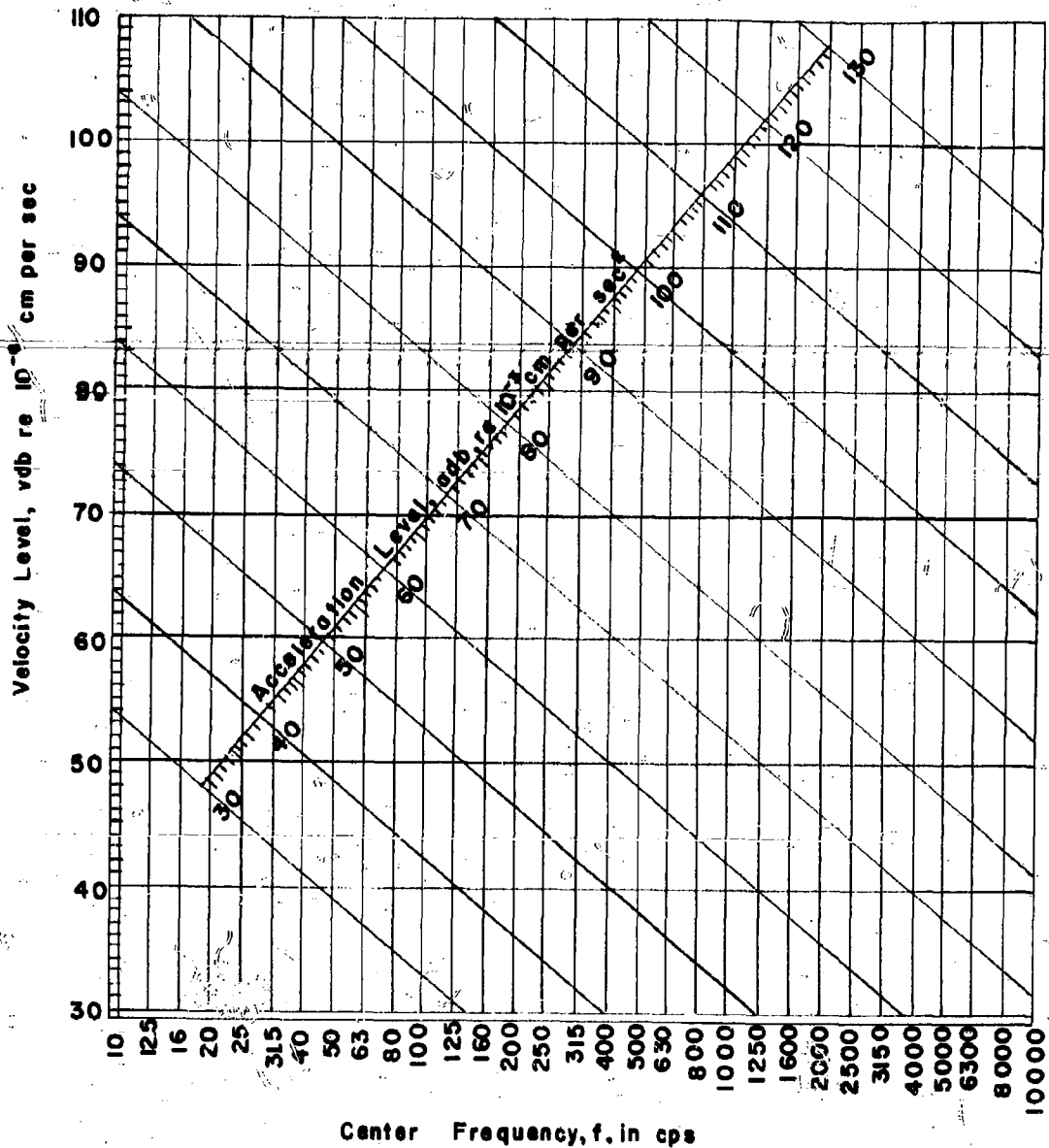
where f = frequency in cycles per second, or by the use of Figure 2-4.

8. **Octave band:** An octave band is a band of frequencies covering a range of 2 to 1, i.e. $f_H/f_L = 2$ where f_H and f_L are the nominal cutoff frequencies of the band.
9. **One-third octave band:** A one-third octave band is a band of frequencies in which the ratio of the extreme frequencies is equal to the cube root of two, i.e. $f_H/f_L = \sqrt[3]{2} = 1.2599$ where f_H and f_L are the nominal cutoff frequencies of the band. NOTE: ASA standard 1/3 octave bands provide for repetition of bands by multiples of 10. They are therefore bands having the characteristic $f_H/f_L = 10^{0.1} = 1.2589$ which for all practical purposes are 1/3 octaves.

10. **Narrow band:** A narrow band is a band whose width is less than one-third octave but not less than one percent of the center frequency.

11. **Band center:** Band center refers to the geometric mean between the extreme frequencies of the band, i.e. $f_c = \sqrt{f_H f_L}$.

FIGURE 2-4
CONVERSION CHART vdb to addb
one third octave band levels



SECTION 3 MAGNETIC NOISE

3.1 INTRODUCTION

Magnetic noise of induction motors has two potential sources: 1) the radial force waves created by the air gap flux density and 2) the magnetostrictive expansion of the core steel. Whereas the force waves are imposed on the air-iron surface of the air gap, the magnetostrictive expansion is an internally generated variation in dimension. Magnetic noise may be categorized by the frequency produced: 1) Twice line frequency and 2) Rotor slot frequency noise. Both potential sources of magnetic noise produce twice line frequency noise (120 cycle noise for 60 cycle motors). However, it will be shown that, for two pole motors where 120 cycle noise is a problem, the 120 cycle magnetostrictive noise is small compared to that produced by the radial force waves. The high frequency magnetostrictive effect will be shown to be negligible. An investigation of the effect of the rotor and stator slot harmonics of the air gap flux density reveals that the radial force waves produce three frequencies approximately equal to $\frac{120R}{P}$ and three approximately equal to $\frac{240R}{P}$. These are termed the primary and secondary rotor slot frequencies, respectively.

After discussing the source of magnetic noise, a treatment of the effect of the following factors on magnetic noise is presented.

- 1) Air Gap Flux Density
- 2) Rotor-Stator Slot Combination
- 3) Rotor and Stator Geometry
- 4) Stator Coil Pitch
- 5) Skew of Rotor Bars
- 6) Grain Orientation of Core Steel
- 7) Annealing of Core Steel

The methods of reducing magnetic noise indicated by these studies are summarized in the conclusion of this section.

3.2 FUNDAMENTAL FLUX AND FLUX FORCE WAVES

In three phase 60 cycle induction motors, each phase winding generates a stationary 60 cycle pulsating magnetomotive force wave (mmf). The three windings are displaced by 120 electrical degrees in space from each other. When the windings are excited by balanced three-phase currents, the generated mmf's will be 120° phase displaced in time. Assuming symmetrical magnetic circuits, the mmf's will produce stationary pulsating magnetic fields of equal magnitude. Because the three stationary fields are both time and space dependent, each may be resolved into two oppositely rotating component fields having a magnitude one-half that of the stationary fields. The resultant field at any point is the sum of the three stationary fields and, therefore, of the six rotating compon-

ents. The three component waves rotating in one direction are displaced in phase by 120° and therefore add vectorially to zero; the three component waves rotating in the opposite direction are in phase and add algebraically. Thus, the three stationary windings combine to create a rotating magnetic field whose magnitude is 3/2 that of each stationary field. (8)^{*}

This field rotates 360 electrical degrees in space during one period of the input frequency (60 cps). The angular velocity of the wave is $\omega = 2\pi f = 120\pi$ electrical radians per second. Since πP electrical radians corresponds to one revolution, the rotational speed of the wave is $120/P$ revolutions per second or $7200/P$ rpm, where $P =$ the number of poles. This speed is called the synchronous speed. The synchronous speed of two-pole motors is 60 rps or 3600 rpm; that of four-pole motors is 30 rps, etc. The lower rotational frequency of motors with more than 2 poles is exactly compensated by the increase in number of cycles of flux around the air gap periphery. Thus the fundamental air gap flux of induction motors has a 60 cycle per second variation regardless of the number of poles. This can also be seen from the fact that the stationary fields which add to form the rotating wave have 60 cycle variation.

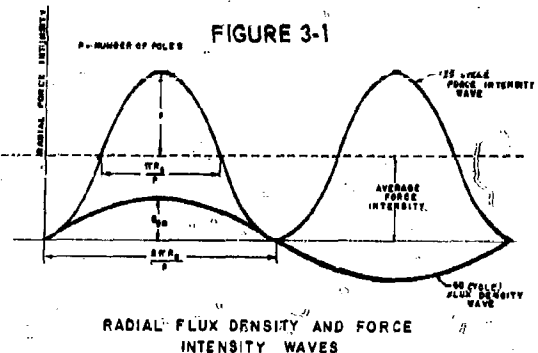


Figure 3-1 shows one cycle (two poles) of the revolving flux density wave in the air gap of an induction motor developed along a straight line. This may be considered as the entire air gap of a two-pole motor, or one-half the developed air gap of a four-pole motor, etc. The flux density as a function of time is given by the expression:

$$B_g = B_{gm} \sin \omega t \quad 3.1$$

$$= B_{gm} \sin 2\pi f t$$

*Numbers in parentheses refer to references listed in the Bibliography.

where B_g = flux density at any point, in lines/sq. in.

B_{gm} = maximum flux density in lines/sq. in.

ω = angular velocity in radians/sec.

f = input frequency = 60 cycles/sec.

The magnetic flux exerts a radial pull across the air gap which is proportional to the square of the flux density. The force intensity (pressure) at any point expressed in MKS rationalized units ($\mu_0 = 4\pi \times 10^{-7}$) is:

$$p_i = B_g^2 / 2\mu_0 \quad (9) \quad 3.2$$

In terms of English units,

$$p_i = 1.388 \times 10^{-8} B_g^2 \quad 3.3$$

where p_i = force intensity in pounds/sq. in.

B_g = flux density in lines/sq. in.

Substituting the expression for B_g (Equation 3.1) into equation 3.3 gives

$$p_i = 1.388 \times 10^{-8} B_{gm}^2 \sin^2 \omega t$$

Since $\sin^2 \omega t = 1/2 (1 - \cos 2\omega t)$

$$p_i = 6.94 \times 10^{-9} B_{gm}^2 - 6.94 \times 10^{-9} B_{gm}^2 \cos 2\omega t \quad 3.4$$

The first term of equation 3.4 is the average force intensity shown in figure 3-1, which remains constant and causes only a static compression of the stator core. The second term is a sinusoidally varying component of twice input frequency or 120 cps. Only the periodically varying component will produce noise and vibration. The single amplitude of the force intensity is

$$p = 6.94 \times 10^{-9} B_{gm}^2 \quad 3.5$$

As the above derivation indicates, it is the flux density and force intensity waves that are interrelated. However, these are usually termed flux and force waves respectively.

It should be noted that this 120 cycle force wave has four zero points per cycle of the revolving flux wave. If the stator core is also developed into a straight line, the core will deflect into a shape similar to the force wave with points of zero deflection, (nodes), at each zero point of the force wave. The number of nodes, m , of stator core deflection is always equal to the number of force poles or, twice the number of flux poles, $2P$.

The number of nodes of vibration is of paramount importance as the deflection will be shown to be inversely proportional to the fourth power of m for a given flux density. This is best illustrated by once again considering the stator lamination ring developed into a straight line. Under this idealized condition, the deflection may be calculated by considering the core as a beam freely supported at each node. The single amplitude deflection for such a beam under a sinusoidally distributed load is given by the expression:

$$d = \frac{WL^3}{2\pi^3 EI} \quad (3) \quad 3.6$$

where d = maximum deflection in inches

W = total load in pounds

L = distance between nodes in inches

E = modulus of elasticity in #/in²
(3×10^7 for steel)

I = bending moment of inertia in inches⁴.

In terms of the stator geometry

$$L = \frac{\pi D_s}{m} \quad I = \frac{h^3 L_g}{12}$$

where D_s = mean diameter of the stator core in inches

m = number of nodes

h = radial depth of the stator core in inches

L_g = axial length at air gap in inches

Substituting these expressions in equation 3.6

$$d = \frac{2W D_s^3}{m^3 h^3 L_g} \times 10^{-7} \text{ inches} \quad 3.7$$

Equation 3.7 reveals that the deflection of the stator core is inversely proportional to the third power of the number of nodes for a given load W . The total load however is inversely proportional to m for a given maximum flux density. The load may be calculated by taking the average value of the force wave over the area of the force pole

$$W = \frac{2}{\pi} \times p \times \frac{2\pi R_g L_g}{m} = \frac{4p R_g L_g}{m}$$

where R_g = radius of the air gap in inches

Substituting the expression for p , given by equation 3.5, results in the total load being

$$W = \frac{2.776 B_{gm}^2 R_g L_g}{m} \times 10^{-8} \text{ pounds} \quad 3.8$$

Combining equations 3.7 and 3.8 results in the expression for the deflection in terms of a given maximum flux density

$$d = \frac{5.55 B_g^2 R_g D_s^3 \times 10^{-15}}{m^4 h^3} \text{ inches} \quad 3.9$$

As stated above, this formula has been derived for the idealized condition of the stator core ring developed into a straight line. The derivation of the actual formulas for varying number of nodes, m , reveals that equation 3.9 is sufficiently accurate for cases where m is equal to or greater than 12 (fundamental force wave for a 6 pole motor). As the number of nodes increases, the core segment under study has less and less curvature. The number of nodes in question is always a multiple of four, since there are four force nodes per flux pole pair. The value of deflection indicated by equation 3.9 must be multiplied by 1.788 for 4 node and 1.188 for 8 node force waves. (10)

Thus the single amplitude deflection of the stator core in terms of the maximum flux density for 4, 8, 12 or more node force waves are

$$4 \text{ nodes} \quad d = 9.92 \frac{B_g m R_g D_s^3}{m^4 h^3} \times 10^{-15} \quad 3.10a$$

$$8 \text{ nodes} \quad d = 6.32 \frac{B_g m^2 R_g D_s^3}{m^4 h^3} \times 10^{-15} \quad 3.10b$$

$$12 \text{ nodes or more} \quad d = 5.55 \frac{B_g m^2 R_g D_s^3}{m^4 h^3} \times 10^{-15} \quad 3.10c$$

The effect of the variables in equation 3.10 will be discussed later in the treatment of methods of reducing magnetic noise. However, the effect of the number of nodes may be used to simplify ensuing derivations. Equation 3.10 shows that the deflection is inversely proportional to the fourth power of the number of nodes for a given flux density while equation 3.7 reveals an inverse third power relationship for a given radial force. Thus, in determining the effect of complex stator core vibration, it is often possible to ignore all frequencies except those with the lowest number of nodes. The rapid increase in deflection with a decrease in the number of nodes is also the reason that a two pole motor has higher 120 cycle noise.

3.3 MAGNETOSTRICTION

Magnetostriction is the effect that certain materials, such as steel, have of expanding very slightly along the axis of magnetization when magnetic flux pass through them. The steel stator core expands equally for flux in a positive or negative direction and thus expands and contracts (cycles) twice for each cycle of flux passing through it, i.e., 120 cps for 60 cycle motors. Since the frequency of magnetostriction-caused noise is the same as that produced by the flux force waves, magnetostriction must be considered a potential source of 120 cycle noise. However, the magnetostrictive deflection of the stator

core of induction motors will be shown to be both in phase opposition and small compared to that produced by the flux force waves.

To illustrate the relative effect of magnetostriction it is necessary to compare the radial deflection produced by the magnetostrictive effect with that caused by the flux force waves. The mechanical stresses in the steel resulting from the surface imposed flux force waves is known to affect the magnitude of the magnetostrictive strain. The effect is slight, however, and in this analysis the two deflections are considered to be independent, i.e., that the deflections may be calculated separately and then superimposed to obtain the total deflection.

The magnetostrictive expansion of the stator occurs both in the teeth and in the core. As the teeth are free to move at the air gap end, they will not exert any force on the stator core. The magnetostrictive expansion of the stator teeth does shorten the air gap slightly at the magnetic poles, but since the tooth flux density rotates with the air gap flux density, this change in air gap length does not affect the radial force wave deflections. The vibration of the stator teeth can produce airborne noise but this is generally small compared to that produced by the deflection of the stator core periphery. Therefore in the following analysis only the stator core magnetostrictive effect is considered.

The magnetostrictive strain or elongation per unit length is a function both of the type of steel and of the flux density through the steel. A curve of the magnetostrictive strain vs. flux density for the non-oriented silicon steel normally used in induction motors was not available. A literature search and consultations with four principal steel companies revealed that although much data has been taken on transformer grade (oriented) steels, no information directly applicable to motor grade steel was available. However, it was determined that for silicon steels, the magnetostrictive strain is very closely proportional to the square of the flux density.

With reasonable accuracy, it is assumed that

$$e_t = K B_c^2 \quad 3.11$$

where e_t = the magnetostrictive strain in the direction of flux flow (tangential to core periphery)

B_c = core flux density at point under consideration

K = constant of proportionality (a function of the type of steel)

It has been observed that the volume of the steel experiences only very minute changes when the body is magnetized. Because of the essentially constant volume, Poisson's ratio approaches the maximum value of one-half. (11) Therefore, the transverse strains

in the axial and radial directions are approximately one-half that in the tangential direction. It should be noted that the transverse strains represent a shrinkage rather than an elongation for positive magnetostrictive strains. Considering elongation as positive, the radial strain is

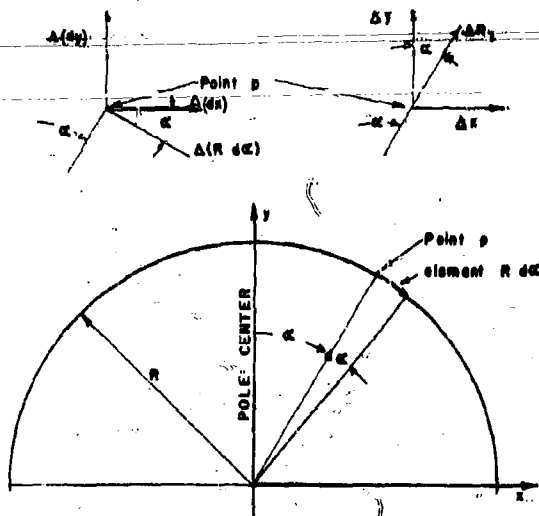
$$\epsilon_r = -1/2 K B_c^2 \quad 3.12$$

The following derivation of the deflection of the stator core due to magnetostriction has been accomplished for a two-pole motor for two reasons:

- 1) Electrical and mechanical degrees are numerically equal, which simplifies the derivation.
- 2) Tests reveal that 120 cycle noise is particularly predominant in two-pole motors.

Figure 3-2 shows one-half of a stator core of a two-pole motor represented as a thin ring of radius, R. The radial deflection will be calculated for the instant when the fundamental flux wave has a pole center coincident with the vertical axis. The angle, α , is measured clockwise from the axis.

FIGURE 3-2



The stator core flux density, B_c , is considered to have a sinusoidal distribution. The maximum core density, B_{cm} , occurs midway between pole centers or at the horizontal or x axis in Figure 3-2. The core density at any point p is given by the expression

$$B_c = B_{cm} \sin \alpha \quad 3.13$$

The tangential and radial magnetostrictive strains are thus

$$\epsilon_t = K B_{cm}^2 \sin^2 \alpha \quad 3.14a$$

$$\epsilon_r = 1/2 K B_{cm}^2 \sin^2 \alpha \quad 3.14b$$

The elongation of a differential element of core circumference, $R d\alpha$, due to the tangential strain is

$$\Delta(R d\alpha) = \epsilon_t R d\alpha \quad 3.15$$

Combining equations 3.14a and 3.15 gives

$$\Delta(R d\alpha) = R K B_{cm}^2 \sin^2 \alpha d\alpha \quad 3.16$$

$$\Delta(R d\alpha) = \text{elongation of element } R d\alpha$$

R = outer radius of core in inches

B_{cm} = maximum core flux density in lines/sq. in.

α = angle measured clockwise from air gap pole center.

The horizontal and vertical components are respectively -

$$\Delta(dx) = R K B_{cm}^2 \sin^2 \alpha \cos \alpha d\alpha$$

$$\Delta(dy) = R K B_{cm}^2 \sin^3 \alpha d\alpha$$

By trigonometric identities it may be shown that

$$\sin^2 \alpha \cos \alpha = 1/4 (\cos \alpha - \cos 3\alpha)$$

$$\text{and } \sin^3 \alpha = 1/4 (3 \sin \alpha - \sin 3\alpha)$$

Therefore

$$\Delta(dx) = 1/4 R K B_{cm}^2 (\cos \alpha - \cos 3\alpha) d\alpha \quad 3.17$$

$$\Delta(dy) = -1/4 R K B_{cm}^2 (3 \sin \alpha - \sin 3\alpha) d\alpha \quad 3.18$$

From considerations of symmetry, it may be seen that points on the core coincident with the horizontal and vertical axes of figure 3-2 will only have radial displacements. Therefore, the total horizontal component of displacement at any point p is the summation of the infinitesimal displacements from $\alpha = 0$ (point of zero horizontal displacement) to α (point p). Thus,

$$\int \Delta(dx) = \Delta x = \int_0^\alpha 1/4 R K B_{cm}^2 (\cos \alpha - \cos 3\alpha) d\alpha$$

$$= 1/4 R K B_{cm}^2 \left[\sin \alpha - 1/3 \sin 3\alpha \right]_0^\alpha$$

Since $\sin(0) = 0$,

$$x = 1/4 R K B_{cm}^2 (\sin \alpha - 1/3 \sin 3\alpha) \quad 3.19$$

Similarly the vertical component of displacement at point p is the summation of the infinitesimal vertical displacements from $\frac{\pi}{2}$ to α .

$$\int \Delta(dy) = \Delta y = -1/4 R K B_{cm}^2 \int_{\pi/2}^{\alpha} (3 \sin \alpha - \sin 3\alpha) d\alpha \quad 3.20$$

$$= -1/4 R K B_{cm}^2 \left[-3 \cos \alpha + 1/3 \cos 3\alpha \right]_{\pi/2}^{\alpha}$$

Since $\cos(\pi/2) = 0$ and $\cos(3\pi/2) = 0$,

$$\Delta y = 1/4 R K B_{cm}^2 (3 \cos \alpha - 1/3 \cos 3\alpha)$$

The vector sum of Δx and Δy is the radial displacement ΔR_r , due to tangential magnetostriction

$$\Delta R_r = \Delta x \sin \alpha + \Delta y \cos \alpha$$

$$= 1/4 R K B_{cm}^2 (\sin \alpha - 1/3 \sin 3\alpha) \sin \alpha + 1/4 R K B_{cm}^2 (3 \cos \alpha - 1/3 \cos 3\alpha) \cos \alpha$$

Using trigonometric identities and simplifying results in the expression

$$\Delta R_r = 1/2 R K B_{cm}^2 (1 + 1/3 \cos 2\alpha) \quad 3.21$$

The elongation of a radial element of height, h , is $\Delta h = h e_r$

The radial deflection, ΔR_r , varies between one-half the height elongation for a thin straight section to the maximum of the entire elongation for a solid cylinder. The radial deflection of a stator core is very nearly that of the minimum limiting condition and may be approximated as

$$\Delta R_r = 1/2 h e_r \quad 3.22$$

Substituting equation 3.14 into equation 3.22 results in the expression for the radial deflection

$$\Delta R_r = -1/4 K h B_{cm}^2 \sin^2 \alpha$$

$$= -1/8 K h B_{cm}^2 (1 - \cos 2\alpha) \quad 3.23$$

The total deflection due to magnetostriction, ΔR , is the sum of the radial and tangential deflection (Equations 3.21 and 3.23).

$$\Delta R = \Delta R_r + R_r$$

$$= 1/2 K B_{cm}^2 \left[R - h/4 + (R/3 + h/4) \cos 2\alpha \right] \quad 3.24$$

The first term of equation 3.24 represents a static expansion of the core and does not contribute to motor noise or vibration. The second term represents a radial motion varying at twice the angle α for a particular instant of time or a radial motion at twice the angular frequency ωt for a given point on the core periphery.

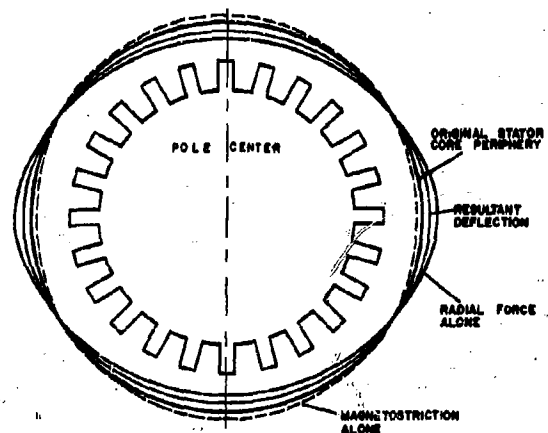
The single amplitude of the magnetostrictive deflection is therefore

$$d_m = 1/2 (R/3 + h/4) K B_{cm}^2 \quad 3.25$$

3.4 COMPARISON OF FORCE WAVE AND MAGNETOSTRICTIVE DEFLECTIONS

The phase displacement of the radial force wave and magnetostrictive deflections of a two pole stator core are illustrated by Figure 3-3. The core is shown for the instant that the air gap magnetic pole centers coincide with the vertical axis. The air gap flux density is maximum along the vertical axis and zero at the horizontal axis. The stator core deflects inward at the magnetic poles and deflects outward between the poles due to the radial force waves. The maximum stator core flux density occurs midway between the poles of air gap flux wave or at the horizontal axis. An examination of equation 3.24 and Figure 3-3 indicates that the magnetostrictive effect will cause the stator core to deflect outward at the vertical axis and inward at the horizontal axis. The $\cos 2\alpha$ term equals +1 for $\alpha = 0$ and -1 for $\alpha = \pi/2$. The radial force wave and the magnetostrictive deflections are identical in form but opposite in direction. The total core deflection is the difference between the maximum deflections due to the two causes. (Equations 3.10 and 3.25).

FIGURE 3-3
Induction Motor Stator Deflection
Two Pole Meter



The relative magnitudes of the two 120 cycle deflections are dependent upon several factors. The most important are:

- 1) The number of poles
- 2) The core and air gap flux densities
- 3) Type of steel
- 4) The stator geometry

Due to the multitude of factors the magnitudes of the deflection may only be calculated for a specific motor design. A 5 HP, 2 Pole, 184 frame dripproof protected motor has been chosen for illustrative purposes.

The radial force wave deflection for a two pole (4 node) motor given by equation 3.10a is repeated here for convenience.

$$d_f = 9.92 \frac{B_{gm}^2 R_g D_s^3}{m^4 h^3} \times 10^{-18} \text{ inches} \quad 3.26$$

The values of the parameters in equation 3.26 for this design are:

$$\begin{aligned} B_{gm} &= 40,000 \text{ lines/sq. in.} & R_g &= 2 \text{ inches} \\ D_s &= 6.58 \text{ inches} & m &= 4 \text{ numeric} \\ h &= 0.883 \text{ inches} \end{aligned}$$

Substituting these values into equation 3.26 reveals the deflection due to radial force waves to be 51.3 microinches.

The deflection of a two pole stator core due to magnetostriction is given by equation 3.25.

$$d_m = 1/2(R/3 + h/4) K B_{cm}^2 \quad (3.25 \text{ repeated})$$

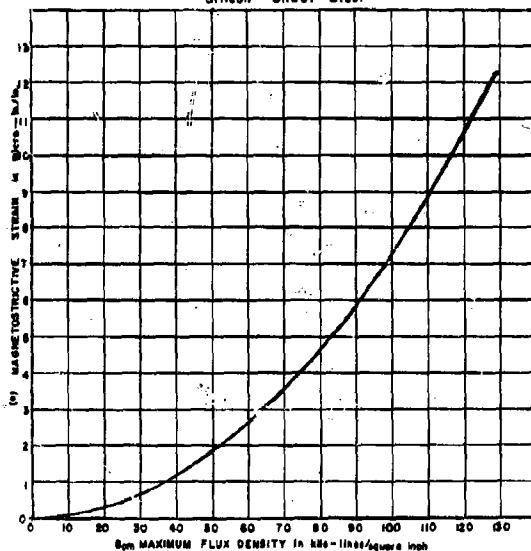
The values of the parameters are:

$$\begin{aligned} R &= 3.73 \text{ in.} & h &= 0.883 \text{ in.} \\ B_{cm} &= 90,000 \text{ lines/sq. in.} \end{aligned}$$

FIGURE 3-4

ASSUMED MAGNETOSTRICTIVE STRAIN VS. FLUX DENSITY

Silicon Sheet Steel



Determining the value of the constant K requires information about the magnetostrictive strain vs. flux density characteristics of the non-oriented stator core steel. As previously mentioned, this information was not available. Figure 3-4 is representative of the maximum magnetostrictive strains exhibited by silicon steels as determined from a survey of the literature. The value of K obtained from this curve is 7.2×10^{-16} . Evaluating equation 3.25 for these values indicates the magnetostrictive deflection to be 4.27 microinches.

Due to the 180° phase displacement, the total 120 cycle deflection is the radial force wave deflection minus the magnetostrictive deflection. For the above examples the total deflection is 47.0 microinches. The magnetostrictive deflection is 8.3%, or one-twelfth the magnitude of the force wave deflection. This corresponds to a 0.75 db decrease in stator core displacement, velocity, or acceleration levels depending upon the units employed.

While the relative effect of magnetostriction will vary with each individual motor design, a general idea of the variation due to motor size may be obtained by investigating the factors relating to stator geometry. Equation 3.25 reveals that the magnetostrictive effect is linearly proportional to the term $(R/3 + h/4)$. Equation 3.26 indicates that the force wave deflection is proportional to $(D_s^3 R_g / h^3)$ for a given number of nodes. Using Allis-Chalmers NEMA two-pole designs as a guide, the ratio of the above factors was calculated for the frame sizes 182 through 405. In all cases the ratios were identical for frame sizes within a frame series of a given diameter.

If these ratios are referred to the 180 series as a base, a frame series factor, F_{fs} , may be obtained.

$$F_{fs} = \frac{\text{ratio for frame series}}{\text{ratio for 180 frame series}}$$

This factor may be used to project the previous 184 frame, 5 HP calculation up through 100 HP. Table 3-1 furnishes the frame series factors and the projected relative magnetostrictive effect as a function of frames series. The magnetostrictive deflection is given in terms of the percentage of radial force wave deflection and as a decibel correction. Only for the 320 series does the correction become appreciably greater than 1 db. An investigation of the stator geometry revealed that this was due to a large radial core thickness which reduced the radial force wave deflection rather than a large magnetostrictive deflection.

TABLE 3-1

Frame Series	180	210	250	280	320	360	400
Frame Series Factor	1	1.04	1.19	1.36	1.66	0.97	0.90
Magnetostrictive Deflection in %	8.3%	8.6%	9.9%	11.3%	13.8%	8.1%	7.5%
Magnetostrictive Deflection in db	0.75db	0.78db	0.91db	1.04db	1.87db	0.73db	0.68db

The fact that the radial force wave and magnetostrictive deflections are in phase opposition suggests the possibility of making them cancel. To do this would require careful attention to the parameters expressed in equations 3.10 and 3.25. The magnetostrictive strain vs. flux density curves for motor grade steel would have to be accurately determined. In addition, it is likely that special steels would have to be developed with larger magnetostrictive strains.

3.5 EFFECT OF FLUX HARMONICS

The derivation of the expression for the magnetostrictive deflection was accomplished by considering only the fundamental of the stator core flux density. The harmonics of the flux density have a much smaller maximum value than the fundamental. As Figure 3-4 indicates, the magnetostrictive strain decreases rapidly for lower flux density. These lower values of magnetostrictive strain also act along a shorter core path. Thus, it may be seen that the magnetostrictive effect of the harmonics is much smaller than that of the fundamental and may be neglected.

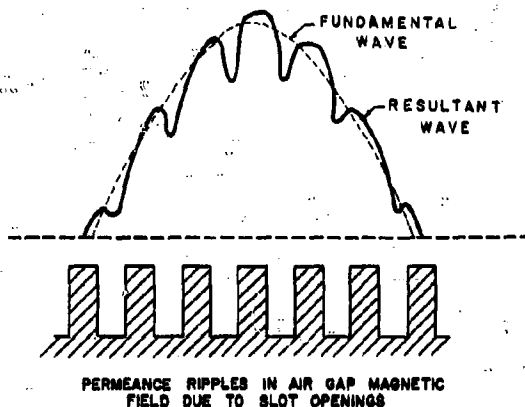
Unlike the harmonics of the core flux density, certain air gap harmonics may be shown to be a significant noise source. In the preceding analysis of the air gap radial force waves, the effect of the harmonics was ignored. The harmonic content of the air gap flux has been the subject of much investigation. (12) It will be sufficient for this treatment to state that most of the air gap harmonics are reduced to sufficiently low values by such methods as proper pitch and distribution of the stator winding and skew of the rotor bars. In addition, the mmf wave of an induction motor contains no harmonics that are a multiple of three due to the three phase winding. However, the rotor and stator slots do create appreciable harmonics by two methods: 1) permeance ripples caused by the slot openings in the steel, and 2) mmf ripples caused by the concentration of current in the slots.

In the discussion of the fundamental flux wave, it was assumed that the permeance of the flux path was uniform around the air gap periphery. Thus a sinusoidal mmf wave produced a sinusoidal flux wave. The presence of slots bordering the air gap causes a variation in the permeance path viewed by the mmf wave. These permeance variations modulate the fundamental flux wave. In Figure 3-5, the fundamental and resultant flux waves are shown above a pictorial representation of the teeth and slot openings. The principal effect of this modulation is the creation of flux harmonics of the order of the number of rotor or stator slots (R and S) respectively.

The concentration of current in the rotor and stator slots causes the magnetomotive force (mmf) wave to be made up of a series of steps. When the fundamental mmf is subtracted from the total, a series of ripples of slot frequency remains. This effect is usually small at no load due to the small stator current

and negligible rotor current. However, it should be noted that even at no load the stator permeance ripples may induce high frequency currents in the rotor bars which will create rotor slot mmf harmonics. This secondary effect is usually reduced to a minimum by proper skewing of the rotor bars.

FIGURE 3-5



The mmf ripples become appreciable under load conditions. As the load on a motor increases, the load currents of both the stator and rotor increase. The load current of the stator sets up a load mmf wave which is displaced 90 electrical degrees from the no load (magnetizing) mmf. The current in the rotor bars set up a mmf wave whose fundamental exactly cancels the fundamental of the stator load mmf. However, both of these mmf waves contain ripples caused by the concentration of current in slots, which do not cancel. As the currents increase with load, these ripples increase proportionately.

The slot harmonics are of such magnitude compared to other harmonics that the air gap field usually may be considered to consist of only the fundamental and the rotor and stator slot harmonics. The mathematical expression for the air gap flux is complicated by the differing speeds of the fundamental and of the slot harmonics. The fundamental wave has P poles and rotates at synchronous speed, $n_s = \frac{7200}{P}$ rpm. The stator slot harmonic wave has 2S poles (S = number of stator slots) and is stationary. The rotor slot harmonic wave has 2R poles (R = number of rotor slots) and travels at rotational speed, $n_r = (1-s) n_s = (1-s) \frac{7200}{P}$ rpm.

In the section dealing with the fundamental flux wave, it was shown that a stationary pulsating wave may be resolved into two oppositely rotating components. The stator slot harmonic wave may thus be represented by two fields, one with 2S-P poles rotating backward and the other with 2S+P poles rotating forward. The respective speeds of these fields are $-\frac{7200}{2S-P}$ and $\frac{7200}{2S+P}$ rpm. The rotating rotor harmonic

wave may be similarly resolved into components. Considering only the fundamental and the stator harmonics, the air gap field may be given by the expression:

$$B_g = B_1 \cos \left(\frac{P}{2} \theta - \omega t \right) \quad 3.27$$

$$+ B_2 \cos \left[\left(S - \frac{P}{2} \right) \theta + \omega t \right] + B_3 \cos \left[\left(S + \frac{P}{2} \right) \theta - \omega t \right]$$

$$+ B_4 \cos \left[\left(R - \frac{P}{2} \right) \theta + \omega t \left(1 - \frac{2R(1-s)}{P} \right) \right]$$

$$+ B_5 \cos \left[\left(R + \frac{P}{2} \right) \theta - \omega t \left(1 + \frac{2R(1-s)}{P} \right) \right] \quad (10)$$

where B_1 = maximum value of fundamental flux density

B_2, B_3 = maximum value of negative and positive rotating components of stator slot harmonic.

B_4, B_5 = maximum value of negative and positive rotating components of rotor slot harmonic.

R, S = number of rotor and stator slots.

P = number of poles

s = slip in per unit

ω = angular velocity $2\pi \times$ input frequency.

θ = angular distance measured from maximum of fundamental.

Equation 3.3 reveals that the force intensity produced by the radial flux is proportional to the square of the flux density. The square of the right hand side of Equation 3.27 contains 30 terms after resolution into single cosine functions. Of these 30 terms, 22 are time varying. Only seven discrete frequencies with varying number of nodes of deflection are produced. The seven frequencies of stator core vibration for 60 cycle motors and the smallest number of nodes of deflection for each frequency are given in Table 3-2.

TABLE 3-2
Stator Core Vibration

Frequency of Vibration	Number of Nodes
1) 120	2P
2) $\frac{120 R (1-s)}{P} - 120$	2R - 2S - 2P
3) $\frac{120 R (1-s)}{P}$	2R - 2S
4) $\frac{120 R (1-s)}{P} + 120$	2R - 2S + 2P
5) $\frac{240 R (1-s)}{P} - 120$	4R - 2P
6) $\frac{240 R (1-s)}{P}$	4R
7) $\frac{240 R (1-s)}{P} + 120$	4R + 2P

The first frequency listed in Table 3-2 is the fundamental force wave previously described. The next three are approximately equal to $\frac{120 R}{P}$ and are often so designated. These may be termed the primary rotor slot frequencies. The rotor slot frequency produced by force waves with the least number of nodes will produce the greatest vibration. If the number of

rotor slots is greater than the number of stator slots ($R > S$), frequency #2 will be the most prominent. Conversely, if $R < S$, frequency #4 predominates. R is never chosen equal to S in order to prevent cogging. The last three frequencies are approximately equal to $\frac{240 R}{P}$ and are termed the secondary or double rotor slot frequencies. Of these three, frequency #5 has the least number of nodes and will predominate.

Tests of many motors indicate that the rotor slot frequency noise is often the highest airborne noise produced. Vibration tests show that the double rotor slot frequency vibration often has the highest db levels. One reason that the double rotor slot frequency predominates in acceleration measurements is that the square of the frequency is reflected in the db levels.

If the expression for the air gap field (Equation 3.27) is referred to the rotational speed of the rotor, the force waves causing the rotor to vibrate may be determined. It can be shown that the rotor will be caused to vibrate at stator slot frequency. Tests of motor vibration of stationary components reveal this frequency to have very low noise levels. Two reasons for this phenomenon are:

- 1) Rotor core is either solid or rigidly attached to the shaft by a spider. The rotor assembly is one of the most rigid motor components and strongly resists deformation.
- 2) Rotor is partially isolated from the stationary components.

It should be remembered that the frequencies of magnetic noise were derived from the expression of the air gap flux of an induction motor. The frequencies produced by other rotating electrical equipment may be quite dissimilar depending upon the harmonic content of the air gap flux density. The possibility that rotor vibrations may be transmitted to the driven unit must also be remembered.

3.6 MEANS OF REDUCING MAGNETIC NOISE

The effective source of induction motor magnetic noise has been shown to be the force waves created by the rotating magnetic field. Since this field is the medium by which power is transmitted from the stator to the rotor, elimination of magnetic noise is not feasible. Magnetic noise may be minimized, however, by several methods. The effect of certain factors on the magnetic noise are described in the following subsections.

3.6.1. Air Gap Flux Density

3.6.2. Rotor-Stator Slot Combination

3.6.3. Rotor and Stator Geometry

3.6.4. Stator Coil Pitch

3.6.5. Skew of Rotor Bars

3.6.6. Grain Orientation of Core Steel

3.6.7. Annealing of Core Steel

3.6.1. Air Gap Flux Density

As Equation 3.10 indicates, the deflection of the stator core is proportional to the square of the air gap flux density. This deflection is transmitted to the motor frame where it both generates airborne noise and is transmitted to the motor feet and thence to the substructure. The factors of transmission and transduction are not necessarily linear. Tests were taken on various motors to determine if a general trend of magnetic noise vs. air gap flux density could be determined. These motors were run at no load with 25, 50, 75, 100, and 125% rated voltage applied. Due to the no load operation the flux density may be assumed proportional to the applied voltage. The vibration acceleration levels for the three axes on the motor feet were recorded. Test data on three representative motors are furnished: 1) a 3 HP, 2 Pole drip proof protected motor, 2) a 5 HP, 2 Pole drip proof protected motor and 3) a 40 HP, 2 Pole totally enclosed fan cooled motor. The adb levels for prominent one-third octave bands that experienced a change in adb levels for these motors are furnished in Tables 3-3, 3-4, and 3-5 respectively.

TABLE 3-3
FLUX DENSITY
3 HP 2 Pole 184 Frame
Vibration Acceleration Levels

Band	Axis	Percent of Rated Voltage				
		25%	50%	75%	100%	125%
63	X	77	78	77	78	78
	Y	83	84	84	84	84
	Z	86	86	86	86	86
125	X	68	68	66	72	73
	Y	67	73	78	83	85
	Z	69	75	78	82	86
4,000	X	89	93	97	101	105
	Y	84	86	88	91	95
	Z	89	92	94	97	101
10,000	X	96	96	97	98	100
	Y	95	96	98	101	103
	Z	96	96	98	100	103
Overall	X	105	105	106	107	109
	Y	101	102	103	104	106
	Z	103	103	104	106	108

Values taken from Spectrograms 3-1 through 3-5.

TABLE 3-4
FLUX DENSITY
5 HP 2 Pole 184 Frame
Vibration Acceleration Levels

Band	Axis	Percent of Rated Voltage				
		25%	50%	75%	100%	125%
63	X	88	88	88	88	88
	Y	85	85	85	85	86
	Z	86	86	86	86	87

Band	Axis	Percent of Rated Voltage				
		25%	50%	75%	100%	125%
125	X	77	79	81	81	83
	Y	67	76	82	86	91
	Z	71	78	83	86	90
1,250	X	92	89	85	86	89
	Y	83	84	86	88	90
	Z	87	85	88	89	92
1,600	X	84	83	83	87	89
	Y	87	89	92	96	98
	Z	92	90	94	97	100
2,000	X	81	82	82	89	92
	Y	84	87	90	90	93
	Z	90	91	94	97	101
4,000	X	87	85	86	87	89
	Y	87	87	87	89	91
	Z	91	91	92	93	95
Overall	X	103	103	103	103	104
	Y	102	103	102	104	105
	Z	104	104	104	106	107

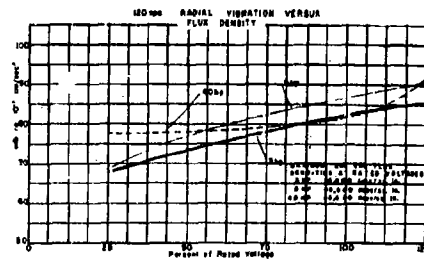
Values taken from Spectrograms 3-6 through 3-10.

TABLE 3-5
FLUX DENSITY
40 HP 2 Pole 364 Frame
Vibration Acceleration Levels

Band	Axis	Percent of Rated Voltage				
		25%	50%	75%	100%	125%
63	X	94	94	94	94	94
	Y	81	81	82	82	83
	Z	84	83	84	85	85
125	X	74	75	73	77	79
	Y	81	80	84	84	91
	Z	75	77	70	82	93
10,000	X	102	102	102	102	102
	Y	116	114	116	116	115
	Z	119	118	119	118	118
Overall	X	109	109	109	110	110
	Y	117	117	118	118	117
	Z	120	120	121	120	120

Values taken from Spectrograms 3-11 through 3-15.

FIGURE 3-6



In Figure 3-6, the average of the 125 cps band adb levels for the radial axes (Y + Z) are plotted versus the applied voltage in percent of rated voltage. The curves for the 3 and 5 HP motors show a slightly decreasing rate of rise whereas the 40 HP curve is linear at low values of flux density but increases rapidly above rated voltage. The maximum air gap flux densities corresponding to rated voltage are 36,000; 40,000; and 28,000 lines per square inch respectively for the 3, 5, and 40 horsepower motors. Thus the rapid increase in vibration of the 40 HP motor does not seem to be due to a numerically high flux density but to non-linear factors of transmission. The different means of construction may be a cause of this variation. The 3 and 5 HP motors are constructed by pressing and tack welding a welded pre-wound stator core into the frame. The 40 HP motor has the stator laminations stacked in the frame and then wound in place.

The effect of flux density on certain rotor slot frequencies may be noted in Tables 3-3 and 3-4. The 3 HP, 2 Pole motor experiences an almost linear increase in vibration in the 4,000 cps band which contains the double rotor slot frequency. The 5 HP, 2 Pole motor, on the other hand, reveals an increase in the 2,000 cps band (rotor slot frequency). The 40 HP motor reveals little change in rotor slot vibration. One reason for this is the smaller relative steel bridge over the rotor slots which is discussed under the effect of slot configuration. Frequencies not listed in these tables experienced slight or no changes.

The variation in the effect of flux density on these motors precludes the determination of an absolute rule. The only recommendation that can be made is the use of the lowest practical flux density consistent with obtaining acceptable motor performance. (The four prototype motors furnished under this contract had maximum air gap flux densities of under 40,000 lines/sq. in.)

3.6.2. Rotor-Stator Slot Combination

The proper selection of stator and rotor slots is probably the most important single aspect of quiet motor design. The number of stator slots is usually chosen a multiple of 3 times the number of poles to give a balanced 3 phase winding. Unbalanced windings are not permissible due to the unbalanced magnetic forces they introduce. This limits the choice of the number of possible stator slots for a particular design to a very few; in some instances there is no choice at all.

The problem simplifies to that of determining the optimum number of rotor slots for a given number of poles and stator slots. Factors other than noise such as elimination of hunting, crawling and cogging eliminate many possible combinations, which are listed in Table 3-6. (13) In all cases the undesirable rotor slots form a band centered about the number of stator slots. Practical considerations limit the maximum and

minimum number of slots that may be used in a rotor of a certain diameter. When all these factors are taken into account, relatively few combinations remain from which the quietest may be selected.

TABLE 3-6

UNDESIRABLE ROTOR-STATOR SLOT COMBINATIONS

Stator Slots	Number of Rotor Slots			
	2 Pole	4 Pole	6 Pole	8 Pole
24	21,22,23,24, 25,26,27	19,20,21,22, 23,24,25,26, 27,28,29	17,18,19,21, 23,24,25,27, 29,30,31	15,16,17,20, 23,24,25,28, 31,32,33
36	33,34,35,36, 37,38,39	31,32,33,34, 35,36,37,38, 39,40,41	29,30,31,33, 35,36,37,39, 41,42,43	27,28,29,32, 35,36,37,40, 43,44,45
48	45,46,47,48, 49,50,51,	43,44,45,46, 47,48,49,50, 51,52,53	41,42,43,45, 47,48,49,51, 53,54,55	39,40,41,44, 47,48,49,52, 55,56,57
54	51,52,53,54, 55,56,57	49,50,51,52, 53,54,55,56, 57,58,59	47,48,49,51, 53,54,55,57, 59,60,61	45,46,47,50, 53,54,55,58, 61,62,63
60	57,58,59,60, 61,62,63	55,56,57,58, 59,60,61,62, 63,64,65	53,54,55,57, 59,60,61,63, 65,66,67	51,52,53,56, 59,60,61,64, 67,68,69
72	69,70,71,72, 73,74,75	67,68,69,70, 71,72,73,74, 75,76,77	65,66,67,69, 71,72,73,75, 77,78,79	63,64,65,68, 71,72,73,76, 79,80,81

TABLE 3-7

PREFERABLE ROTOR-STATOR SLOT COMBINATIONS

Stator Slots	Number of Rotor Slots			
	2 Pole	4 Pole	6 Pole	8 Pole
24	32 34 (12)(16)	32 34 (8)(12)	32 36 (4)(12)	---
36	26 28 44 (16)(12)(12)	26 28 44 (12)(8)(8)	46 48 (8)(12)	48 52 (8)(16)
48	38 40 56 (16)(12)(12)	38 40 56 (12)(8)(8)	58 60 64 68 (8)(12)(20)(28)	58 64 (4)(16)
54	46 62 (12)(12)	46 62 (8)(8)	42 66 (4)(12)	38 40 66 70 (16)(12)(8)(16)
60	52 68 78 (12)(12)(32)	44 46 52 76 (24)(20)(8)(24)	44 48 72 (20)(12)(12)	44 76 (16)(16)
72	---	---	60 (12)	56 58 (16)(12)

From a noise viewpoint, the optimum number of rotor slots for any pole-stator slot combination is that which produces deflections having the greatest number of nodes. For the primary rotor slot frequencies (Numbers 2, 3, and 4 in Table 3-2); this requires the largest practicable difference in the number of rotor and stator slots. For the double rotor slot frequencies, a large number of rotor slots are required. Table 3-7 lists rotor-stator slot combinations frequently used. The numbers in parenthesis are the minimum number of nodes of deflection of the primary rotor slot frequencies. The combinations with large numbers in parenthesis are preferred. Where more than one number of rotor slots produce the same number of nodes of primary rotor slot frequency vibration, the larger should be chosen to reduce the double rotor slot frequency vibration.

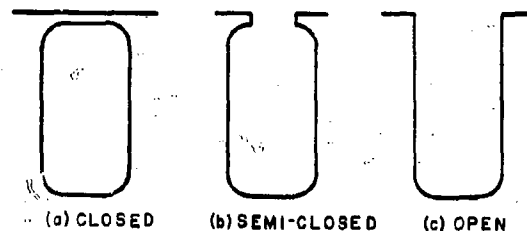
3.6.3. Rotor and Stator Geometry

Various factors related to the geometry of the rotor and stator effect the magnitude of magnetic noise produced by an induction motor. Equation 3.10 reveals the deflection of the stator core to be proportional to $\frac{R_a D_s^3}{h}$, where R_a is the air gap radius, D_s is the mean diameter of the stator core, and h is the radial depth of the core. The deflection may be minimized by reducing the values of R_a and D_s or increasing the value of h . The air gap radius is not easily reduced; nor can the core diameter be decreased without greatly decreasing the core depth. The principal reduction of stator core deflection may be accomplished by increasing the radial depth of the stator core, h . This increased core depth will cause the mean diameter to increase slightly but the overall effect will be a reduction of stator core vibration.

The h^3 term is introduced into Equation 3.10 by the bending moment of inertia of the core. Therefore, any design change that stiffens the core will increase the effective value of h . In the derivation of this equation, any stiffening effect of the stator teeth or motor frame was not considered. The stator teeth will normally have little influence but the frame can help to stiffen the stator core. Continuous peripheral contact between the core and frame or the use of circular rather than axial ribs will result in a larger bending moment of inertia and thus less stator core deflection.

Squirrel cage induction motors have either closed or semi-closed rotor slots as shown in Figure 3-7, a and b, and semi-closed or open slots (b and c). The partial or complete steel bridge over the slots decreases the permeance variation as sensed by the opposing member. The decrease in permeance variation will result in lower magnitudes of slot harmonics of the air gap flux density wave, as expressed in Equation 3.27. The amount of the decrease may vary from appreciable to negligible, depending upon the motor dimensions.

FIGURE 3-7
Slot Configuration



A closed rotor slot causes less permeance variation than a semi-closed slot. However, the thickness of the steel bridge is dependent upon manufacturing tolerances and mechanical strength requirements and is often kept to a minimum to reduce the undesirable rotor slot leakage reactance. As a result the bridge thickness does not increase at the same rate as the motor size. The smaller relative bridge thickness of larger motors may become saturated with leakage flux even at no load. As the steel bridge saturates, the permeance variation approaches that of a completely open slot, Figure 3-7c. Under such circumstances, the closed slot may not appreciably reduce magnetic noise. A discussion of the effect of motor load upon this phenomenon is presented in Section 7. Since the use of closed slots never causes an increase in noise it is recommended that rotors with closed slot configuration be used.

For similar reasons, stators should utilize semi-closed rather than open slot configuration. The width of the slot opening should be kept to a minimum. The ability to wind the motor will determine the minimum opening that may be used. For noise critical applications, where an increase in winding time and therefore cost is permissible, the minimum opening may be established as twice the thickness of the slot liner plus the diameter over insulation of the largest wire size plus 20 mils clearance. For motors built in frames larger than 286 frame, the clearance should be increased to 30 mils.

The length of the air gap also affects the permeance variation; the longer the air gap, the less variation is sensed by the opposing member. The length of air gap is also dependent on design criteria other than noise. The merits of increasing the air gap to reduce the slot harmonic magnetic noise must be compared to the corresponding decrease in power factor and efficiency as well as an increase in starting current. If both closed rotor slots and stator slots with the minimum openings are used, it is felt that air gap lengths used for NEMA motors will be sufficient. For example, NEMA motors built on the 180 frame series have air gaps of .014 to .018"; those built on the 360 series have .025 to .040" air gaps. The air gap length within a frame series increases with a decrease in number of poles.

3.6.4. Stator Coil Pitch

In the discussion of the air gap flux harmonics, it was stated that harmonics other than the slot harmonics are reduced by the pitch and distribution of the stator windings. The distribution factor for each harmonic is a direct function of the number of stator slots. As previously mentioned, the number of stator slots is often fixed by physical limitations and the necessity of having a multiple of 3P. However, a choice in the stator coil pitch usually exists. The pitch ratio should be selected to give small pitch factors for the lower order air gap harmonics. Due to the step function of the induced mmf wave, the lower order harmonics predominate (except for the slot harmonics).

The pitch factor for the nth harmonic is given by the expression

$$K_{pn} = \cos n(1-\text{Pitch Ratio}) 90^\circ \quad 3.28$$

In Table 3-8, the pitch factor for the fundamental and the fifth, seventh and eleventh harmonics are given for various pitch ratios. Due to symmetry there are no even harmonics. The third harmonic and all harmonics a multiple of three are not present in three phase motors. Thus the optimum pitch ratio is that producing low pitch factors for the fifth and higher harmonics. Usually only the fifth and seventh harmonic pitch factors need be considered.

TABLE 3-8
HARMONIC PITCH FACTORS

Dec.	Slots Per Pole										Pitch Factor				
	3	4	6	8	9	10	12	15	18	21	24	Kp1	Kp5	Kp7	Kp11
1	1	1	1	1	1	1	1	1	1	1		1.000	1.000	1.000	1.000
.958											23/24	.996	.947	.897	.752
.952											20/21	.997	.951	.901	.802
.944											17/18	.996	.956	.904	.774
.933											14/15	.995	.966	.913	.802
.917											11/12	.991	.979	.926	.831
.905											10/11	.989	.983	.930	.845
.900											9/10	.988	.987	.934	.858
.887					8/9						16/18	.985	.983	.932	.862
.872					7/8						21/24	.981	.980	.931	.864
.857											13/15	.978	.978	.930	.865
.857											12/14	.978	.978	.930	.865
.853											10/12	.976	.976	.929	.862
.853											9/11	.976	.976	.929	.862
.850											17/21	.975	.975	.928	.861
.850											15/18	.975	.975	.928	.861
.847											12/15	.974	.974	.928	.861
.847											11/14	.974	.974	.928	.861
.846											10/13	.974	.974	.928	.861
.846											9/12	.974	.974	.928	.861
.843											17/18	.974	.974	.928	.861
.843											16/21	.974	.974	.928	.861
.843											15/24	.974	.974	.928	.861
.843											14/21	.974	.974	.928	.861
.843											13/21	.974	.974	.928	.861
.843											12/24	.974	.974	.928	.861
.843											11/24	.974	.974	.928	.861
.843											10/24	.974	.974	.928	.861
.843											9/24	.974	.974	.928	.861
.843											8/24	.974	.974	.928	.861
.843											7/24	.974	.974	.928	.861
.843											6/24	.974	.974	.928	.861
.843											5/24	.974	.974	.928	.861
.843											4/24	.974	.974	.928	.861
.843											3/24	.974	.974	.928	.861

3.6.5. Skew of Rotor Bars

The practice of skewing either the rotor or stator slots with respect to the axis of rotation to reduce noise and provide for smooth acceleration has become so prevalent that the vast majority of induction motors are skewed. Authorities agree that skewing reduces magnetic noise, but there is no clear agreement on the optimum amount of skew. In addition, practically all the literature refers to the effect of skew on only the overall airborne sound pressure levels; little of nothing is said about structureborne noise or frequency analysis. It was the object of this study to investigate these areas.

The degree of skew affects the performance of a motor as well as the noise and vibration. In fact, the rapid decay of motor performance with increasing skew is generally the factor which limits the amount a motor may be skewed. Therefore, it was necessary to determine and to relate the effects of skew on both motor performance and noise. The effect of skew shows up principally in the parameters of the skewed member (rotor) and only slightly in the non-skewed member (stator) through mutual inductance. (14) The parameter most affected is the rotor leakage reactance which contains a factor $(1 + SK^2)$ where

$$SK = X/\tau$$

SK = skew in "rotor slots"

X = radial displacement of ends of rotor bars

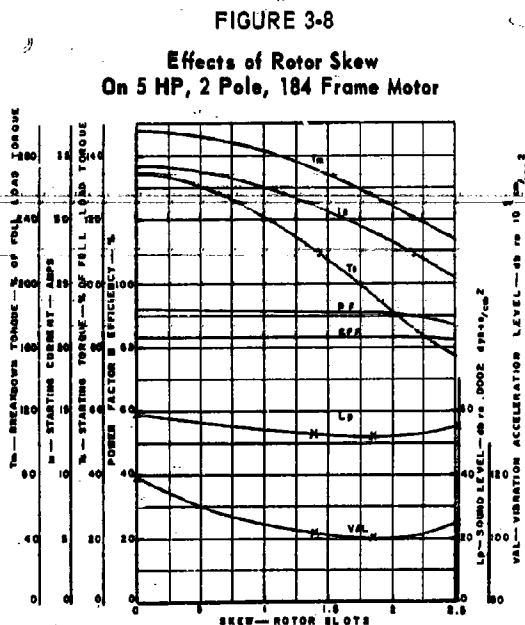
τ = rotor slot pitch measured in same units as X

Therefore, skew is expressed in terms of number of rotor slots for this study.

A 5 HP, 2 pole, 184 frame motor design was used for this study. Performance factors such as breakdown torque, starting current, starting torque, power factor and efficiency were calculated for various amounts of rotor skew. Although several methods of calculating induction motor reactances are used, the degree of skew was considered to affect only the rotor leakage reactance with regard to performance calculations. This method has been found to correlate very well with actual tests. Other parameters, such as the rotor resistance, also change slightly. This change is small and may be ignored without unduly sacrificing accuracy.

Much ambiguity exists in the technical literature with respect to the effect of skew on motor noise. (15,16) Calculation of the noise produced by varying amounts of skew cannot accurately be made. Therefore, the above motor was built with four rotors, identical except for the amount of skew. These rotors had 0, 1.41, 1.86, and 2.50 rotor slots skew respectively. Airborne and structureborne noise measurements were taken of the motor with all four rotors.

Figure 3-8 shows the calculated performance factors and the measured overall noise levels for this motor for skews ranging from zero to 2.5 rotor slots. The breakdown torque, starting torque and starting current can be seen to drop off quite sharply as the amount of skew is increased. The full load power factor and efficiency curves show little change until an extreme amount of skew is used. Two curves of test data are plotted to indicate the overall noise level of the motor with respect to skew. The sound pressure level curve, L_p , is the overall reading taken at three feet from the front end (opposite the shaft extension) of the motor. The vibration acceleration level curve, VAL, is a plot of the average of the overall levels for the three axes on the motor feet. These noise curves reveal a gradual increase to a broad valley followed by a more rapid increase.



A clearer picture of the effect of skew on magnetic noise may be obtained by inspecting the one-third octave sound pressure and acceleration levels listed in Tables 3-9 and 3-10, respectively. Since magnetic noise first appears as motor vibration, Table 3-10 is the more indicative. The low frequencies reveal a varying pattern with respect to increasing skew. The 63 cps X-Axis vibration decreases sharply as does the 125 cps X-Axis band. The 125 cps band shows a more gradual decrease in the radial (Y & Z) axes. The 200 cps band has a sporadic variation. This table reveals that the primary effect of increasing skew shows up in the frequency bands above 2,000 cps. All of these bands have a variation similar to the VAL curve of Figure 3-8.

TABLE 3-9
SKEW TEST
5 HP 2 Pole
Sound Pressure Levels

Band	0 RS	1.41 RS	1.86 RS	2.5 RS
125	35	29	30	28
250	39	34	33	38
315	49	42	40	43
800	52	42	42	48
1,250	49	41	42	45
4,000	44.5	31.5	33	36
5,000	40	34.5	36.5	34.5
Overall	59	53	52	55

Values taken from Spectrograms 3-16 and 3-17.

TABLE 3-10
SKEW TEST
5 HP 2 Pole
Vibration Acceleration Levels

Band	Axis	0 RS	1.41 RS	1.86 RS	2.5 RS
63	X	95.5	80	77	74
	Y	84	79.5	84	85
	Z	80	75.5	83	86
125	X	97	71	75	*
	Y	87	83	83	82
	Z	85	83	82	81
200	X	83	74	87	80
	Y	74	73	77	72
	Z	74	70	*	*
2,000	X	101	94	92	96
	Y	103	94	92.5	98
	Z	97	88	89	96
2,500	X	100	93	91.5	95
	Y	101.5	93	90	94
	Z	94	85	85	88
4,000	X	107	94	91	93
	Y	107	90	86	89
	Z	109	90	88	91
8,000	X	108	88.5	82	92
	Y	112	91.5	88	98
	Z	105.5	86	87	96
10,000	X	122	100.5	97	102.5
	Y	110	92.5	91	98
	Z	117	93.5	97	101
Overall	X	124	105	101	107
	Y	115	101	99	104
	Z	118	99	99	104.5

*Values less than 70 adb were below range of recording paper.

Values taken from Spectrograms 3-18 through 3-21.

Of the low frequency bands, only the 125 cps radial axes band reflect magnetic noise variation; the others reflect a change in bearing noise. The bearings used in this test had large internal clearances and were not initially preloaded. The skew of the rotor bars produces an axial component of the force on the rotor bars created by the magnetic field and the rotor bar currents. This axial force increases skew, and preloads one motor bearing similar to the manner described in Section 7 on the effects of motor load. The rotational frequency noise (60 cps) decreases due to the taking up of the internal clearances which improve the concentricity of the air gap. The 125 cps band variation in the X-Axis is the second harmonic of this rotational frequency change. The erratic variation of the 200 cps band is due to variation in preload force on the bearing. This variation is quite similar to that of the same band obtained in the preload amount test (Table 4-2, Section 4). It will be shown in Section 4 that the preload force may be adjusted to result in minimum bearing noise. These variations in bearing noise are therefore extraneous to this study of magnetic noise and may be ignored. Thus, only the high frequency and the 125 cps radial axes bands reflect variation in magnetic noise.

The initial decrease in magnetic noise with an increase in skew is due to the reduction of the rotor slot harmonics. At zero skew, the flux pulsations caused by segments along the axial length of the rotor slots are in space phase. As the skew is increased, the phase difference between the pulsations of the segments becomes greater. To the extent that the stator core may be considered as a unit rather than as individual laminations, the effective rotor slot harmonic may be considered the phasor sum of the pulsations of all segments along the length of the rotor slots. An increase in skew causes a greater phase displacement and thus a lower effective rotor slot harmonic. Under these assumptions, a skew of one rotor slot would eliminate deflection caused by force waves set up by the rotor slot harmonic. Figure 3-8 and Table 3-10 indicate the minimum slot frequency noise is achieved at higher values of skew. This suggests that the stator core reacts to the skewed force wave neither as individual lamination nor as a solid core but as some intermediate structure. The decrease in 120 cycle magnetic noise reflected in the radial axes 125 cps band is also due to the reduction in rotor slot harmonic. Referring to Equation 3.27 the cross multiplication of the oppositely rotating rotor slot harmonics can be seen to produce 120 cps vibration with the same number of nodes as the square of the fundamental. The maximum flux densities of the slot harmonics are much smaller than the fundamental and the decrease in the 120 cps vibration is thus much less than that of the rotor slot frequencies.

At values of skew greater than 2 rotor slots the magnetic noise produced by the rotor slot harmonics

increases. There are several potential reasons for this increase.

1. The skew has increased to the point that the actual phase displacements of the stator core vibration from end to end are greater than 360° and are causing a greater total deflection.
2. The increase in skew results in a large leakage flux, decreasing the flux linking the rotor. The rotor bar currents must therefore increase to supply the no load losses of the motor. The increased rotor currents cause an increased mmf and permeance ripples in the same manner as the rotor bar load currents described in Section 7.

The relative effect of these factors was not evaluated, since the deterioration of motor performance is sufficient to prohibit this large amount of skew. However it is important that a noise minimum exists.

These noise measurements reveal that there is an optimum amount of rotor bar skew. For this motor, it does not occur at either one rotor bar skew or one stator slot skew (1.4 rotor slots for this particular motor). Both of these amounts are often proposed as optimum values in the literature. The optimum point for this motor is between 1.75 and 2.0 rotor slots skew. The amount of skew has also been determined to affect the entire frequency spectrum of the motor rather than only isolated frequencies.

The extent to which a stator core will deflect as a unit rather than as individual punchings is dependent upon the construction of the stator core. Thus the analytical determination of the optimum skew for an induction motor is not possible for the general case. However, this study reveals that the optimum skew is not critical; that the minimum noise occurs at the bottom of a broad valley. An amount of skew that will result in near minimum magnetic noise may be selected analytically. The absolute minimum may be determined by test of several rotors with varying amounts of skew.

Skewing less than one rotor slot is not only ineffective in appreciably reducing the unit's noise and vibration, but is also insufficient to minimize the stray load losses and the probability of encountering cogging or crawling during acceleration. On the other hand, the rapid decay of performance with respect to skew precludes the use of an amount of skew appreciably greater than 1.5 rotor slots. As a first approximation, it is suggested that the rotor be skewed one rotor or stator slot, whichever produces the greater angle. An examination of the slot combinations listed in Table 3-7 reveals that one stator slot pitch never exceeds 1.5 rotor slots. For the test motor, this method would recommend 1.4 rotor slots skew (1 stator slot) which results in near minimum motor noise without too great a sacrifice of motor performance.

One aspect of this test requires further explanation. Table 3-10 reveals that in the high frequency region not only the primary and secondary rotor slot

frequencies (approximately 2,000 & 4,000 cps, respectively) are affected by the amount of skew, but also harmonics of these frequencies. These harmonics are introduced by the variation in permeability of the core steel described in the next two subsections. Thus the 8,000 & 10,000 cps bands reflect magnetic noise at low values of skew. The skew angle affects the harmonics to a greater degree than the primary rotor slot frequencies. At higher skews the magnetic noise levels in the high frequency bands falls below that noise produced by the bearings. Throughout this report, it will be noted that the 8,000 & 10,000 cps bands usually reflect variation in bearing noise since the motors under test had skewed rotors.

3.6.6. Grain Orientation of Core Steel

In the evaluation of the effect of grain orientation on motor noise, two external sources of information were consulted. A thorough literature search was undertaken and steel companies supplying electrical sheet steel were consulted. The data on orientation in the technical literature is concerned only with the magnetostrictive effect and specifically, with regard to transformers. Contact was made with four steel companies to determine if studies were underway but not yet reported in the literature. None of these companies had investigated the effect under question but one company has begun an experimental study on the varying permeability of the sheet steel as a function of angle with respect to rolling direction. This is a prerequisite step to any thorough study and lacking such information, only a preliminary investigation could be made. General information and certain theories developed in this study are given below.

The effect of orientation is caused by the crystal structure of the steel and the rolling process used in making the steel into sheets. Steel is composed of crystals or "grains". Within the grains, the atoms are arranged in systematic order. At the boundary between grains, there exists a disorganization of atoms. Magnetic flux finds it easy to transverse a crystal but the disorganization of atoms at the grain boundary causes a barrier. Rolling the steel causes the crystals to elongate in the direction of roll. Thus, flux traveling in the direction of roll crosses fewer grain boundaries and thus encounters less resistance to the flux (reluctance). The steel is said to have a high permeability in this direction of roll.

Most electrical sheet steel used in induction motors is termed "non-oriented" while steel supplied mainly for transformer use is termed "grain-oriented". Actually non-oriented steel is made only somewhat less oriented than the transformer grade by rolling the sheets in two directions at right angles to each other. The grain-oriented steel has a permeability at right angles to the roll direction (lateral) one-tenth, or less, of the permeability in the roll (transverse)

direction. The non-oriented steel has a lateral permeability of 80 - 85% of the transverse permeability. The transverse permeability of motor grade steel is lower due to the bi-directional rolling operation. The permeability of motor grade steel at a 45° angle to roll is believed to be lower than in either the lateral or transverse directions but exact values are not available.

This variation in permeability results in what may be termed a "pole" effect. There exists an inherent tendency for flux to form a strong pair of poles in the transverse direction with a somewhat weaker pair of poles in the lateral direction and with "valleys" in between all four poles. This pole effect causes, in theory, second and fourth harmonics of all air gap fluxes, such as the slot harmonics, as well as the fundamental.

To determine if orientation is important in an induction motor, a 3 HP, 2 pole motor was built with two sample stator cores of motor grade steel. One of these cores had all stator punchings lined up with respect to the direction of roll (oriented) and the other had each punching rotated 45° with respect to the adjacent punching (non-oriented). With 120 punchings in the 3 inch long core, the varying permeabilities of the second core were averaged and resulted in a highly uniform permeability. The cores were wound identically and tested with the same motor frame and other components.

Table 3-11 lists the vibration acceleration levels for this test. These band levels indicate the non-oriented core to result in an appreciably lower axial X-axis vibration in the frequency bands below 250 cps. The radial (Y and Z) axes show a smaller decrease. The rotor slot frequency (2,000 cps) increases slightly but the double rotor slot frequency (4,000 cps band) experiences a 5.5 adb decrease in the radial axes and a 2. adb decrease in the X-axis. The 8,000 and 10,000 bands reflect an increase in bearing noise due to deterioration of the bearings.

This test indicates that the non-oriented stator core experiences less vibration than the oriented core. It is especially interesting that the decrease in vibration takes place in the shaft axis for harmonics of the fundamental flux wave and the radial axes for the second harmonic of the rotor slot frequency. The variation in direction is not fully understood at this time. However, since elimination of orientation reduces magnetic noise, the stator core should be so constructed to minimize variation in permeability. If the number of stator slots is a multiple of 8, the successive laminations should be rotated in steps of 45° (one-eighth revolution). For stators with 54 or 60 slots, the laminations should be rotated in steps of 90°.

TABLE 3-11
Grain Orientation
Vibration Acceleration Levels

Band	Axis	Oriented Core	Non-Oriented Core
63	X	86	74
	Y	78	75
	Z	73	74
125	X	89.5	76
	Y	81	78
	Z	81	78
200	X	85	77
	Y	71	71
	Z	65	67
250	X	78	73
	Y	67	65
	Z	72	67
2,000	X	90	90
	Y	90	91
	Z	87	91
4,000	X	89	87
	Y	91.5	86
	Z	97.5	92
8,000	X	92	96
	Y	94	94
	Z	93	98
10,000	X	91	98
	Y	93	96
	Z	92	98
Overall	X	103	104
	Y	101	102
	Z	103	104

Values taken from Spectrograms 3-22 and 3-23.

3.6.7. Annealing of Core Steel

A test was conducted to determine the effect that annealing rotor and stator punchings has on induction motor noise. Many manufacturers use annealed laminations to take advantage of the lower core loss of annealed steel. During annealing, the crystal grains enlarge in the direction of roll. The resulting decrease in grain boundaries increases the permeability in that direction. However, the difference between roll and transverse directions becomes greater.

The 3 HP, 2 pole motor design was again used for this test. Two stator cores were built with punching aligned with respect to the direction of roll: one of annealed steel, the other of non-annealed steel. Table 3-12 lists the prominent acceleration levels for the X, Y, and Z axes and the stator core for these two motors. The rotational frequency indicated in the 63 cps band shows a sporadic variation, as does the 1,250 cps band. The 2,000 cps band containing the

rotor slot frequency shows an average 4 db lower acceleration level for the non-annealed core. The double rotor slot frequency (4,000 cps band) reveals an even greater change especially on the stator core. The 8,000 and 10,000 cps bands reveal an average 20 db decrease of stator core vibrations for the non-annealed core. This effect reveals itself to only a minor degree on the three axes on the motor feet. These high frequency magnetic-induced stator vibrations are greatly attenuated in the transmission to and through the motor frame. Thus while the stator core has a high level of 8,000 or 10,000 cps magnetic vibration, this has only a nominal effect on the motor noise as normally measured on the feet. The high frequency bearing noise, on the other hand, is more easily transmitted to the feet due to the continuous peripheral contact between the bearings and the bearing housing. Thus the 8,000 and 10,000 cps magnetic noise revealed in this test does not invalidate the statements made elsewhere that these frequency bands normally reflect bearing noise.

TABLE 3-12
Annual Stator Core Test
Vibration Acceleration Levels

Band	Axis	Annealed Core	Non-Annealed Core
63	X	82	82
	Y	74	79
	Z	82	81
	Core	75	75
1,250	X	80	88
	Y	86	86
	Z	82	79
	Core	79	78
2,000	X	85	79
	Y	84	85
	Z	95	90
	Core	90	84
4,000	X	89	88
	Y	98	94
	Z	96	90
	Core	112	92
8,000	X	96	93
	Y	99	93
	Z	103	101
	Core	104	83
10,000	X	98	100
	Y	105	100
	Z	101	98
	Core	102	80
Overall	X	105	105
	Y	108	104
	Z	108	105
	Core	115	103

Values taken from Spectrograms 3-24 through 3-27.

TABLE 3-13

**Anneal Rotor Core Test
Vibration Acceleration Levels**

Band	Axis	Annealed Core	Non-Annealed Core
63	X	95	97
	Y	89	91
	Z	81	89
	Core	89	88
2,000	X	98	97
	Y	98	96
	Z	90	90
	Core	87	88
4,000	X	94	92
	Y	100	96
	Z	100	98
	Core	92	92
6,000	X	91	88
	Y	88	86
	Z	86	85
	Core	97	89
8,000	X	96	96
	Y	94	92
	Z	88	88
	Core	82	87
Overall	X	106	105
	Y	106	104
	Z	104	103
	Core	104	101

Values taken from Spectrograms 3-28 through 3-31.

A similar test was conducted to determine the effect of annealing rotor punchings on motor noise. Two rotor cores were built for the 3 HP motor similar to the stator cores previously described. As Table 3-13 indicates, the non-annealed rotor core caused slightly less vibration (an average 2 adb overall reduction). The greatest difference was 8 adb recorded on the core at 6,000 cps. There are two reasons that annealing of rotor punchings has less effect than annealing of stator punchings.

- 1) The skewing of rotor punchings reduces the pole effect slightly.
- 2) At no load, the rotor is rotating at almost synchronous speed. The rotor pole effect therefore, only modifies the synchronous flux wave to a slight degree.

These two tests indicate that annealing of aligned punchings increases the pole effect caused by grain orientation and, therefore, introduces harmonics of the stator core vibrations. However, if the stator and rotor punchings are rotated in the manner described in the previous test, the pole effect is not present and annealing will not cause an increase in motor noise. Annealed punchings should be used only if the punchings are staggered to minimize variation in permeability.

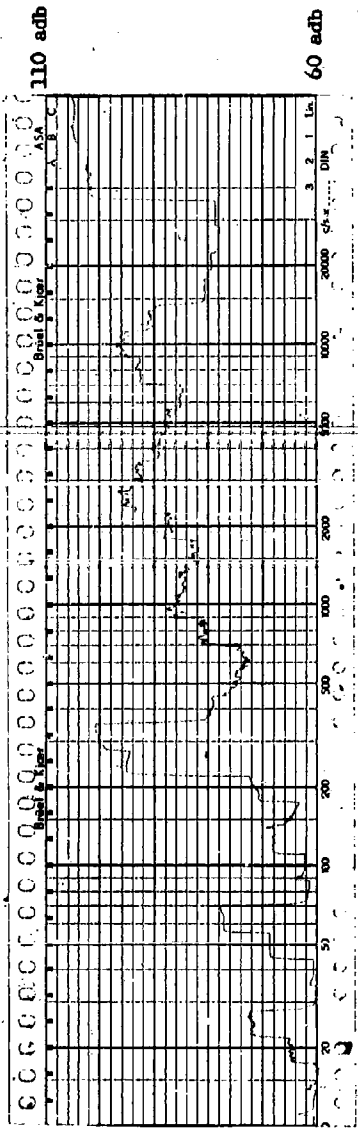
3.7 CONCLUSION

The predominant source of induction motor magnetic noise has been shown to be the radial force waves set up by the air gap flux density. The importance of the frequencies produced has been proved to be inversely proportional to the fourth power of the number of nodes of the force wave producing the frequency for a given flux density. The frequencies and the smallest number of nodes producing each frequency are given in Table 3-2.

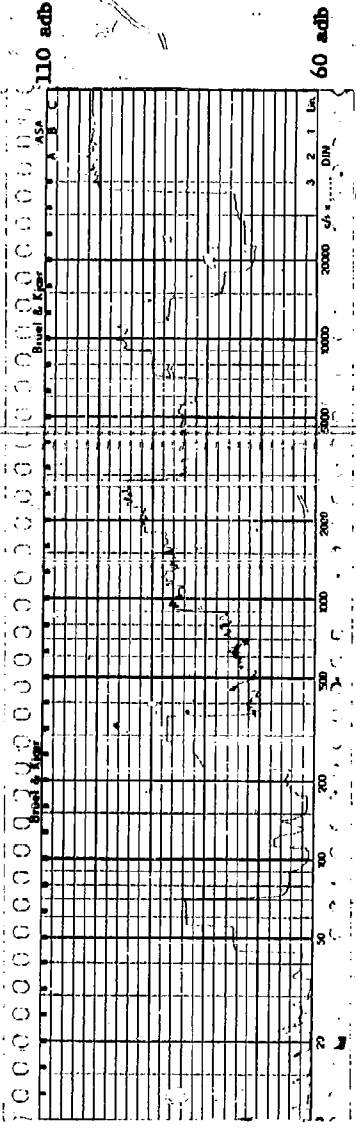
The steps that may be taken to reduce magnetic noise are these:

1. Use of low air gap flux densities. Maximum density of 40,000 lines per square inch is recommended. However, a low flux density is not consistent with compact motor design.
2. Selection of proper rotor-stator slot combination to produce high node force waves. Acceptable combinations are listed in Table 3-7.
3. Increase in actual or effective radial thickness of stator core. Effective thickness is increased by frame modification such as circumferential ribs.
4. Use of closed rotor slots and narrow neck semi-closed stator slots.
5. Selection of stator coil pitch to minimize 5th and 7th harmonic of air gap flux density.
6. Skewing rotor bars one rotor slot or one stator slot, whichever is the greater amount of skew.
7. Rotation of successive stator core laminations to minimize permeance variation due to grain orientation. Punchings should be rotated preferably by 45° steps or, if the number of stator slots prevents this, by 90° steps.
8. Laminations should be annealed only if punchings are rotated as specified in 7.

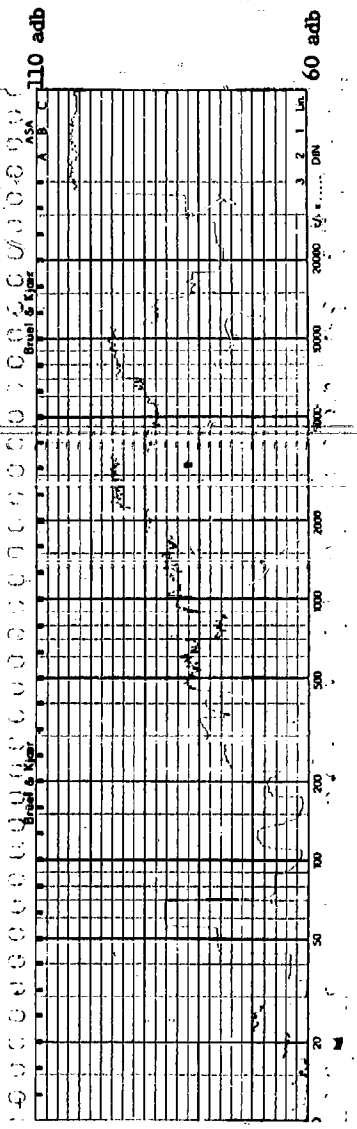
J



Flux Density
 3 HP 2 Pole
 184 Frame Open
 22 April 1960
 Structureborne
 25% Rated Voltage
 X-Axis

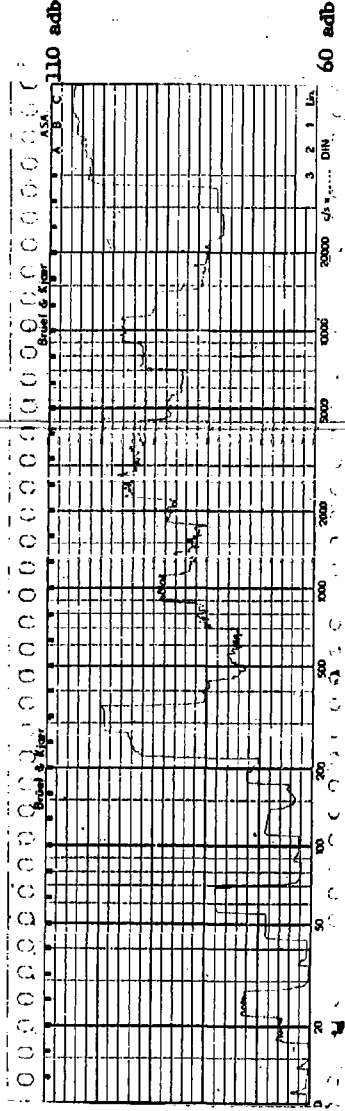


Flux Density
 3 HP 2 Pole
 184 Frame Open
 22 April 1960
 Structureborne
 25% Rated Voltage
 X-Axis

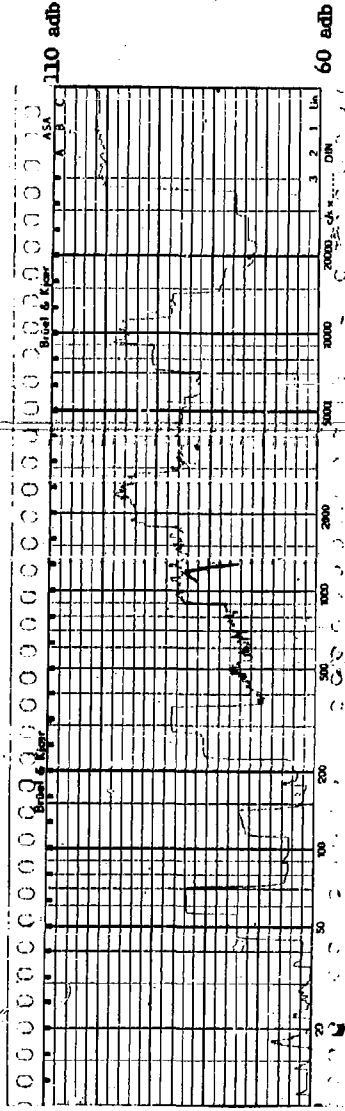


Flux Density
 3 HP 2 Pole
 184 Frame Open
 22 April 1960
 Structureborne
 25% Rated Voltage
 Z-Axis

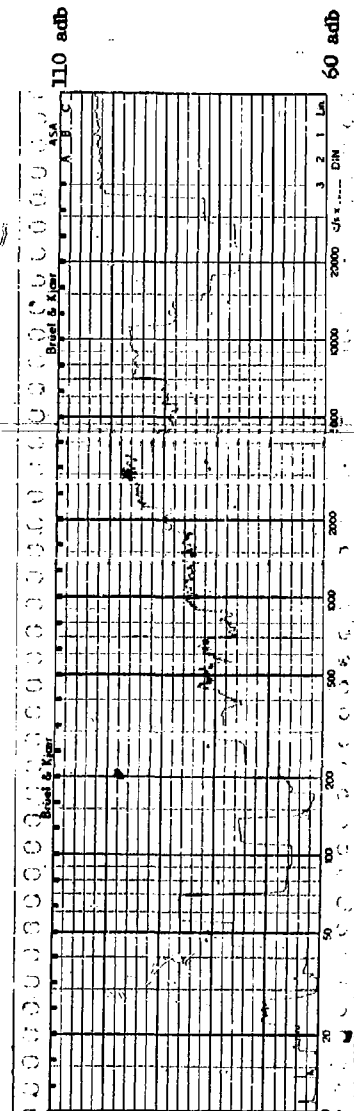
Flux Density
 3 HP 2 Pole
 184 Frame Open
 22 April 1960
 Structureborne
 50% Rated Voltage
 I-Axis



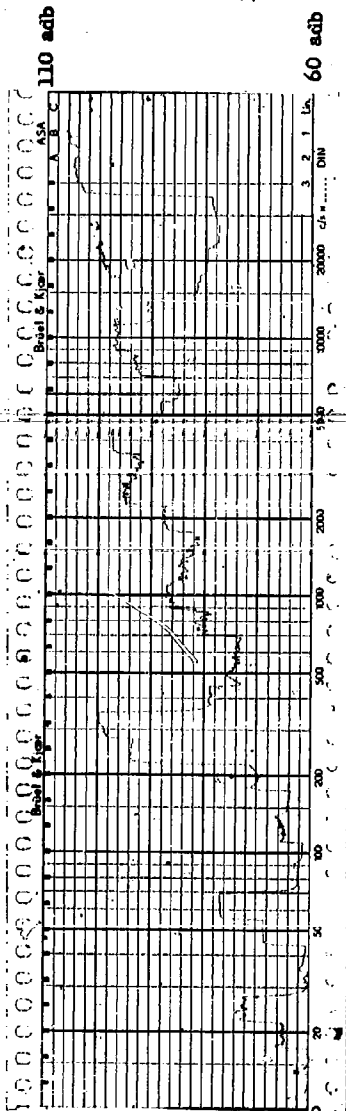
Flux Density
 3 HP 2-Pole
 184 Frame Open
 22 April 1960
 Structureborne
 50% Rated Voltage
 Y-Axis



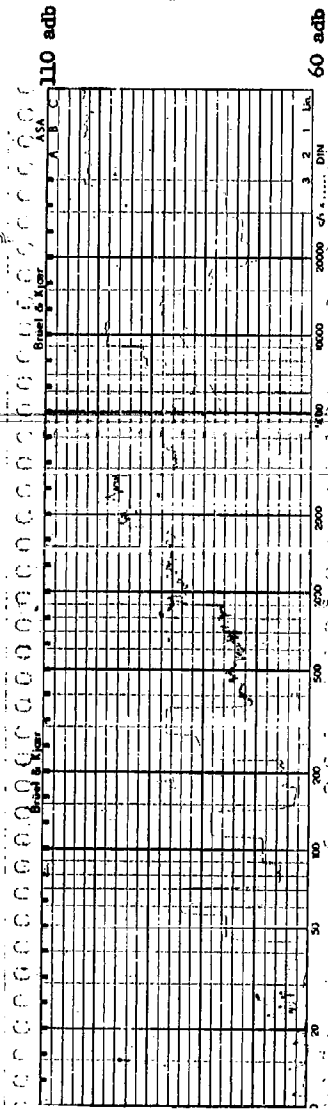
Flux Density
 3 HP 2 Pole
 184 Frame Open
 22 April 1960
 Structureborne
 50% Rated Voltage
 Z-Axis



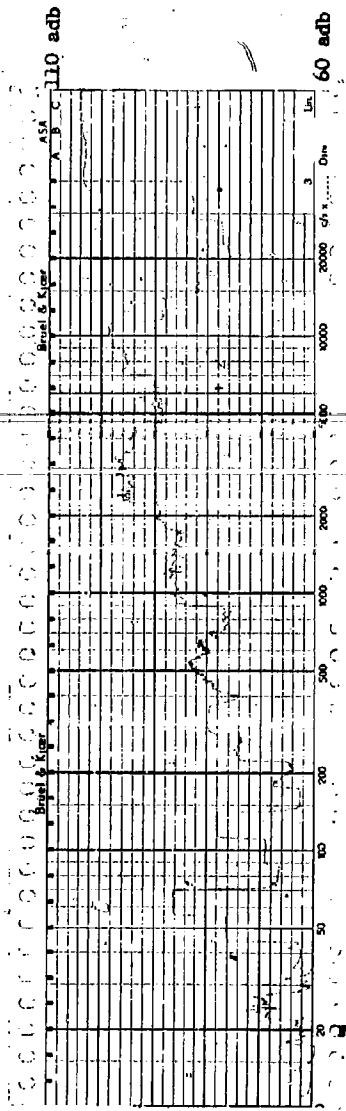
Flux Density
3 HP 2 Pole
184, Frame Open
22 April 1960
Structureborne
75% Rated Voltage
X-Axis

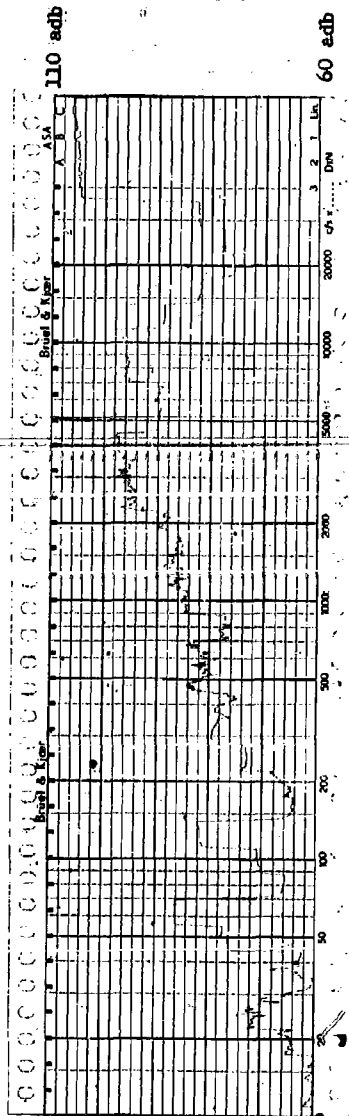
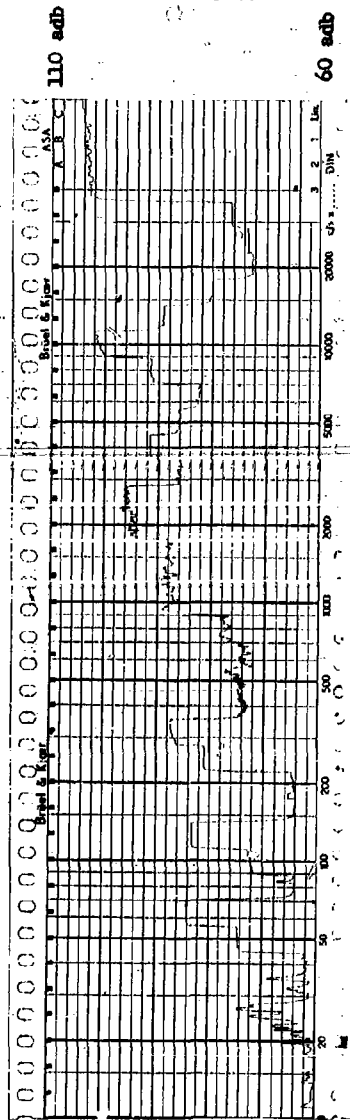
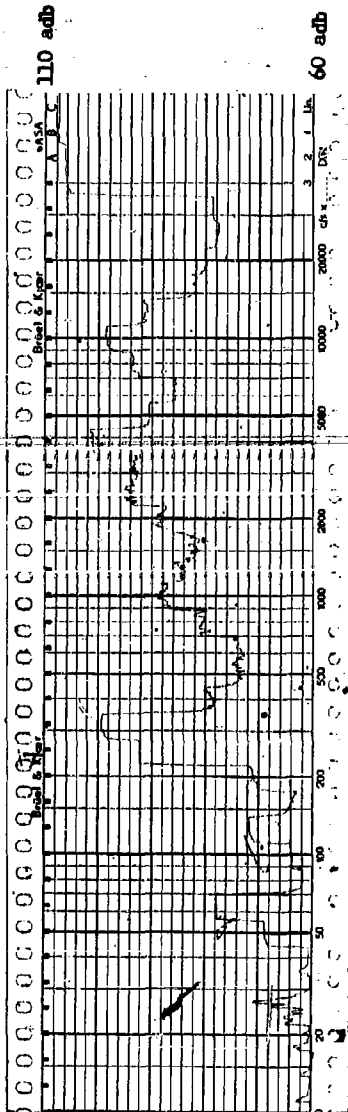


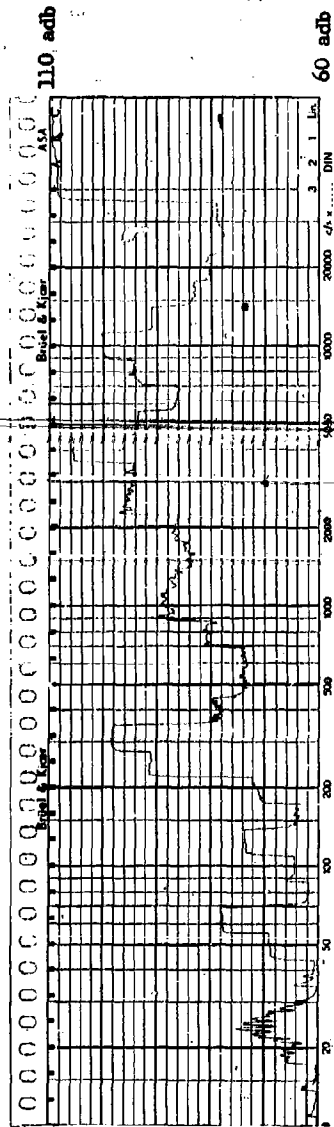
Flux Density
3 HP 2 Pole
184, Frame Open
22 April 1960
Structureborne
75% Rated Voltage
Y-Axis



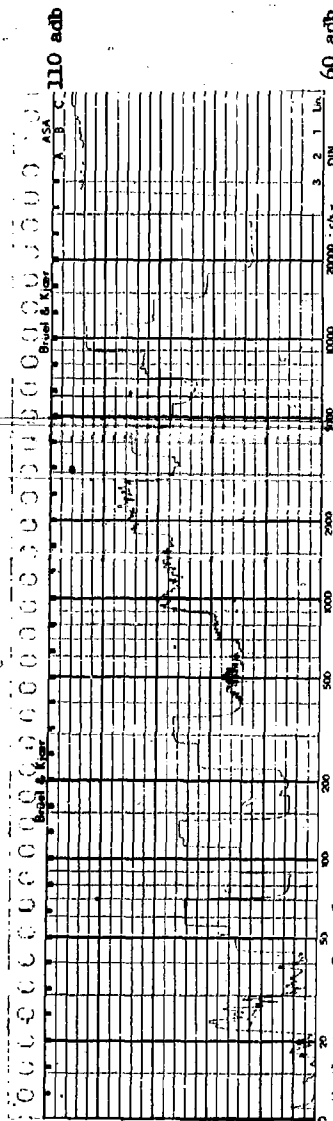
Flux Density
3 HP 2 Pole
184, Frame Open
22 April 1960
Structureborne
75% Rated Voltage
Z-Axis



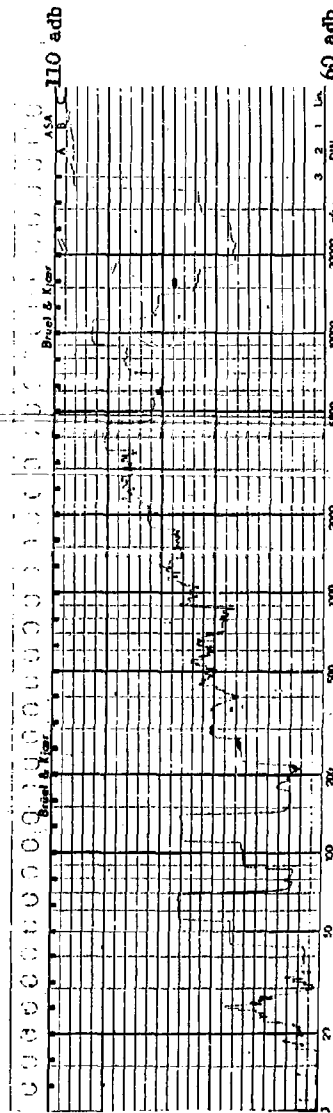




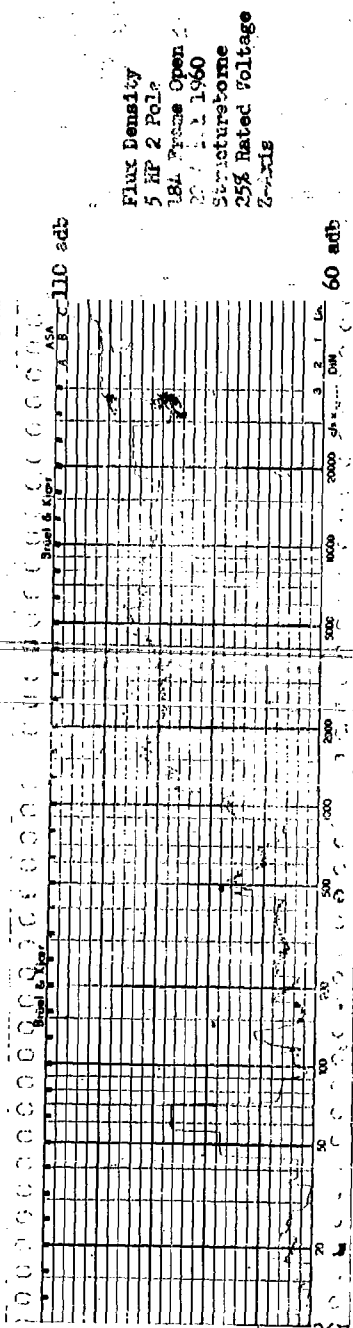
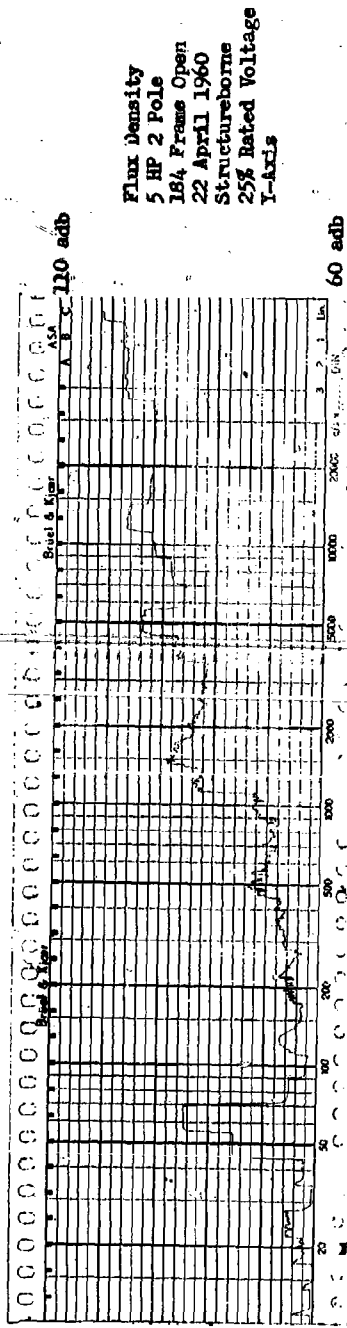
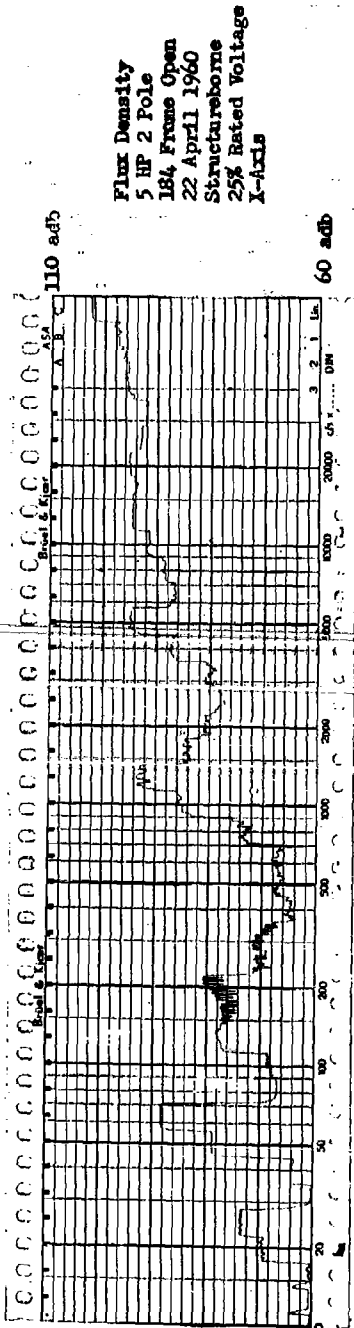
Flux Density
 3 HP 2 Pole
 184 Frame Open
 22 April 1960
 Structureborne
 125% Rated Voltage
 X-Axis



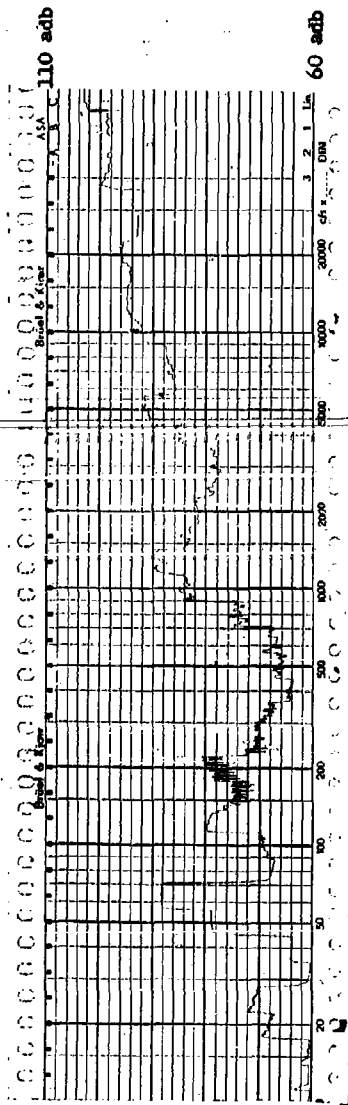
Flux Density
 3 HP 2 Pole
 184 Frame Open
 22 April 1960
 Structureborne
 125% Rated Voltage
 Y-Axis



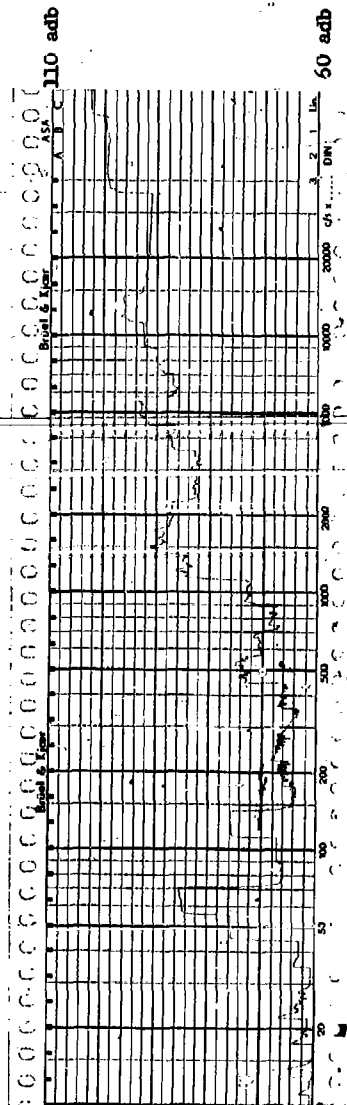
Flux Density
 3 HP 2 Pole
 184 Frame Open
 22 April 1960
 Structureborne
 125% Rated Voltage
 Z-Axis



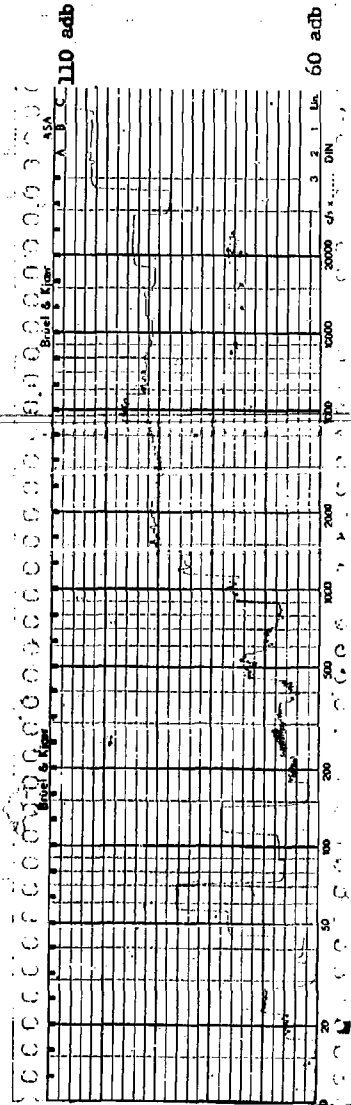
Flux Density
5 HP 2 Pole
184, Frame Open
22 April 1960
Structureborne
50% Rated Voltage
Y-Axis

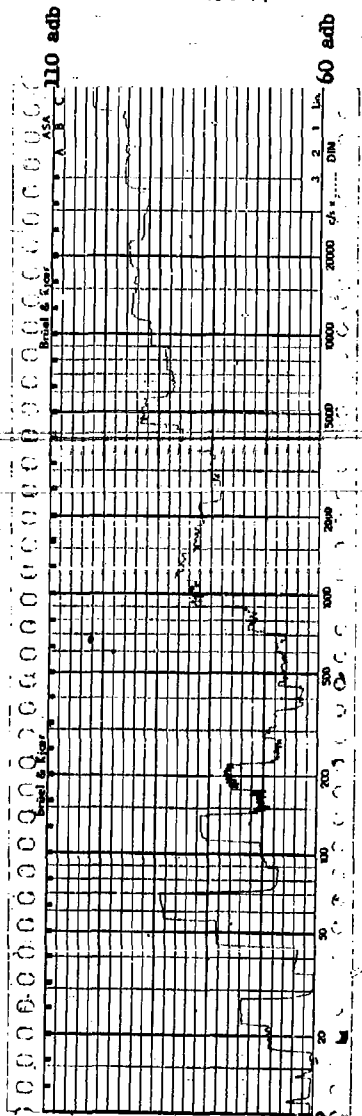


Flux Density
5 HP 2 Pole
184, Frame Open
22 April 1960
Structureborne
50% Rated Voltage
Y-Axis

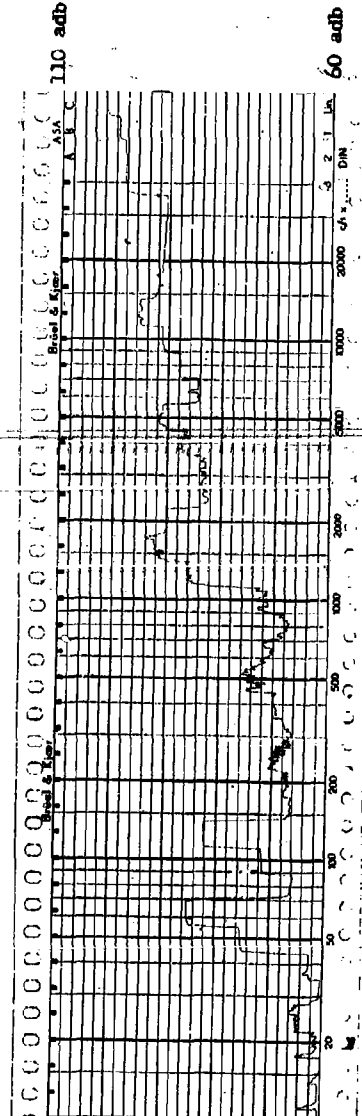


Flux Density
5 HP 2 Pole
184, Frame Open
22 April 1960
Structureborne
50% Rated Voltage
Z-Axis

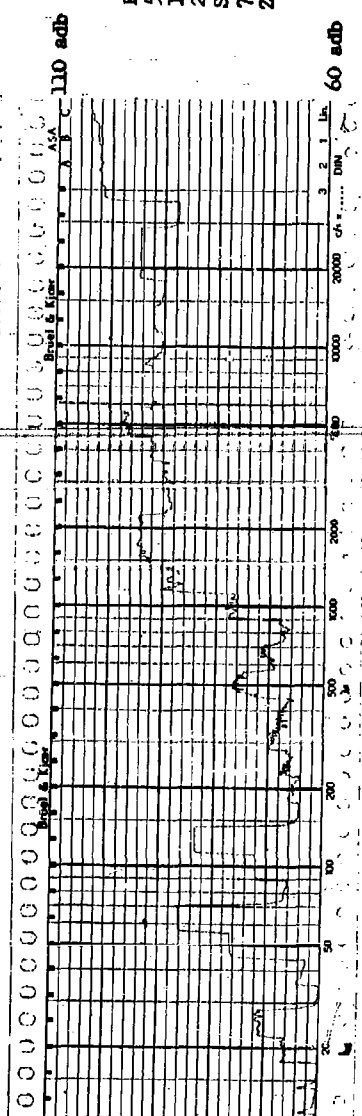




Flux Density
 5 HP 2 Pole
 184 Frame Open
 22 April 1960
 Structureborne
 75% Rated Voltage
 X-Axis

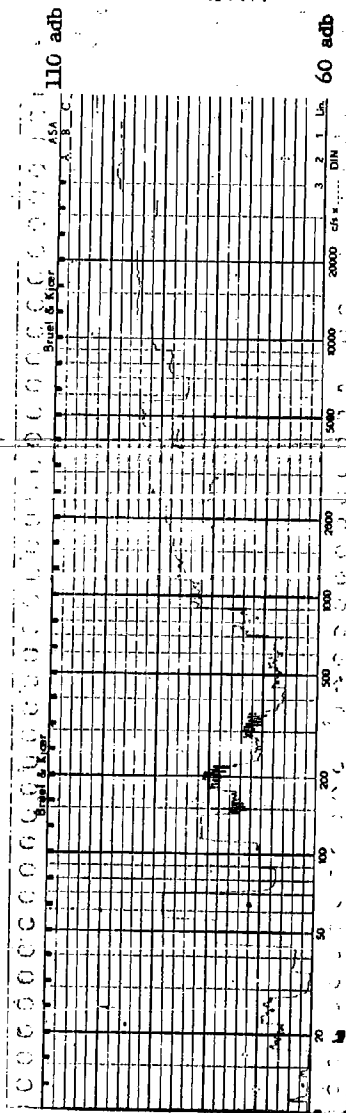


Flux Density
 5 HP 2 Pole
 184 Frame Open
 22 April 1960
 Structureborne
 75% Rated Voltage
 Y-Axis

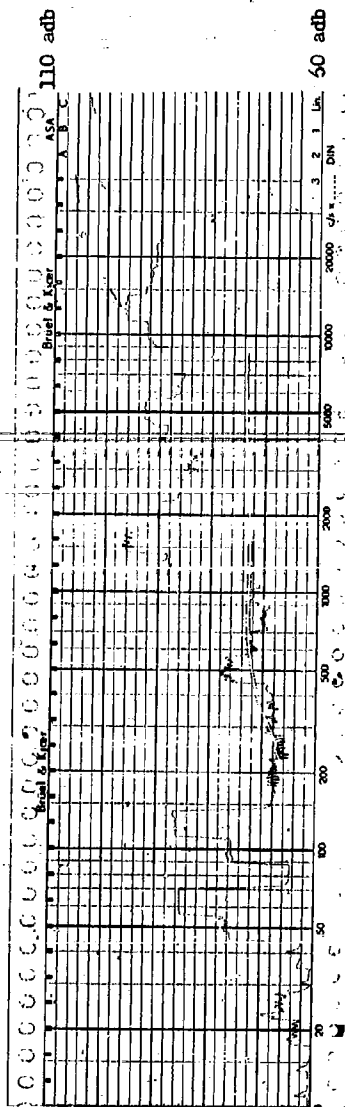


Flux Density
 5 HP 2 Pole
 184 Frame Open
 22 April 1960
 Structureborne
 75% Rated Voltage
 Z-Axis

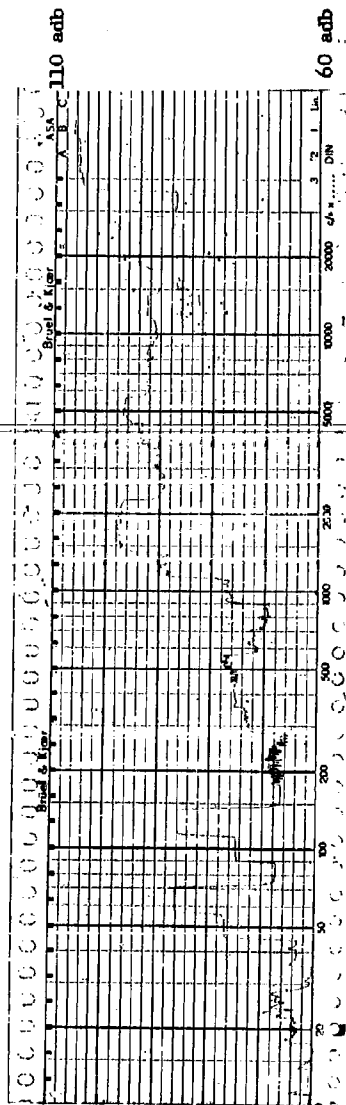
Flux Density
5 HP 2 Pole
184 Frame Open
22 April 1960
Structureborne
100% Rated Voltage
X-Axis

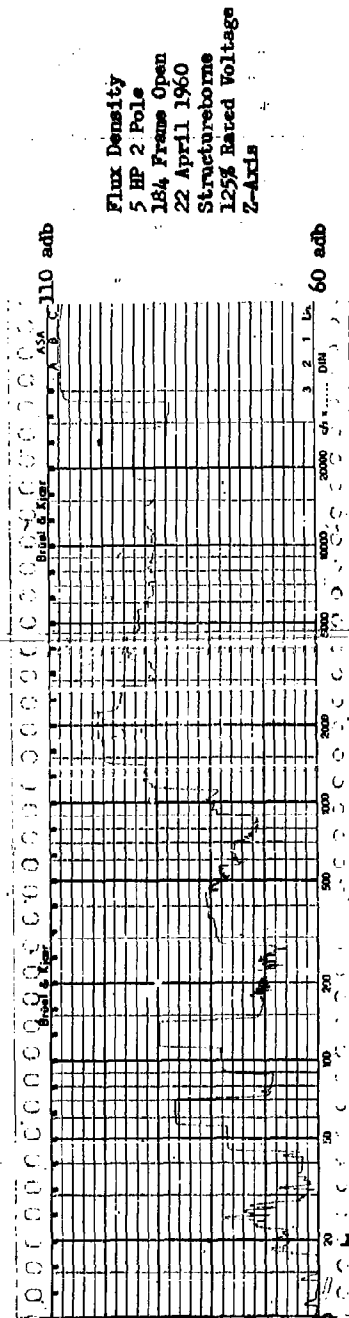
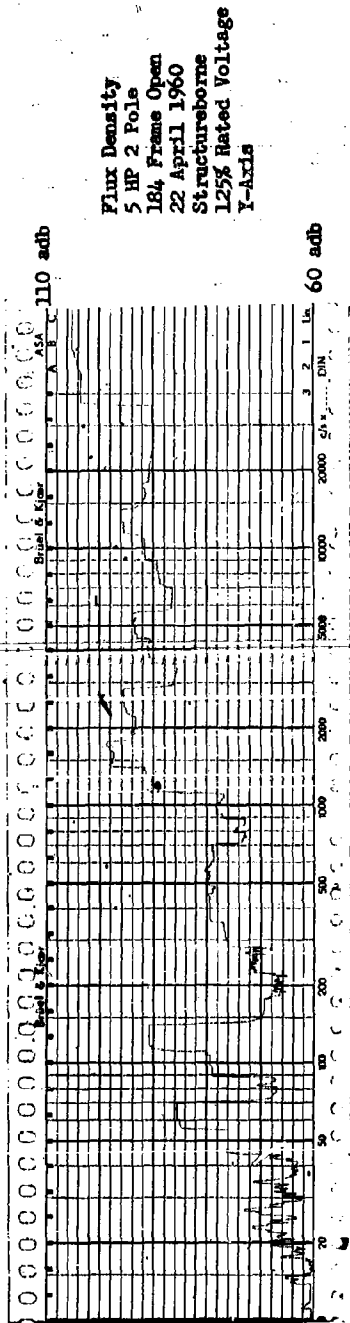
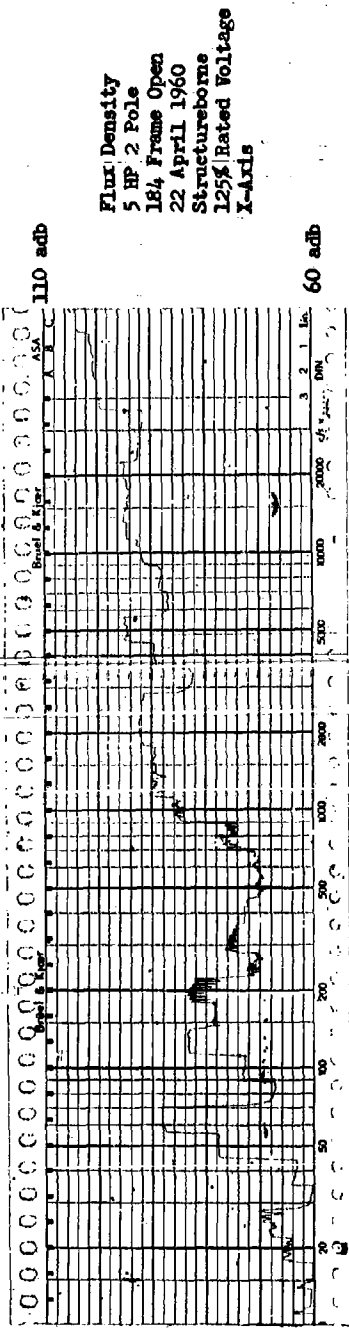


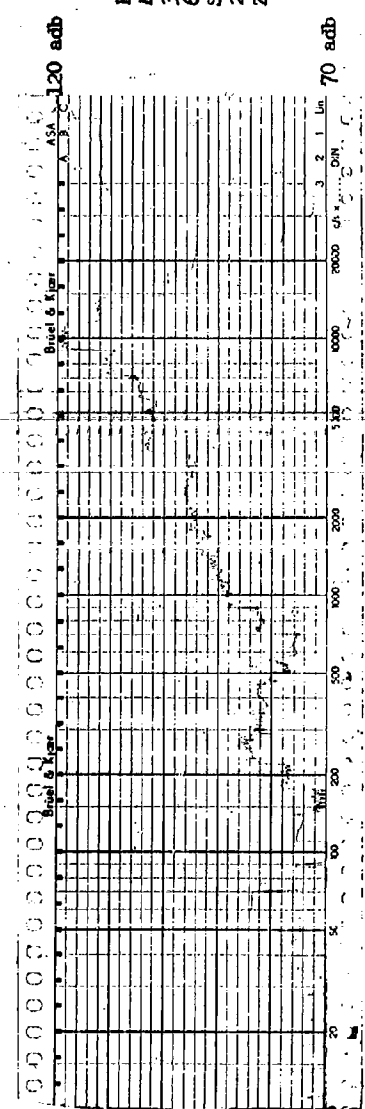
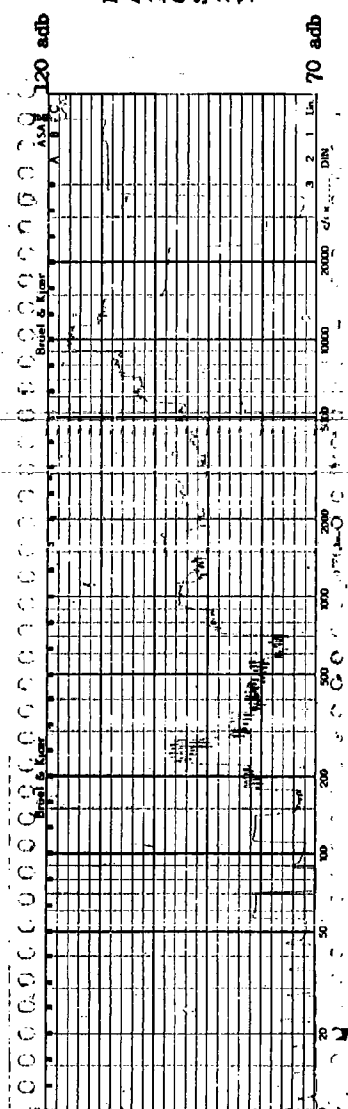
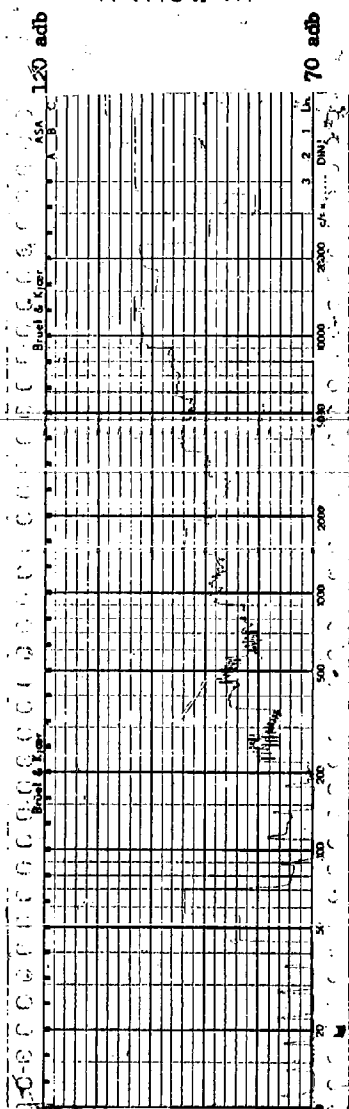
Flux Density
5 HP 2 Pole
184 Frame Open
22 April 1960
Structureborne
100% Rated Voltage
Y-Axis



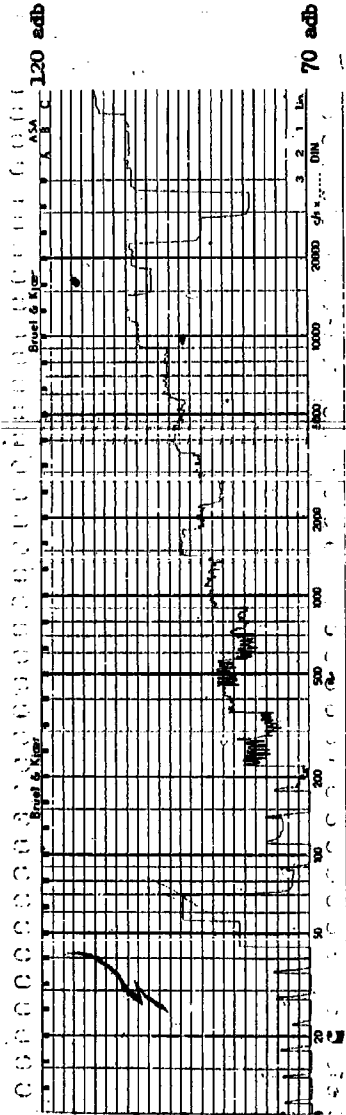
Flux Density
5 HP 2 Pole
184 Frame Open
22 April 1960
Structureborne
100% Rated Voltage
Z-Axis



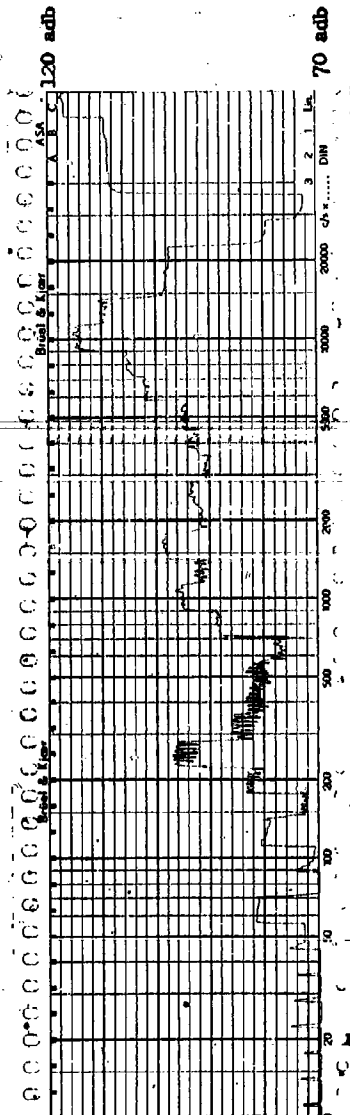




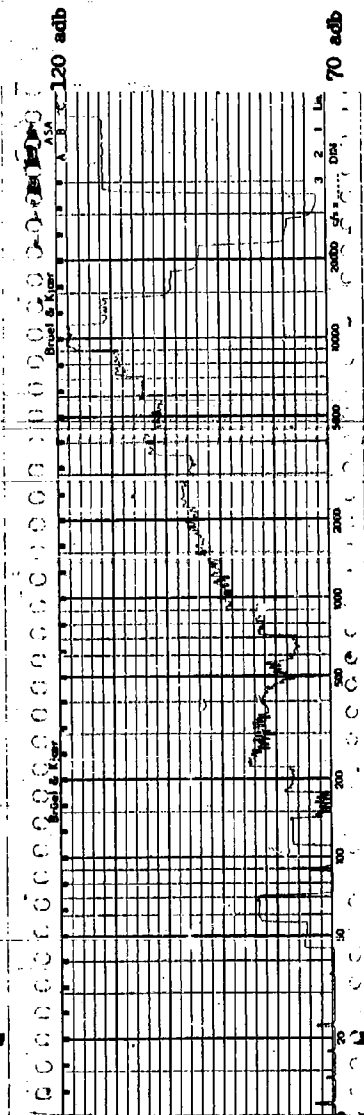
Flux Density
 40 HP 2 Pole
 364 Frame TEFC
 6 July 1960
 Structureborne
 50% Rated Voltage
 X-Axis



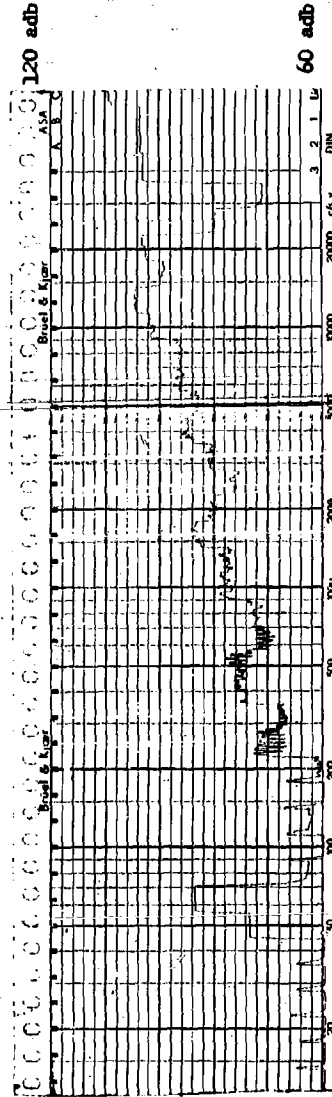
Flux Density
 40 HP 2 Pole
 364 Frame TEFC
 6 July 1960
 Structureborne
 50% Rated Voltage
 Y-Axis



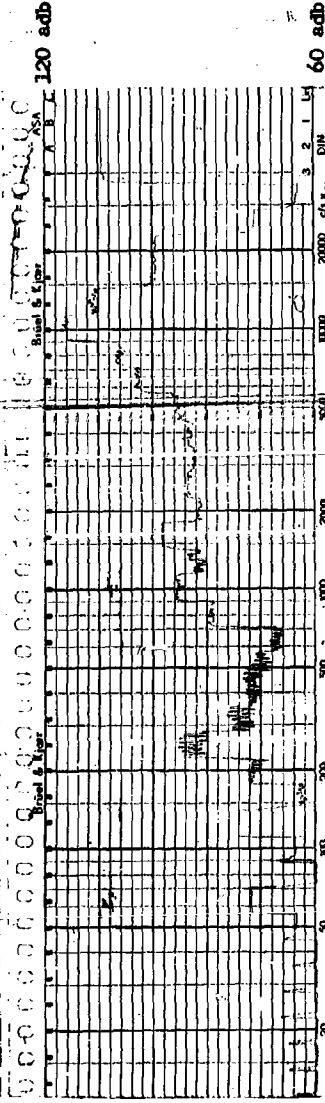
Flux Density
 40 HP 2 Pole
 364 Frame TEFC
 6 July 1960
 Structureborne
 50% Rated Voltage
 Z-Axis



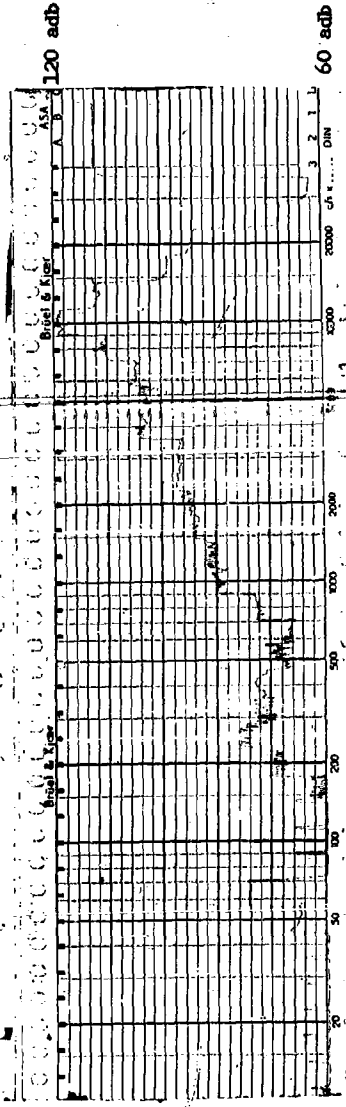
Flux Density
40 HP 2 Pole
364 Frame TEFC
6 July 1960
Structureborne
75% Rated Voltage
Y - Axis



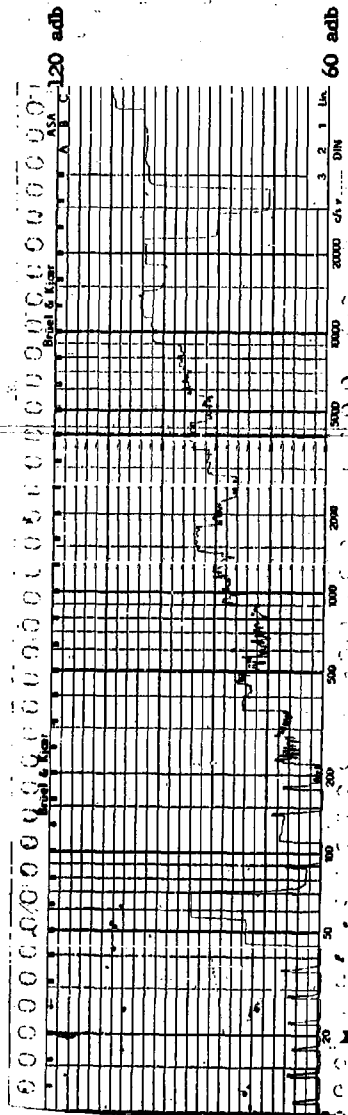
Flux Density
40 HP 2 Pole
364 Frame TEFC
6 July 1960
Structureborne
75% Rated Voltage
Y - Axis



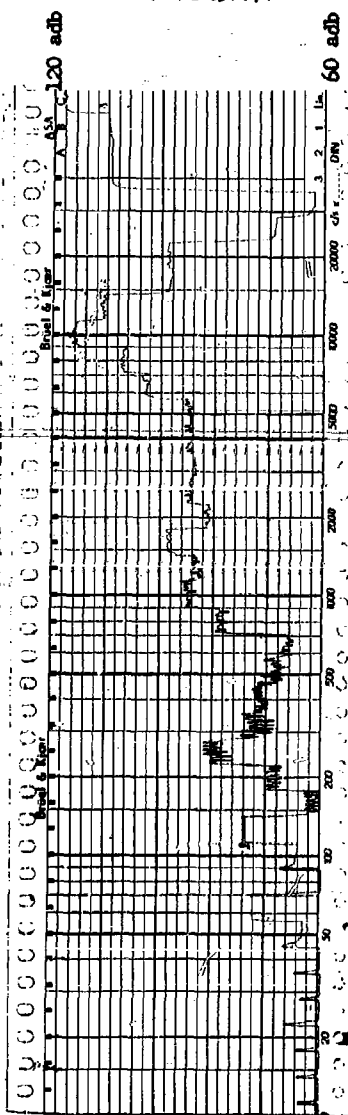
Flux Density
40 HP 2 Pole
364 Frame TEFC
6 July 1960
Structureborne
75% Rated Voltage
Z - Axis



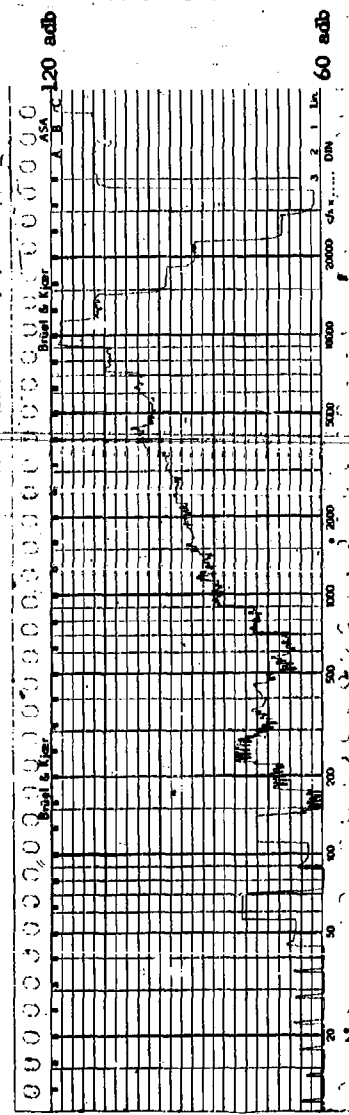
Flux Density
 40 HP 2 Pole
 364 Frame TEFC
 6 July 1960
 Structureborne
 100% Rated Voltage
 X - Axis

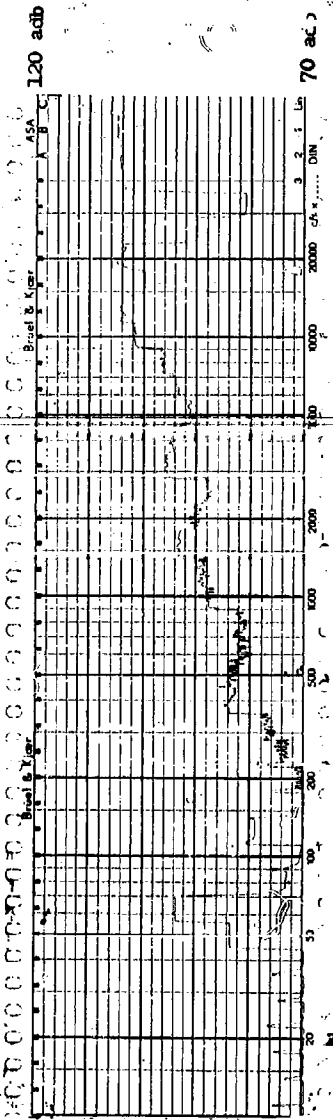


Flux Density
 40 HP 2 Pole
 364 Frame TEFC
 6 July 1960
 Structureborne
 100% Rated Voltage
 Y - Axis

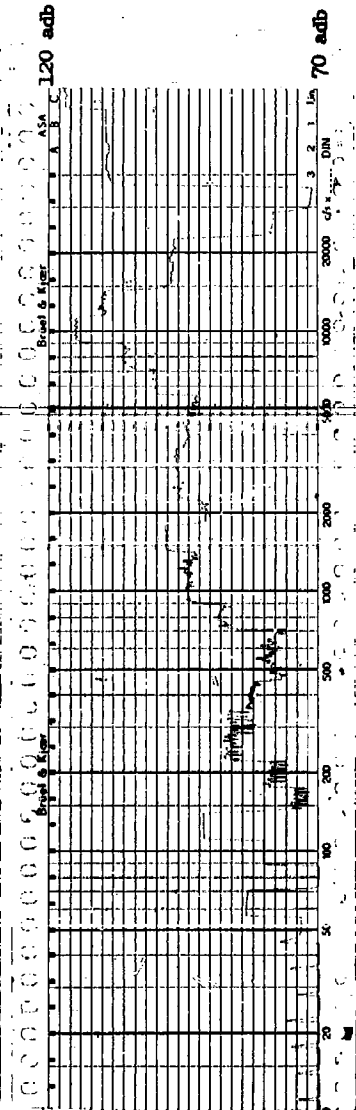


Flux Density
 40 HP 2 Pole
 364 Frame TEFC
 6 July 1960
 Structureborne
 100% Rated Voltage
 Z - Axis

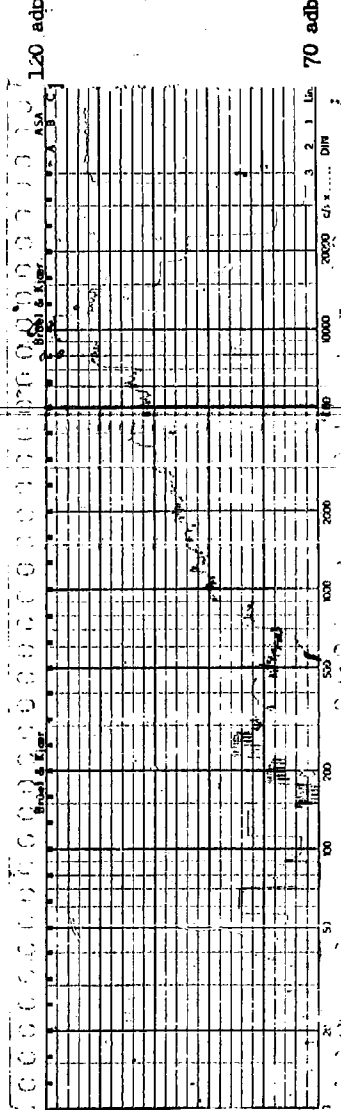




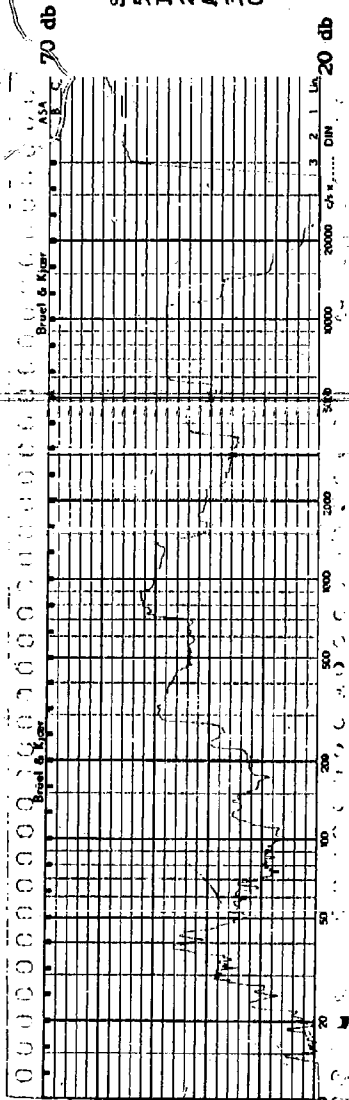
Flux Density
 40 HP 2 Pole
 364 Frame TEFC
 6 July 1960
 Structureborne
 125% Rated Voltage
 X - Axis



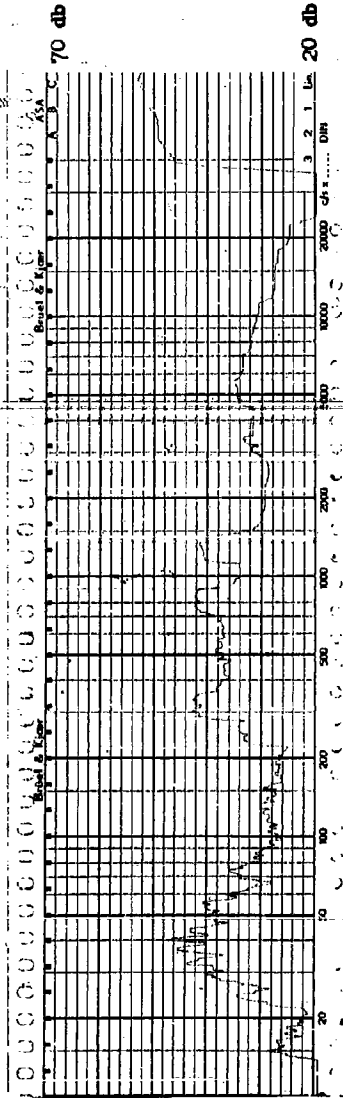
Flux Density
 40 HP 2 Pole
 364 Frame TEFC
 6 July 1960
 Structureborne
 125% Rated Voltage
 Y - Axis



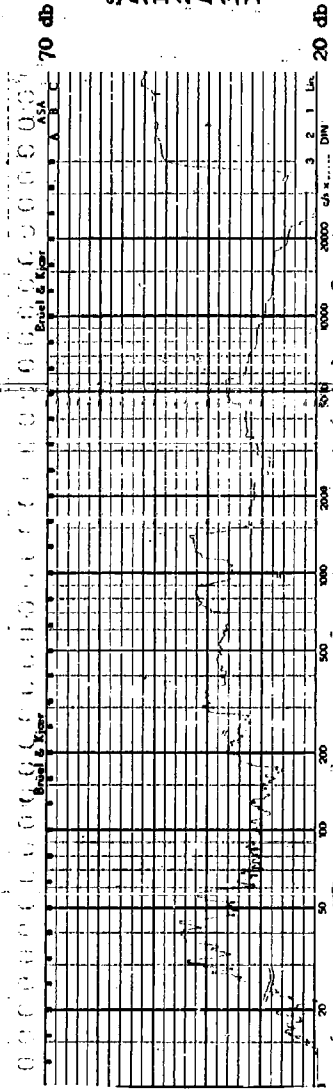
Flux Density
 40 HP 2 Pole
 364 Frame TEFC
 6 July 1960
 Structureborne
 125% Rated Voltage
 Z - Axis



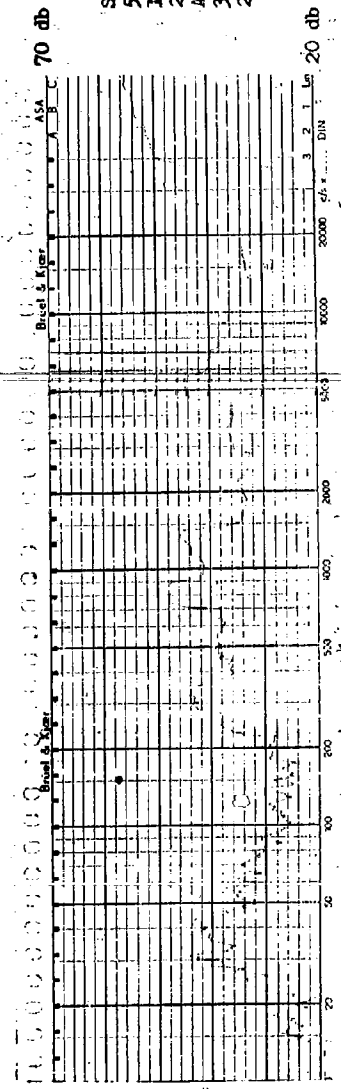
Skew Test
5 HP 2 Pole
184 Frame Open
27 April 1960
Airborne
3 Ft. Front End
0 Skew



Skew Test
5 HP 2 Pole
184 Frame Open
27 April 1960
3 Ft. Front End
1.41 ES Skew

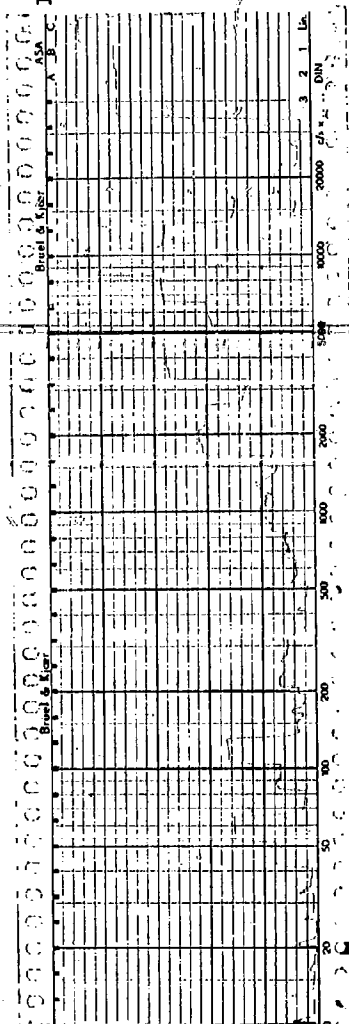


Skew Test
 5 HP 2 Pole
 184 Frame Open
 27 April 1960
 Airborne
 3 Ft. Front End
 1.86 RS Skew



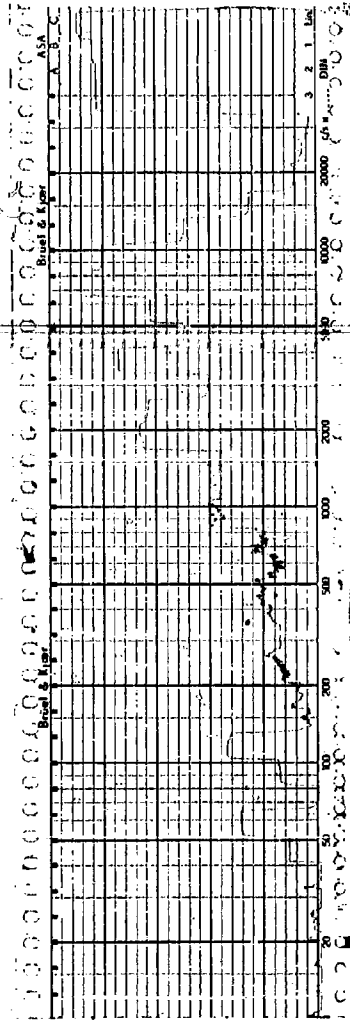
Skew Test
 5 HP 2 Pole
 184 Frame Open
 27 April 1960
 Airborne
 3 Ft. Front End
 2.5 RS Skew

130 adb



Skew Test
5 HP 2 Pole
184 Frame Open
17 Feb. 1960
Structureborne
0 Skew
X-Axis

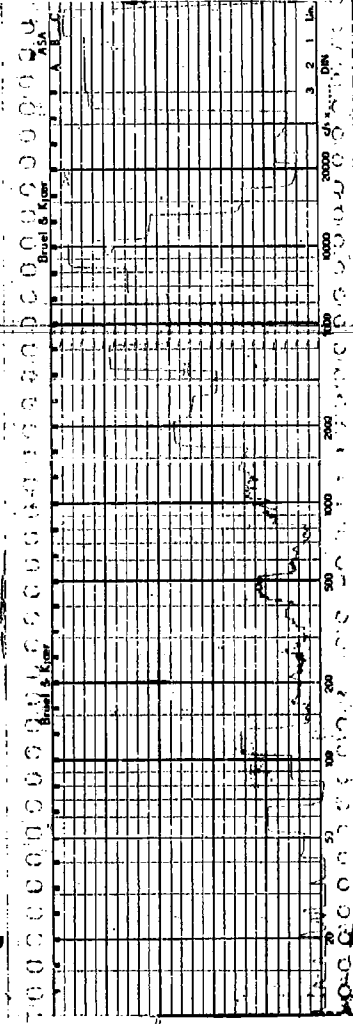
80 adb



Skew Test
5 HP 2 Pole
184 Frame Open
17 Feb. 1960
Structureborne
0 Skew
Y-Axis

120 adb

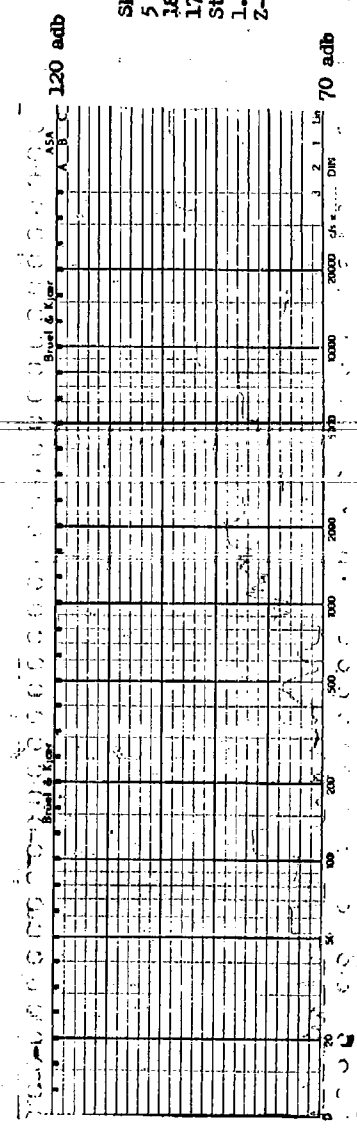
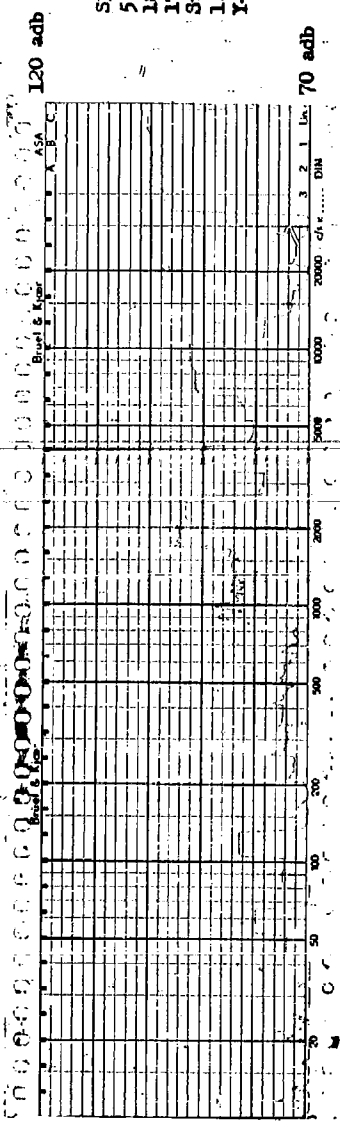
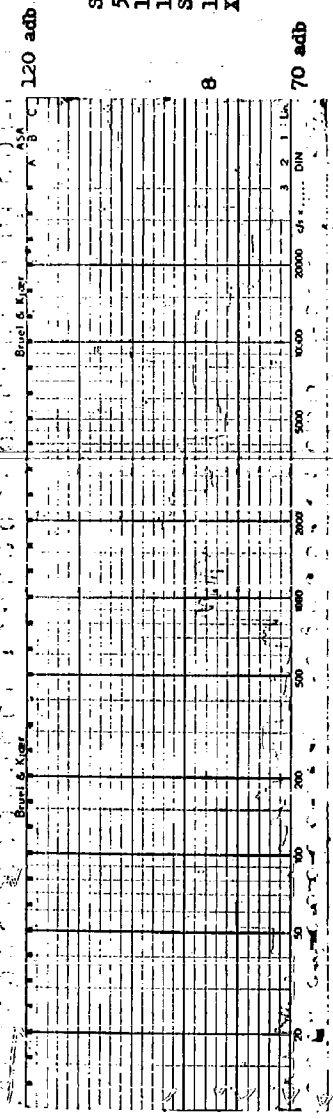
70 adb

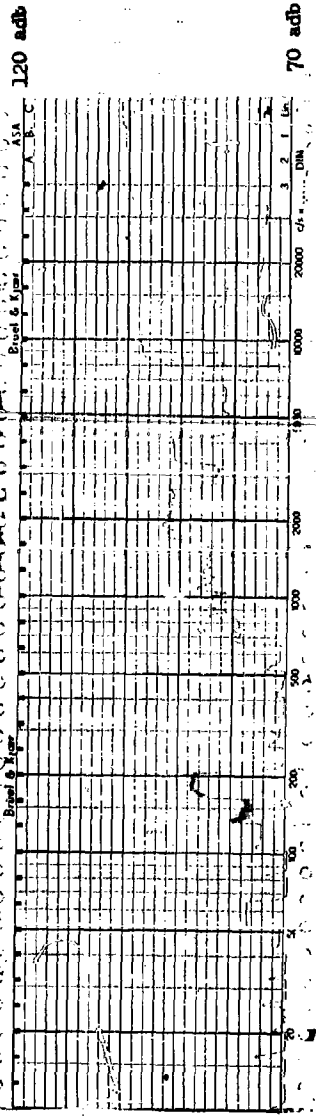


Skew Test
5 HP 2 Pole
184 Frame Open
17 Feb. 1960
Structureborne
0 Skew
Z-Axis

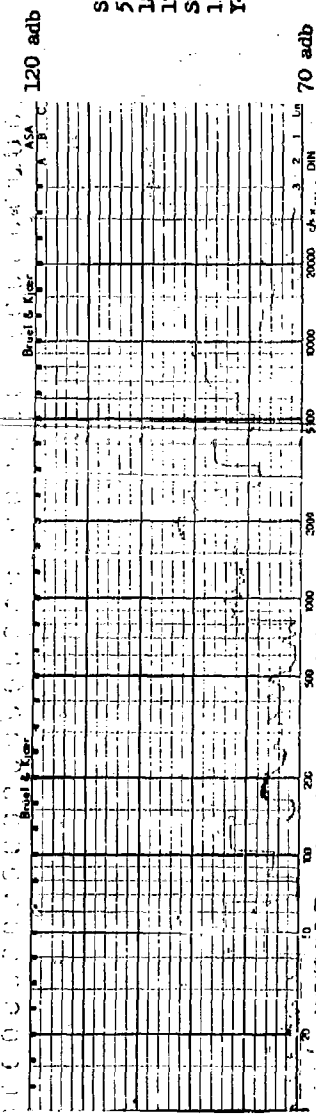
120 adb

70 adb

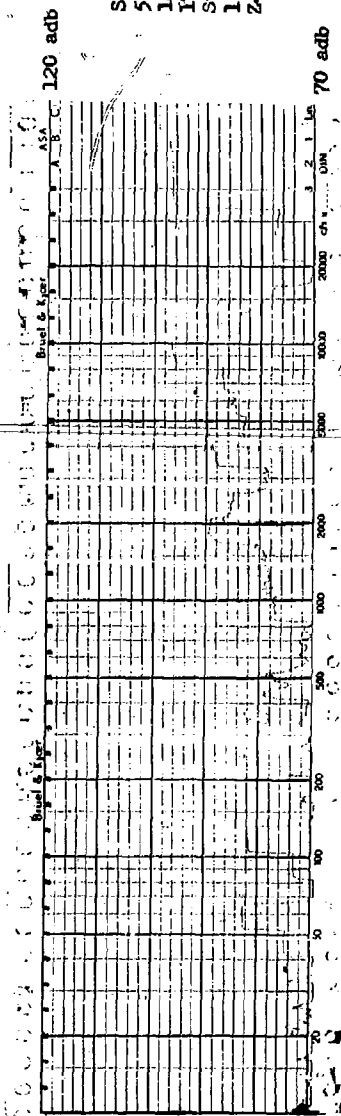




Skew Test
 5 HP 2 Pole
 184 Frame Open
 17 Feb. 1960
 Structureborne
 1.86 RS Skew
 X-Axis



Skew Test
 5 HP 2 Pole
 184 Frame Open
 17 Feb. 1960
 Structureborne
 1.86 RS Skew
 Y-Axis



Skew Test
 5 HP 2 Pole
 184 Frame Open
 17 Feb. 1960
 Structureborne
 1.86 RS Skew
 Z-Axis

120 adb

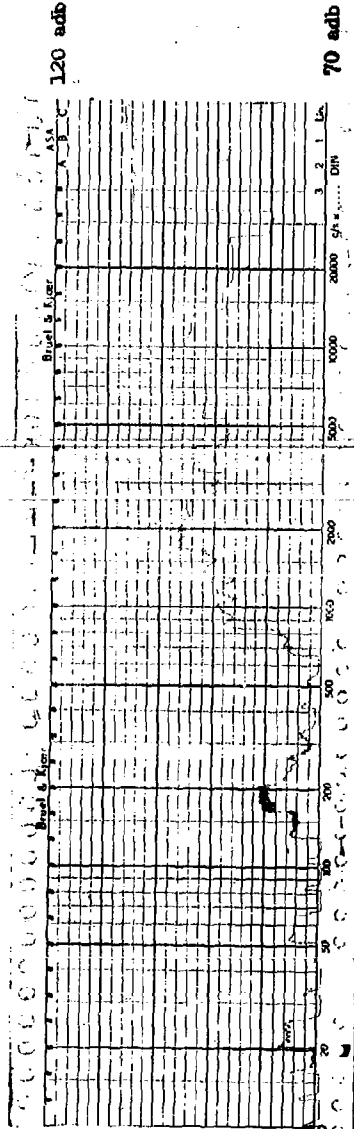
70 adb

120 adb

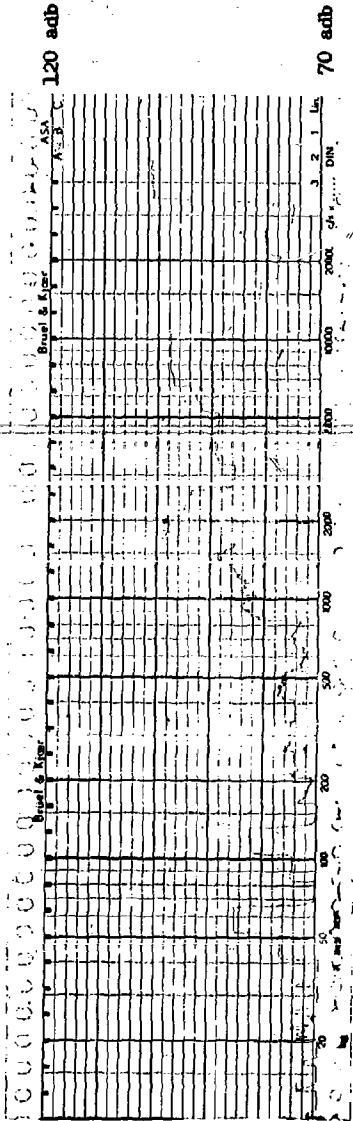
70 adb

120 adb

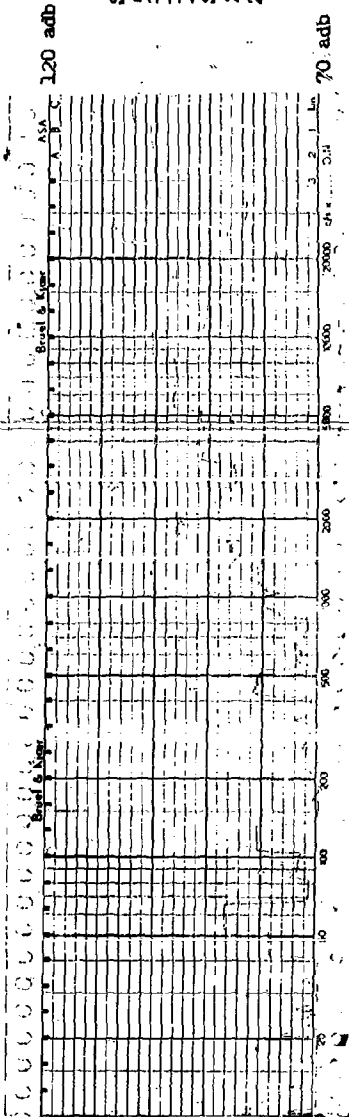
70 adb



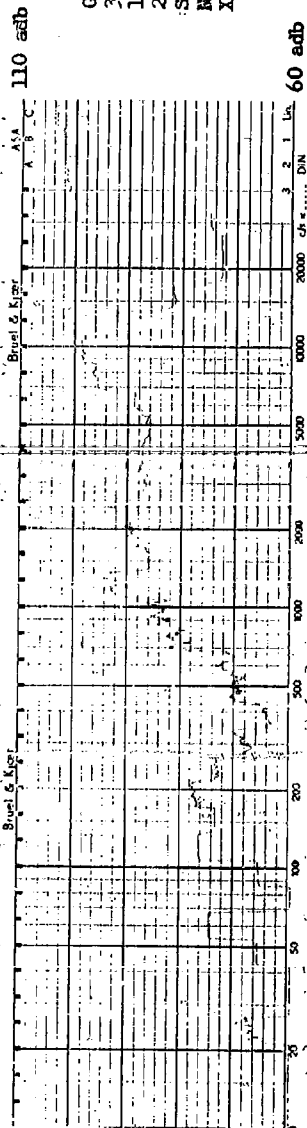
Skew Test
 5 HP 2 Pole
 184, Frame Open
 17 Feb. 1960
 Structureborne
 2.5 RS Skew
 Y-Axis



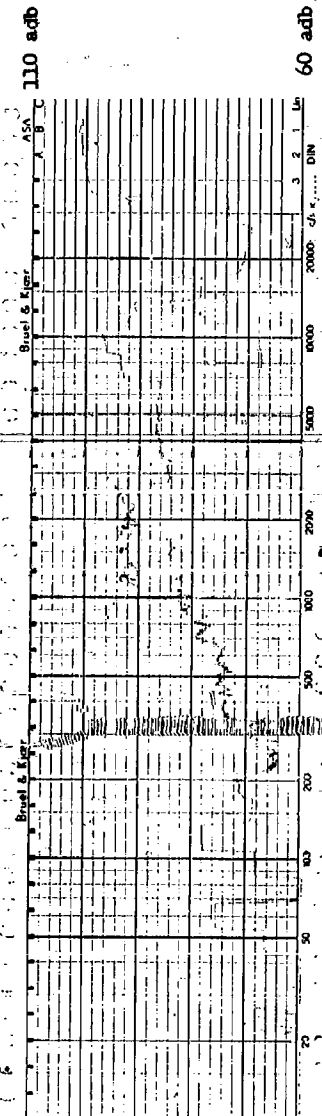
Skew Test
 5 HP 2 Pole
 184, Frame Open
 17 Feb. 1960
 Structureborne
 2.5 RS Skew
 Y-Axis



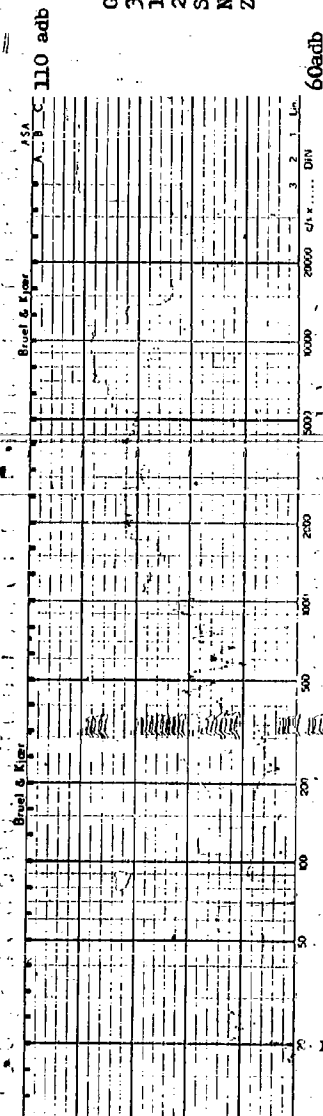
Skew Test
 5 HP 2 Pole
 184, Frame Open
 17 Feb. 1960
 Structureborne
 2.5 RS Skew
 Z-Axis



Grain Orientation
 3 HP 2 Pole
 184 Frame Open
 29 Jan. 1960
 Structureborne
 Non-oriented Core
 X-axis

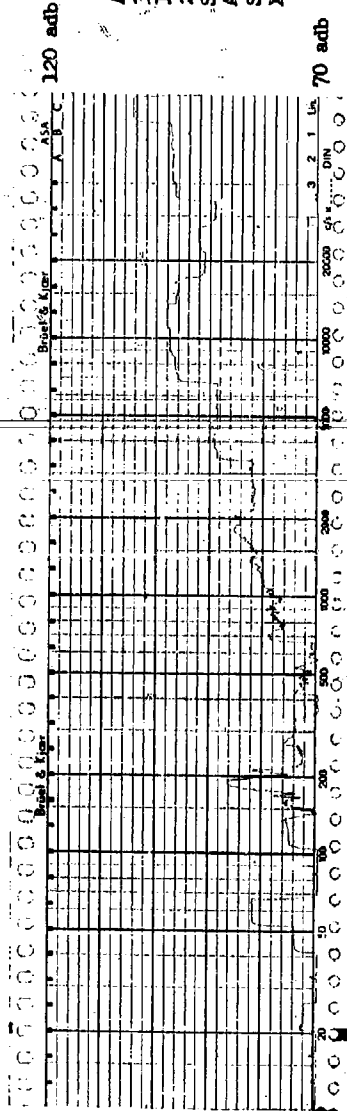


Grain Orientation
 3 HP 2 Pole
 184 Frame Open
 29 Jan. 1960
 Structureborne
 Non-oriented Core
 Y-axis

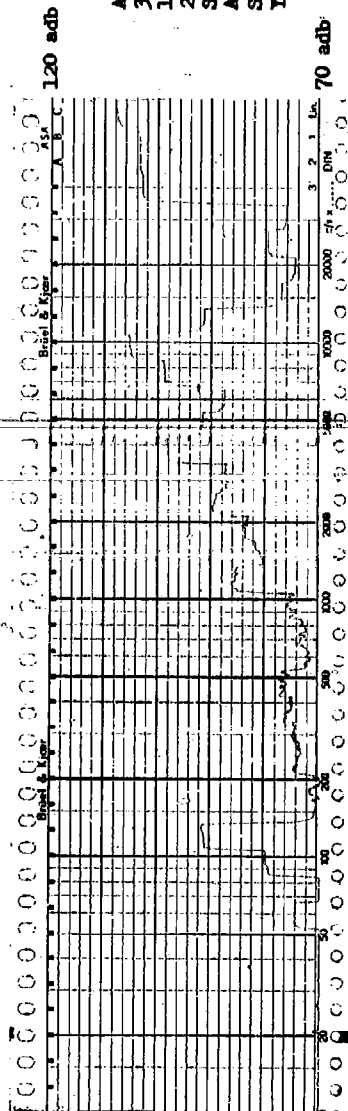


Grain Orientation
 3 HP 2 Pole
 184 Frame Open
 29 Jan. 1960
 Structureborne
 Non-oriented Core
 Z-axis

Anneal Test
3 HP 2 Pole
184 Frame Open
22 Sept. 1960
Structureborne
Annealed
Stator Core
Y-Axis

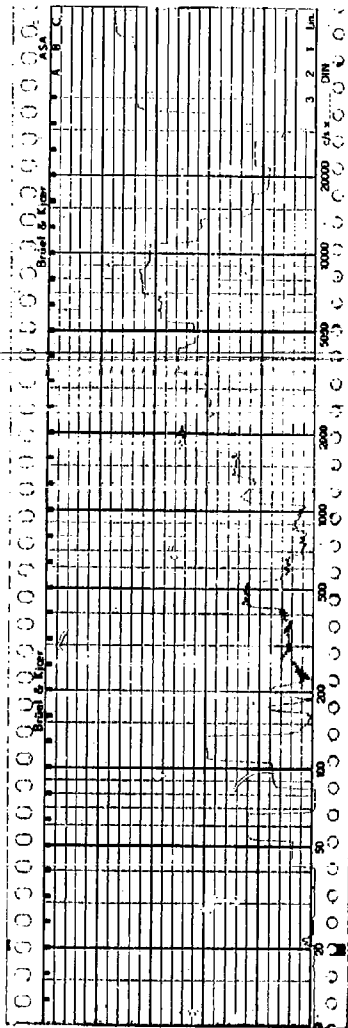


Anneal Test
3 HP 2 Pole
184 Frame Open
22 Sept. 1960
Structureborne
Annealed
Stator Core
Y-Axis



Anneal Test
3 HP 2 Pole
184 Frame Open
22 Sept. 1960
Structureborne
Annealed
Stator Core
Z-Axis

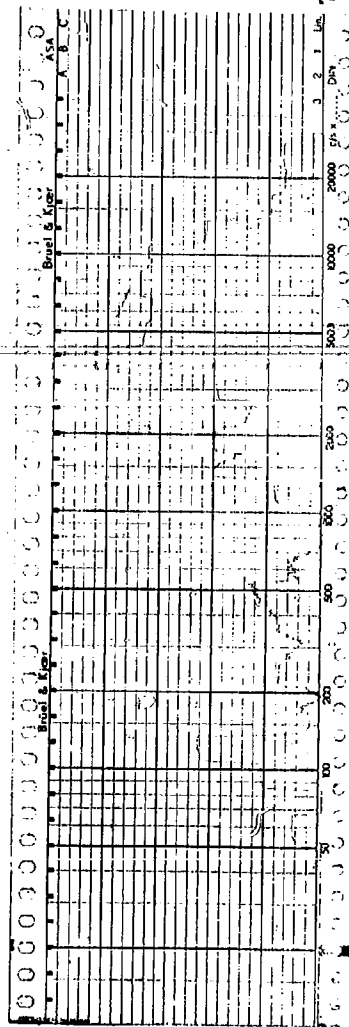
120 adb



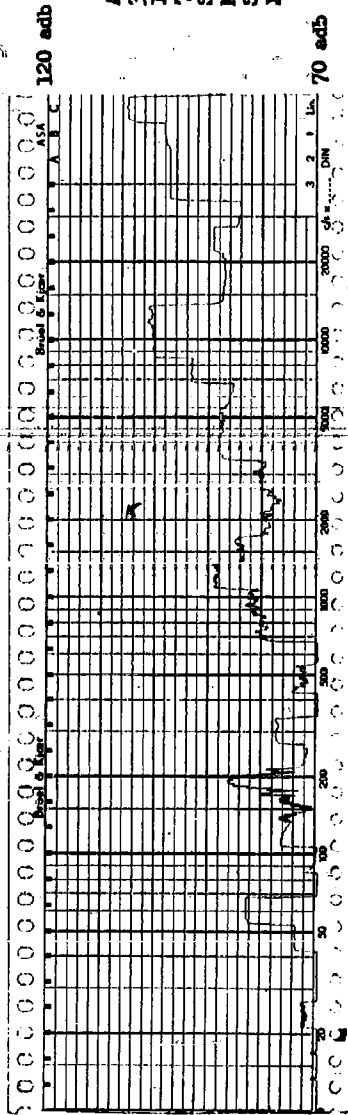
70 adb

Anneal Test
3 HP 2 Pole
184 Frame Open
22 Sept. 1960
Structureborne
Annealed
Stator Core
Core

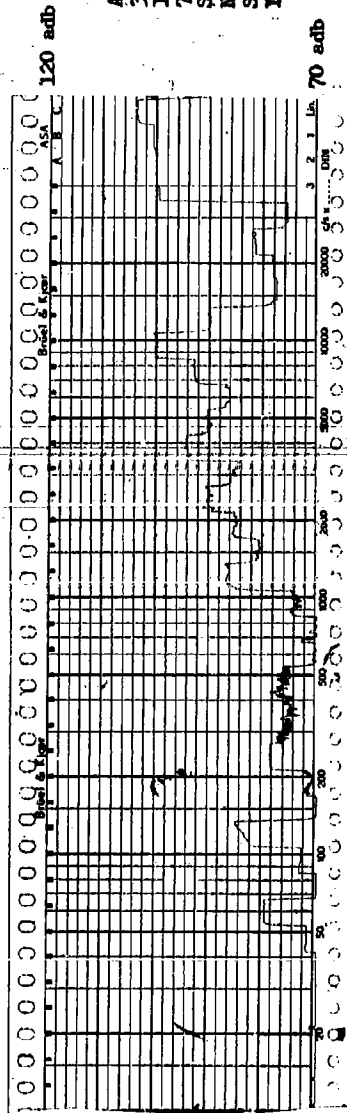
120 adb



70 adb

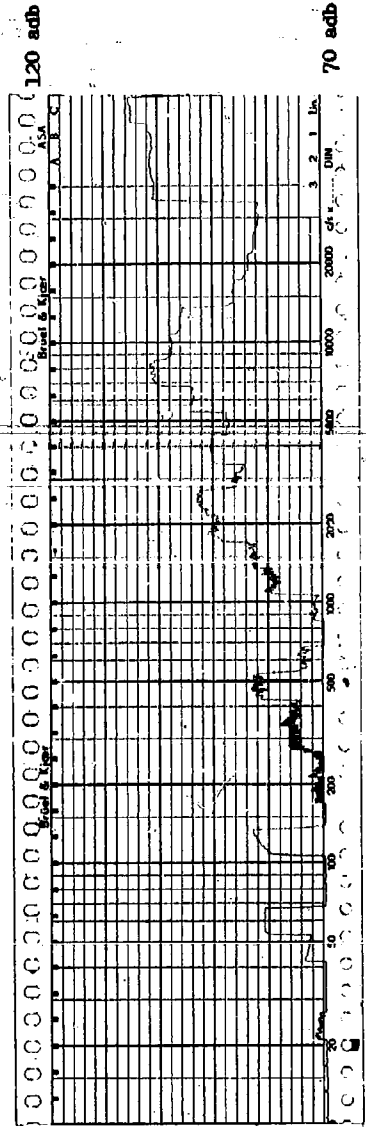


Anneal Test
 3 HP 2 Pole
 184, Frame Open
 7 Sept. 1960
 Structureborne
 Non-annealed
 Stator Core
 X-Axis

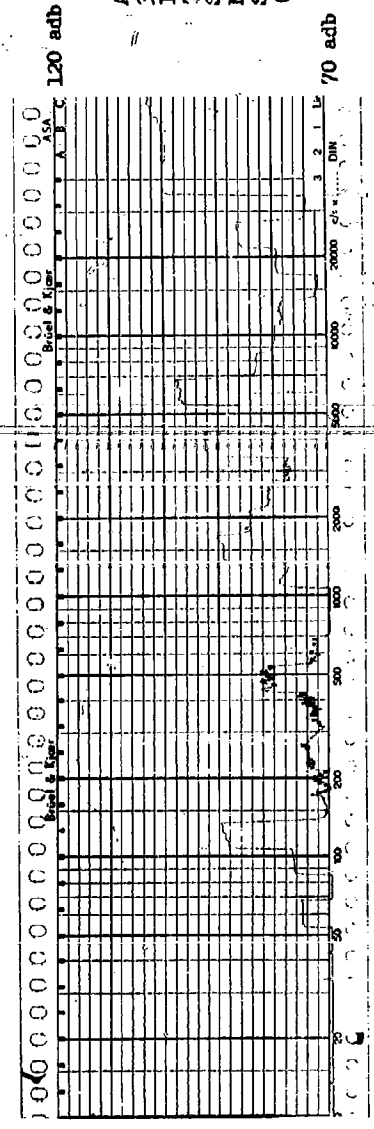


Anneal Test
 3 HP 2 Pole
 184, Frame Open
 7 Sept. 1960
 Structureborne
 Non-annealed
 Stator Core
 X-Axis

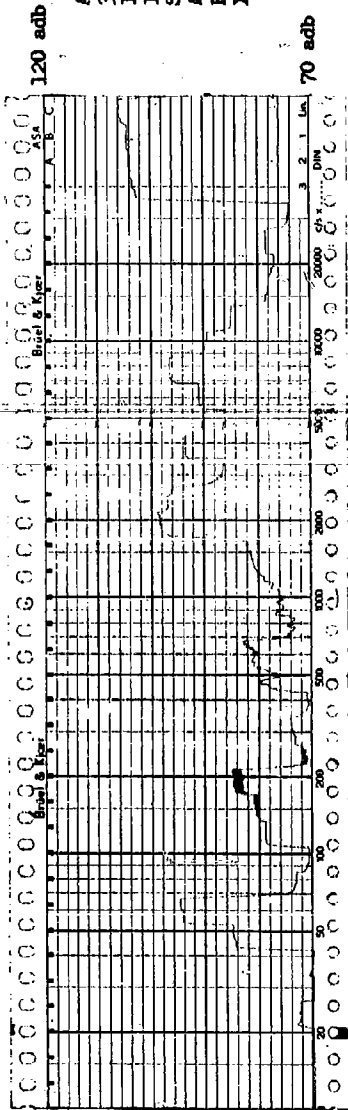
Anneal Test
 3 HP 2 Pole
 184 Frame Open
 7 Sept. 1960
 Structureborne
 Non-annealed
 Stator Core
 Z - Axis



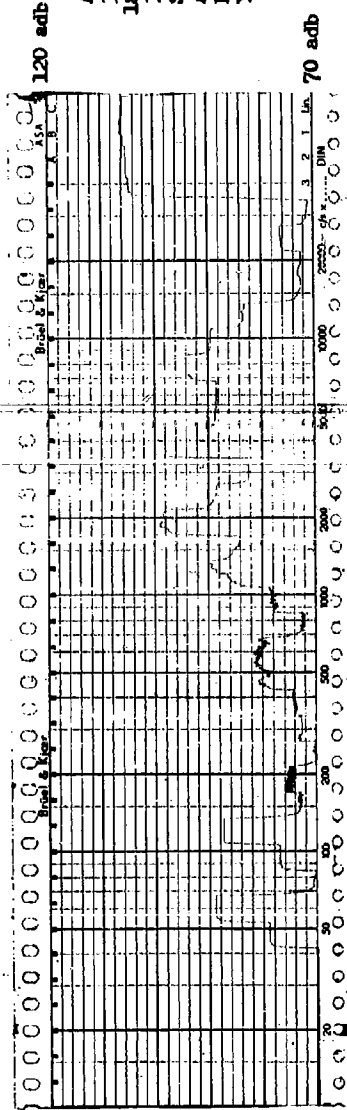
Anneal Test
 3 HP 2 Pole
 184 Frame Open
 7 Sept. 1960
 Structureborne
 Non-annealed
 Stators Core
 Core

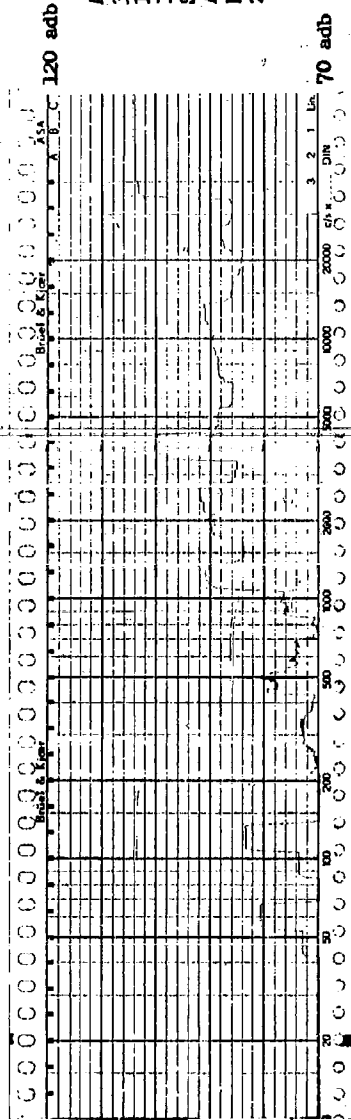


Anneal Test
 3 HP 2 Pole
 184, Frame Open
 16 Nov. 1960
 Structureborne
 Annealed
 Rotor Core
 Y-Axis

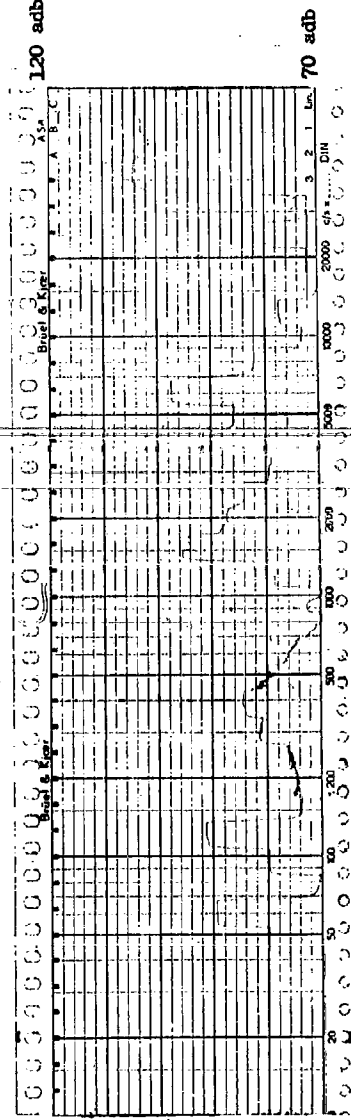


Anneal Test
 3 HP 2 Pole
 184, Frame Open
 16 Nov. 1960
 Structureborne
 Annealed
 Rotor Core
 Y-Axis

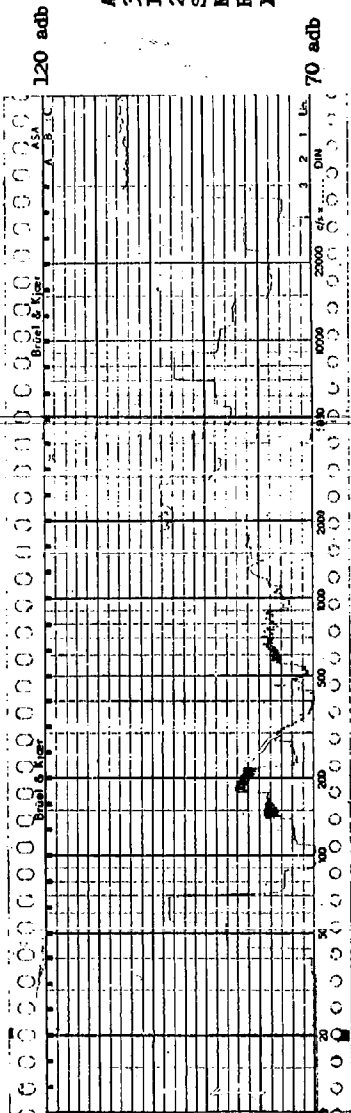




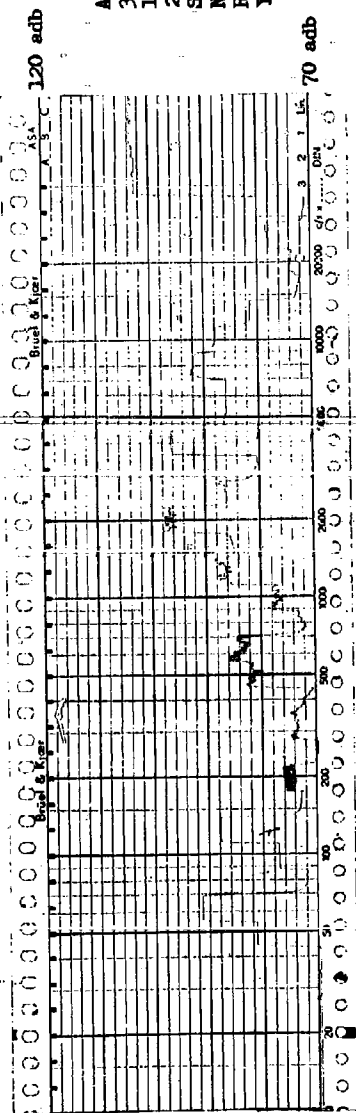
Anneal Test
 3 HP 2 Pole
 184, Frame Open
 16 Nov. 1960
 Structureborne
 Annealed
 Rotor Core
 Z-Axis



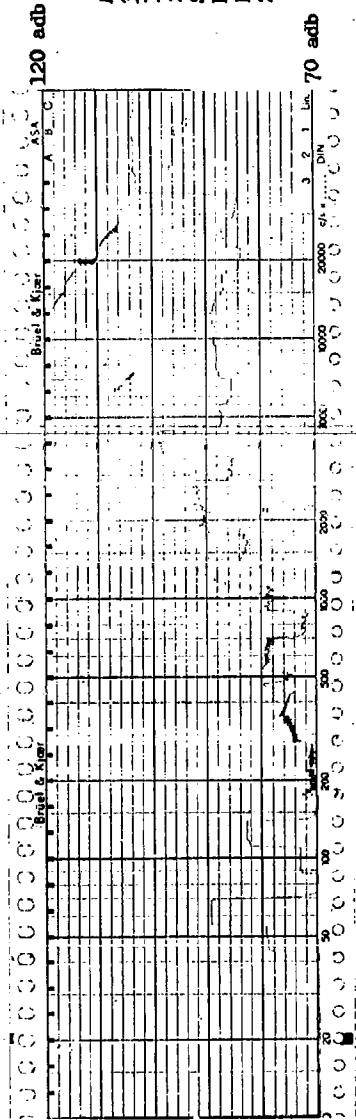
Anneal Test
 3 HP 2 Pole
 184, Frame Open
 16 Nov. 1960
 Structureborne
 Annealed
 Rotor Core
 Core



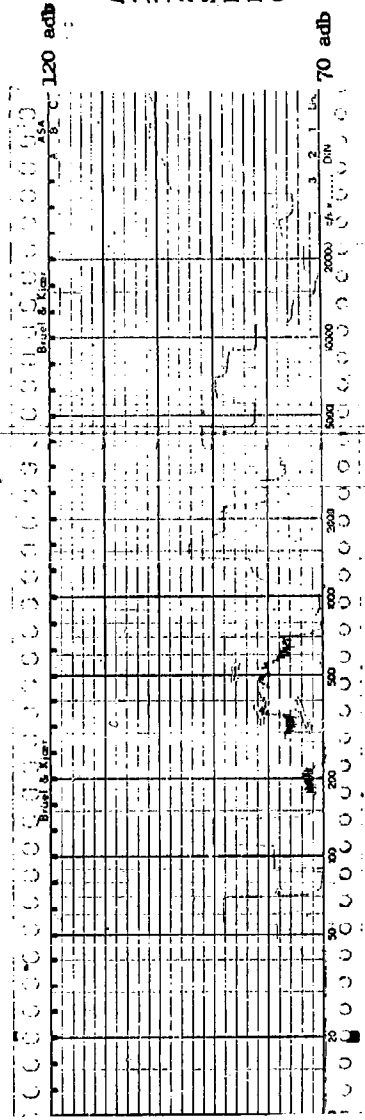
Anneal Test
3 HP 2 Pole
184 Frame Open
23 Nov. 1960
Structureborne
Non-annealed
Rotor Core
X-Axis



Anneal Test
3 HP 2 Pole
184 Frame Open
23 Nov. 1960
Structureborne
Non-annealed
Rotor Core
Y-Axis



Anneal Test
 3 HP 2 Pole
 184 Frame Open
 23 Nov. 1960
 Structureborne
 Non-annealed
 Rotor Core
 Z-Axis



Anneal Test
 3 HP 2 Pole
 184 Frame Open
 23 Nov. 1960
 Structureborne
 Non-annealed
 Rotor Core
 Core

SECTION 4

BEARING NOISE

4.1 INTRODUCTION

The bearings used in induction motors are a source of noise and vibration because of the sliding or rolling contact of bearing components. Two types of bearings are commonly used: sleeve bearings and ball bearings. The former type has sliding contact between components, while the latter has a combination of rolling and sliding contact. (17)* The relative merits of these two types are discussed and form the basis for the recommendation of using ball bearings for multi-purpose motors. Various studies of ball bearings and the means available to the motor manufacturer of reducing ball bearing noise are reported: The effect of the following factors on bearing noise were studied:

- 1) bearing preload
- 2) shaft-bearing interference fit
- 3) bearing locknut
- 4) bearing lubricant

Recommendations for minimizing bearing noise are summarized in the conclusion.

4.2 SLEEVE BEARINGS

A sleeve bearing consists of a rotating journal or shaft in a stationary sleeve of special wearing material whose bore is several mils larger than the shaft diameter. A thin film of liquid lubricant (usually oil) is provided to reduce the sliding friction between the opposing members. This simplicity of construction underlies the general belief that sleeve bearings are quiet compared to ball bearings. However, certain modifications are usually made in the basic sleeve bearing design to maintain the lubricant film and thereby to improve the bearing performance. These modifications generally result in an increase in bearing noise. Sleeve bearings may be divided into two categories based on whether rotation of the shaft is necessary to maintain the lubricant film; i.e., static film bearings and dynamic film bearings.

In a static film bearing the lubricating fluid is put under pressure from an external source such as a pump and then fed to the bearing surface by means of certain cavities or slots provided in bearing surface. This pressurized film which separates the bearing components and eliminates metal-to-metal contact, is independent of journal rotation. The slotting of a sleeve bearing produces an additional noise frequency which is N times the rotation frequency:

$$f_{bs} = N \times f_r \approx \frac{120N}{P} \quad 4.1$$

*Numbers in parenthesis refer to references listed in the Bibliography.

where f_{bs} = the bearing slot frequency
 f_r = the rotational frequency
 N = number of bearing slots
 P = number of poles

The external system needed to pressurize the liquid is also a noise source. In the comparison of the noise produced by differing types of bearings both the bearing and the means of lubrication must be considered.

A dynamic fluid film bearing is based on the eccentric pump action inherent in a sleeve bearing. Just as a common pump must turn to produce a pressure, the journal in a dynamic film bearing must turn to pressurize the liquid. The pressurized liquid is capable of transmitting sufficient force to lift the journal from the mating sleeve. The lubricant film may be considered as a series of laminar layers. The innermost layer of the liquid will whirl around with the journal; the outermost layer will be stationary on the sleeve surface. The viscosity of the liquid will determine the ease of relative motion of layers between these two. Note that without relative motion, there is no pressure and thus no support from the liquid. At standstill, the liquid is pressed out from the two bearing members, and during a subsequent starting there will be metal-to-metal contact and therefore wear.

A dynamic film bearing also has grooves or slots cut into the sleeve to distribute the lubricant to the bearing surface. The frequency of the noise produced by these slots is that given by equation 4.1. Various means of feeding the lubricant to the bearing grooves are used:

- 1) Gravity Feeding
- 2) Wick Feeding
- 3) Flood Lubrication
- 4) Pressure Feed (from an internal or self-driven system)
- 5) Oil-Ring Feed

The noise produced by these lubrication systems varies from slight to considerable. The more exacting the load requirements, the more complex and noisy the lubrication system will be.

Certain low noise aspects of sleeve bearings for integral horsepower motors may be utilized to a greater extent in the near future. New sleeve materials having low coefficients of friction and sufficient dimensional rigidity may eliminate the need for lubricated sleeve bearings or ball bearings in many applications. Among the materials currently used only for special motors, but under evaluation for broader applications, are filled and unfilled thermoplastic resins, thermosetting resins, and several sintered metals having a partial fill and coating of plastic.

Preliminary studies indicate that these non-lubricated bearings will have a noise spectrum that differs greatly from a static or dynamic film lubricated

sleeve bearing. The sliding contact between two solid bodies will produce minute, high frequency, vibrations regardless of low coefficient of friction and proper surface finish, while the interlaminar flow of a lubricant is ideally smooth. On the other hand, a non-lubricated sleeve bearing has two decided advantages: 1) the sleeve materials are normally poor vibration transmitters, particularly in the higher frequency bands, and 2) the provisions for constantly maintaining a lubricant in the bearing gap are eliminated.

Non-lubricated sleeve bearings, therefore, will create very little motor vibration while airborne noise in the higher frequencies will be present to a degree varying with the wearing characteristics of the selected sleeve material. A comparison of the noise-producing aspects of this type bearing to those of a ball bearing can only be made when the numerous sleeve materials have been evaluated and developed for application in the integral horsepower frames. At that time an establishment of the functional and noise-producing relationship between non-lubricated and special ball bearings is recommended.

4.3 BALL BEARINGS

Anti-friction bearings use a train of rolling elements such as balls to essentially replace sliding friction with a much lower friction consisting mostly of rolling friction and a small amount of sliding between the balls and raceways. Ball bearings with their numerous components moving relative to each other have long been recognized as a motor noise source. These bearings produce both random frequency and discrete frequency noise. Random frequency noise and vibration is caused by the balls rattling within the raceway clearances and sliding on the raceways. The discrete frequencies of noise are produced by irregularities of the ball bearing components and may be determined if the bearing geometry and the shaft speed are known. (18)

The following symbols are defined:

r_i = radius of inner raceway

r_o = radius of outer raceway

r_E = radius of rolling elements

r_T = radius of train of rolling elements

E = number of rolling elements (numeric)

n_R = speed of inner raceway or shaft in rpm.

n_T = speed of train of rolling elements in rpm.

n_E = spin (rotational speed) of rolling elements in rpm.

f_R = fundamental rotational frequency of shaft in cps.

f_T = fundamental rotational frequency of train in cps.

f_E = fundamental rotational frequency of rolling elements in cps.

f_i = frequency due to inner raceway in cps.

f_o = frequency due to outer raceway in cps.

P = number of poles

According to the geometry of the bearings, the radii are interrelated as follows:

$$r_T = r_i + r_E$$

Clearance is neglected here because the nominal dimensions provide sufficiently accurate data for the calculation of frequencies. The speed of the train of rolling elements and the rotational speed of the elements may be calculated as follows:

$$n_T = n_R \frac{r_i}{r_i + r_o}$$

$$n_E = \frac{r_o}{r_E} \times n_T$$

The five most prominent discrete frequencies produced by ball bearings are listed below.

1) The fundamental rotational frequency which appears at the slightest unbalance or eccentricity of the inner race is

$$f_R = n_R / 60 \text{ cps} \quad 4.2$$

2) Any irregularity of a rolling element or the cage causes noise with a frequency,

$$f_T = n_T / 60 \text{ cps} \quad 4.3$$

3) The spin frequency of a rolling element is

$$f_E = n_E / 60 \text{ cps} \quad 4.4$$

Any rough spot or indentation of an element causes a frequency component $f_{E'} = 2 f_E$ because the spot hits the inner and outer race alternately.

4) Another frequency occurs if there is an irregularity (high spot or indentation) on the inner raceway

$$f_i = E (n_R - n_T) / 60 \text{ cps} \quad 4.5$$

In the case of many spots, the harmonics of f_i will be more pronounced.

- 5) The fifth frequency component depends upon the existence of irregularities on the outer raceway.

$$f_o = E n_T / 60 \text{ cps} \quad 4.6$$

The speed of the train of rolling elements, n_T , is roughly 1/2 the rotational speed, n_R . Equations 4.5 and 4.6 may be approximated by the expression:

$$f_i \approx f_o \approx \frac{E/2 \times n}{60} R = \frac{60E}{P} \text{ cps} \quad 4.7$$

Since the bearing noise is produced by irregularities of the bearing components, it follows that reduction of bearing noise requires a reduction in component irregularities. The means of manufacturing quiet ball bearings is beyond the scope of this study. However, the optimum utilization of quiet ball bearings is treated later in this section.

4.4 RELATIVE ADVANTAGES OF SLEEVE AND BALL BEARINGS

A sleeve bearing is inherently quieter than a ball bearing. The advantage of a sleeve bearing lies in its simplicity of design which utilizes a minimum number of components. One disadvantage results from the diametral clearance which is initially several mills in magnitude. Under load, the shaft rides up the side of the sleeve; thus the relative position of the rotor with respect to the stator is both a function of the load and the condition of the bearing. This variation is undesirable since an eccentric air gap results in unbalance magnetic forces. A more important disadvantage of sleeve bearings lies in the methods required to maintain the lubricating film between the shaft and the sleeve.

The major advantage of ball bearings is their high performance qualities. They can be used for applications involving high speeds, high radial and thrust loads, and frequent starts with prolonged idle periods. Ball bearings usually are grease lubricated, thus eliminating noise produced by lubricant feeding devices. The internal clearance in a ball bearing is less than one mil and does not increase with bearing use, thus eliminating one factor in maintaining a uniform air gap. The disadvantage of ball bearings is their numerous components moving at differing speeds. The noise produced by ball bearings is dependent upon the sphericity of the balls and the surface finishes of the components. Recently ball bearing manufacturers have perfected manufacturing techniques to the point that they can produce ball bearings meeting the anderson requirements of MIL-B-17931A, Amendment 2, dated 16 September 1959. The anderson is a unit of measure which represents the vibrational velocity in the radial direction in microinches per radian of revolution of the bearing. The magnitude of the improve-

ment in bearing noise is considerable, since this amendment essentially reduced the permissible vibration by 50%.

The decision as to which type bearing to use will depend upon the application of the motor. If the motor is designed for a specific use where the radial and thrust loads on the bearing are both known and not excessive, sleeve bearings are recommended. If, however, the motor is a general design for multi-purpose applications or if the bearing loads or speed are high, ball bearings meeting Amendment 2 of MIL-B-17931A are recommended.

Bearing manufacturers are presently attempting to solve the problem of producing shielded or sealed bearings meeting Amendment 2. The raceways of such bearings are honed or specially ground to obtain an eccentricity of less than 25 millionths of an inch. The grooves for the seals or shields are too narrow (about 1/32") for grinding and must be cut. The necessary heat treatment of the bearing results in an out-of-roundness of these grooves. The shield or seal, which is crimped or pressed into the outer race, tend to deform the raceway to correct this out-of-roundness. Because of the thinness of the outer raceway, the force exerted by the shield is sufficient to cause deformation of the order of 500 millionths of an inch, or 20 times the raceway tolerances. To eliminate the deleterious effect of these warped raceways, only open bearings were used in the following studies and in the prototype units.

4.5 MEANS OF REDUCING BALL BEARING NOISE

Various studies were made of ball bearings and the means available to the motor manufacturer of reducing bearing-caused motor noise. With the exception of the first study of three classes of bearings, all tests were conducted with bearings meeting Amendment 2 of MIL-B-17931A. The test data furnished is that taken on several 3 HP, 2 Pole, 184 frame open motors. The effects of following factors were studied:

4.5.1 Bearing Preload

- a) Effect of preloading three classes of bearings
- b) Amount of preload force
- c) Type of thrust washer

4.5.2 Shaft-Bearing Interference Fit

4.5.3 Bearing Locknut

4.5.4 Bearing Lubricant

4.5.1 Bearing Preload

4.5.1a Effect of Preloading Three Classes of Bearings

One of the best known methods of reducing ball bearing noise is the use of a thrust washer to axially preload the bearings. This washer acts as a spring to exert a force on the outer race of the ball bearing. The reactive force is supplied by the shaft pressing against the inner race of the bearing. This force couple across the bearings takes up the internal clearances and causes each ball to follow the same

path on each bearing raceway.

Three classes of bearings meeting FF-B-171, Amendment 1, and Amendment 2 of MIL-B-17931A respectively were investigated. For the non-preloaded condition, the test motor had axial end play as specified in MIL-M-17060B. For the preloaded condition, a bearing housing modified to accommodate a thrust washer was substituted for the original one. Except for the bearings, the same components were used in the three tests.

Table 4-1 lists the vibration acceleration levels for prominent one-third octaves and the overall readings for this study. For the first two classes of bearings, preloading has detrimental effect with the principal exception of the rotational frequency vibration (63 cps band) along the shaft axis. On the other hand, preloading bearings meeting Amendment 2, MIL-B-17931A results in an appreciable decrease in vibration in all prominent frequencies and an average 5 adb overall reduction. Note especially the 14 adb decrease in the 4000 cps X - axis vibration. This is especially interesting as the 4000 cps band primarily reflects the double rotor slot frequency. (See Section 3.)

TABLE 4-1

Effect Of Preload On Bearings
184 Frame 2 Pole Motor
Vibration Acceleration Levels

Band	Axis	FF-B-171		Amendment 1 MIL-B-17931A		Amendment 2 MIL-B-17931A	
		Unloaded	Loaded	Unloaded	Loaded	Unloaded	Loaded
63	X	85	80	89	85	81	80
	Y	82	82	86	84	78	78
	Z	81	78	82	84	76	76
200	X	73	86	79	92	*	74
	Y	66	72	81	85	74	*
	Z	66	68	80	80	72	*
2000	X	95	95	94	95	91	89
	Y	94	97	96	100	95	90
	Z	96	94	93	97	93	91
4000	X	102	100	94	96	100	86
	Y	91	92	95	95	89	87
	Z	96	98	96	97	97	97
10,000	X	101	100	101	101	100	93
	Y	104	106	101	102	106	101
	Z	102	104	100	104	102	98
Overall	X	109	109	107	107	107	101
	Y	108	109	106	109	108	103
	Z	108	110	106	109	106	103

* Values less than 70 adb were below range of recording paper for Spectrograms 4-3 through 4-6.

Values taken from Spectrogram 4-1 through 4-6.

These tests reveal that preloading all three types of bearings eliminates noise caused by the balls

rattling within the raceways and cage and improves balance by the removal of bearing looseness. But, preloading also causes the balls to closely follow the surfaces of the raceways. If the surface finish of the raceways and the sphericity of the balls are of high quality, then the bearing will run smoothly and thus quietly. However, if the surface and balls are not of this high quality, preloading may cause the balls to follow surface irregularities that they otherwise might have skimmed over. The reason for the large reduction in 4000 cps shaft axis vibration is not known.

During these tests the bearings were run with the amount of preload force indicated by rule-of-thumb that the preload force in pounds should be five times the bore size i.e., 25 pounds for an O5 bearing. It was observed that the 200 cps band is erratic and highly sensitive to the amount of preload force. A test to determine the optimum amount of preload force became necessary.

4.5.1b Amount of Preload Force

For this test, one bearing housing was milled out to accommodate an uncompressed thrust washer. Successive tests were made with an increasing number of shims placed behind the thrust washer. The preload force was determined by measuring the minimum force applied to the shaft that would cause the rotor to move axially. This measured force includes the frictional resistance of the bearing O.D. sliding within the housing bore as well as the preload force. This frictional resistance is of the order of a few pounds and, as Figure 4-1 shows, remains constant. The linear characteristic of the thrust washer over the normal operating range could only result in the straight line portion of the curve shown in Figure 4-1 if the frictional force were constant. As the frictional force is both small and constant, the measured force has been considered to be equal to the preload force.

FIGURE 4-1

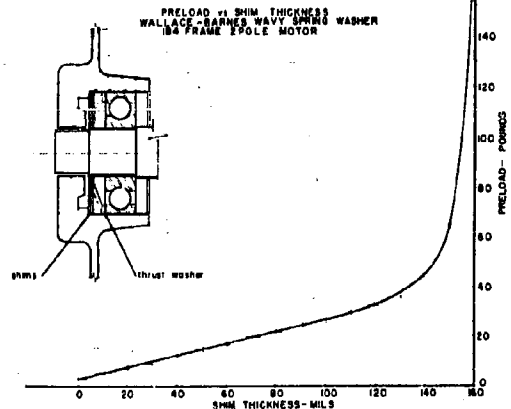


Table 4-2 lists the adb levels for important one-third octaves for various amounts of preload force. The 200 cps band shows an initial decrease, then a gradual increase reaching a peak at 21.5 pounds preload followed by a gradual decrease. This is especially prominent in the X-axis readings. The other bands show an initial decrease and then either remain essentially the same or increase very gradually until excessive preload force (above 60 pounds) is applied. These large forces cause an abrupt increase in vibration. The bearings were permanently damaged and subsequent lowering of the preload force did not result in lower vibration levels.

The initial decrease noted in all frequency bands is due to the removal of internal bearing clearance. Since the thrust washer was originally uncompressed, the initial measured force was all frictional resistance. The minimum vibration levels occur when the bearing is only slightly preloaded. All bands other than the 200 cps band either remain constant or rise so slightly that the range of 7 to 27 pounds effectively results in the same noise production, i.e., a broad minimum exists. The 200 cps band, however, shows an increase of 20 adb in the X-axis reaching a maximum at 21.5 pounds preload. This band, which has been termed "preload band" due to its sensitivity to the amount of preload, narrows the acceptable range of preload force to between 7 and 12 pounds. Note that the 25 lbs. indicated by the rule-of-thumb previously mentioned causes near maximum vibration in the 200 cps band. This test indicates the optimum preload force to be the minimum force that takes up the internal bearing clearances.

The usual method of preloading bearings is to machine the bearing housing to accommodate a thrust washer as used in the preceding test. The preload force is determined by the amount the thrust washer

must be compressed to assemble the motor. The normal end play tolerances are such that maintaining the small amount of preload force indicated by the previous study is difficult. In addition, the optimum preload force has been determined for only one size and make of bearing. Additional testing is required to determine if the results of this test are indicative of other sizes and makes.

A means of adjusting the amount of preload after motor assembly is shown in Figure 4-2. Use of such a device eliminates relying on previous test and compensates for production variation. The preload force is adjusted by screwing the preload adjuster in or out, thus varying the compression of the thrust washer. A locknut is used to lock the preload adjuster in the position resulting in minimum noise.

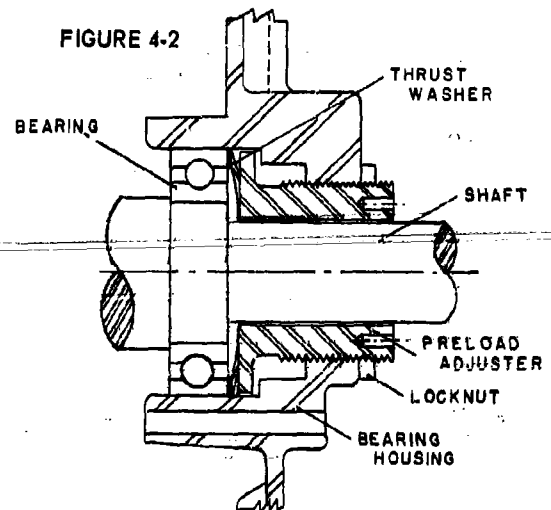


TABLE 4-2
Preload Amount
Vibration Acceleration Levels

Band	Axis	Preload Force in Pounds																	
		2.5	5.5	7	9	11.5	14.5	16.5	19.5	21.5	24	26.5	29.5	32	35.5	44.5	65	100	155
200	X	73	73	74	76	80	85	88	91	93	92.5	92	86	84	82	78	76	74	
	Y	80	73	*	*	71	73	75	76	79	78.5	78	76	74	73	*	*	*	
	Z	71	71	*	*	*	70	72	73	74	74	75	72	72.5	71	*	*	*	
500	X	83	82	71	*	*	*	70	*	*	70	*	*	71	71	72	72	72	
	Y	82	79	76	75	76	76	77	75	75	75	75	73	74	74	80	78	81	
	Z	88	78	80	80	79	78	79	79	78	79	77	79	78	81	79	84	84	
1250	X	98	96	89	82	82	83	82	83	81	84	81	82	80	82	83	84	85	
	Y	100	100	91	86	83	85	83	84	83	84	85	86	86	84	83	87	88	
	Z	98	97	88	82	81	80	81	79	81	83	82	83	82	81	82	84	86	
2000	X	103	99	94	86	87	87	88	88	89	89	90	91	90	90	94	96		
	Y	104	102	95	90	92	91	91.5	90.5	91	92	93	92	91	93	93	96		
	Z	101	100	92	88	88	88	89	89	90	90	90	90	89	90	91	94		
4000	X	95	99	95	98	96	95	93	94	93	93	96	97	94	95	97	96		
	Y	93	91	90	90	89	88	88	88	88	88	89	90	90	90	90	93		
	Z	97	98	92	94	92	94	91	91.5	91	92	94	94	94	96	94	97		
10,000	X	100	92	88	89	90	93	90	89	91	93	91	91	96	95	91	91		
	Y	103	103	96	96.5	97	99	98	100	98	99	99	98	100	98	99	100		
	Z	100	97	92	96	98	92	94	94	95	95	100	95	95	96	97	97		
Overall	X	108	107	103	101	101	101	100	101	101	101	101	102	101	101	104	105		
	Y	109	109	102	100	101	101	101	101	100	102	102	102	102	102	102	104		
	Z	108	108	101	102	102	101	100	101	101	101	103	102	102	102	103	106		

* Values less than 70 adb were below the range of recording paper.

Values taken from Spectrograms 4-7 through 4-24.

4.5.1c Type of Thrust Washer

A test was conducted to determine if the type of thrust washer had any effect on bearing noise. A wavy spring washer having three point contact with the bearing outer race and a Belleville washer having continuous contact with the outer race were tested. Since the spring constants of the two washers are different, a bearing housing was milled out to accommodate either uncompressed thrust washer. By adding a different number of shims, the preload force was adjusted to 12 pounds for each test. Spectrograms of the motor vibration were practically identical, (Spectrograms 4-25 through 4-28.) indicating that the type of thrust washer used has no effect on bearing noise.

4.5.2 Shaft-Bearing Interference Fit

It is necessary that the inner ring of a ball bearing be tight enough to prevent turning under load. This is accomplished by an interference fit between the shaft and bearing or by means of a locknut; or a combination of both may be used. When the bearing has a tight fit on the shaft, the inner race expands. A study

was made to determine the effect that this expansion has on the bearing noise. The bearing bore dimensions of the test motor were measured to be 1.1810 inches. Three special shafts were made, having bearing seats 1.1811, 1.1816, and 1.1821 inches in diameter, respectively. The resulting amounts of interference (.0001", .0006" and .0011") cover the range obtained using ABEC-1 grade bearings and tolerances. Vibration readings were taken of a motor with the bearings on the shaft with the smallest interference fit. The bearings were then carefully removed, the second shaft substituted in the rotor assembly, the rotor rebalanced, and the bearings carefully pressed on the new shaft. The same procedure was used in changing to the .0011" interference fit shaft.

Table 4-3 indicates the vibration levels for all three conditions for the (X,Y,Z) axes on the motor feet as well as axial readings taken on the rear and front bearing housings (designated as R and F in Table 4-4). Once again, the 200 cps band X-axis reflects the effect of slight variations in the amount of preload force. This test reveals that minimum bearing noise results from the minimum bearing-shaft interference. It is recommended that a light press fit of between 0.0001" and 0.0003" be used.

The 0.0004" bore tolerance of an ABEC-1 grade bearing would require that the bearings be individually measured and selected. Use of higher ABEC grade bearings reduces this variation and is more compatible with the internal tolerances necessary to meet Amendment 2 of MIL-B-17931A.

TABLE 4-3

Bearing - Shaft Interference
Vibration Acceleration Levels

Band	Axis	0.1 Mil	0.6 Mil	1.1 Mil
63	X	85	94	95
	Y	84	95	98
	Z	84	94	97
	R	75	84	89
	F	82	93	94
200	X	73	83	74
	Y	72	75	73
	Z	70	71	74
	R	70	85	75
	F	72	86	73
800	X	74	76	79
	Y	73	75	76
	Z	71	73	73
	R	90	107	103
	F	88	90	91
1250	X	88	86	90
	Y	89	91	92
	Z	86	86	89
	R	97	102	105
	F	92	93	96
10,000	X	96	90	96
	Y	102	100	106
	Z	99	94	100
	R	105	102	106
	F	101	101	102
Overall	X	104	105	106
	Y	105	105	108
	Z	106	106	108
	R	107	112	112
	F	106	110	111

Values taken from Spectrograms 4-29 through 4-34.

4.5.3 Bearing Locknut

The light press fit recommended by the previous test may be insufficient to keep the bearing inner race from rotating on the shaft. If this proves to be true, it is recommended that a bearing locknut be used rather than a tighter press fit. A test of a motor equipped with 305 bearings revealed a negligible change in bearing noise as the torque on the locknut was increased from zero to 12 lb. ft. See spectrograms 4-35 through 4-38.

It should be remembered that preloading of the bearings forces the inner race up against the shaft shoulder and this also tends to prevent rotation of the bearing on the shaft. The disadvantage of using bearing locknuts is the possibility that they may be overtightened and deform the bearing raceway. Bearing locknuts should only be used where necessary to prevent slipping of the bearing on the shaft.

4.5.4 Bearing Lubricant

Two tests were made of the effect on motor noise of bearing lubricant. The first concerned the cleanliness of the grease used; the second was a test of the relative quietness of three high temperature greases. For the first test, two samples of the brand grease were used. The first was a particularly clean sample

and the second was a sample rejected for high dirt content. The dirt counts of the two samples are furnished in Table 4-4 with the limits set by the bearing manufacturer.

TABLE 4-4

Particle Size	Dirt Count			
	5 to 20 μ .0002" to .0008"	21 to 50 μ .0008" to .002"	51 to 75 μ .002" to .003"	Over 75 μ Over .003"
Maximum Number Particles Permitted	5000	2000	50	0
Clean Grease	468	59	0	0
Reject Grease	7652	526	1.68	0

The dirt content permitted by the manufacturer is less than that allowed by certain military specifications. For example, MIL-L-3545 sets the following limits.

Particle Size	Number Permitted
25 μ or above	7,500
75 μ or above	1,600
125 μ or above	0

Note that both grease meet the military requirements. The test motor was vibration tested with the open bearings consecutively lubricated as follows:

- 1) light machine oil
- 2) clean grease
- 3) light machine oil
- 4) reject grease
- 5) light machine oil

The following method was used to remove one lubricant and replace it with another. The bearings were not removed but cleaned on the shaft. The entire rotor assembly was submerged in clean solvent and the bearings rotated by hand. The bearings were then forced-air dried and the process repeated with new solvent. The bearing grease cavity and end caps were similarly cleaned. The grease was placed in bearings and grease cavities with a clean stainless steel spatula. The grease cavities of the bearing housings and end caps were half filled with grease and the bearings were one-third filled. In Table 4-5, the prominent one-third octave vibration levels are shown for the three axes on the motor feet and for two axes parallel to the shaft and measured on the rear bearing housing and rear housing hub respectively. The reject grease caused an increase in the middle frequency range varying from slight to 20 adb in the 1250 cps one-third octave band. Another interesting feature of this test is that cleaning the bearing lubricated with the clean grease and replacing the machine oil essentially duplicated the first machine oil readings. The dirt in the reject grease possibly damaged the bearing surfaces since a similar replacement of the reject grease with light machine oil did

not reduce the vibration to the previous levels. It is recommended that lubricant with extremely low dirt content be used.

TABLE 4-5

Effect Of Grease Dirt Count
Vibration Acceleration Levels

Band	Axis	Oil	Clean Grease	Oil	Reject Grease	Oil
63	X	78	81	78	81	78
	Y	83	83	82	83	82
	Z	86	85	86	86	84
	Hsg. Hub.	76 *	78 76	76 *	80 74	79 *
1250	X	88	86	90	94	86
	Y	86	87	86	85	87
	Z	85	85	83	88	83
	Hsg. Hub.	81 94	80 90	80 90	97 110	78 92
2000	X	81	81	80	88	80
	Y	86	85	86	89	86
	Z	89	89	85	87	86
	Hsg. Hub.	80 78	81 74	77 73	78 85	76 79
4000	X	87	87	87	92	89
	Y	97	97	96	99	97
	Z	92	89	86	89	86
	Hsg. Hub.	92 82	81 79	89 79	88 92	86 80
10,000	X	98	99	92	97	96
	Y	95	96	96	92	90
	Z	92	93	92	92	93
	Hsg. Hub.	96 94	98 97	98 95	103 97	100 96
Overall	X	100	102	100	104	103
	Y	102	102	102	105	103
	Z	101	102	101	104	102
	Hsg. Hub.	102 103	105 105	103 102	111 114	106 108

*Values less than 70 adb were below range of recording paper.

Values taken from Spectrograms 4-39 through 4-48.

Care must also be taken to maintain the cleanliness of the lubricant. Improper relubrication can permanently damage the ball bearing surfaces. The grease used for relubrication should have as low a dirt count as the original. Extreme care should be exercised so that no impurities from the grease openings or the surroundings can pollute the lubricant. The housing-bearing-end cap grease cavity should never be completely filled. If the bearings are re-greased while the motor is not running, the bearings will be completely flooded with grease. The viscous friction of the balls churning through the grease causes overheating. This heat will melt the grease, which will then flow out into the motor. However, operation at high temperature and with the soap particles as well as the oil in the path of rotating balls will result in permanent surface damage. The dangers of overlubrication are great enough that it is recommended that the bearings be relubricated as seldom

as possible. If relubrication is necessary, a high degree of cleanliness must be maintained. Although it is not normal practice for shielded bearings, an open bearing should be relubricated with a limited amount of grease with the motor running.

The relative quietness of three high temperature greases were tested. The greases were replaced in the same manner as in the previous test. Table 4-6 furnishes the adb levels for the prominent one-third octaves for the following consecutive lubricants:

- 1) light machine oil
- 2) Andok 260 Grease
- 3) light machine oil
- 4) Aeroshell 5A Grease
- 5) light machine oil
- 6) Texas TG 3007 Grease
- 7) light machine oil

The difference between the three greases was not great but the Aeroshell 5A appeared to cause less vibration. This grease was used as the bearing lubricant for the prototype motors.

TABLE 4-6
Grease Type Test
Vibration Acceleration Levels

Band	Axis	Oil	Andok 260 Oil	Aeroshell 5A Oil	Texas 3007 Oil	Oil		
125	X	75	81	84	96	83	91	81
	Y	84	81	85	90	91	85	86
	Z	80	86	86	92	84	86	86
	Hsg.	76	83	83	95	88	81	85
	Hub	78	80	85	100	88	80	85
200	X	87	86	89	75	84	79	83
	Y	83	74	80	72	79	73	78
	Z	83	70	71	*	71	71	72
	Hsg.	86	88	88	78	87	76	89
	Hub	79	86	86	80	83	74	83
1000	X	93	88	84	85	87	85	85
	Y	95	90	87	87	87	87	86
	Z	90	88	85	85	86	85	84
	Hsg.	98	98	98	91	95	93	96
	Hub	109	107	99	102	103	93	95
2000	X	103	102	98	95	97	94	97
	Y	102	99	103	98	99	98	101
	Z	99	98	95	92	96	95	96
	Hsg.	87	88	87	75	88	78	93
	Hub	95	92	92	82	90	88	92
10,000	X	91	88	94	91	96	95	95
	Y	99	98	95	94	96	95	96
	Z	93	91	98	96	98	96	96
	Hsg.	101	98	102	100	102	101	97
	Hub	93	90	102	96	98	100	100
Overall	X	108	106	106	105	106	105	106
	Y	107	107	108	104	106	106	107
	Z	108	107	106	103	105	104	105
	Hsg.	107	108	106	106	107	106	106
	Hub	112	112	111	110	110	111	110

*Values less than 70 adb were below range of recording paper.

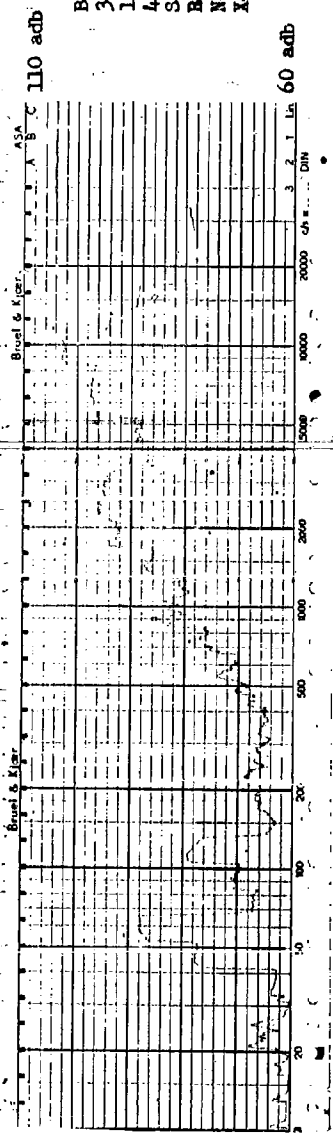
Values taken from Spectrograms 4-49 through 4-62.

It was noted that all three greases resulted in less noise than the light machine oil. This was somewhat unexpected since grease is composed of mineral oil and soap. The soap acts only as a carrier of the lubricant and once the grease has been channeled, the bearing is lubricated by an oil film. Soap particles that migrate into the path of the balls are either thrown out or the balls must roll over the obstruction. Either way noise is produced. Perhaps grease lubricated bearings are quieter than oil lubricated bearings because the grease also acts as a damping agent.

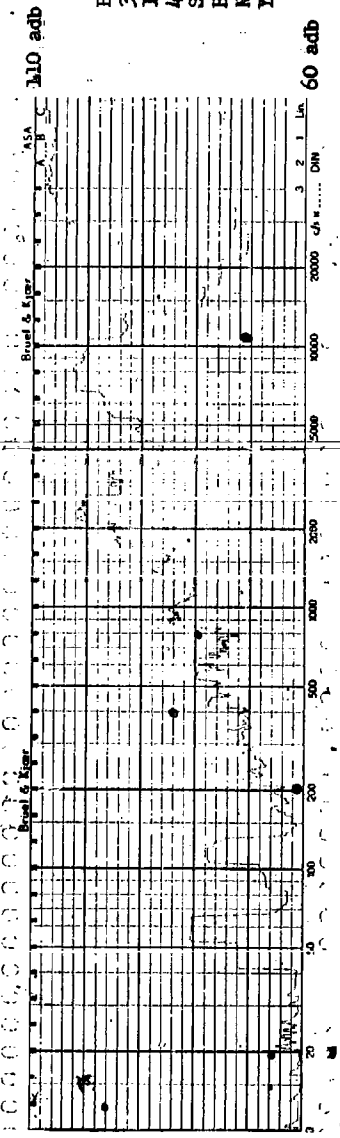
4.6 CONCLUSION

An appraisal of the application of sleeve bearings to squirrel-cage induction motors in the 1-100 HP range indicates the probability of attaining noise reduction when the bearing is designed to a particular speed and a moderate radial or thrust loading. The design and means for noise reduction of these bearings, either lubricated or non-lubricated, were not included in this study. Ball bearings meeting the anderson limits of Amendment 2 of MIL-B-17931A are recommended for motors designed for general applications, heavy external loading, or prolonged periods at rest. The following recommendations are made to minimize ball bearing caused motor noise:

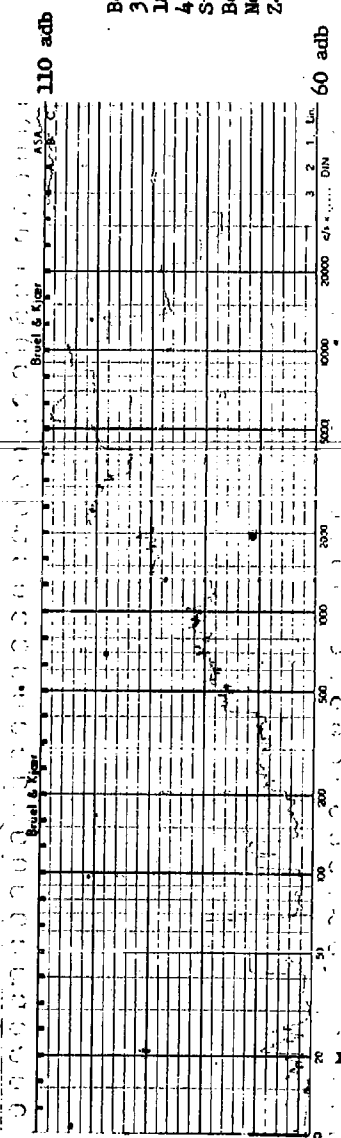
- 1) Use of ball bearings meeting Amendment 2 of MIL-B-17931A.
- 2) Ball bearings should be preloaded by use of a thrust washer.
- 3) The amount of preload force should be the minimum that takes up the internal clearance. If means for adjusting the preload are provided, the preload should be adjusted to give minimum motor noise.
- 4) An interference fit of between 0.0001 and 0.0003 is recommended for the shaft-bearing fit. Use of ABEC-5 or higher bearings is an aid in obtaining the light press fit and is more compatible with the internal tolerance necessary to produce a low vibration bearing.
- 5) Where bearing locknuts must be used, they should be no tighter than necessary to prevent rotation of the inner raceway on the shaft.
- 6) The dirt count should be determined for sample quantities of grease used in service or at place of motor manufacture. It is recommended that limit as to the maximum dirt count permissible for lubrication of low vibration bearings be established.



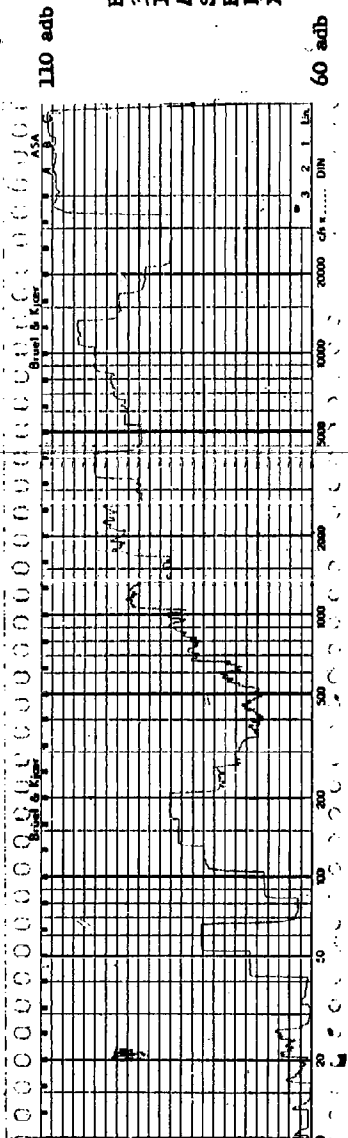
Bearing Type Test
 3 HP 2 Pole
 184 Frame Open
 4 Feb. 1960
 Structureborne
 Bearing FF-B-171
 Not Preloaded
 X-Axis



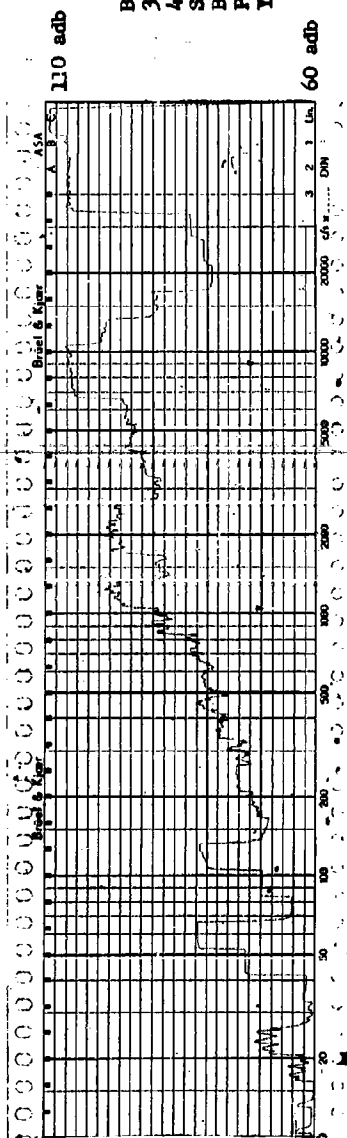
Bearing Type Test
 3 HP 2 Pole
 184 Frame Open
 4 Feb. 1960
 Structureborne
 Bearing FF-B-171
 Not Preloaded
 Y-Axis



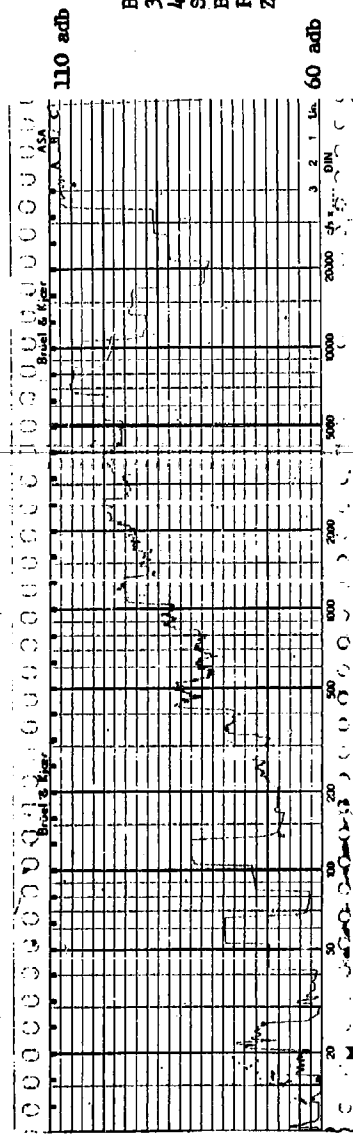
Bearing Type Test
 3 HP 2 Pole
 184 Frame Open
 4 Feb. 1960
 Structureborne
 Bearing FF-B-171
 Not Preloaded
 Z-Axis



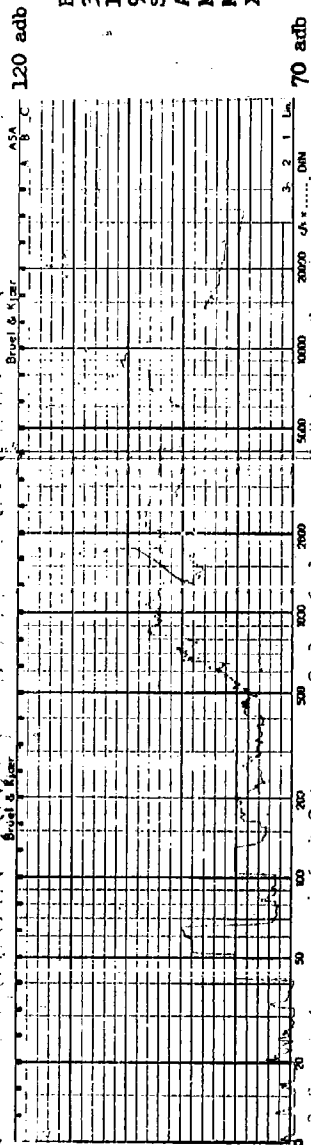
Bearing Type Test
 3 HP 2 Pole
 184 Frame Open
 4 Feb. 1960
 Structureborne
 Bearing FF-B-171
 Preloaded
 X-Axis



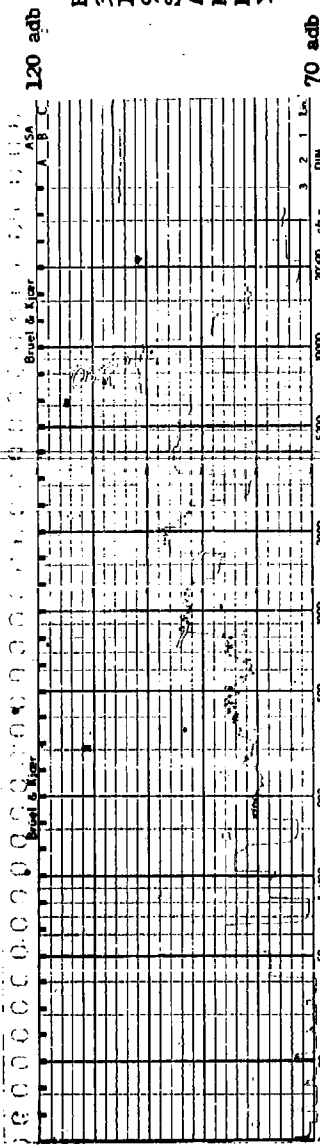
Bearing Type Test
 3 HP 2 Pole
 4 Feb. 1960
 Structureborne
 Bearing FF-B-171
 Preloaded
 Y-Axis



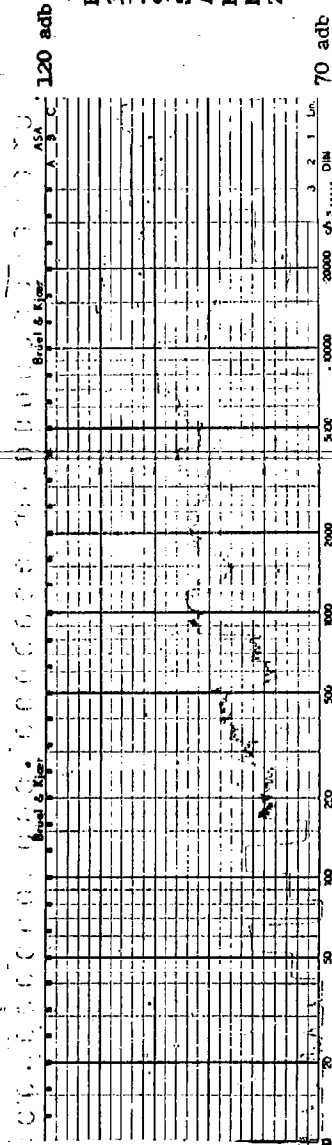
Bearing Type Test
 3 HP 2 Pole
 4 Feb. 1960
 Structureborne
 Bearing FF-B-171
 Preloaded
 Z-Axis



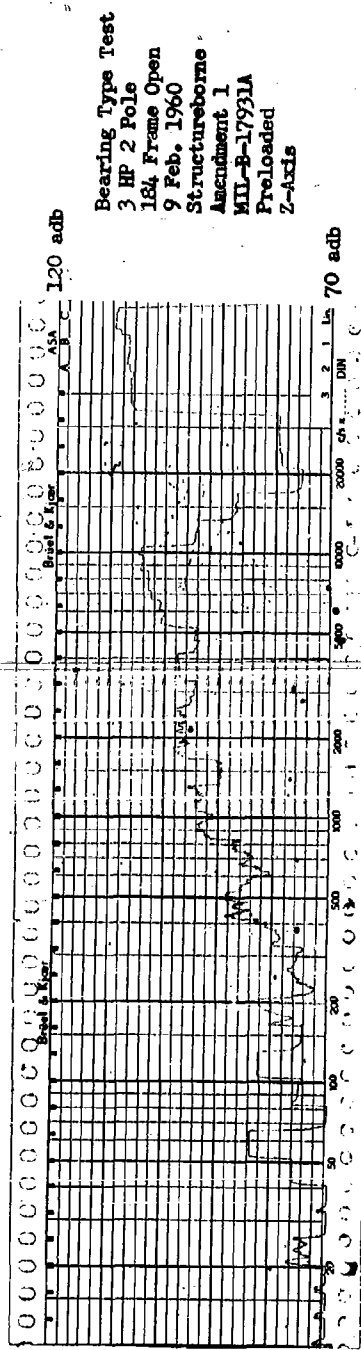
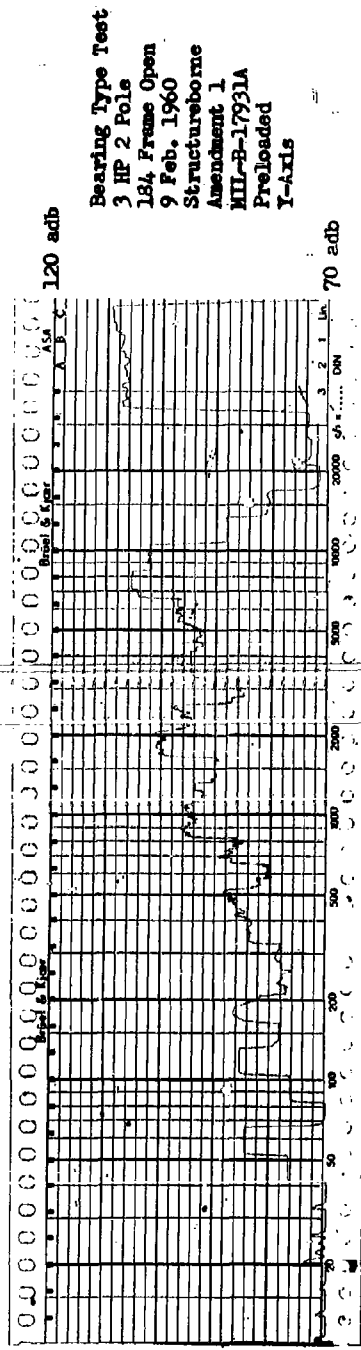
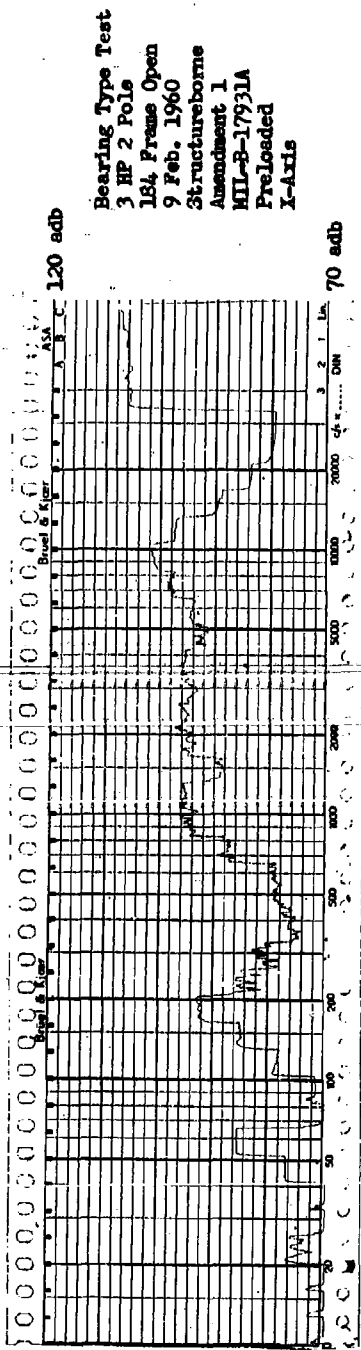
Bearing Type Test
 3 HP 2 Pole
 184, Frame Open
 9 Feb. 1960
 Structureborne
 Amendment 1
 MIL-B-17931A
 Not Preloaded
 X-Axis

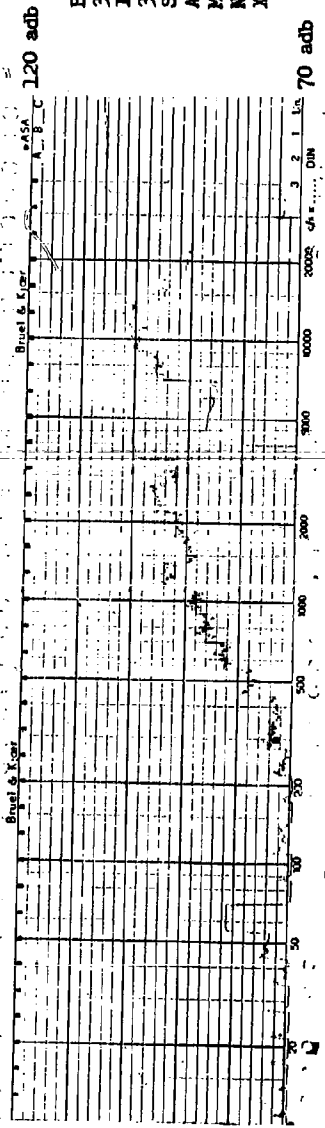


Bearing Type Test
 3 HP 2 Pole
 184, Frame Open
 9 Feb. 1960
 Structureborne
 Amendment 1
 MIL-B-17931A
 Not Preloaded
 Y-Axis

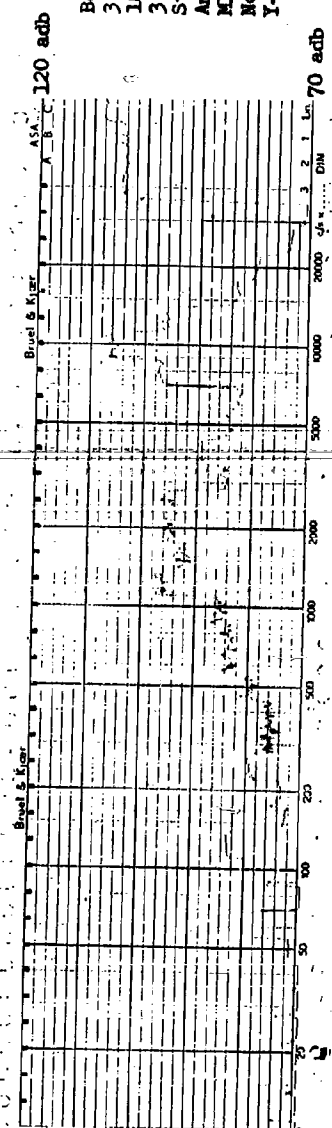


Bearing Type Test
 3 HP 2 Pole
 184, Frame Open
 9 Feb. 1960
 Structureborne
 Amendment 1
 MIL-B-17931A
 Not Preloaded
 Z-Axis

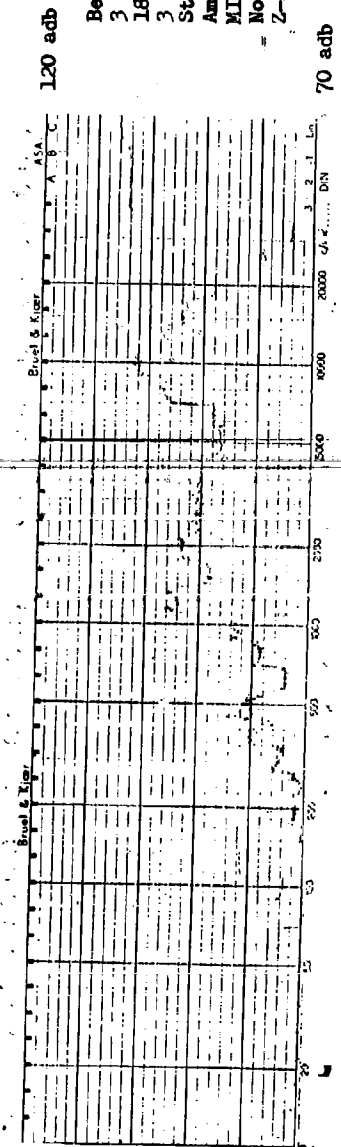




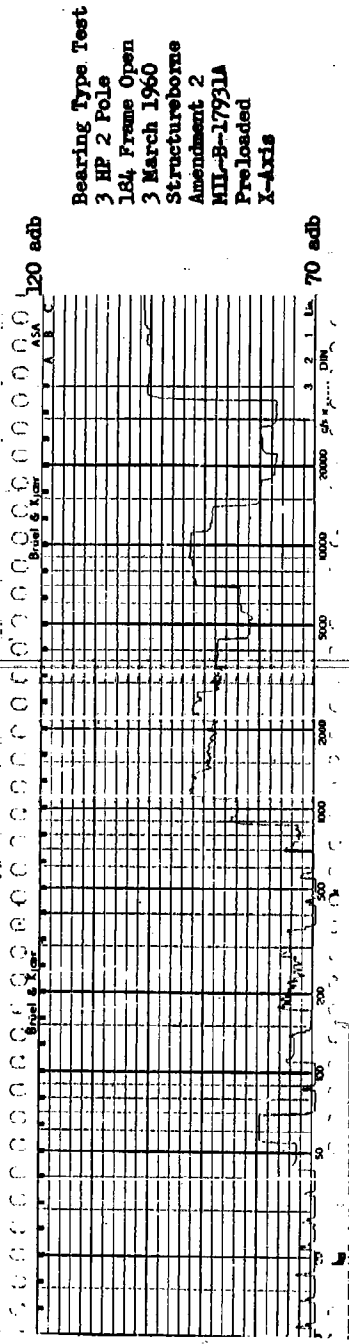
Bearing Type Test
 3 HP 2 Pole
 184 Frame Open
 3 March 1960
 Structureborne
 Amendment 2
 MIL-B-17931A
 Not Preloaded
 X-Axis



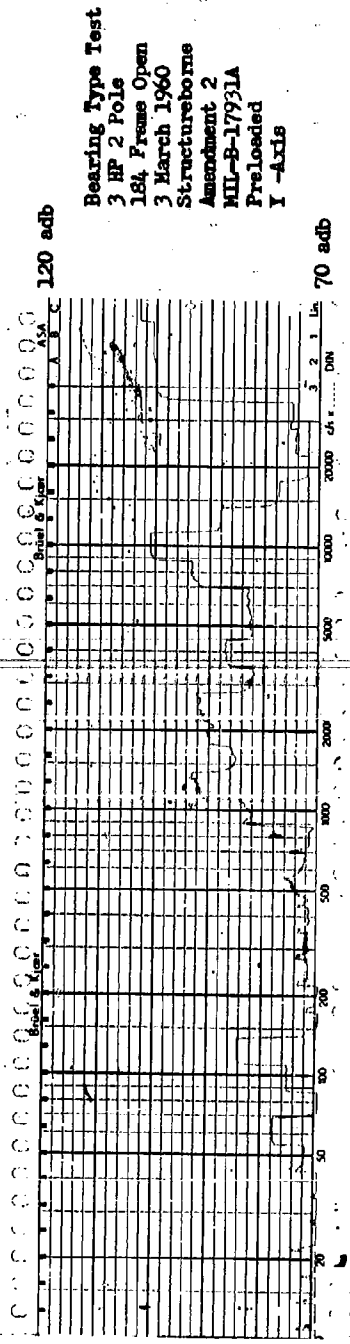
Bearing Type Test
 3 HP 2 Pole
 184 Frame Open
 3 March 1960
 Structureborne
 Amendment 2
 MIL-B-17931A
 Not Preloaded
 Y-Axis



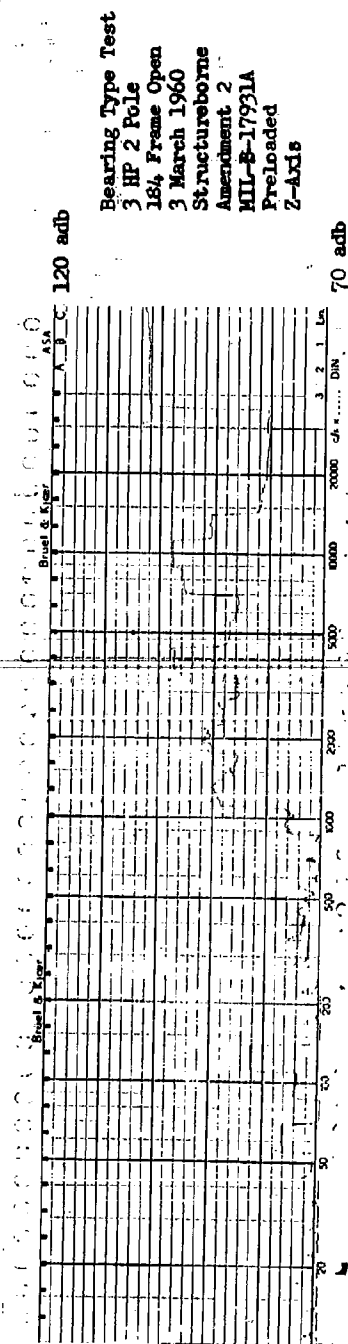
Bearing Type Test
 3 HP 2 Pole
 184 Frame Open
 3 March 1960
 Structureborne
 Amendment 2
 MIL-B-17931A
 Not Preloaded
 Z-Axis



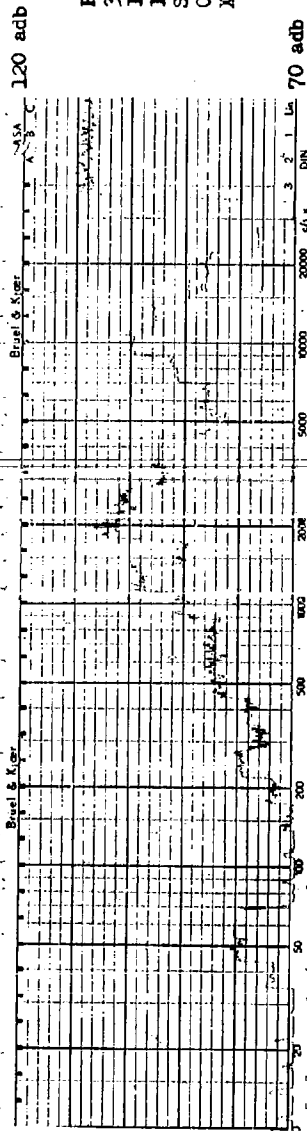
Bearing Type Test
 3 HP 2 Pole
 184 Frame Open
 3 March 1960
 Structureborne
 Amendment 2
 MIL-B-17931A
 Preloaded
 X-Axis



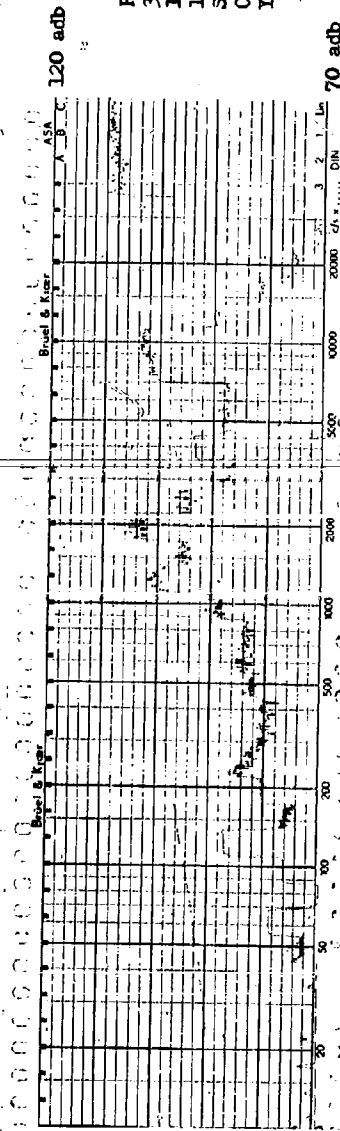
Bearing Type Test
 3 HP 2 Pole
 184 Frame Open
 3 March 1960
 Structureborne
 Amendment 2
 MIL-B-17931A
 Preloaded
 Y-Axis



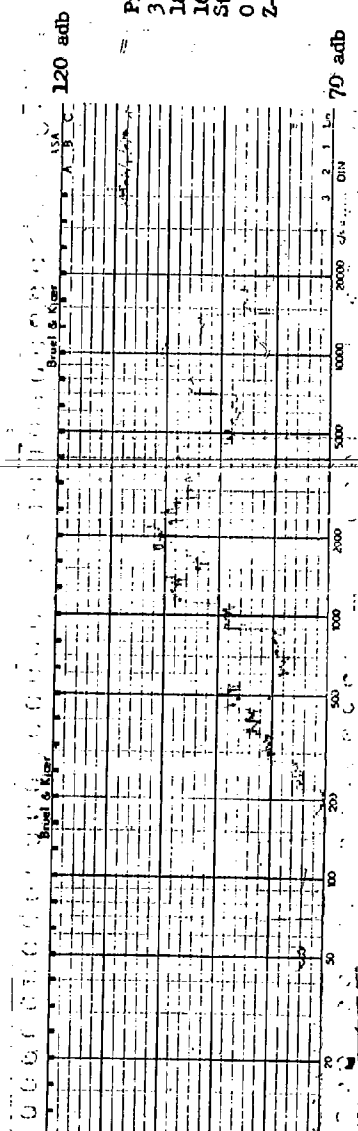
Bearing Type Test
 3 HP 2 Pole
 184 Frame Open
 3 March 1960
 Structureborne
 Amendment 2
 MIL-B-17931A
 Preloaded
 Z-Axis



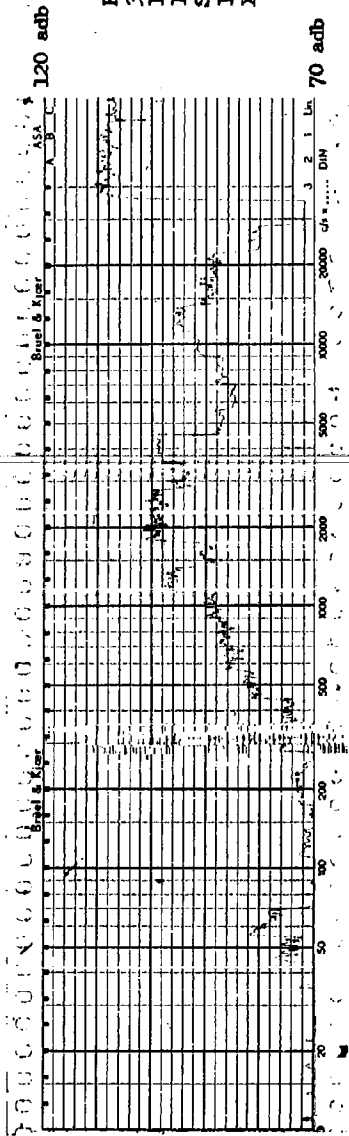
Preload Amount Test
 3 HP 2 Pole
 184 Frame Open
 16 May 1960
 Structureborne
 0 Mils 2.5 lbs.
 X-Axis



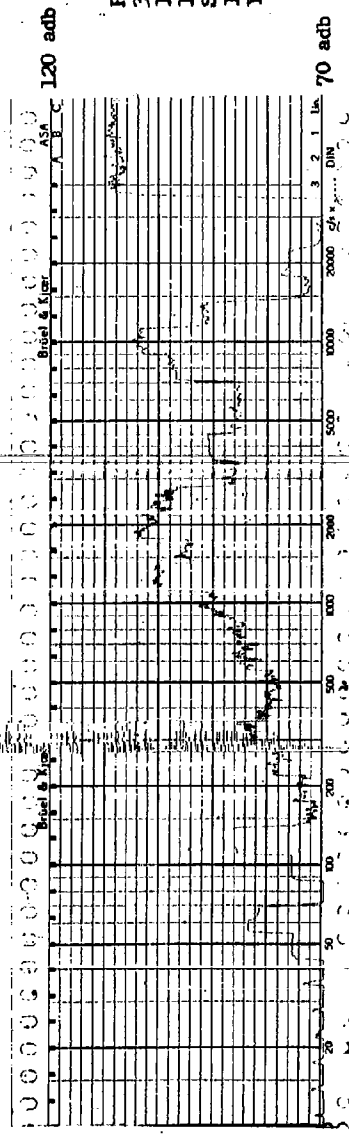
Preload Amount Test
 3 HP 2 Pole
 184 Frame Open
 16 May 1960
 Structureborne
 0 Mils 2.5 lbs.
 Y-Axis



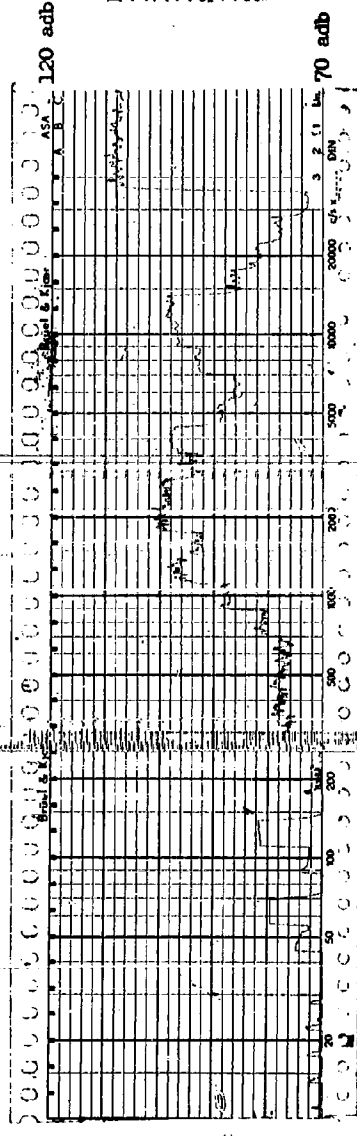
Preload Amount Test
 3 HP 2 Pole
 184 Frame Open
 16 May 1960
 Structureborne
 0 Mils 2.5 lbs.
 Z-Axis



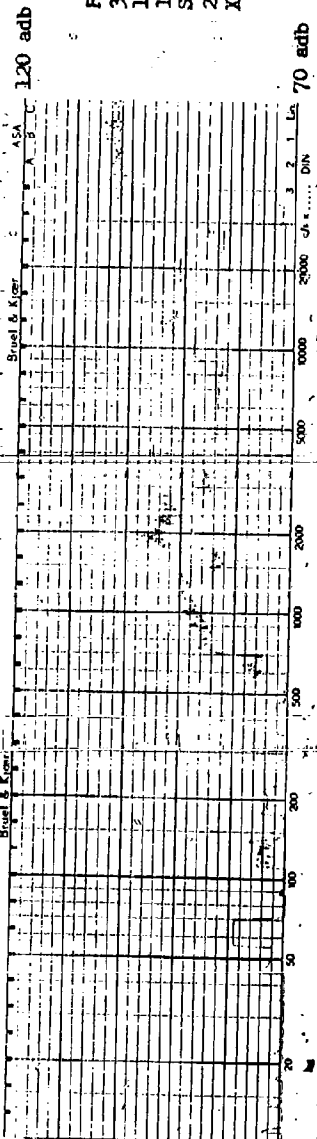
Preload Amount Test
3 HP 2 Pole
184 Frame Open
16 May 1960
Structureborne
10 Mills 5.5 lbs.
X-Axis



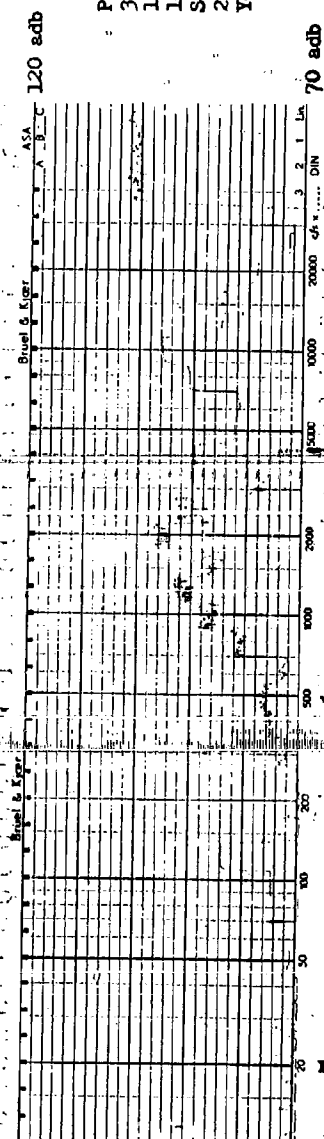
Preload Amount Test
3 HP 2 Pole
184 Frame Open
16 May 1960
Structureborne
10 Mills 5.5 lbs.
Y-Axis



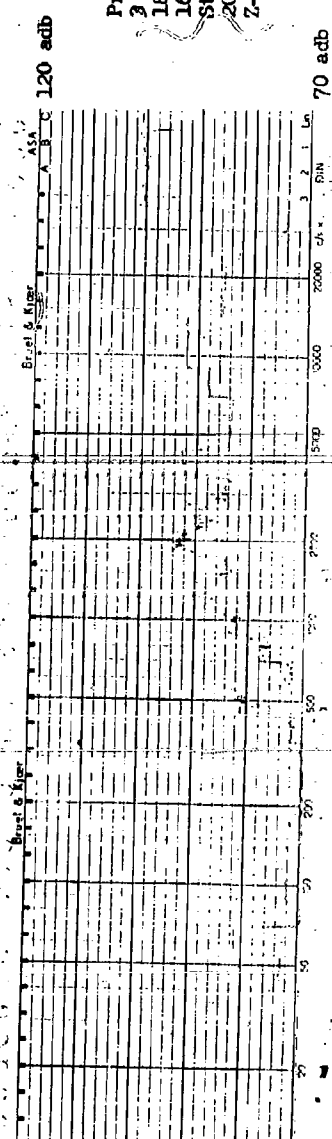
Preload Amount Test
3 HP 2 Pole
184 Frame Open
16 May 1960
Structureborne
10 Mills 5.5 lbs.
Z-Axis



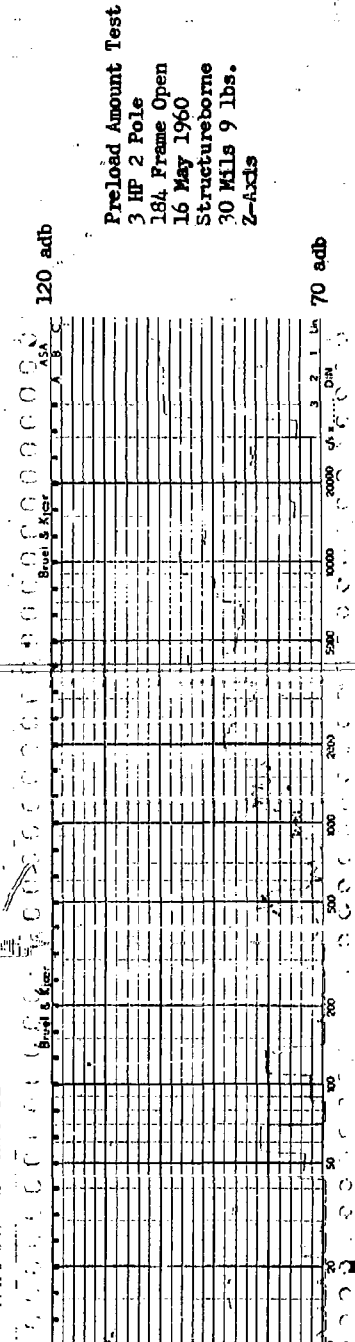
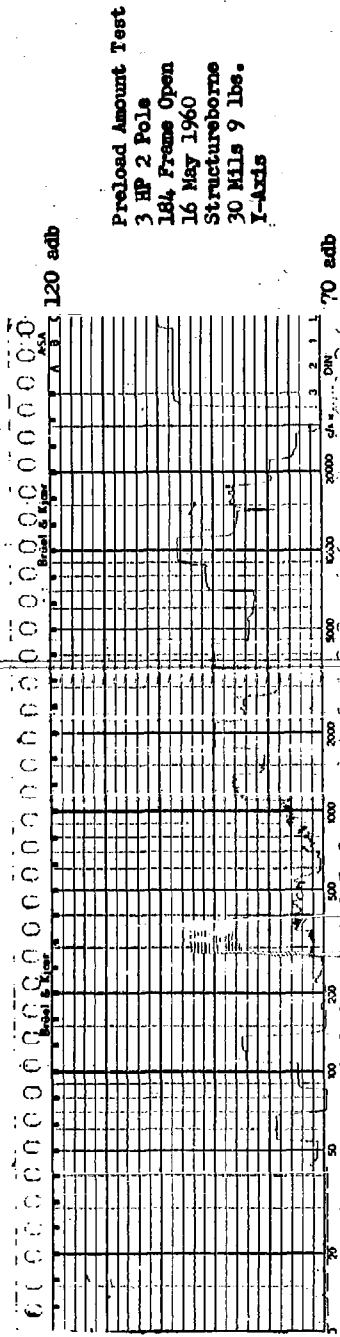
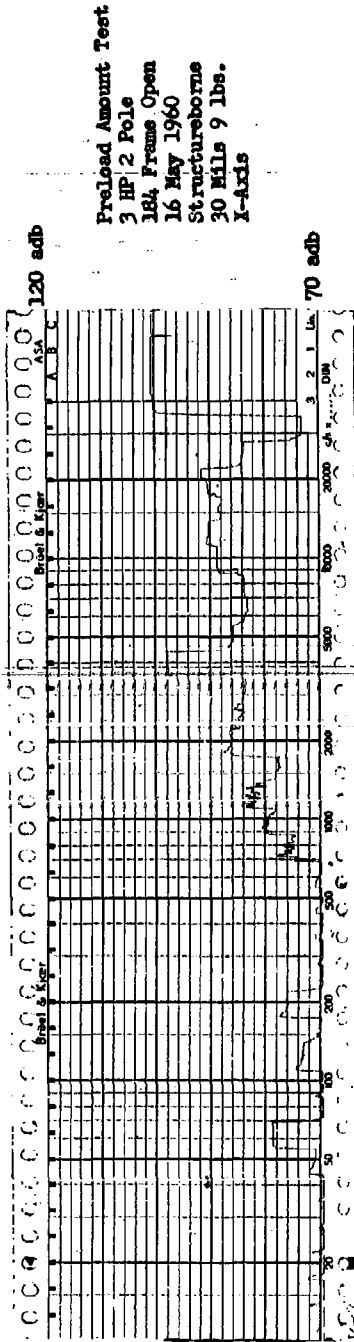
Preload Amount Test
 3 HP 2 Pole
 184, Frame Open
 16 May 1960
 Structureborne
 20 Mils 7 lbs.
 X-Axis

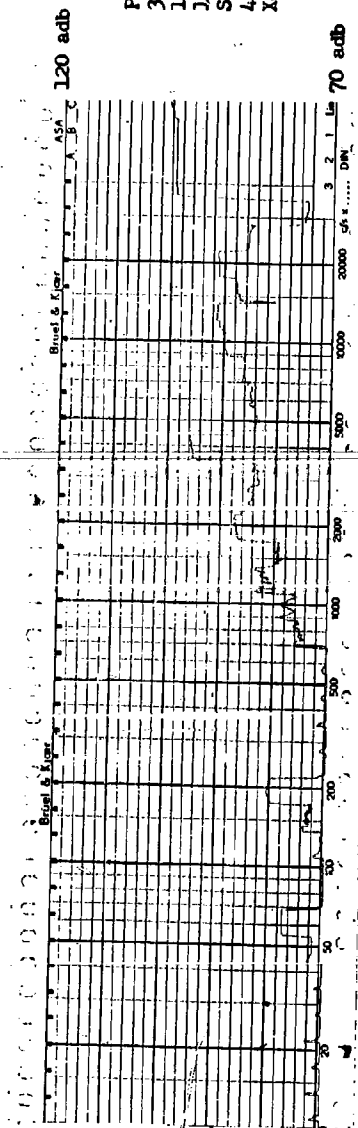


Preload Amount Test
 3 HP 2 Pole
 184, Frame Open
 16 May 1960
 Structureborne
 20 Mils 7 lbs.
 Y-Axis

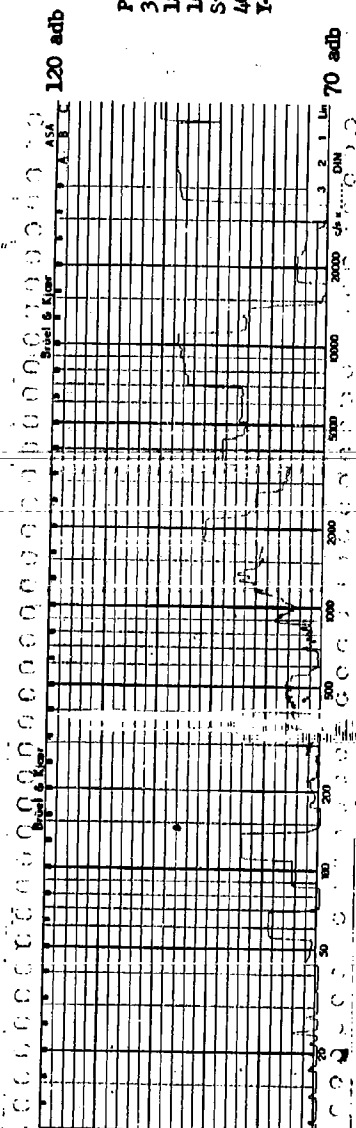


Preload Amount Test
 3 HP 2 Pole
 184, Frame Open
 16 May 1960
 Structureborne
 20 Mils 7 lbs.
 Z-Axis

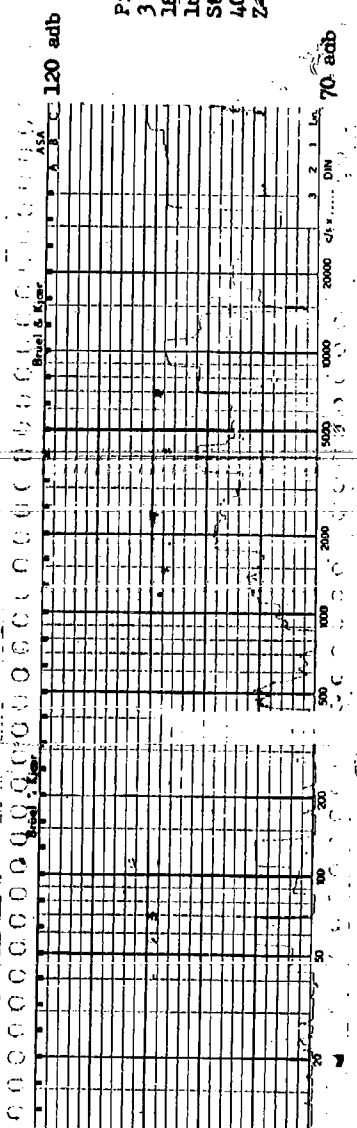




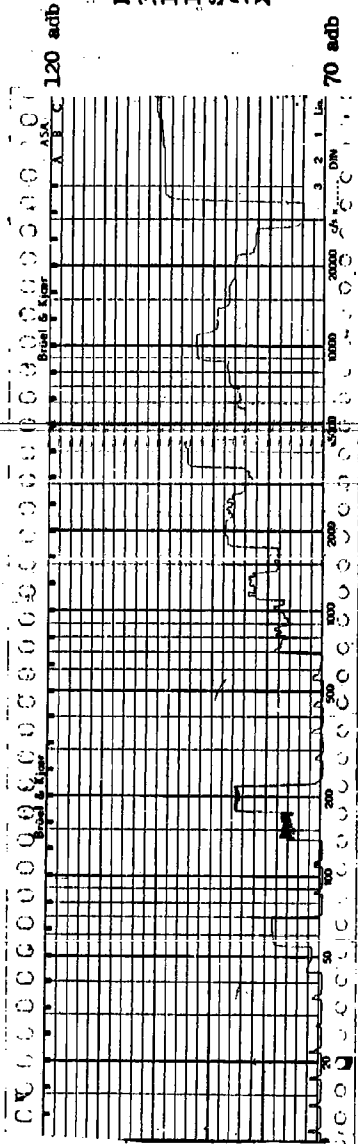
Preload Amount Test
 3 HP 2 Pole
 184 Frame Open
 16 May 1960
 Structureborne
 40 Mills 11.5 lbs.
 X-Axis



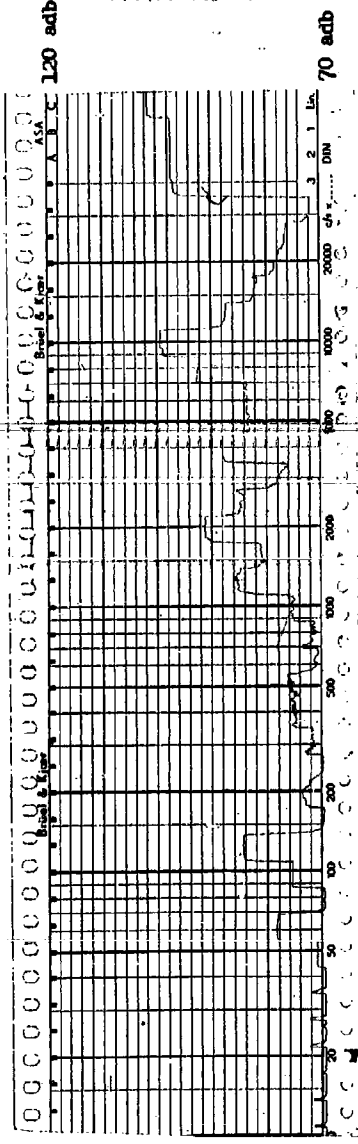
Preload Amount Test
 3 HP 2 Pole
 184 Frame Open
 16 May 1960
 Structureborne
 40 Mills 11.5 lbs.
 Y-Axis



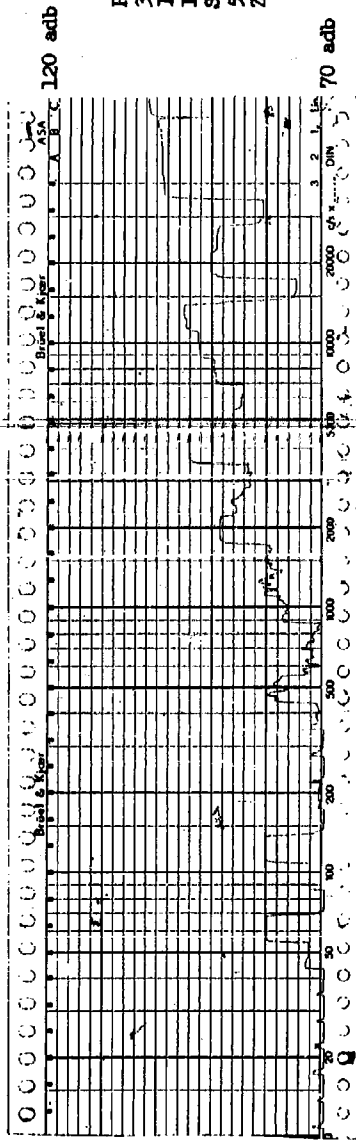
Preload Amount Test
 3 HP 2 Pole
 184 Frame Open
 16 May 1960
 Structureborne
 40 Mills 11.5 lbs.
 Z-Axis



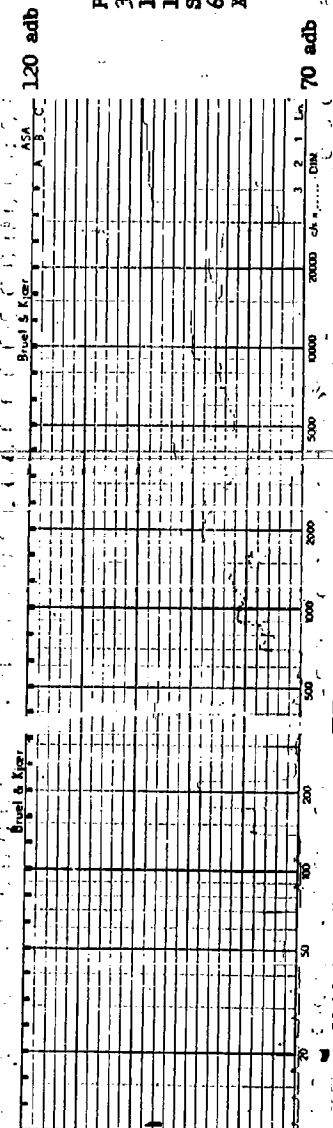
Preload Amount Test
 3 HP 2 Pole
 184 Frame Open
 16 May 1960
 Structureborne
 50 Mils 14.5 lbs.
 X-Axis



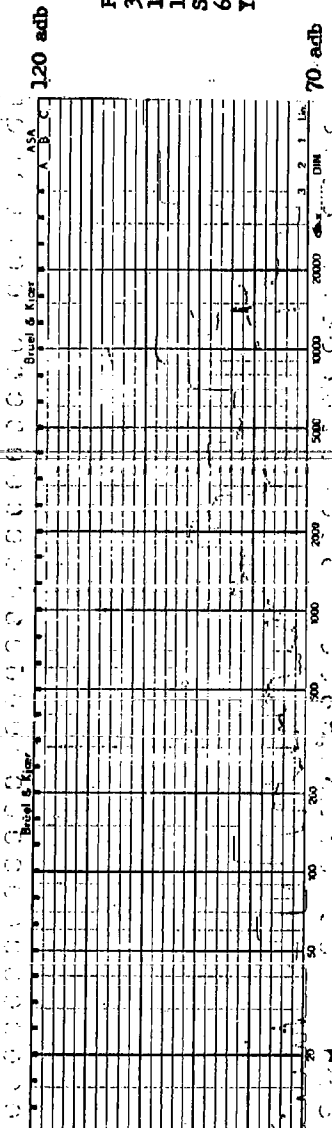
Preload Amount Test
 3 HP 2 Pole
 184 Frame Open
 16 May 1960
 Structureborne
 50 Mils 14.5 lbs.
 Y-Axis



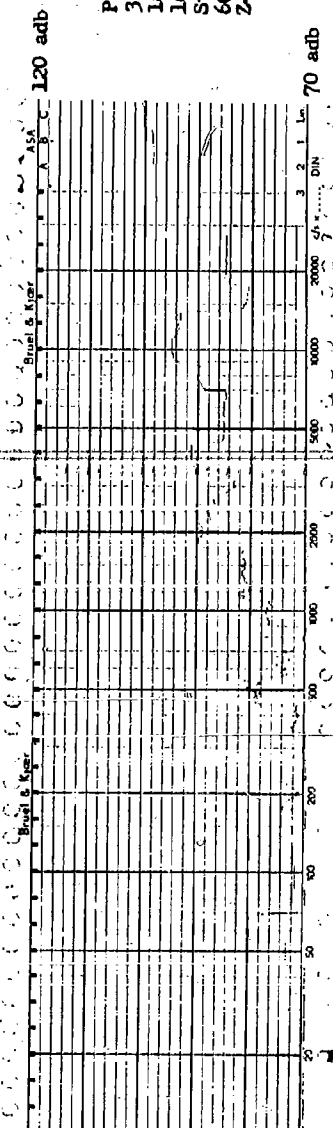
Preload Amount Test
 3 HP 2 Pole
 184 Frame Open
 16 May 1960
 Structureborne
 50 Mils 14.5 lbs.
 Z-Axis



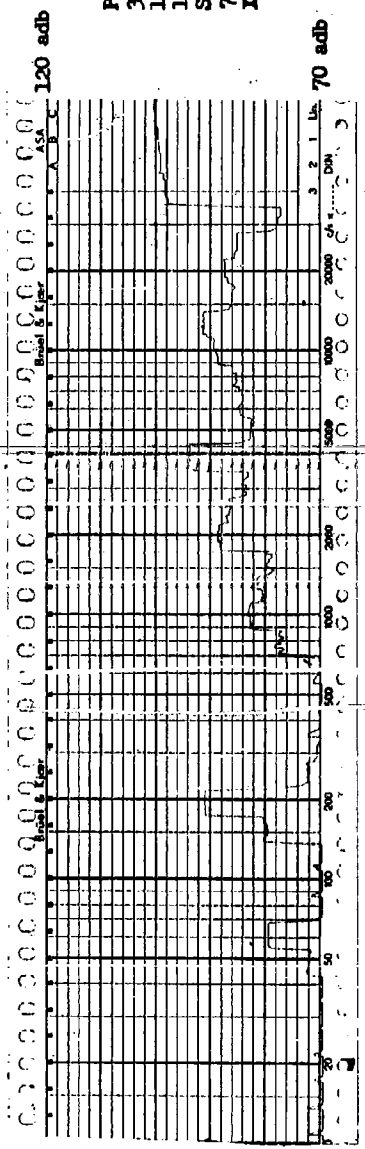
Preload Amount Test
 3 HP 2 Pole
 184 Frame Open
 16 May 1960
 Structureborne
 60 Mills 16.5 lbs.
 X-Axis



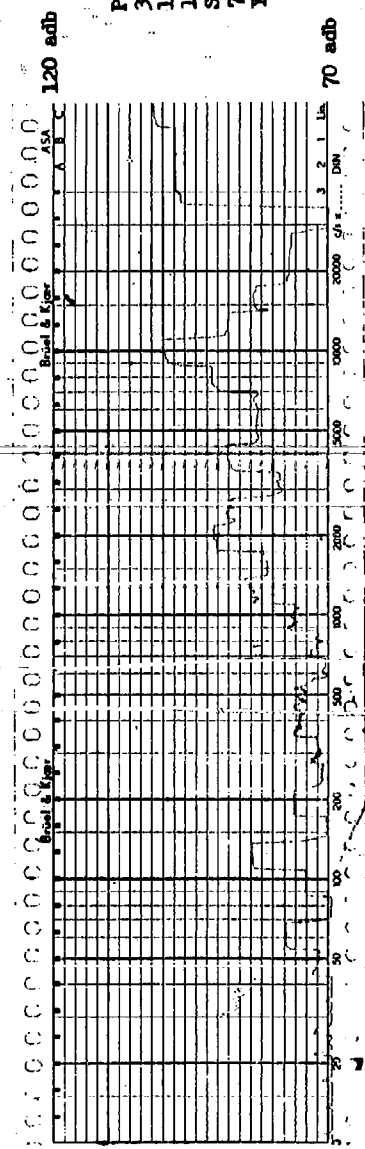
Preload Amount Test
 3 HP 2 Pole
 184 Frame Open
 16 May 1960
 Structureborne
 60 Mills 16.5 lbs.
 Y-Axis



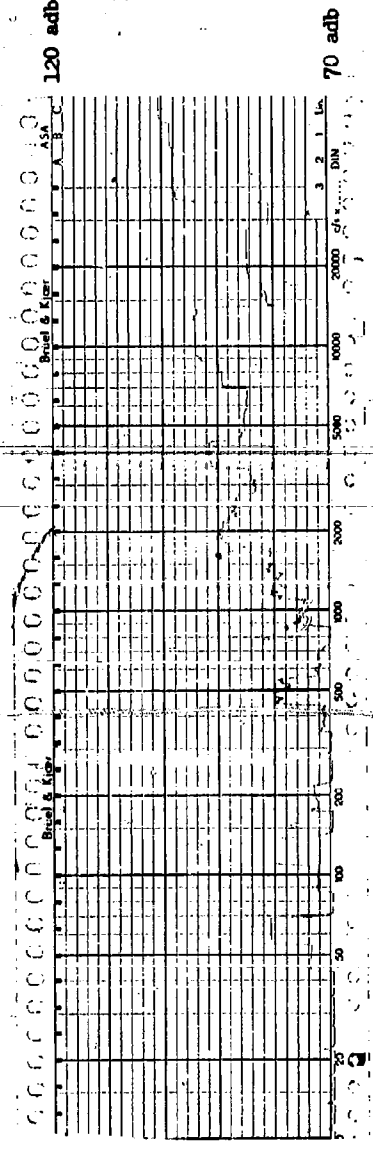
Preload Amount Test
 3 HP 2 Pole
 184 Frame Open
 16 May 1960
 Structureborne
 60 Mills 16.5 lbs.
 Z-Axis



Preload Amount Test
 3 HP 2 Pole
 184, Frame Open
 16 May 1960
 Structureborne
 70 Mils 19.5 lbs.
 Y-Axis

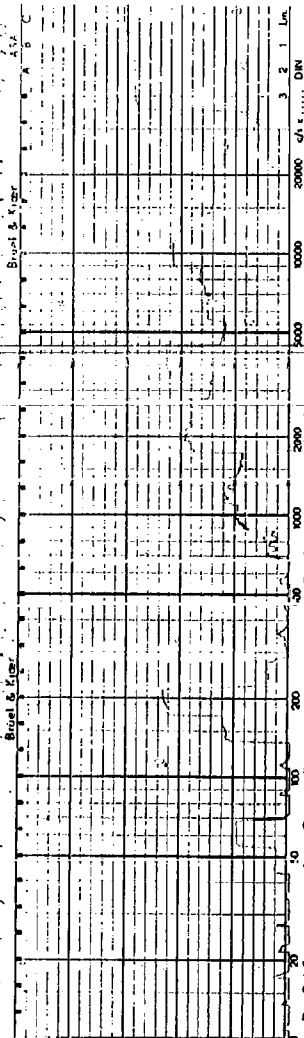


Preload Amount Test
 3 HP 2 Pole
 184, Frame Open
 16 May 1960
 Structureborne
 70 Mils 19.5 lbs.
 Y-Axis



Preload Amount Test
 3 HP 2 Pole
 184, Frame Open
 16 May 1960
 Structureborne
 70 Mils 19.5 lbs.
 Z-Axis

L20 adb

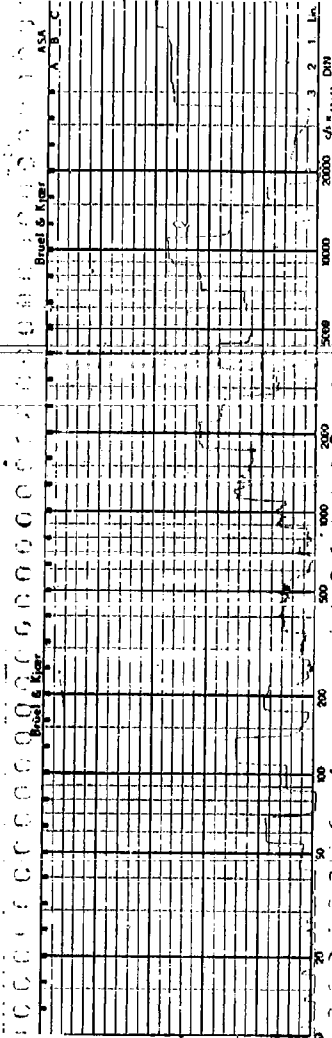


Preload Amount Test

3 HP 2 Pole
184, Frame Open
16 May 1960
Structureborne
80 Mils 21.5 lbs.
X-Axis

70 adb

L20 adb

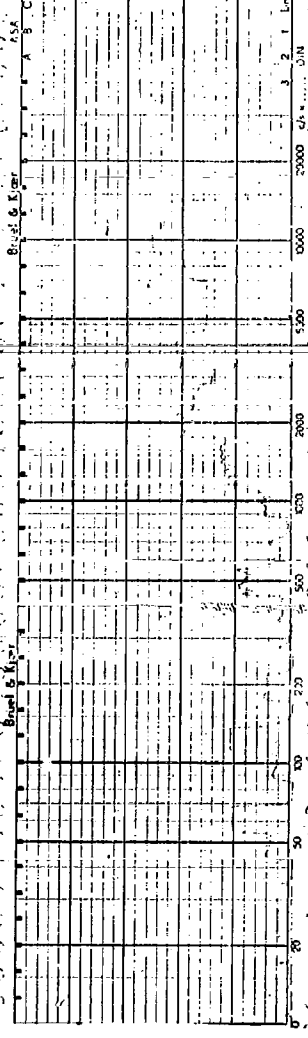


Preload Amount Test

3 HP 2 Pole
184, Frame Open
16 May 1960
Structureborne
80 Mils 21.5 lbs.
Y-Axis

70 adb

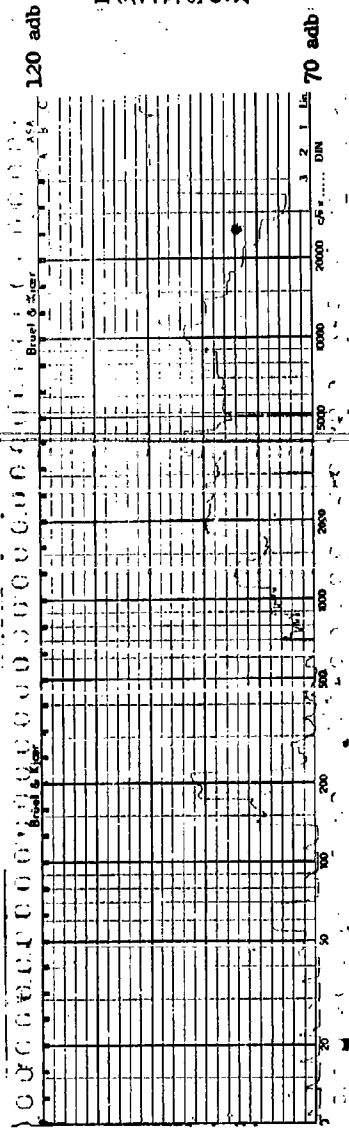
L20 adb



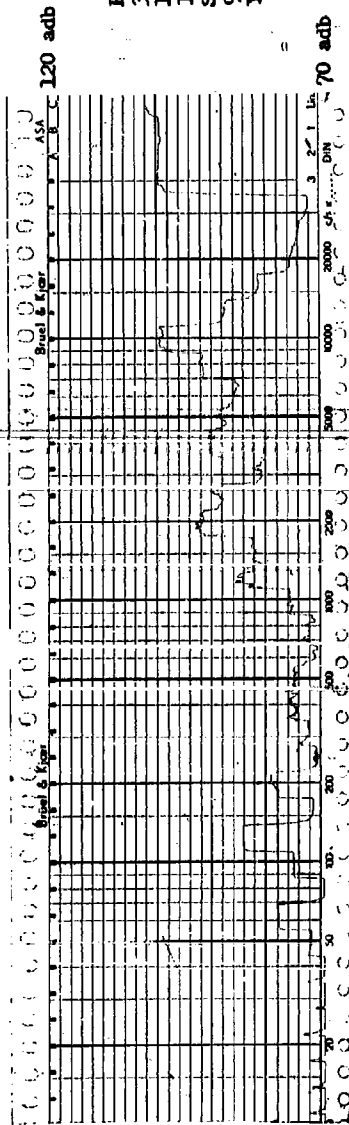
Preload Amount Test

3 HP 2 Pole
184, Frame Open
16 May 1960
Structureborne
80 Mils 21.5 lbs.
Z-Axis

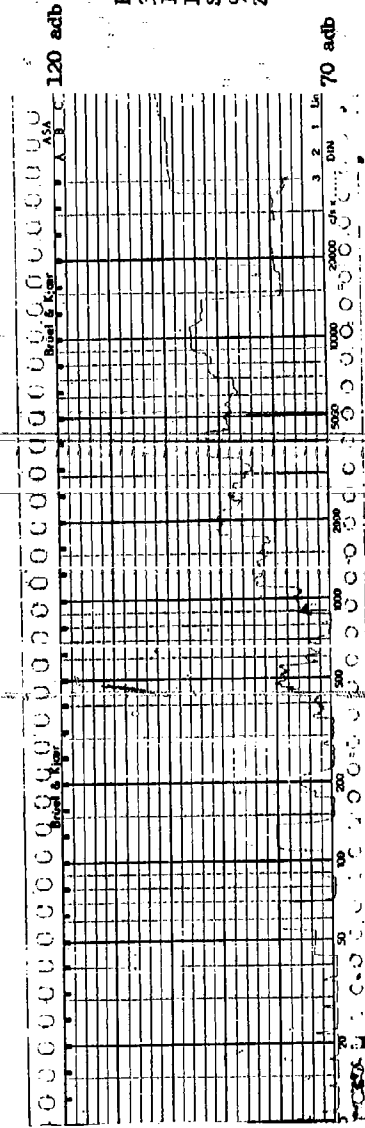
70 adb



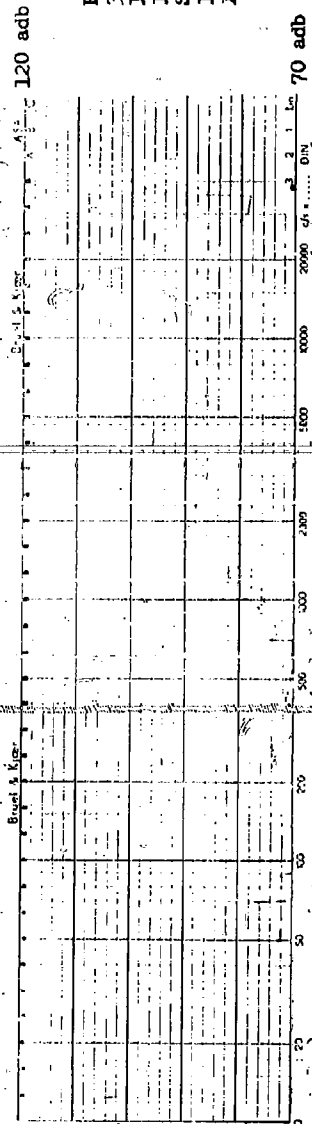
Preload Amount Test
3 HP 2 Pole
184 Frame Open
16 May 1960
Structureborne
90 Mils 24 lbs.
X-Axis



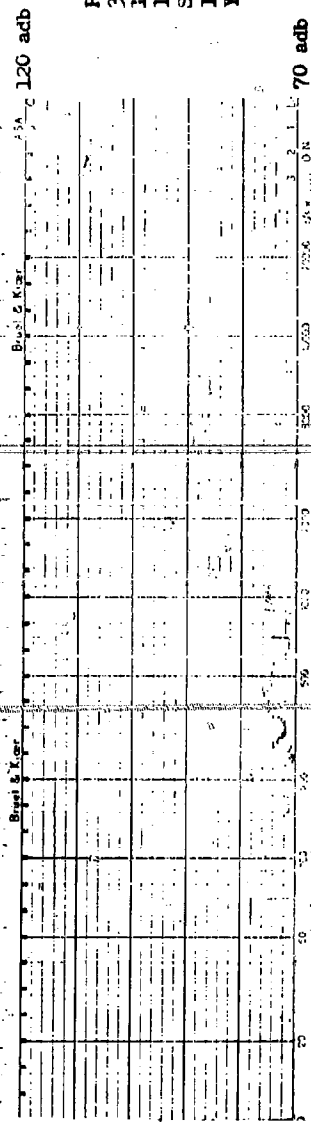
Preload Amount Test
3 HP 2 Pole
184 Frame Open
16 May 1960
Structureborne
90 Mils 24 lbs.
Y-Axis



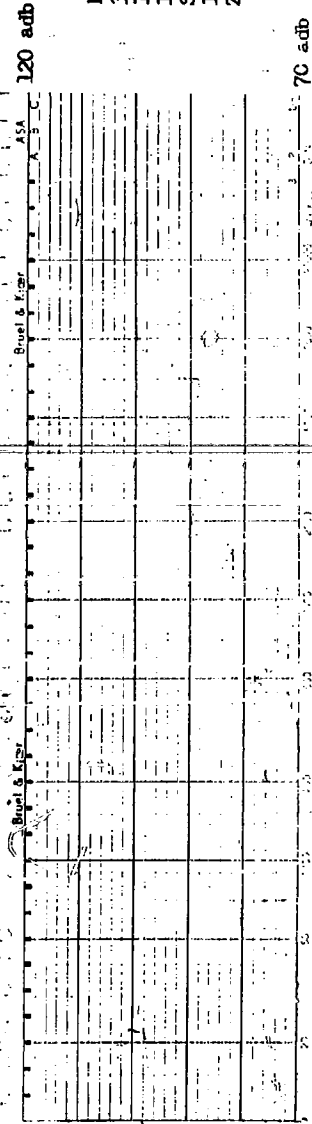
Preload Amount Test
3 HP 2 Pole
184 Frame Open
16 May 1960
Structureborne
90 Mils 24 lbs.
Z-Axis



Preload Amount Test
 3 HP 2 Pole
 184 Frame Open
 16 May 1960
 Structureborne
 100 Mils 26.5 lbs.
 X-Axis



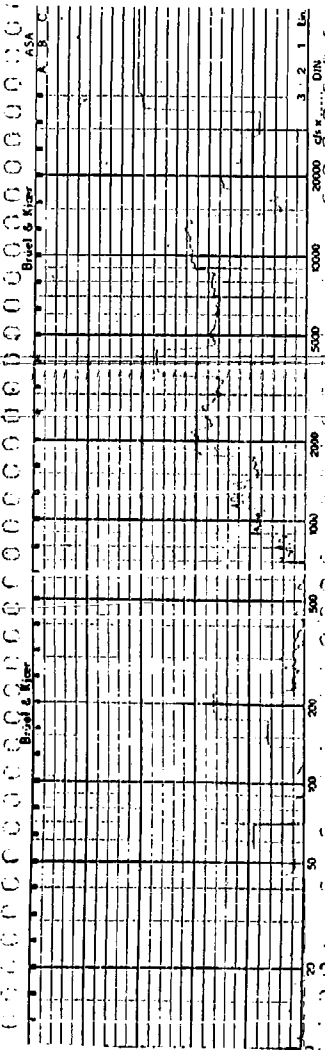
Preload Amount Test
 3 HP 2 Pole
 184 Frame Open
 16 May 1960
 Structureborne
 100 Mils 26.5 lbs.
 Y-Axis



Preload Amount Test
 3 HP 2 Pole
 184 Frame Open
 16 May 1960
 Structureborne
 100 Mils 26.5 lbs.
 Z-Axis

120 adb

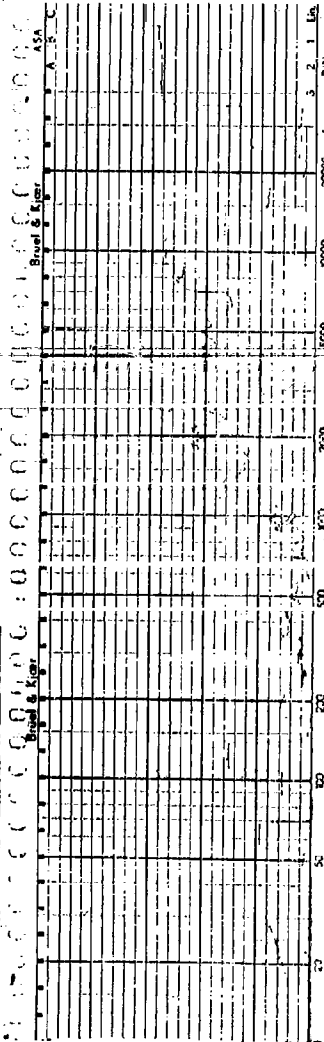
Preload Amount Test
3 HP 2 Pole
184, Frame Open
16 May 1960
Structureborne
110 Mills 29.5 lbs.
X-Axis



70 adb

120 adb

Preload Amount Test
3 HP 2 Pole
184, Frame Open
16 May 1960
Structureborne
110 Mills 29.5 lbs.
Y-Axis



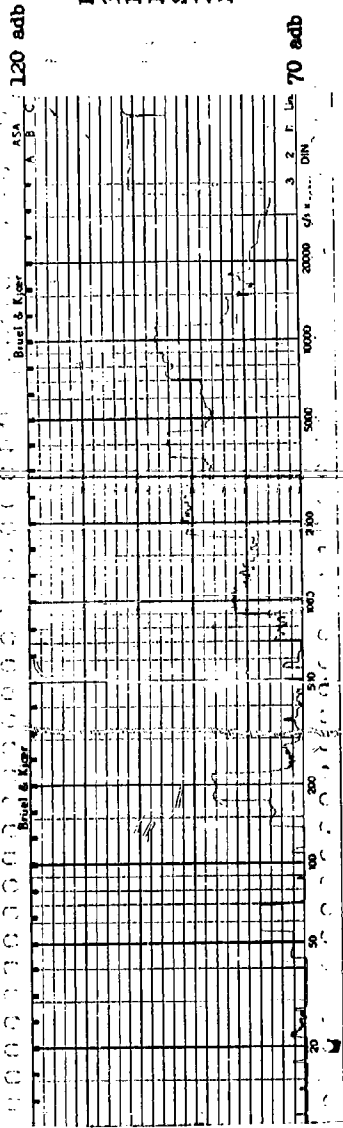
70 adb

120 adb

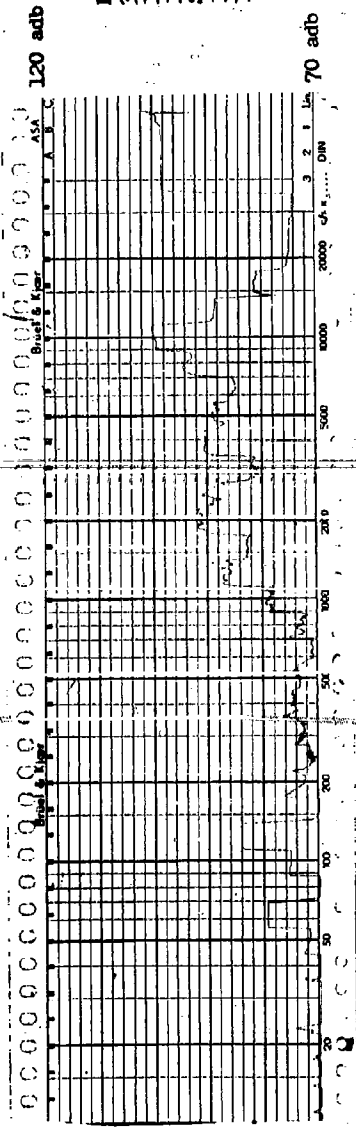
Preload Amount Test
3 HP 2 Pole
184, Frame Open
16 May 1960
Structureborne
110 Mills 29.5 lbs.
Z-Axis



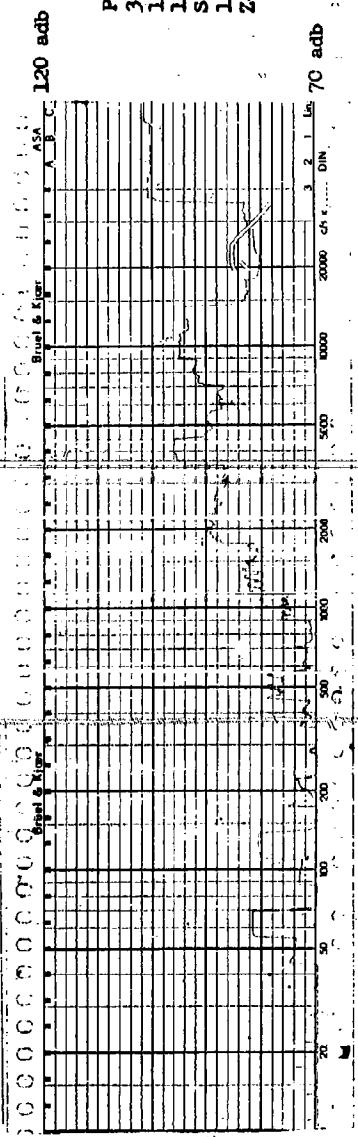
70 adb



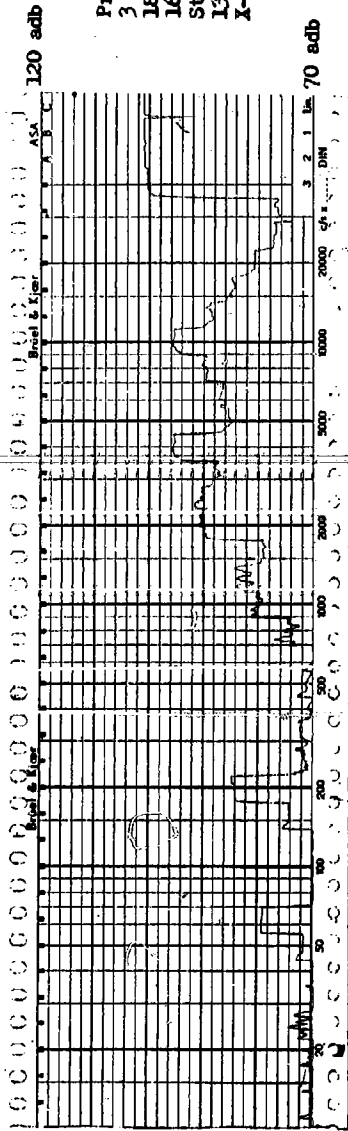
Preload Amount Test
 3 HP 2 Pole
 184 Frame Open
 16 May 1960
 Structureborne
 120 Mils 32 lbs.
 X-Axis



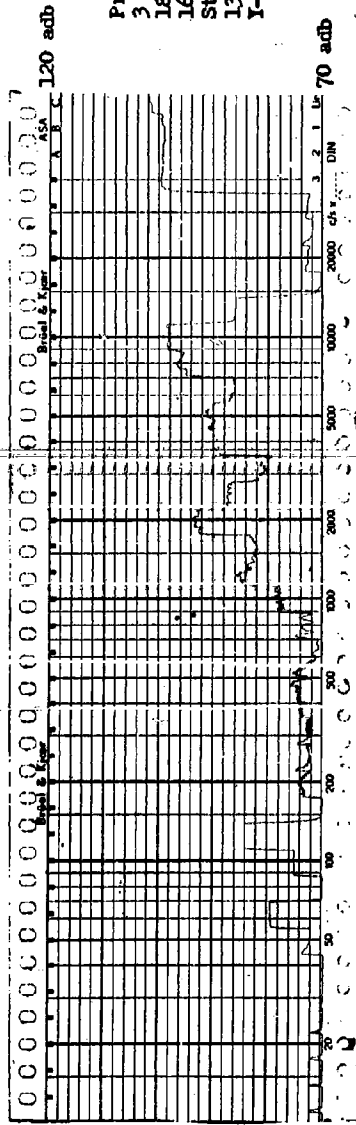
Preload Amount Test
 3 HP 2 Pole
 184 Frame Open
 16 May 1960
 Structureborne
 120 Mils 32 lbs.
 Y-Axis



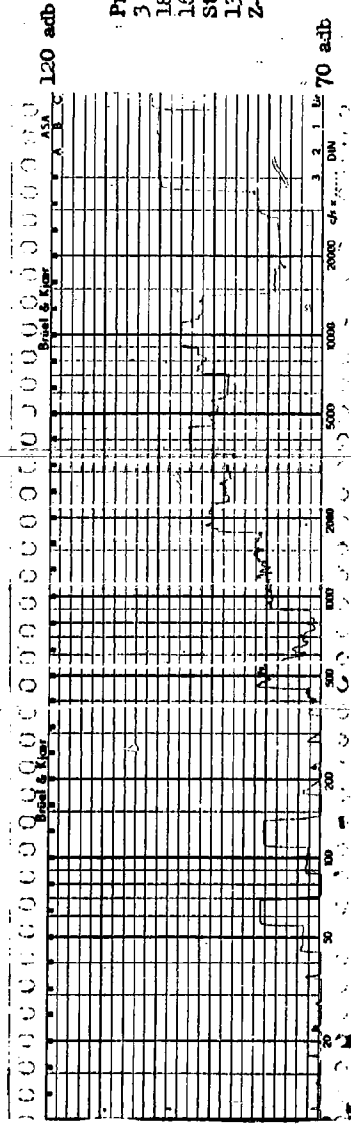
Preload Amount Test
 3 HP 2 Pole
 184 Frame Open
 16 May 1960
 Structureborne
 120 Mils 32 lbs.
 Z-Axis



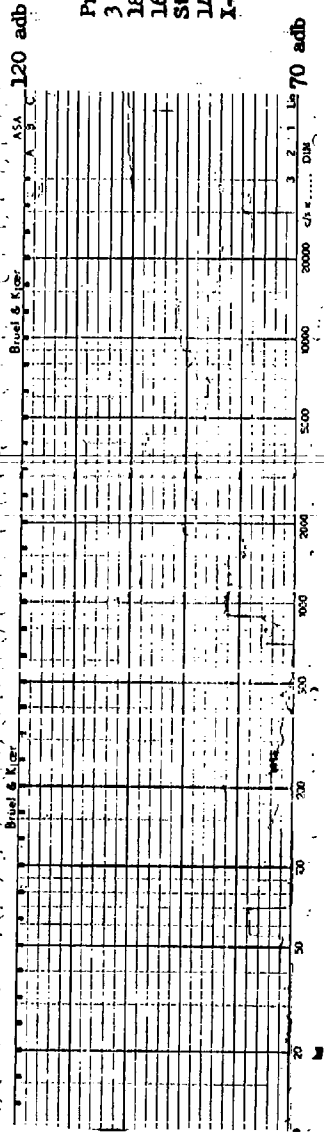
Preload Amount Test
 3 HP 2 Pole
 184 Frame Open
 16 May 1960
 Structureborne
 130 Mills 35.5 lbs.
 X-Axis



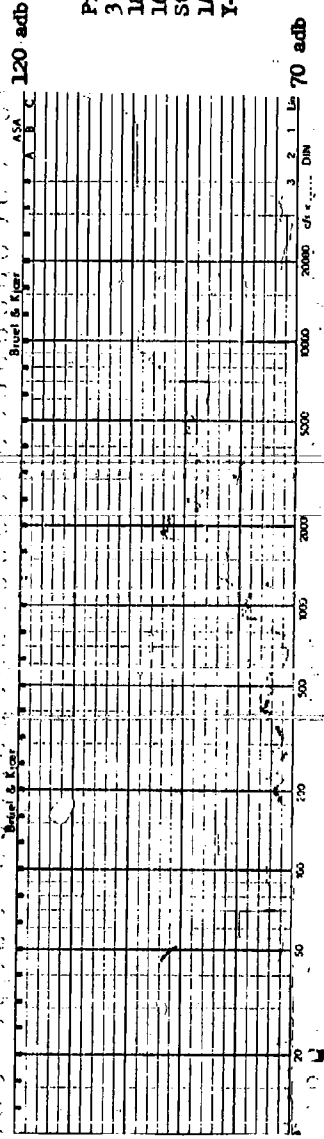
Preload Amount Test
 3 HP 2 Pole
 184 Frame Open
 16 May 1960
 Structureborne
 130 Mills 35.5 lbs.
 Y-Axis



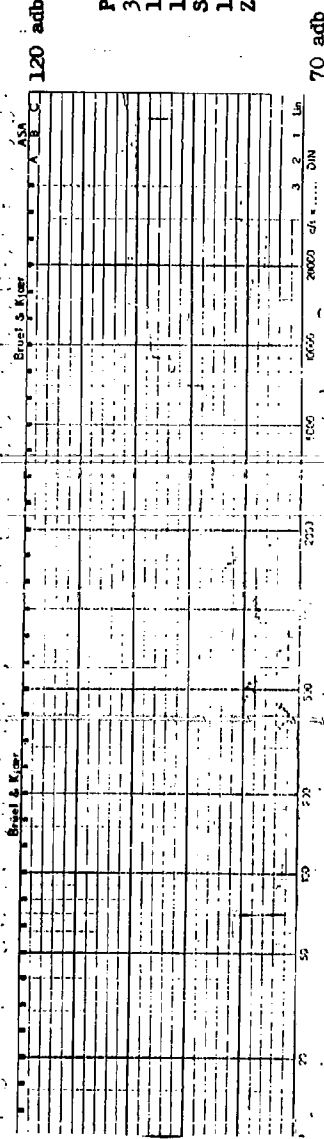
Preload Amount Test
 3 HP 2 Pole
 184 Frame Open
 16 May 1960
 Structureborne
 130 Mills 35.5 lbs.
 Z-Axis



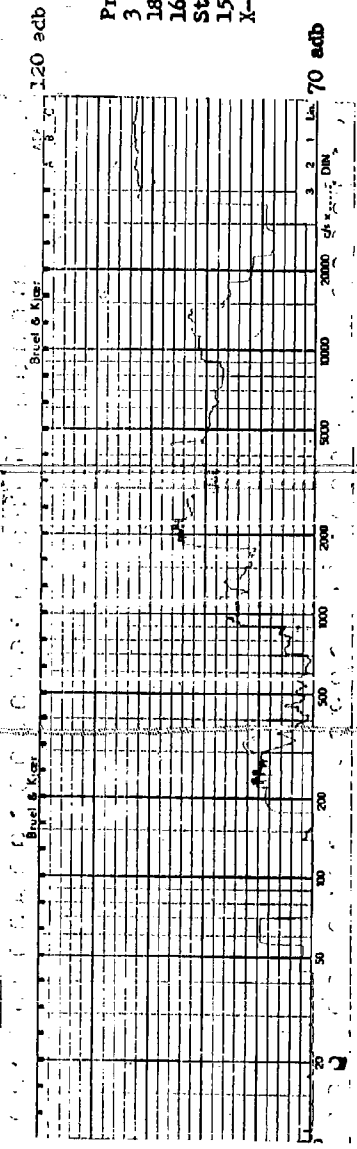
Preload Amount Test
 3 HP 2 Pole
 184 Frame Open
 16 May 1960
 Structureborne
 140 Mils 44.5 lbs.
 X-Axis



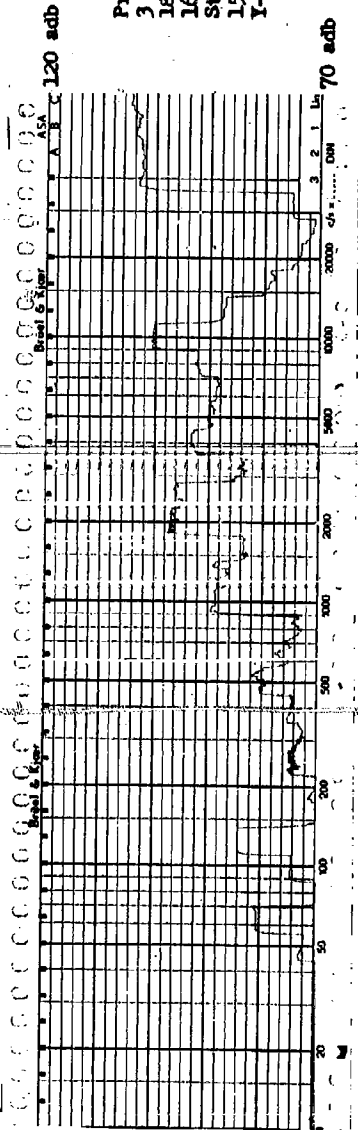
Preload Amount Test
 3 HP 2 Pole
 184 Frame Open
 16 May 1960
 Structureborne
 140 Mils 44.5 lbs.
 Y-Axis



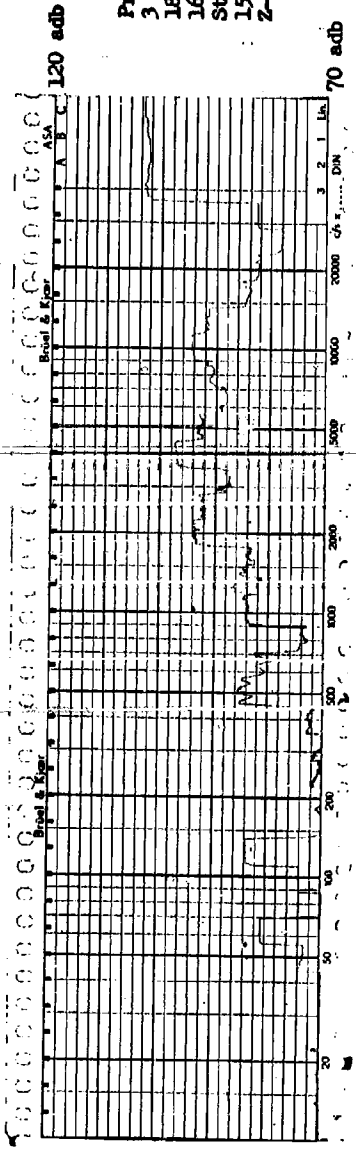
Preload Amount Test
 3 HP 2 Pole
 184 Frame Open
 16 May 1960
 Structureborne
 140 Mils 44.5 lbs.
 Z-Axis



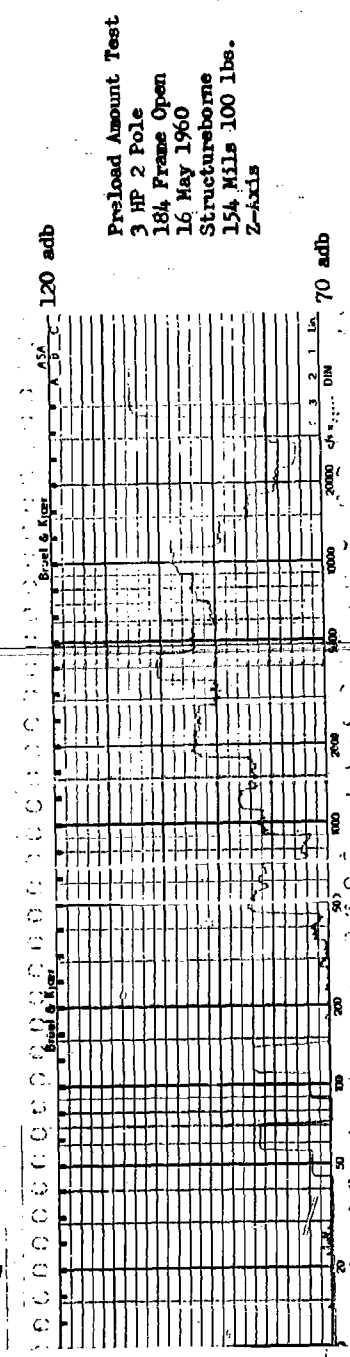
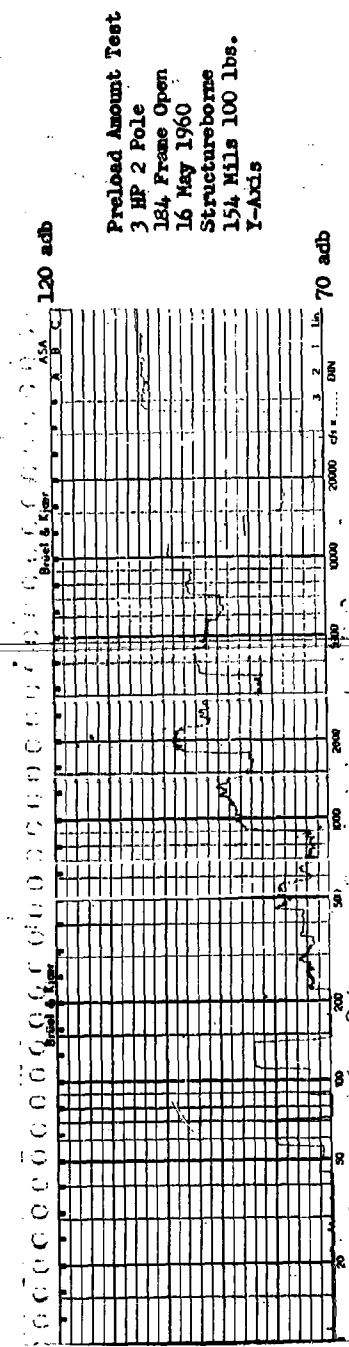
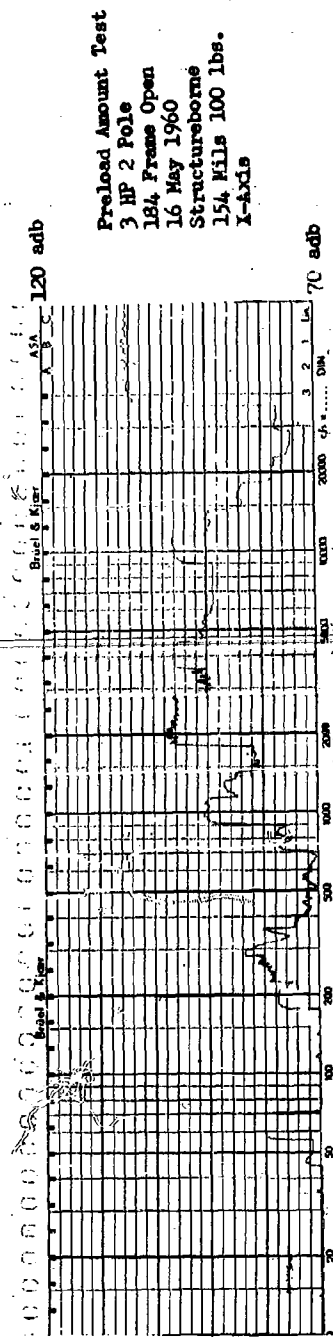
Preload Amount Test
 3 HP 2 Pole
 184 Frame Open
 16 May 1960
 Structureborne
 150 Mils 65 lbs.
 X-Axis

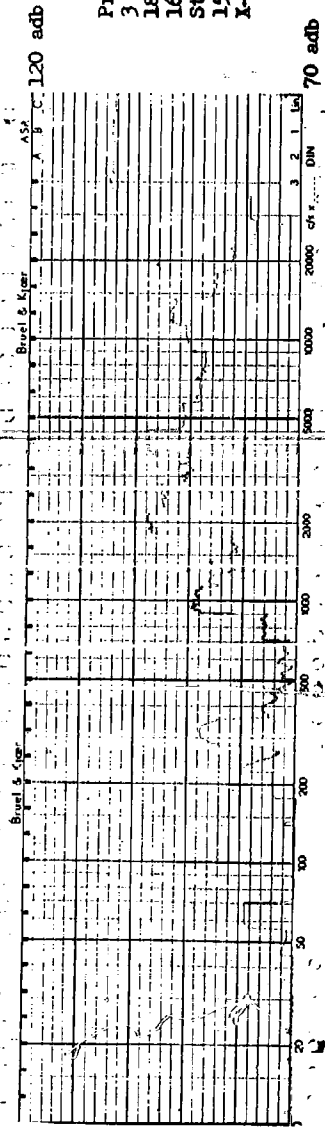


Preload Amount Test
 3 HP 2 Pole
 184 Frame Open
 16 May 1960
 Structureborne
 150 Mils 65 lbs.
 Y-Axis

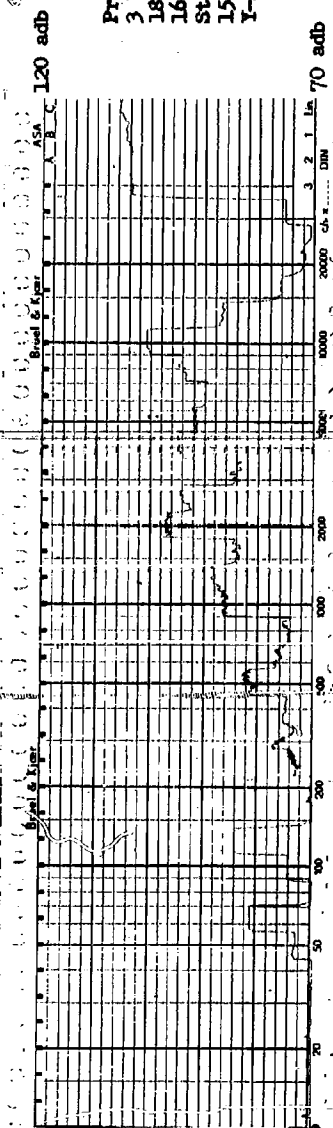


Preload Amount Test
 3 HP 2 Pole
 184 Frame Open
 16 May 1960
 Structureborne
 150 Mils 65 lbs.
 Z-Axis

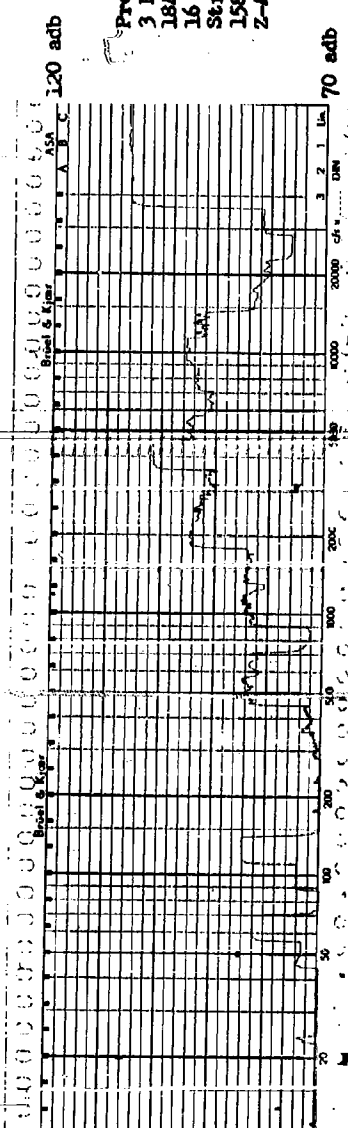




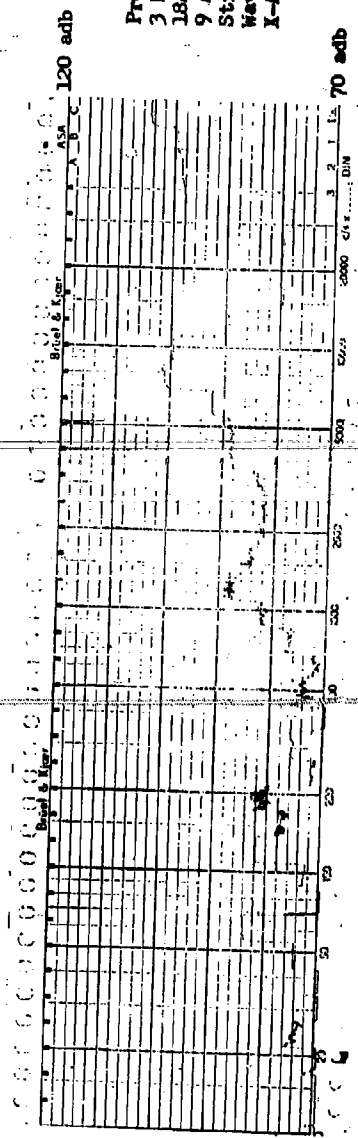
Preload Amount Test
 3 HP 2 Pole
 184, Frame Open
 16 May 1960
 Structureborne
 158 Mils 155 lbs.
 X-Axis



Preload Amount Test
 3 HP 2 Pole
 184, Frame Open
 16 May 1960
 Structureborne
 158 Mils 155 lbs.
 Y-Axis



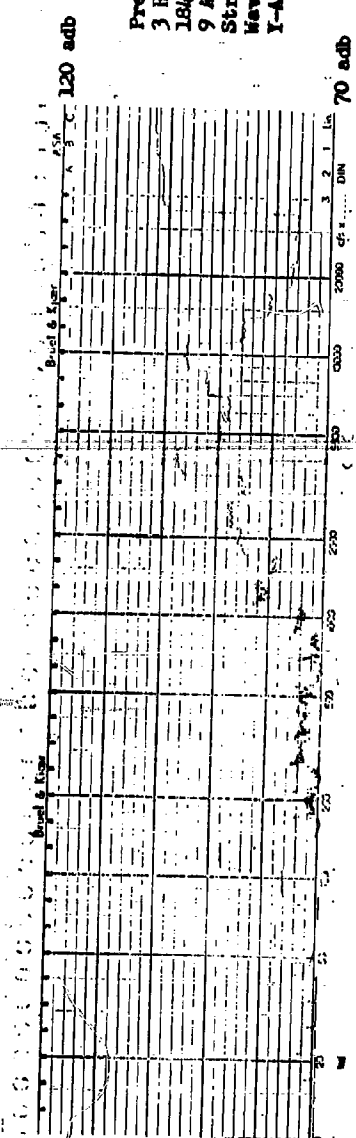
Preload Amount Test
 3 HP 2 Pole
 184, Frame Open
 16 May 1960
 Structureborne
 158 Mils 155 lbs.
 Z-Axis



120 adb

70 adb

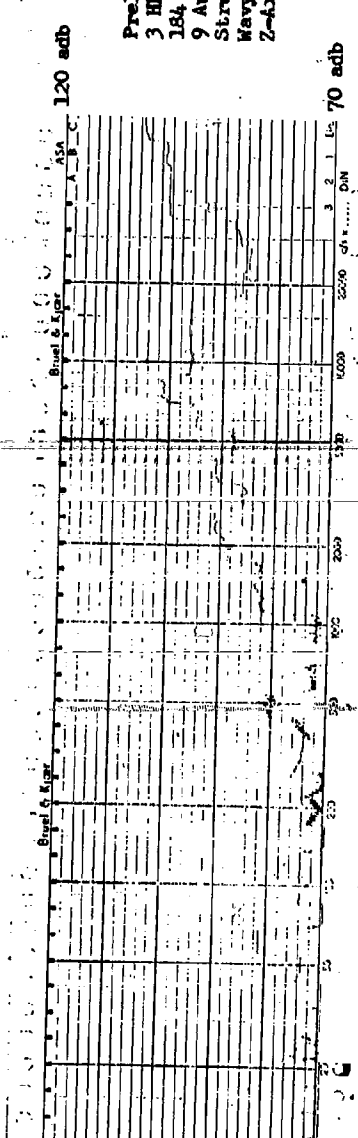
Preload Type Test
 3 HP 2 Pole
 184 Frame Open
 9 August 1960
 Structureborne
 Navy Spring Washer
 X-Axis



120 adb

70 adb

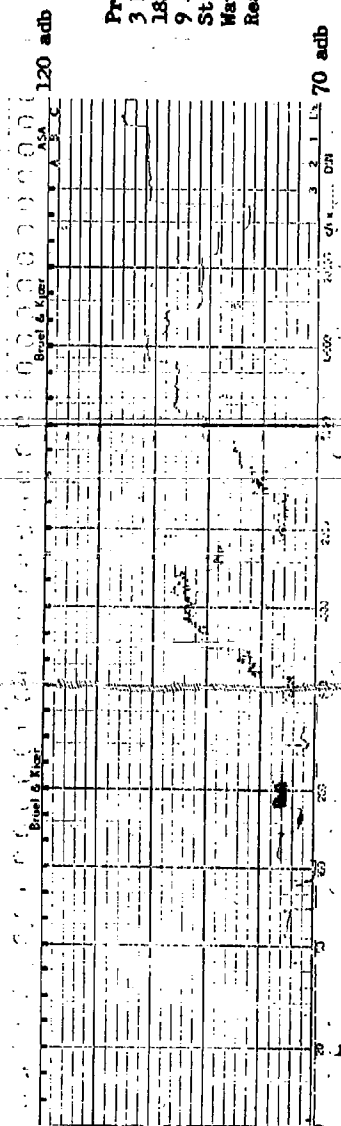
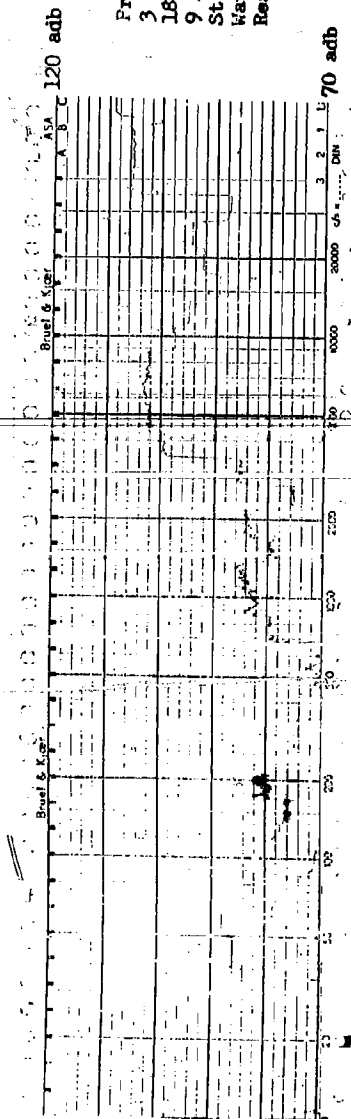
Preload Type Test
 3 HP 2 Pole
 184 Frame Open
 9 August 1960
 Structureborne
 Navy Spring Washer
 X-Axis

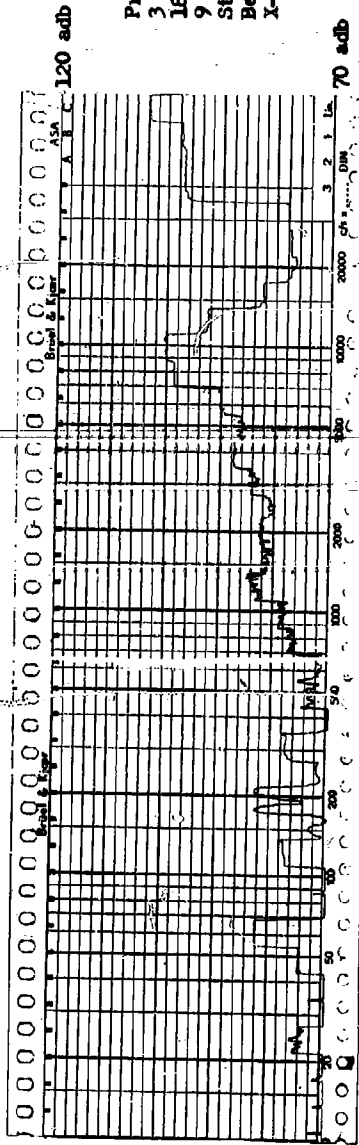


120 adb

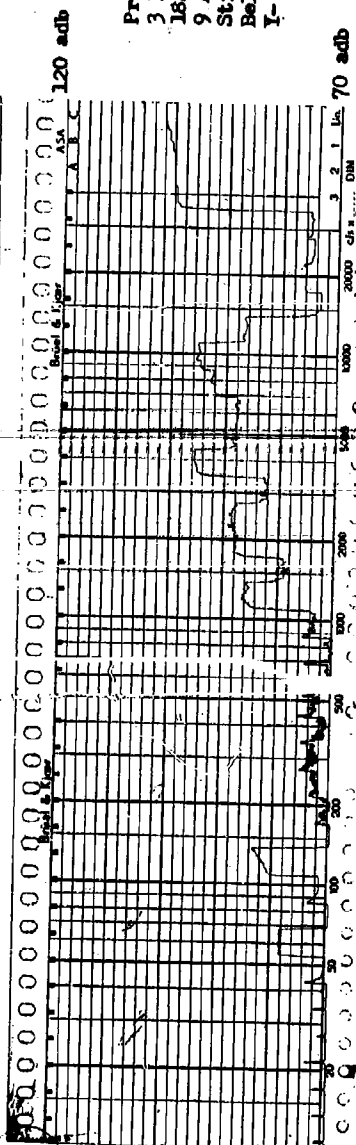
70 adb

Preload Type Test
 3 HP 2 Pole
 184 Frame Open
 9 August 1960
 Structureborne
 Navy Spring Washer
 Z-Axis

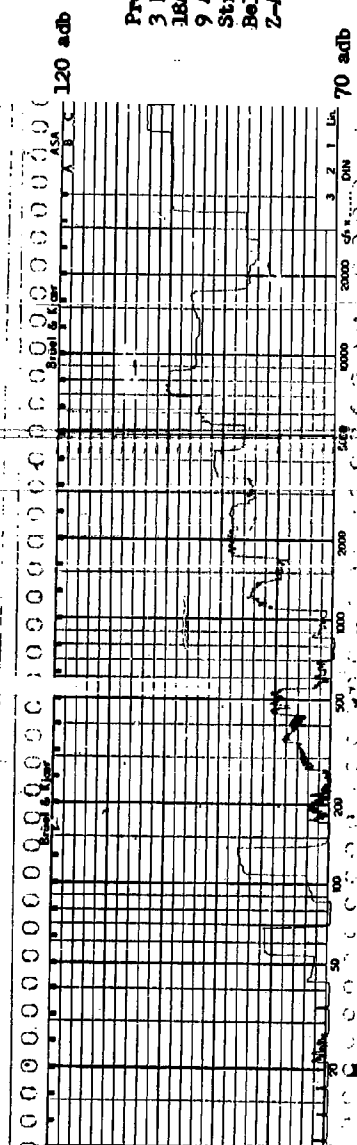




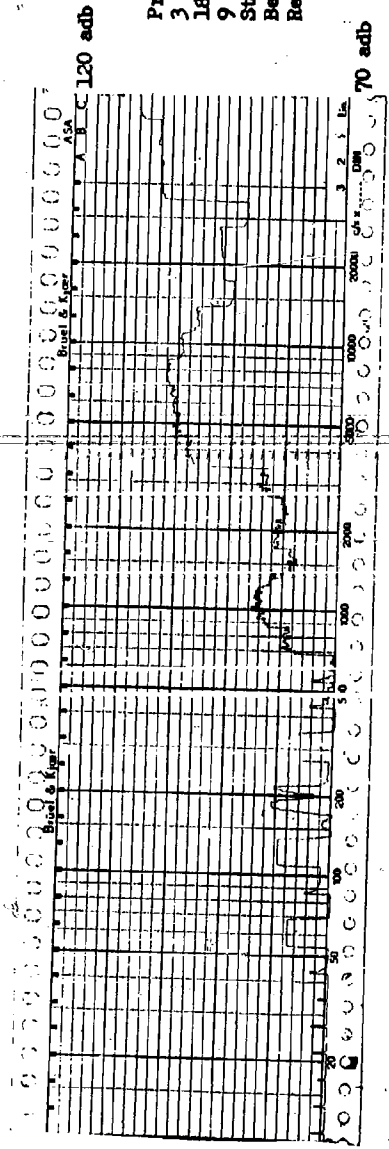
Preload Type Test
 3 HP 2 Pole
 184 Frame Open
 9 August 1960
 Structureborne
 Belleville Washer
 X-Axis



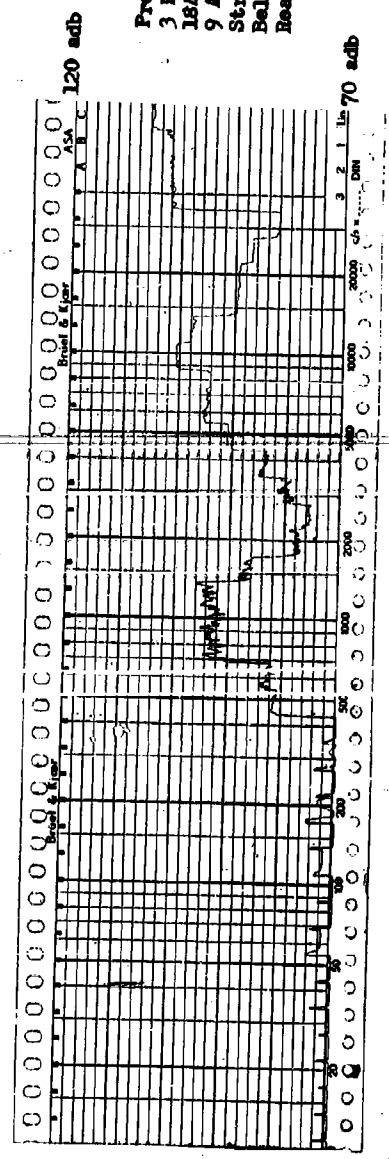
Preload Type Test
 3 HP 2 Pole
 184 Frame Open
 9 August 1960
 Structureborne
 Belleville Washer
 Y-Axis



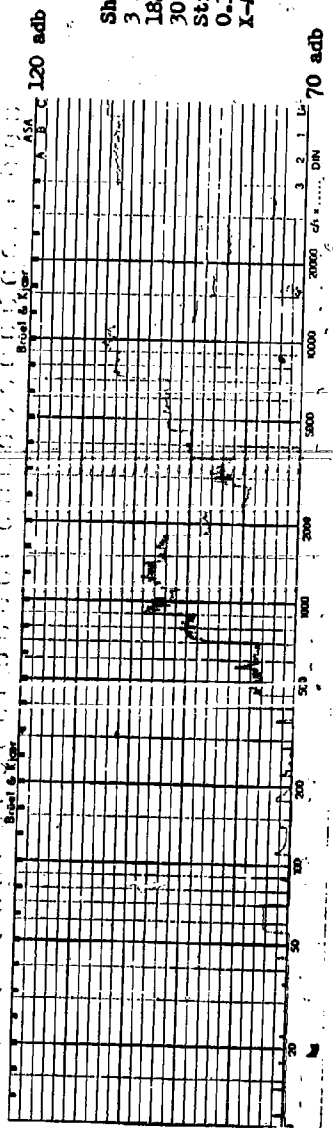
Preload Type Test
 3 HP 2 Pole
 184 Frame Open
 9 August 1960
 Structureborne
 Belleville Washer
 Z-Axis



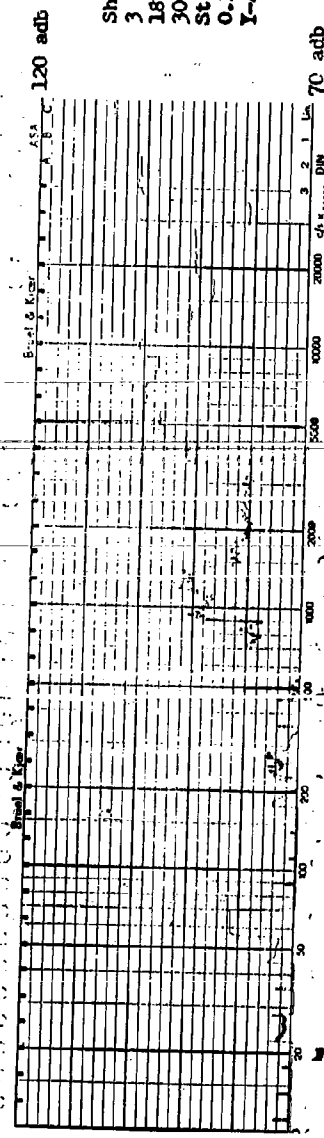
Preload Type Test
 3 HP 2 Pole
 184 Frame Open
 9 August 1960
 Structureborns
 Belleville Washer
 Rear Erg. Hsg.



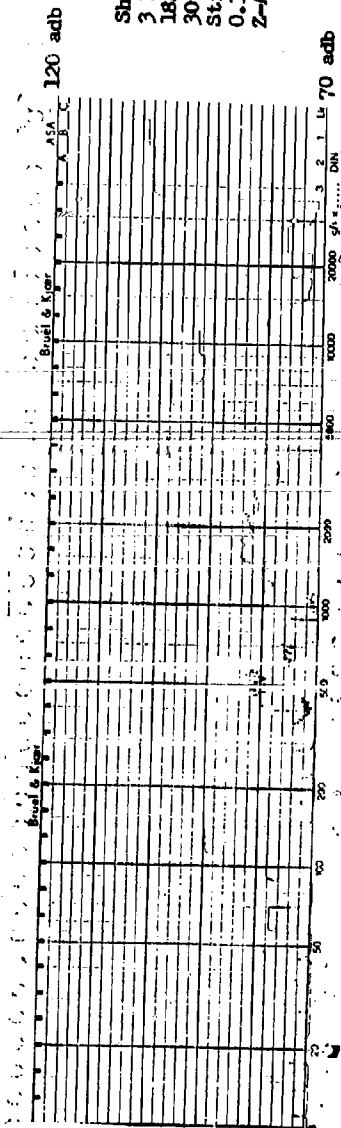
Preload Type Test
 3 HP 2 Pole
 184 Frame Open
 9 August 1960
 Structureborns
 Belleville Washer
 Rear Bearing



Shaft Bearing Fit
 3 HP 2 Pole
 184 Frame Open
 30 June 1960
 Structureborne
 0.1 Mil Interference
 X-Axis

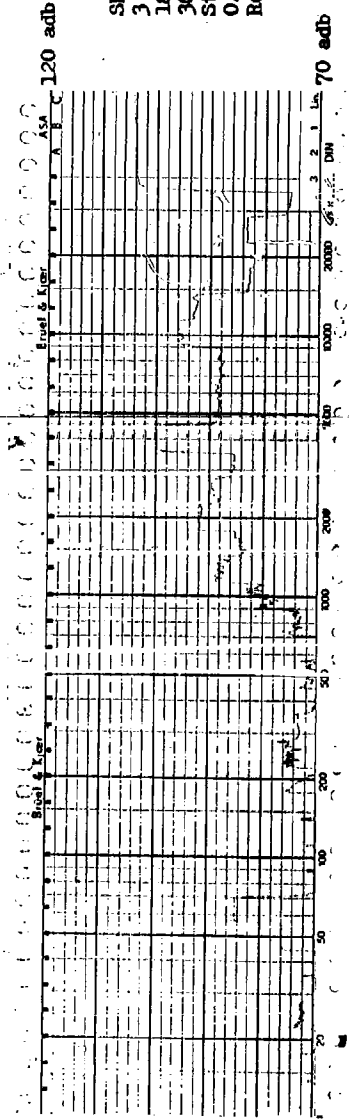


Shaft Bearing Fit
 3 HP 2 Pole
 184 Frame Open
 30 June 1960
 Structureborne
 0.1 Mil Interference
 Y-Axis

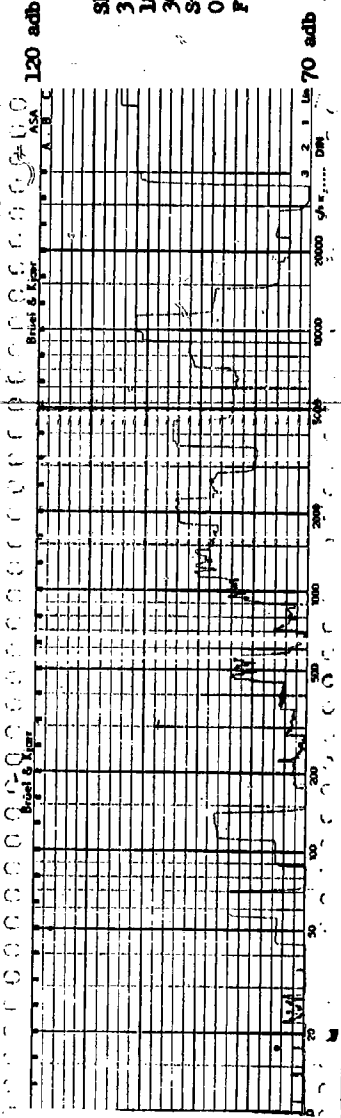


Shaft Bearing Fit
 3 HP 2 Pole
 184 Frame Open
 30 June 1960
 Structureborne
 0.1 Mil Interference
 Z-Axis

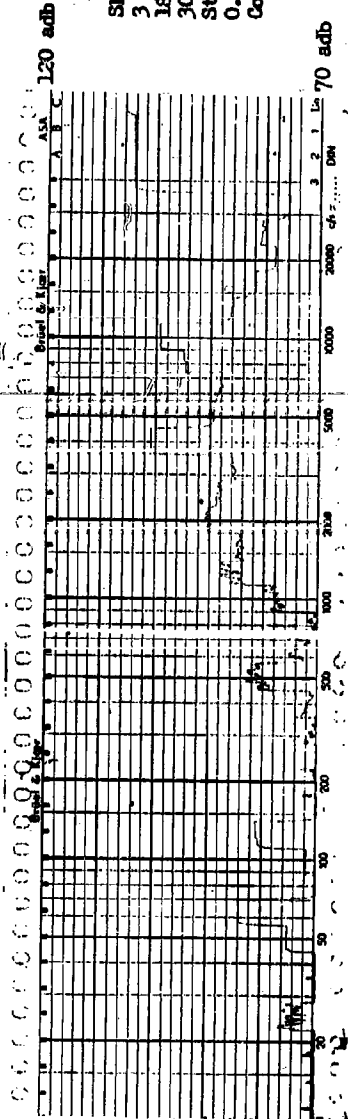
7-29



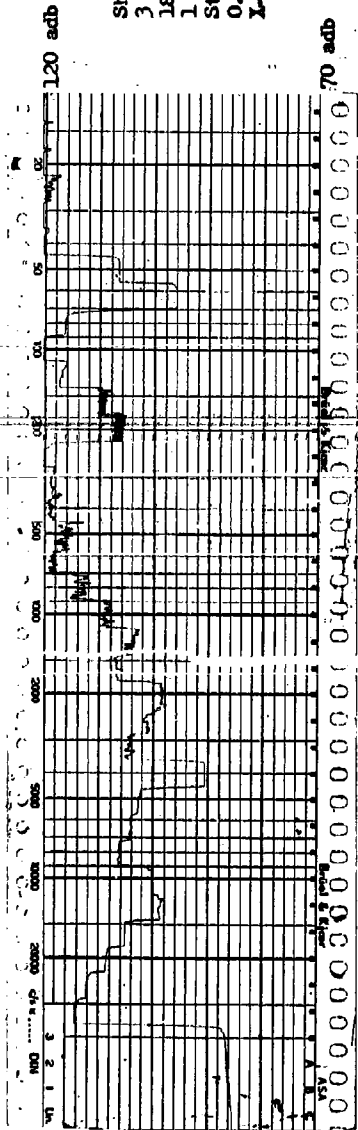
Shaft Bearing Fit
 3 HP 2 Poles
 184 Frame Open
 30 June 1960
 Structureborne
 0.1 Mil Interference
 Rear Bearing



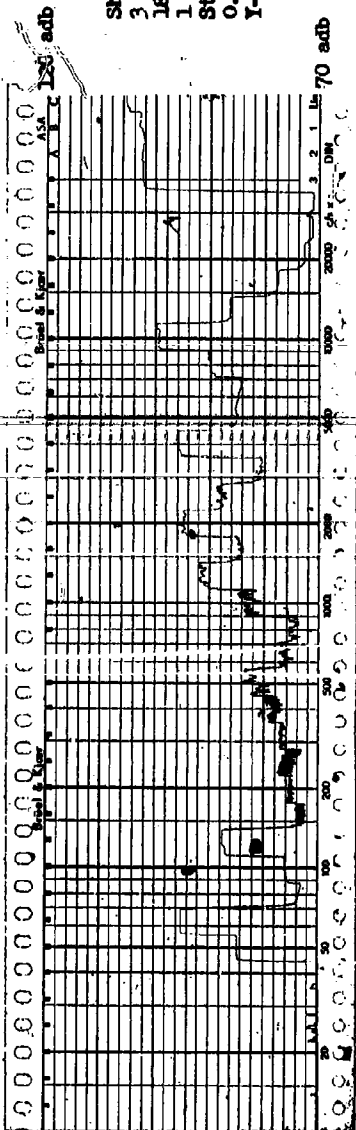
Shaft Bearing Fit
 3 HP 2 Poles
 184 Frame Open
 30 June 1960
 Structureborne
 0.1 Mil Interference
 Front Brg. Hsg.



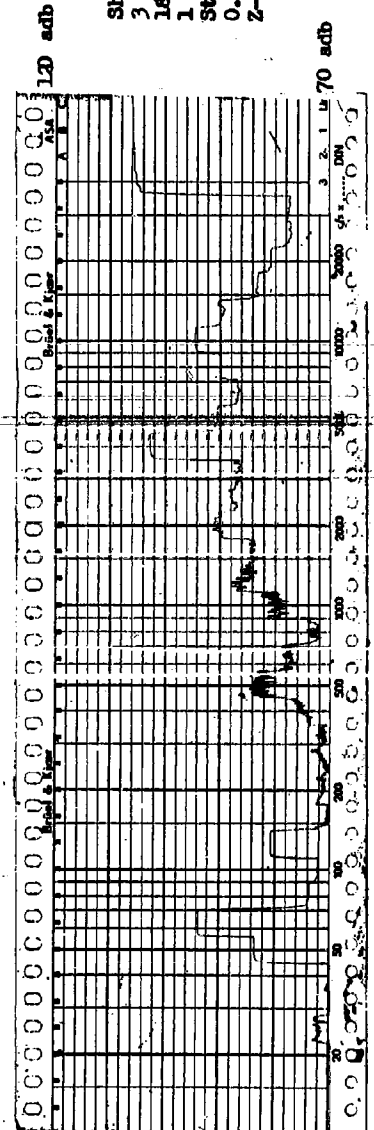
Shaft Bearing Fit
 3 HP 2 Poles
 184 Frame Open
 30 June 1960
 Structureborne
 0.1 Mil Interference
 Core



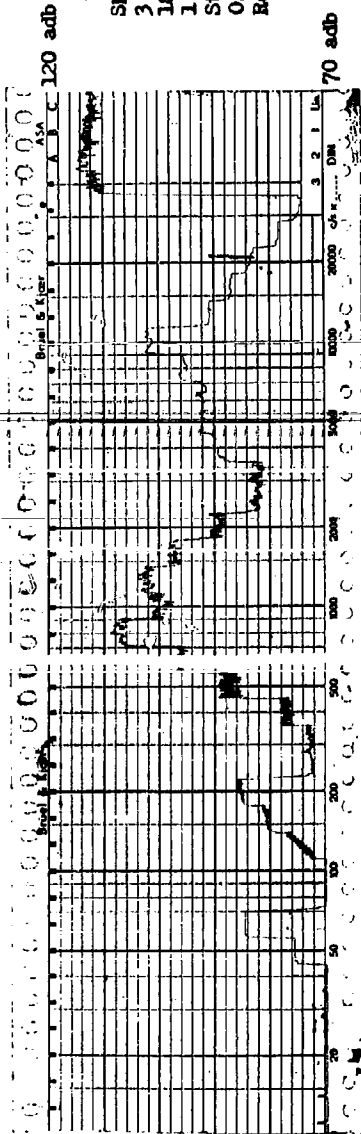
Shaft Bearing Fit
 3 HP 2 Pole
 184 Frame Open
 1 July 1960
 Structureborne
 0.6 Mil Interference
 X-Axis



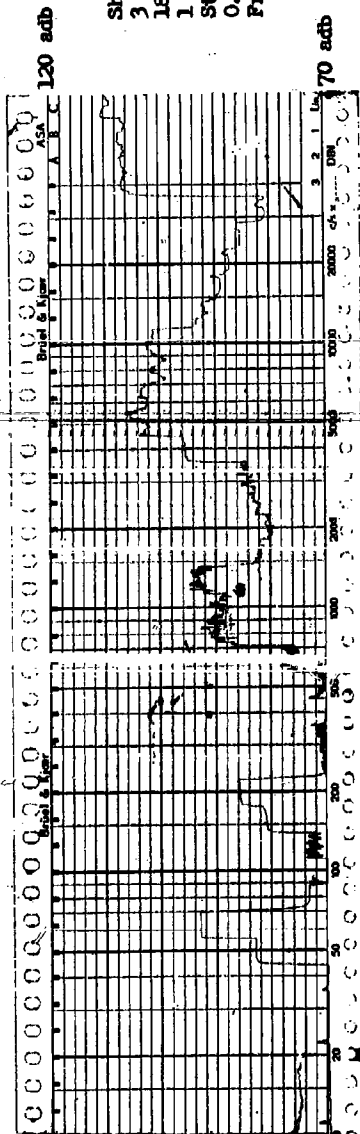
Shaft Bearing Fit
 3 HP 2 Pole
 184 Frame Open
 1 July 1960
 Structureborne
 0.6 Mil Interference
 Y-Axis



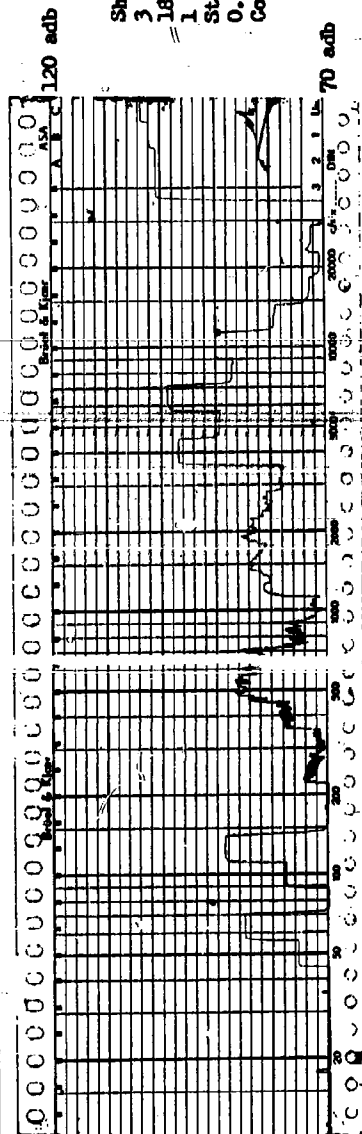
Shaft Bearing Fit
 3 HP 2 Pole
 184 Frame Open
 1 July 1960
 Structureborne
 0.6 Mil Interference
 Z-Axis



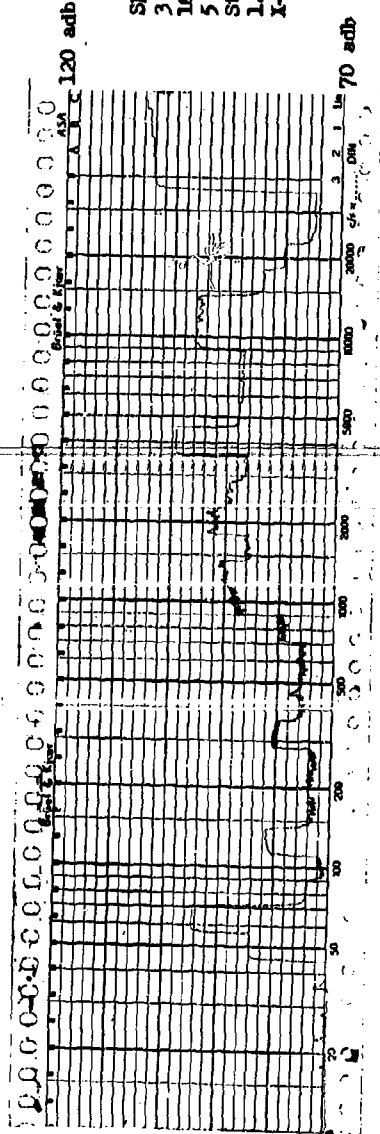
Shaft Bearing Fit
 3 HP 2 Pole
 184 Frame Open
 1 July 1960
 Structureborne
 0.6 Mill Interference
 Rear Bearing



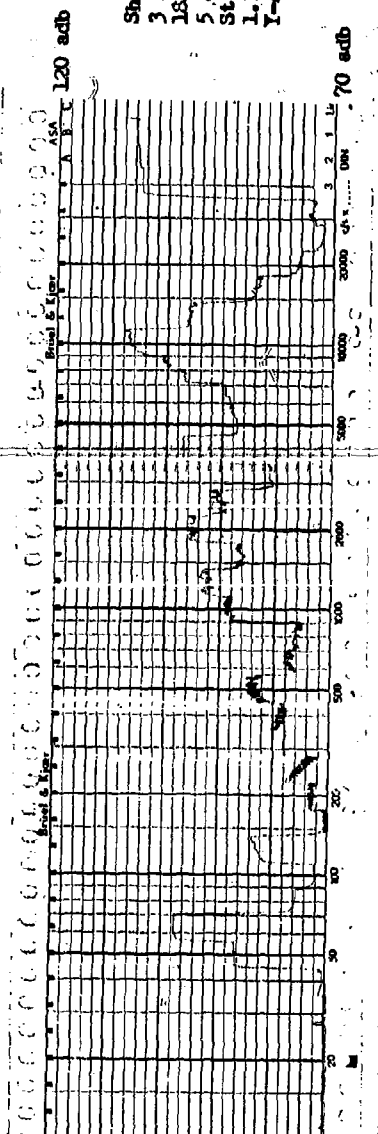
Shaft Bearing Fit
 3 HP 2 Pole
 184 Frame Open
 1 July 1960
 Structureborne
 0.6 Mill Interference
 Front Brg. Hsg.



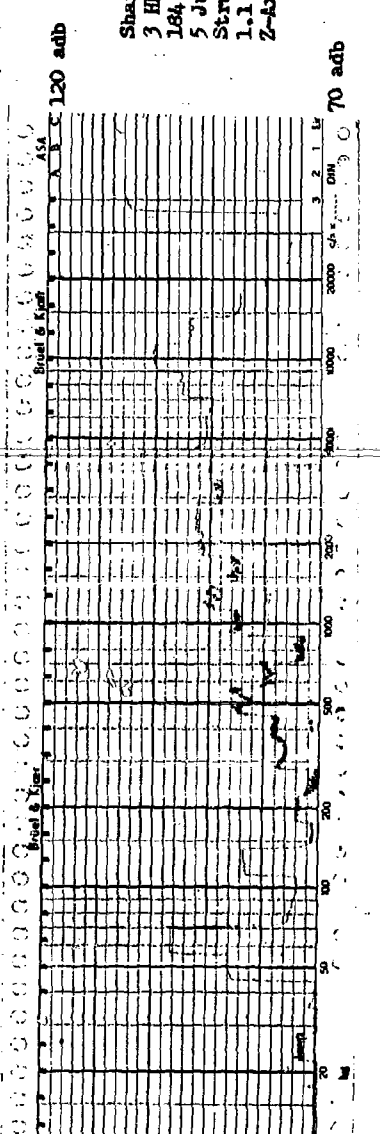
Shaft Bearing Fit
 3 HP 2 Pole
 184 Frame Open
 1 July 1960
 Structureborne
 0.6 Mill Interference
 Core



Shaft Bearing Fit
 3 HP 2 Pole
 184 Frame Open
 5 July 1960
 Structureborne
 1.1 Mil Interference
 X-axis

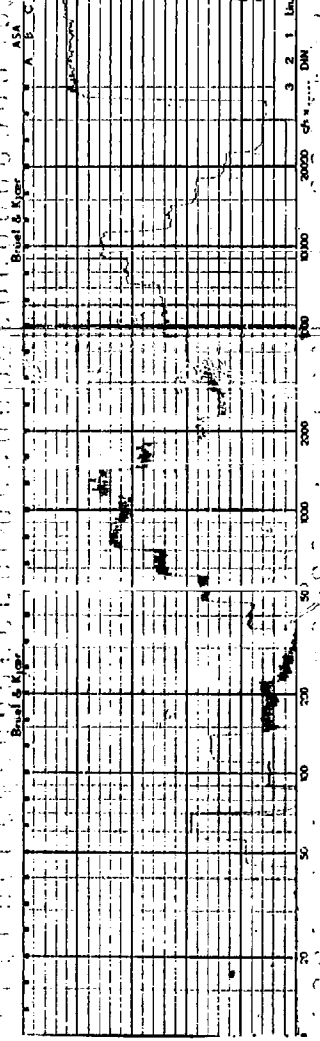


Shaft Bearing Fit
 3 HP 2 Pole
 184 Frame Open
 5 July 1960
 Structureborne
 1.1 Mil Interference
 Y-axis



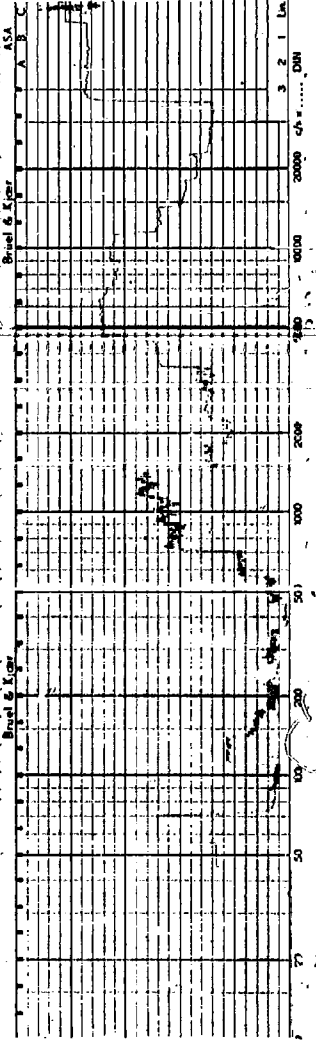
Shaft Bearing Fit
 3 HP 2 Pole
 184 Frame Open
 5 July 1960
 Structureborne
 1.1 Mil Interference
 Z-axis

120 adb



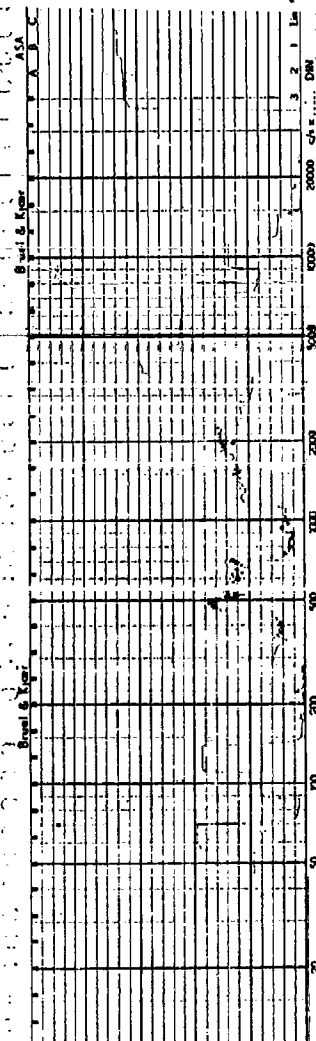
Shaft Bearing Fit
 3 HP 2 Pole
 184 Frame Open
 5 July 1960
 Structureborne
 1.1 Mil Interference
 Rear Bearing

120 adb

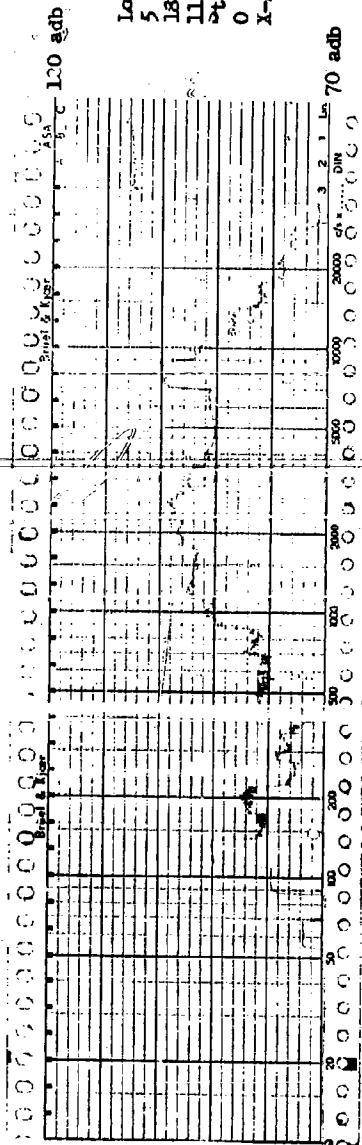


Shaft Bearing Fit
 3 HP 2 Pole
 184 Frame Open
 5 July 1960
 Structureborne
 1.1 Mil Interference
 Front Brg. Hsg.

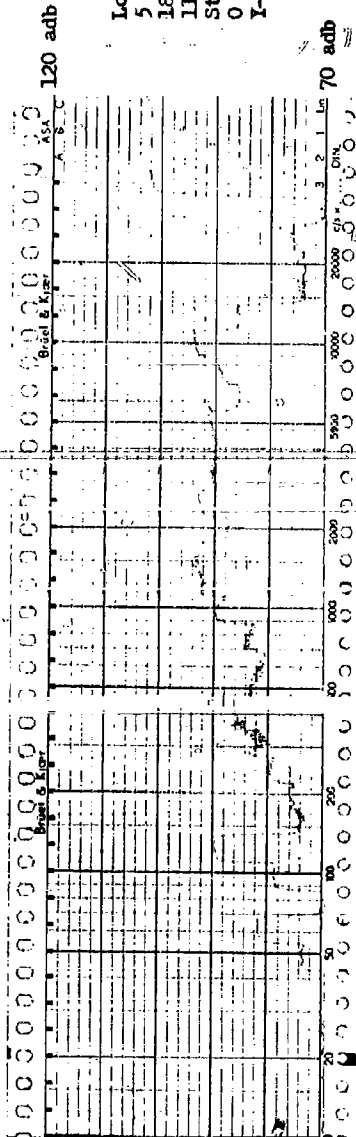
120 adb



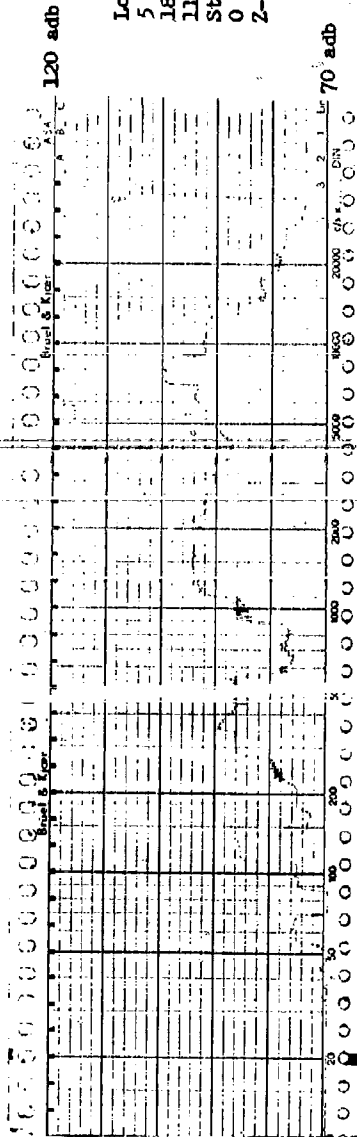
Shaft Bearing Fit
 3 HP 2 Pole
 184 Frame Open
 5 July 1960
 Structureborne
 1.1 Mil Interference
 Core



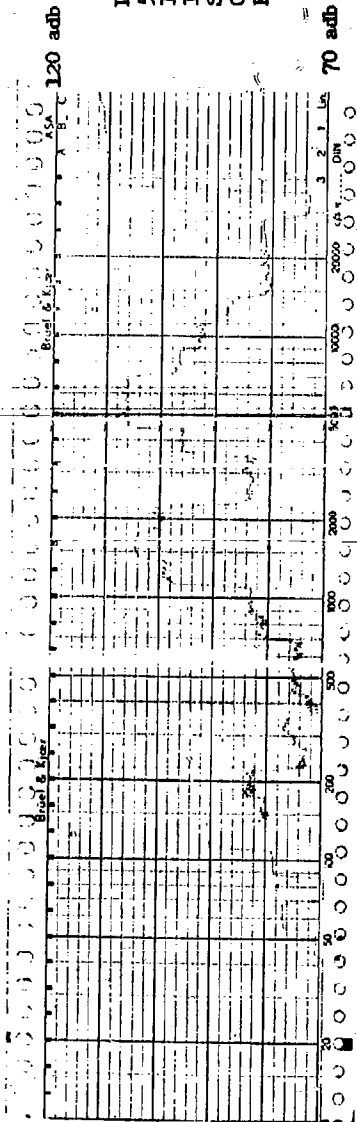
Locknut Test
 5 HP 2 Pole
 184, Frame Open
 11 Nov. 1960
 Structureborne
 0 lb-ft torque
 X-Axis



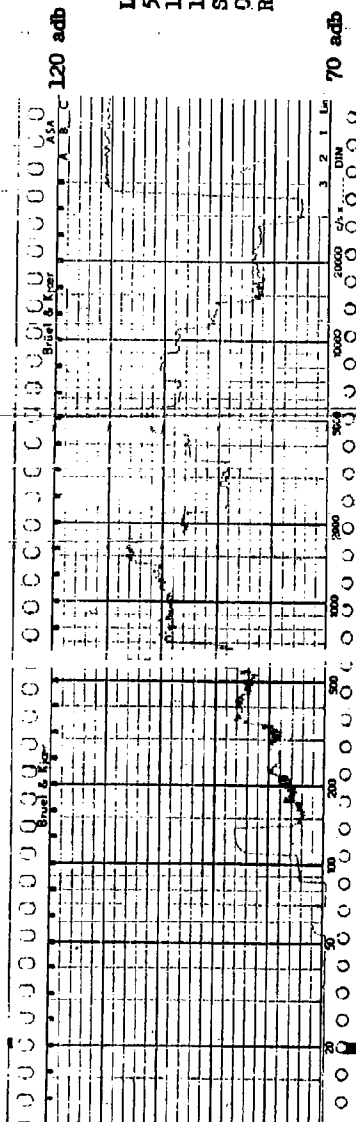
Locknut Test
 5 HP 2 Pole
 184, Frame Open
 11 Nov. 1960
 Structureborne
 0 lb-ft torque
 Y-Axis



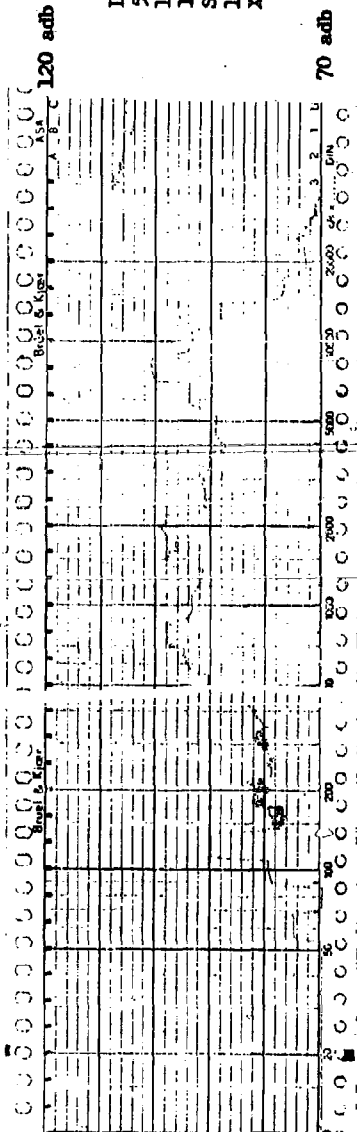
Locknut Test
 5 HP 2 Pole
 184, Frame Open
 11 Nov. 1960
 Structureborne
 0 lb-ft torque
 Z-Axis



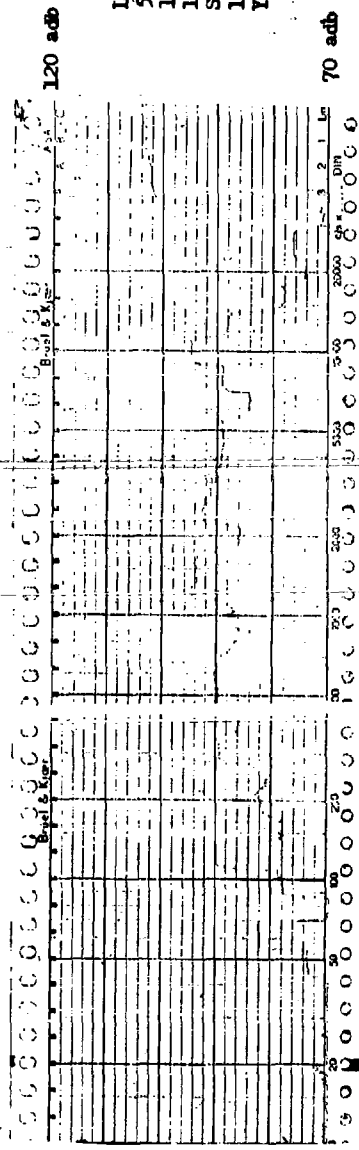
Locknut Test
 5 HP 2 Pole
 184 Frame Open
 11 Nov. 1960
 Structureborne
 0 lb-ft torque
 Front Brg.



Locknut Test
 5 HP 2 Pole
 184 Frame Open
 11 Nov. 1960
 Structureborne
 0 lb-ft torque
 Rear Brg. Hub



Locknut Test
 5 HP 2 Pole
 184 Frame Open
 11 Nov. 1960
 Structureborne
 12 lb-ft torque
 X - Axis



Locknut Test
 5 HP 2 Pole
 184 Frame Open
 11 Nov. 1960
 Structureborne
 12 lb-ft torque
 Y - Axis

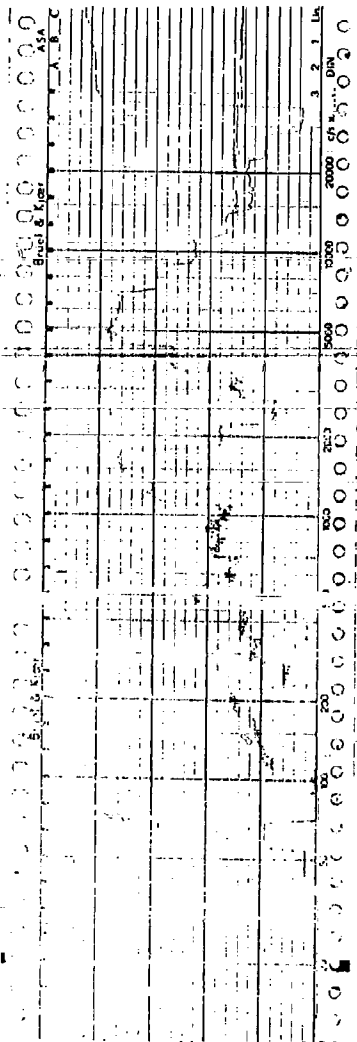


Locknut Test
 5 HP 2 Pole
 184 Frame Open
 11 Nov. 1960
 Structureborne
 12 lb-ft torque
 Z - Axis

120 adb

Locknut Test
5 HP 2 Pole
184, Frame Open
11 Nov. 1960
Structureborne
12 lb-ft torque
Front Brg.

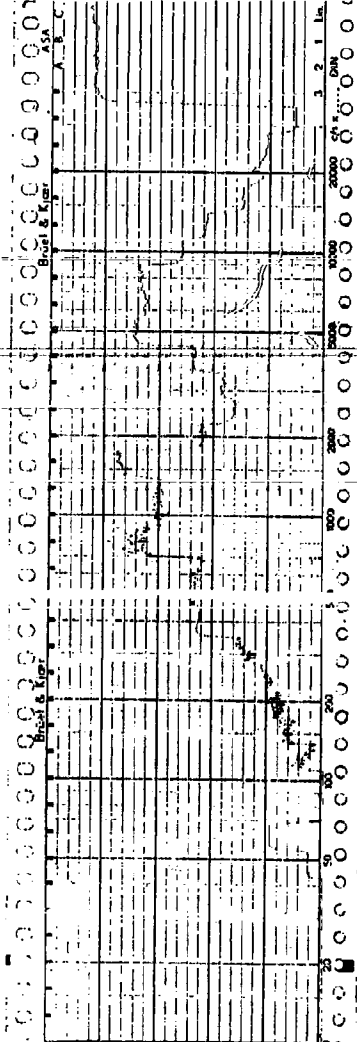
70 adb

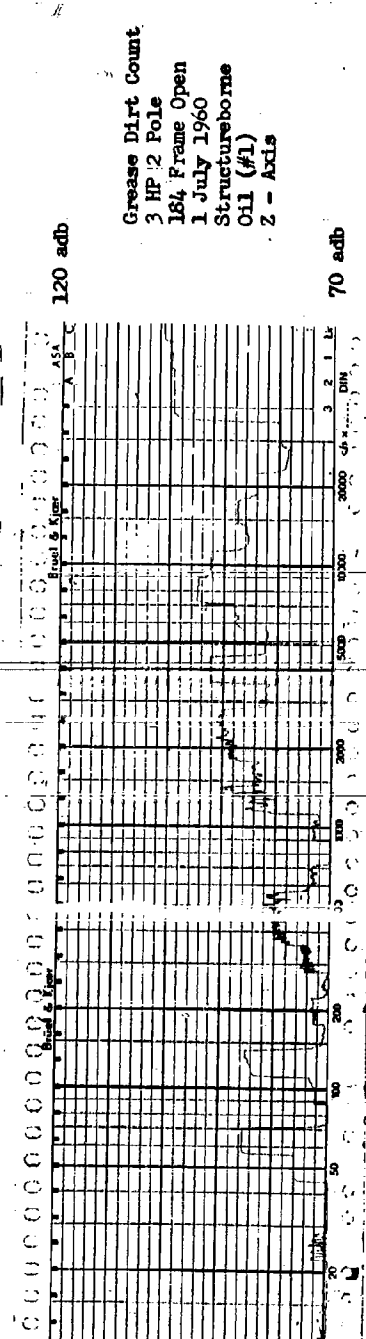
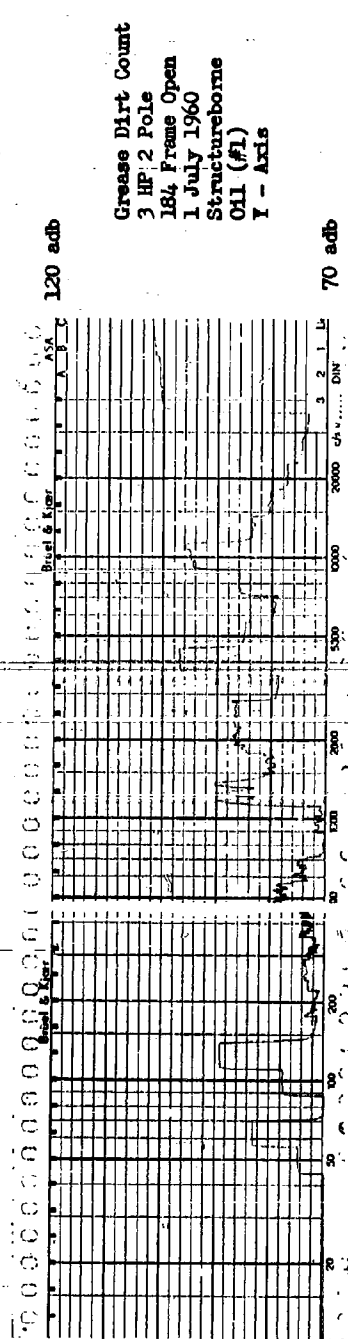
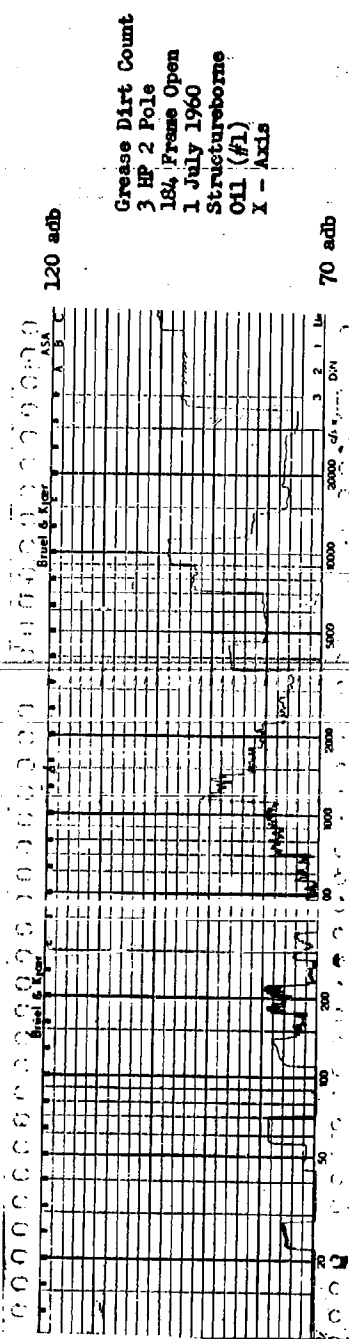


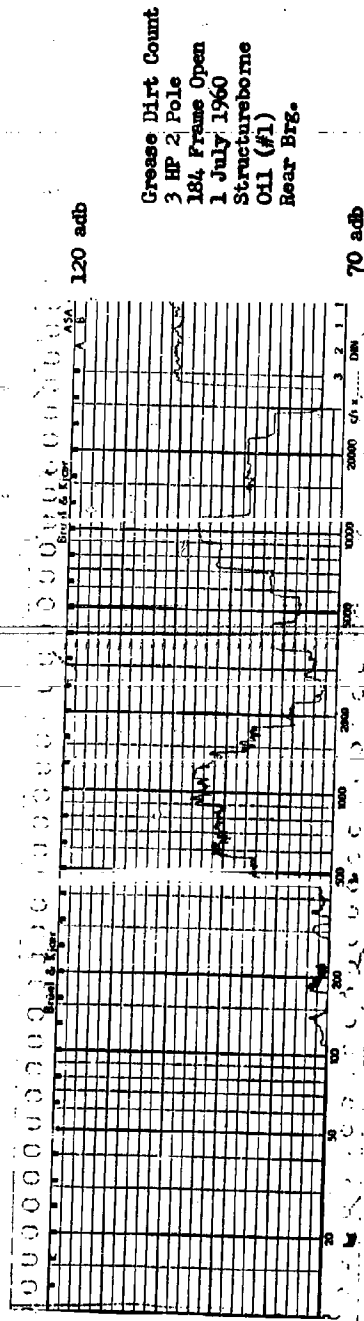
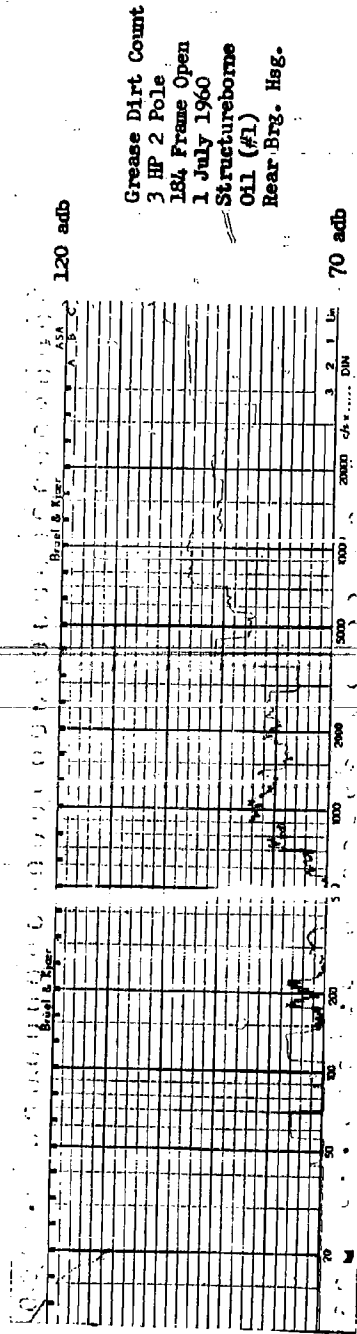
120 adb

Locknut Test
5 HP 2 Pole
184, Frame Open
11 Nov. 1960
Structureborne
12 lb-ft torque
Rear Brg. Hub

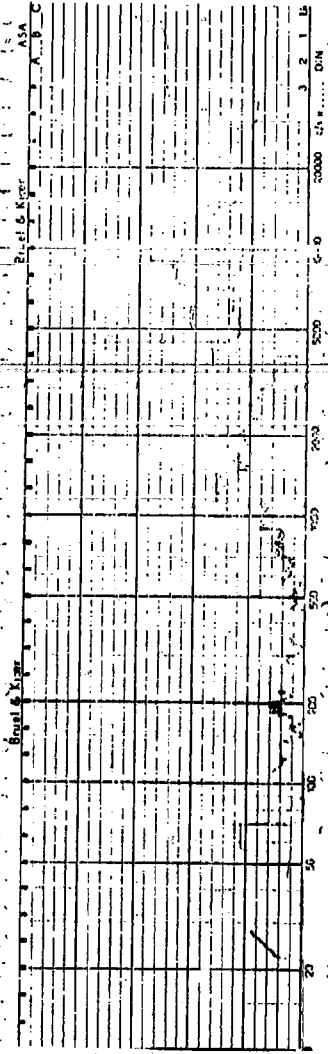
70 adb







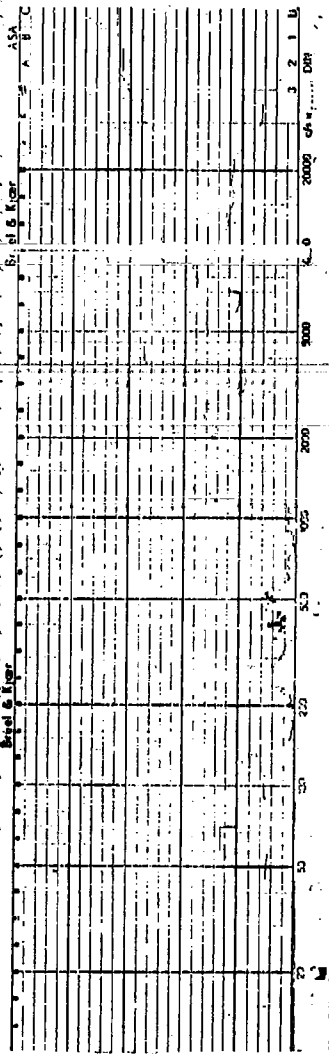
120 adb



Grease Dirt Count
3 HP 2 Pole
184 Frame Open
5 July 1960
Structureborne
Clean Grease (#2)
X - Axis

70 adb

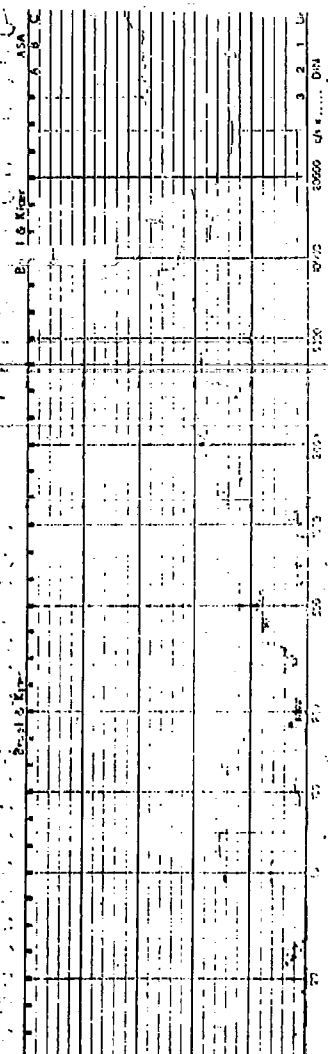
120 adb



Grease Dirt Count
3 HP 2 Pole
184 Frame Open
5 July 1960
Structureborne
Clean Grease (#2)
Y - Axis

70 adb

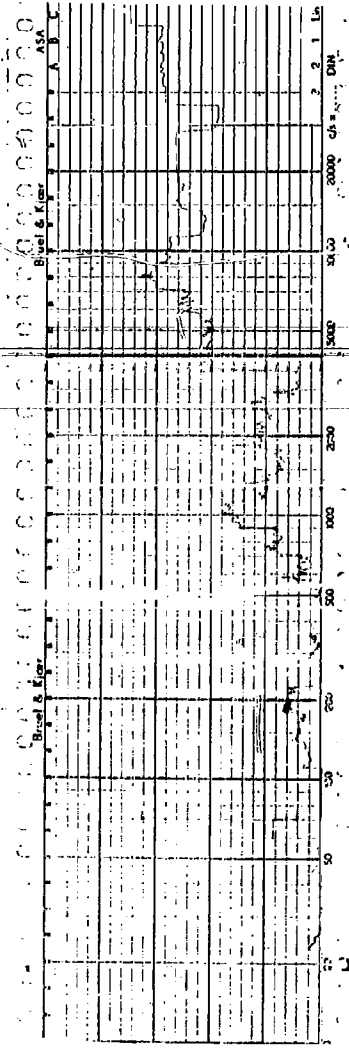
120 adb



Grease Dirt Count
3 HP 2 Pole
184 Frame Open
5 July 1960
Structureborne
Clean Grease (#2)
Z - Axis

70 adb

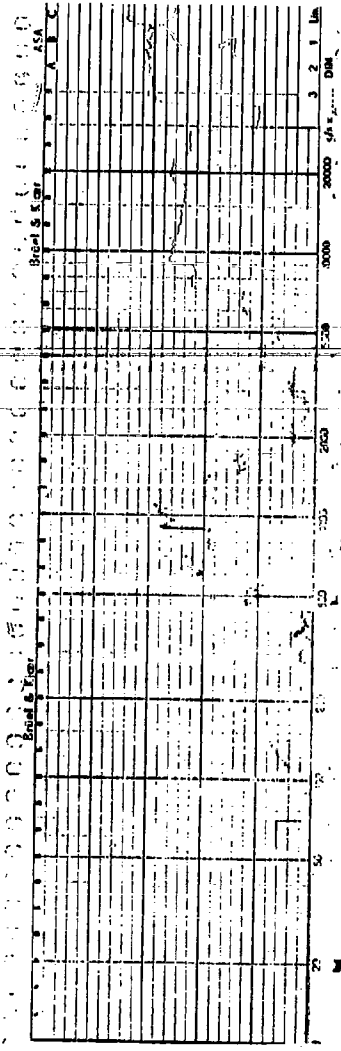
120 adb



Grease Dirt Count
 3 HP 2 Pole
 184, Frame Open
 5 July 1960
 Structureborne
 Clean Grease (#2)
 Rear Brg. Hdg.

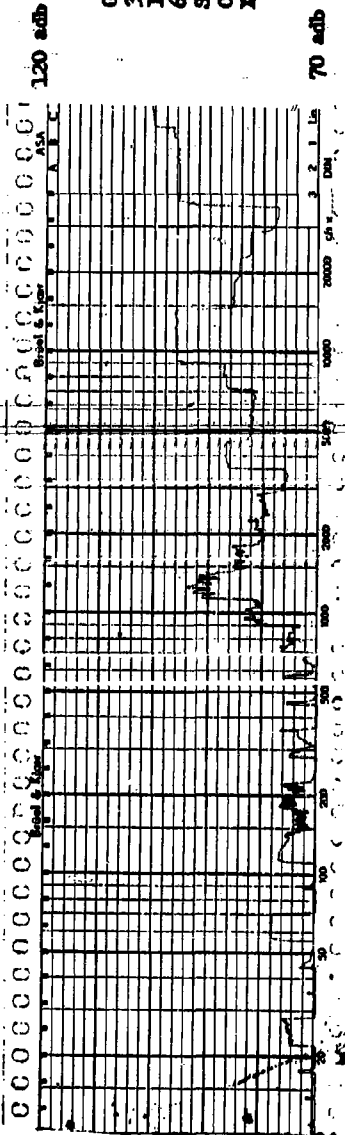
70 adb

120 adb

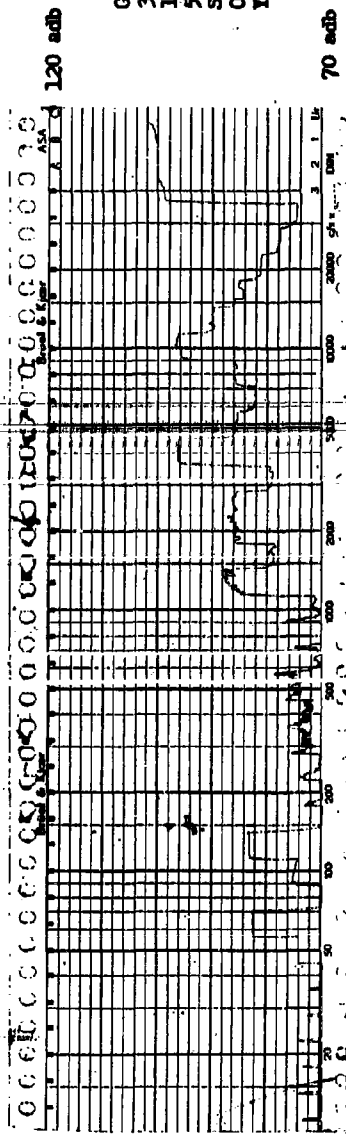


Grease Dirt Count
 3 HP 2 Pole
 184, Frame Open
 5 July 1960
 Structureborne
 Clean Grease (#2)
 Rear Brg.

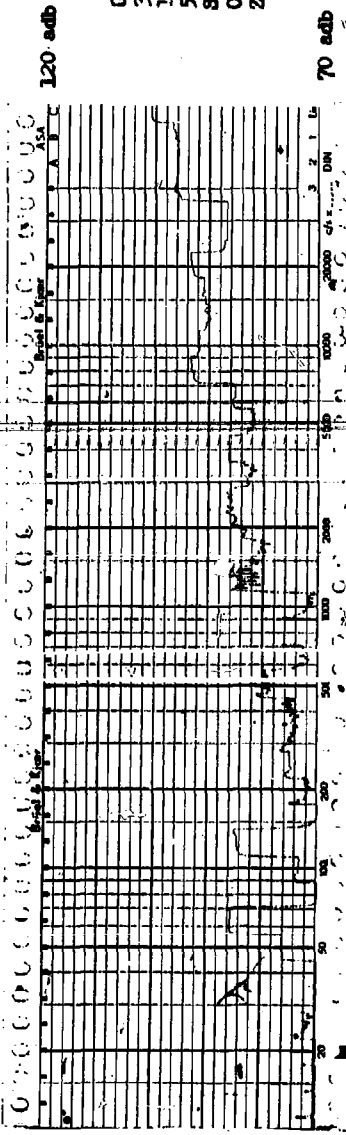
70 adb



Grease Dirt Count
 3 HP 2 Pole
 184, Frame Open
 6 July 1960
 Structureborne
 Oil (#3)
 X - Axis

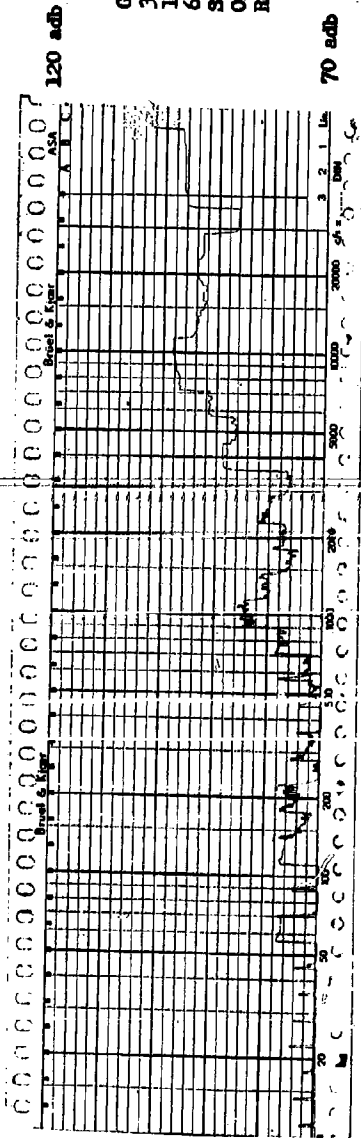


Grease Dirt Count
 3 HP 2 Pole
 184, Frame Open
 5 July 1960
 Structureborne
 Oil (#3)
 Y - Axis

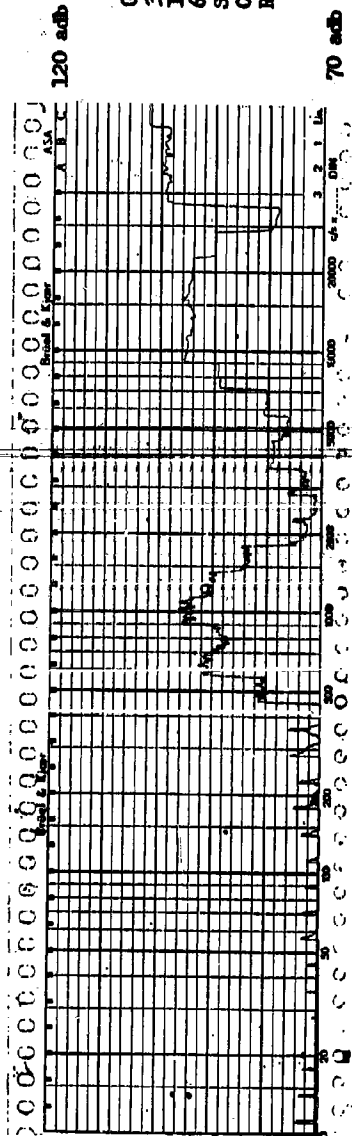


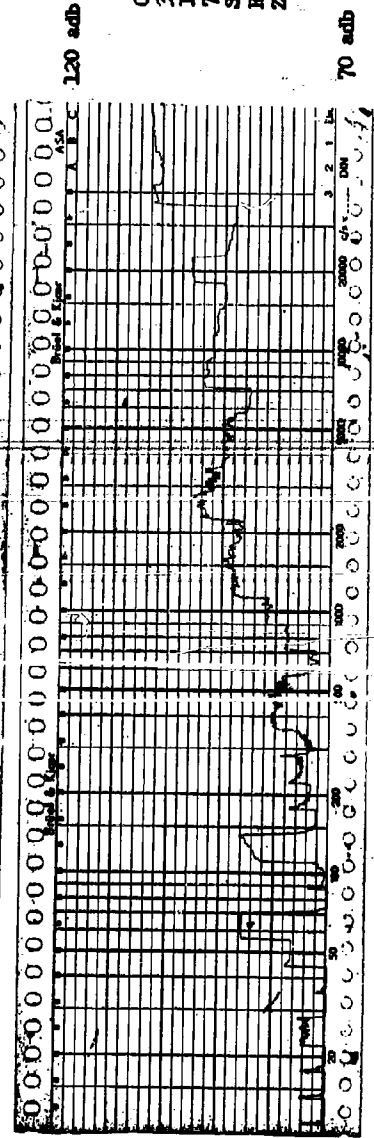
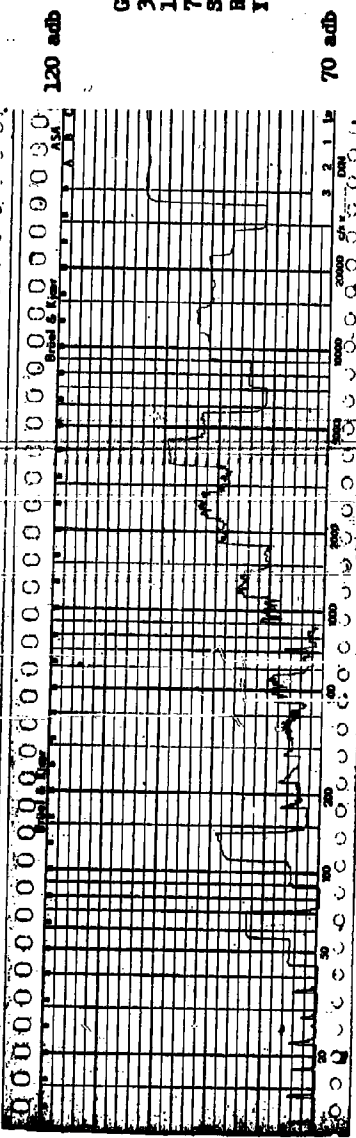
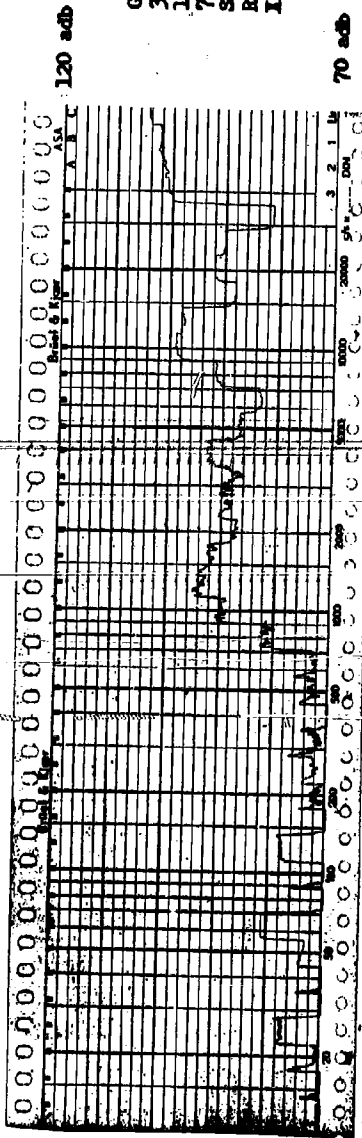
Grease Dirt Count
 3 HP 2 Pole
 184, Frame Open
 5 July 1960
 Structureborne
 Oil (#3)
 Z - Axis

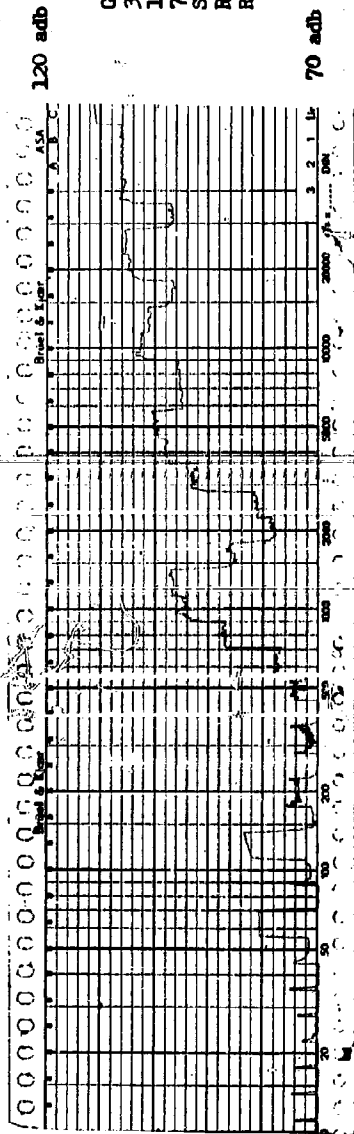
Grease Dirt Count
3 HP 2 Pole
184 Frames Open
6 July 1960
Structureborne
Oil (#3)
Rear Brg. Hag.



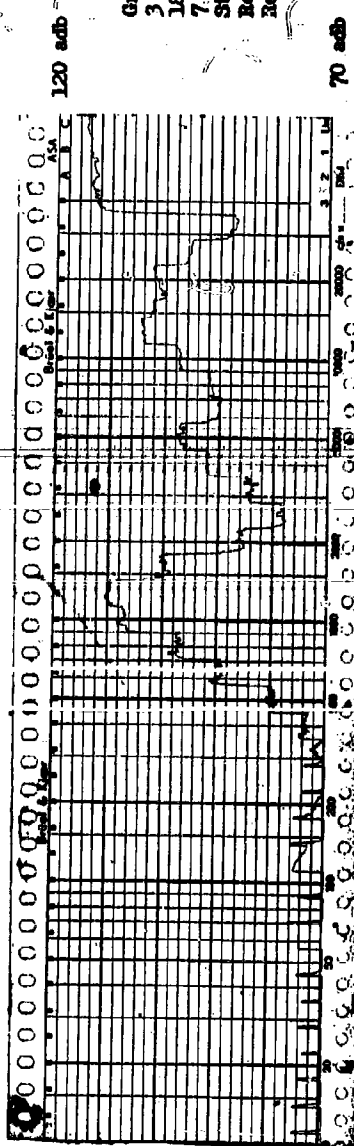
Grease Dirt Count
3 HP 2 Pole
184 Frames Open
6 July 1960
Structureborne
Oil (#3)
Rear Brg.



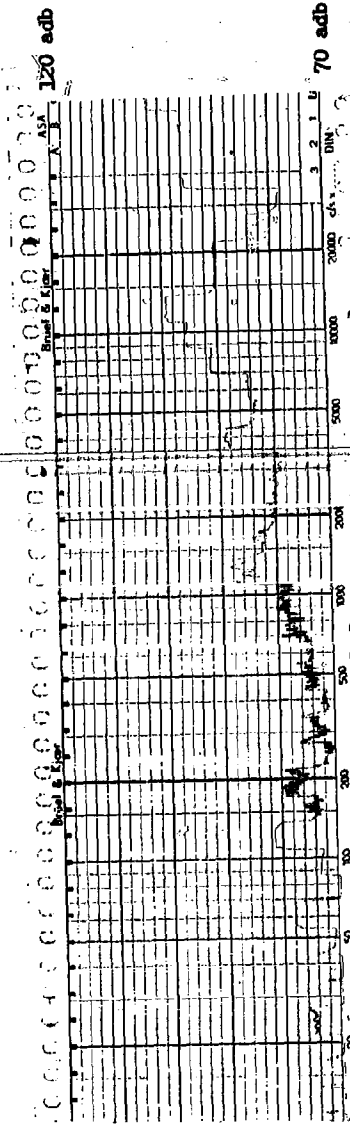




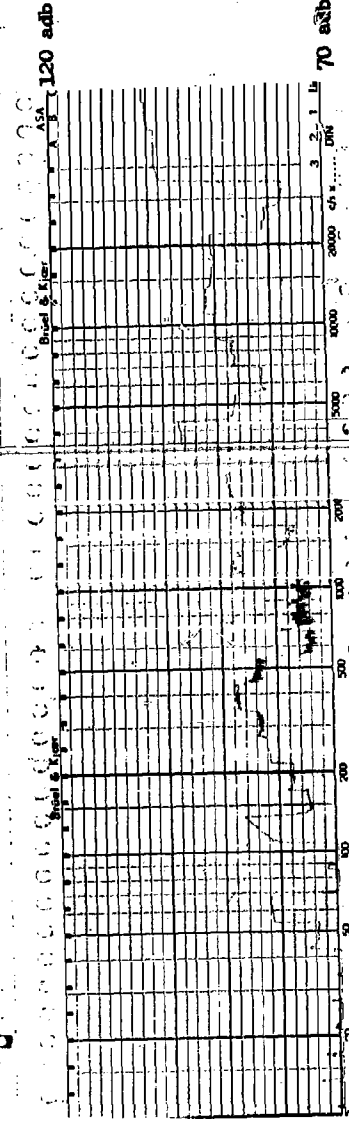
Grease Dirt Count
 3 HP 2 Poles
 184 Frame Open
 7 July 1960
 Structureborne
 Reject Grease (#4)
 Rear Brg. Hsq.



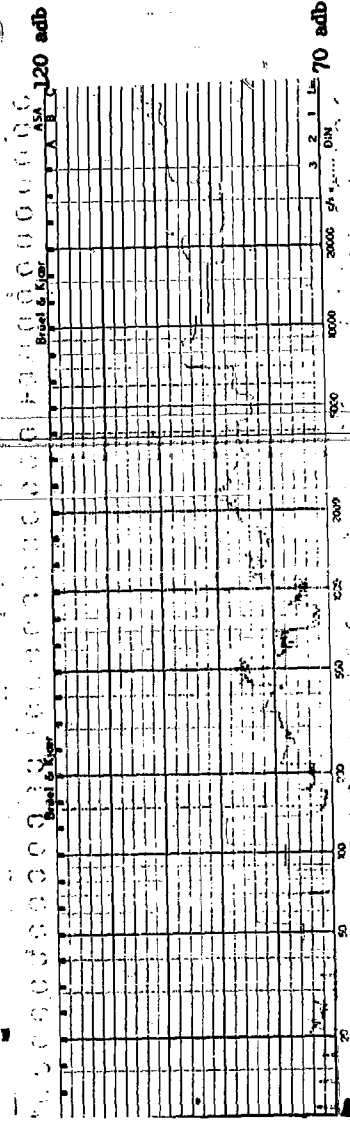
Grease Dirt Count
 3 HP 2 Poles
 184 Frame Open
 7 July 1960
 Structureborne
 Reject Grease
 Rear Brg.



Grease Dirt Count
 3 HP 2 Pole
 184 Frame Open
 11 July 1960
 Structureborne
 Oil (#5)
 X - Axis

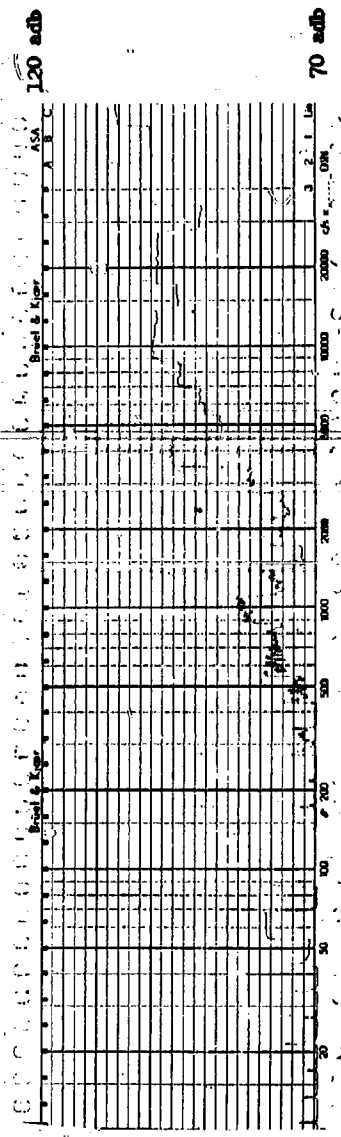


Grease Dirt Count
 3 HP 2 Pole
 184 Frame Open
 11 July 1960
 Structureborne
 Oil (#5)
 Y - Axis



Grease Dirt Count
 3 HP 2 Pole
 184 Frame Open
 11 July 1960
 Structureborne
 Oil (#5)
 Z - Axis

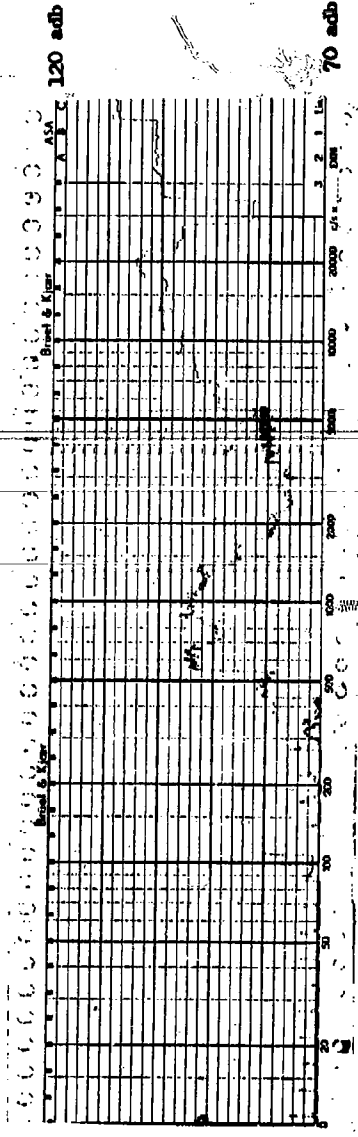
Grease Dirt Count
3 HP 2 Fole
184, Frame Open
11 July 1960
Structureborne
Oil (#5)
Rear Brg. Hsg.



120 adb

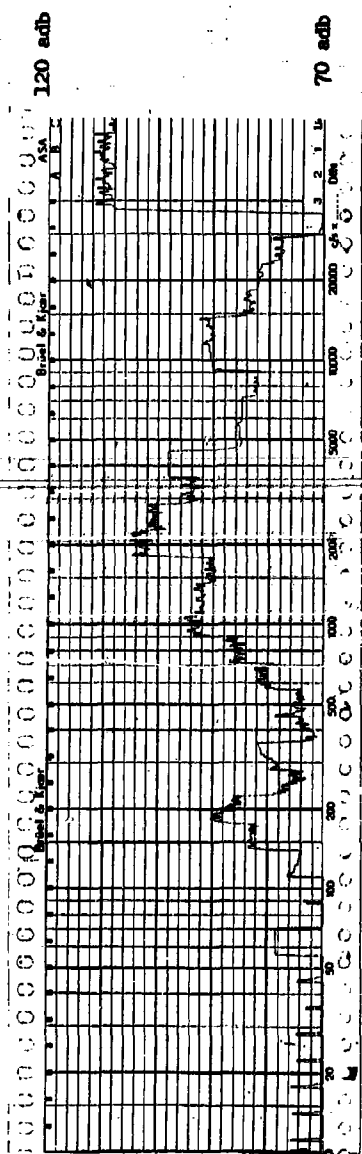
70 adb

Grease Dirt Count
3 HP 2 Fole
184, Frame Open
11 July 1960
Structureborne
Oil (#5)
Rear Brg.

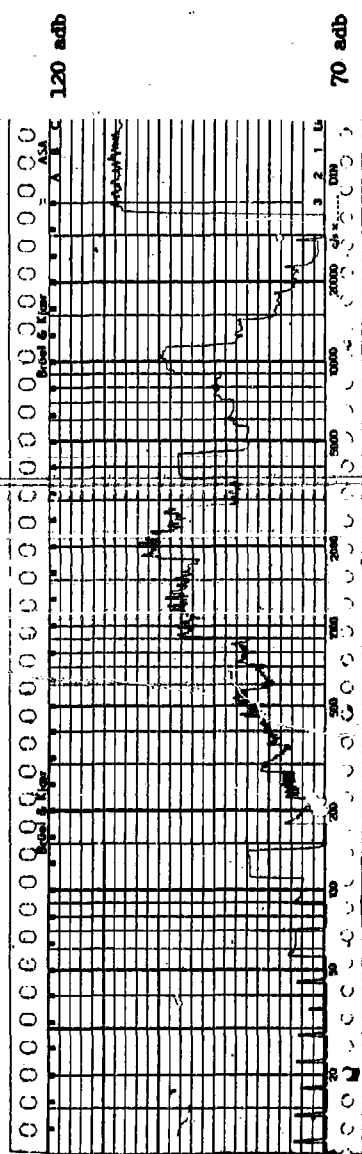


120 adb

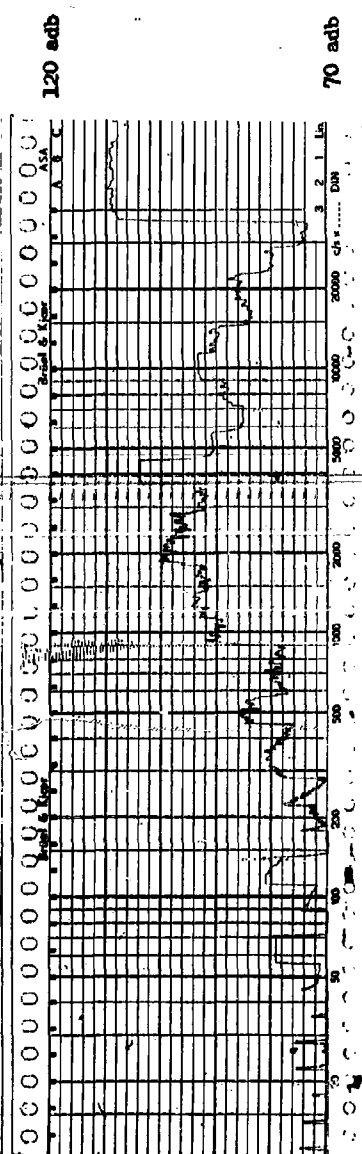
70 adb



Grease Test
 3 HP 2 Pole
 184 Frame Open
 7 July 1960
 Structureborne
 Oil (#1)
 X - Axis



Grease Test
 3 HP 2 Pole
 184 Frame Open
 7 July 1960
 Structureborne
 Oil (#1)
 X - Axis

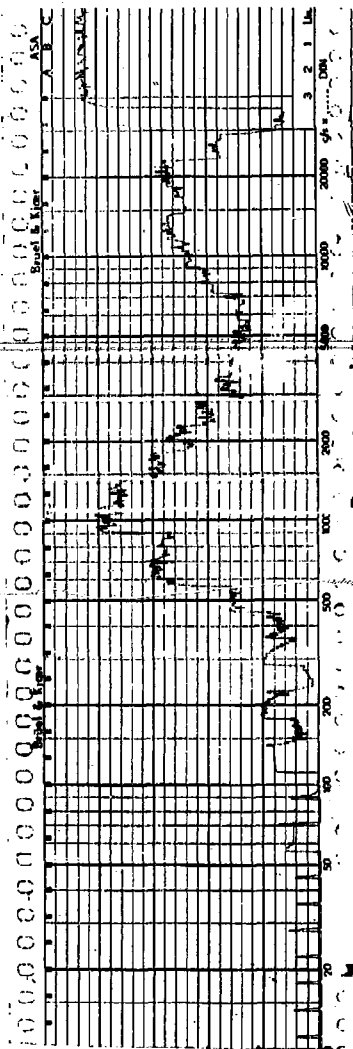


Grease Test
 3 HP 2 Pole
 184 Frame Open
 7 July 1960
 Structureborne
 Oil (#1)
 Z - Axis

4-41

Grease Test
3 HP 2 Pole
184 Frame Open
7 July 1960
Structureborne
Oil (#1)
Front Brg. Hsg.

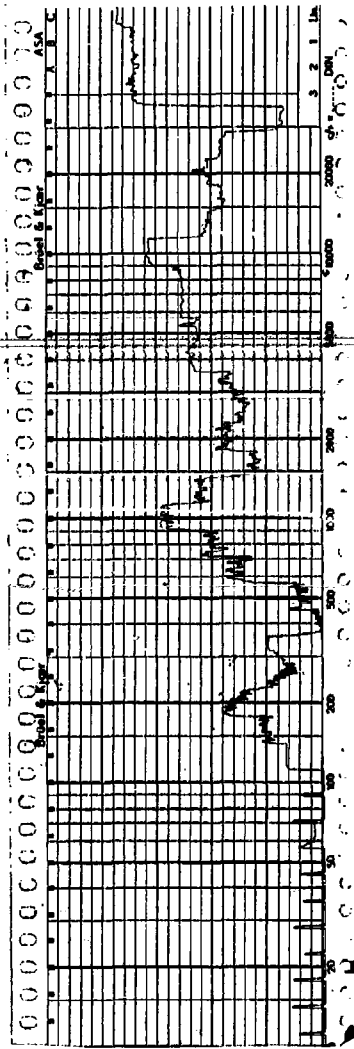
120 adB



70 adB

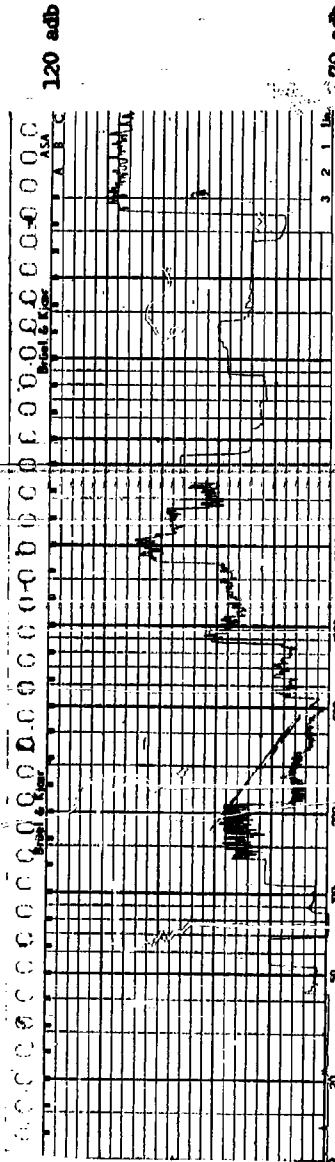
Grease Test
3 HP 2 Pole
184 Frame Open
7 July 1960
Structureborne
Oil (#1)
Rear Brg.

120 adB

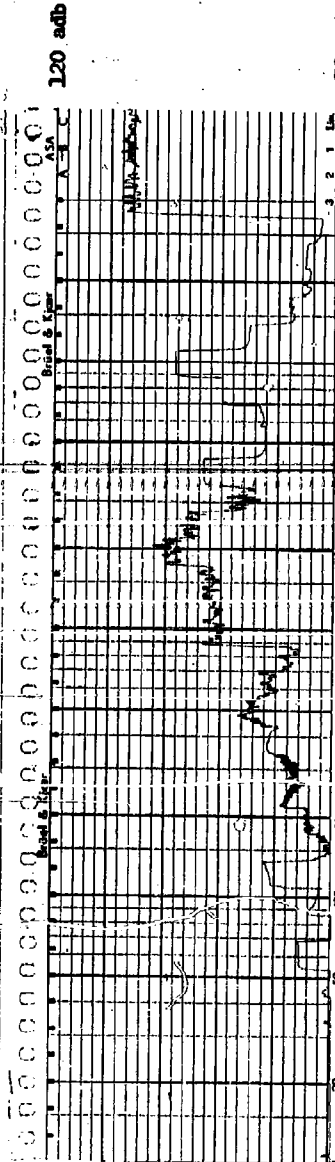


70 adB

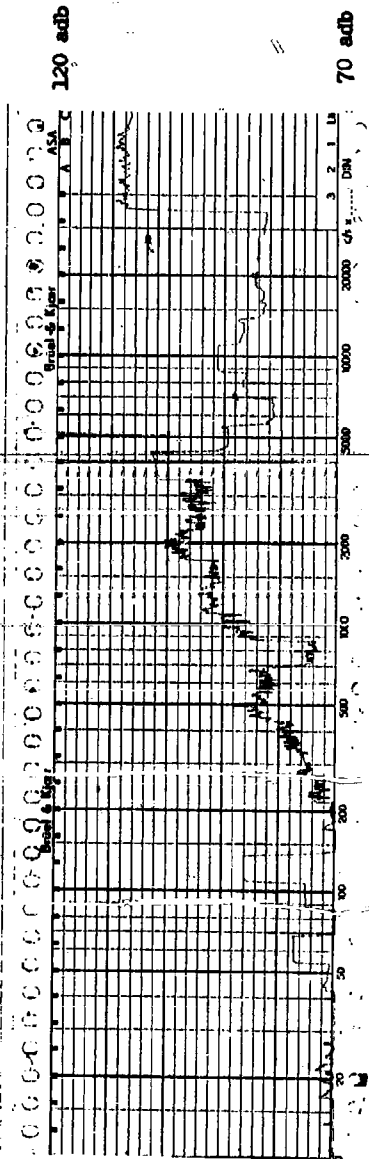
Grease Test
3 HP 2 Pole
184, Frame Open
11 July 1960
Structureborne
Andok 260 (#2)
X - Axis



Grease Test
3 HP 2 Pole
184, Frame Open
11 July 1960
Structureborne
Andok 260 (#2)
Y - Axis



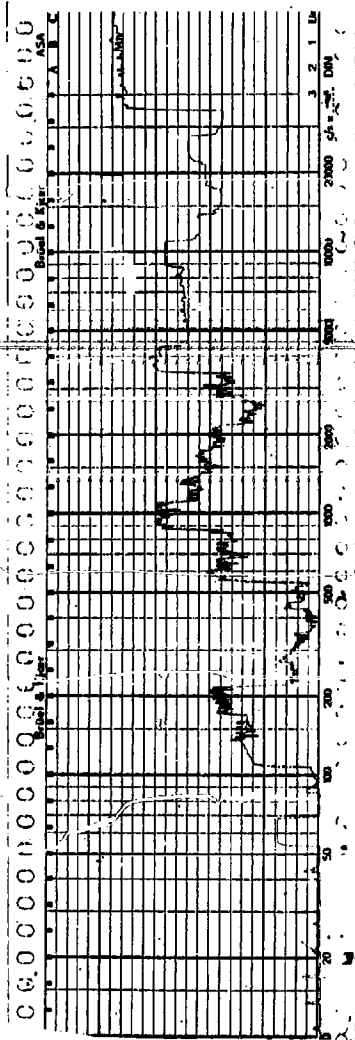
Grease Test
3 HP 2 Pole
184, Frame Open
11 July 1960
Structureborne
Andok 260 (#2)
Z - Axis



Grease Test
3 HP 2 Pole
184 Frame Open
11 July 1960
Structureborne
Amdok 260 (#2)
Front Brg. Hag.

120 adB

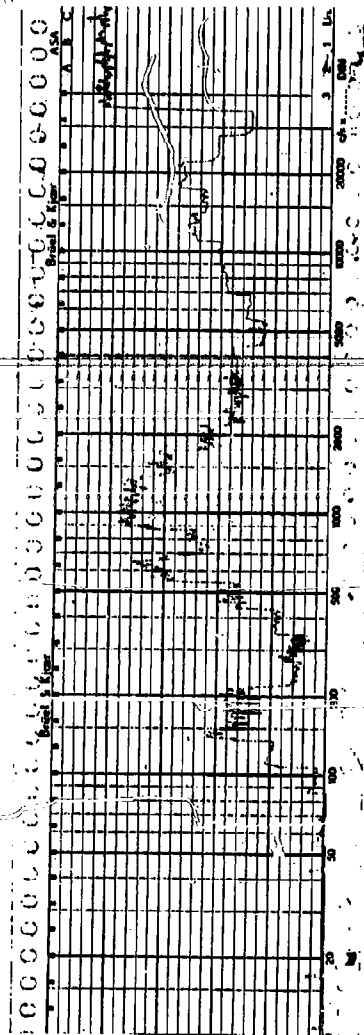
70 adB



Grease Test
3 HP 2 Pole
184 Frame Open
11 July 1960
Structureborne
Amdok 260 (#2)
Rear Bearing

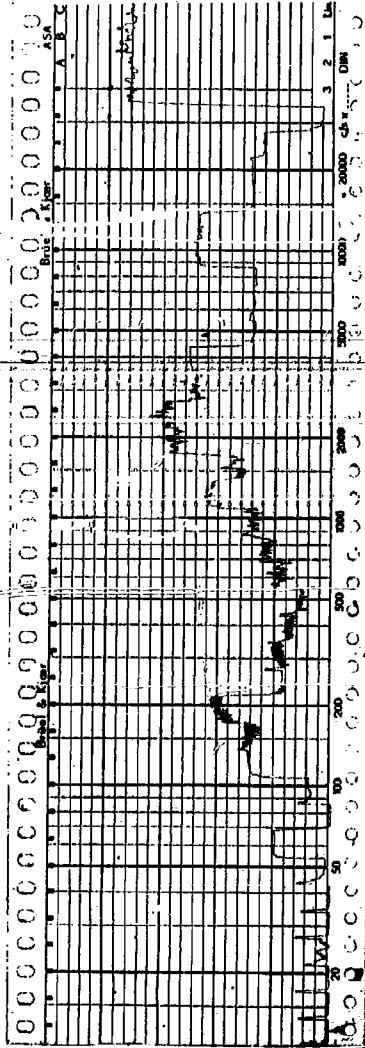
120 adB

70 adB



Grease Test
3 HP 2 Pole
184, Frame Open
12 July 1960
Structureborne
Oil (#3)
Y - Axis

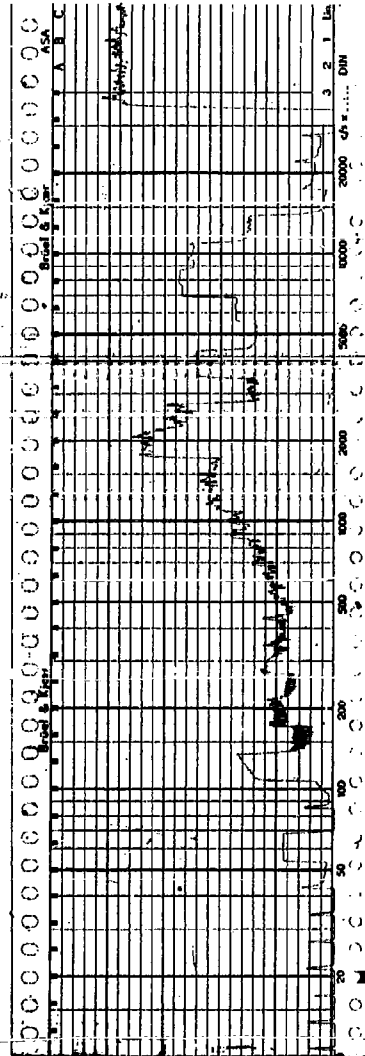
120 adb



70 adb

Grease Test
3 HP 2 Pole
184, Frame Open
12 July 1960
Structureborne
Oil (#3)
Y - Axis

120 adb

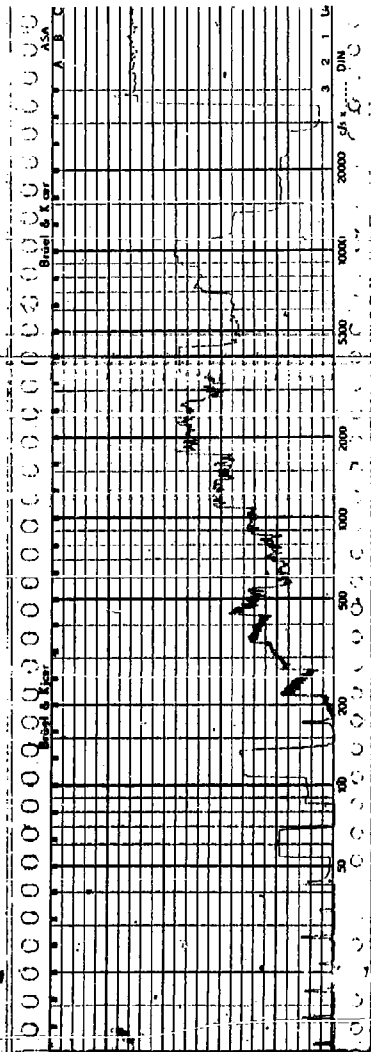


70 adb

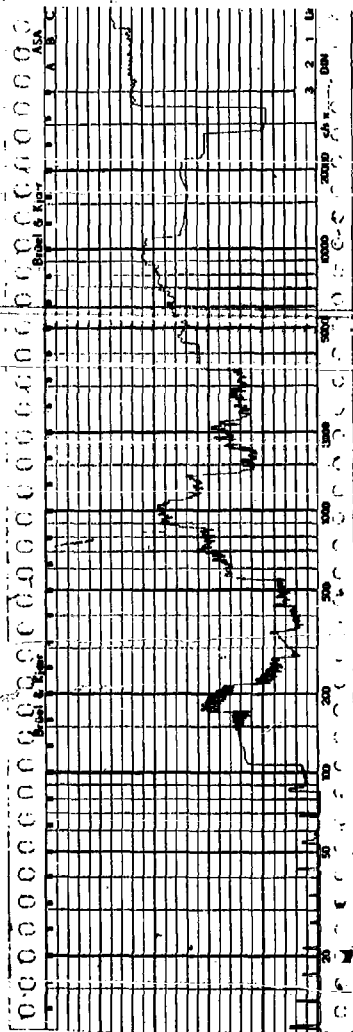
120 adb

Grease Test
3 HP 2 Pole
184, Frame Open
12 July 1960
Structureborne
Oil (#3)
Z - Axis

70 adb



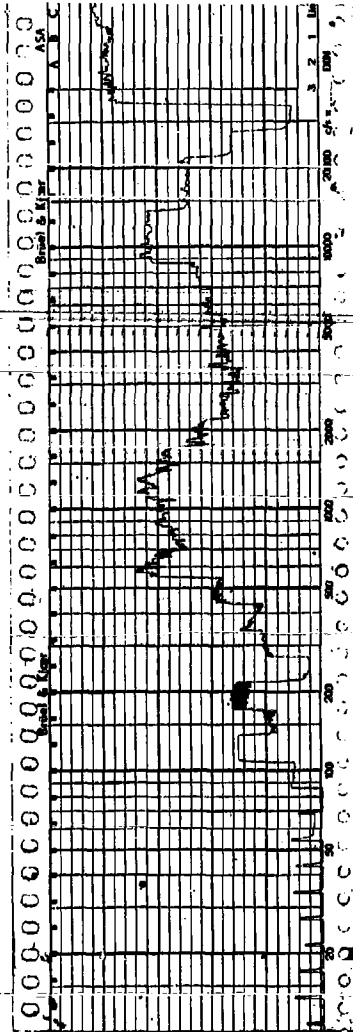
120 adb



Grease Test
3 HP 2 Pole
184, Frame Open
12 July 1960
Structureborne
Oil (#3)
Front Brg. Hng.

70 adb

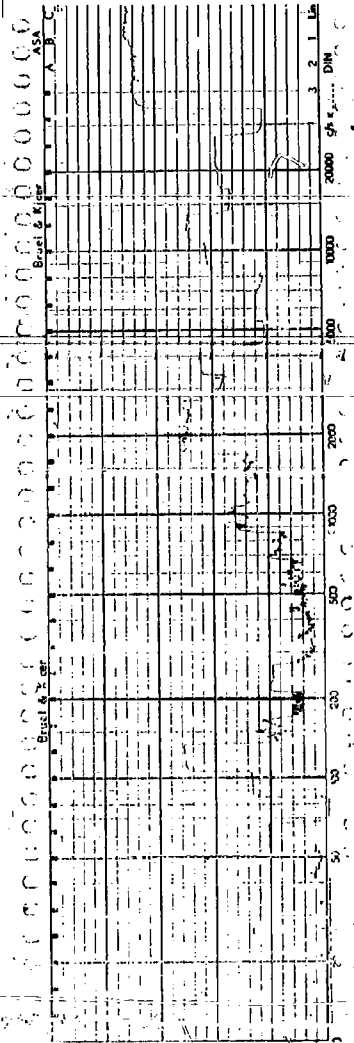
120 adb



Grease Test
3 HP 2 Pole
184, Frame Open
12 July 1960
Structureborne
Oil (#3)
Bear Bearing

70 adb

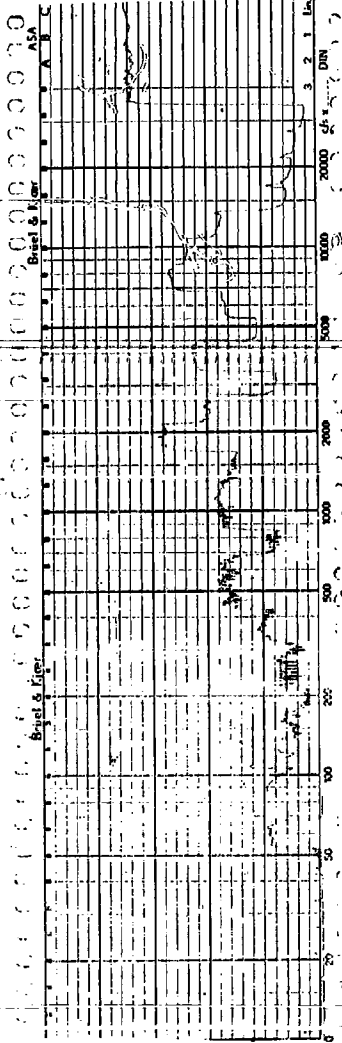
120 adb



Grease Test
3 HP 2 Pole
184, Frame Open
13 July 1960
Structureborne
Aeroshell (#4)
Y - Axis

70 adb

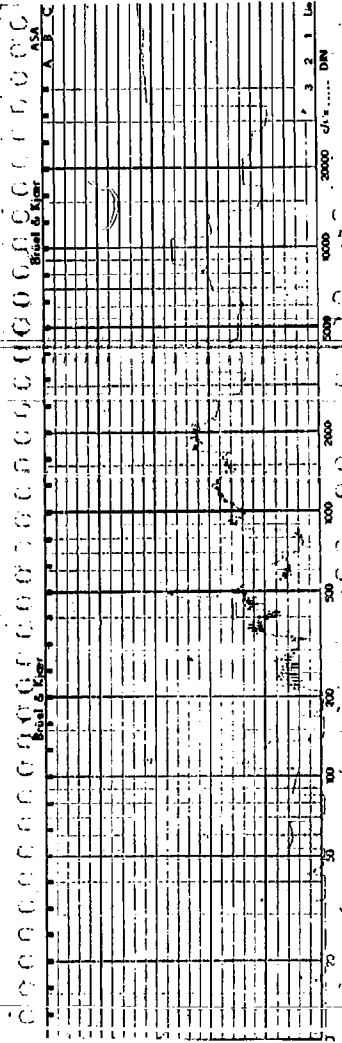
120 adb



Grease Test
3 HP 2 Pole
184, Frame Open
13 July 1960
Structureborne
Aeroshell (#4)
Y - Axis

70 adb

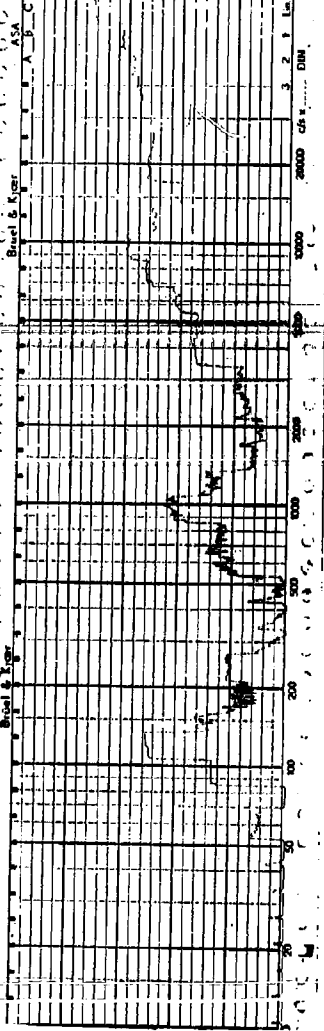
120 adb



Grease Test
3 HP 2 Pole
184, Frame Open
13 July 1960
Structureborne
Aeroshell (#4)
Z - Axis

70 adb

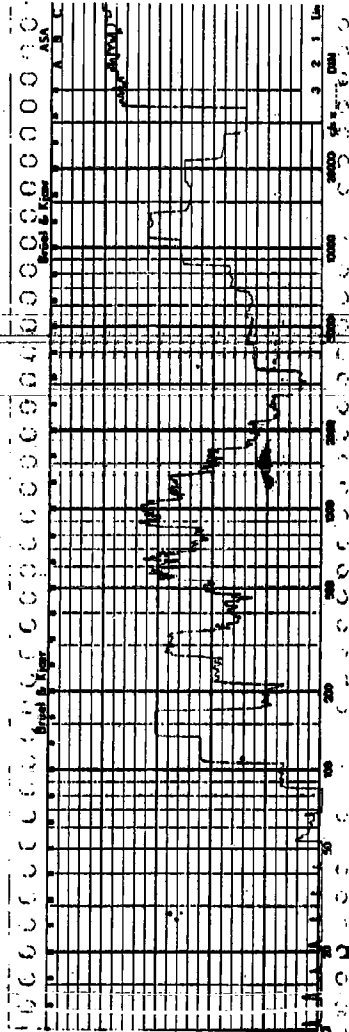
120 adb



70 adb

Grease Test
 3 HP 2 Pole
 184 Frame Open
 13 July 1960
 Structureborne
 Aeroshell (#4)
 Front Brg. Hsg.

120 adb

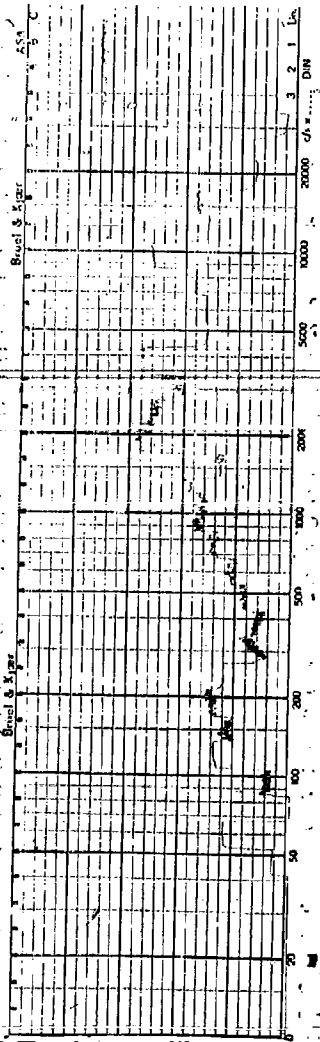


70 adb

Grease Test
 3 HP 2 Pole
 184 Frame Open
 13 July 1960
 Structureborne
 Aeroshell (#4)
 Rear Bearing

Grease Test
 3 HP 2 Pole
 184 Frame Open
 13 July 1960
 Structureborne
 Oil (#5)
 X - Axis

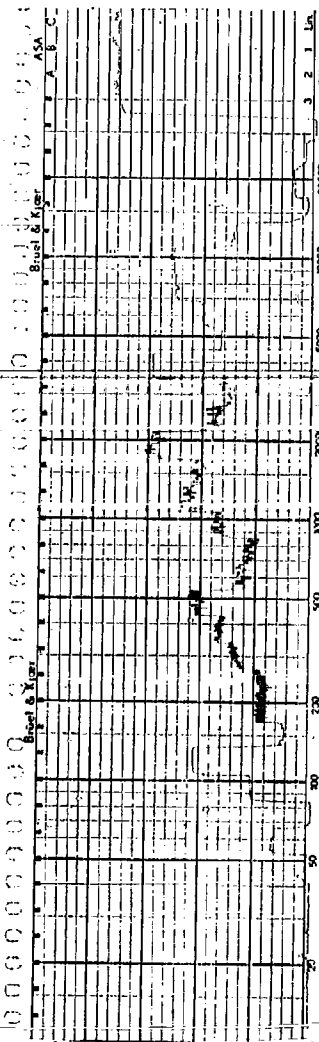
120 adb



70 adb

Grease Test
 3 HP 2 Pole
 184 Frame Open
 13 July 1960
 Structureborne
 Oil (#5)
 Y - Axis

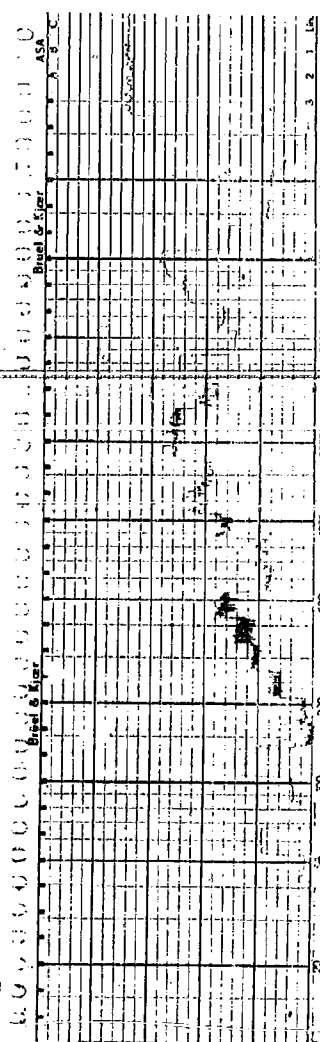
120 adb



70 adb

Grease Test
 3 HP 2 Pole
 184 Frame Open
 13 July 1960
 Structureborne
 Oil (#5)
 Z - Axis

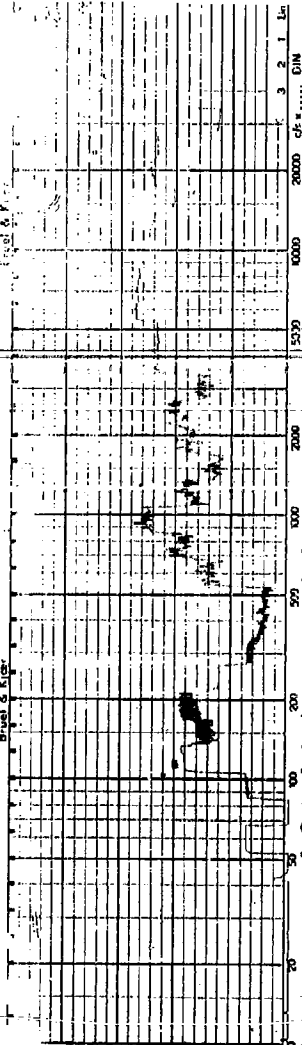
120 adb



70 adb

Grease Test
 3 HP 2 Pole
 184 Frame Open
 13 July 1960
 Structureborne
 Oil (#5)
 Front Brg. Hsg.

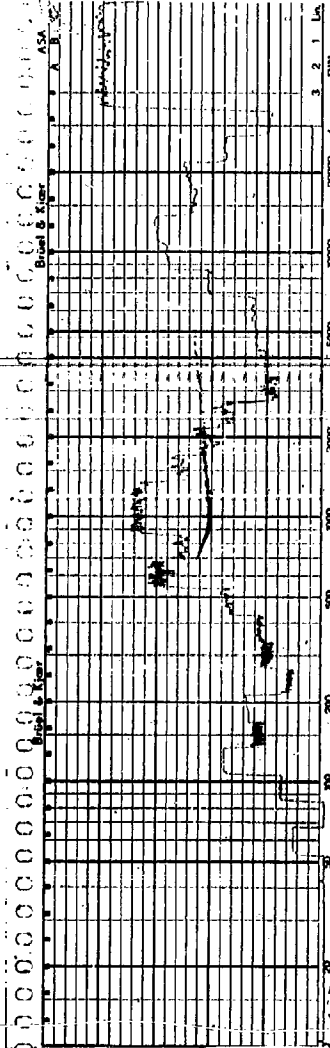
120



70 adb

Grease Test
 3 HP 2 Pole
 184 Frame Open
 13 July 1960
 Structureborne
 Oil (#5)
 Rear Brg.

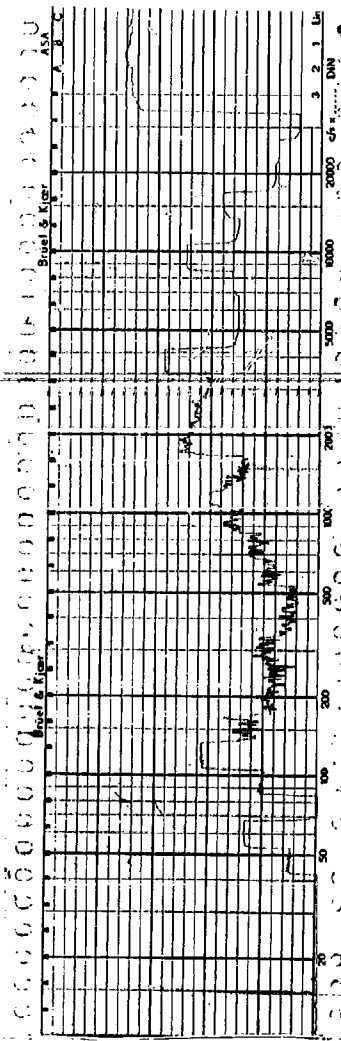
120 adb



70 adb

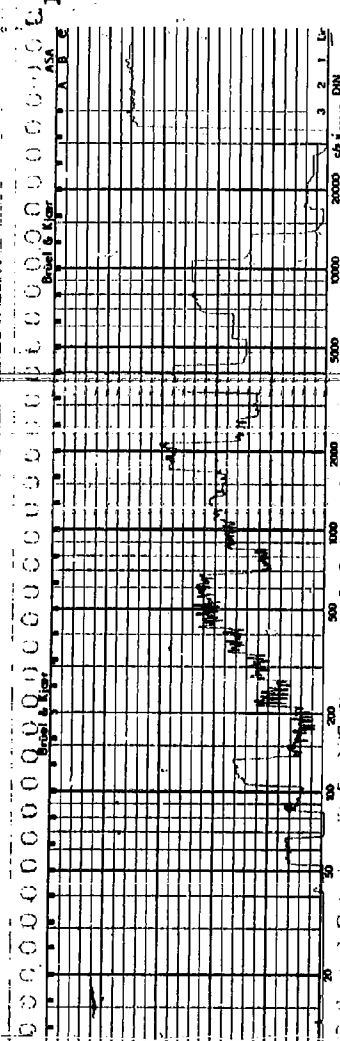
Grease Test
3 HP 2 Pole
184, Frame Open
15 July 1960
Structureborne
Texas TG 3007 (#6)
X - Axis

120 adB



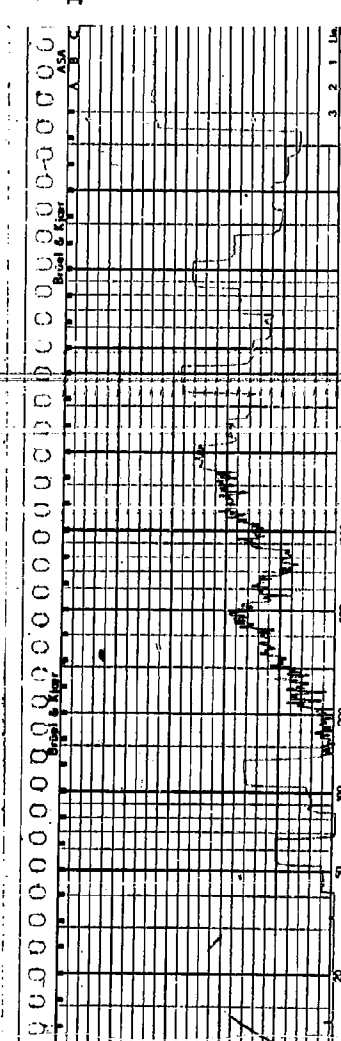
70 adB

120 adB



70 adB

120 adB



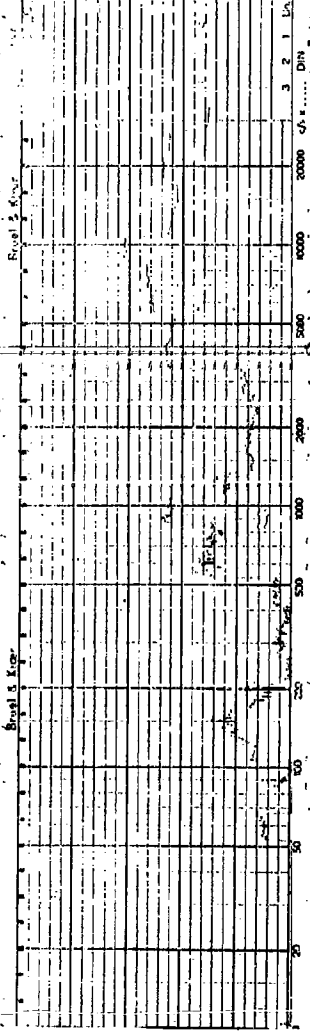
70 adB

Grease Test
3 HP 2 Pole
184, Frame Open
15 July 1960
Structureborne
Texas TG 3007 (#6)
Y - Axis

Grease Test
3 HP 2 Pole
184, Frame Open
15 July 1960
Structureborne
Texas TG 3007 (#6)
Z - Axis

Grease Test
 3 HP 2 Pole
 184 Frame Open
 15 July 1960
 Structureborne
 Texas TG 3007 (#6)
 Front Brg. Hsg.

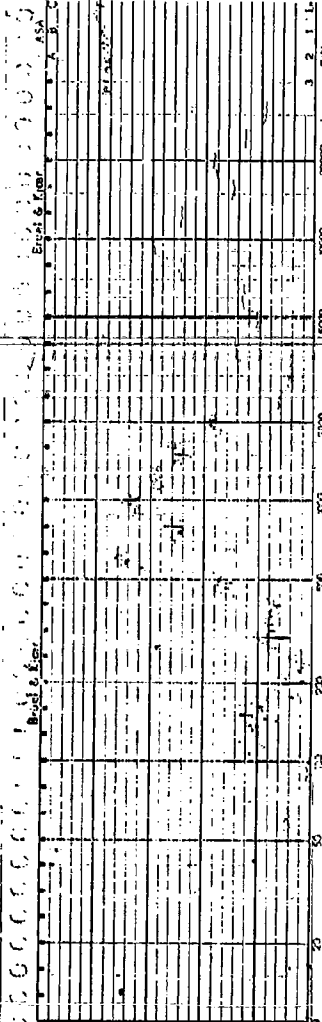
120 adb



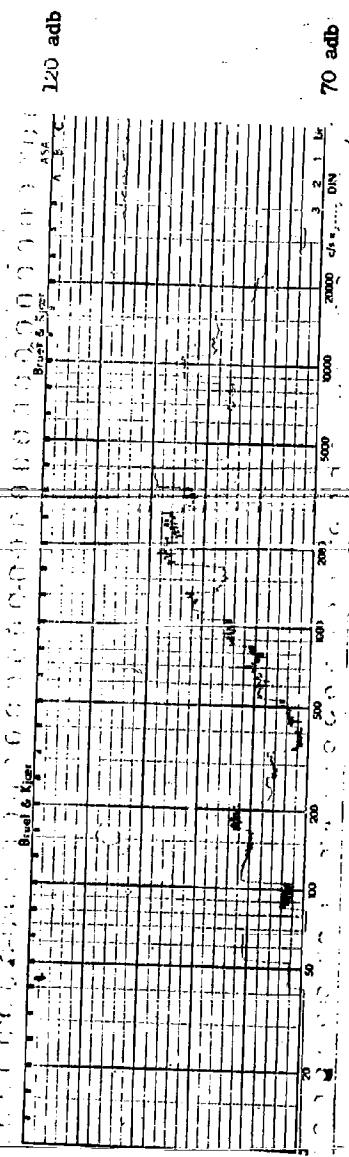
70 adb

Grease Test
 3 HP 2 Pole
 184 Frame Open
 15 July 1960
 Structureborne
 Texas TG 3007 (#6)
 Rear Brg.

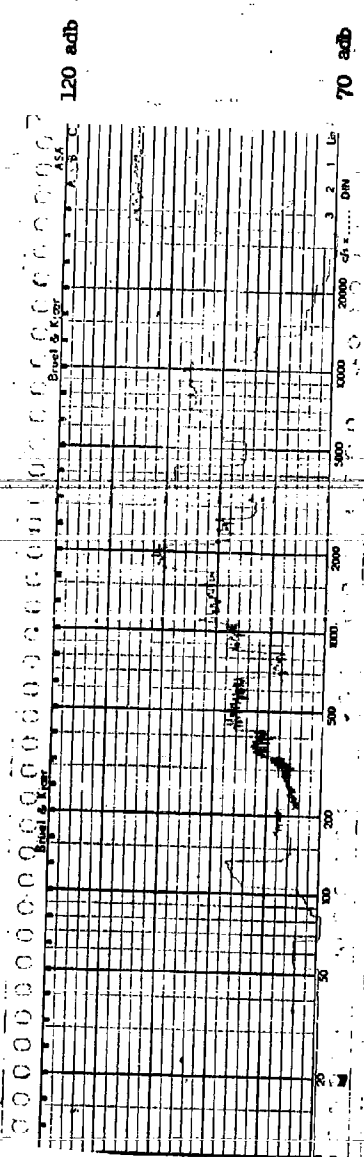
120 adb



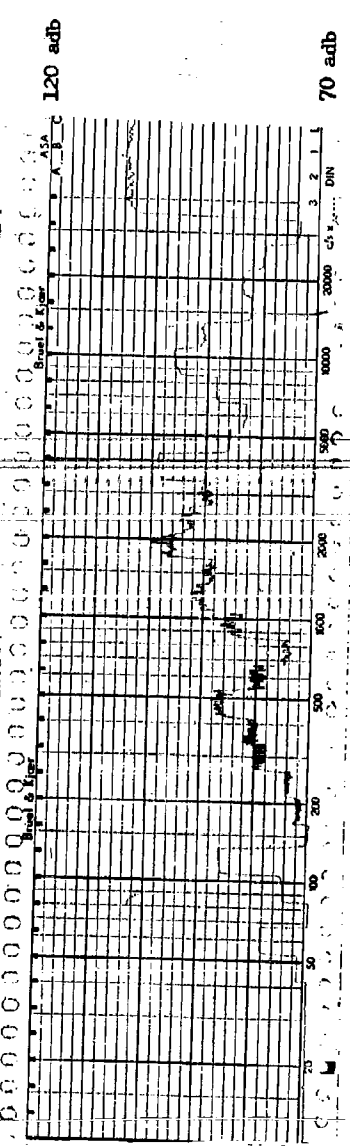
70 adb



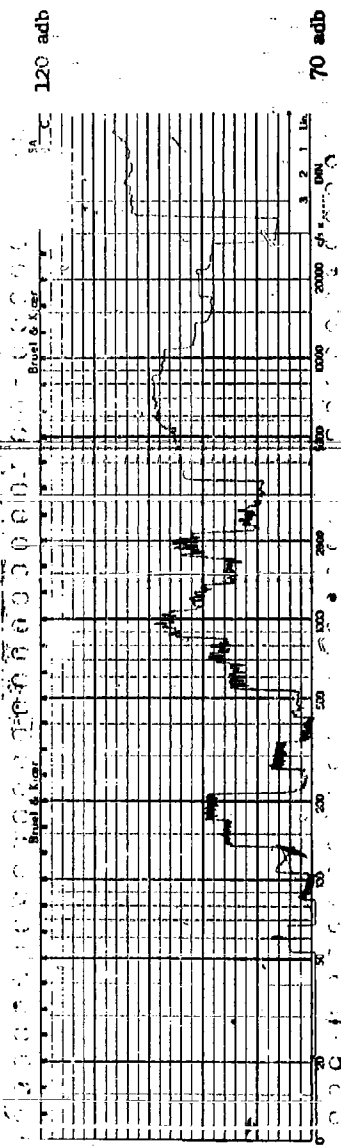
Grease Test
 3 HP 2 Pole
 184 Frame Open
 18 Jul. 1960
 Structureborne
 Oil (#7)
 X - Axis



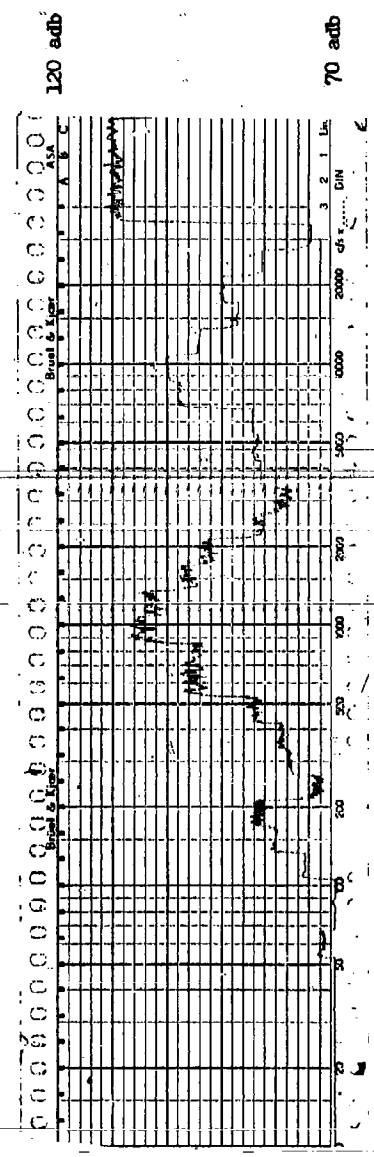
Grease Test
 3 HP 2 Pole
 184 Frame Open
 18 July 1960
 Structureborne
 Oil (#7)
 Y - Axis



Grease Test
 3 HP 2 Pole
 184 Frame Open
 18 July 1960
 Structureborne
 Oil (#7)
 Z - Axis



Grease Test
 3 HP 2 Pole
 184, Frame Open
 18 July 1960
 Structureborne
 Oil (#7)
 Front Bearing Hsg.



Grease Test
 3 HP 2 Pole
 184, Frame Open
 18 July 1960
 Structureborne
 Oil (#7)
 Rear Bearing

SECTION 5 FAN NOISE

5.1 INTRODUCTION

Fan noise differs from the majority of motor noise in that it is created in the airstream rather than in the motor components. Thus this noise is created as airborne noise rather than as vibration. For fan noise to appear as motor vibration, a transducing element is required. Vibration tests of drip-proof protected and totally-enclosed motors with and without fans indicate that motor components do not readily transduce this fan noise into vibration.

Fan noise has received considerable attention in the past, not only with respect to electric motors, but other types of equipment such as blowers and air conditioning units. The method of reducing fan noise are generally well known and will only be reviewed in this section where they apply to specific noise-producing areas in drip-proof protected and totally enclosed motors.* In addition, special fan dimensions and configurations were fabricated and tested to establish the degree of noise reduction attainable by deviating from high production, bi-directional fan designs.

Fan noise consists of three principal components which are treated in the following subsections:

5.2 Turbulence Effect

5.3 Siren Effect

5.4 Whistling Effect

The means of reducing fan noise are summarized in the conclusion of this section.

5.2 TURBULENCE EFFECT

Air turbulence noise is random frequency noise caused by vortices in the airstream, or, more specifically, any lateral component of air velocity. The air turbulence may be produced by either the fans moving relative to the airstream or the airstream moving relative to a stationary member. Minimizing this noise calls for the elimination of sharp edges and burrs on all parts in contact with the airstream. It requires aerodynamically designed fans, fan bowls, and, in fact, the entire airstream path. The airstream path through a drip-proof protected motor does not lend itself to aerodynamic design to the degree that the airstream over a totally-enclosed motor does. Therefore, minimizing the air turbulence effect of these two types of motors is treated separately.

5.2.1 Drip-proof Protected Motors

Drip-proof protected motors are cooled by air drawn into the interior of the motors and over the exposed winding and core by internal fans. Most manu-

*For a more extensive treatment of fan noise in general, the reader is referred to Chapter 25, Handbook of Noise Control (Reference 18 in Bibliography).

facturers use fan blades cast as an integral part of the rotor end ring, and these fan blades are invariably of a purely radial design. This construction is dictated by the desirability of the bi-directional operation.

Two cooling methods are presently used: end-to-end and end-to-center. In the end-to-end method, the cooling air is drawn in through one bearing housing and exhausted out the other bearing housing, which does not contain an air deflector. The rotor fan blades at this end serve only to prevent dead air spaces and resulting hot spots. In end-to-center construction, air is drawn in through both bearing housings and exhausted through openings in the motor frame. This method results in more uniform cooling; therefore, less air is needed.

The most effective way of reducing fan noise is to reduce the amount of air drawn in by the fan. Low current and flux densities should be incorporated into the motor design. Also, sufficient steel and iron must be used to conduct the internally generated heat away to the exterior of the motor, where the motor may lose this heat by convection and radiation. The rate of heat transfer is a function of the temperature difference between motor and the surrounding atmosphere i.e., the temperature rise. A quiet motor should be designed to operate at a temperature near the insulation class limit to fully utilize the insulation and to optimize the efficiency of heat removal.

Economy of manufacture has prompted industry to use one rotor end ring die for motors with more than one rating or speed, i.e., a four and a six pole motor may have the same fan. This results in economical construction rather than the most quiet or most efficient cooling system. The optimum fan blade length is a function of many variables such as the physical geometry of the air path, the amount of heat generated, and the amount of heat removed by radiation or conduction. A general formula for determining the length of fan blade would be complex and can better be determined experimentally. The experimental method consists of multiple heat runs with varying fan blade lengths.

This method is illustrated by the following test of the effect of shortening the axial length of cast rotor fan blades of two motors:

- 1) a 3 HP, 2 Pole, 184 frame open motor and
- 2) a 3 HP, 4 Pole, 184 frame open motor

The two pole rotor core had a 4 inch O.D. and was 3 inches long. The corresponding four pole dimensions were 4½ and 3½ inches respectively. The airborne noise and temperature rises were measured for the original fan blade lengths and for various fractions of these lengths.

The airborne noise produced by these motors at varying fan blade lengths was so nearly identical that only the curve for the two pole motor is plotted in

Figure 5-1. The airborne noise curve is a plot of the overall sound pressure levels recorded 3 feet from the front end of the motor which are representative of those recorded at other positions. (See Spectrograms 5-1 & 5-2) Reducing the fan blade length resulted in a decrease in airborne noise except at zero length. This increase in noise is probably caused by the balancing method. Since the balancing lugs were also removed for the zero length test, holes were drilled in the end ring. These spectrograms reveal that the predominant peaks of airborne noise most effectively reduced by shortening the die cast rotor fan blades were at 250 and 800 cps bands. The latter frequency band was the highest in the sound pressure level spectrum, and a reduction of this band, therefore, results in a corresponding decrease in the overall level.

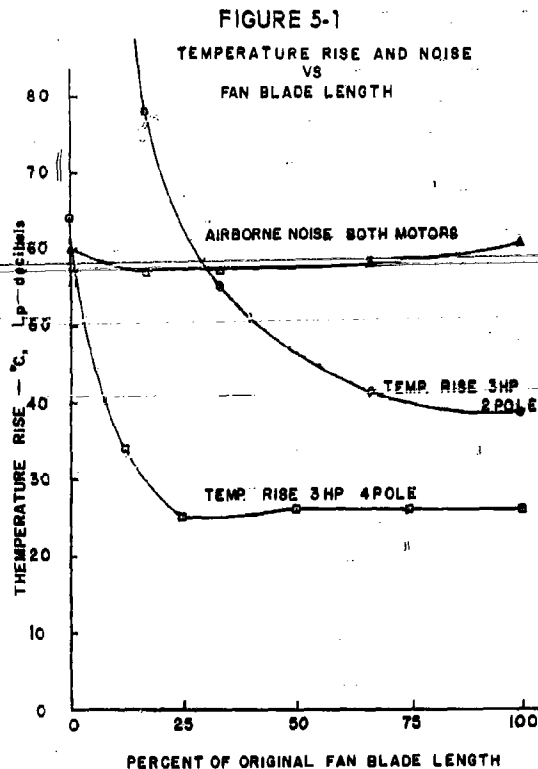


Figure 5-1 reveals that the temperature rise vs. fan blade curve of the four pole motor has an initial sharp decrease, rises slightly, and then becomes level. Notice that the motor has a slightly lower temperature rise at 25% fan blade length as with the original fan blades. The 25% fan blade length moves a volume of air at a velocity sufficient to remove the heat at the same rate as it is generated. The remaining 75% serves only to create additional fan noise and windage losses. This minimum temperature rise occurring between the steeply sloped and the level sections has been observed on a number of units and is always

only a few degrees below the "level" temperature rise. Thus, this minimum is mainly of academic interest. However, it illustrates the ineffectiveness in increasing the fan blade length beyond a certain point.

Note that this motor not only has excess fan blade length but also operates at a temperature considerably below the insulation class limit (40°C for a class A motor). Therefore, for minimum noise the fan blades should be shortened to less than 25% of the original length. Because of the steepness of the curve in this region a tolerance for production variation should be used.

The temperature rise curve of the two pole motor closely resembles and expanded curve of the 0 to 25% region of the four pole motor. This two pole motor illustrates a motor with the optimum fan blade length for class A insulation. If this motor had class B insulation the fan blade should be shortened to 30% - 40% of the original length to take advantage of the 4db decrease in sound pressure level.

It is recommended that the fan blade length of dripproof protected motors be chosen to result in a temperature rise slightly under the insulation class limit to allow for production variation. New end ring dies can be made, or the fan blades made by existing end ring dies may be shortened at the same time the motor is turned down for the air gap.

An attempt to realize less fan noise was made by limiting the motor to one direction of rotation. Several backwardly inclined fabricated fans were fastened to the rotor of the two pole motor which had the fan blades removed, as shown in Figure 5-2. Table 5-1 reveals that these units produced almost identical airborne readings for various temperature rises as those for the standard (radial, die-cast) fan. The 15 and 60 degree designations in Table 5-1 refer to the intersection angle between tangents at the extreme ends of the curved blades.

FIGURE 5-2

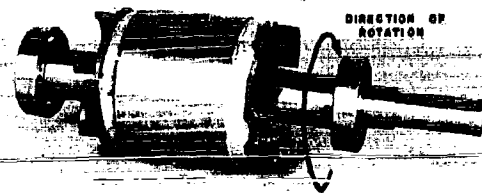


TABLE 5-1
Unidirectional Fans for Dripproof Motors
Sound Pressure Levels

Band	Axis	Radial	Backward 15°	Inclined 60°
200	Front	37	40	35
	Side	36	35	32
250	Front	46	47	44
	Side	44	43	42
315	Front	52	52	52
	Side	52	52	54
400	Front	50	50	46
	Side	51	52	47
800	Front	49	48	44
	Side	53	51	49
Overall	Front	59	59	58
	Side	60	60	59

Values taken from Spectrograms 5-3 through 5-5.

The lower air velocity and turbulence over the trailing edges of a backwardly inclined fan blade, as opposed to a radial blade, should result in a quieter operation with unidirectional fans. The reason all test data failed to reveal this noise reduction lies in the airstream path of a dripproof induction motor. The turbulence through and around the air deflectors and irregular end windings, over the stator core, and between the ribs supporting the stator assembly is large compared to the fan turbulence and cannot be eliminated. It can only be minimized through the optimization of heat flow as previously described. Unidirectional fans for dripproof protected motors do not appear to cause any reduction of noise.

5.2.2 Totally-Enclosed, Fan Cooled Motors

TEFC motors are cooled by an external fan which blows air over the motor surface. The frame and bearing housings are often ribbed to provide a large cooling surface. This air flow path can be streamlined. The greatest improvement can be realized by an aerodynamic design of the fan and fan bowl. Use of a purely centrifugal fan causes two abrupt changes in the air stream. First, when the air drawn into the fan bowl has its direction changed from axial to spiral. Second, when the spiral airstream strikes the fan bowl, and becomes helical in shape.

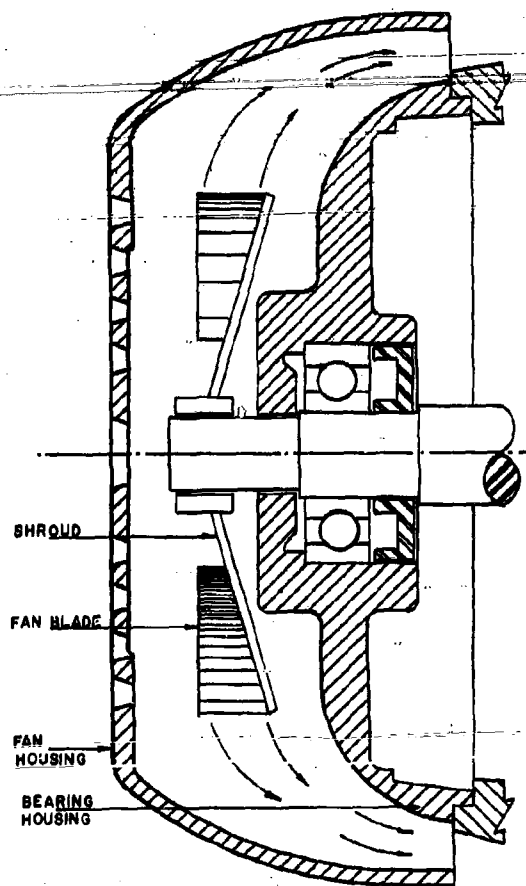
While more than one solution is possible, the use of a fabricated unidirectional fan (Figure 5-3) and properly shaped fan bowl has been found to be highly effective. This fan relies upon a conical-shaped shroud to cause the airstream to make only a partial change to a helical direction. The backwardly curved fan blades direct the air spirally outward with a minimum of air turbulence. The fan bowl is so shaped that in conjunction with the bearing housing, the airstream is gradually directed over the surface of

the motor as shown in Figure 5-4. Spectrogram 5-6 reveals the use of such a combination to result in a 7db decrease of the overall noise produced by a 40 HP motor over that produced by the propeller type unidirectional fan, originally used.

FIGURE 5-3



FIGURE 5-4



5.3 SIREN EFFECT

The siren effect is caused by the tips of the fan blades, or other components acting as fan blades, passing close to a series of protruding stationary members. The frequency of fan blade noise is the rotational frequency times the number of fan blades.

$$f_{fb} = \frac{\text{RPM}}{60} B \approx \frac{120 B}{P}$$

where f_{fb} = fan blade frequency in cps

B = number of fan blades

P = number of poles

The fan housing of totally enclosed motors amplifies the second harmonic of f_{fb} which often becomes the highest airborne noise frequency.

The number of fan blades should be chosen to avoid any prominent frequencies of noise produced by other sources. It can be seen from the above equation that, if the number of fan blades is the same as the number of poles, 120 cps noise will be produced. Since 120 cps noise and vibration will always be produced by the force waves of 60 cps induction motors, the number of fan blades should never equal the number of poles. It was shown in Section 4 that ball bearings produce two frequencies which may be approximated by the expression $F = E \times \frac{1}{2}$ (Equation 4-7). To prevent adding to the levels at this frequency, the number of fan blades should not equal half the number of rolling elements. In addition to avoiding discrete frequencies, the fan blade frequency should not lie within any prominent band of frequencies such as the preload band, or the number of blades should not equal $f_c \times P/120$ where f_c equals the center frequency of the objectionable band.

In dripproof protected motors, rotor fan blades do not normally pass close enough to any stationary irregularity to produce an appreciable siren effect. Even in totally-enclosed motors with external fans, the siren effect may be eliminated by increasing the clearance between the fans and stationary parts. It is recommended that the bearing housing at the fan end not have external ribs.

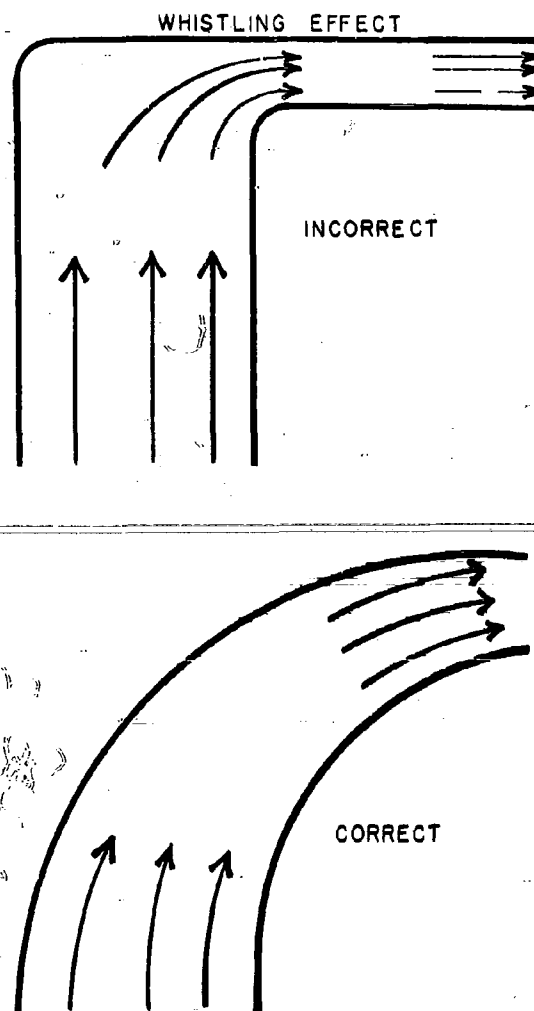
A treatment of the siren effect caused by radial rotor and stator air ducts, utilized in motors above 100 HP, may be found in the 1957 AIEE Transactions. (See reference 19 in the Bibliography)

5.4 WHISTLING EFFECT

Any constriction, especially a sudden one, of the airstream path produces a whistling effect. The frequency of this whistle is dependent upon many factors such as the size of the constriction and the volume of air. The necessary preventive (or corrective) measures are elimination of constrictions and rounding the

edges of unremovable obstructions. Figure 5-5 illustrates the elimination of causes of whistling noise.

FIGURE 5-5



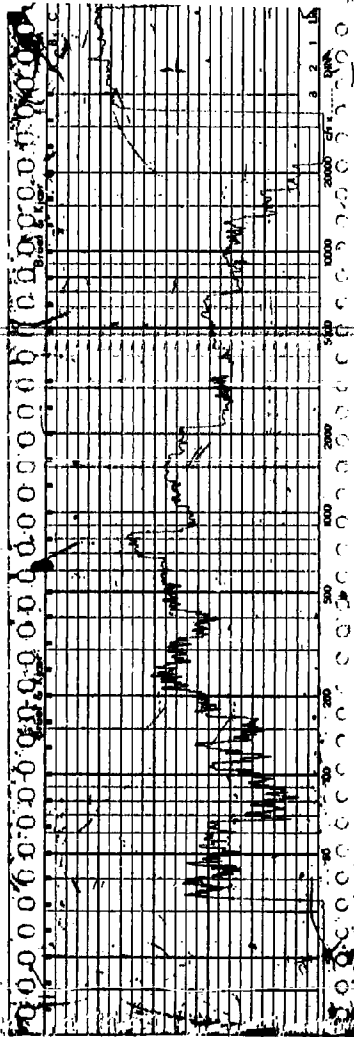
5.5 CONCLUSION

Fan noise of induction motors may be minimized by these means:

- 1) The number of fan blades should be chosen to avoid producing the same frequency noise as produced by other sources. The important combination to be avoided are:
 - a. Number of fan blades equal to number of poles (120 cps).
 - b. Number of fan blades equal to $\frac{1}{2}$ number of rolling elements in the ball bearing.

- c. Number of fan blades equal to $f_c P / 120$ where f_c equals the center frequency of any objectionable band.
An odd number of blades minimizes pulsations caused by blades passing near symmetrically located ribs, etc.
- 2) Within the range of acceptable performance, cost and weight, the amount of cooling air necessary will be reduced by:
 - a. Use of low current and flux densities to minimize generated heat.
 - b. Use of sufficient iron and steel to convey generated heat to motor frame.
 - c. Full load operation at a temperature near the insulation class limit.
 - d. Use of higher temperature insulation systems.
 - 3) The more efficient end-to-center cooling method should be used for dripproof protected motors.
 - 4) The minimum axial length of fan blades of dripproof protected motors should be determined for each motor design for noise-sensitive applications.
 - 5) Use of a backwardly inclined conical shroud behind the fan of a 40 HP, 2 pole totally-enclosed motor reduced the overall sound pressure level by 7db. A similar shroud design is recommended for both unidirectional and bi-directional fans on totally-enclosed, fan-cooled motors.
 - 6) Clearance between fans and stationary parts should be sufficient to prevent a siren effect. The wide range of motor sizes, speeds, and constructions precludes the determination of a numerical value for a permissible minimum clearance. Greater attention to this factor is needed for externally fan cooled motors than for dripproof protected motors with integral fan blade - endring construction.
 - 7) Sharp turns and constrictions in the airstream path should be eliminated. The areas that require special attention are:
 - a. The external fan housing opening and exhaust.
 - b. The intake and exhaust ports of dripproof protected motors. Screening with a large percentage of open area should be used.
 - c. Area between air deflector and end turns.
 - 8) Sharp edges in the airstream path should be eliminated. Parts in contact with high velocity air should be given prime consideration.
 - a. The fan should be smooth and free from burrs, blow holes, etc.
 - b. The fan bowl should present no sharp edges to the airstream. A cast fan bowl is preferable to a fabricated sheet steel one. If sheet steel is used, the edges should be rounded during the stamping process and coated with plastic or a similar material.

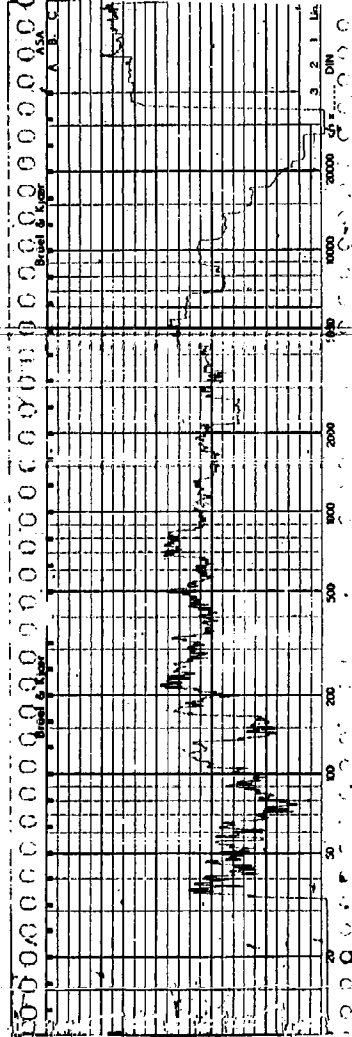
70 db



20 db

Fan Blade Length
 3 HP 2 Pole
 184, Frame Open
 26 August 1959
 Airborne
 3 Ft. Front End
 Full Fan Blade

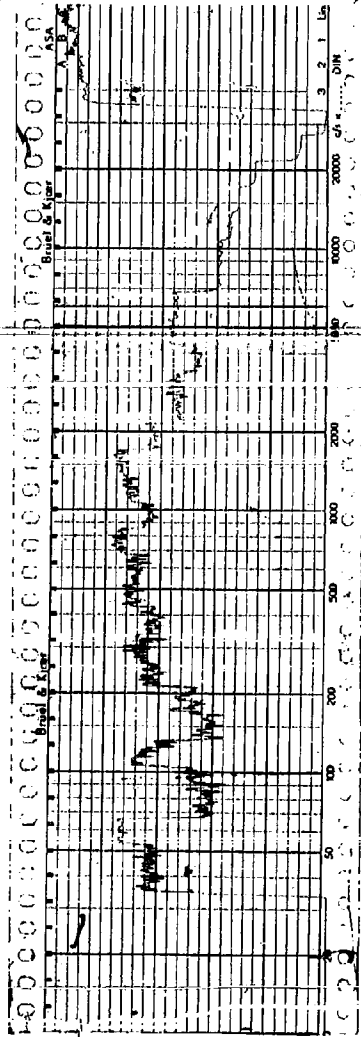
70 db



20 db

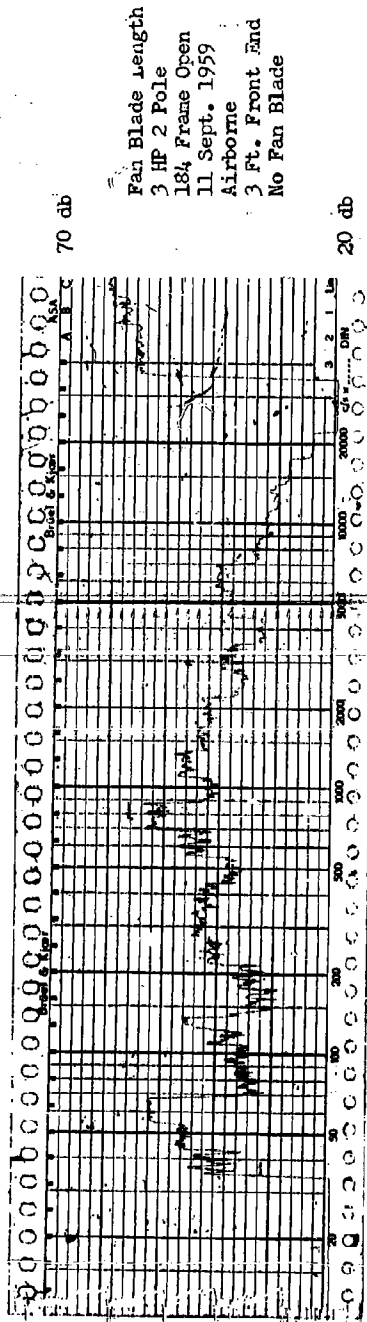
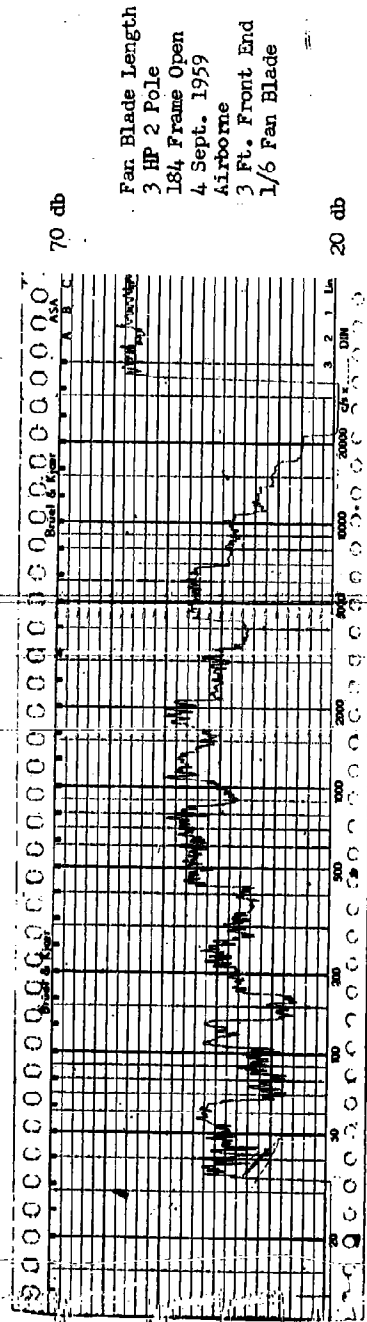
Fan Blade Length
 3 HP 2 Pole
 184, Frame Open
 31 August 1959
 Airborne
 3 Ft. Front End
 2/3 Fan Blade

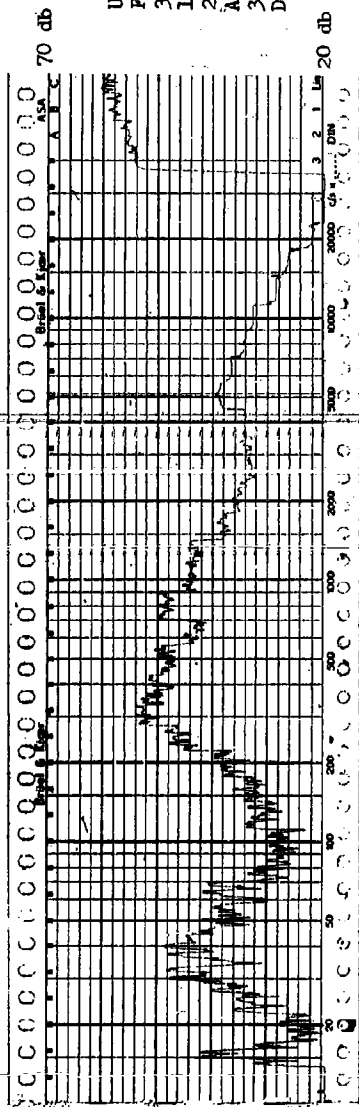
60 db



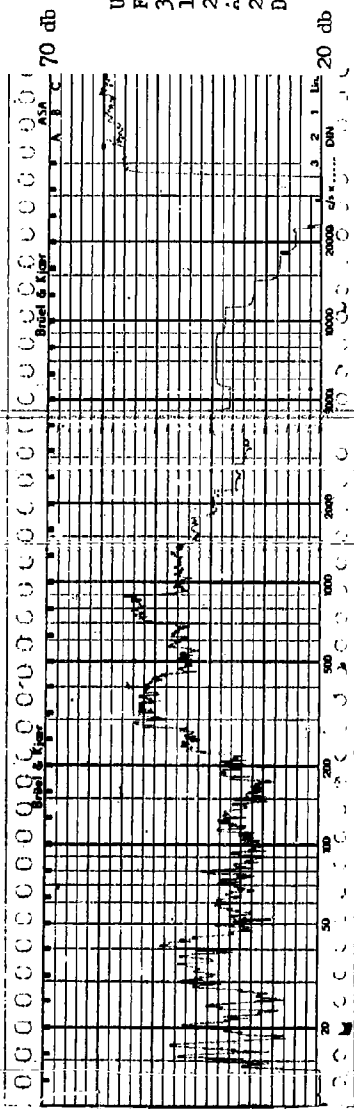
10 db

Fan Blade Length
 3 HP 2 Pole
 184, Frame Open
 2 Sept. 1959
 Airborne
 3 Ft. Front End
 1/3 Fan Blade

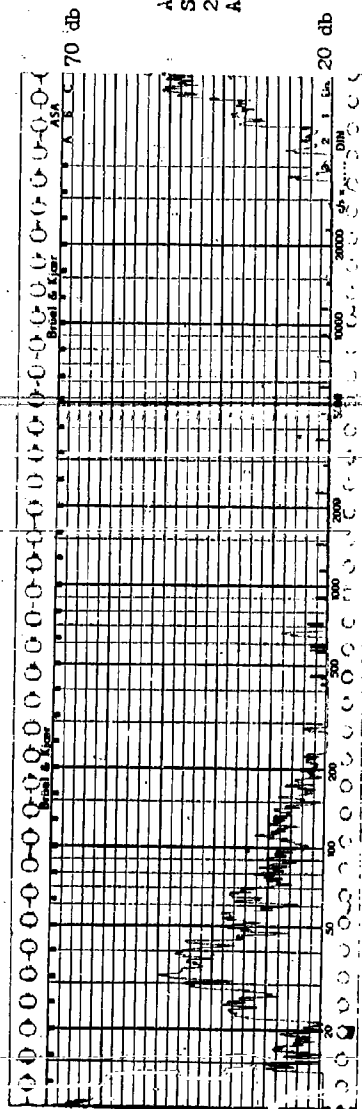




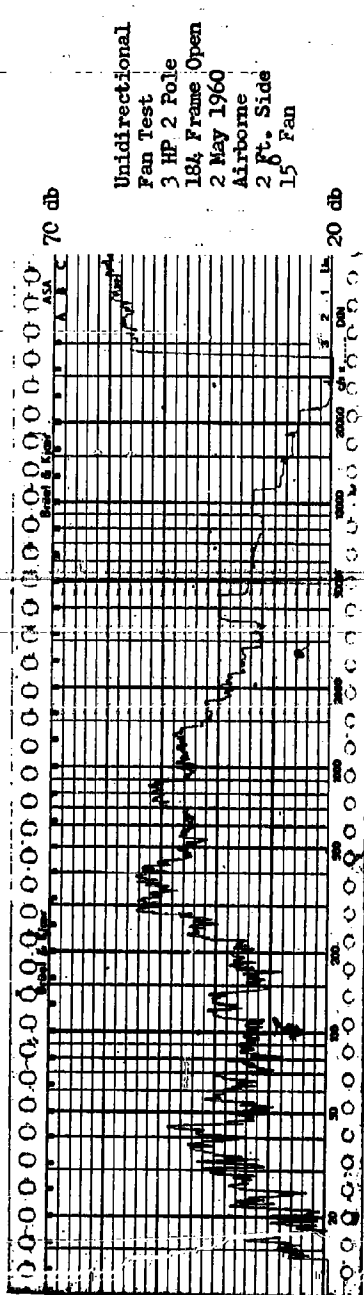
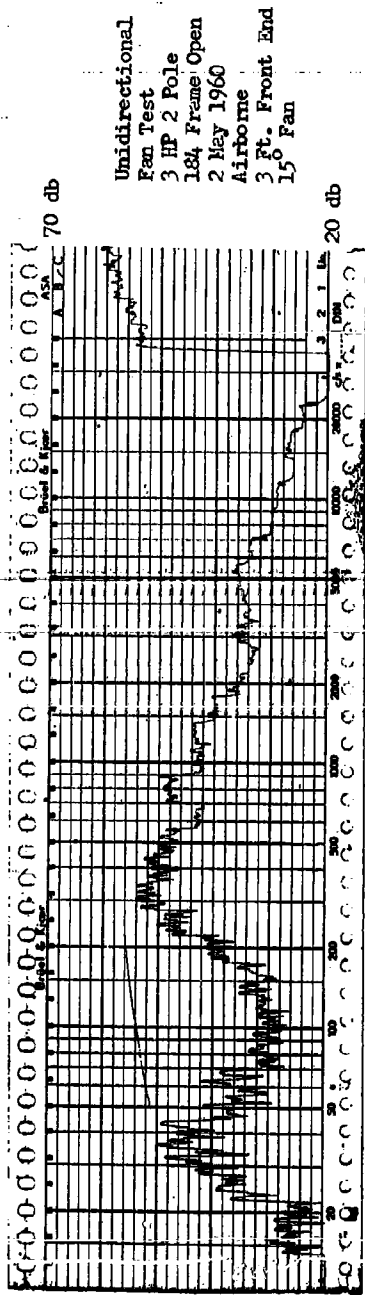
Unidirectional
 Fan Test
 3 HP 2 Pole
 184 Frame Open
 2 May 1960
 Airborne
 3 Ft. Front End
 Die Cast Fan

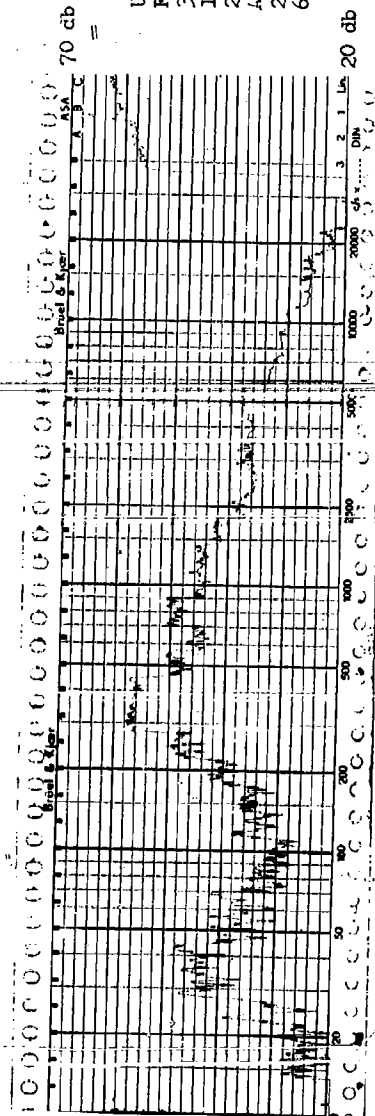
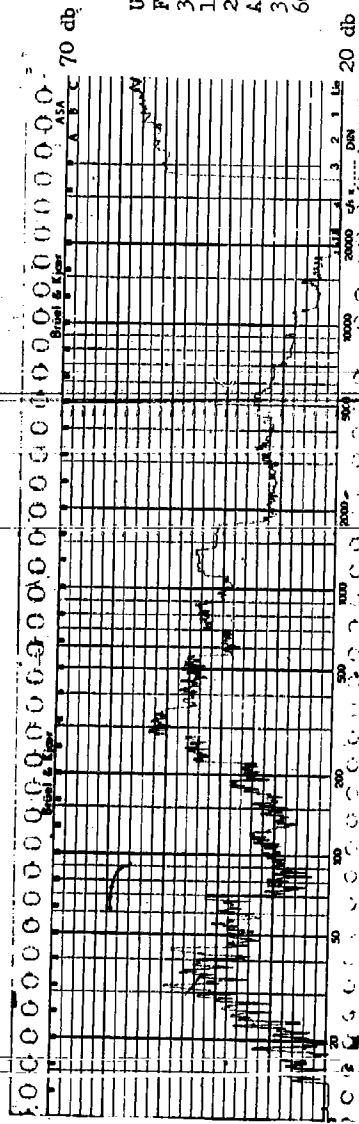


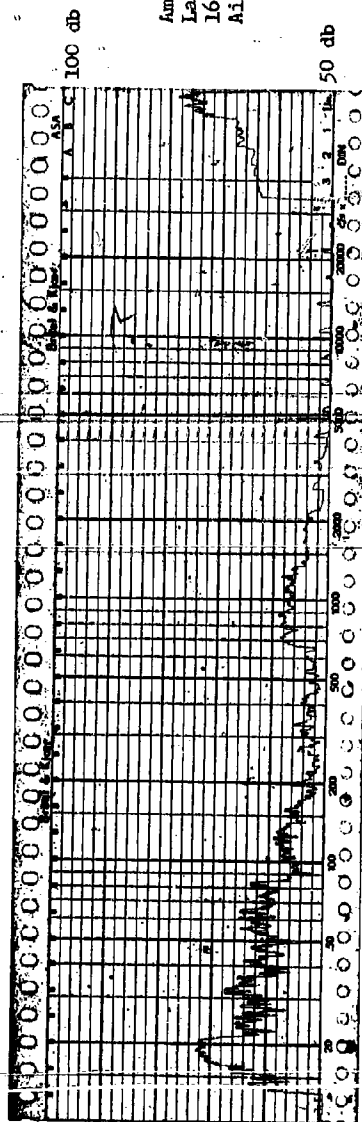
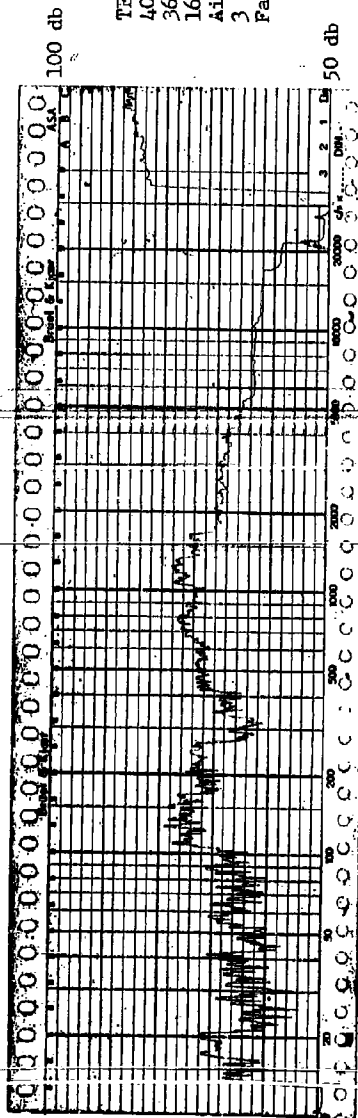
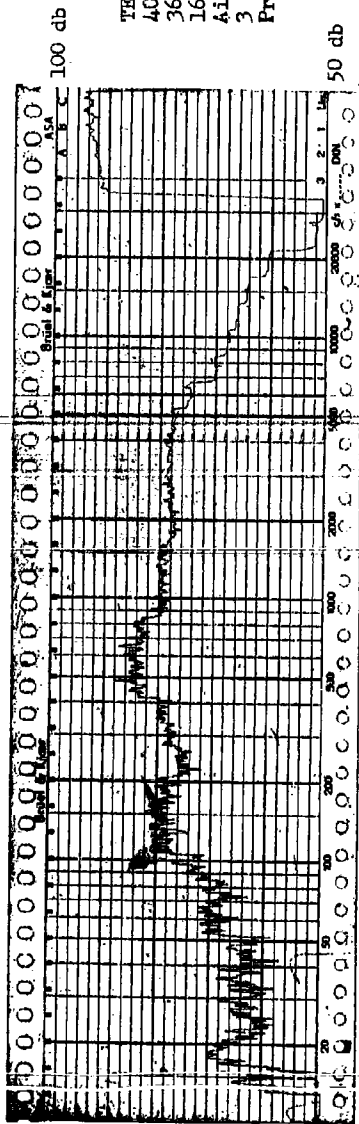
Unidirectional
 Fan Test
 3 HP 2 Pole
 184 Frame Open
 2 May 1960
 Airborne
 2 Ft. Side
 Die Cast Fan



Ambient
 Sound Room
 2 May 1960
 Airborne







SECTION 6 UNBALANCE NOISE

6.1 INTRODUCTION

At the commencement of this contract, extensive studies of the effect of motor unbalance were planned by the Naval Engineering Experimental Station. It was decided to concentrate on other aspects of motor noise rather than duplicate this work. However, certain preliminary work was necessary to relate unbalance with other motor noise sources. A discussion of this work and of the causes of unbalance noise are presented in this section.

Unbalance primarily produces rotational frequency noise. The rotational frequency of a 60 cycle induction motor at any load is

$$f_r = 120 \times \frac{(1-s)}{P}$$

where f_r = rotational frequency in cycles per second

s = slip in per unit

P = number of poles

The unbalance noise produced by two pole motors is approximately 60 cycle noise; that produced by four pole motors is nearly 30 cycles; etc. The second harmonic of rotational frequency has been observed under conditions of extreme unbalance.

6.2 CAUSE OF UNBALANCE NOISE

In rotating machinery, unbalance noise is produced by an unequal weight distribution of the rotating member around the axis of rotation. This uneven weight distribution of the rotor assembly of induction motors is caused by

- 1) Voids in cast aluminum bars and end rings
- 2) Non-uniformity of core steel
- 3) Keyways
- 4) Out-of-roundness of machined surfaces
- 5) Eccentricity of machined surfaces with axis of rotation
- 6) Eccentric location of slots

In addition, lack of shaft rigidity and looseness of fits will permit rotor assembly to deflect under unbalanced magnetic forces. This deflection will rotate with the rotating flux wave, thus creating a cam effect.

6.3 RELATIVE EFFECT OF UNBALANCE NOISE

The degree of balance is usually specified in terms of the motor vibration caused by the unbalance. The dynamic balance vibration is measured on the bearing housing in the direction giving the maximum amplitude. Table 6-1 lists the maximum allowable

amplitude of this vibration as specified in MIL-M-17060B. Note that the vibration is specified in displacement units (mils), whereas the unit of acceleration decibels is coming into prominence for vibration measurement. Displacement values may be converted into acceleration levels at a specified frequency but the frequency bandwidth of balance vibration measurement is not specified.

TABLE 6-1
Dynamic Balance Vibration

Weight of motors Pounds	Maximum allowable total amplitude		
	Standard balance Mils	Precision balance Mils	Super-precision balance Mils
Up to 350	1.0	0.5	0.2
From 351 to 800	1.5	0.75	0.3
From 801 to 2,000	2.0	1.0	0.4
From 2,001 and up	3.0	1.5	--

A test was conducted to determine the relationship between balance measurements taken with an IRD dynamic balancing device on the bearing housing and readings taken there and at other places with the Bruel & Kjaer equipment described in Section 2. A 5 HP, 2 Pole, 184 frame open motor was equipped with special bearing housings to permit addition of balance weights to the end ring lugs without motor disassembly. This motor had initial displacement measurements of .25 and .20 mils on the front and rear bearing housing hubs respectively. Weights were added to the rear end ring to increase the unbalance at that end while the displacement at the front end was maintained at .25 mils. Acceleration readings were taken with the B & K equipment on the three axis on the motor feet and an axial and a radial axes on the rear bearing housing hub. The radial hub reading was taken at the same point as the displacement readings. The test data for rear bearing hub displacements of .20, .45, .85, and 1.70 mils respectively are furnished in Table 6-2.

TABLE 6-2
Balance Test
Vibration Acceleration Levels

Band	Axis	Rear Bearing Hub Displacement in Mils			
		.20	.45	.85	1.70
63	X	85	93	97	102
	Y	78	83	90	105
	Z	82	86	90	105
	Axial	79	78	81	82
	Radial	81	94	102	107
125	X	78	79	78	79
	Y	89	88	88	89
	Z	79	80	80	82
	Axial	75	74	79	83
	Radial	79	80	72	74

Continued on next page

Band	Axis	Rear Bearing Hub Displacement in Mils			
		.20	.45	.85	1.70
200	X	88	89	84	80
	Y	*	71	*	*
	Z	72	71	72	71
	Axial	84	80	80	80
	Radial	78	72	73	74
500	X	77	76	78	78
	Y	83	82	79	82
	Z	87	82	83	82
	Axial	97	98	99	99
	Radial	100	104	99	105
2000	X	89	88	87	86
	Y	93	94	88	88
	Z	97	96	96	96
	Axial	84	84	83	83
	Radial	89	88	89	90
4000	X	91	92	91	92
	Y	98	98	96	96
	Z	96	97	97	93
	Axial	85	84	84	85
	Radial	90	89	89	88
8000	X	102	102	103	104
	Y	98	97	94	97
	Z	100	101	101	102
	Axial	101	91	91	91
	Radial	102	103	102	101
Overall	X	106	106	107	109
	Y	105	105	105	105
	Z	106	106	106	107
	Axial	110	111	110	110
	Radial	109	112	112	115

*Values less than 70 odb were below range of recording paper.

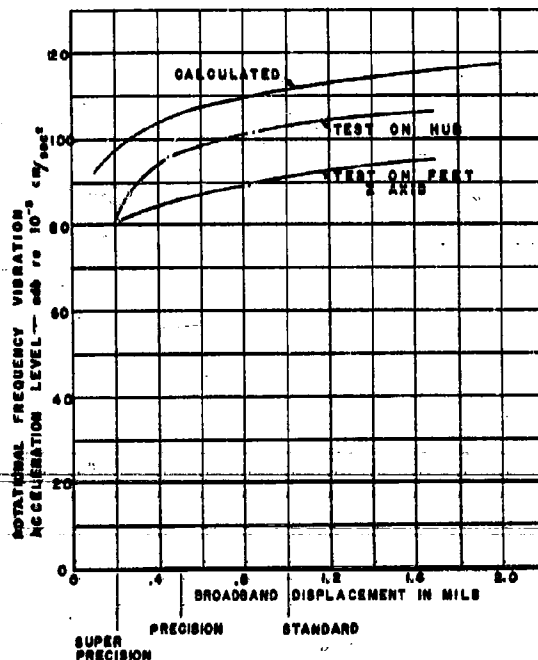
Values taken from Spectrograms 6-1 through 6-8.

The rotational frequency of this two pole motor lies within the 63 cps one-third octave. An investigation of the odb levels for this frequency band reveals that the radial axes (Y, Z, and Radial Hub) experience a greater change than the axial axes (X and Axial Hub). The 125 cps band shows little change on the X, Y, & Z axes while the hub axes reflect the time variation of 120 cycle noise explained in Section 7.3. The only remaining band with appreciable variation is the 200 cps band which once again reflects variation in preload force.

The 63 cps levels for the radial hub and Z axes are plotted as a function of the displacement measurements in Figure 6-1. The balance designations "super-precision", "precision", and "standard" are those listed in Military Specifications MIL-M-17060B for motors weighing less than 350 pounds. Note that the vibration decreases sharply in the region between the "precision" and the "super-precision" designations. Unfortunately, the achievement of a higher degree of balance also becomes more difficult in this region. The "hub" curve is lower than the calculated curve obtained by converting the displacement values to odb at the rotational frequency, 60 cps. This indicates the displacement values are broadband in nature

and are reflecting vibration of other than the rotational frequency which the 63 cps odb levels do not. The drop in odb values from the hub readings to those taken on the feet show the attenuation characteristic of the housing and yoke as a function of bearing hub displacement.

FIGURE 6-1



- This test reveals two points worthy of note.
- 1) Conversion of displacement levels to odb levels cannot be made with sufficient accuracy unless filters are used to reduce frequency band of balancing equipment.
 - 2) The bearing housings and yoke have a non-linear attenuation characteristics. Thus while specification of bearing housing hub movement is indicative of the unbalance vibration transmitted to the load, it is not necessarily indicative of the unbalance vibration transmitted to the substructure from the motor feet.

6.4 REDUCTION OF UNBALANCE NOISE

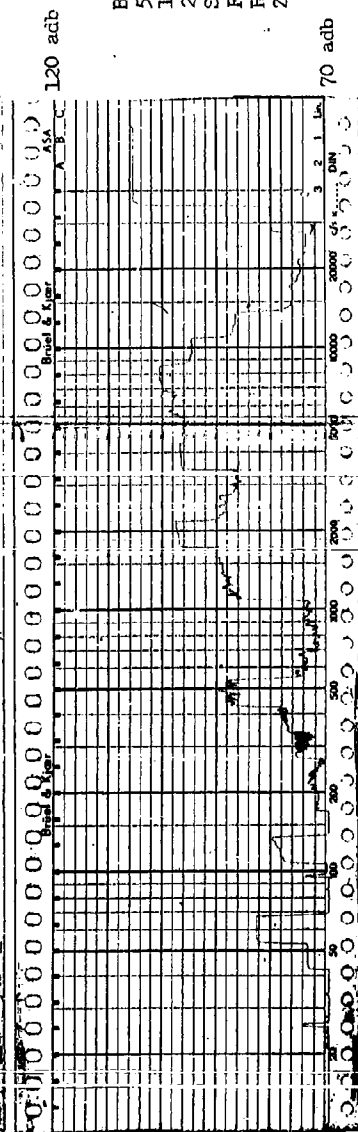
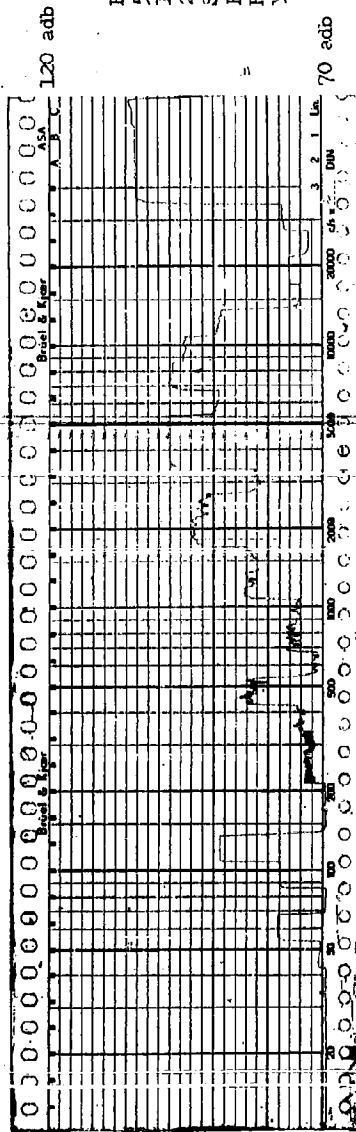
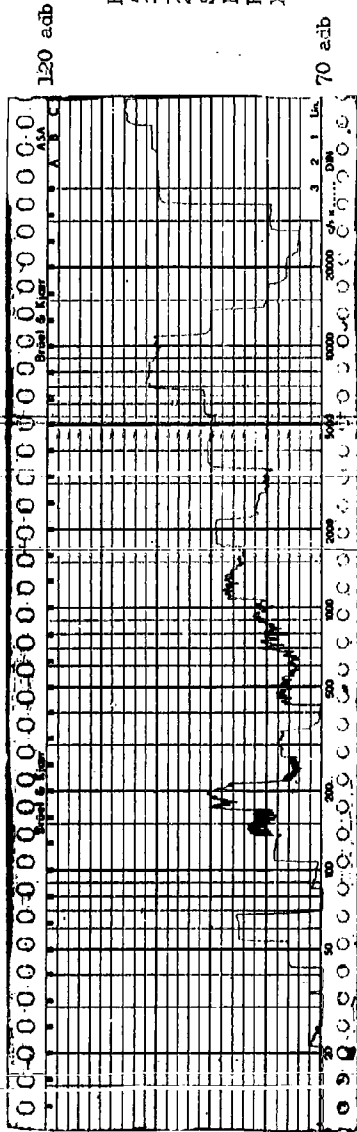
Reduction of unbalance noise falls into two categories: preventive and corrective actions. The preventative steps that may be taken are careful attention to tolerances and providing sufficient shaft rigidity to resist deflection under unbalanced magnetic forces. However certain sources of unbalance, such as small voids in the cast aluminum are difficult to control. Thus, there must be a method of correcting this uneven weight distribution. This is accomplished by either adding or removing weight at

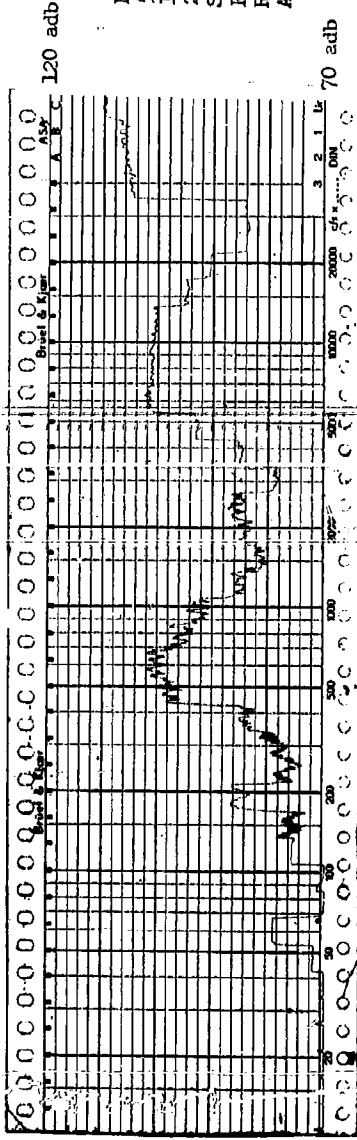
various points around the axis of rotation. Die-cast induction motors are usually balanced by the addition of small weights to lugs or cavities provided on the rotor end rings. In addition, motors for ultra-quiet application are often provided with external balance rings to facilitate in-place-balancing at the load site. The prototype motors were equipped with external balance rings and certain observations about their use are included in Section 9.

6.5 CONCLUSION

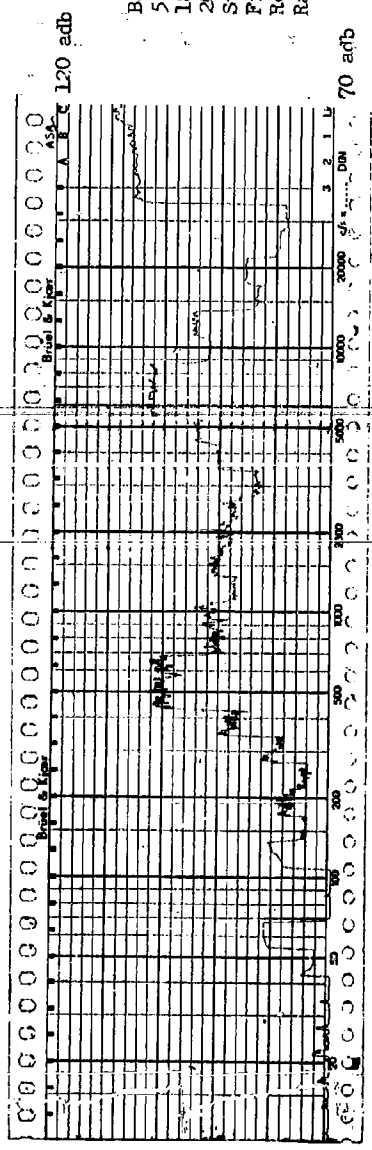
This section treats only a preliminary study of unbalance noise. The cause and nature of unbalance noise are described but the methods of reducing un-

balance are only outlined. As previously indicated, this phase of motor noise was not to be studied in detail here because of other scheduled work. It should be noted that of the four sources of motor noise, only unbalance may be directly attacked. Whereas the magnetic fields, bearings and fans are all necessary for motor operation, unbalance is a byproduct of manufacturing variations. The theory of reducing unbalance noise is exceedingly simple: Reduce the unbalance of the rotating component. However, the achievement and maintenance of the reduced value of unbalance becomes very difficult at low values of unbalance. The balancing work performed on the prototype motors (Section 9) is an example of the difficulties one may encounter.

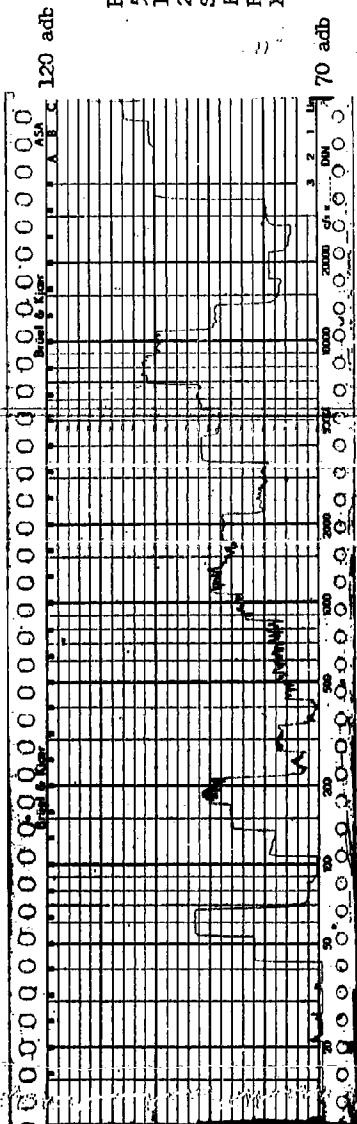




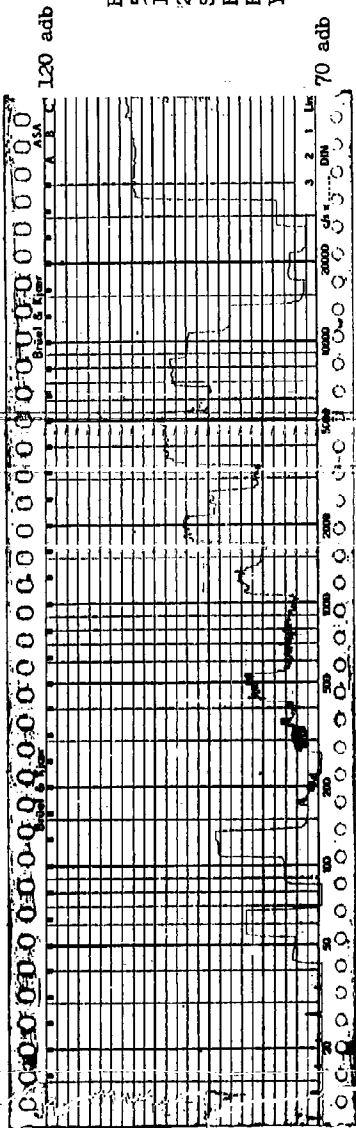
Balance Test
 5 HP 2 Pole
 184 Frame Open
 20 July 1960
 Structureborne
 Front .25 mills
 Rear .20 mills
 Axial Hub



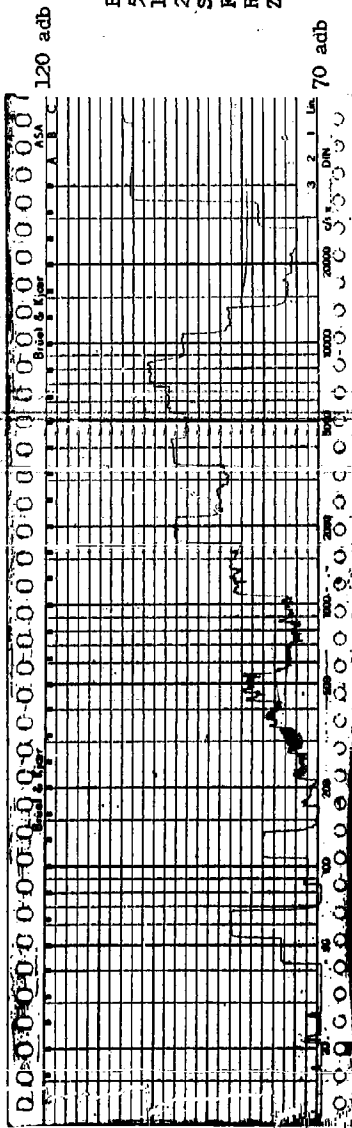
Balance Test
 5 HP 2 Pole
 184 Frame Open
 20 July 1960
 Structureborne
 Front .25 mills
 Rear .20 mills
 Radial Hub



Balance Test
 5 HP 2 Pole
 184 Frame Open
 20 July 1960
 Structureborne
 Front .25 mils
 Rear .45 mils
 X-Axis

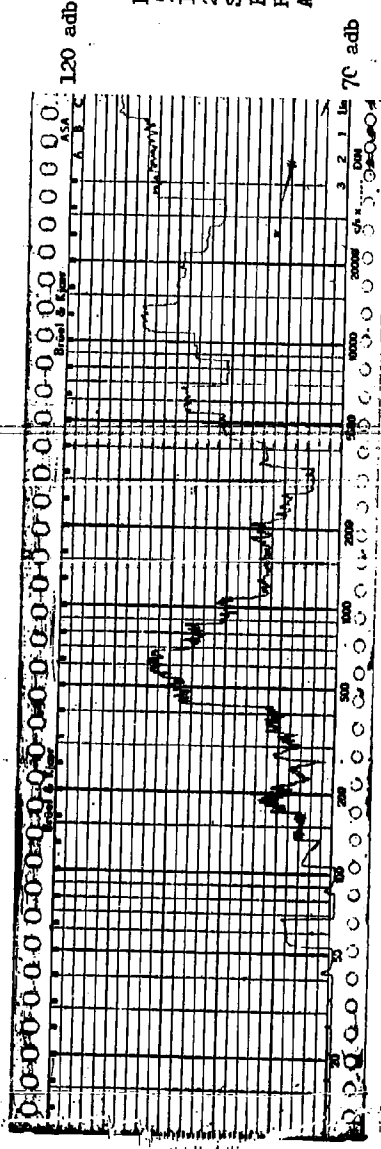


Balance Test
 5 HP 2 Pole
 184 Frame Open
 20 July 1960
 Structureborne
 Front .25 mils
 Rear .45 mils
 Y-Axis

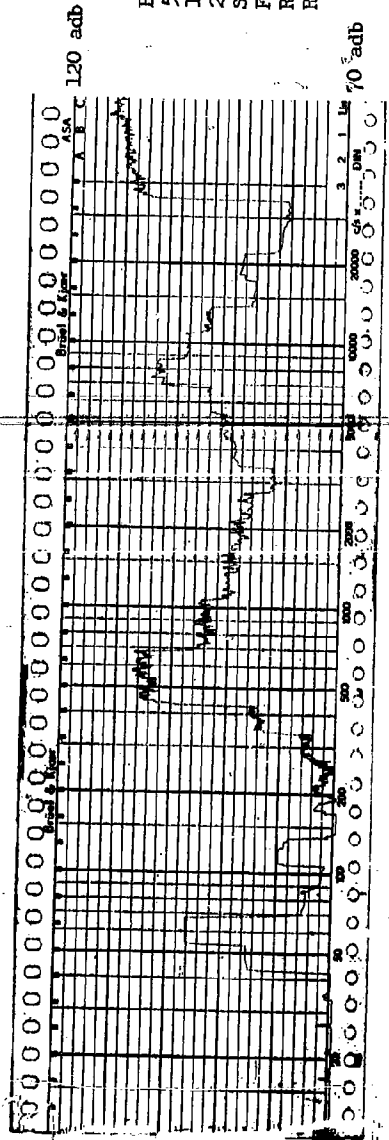


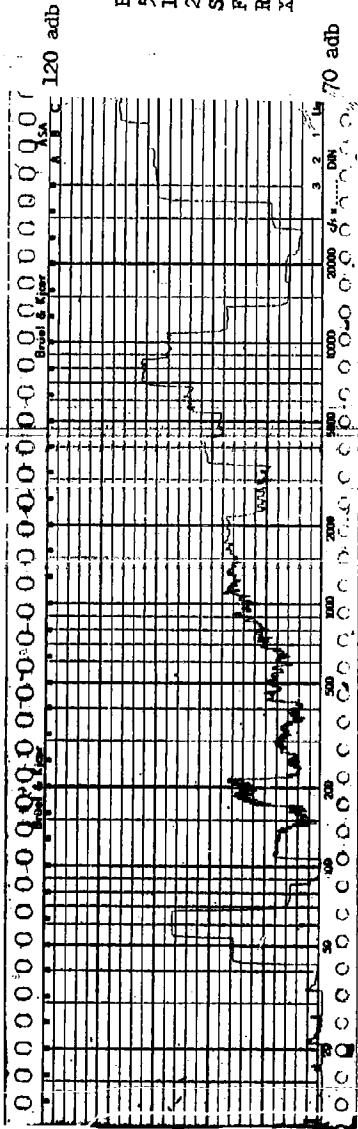
Balance Test
 5 HP 2 Pole
 184 Frame Open
 20 July 1960
 Structureborne
 Front .25 mils
 Rear .45 mils
 Z-Axis

Balance Test
 5 HP 2 Pole
 184 Frame Open
 20 July 1960
 Structureborne
 Front .25 mils
 Rear .45 mils
 Axial Hub

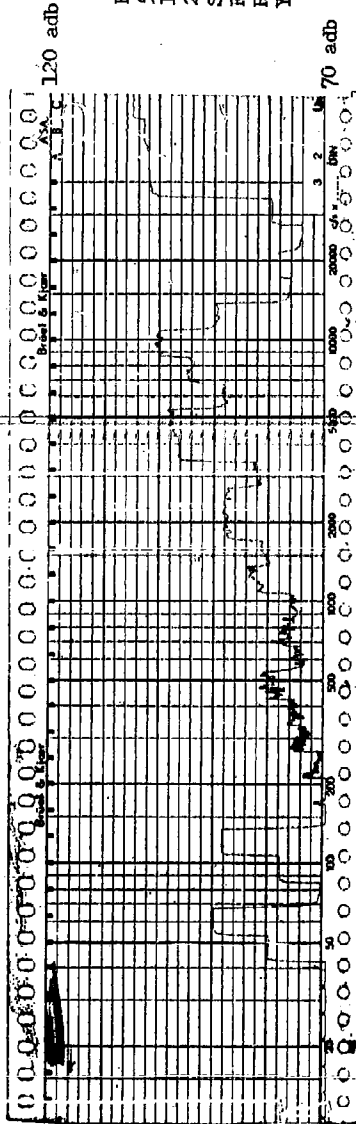


Balance Test
 5 HP 2 Pole
 184 Frame Open
 20 July 1960
 Structureborne
 Front .25 mils
 Rear .45 mils
 Radial Hub

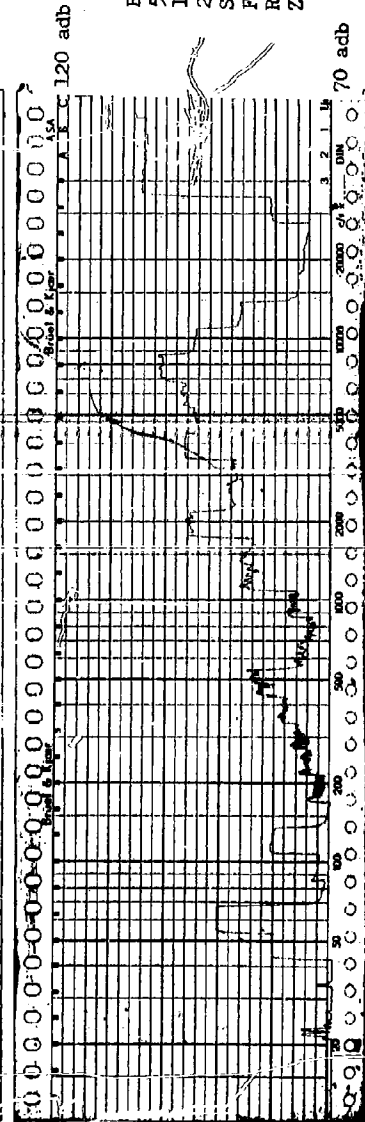




Balance Test
 5 HP 2 Pole
 184 Frame Open
 20 July 1960
 Structureborne
 Front .25 mills
 Rear .85 mills
 X-Axis

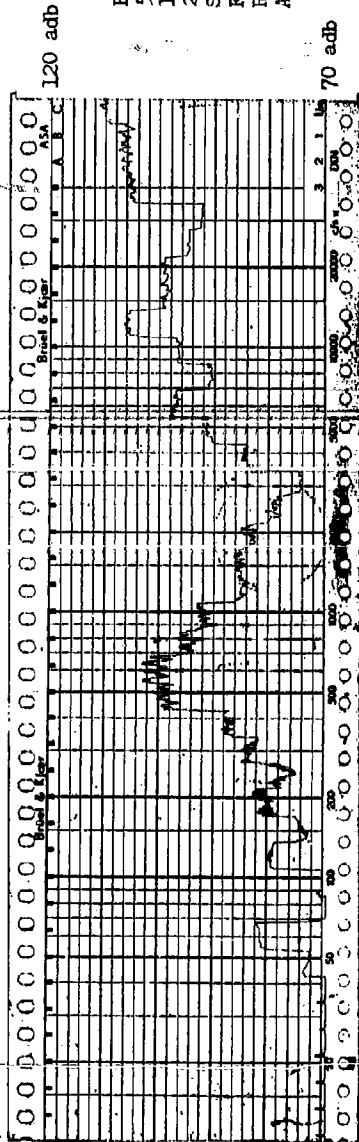


Balance Test
 5 HP 2 Pole
 184 Frame Open
 20 July 1960
 Structureborne
 Front .25 mills
 Rear .85 mills
 Y-Axis

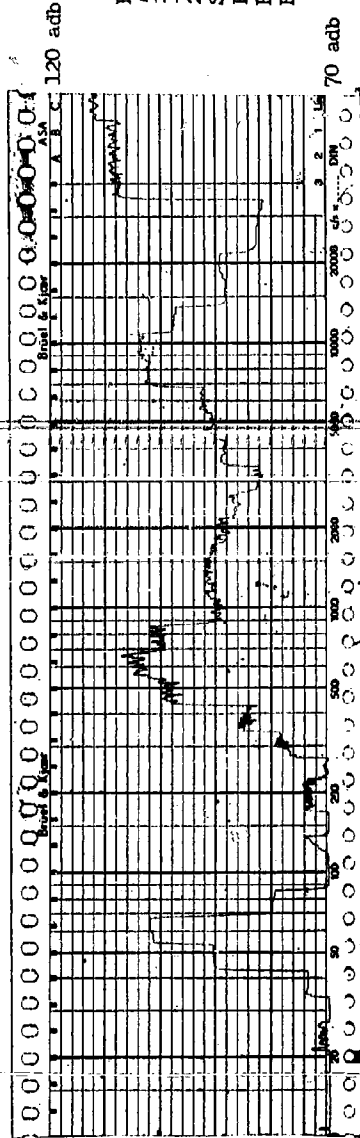


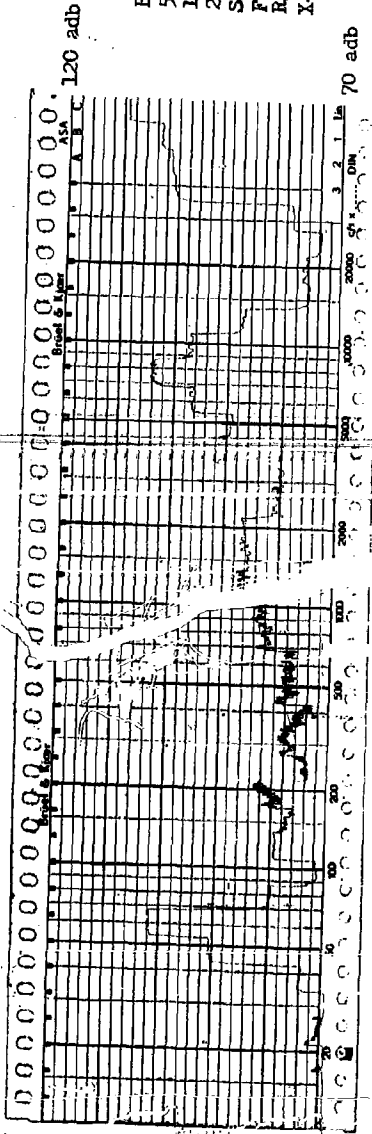
Balance Test
 5 HP 2 Pole
 184 Frame Open
 20 July 1960
 Structureborne
 Front .25 mills
 Rear .85 mills
 Z-Axis

Balance Test
 5 HP 2 Pole
 184 Frame Open
 20 July 1960
 Structureborne
 Front .25 mils
 Rear .85 mils
 Axial Hub



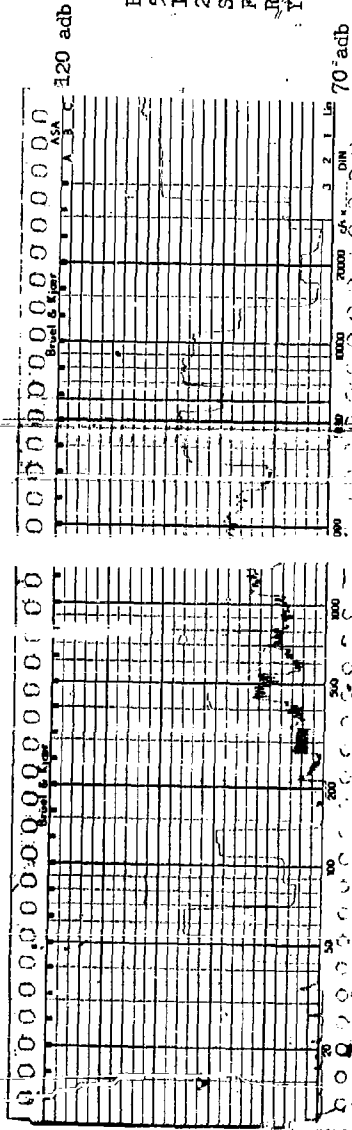
Balance Test
 5 HP 2 Pole
 184 Frame Open
 20 July 1960
 Structureborne
 Front .25 mils
 Rear .85 mils
 Radial Hub





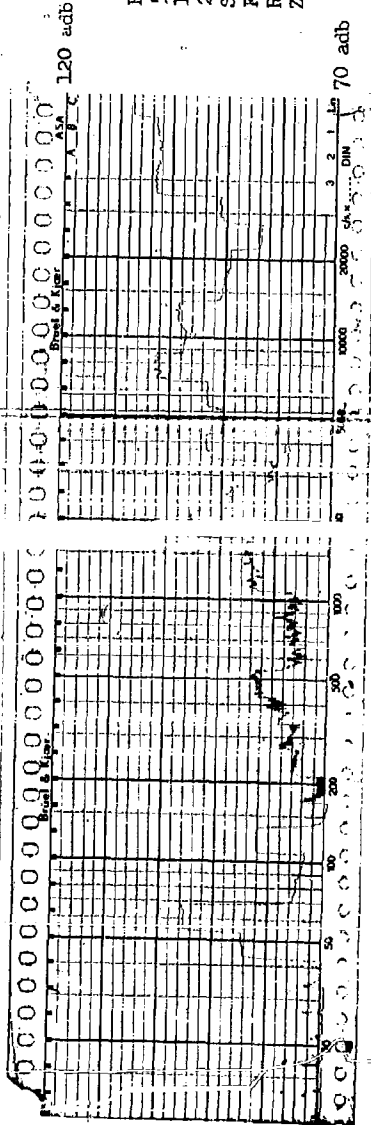
Balance Test
 5 HP 2 Pole
 184 Frame Open
 20 July 1960
 Structureborne
 Front .25 mills
 Rear 1.70 mills
 X-Axis

70 adb



Balance Test
 5 HP 2 Pole
 184 Frame Open
 20 July 1960
 Structureborne
 Front .25 mills
 Rear 1.70 mills
 Y-Axis

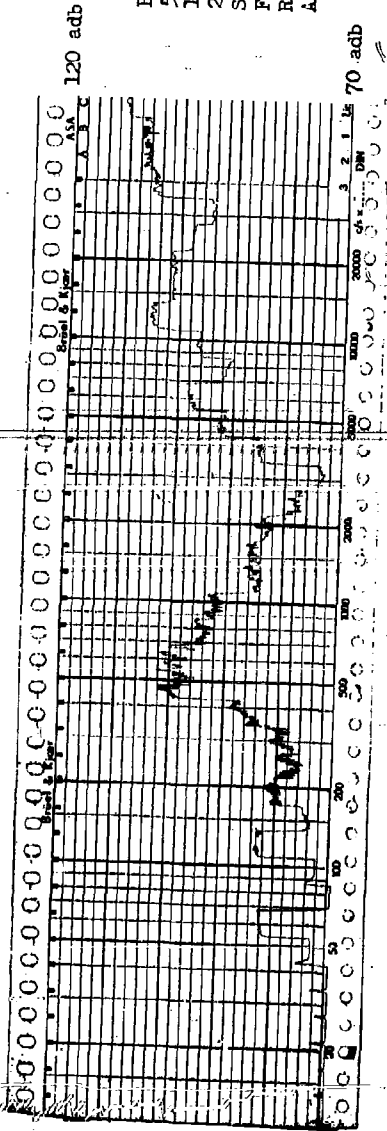
70 adb



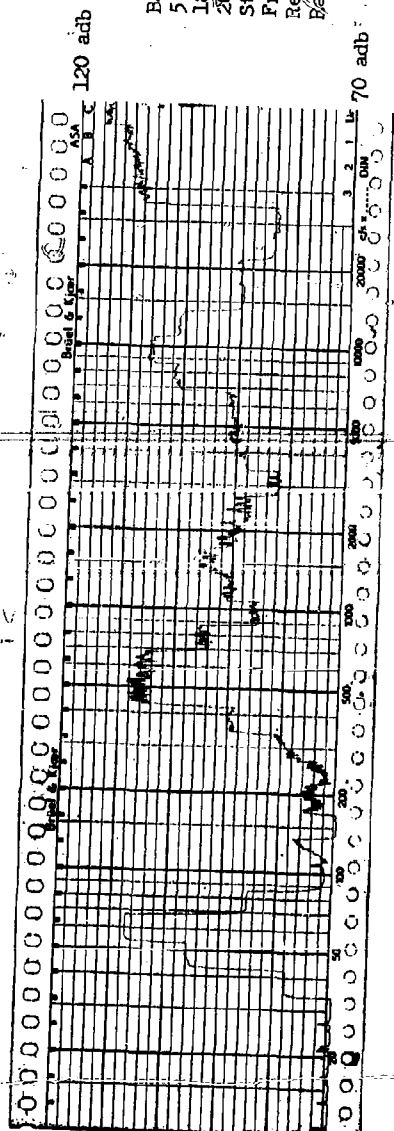
Balance Test
 5 HP 2 Pole
 184 Frame Open
 20 July 1960
 Structureborne
 Front .25 mills
 Rear 1.70 mills
 Z-Axis

70 adb

Balance Test
 5 HP 2 Pole
 184 Frame Open
 20 July 1960
 Structureborne
 Front .25 mills
 Rear 1.70 mills
 Axial Hub



Balance Test
 5 HP 2 Pole
 184 Frame Open
 20 July 1960
 Structureborne
 Front .25 mills
 Rear 1.70 mills
 Radial Hub



SECTION 7 EFFECT OF LOAD

7.1 INTRODUCTION

The degree of load may be shown to affect all four principal classifications of motor noise: magnetic, bearing, fan and unbalance. Few references in the technical literature consider the change in noise due to load, and no comprehensive treatment is available. The effects of load are shown to be dependent upon many factors, and methods of minimizing the difference between load and no load noise are presented. A proposed test procedure for determining this noise difference is also presented.

7.2 TEST MOTORS

Tests were conducted on two 5 HP, 2 Pole motors and one 40 HP, 4 Pole motor under varying load conditions. The 5 HP motors were connected to a dynamometer with a flexible rubber coupling and were isolated from the dynamometer base with 10 cycle Barry mounts. Figures 7-1 and 7-2 show the dynamometer test site and the rubber coupling, respectively. The 40 HP unit was also mounted on 10 cycle isolators. However, a flexible metal coupling was used due to the higher power transmission. The motors were tested under these conditions: (1) Uncoupled from the dynamometer (no load), (2) driving the uncoupled dynamometer (minimum load), (3) at full rated load. Tables 7-1 and 7-2 show the vibration acceleration levels for prominent one-third octaves and the overall reading for the 184 frame open, and the 213 frame, totally-enclosed, 5 HP motors. Levels for the 40 HP open motor are given in Table 7-3. The causes of the vibration changes listed in these three tables are discussed under the classifications of noise experiencing the change.

FIGURE 7-1

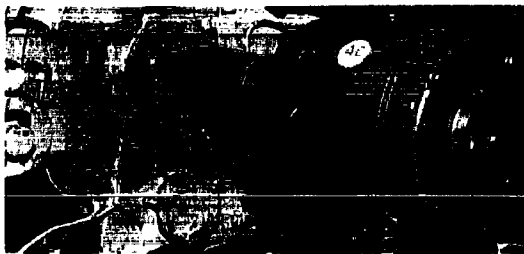


FIGURE 7-2

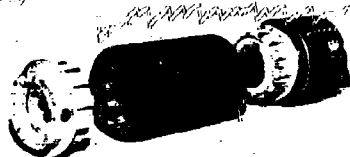


TABLE 7-1

Load Test
5 HP 2 Pole 184 Frame
Vibration Acceleration Levels

Band	Axis	No Load	Minimum Load	Full Load
63	X	86	103	100
	Y	85	96	94
	Z	88	102	98
200	X	78	84	83
	Y	71	77	76
	Z	74	80	81
1250	X	80	82	89
	Y	86	81	94
	Z	93	91	101
1600	X	85	90	94
	Y	90	91	103
	Z	93	99	108
2000	X	85	84	94
	Y	92	94	102
	Z	96	101	107
4000	X	81	83	91
	Y	83	87	95
	Z	95	90	94
Overall	X	101	106	107
	Y	103	104	108
	Z	109	109	113

Values taken from Spectrograms 7-1 through 7-3.

TABLE 7-2

Load Test
5 HP 2 Pole 213 Frame
Vibration Acceleration Levels

Band	Axis	Minimum Load	Full Load
63	X	93	98
	Y	91	97
	Z	91	96
250	X	96	88
	Y	90	87
	Z	95	85
2000	X	100	101
	Y	101	104
	Z	100	103
2500	X	103	103
	Y	106	100
	Z	100	103
5000	X	93	94
	Y	85	93
	Z	90	100
Overall	X	112	112
	Y	110	114
	Z	112	114

Values taken from Spectrograms 7-4 and 7-5.

TABLE 7-3

Load Test
40 HP 4 Pole 364 Frame
Vibration Acceleration Levels

Band	Axis	No Load	Minimum Load	Full Load
125	X	73	76	89
	Y	70	71	73
	Z	73	73	72
160	X	78	81	93
	Y	*	*	*
	Z	72	70	71
315	X	71	72	77
	Y	73	85	92
	Z	84	76	80
500	X	99	86	82
	Y	86	87	84
	Z	86	85	82
2000	X	105	103	99
	Y	109	106	105
	Z	113	107	105
2500	X	96	99	94
	Y	103	108	105
	Z	104	109	108
Overall	X	108	109	108
	Y	110	111	110
	Z	115	113	113

* Values less than 70 adb were below range of recording paper.

Values taken from Spectrograms 7-6 through 7-8.

7.3 MAGNETIC NOISE

The effect of load may cause the slot frequency magnetic noise of an induction motor to either increase or decrease. Factors which cause an amplification of slot frequency noise are increased rotor and stator load currents, and the increase in apparent permeability variation due to the rotor slots. The factor which tends to decrease slot frequency noise is the reduction of magnetizing flux with increasing load. Depending upon which factor is the most pronounced, the magnetic noise may be either amplified or attenuated.

As the load on a motor increases, the load currents of both the stator and rotor increase. The load current of the stator sets up a load mmf wave which is displaced 90 electrical degrees from the no load (magnetizing) mmf. The current in the rotor bars set up a mmf wave whose fundamental exactly cancels the fundamental of the stator load mmf. However, both of these mmf waves contain ripples caused by the concentration of currents in slots, which do not cancel. As the currents increase with load, these ripples increase proportionately. It is shown in Section 3 that these ripples cause flux force waves which cut the stator at the frequencies shown in Table 7-4.

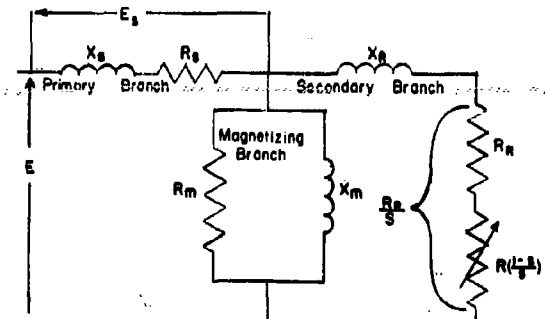
The effect of the type of rotor slot configuration

on the permeance ripples is also discussed in Section 3. The partial or complete steel bridge over a semiclosed or closed slot causes an apparent decrease in the permeance variation of the rotor slot as sensed by the stator. At no load, this steel bridge is carrying only the small component of the stator-generated flux that leaks across the rotor bridge. Under load, the rotor bar currents produce rotor leakage flux, which crosses and tends to saturate the slot bridge. As the bridge saturates, the permeance ripples approach those of the open slot configuration. Thus, the permeance ripples and the rotor slot frequency noise can increase with load.

A third factor may result in a reduction in magnetic noise. The magnetizing current of an induction motor decreases as the motor load is increased. This is best illustrated by the use of the exact equivalent circuit, Figure 7-3, where the magnetizing branch lies between the primary (stator) and the secondary (rotor) branches. The increased current due to load causes a greater resistance and reactance drop, E_s , across the primary with a resultant decrease in voltage ($E-E_s$) across the magnetizing branch. The total flux per pole is proportional to this voltage and the resultant variation as a function of load will depend upon the degree of saturation in the magnetic circuit. Whether load will increase or decrease the overall magnetic noise depends on which of the three factors predominate.

FIGURE 7-3

EXACT INDUCTION MOTOR
EQUIVALENT CIRCUIT



Although the 184 frame motor's overall vibration increased by only 4 adb, the one-third octaves containing the rotor slot frequencies indicated an increase of up to 12 adb. The three primary rotor slot frequencies (Numbers 2, 3 and 4 in Table 7-4) are 1920, 1800, and 2040 cps. At no load, these are all contained within the 2000 cps one-third octave. The 1800 cps noise (which is most prominent since $R > S$) also appears in the 1600 cps one-third octave, as 1800 cps is near the boundary between the two one-third octaves. At full load, the frequencies become 1850, 1730, and 1970 cps respectively due to the de-

crease in motor speed. Under this condition the frequencies are almost evenly divided between the two bands. The next largest increase occurs in the 4000 cps band which contains the secondary rotor slot frequencies. This motor's large change in magnetic noise under load is attributed to its closed-slot-configuration rotor slots. This causes a maximum permeance variation between minimum and full load, and therefore, an increase of twice slot frequency noise.

TABLE 7-4
Stator Core Vibration

	Frequency of Vibration	Number of Nodes
1.	120	2P
2.	$\frac{120 R (1-s)}{P} \dots 120$	2R - 2S - 2P
3.	$\frac{120 R (1-s)}{P}$	2R - 2S
4.	$\frac{120 R (1-s)}{P} + 120$	2R - 2S + 2P
5.	$\frac{240 R (1-s)}{P} - 120$	4R - 2P
6.	$\frac{240 R (1-s)}{P}$	4R
7.	$\frac{240 R (1-s)}{P} + 120$	4R + 2P

The 213 frame motor reveals a different pattern of vibration change with load. The primary slot frequencies of this motor (1920, 2040, and 2160 cps at no load) all remain within the 2000 cps one-third octave and increase only very slightly. This small increase of rotor slot noise, as compared to the preceding case, is due to the rotor having a semi-closed slot. Therefore, the variation from no load to full load was minimized.

The 40 HP motor is an example of a motor experiencing a decrease in magnetic noise with an increase in load. Since this magnetic noise was the most prominent, the overall noise level also decreased. This decrease in magnetic noise is due to the decrease in magnetizing flux. The permeance ripples produced by this motor did not increase because of two factors.

- (1) Semi-closed rotor slots were utilized.
- (2) The thickness of the partial steel bridge over the rotor slots does not increase appreciably for large diameter motors.

The combination of these factors resulted in an effective open slot at any load.

The effect of load on the 120 cycle magnetic noise could not be determined on the test motor for various reasons. The pre-load band of the 40 HP, 4 Pole motor was reflected in the 125 cps one-third magnetic noise.

The change in the 120 cycle noise of the two

pole motors under load was insufficient to register above an inherent variation in this frequency noise. In two pole motors whose torque is low compared to their horsepower, operation at no load can cause a time variation of twice line frequency noise. When these motors have small no load losses, the rotor will rotate at almost synchronous speed. For example, a 40 HP, two-pole, totally-enclosed motor with the fan removed was observed to slip only one revolution every three minutes at no load. The variation in permeance of the rotor steel due to rolling (described in Section 3) will rotate at slip frequency with respect to the synchronous wave. Thus the minimum reluctance path will coincide with the synchronous wave at twice slip frequency. This time variation in rotor permeability will modulate the amplitude of the fundamental flux wave and thus the 120 cycle magnetic noise generated by this flux wave.

A similar phenomenon, common in two pole motors, produces a beat frequency effect at twice slip frequency similar to the modulation of the 120 cycle noise described above. This beat effect is caused by the alternate aiding and bucking of noise sources producing twice line frequency and twice rotational frequency. (20)* The addition of fairly small loads such as the air flow resistance to the external fan increases the slip frequency and reduces these two effect appreciably. At moderate loads, these phenomena disappear completely. (See Spectragrams 7-9 and 7-10.)

7.4 BEARING NOISE

The standard straight line skew of rotor bars normally used in induction motor design, in conjunction with the slowing down of the rotor under load causes a variation in the amount of axial force on the bearings. This is true whether or not the bearings are initially preloaded. The variation in preload can cause either an increase or decrease in the amount of noise produced by initially preloaded precision bearings and will cause an amplification of the noise produced by non-preloaded standard bearings.

As motor load is increased, the rotor slows down relative to the synchronous flux wave. The rotor bars "cut" the flux wave at a greater rate. This produces a force, F, on each rotor bar which is perpendicular to the bar.

$$F = K B l i \quad 7.1$$

where F = normal force
K = constant of proportionality
B = flux density
l = length of conductor
i = current in conductor

*Number in parentheses refer to references listed in the Bibliography.

If Θ is the angle of rotor bar skew, $F \cos \Theta$ is the tangential component which supplies the motor torque. $F \sin \Theta$ is an axial component, hereafter termed F_a . This axial force is readily computed for any load and speed if the rotor dimensions are known.

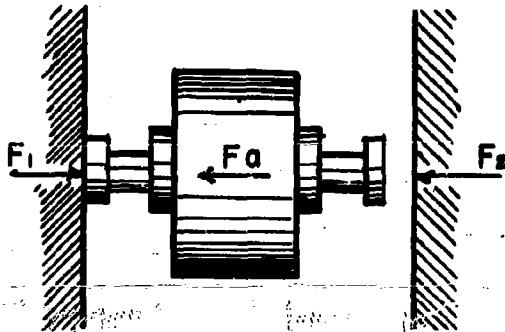
$$F_a = \frac{5,250 \text{ HP} \tan \Theta}{n r} \quad \text{lbs} \quad 7.2$$

where F_a = axial force in pounds
 HP = load in horsepower
 Θ = skew angle
 n = motor speed in rpm
 r = rotor radius in feet

This axial force may vary the preload force on the bearings in one of four manners, depending upon the manner of initial preloading. In this discussion, the subscript 1 indicates terms referring to the bearing at which the axial force is directed; subscript 2 refers to the opposite bearing.

F_a = axial force due to load
 F_i = initial preload force for both bearings.
 F_1 = preload force under load for bearing #1.
 F_2 = preload force under load for bearing #2.
 K_1 = spring constant of spring washer #1
 K_2 = spring constant of spring washer #2
 X_1 = initial deflection of spring washer #1
 X_2 = initial deflection of spring washer #2

Condition 1: Bearings not preloaded, i.e., $F_i = 0$.



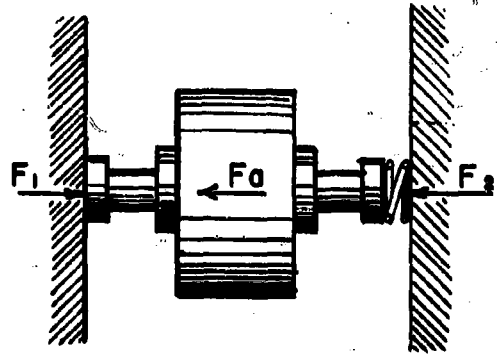
Shaft is free to move and moves in direction of F_a . After shaft has taken up the end play.

$$F_1 = F_a \quad F_2 = 0 \quad 7.3$$

Condition 2: Spring washer at bearing #2, i.e.,

$$F_i = K_2 X_2$$

(Note F_i preloads both bearings)



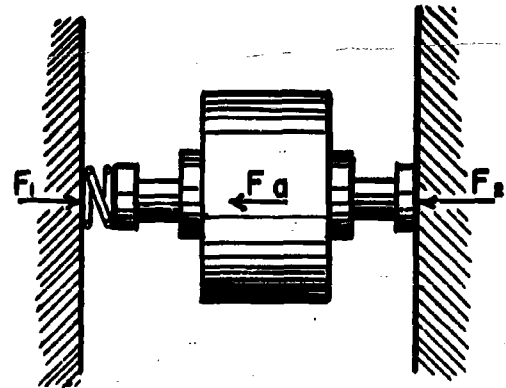
Shaft is not free to move, therefore, spring #2 remains compressed the same amount.

$$F_1 = F_i + F_a \quad F_2 = F_i \quad 7.4$$

Condition 3: Spring washer at bearing #1, i.e.,

$$F_i = K_1 X_1$$

(Again F_i preloads both bearings)



If $F_a < F_i$ which is the normal case,

$$F_1 = F_i \quad F_2 = F_i - F_a \quad 7.5a$$

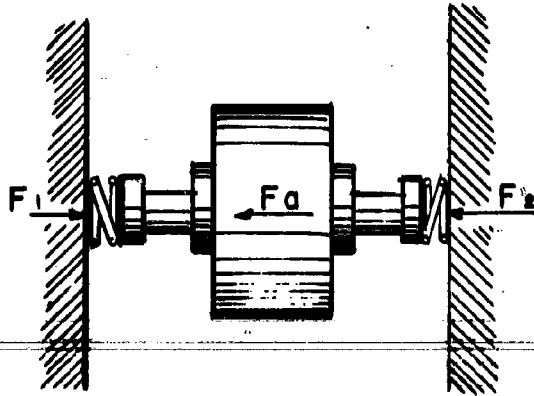
If $F_a > F_i$ the shaft will move

$$F_1 = F_a \quad F_2 = 0 \quad 7.5b$$

Condition 4: spring washers at both bearings, i.e.,

$$F_1 = K_1 X_1 = K_2 X_2$$

The amount of initial preload on each bearing must be the same for there to be no net force on the shaft. If dissimilar spring washers are used ($K_1 \neq K_2$) due to different size bearings, the washers will deflect amounts inversely proportional to their spring constants.



Shaft moves a distance X , due to force, F_a .

$$F_1 = K_1 (X_1 + X) \quad F_2 = K_2 (X_2 - X)$$

$$\text{but } F_1 - F_2 = F_a$$

$$\text{therefore, } F_1 = F_a + F_2 \frac{K_1}{K_1 + K_2}$$

$$F_2 = F_1 - F_a \frac{K_2}{K_1 + K_2} \quad 7.6$$

This variation in preload amount may vary the bearing noise in either direction. As is discussed in Section 4, there is a preload band of frequencies which occurs in the range between 150 and 250 cps. This band was shown to be highly dependent upon the amount of preload. The 213 frame motor was preloaded in the manner of condition #2. The full load axial force was calculated to be 5.9 pounds using Equation 7.2. The initial preload was approximately 25 pounds, which was subsequently found to result in near maximum preload noise. The decrease of 8 to 10 adb of the 250 cps one-third octave correlates quite well with the data furnished in Table 4-2 in Section 4.

The preload band of the bearings in the 40 HP motor lies within the 120 and 160 cps one-third oc-

taves. These bands showed an increase of 12-13 adb on the X-axis (parallel to the shaft). The second harmonic appears in the 315 cps band. This motor had standard electric motor grade bearings which were not preloaded (Condition #1). As explained in Section 4, preloading of standard bearings (FF-B-171) often results in an increase in motor vibration.

7.5 FAN NOISE

Motor load has only a nominal effect on fan noise. This slight effect is due to the decreased rotating speed of the rotor, which diminishes the amount of air pumped. See Section 5. The frequency of fan noise, like most motor noise, is decreased by the percentage of slip.

7.6 UNBALANCE NOISE

It was noted that the unbalance noise of the motors tested varied with load. The 184 frame motor experienced about 3 adb less rotational frequency (63 cps band) noise at full load than at minimum load. The 213 frame motor reveals a decrease of 5 adb for the same load change. The 40 HP unit, on the other hand, did not experience a change in rotational frequency noise. These variations may be the result of the magnetic pull on the dynamometer rotor which was transmitted back to the motor. The motor-dynamometer combination was not dynamically balanced as a unit at minimum load; thus, no conclusions of this part of the study can be made.

7.7 CONCLUSION

This study reveals that no load noise tests of an induction motor are not, in general, indicative of the motor vibration at full or even partial load. The frequencies of most electro-mechanical noise will become:

$$f_{fl} = f_{nl} (1-s)$$

where f_{fl} = frequency of noise under load

s = motor slip in per unit

f_{nl} = no load frequency of noise

The amplitude of the vibration may increase or decrease depending upon the source of the noise and other conditions.

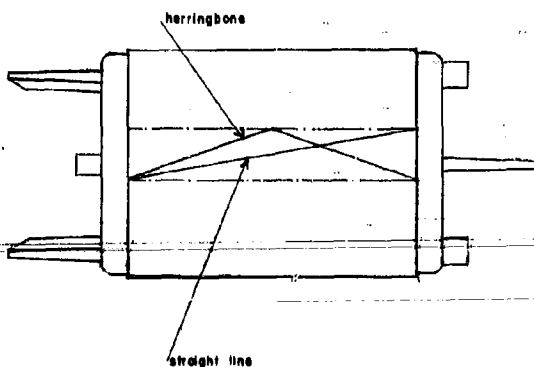
Increase in motor vibration due to load may be minimized by:

- 1) Using herringbone skewed rotors. The two straight line skew segments will produce axial forces equal in magnitude and opposite in

direction and thereby cancel each other.* This permits the optimum preload force on the bearings to be set at no load and to be independent of load. The amount of skew is determined by the maximum peripheral displacement of the rotor bars. Therefore, the equivalent herringbone skew for a standard straight line skew requires that each half of the rotor bars have an angle whose tangent is twice that of the straight line skew rotor bars, as shown in Figure 7.4.

FIGURE 7-4

EQUIVALENT STRAIGHT LINE
and HERRINGBONE SKEW



- 2) If herringbone skew cannot be used, amount and manner of preload must be selected such that an increase in preload as calculated by Equation 7.2 will not cause an increase in vibration. The vibration vs. preload characteristics will have to be determined for each size of bearing used and, until consistency is verified, for individual bearings.
- 3) Use of as large an air gap as is consistent with meeting necessary starting current and

*Another cause of axial movement, significant only under starting conditions, is a result of an initial axial misalignment of the rotor and stator magnetic centers. The rotor end rings will encounter unbalanced transient fields. The rotor will move in the direction of the end ring farthest from the stator magnetic center.

power factor requirements. As shown in Section 3, a large air gap minimizes the effect of permeance ripples which increase the load.

- 4) The variation of motor noise due to load demonstrated in Tables 7-1, 7-2, and 7-3 indicates the need for noise testing under load conditions. Measurement of motor noise under load presents the problem of isolating the noise of the loading device. It is recommended that full load testing be done in the following manner:

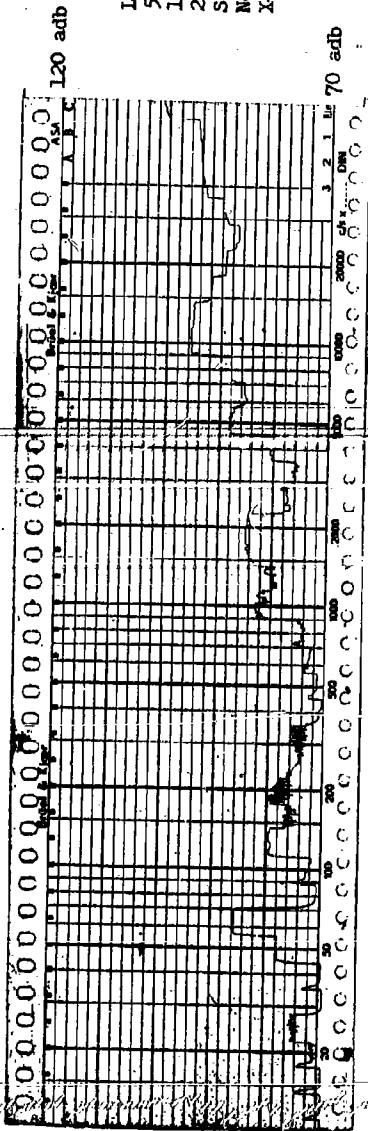
1. With motor isolated to highest degree obtainable, take noise measurements at load site, such as dynamometer, under no load conditions (uncoupled).
2. Take noise measurements with motor connected to load with a flexible coupling (rubber, if possible) and driving a minimum load such as an unexcited dynamometer.
3. Take noise measurements with motor at full load (excited dynamometer).

The corrected full load reading is:

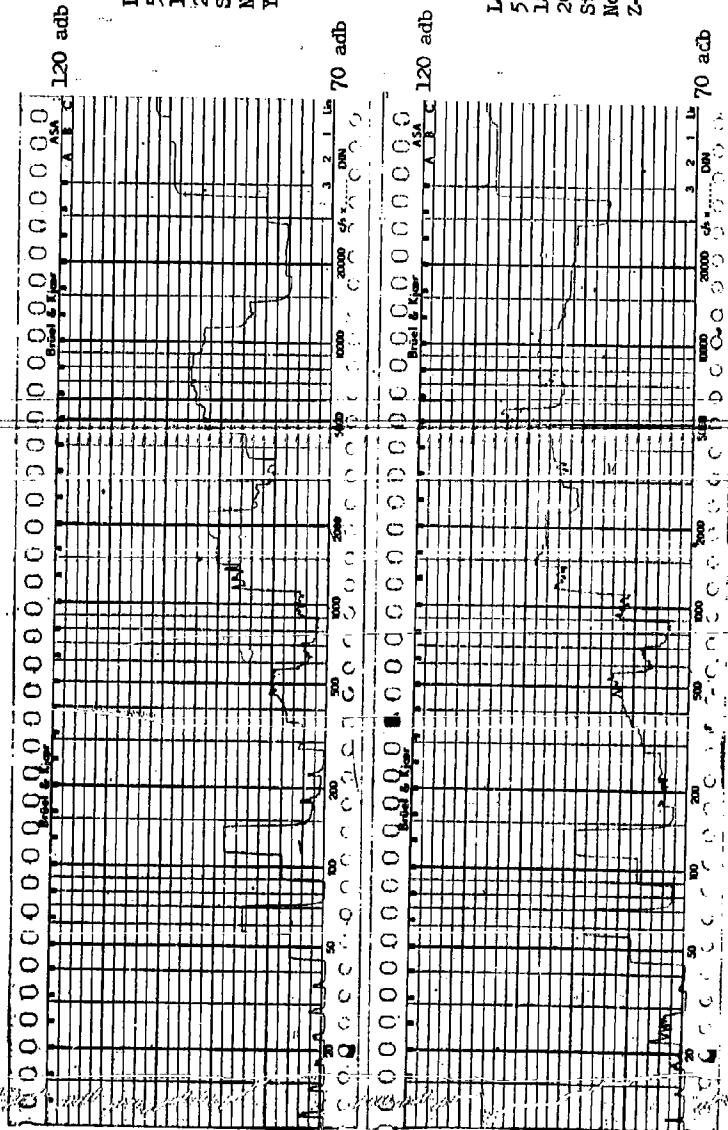
$$\text{Reading 1} + (\text{Reading 3} - \text{Reading 2})$$

This method relies on the isolation used (such as mounts, couplings, separate foundations, rooms, etc.) to minimize the noise change in the loading device due to load rather than the total noise produced by the loading device. The difference between the first two readings is assumed to be caused by the dynamometer since the motor is only slightly loaded by the dynamometer's windage and friction losses. (The 5 HP motors in this study were supplying only 0.35 HP when they were driving an unexcited 15 HP dynamometer.)

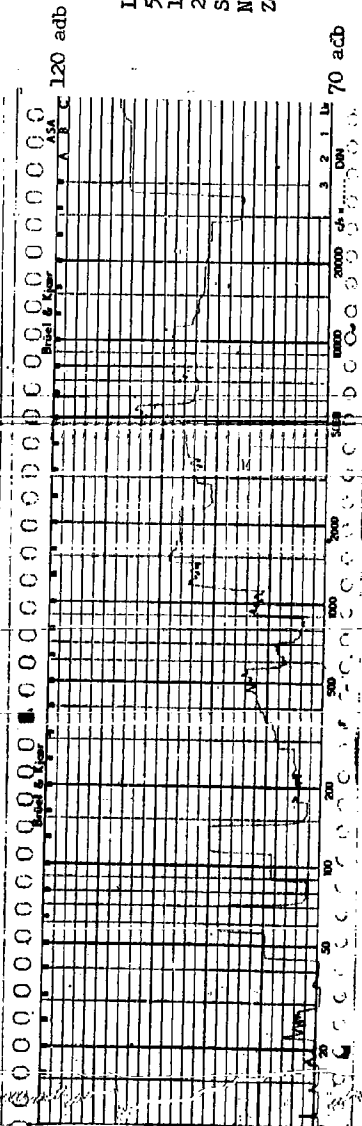
- 5) This study indicates that a motor with semi-closed rotor slots experiences less increase in vibration with respect to load than does a motor with closed slots. However, the permeance variation due to a closed slot under load conditions only approaches that of a semi-closed slot. The closed slot causes a greater increase in vibration with load only because it is quieter at no load. Use of a closed rotor slot rather than a semi-closed slot is recommended.



Load Test 1
5 HP 2 Pole
184 Frame Open
20 April 1960
Structureborne
No Load
X-Axis

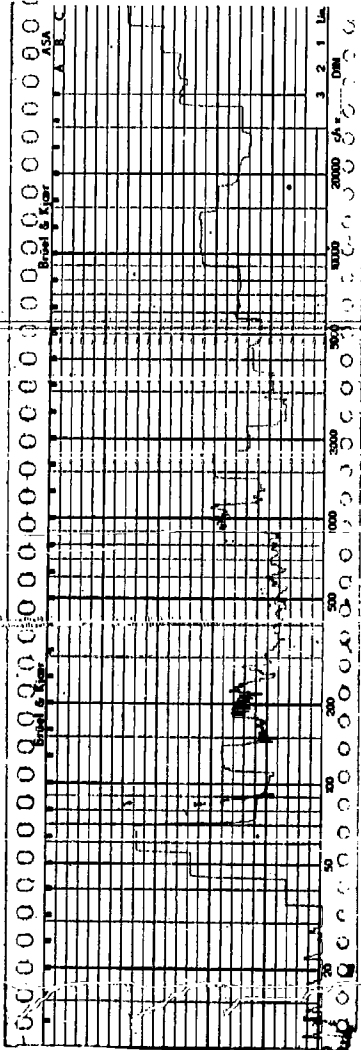


Load Test 1
5 HP 2 Pole
184 Frame Open
20 April 1960
Structureborne
No Load
Y-Axis



Load Test 1
5 HP 2 Pole
184 Frame Open
20 April 1960
Structureborne
No Load
Z-Axis

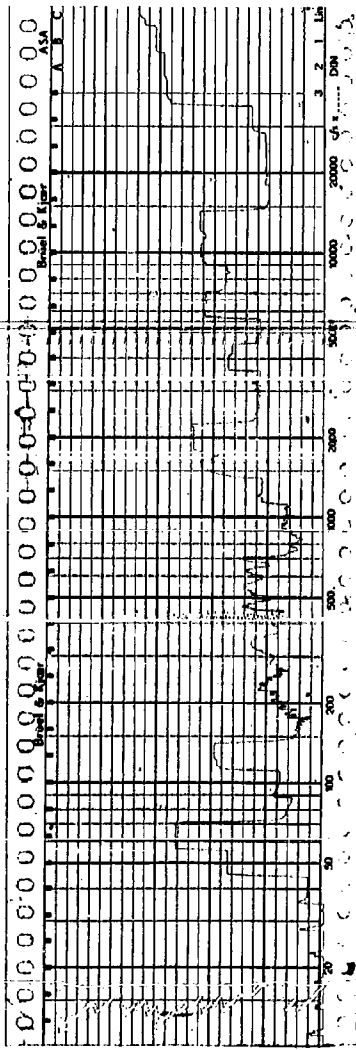
120 adb



Load Test 1
5 HP 2 Pole
184 Frame Open
20 July 1960
Structureborne
Minimum Load
X-Axis

70 adb

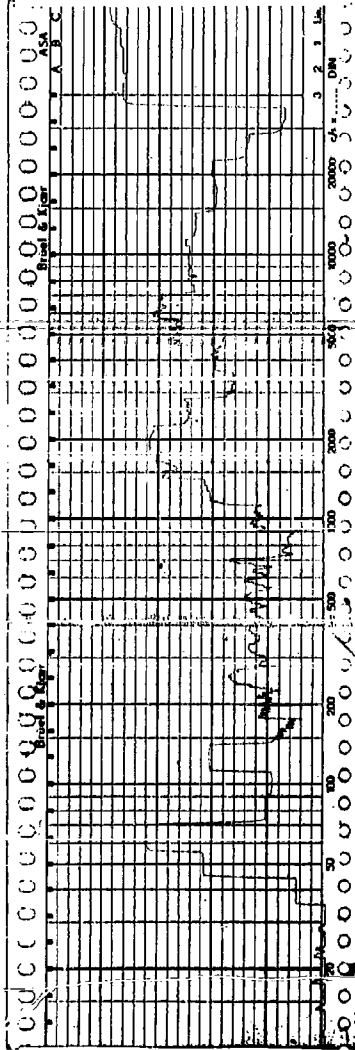
120 adb



Load Test 1
5 HP 2 Pole
184 Frame Open
20 July 1960
Structureborne
Minimum Load
Y-Axis

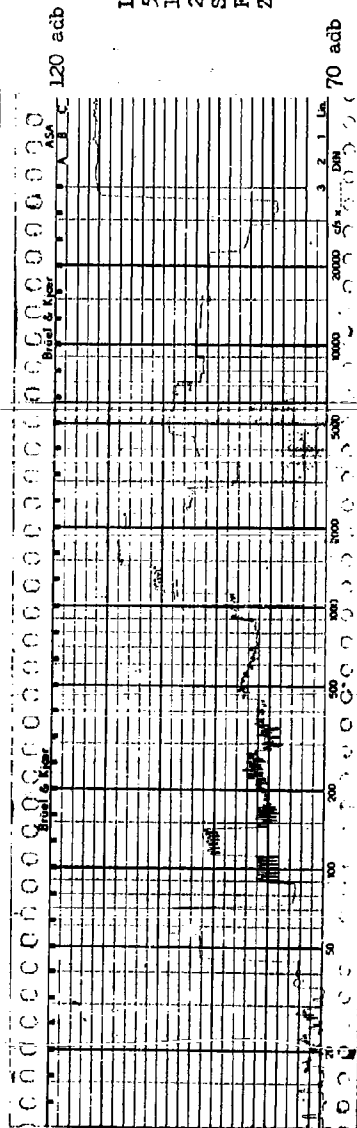
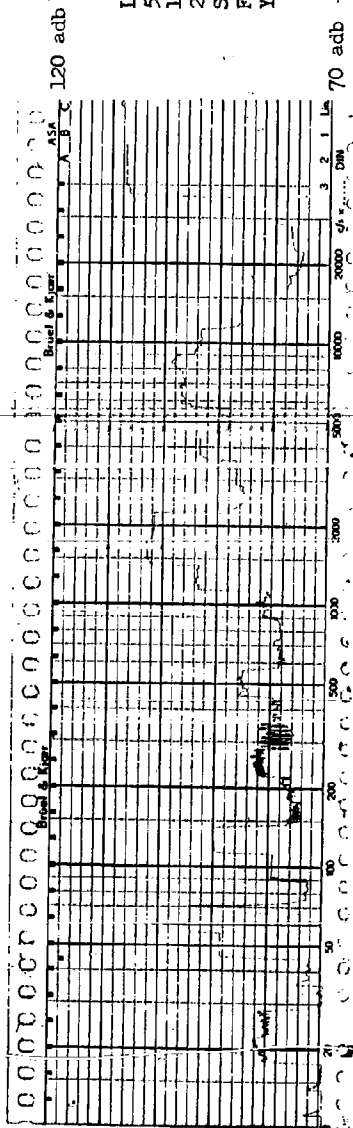
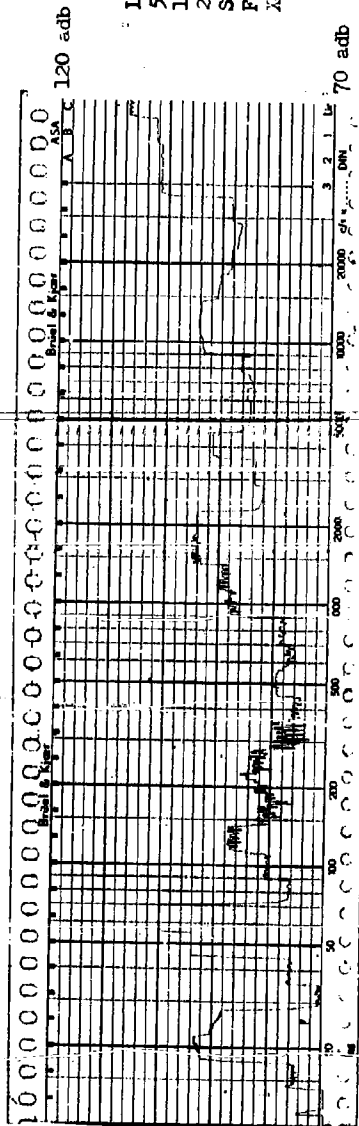
70 adb

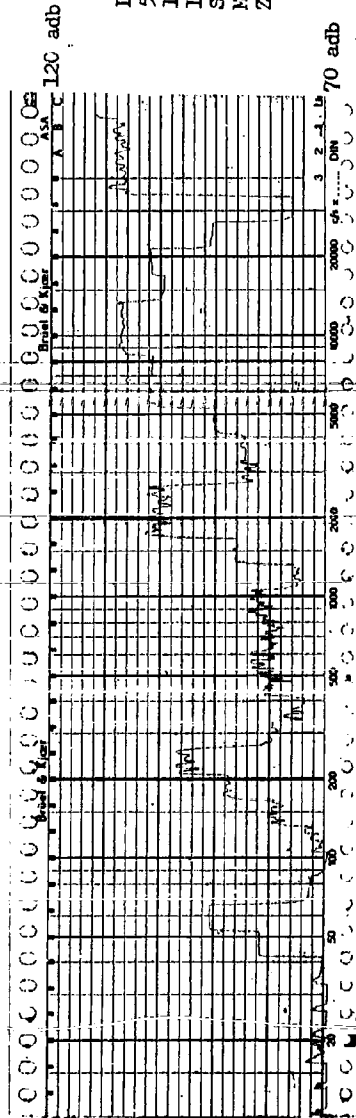
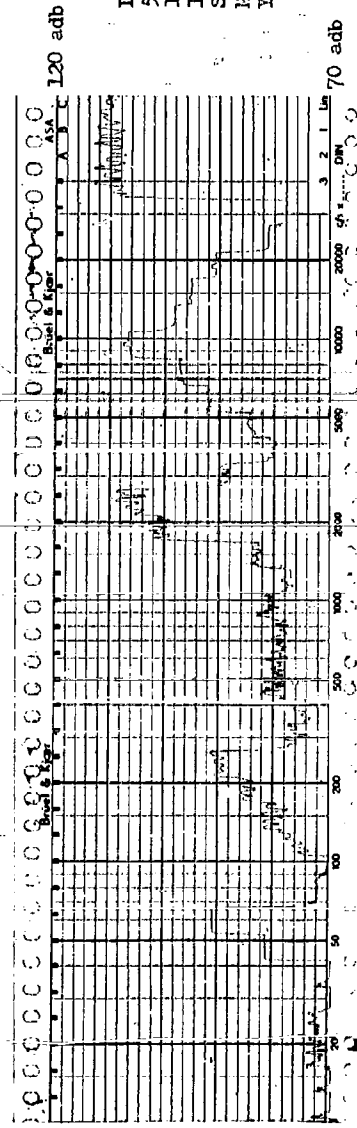
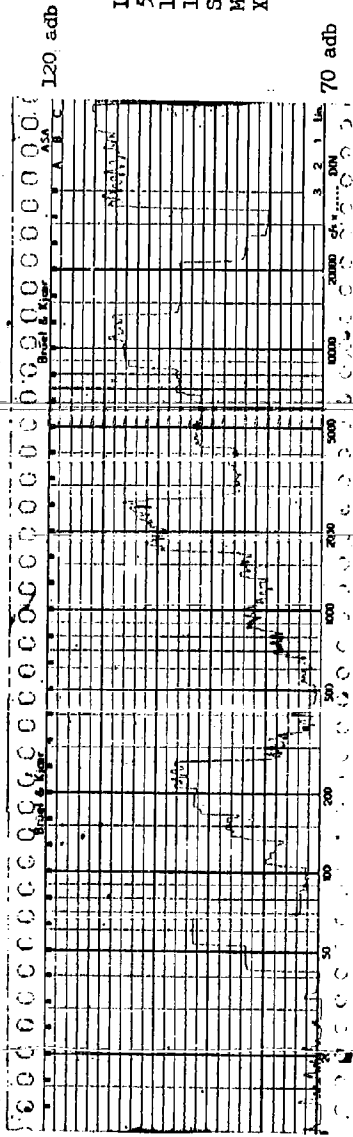
120 adb

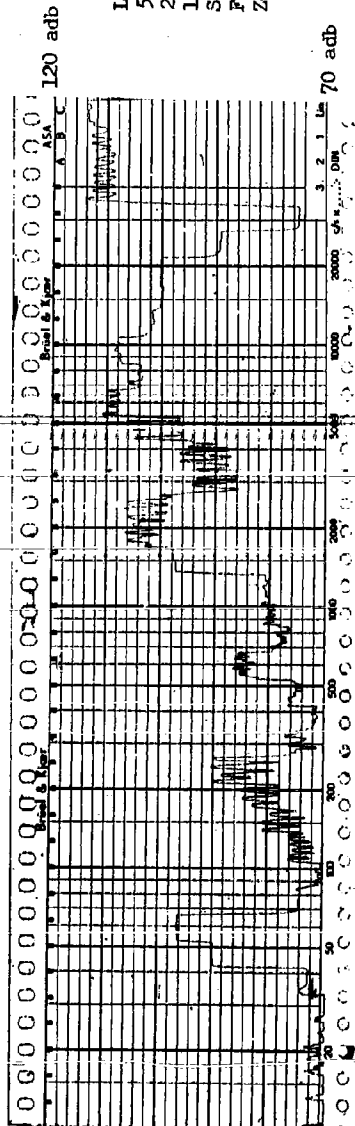
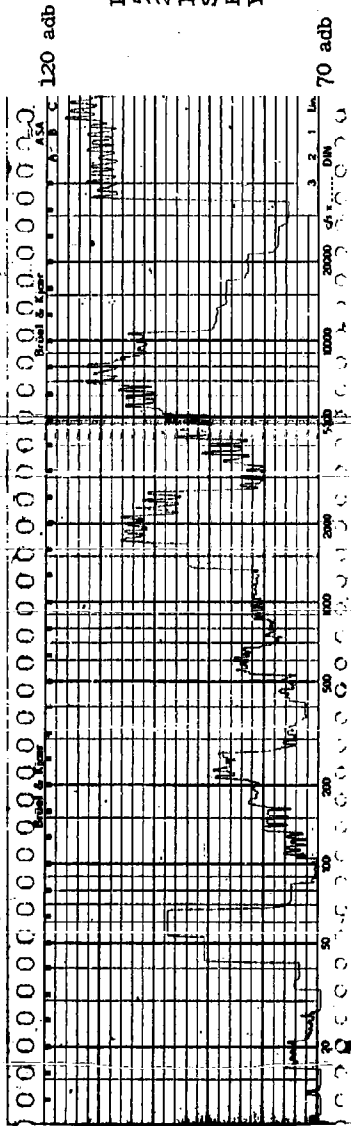
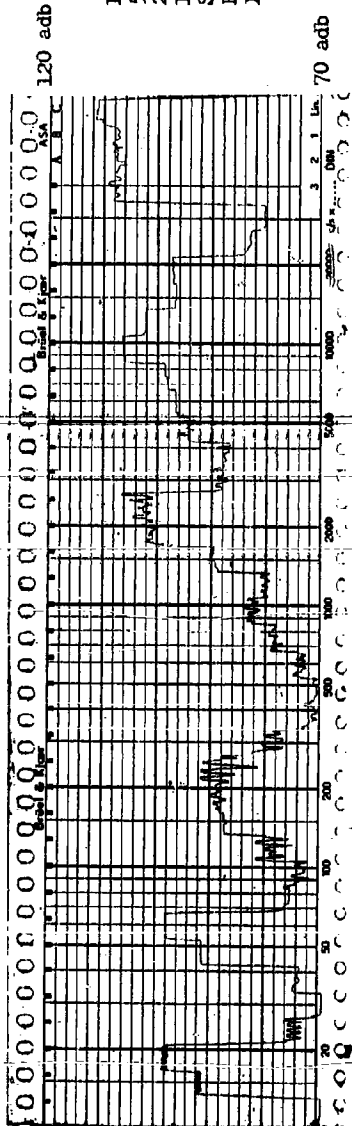


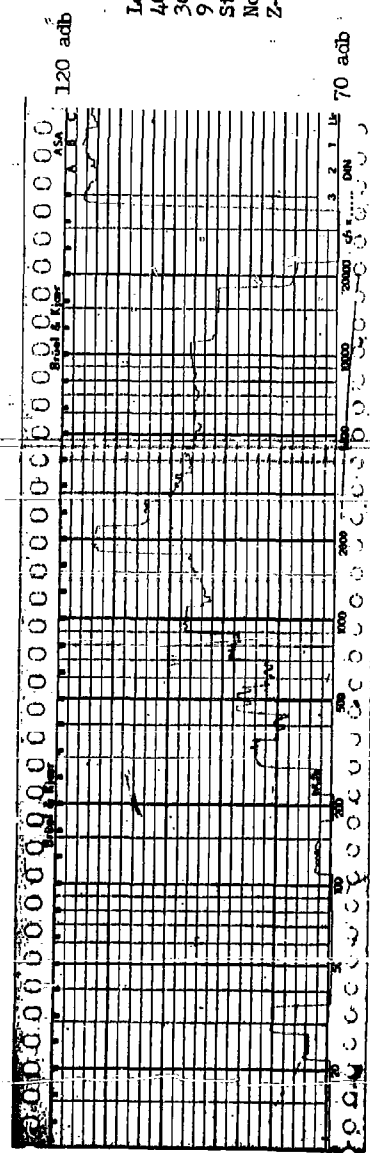
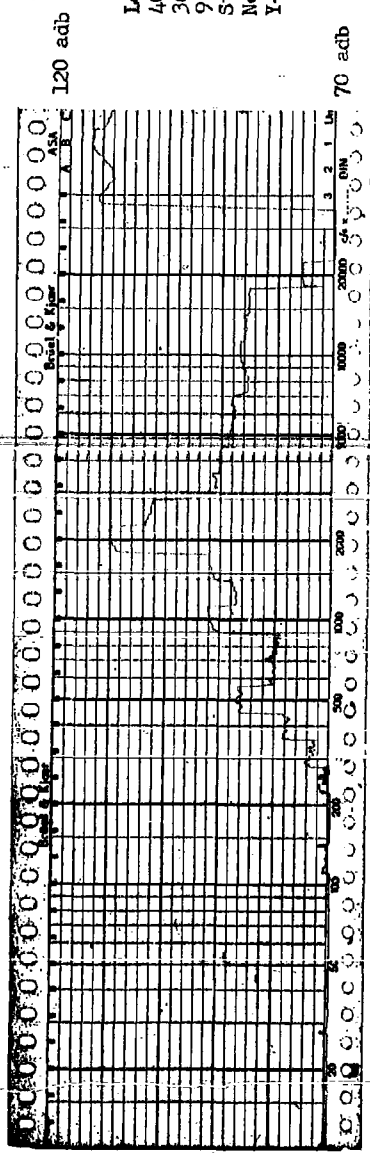
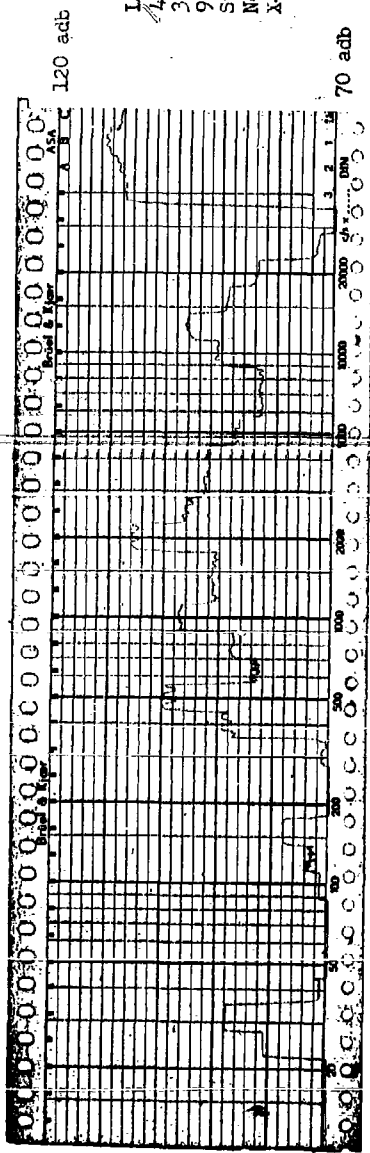
Load Test 1
5 HP 2 Pole
184 Frame Open
20 July 1960
Structureborne
Minimum Load
Z-Axis

70 adb



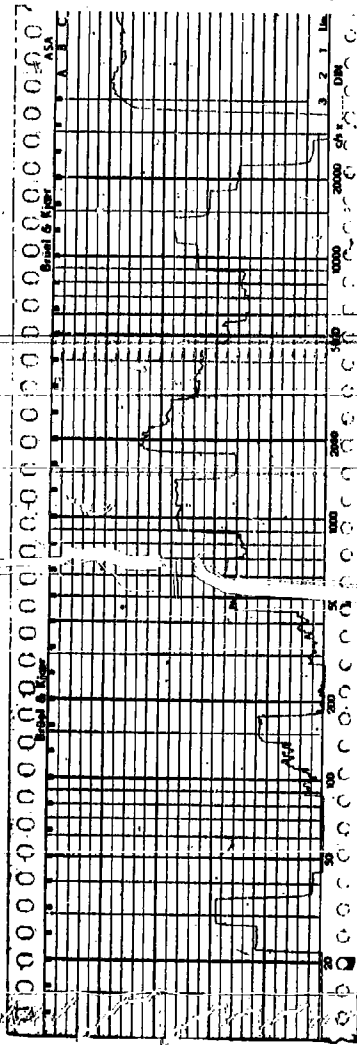






 Load Test 3
 40 HP 4 Pole
 364 Frame Open
 9 May 1960
 Structureborne
 Minimum Load
 X-Axis

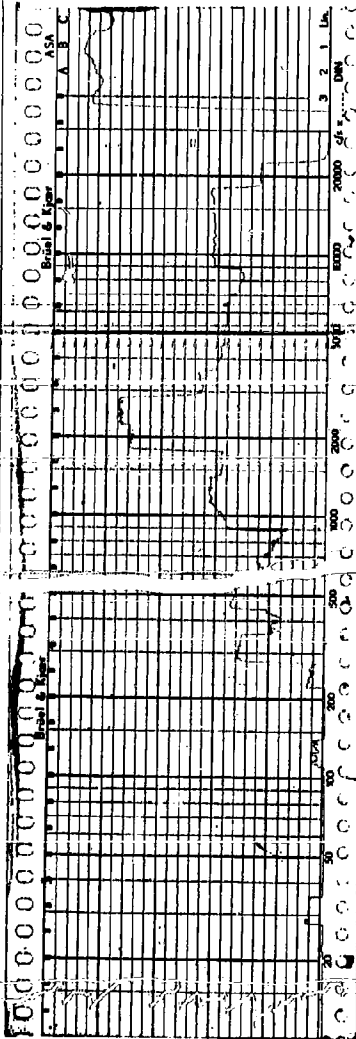
120 adb



70 adb

 Load Test 3
 40 HP 4 Pole
 364 Frame Open
 9 May 1960
 Structureborne
 Minimum Load
 Y-Axis

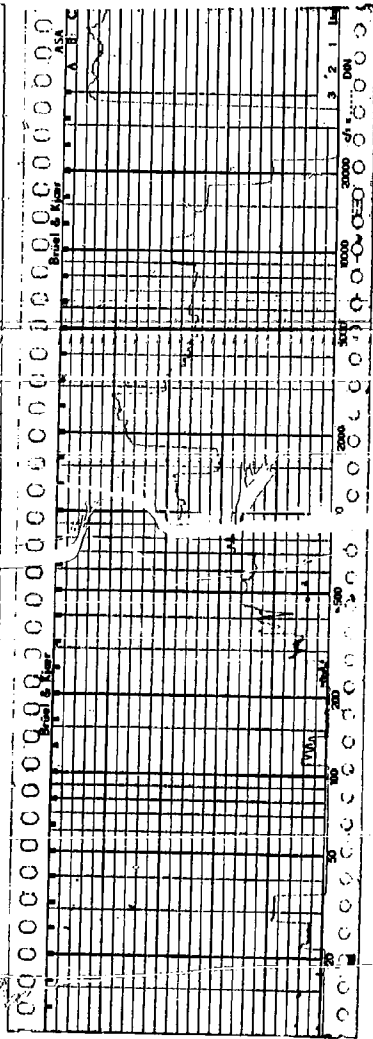
120 adb



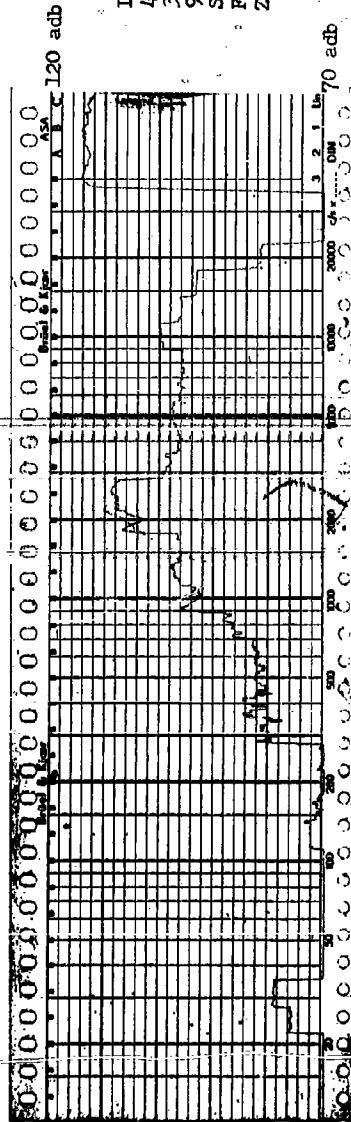
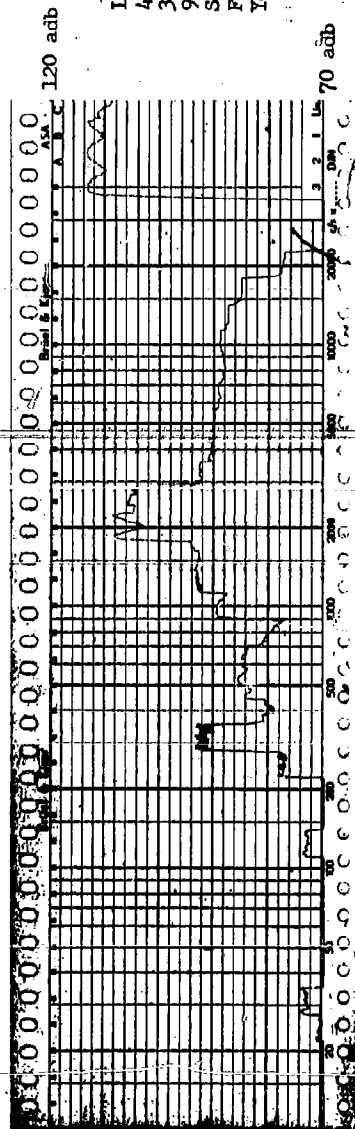
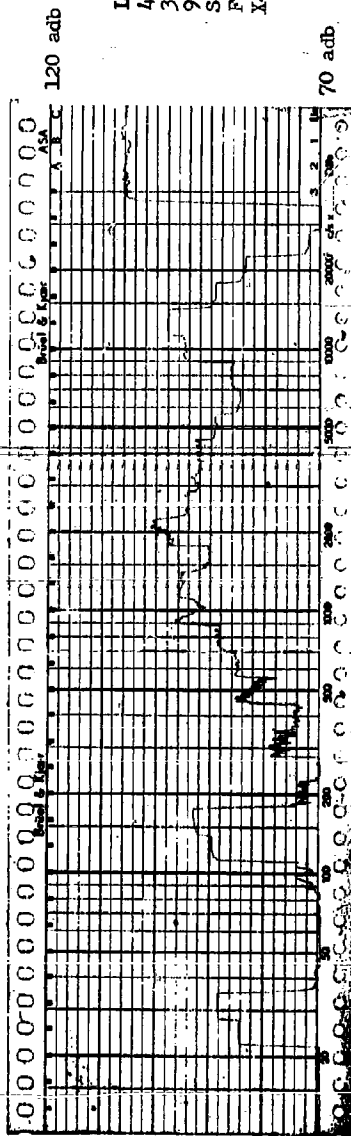
70 adb

 Load Test 3
 40 HP 4 Pole
 364 Frame Open
 9 May 1960
 Structureborne
 Minimum Load
 Z-Axis

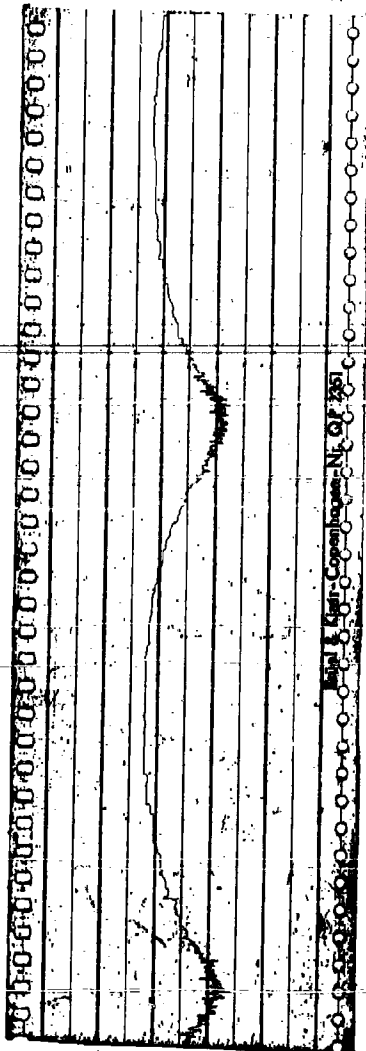
120 adb



70 adb



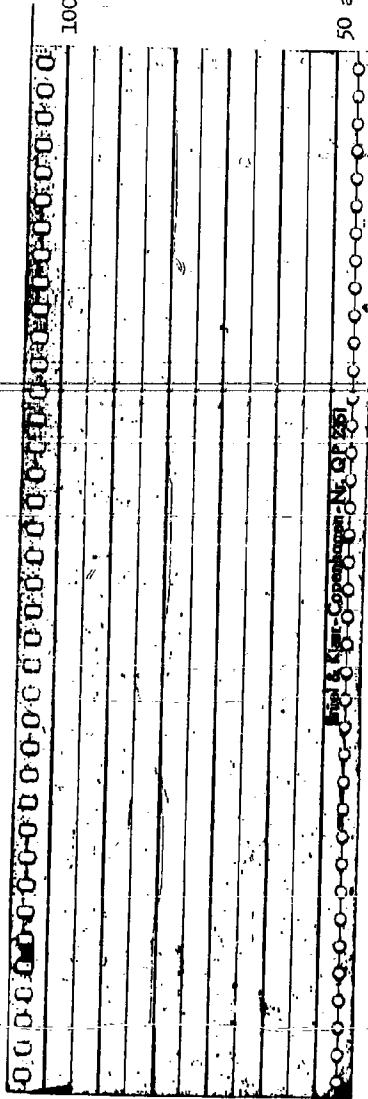
100 adb



Fluctuation of
125 cps band
40 HP 2 Pole
364 Frame TFC
1 June 1960
Structureborne
Paper speed 1 mm/sec
Motor speed 3599.57 RPM

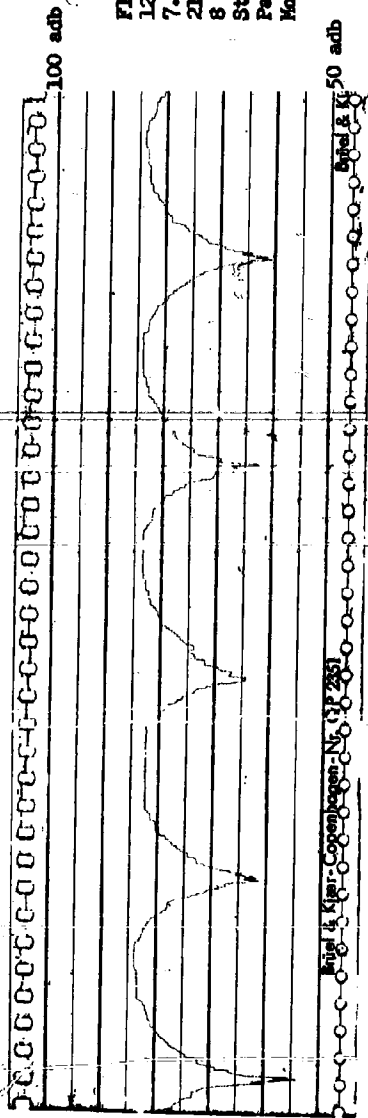
50 adb

100 adb



Fluctuation of
125 cps band
40 HP 2 Pole
364 Frame TFC
1 June 1960
Structureborne
Paper speed 1 mm/sec
Motor speed 3594.4 RPM

50 adb



Fluctuation of
 125 cps band
 7.5 HP 2 Pole
 215 Frame Open
 8 June 1960
 Structureborne
 Paper speed 1 mm/sec
 Motor speed 3598.75 RPM

SECTION 8

MISCELLANEOUS STUDIES

8.1 INTRODUCTION

This section deals with two important aspects of motor noise. One, various factors in induction motor construction can either amplify or attenuate the noise produced by the four sources previously discussed. The effect of these construction factors is considerable and, thus, of as great an importance as the sources themselves. The following construction factors are treated in the indicated sub-sections.

8.2 Tolerances

8.3 Frame Materials and Rigidity

The second aspect treated in this section is that of attenuation devices. If the desired level of motor noise cannot be achieved by reduction of the noise source, then the noise produced by the source must be attenuated between the point of generation and where it becomes objectionable. The following attenuation devices were studied.

8.4 Damping Compounds

8.5 Encapsulation Compounds

8.6 Internal Isolation

8.2 TOLERANCES

Manufacturing tolerances can affect motor noise in several ways. The most important are:

- 1) Eccentricity of the airgap causes unbalanced magnetic forces which result in magnetic noise.
- 2) Non-parallelism of the rotational axis with the bearing housing bores causes deformation of the bearing and resulting in bearing noise.
- 3) A tight fit between bearing and shaft also deforms the bearing and increases bearing noise.

No less than twelve manufacturing tolerances affect the concentricity of the air gap excluding internal bearing tolerances. These tolerances apply to the rotor and stator air gap surfaces and one for each mating part of the following five fits: stator core - yoke, yoke - bearing housing, bearing housing - bearing, bearing - shaft, and shaft - rotor core. These tolerances can cause the magnetic axes of the rotor and stator to diverge. Similarly six tolerances affect the alignment of the axes of the bearing housing bores after motor assembly: One for each housing bore, housing OD, and yoke fit. Misalignment causes the rotor axis to be non-parallel to both bearing housing bores and, therefore, the bearing inner races are non-parallel to the outer races.

A 40 HP, 2 Pole, 364 frame TEFC motor was chosen for the investigation of the vibration caused by these misalignments. This motor was supplied with special bearing housings permitting adjustment

and measurement of the air gap at both ends of the motor. The motor was first tested with a concentric 36 mil air gap. Then the rotor was adjusted such that the rotor axis was 8 mils below and parallel to the stator axis. Next the rotor was adjusted so that its axis was 8 mils above the stator axis at the front end of the air gap and 8 mils below at the rear end. Finally the rotor was adjusted to give a uniform 36 mil air gap again.

Vibration readings for these conditions are given in Table 8-1. The F and R axes are parallel to the shaft, and on the front and rear bearing housings, respectively. Moving the rotor 8 mils off center caused a general increase in high frequency noise. The variation ranged from a 2 adb decrease to a 12 adb increase. This general increase is due to an amplification of the rotor slot frequencies and to the introduction of additional harmonic magnetic fields caused by the air gap eccentricity.

TABLE 8-1
Effect of Eccentric Air Gap
Vibration Acceleration Levels

Band	Axis	8 Mil		6 Mil	
		Concentric	Parallel	Non-parallel	Concentric
63	X	94	94	94	94
	Y	80	80	79	82
	Z	83	84	86	87
	F	88	86	86	88
5000	R	90	88	89	88
	X	88	92	91	92
	Y	91	97	94	93
	Z	100	103	103	100
8000	F	96	98	98	98
	R	97	97	97	97
	X	90	96	98	96
	Y	101	113	114	106
10,000	Z	107	109	114	106
	F	116	116	122	110
	R	120	122	119	116
	X	95	103	104	101
Overall	Y	109	108	111	114
	Z	108	115	114	115
	F	112	123	126	126
	R	118	116	116	129
Overall	X	106	109	108	109
	Y	111	116	116	116
	Z	113	117	118	117
	F	119	124	127	127
Overall	R	123	124	122	130

Values taken from Spectrograms 8-1 through 8-8.

Changing the rotor axis from a parallel off-center alignment to the non-parallel alignment resulted in a very slight increase in vibration levels. The increase in bearing noise due to non-parallel bearing races was balanced by a decrease in magnetic noise, although the magnetic noise remained greater than for the concentric condition. The average eccentricity of the air gap was only half that of the previous test since the rotor and stator axes crossed at the midpoint of the cores. The bearings were permanently

damaged by operation under non-parallel conditions as evidenced by the high vibration levels after readjustment to a concentric air gap.

While the increase in noise was appreciable in these tests the eccentricity of the air gap was also considerable. The 8 mil change in rotor axis placement resulted in air gap measurements of 44-36-28-36 measured at 90° intervals starting at the top. This variation is larger than would result from normal tolerances. The variation can be held to reasonable limits by the following methods:

- 1) Performing all machining operations on one component at the same time, thereby maintaining concentricity of turns and bores.
- 2) Decreasing the tolerance allowances of the bearing housing bores. An ABEC-5 or higher tolerance is recommended.
- 3) Preloading bearings to take up the internal bearing tolerances.
- 4) Use of a light press fit (1 to 2 mil interference) between the bearing housings and frame.

Other measures, such as both boring out the bearing housings and grinding the stator bore when each part is assembled into the frame, can be taken as additional precautions but the measures listed above are considered sufficient to control the air gap concentricity.

~~The above study deals exclusively with those tolerances which affect the air gap concentricity. Additional tolerance studies were conducted in conjunction with the construction of the prototype motors and are reported in Section 9.3.1.~~

8.3 FRAME MATERIALS AND RIGIDITY

A test was conducted to determine the relative merits, as far as noise, is concerned, of three materials used for cast components. The casting materials tested were nodular iron, cast steel, and aluminum. A 7-1/2 HP, 2 Pole, 213 frame TEFC motor was used for this study. The same stator and rotor assemblies were consecutively assembled into the frames and bearing housings cast of the different materials. The castings were made from patterns which were identical except for shrinkage compensation. Results of this test are furnished in Table 8-2. These vibration acceleration levels indicate that nodular iron is preferable.

In addition to the attenuation and transmission of vibration through frame materials, the motor components must have sufficient rigidity to resist deformation caused by magnetic forces, weight of rotor assembly, etc. A rigid component is not necessarily a heavy one, although adding material is one method of attaining rigidity. Assuming a constant applied force, the acceleration of the vibratory motion is inversely proportional to the mass of the unit. In terms of decibels, a doubling of the weight of a unit will decrease the adb levels by 6 adb, if the added weight is inert. If, however, the heavier unit has a higher horsepower rating, this is not true. Generally speak-

ing, the vibration remains essentially constant as the size of the unit increases.

TABLE 8-2

Frame Material Study
Vibration Acceleration Levels

Band	Axis	Nodular Iron	Cast Steel	Aluminum
63	X	94	98	99
	Y	92	87	92
	Z	91	87	91
2000	X	87	87	95
	Y	86	91	102
	Z	86	94	104
2500	X	97	100	86
	Y	90	104	98
	Z	99	103	96
6300	X	100	97	97
	Y	94	92	95
	Z	99	100	110
10,000	X	107	111	101
	Y	102	106	107
	Z	102	109	105
Overall	X	110	113	108
	Y	105	113	111
	Z	109	114	112

Values taken from Spectrograms 8-9 through 8-11.

~~Changing the acceleration levels of a specific unit by adding inert weight is ineffective since the transmitted force remains the same. If, however, the unit is made more rigid by the added weight, a net gain will result. Material added in the form of ribs on the yoke or bearing housings decreases the vibration more than would result from the mere weight increase. (21) In specific instances, a component may be redesigned for greater rigidity without a weight increase or even with a weight decrease. Usually, however, some increase in weight may be expected.~~

Variations among the mechanical designs of different frame sizes and different manufacturers precludes specific recommendations. The following general recommendations regarding the frame materials and frame rigidity are made.

- 1) Nodular iron castings are preferable to cast steel and aluminum for attenuating the overall vibration produced in an induction motor. The differences in these materials is particularly noticeable at frequencies above 2000 cps.
- 2) The attenuating characteristics of the frame are greater at higher values of vibration. (See Section 6, Figure 6-1)
- 3) Ribbing of housings and yokes will increase their rigidity and reduce their vibration and the airborne noise generated by this vibration. Several important aspects about ribbing must be considered:
 - a. Use of circular rather than axial ribs will cause a greater reduction of deflections due to radial air gap forces.
 - b. Ribs should not interrupt a high velocity air stream. For example, the fan end bear-

ing housing of TEFC motors should not be externally ribbed.

8.4 DAMPING COMPOUNDS

A study was made of the feasibility of using damping compounds on motor components. These compounds, usually of either a tar or plastic base, are applied to the metal surfaces. Any vibration of the metal results in a stretching and contracting of the metal surface and therefore of the coating. This flexing of the compound dissipates some of the vibratory motion in the form of heat. These compounds are particularly effective when applied to large, thin, unsupported plates. The purpose of this study was to determine if these compounds were effective on cast motor components whose shapes are quite dissimilar from a flat unsupported plate.

Tests were conducted on bearing housings and air deflectors of open motors and fan housings of totally enclosed, fan cooled motors. The housings were of cast iron while the air deflectors were stamped from sheet steel. Four sets of components were prepared. The first set was not coated, the other three were coated with H.L. Blachford's *Aquaplas*, Minnesota Mining and Manufacturing Company's compounds *EC-244* and *1378*, respectively. Before assembling the components into the test motors, the components were hung from a wire and then struck. It was observed that the uncoated air deflectors produced a pronounced ring effect, while the coated ones did not, indicating that all three compounds drastically reduced the vibration decay time of this part. The cast bearing & fan housings produced little "ring" in either the coated or uncoated condition.

A 3 HP, 2 Pole, 184 frame open motor was successively equipped with the four sets of bearing housings and air deflectors. Table 8-3 shows the negligible change in vibration acceleration levels due to the coatings. Table 8-4 indicates the airborne noise was also unaffected by the use of damping compounds. This is attributed to the following reasons:

- 1) The structurally complex shape of the components.
- 2) The relatively thick cast construction.
- 3) Assembly of components into motor increased their rigidity. Thus, while the noise generating characteristics of the air deflectors were greatly changed, there was no discernable change in motor noise.

TABLE 8-3
Bearing Housing Coatings
Vibration Acceleration Levels

Band	Axis	No Coating	Aquaplas	EC-244	1378
63	X	81.5	77	80	84
	Y	83	82	82.5	83
	Z	82.5	82.5	81.5	83
125	X	76	78	73.5	84
	Y	85.5	84	86	84
	Z	83	81.5	79	81

Band	Axis	No Coating	Aquaplas	EC-244	1378
160	X	82	78	85	86
	Y	73	75	75	76
	Z	70	73	70	73
200	X	85	79	88	87
	Y	74	77.5	77.5	75
	Z	72	75	71	75
1,250	X	85	85	87	86
	Y	91	90	92	92
	Z	89	86	89	88.5
2,000	X	90	92	91	94
	Y	94	94	96	96
	Z	91	91	92	92
4,000	X	95	97	98	94
	Y	91	91	92	89
	Z	98	99	99	96.5
10,000	X	98	100	94	100
	Y	99	100	96	101
	Z	98	103	97.5	102
Overall	X	103	105	103	104
	Y	103	105	103	104
	Z	104	106	104	105

Values taken from Spectrograms 8-12 through 8-15.

TABLE 8-4
Bearing Housing Coatings
Sound Pressure Levels

Band	No Coating	Aquaplas	EC-244	1378
315	48	47	52	51
1,000	49	52	49	50
5,000	37	40	42	39
Overall	58	59	58.5	58

Values taken from Spectrograms 8-16 and 8-17

Table 8-5 shows the airborne sound levels for a 5 HP, 2 Pole, 213 frame TEFC motor supplied with the four fan housings previously described. The fan housings are simpler in construction than the bearing housings, have thinner walls, and only three point rather than continuous contact with the frame. These factors, in conjunction with the possibility of the porous compounds absorbing some of the fan-caused airborne noise, prompted this test. As Table 9-5 indicates, the effect of the compounds is again negligible. Therefore, it is concluded that the use of damping compounds on cast or small fabricated motor components will not reduce motor noise. This conclusion will not apply to sheet metal enclosures mounted on the motor frame.

TABLE 8-5
Fan Housing Coatings
Sound Pressure Levels

Band	No Coating	Aquaplas	EC-244	1378
63	61	60	62	60
800	70	70	70	70
2,500	63	62	62	62
Overall	78	78	77	78

Values taken from Spectrograms 8-18 and 8-19

8.5 ENCAPSULATION COMPOUNDS

Airborne and structureborne noise tests were conducted to determine the effects of encapsulation compounds on motor noise. Use of these compounds to seal off the motor windings from the environment is becoming widespread. The encapsulation method for the test motors utilized molds to insure complete fill of the winding and end turns. The encapsulation material used was Epoxylite's compound #293-12.

A 3 HP, 4 Pole, 184 frame dripproof protected motor was used for the airborne test. Airborne readings were taken at eight points around the motor before and after encapsulation of the motor windings. The spectrograms (8-20 thru 8-25) reveal an appreciable change in the directivity of various frequencies but the average levels remain essentially constant. Although the presence of the encapsulation material neither increase nor decreases airborne noise, the directivity of airborne noise is appreciably changed because the air flow path is changed.

The vibration test was conducted on a 2 HP, 4 Pole, 182 frame open motor. Table 8-6 lists the prominent 1/3 octave vibration acceleration levels for two vertical axes: (1) the Z-axis on the motor feet, and (2) an axis on the stator core. The stator core axis was recorded in order to closely reflect any change in core vibration due to the stator coil encapsulation. The primary rotor slot frequencies of this motor reflects in both the 1000 and 1250 cps bands. The two axes in these bands reveal an average 6 db decrease caused by the encapsulation. The spectrograms for the encapsulated motor also reflect spurious changes due to bearing deterioration which caused an increase in the 31.5 and 8000 cps bands on the Z-axis. Both the 31.5 cps band, which contains the rotational frequency (30 cps), and the 8000 band often reflect bearing noise. The core axis shows a decrease in these bands indicating the changes do not originate in the stator core. Since the change was so clearly a result of a defective bearing, the test was not repeated.

TABLE 8-6 Encapsulation Test
Vibration Acceleration Levels

Band	Axis	Unencapsulated	Encapsulated
31.5	Z	75	80
	Core	76	73
125	Z	72	70
	Core	77	75
1000	Z	104	96
	Core	99	96
1250	Z	107	101
	Core	110	104
8000	Z	97	103
	Core	101	98
Overall	Z	112	109
	Core	112	108

Values taken from Spectrograms 8-26 and 8-27.

The 6 db decrease in magnetic noise may be caused by two factors: (1) the epoxy encapsulation material completely fills the stator slots. If the compound is sufficiently rigid, this will add to the stator core and tooth rigidity and, thus, reduce the deflections caused by the magnetic force waves. (2) the presence of encapsulation around the end turns and through the slots can act as either a rigid support or a damping agent depending upon the rigidity of the material.

The 6 db decrease obtained using the Epoxylite epoxy compound is sufficiently large that further work in this field is warranted. It is recommended that a study be made to optimize the encapsulation compound to a maximum reduction of magnetic noise.

An encapsulation insulation system has recently been developed that can withstand occasional submergence in salt water (BuShips Contract NOBS 72314). Incorporation of this development with the vibration reduction caused by encapsulation suggests the feasibility of utilizing quieter encapsulated motors in many applications now requiring totally enclosed motors.

8.6 INTERNAL ISOLATION

The feasibility of providing internal isolation material between the stator core and frame was investigated. The fundamental theory of vibration isolation and the problems of providing internal isolation are treated. Tests of a sample isolation system indicate a large decrease in motor vibration, especially in the high frequencies.

Any isolation material has a transmissibility versus frequency characteristic similar to that shown in Figure 8-1. The equation for this curve can be given exactly for steel springs because they have straight line load deflection characteristics and negligible damping.

$$T = \frac{F_t}{F_d} = \frac{1}{\left(\frac{f_d}{f_n}\right)^2 - 1} \quad 8.1$$

where T = transmissibility
 F_t = force transmitted through the resilient mounting.
 F_d = disturbing force in same units as F_t .
 f_d = frequency of disturbing vibration in cycles per second.
 f_n = natural frequency of the resiliently mounted system in cps.

The natural frequency of the resiliently mounted system, f_n , is

$$f_n = \frac{188}{60} \sqrt{\frac{1}{d}} \quad 8.2$$

but $d = \frac{W}{k}$

$$f = \frac{188}{60} \sqrt{\frac{k}{W}} \quad 8.3$$

where d = static deflection of the resilient mounting in inches.
 k = spring constant or stiffness factor of the mounting in pounds per inch of deflection.
 W = weight on the mounting in pounds.

As indicated above, these equations are exact only for steel springs or the equivalent. For rubber and neoprene, 50% of the static deflection may be used when calculating f_n . (22)

constant, k , will lower the peak at f_n and raise the transmissibility beyond $\sqrt{2} f_n$, until the extreme case of no isolation results in a horizontal line through unity transmissibility.

Because the use of any isolation material results in an amplification of all frequencies below $\sqrt{2} f_n$, it is imperative that f_n be equal or less than the lowest frequency vibration of importance. In induction motors, this frequency is the rotational frequency, f_r . Therefore, the natural frequency must meet the following condition:

$$f_n < \frac{f_r}{\sqrt{2}}$$

$$\text{or } f_n < \frac{120(1-s)}{\sqrt{2} P} \quad 8.4$$

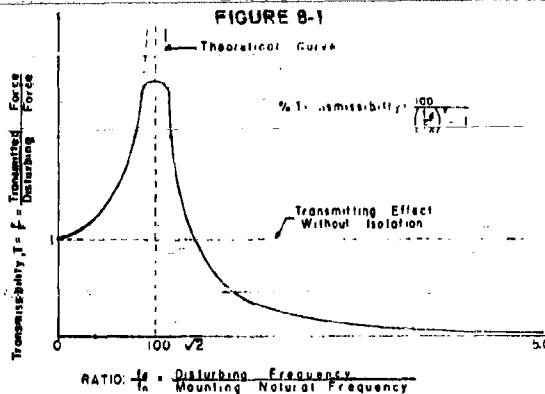
Since the isolation must be effective at no load ($s = 0$) as well as full load, Equation 8.4 may be simplified.

$$f_n < \frac{85}{P} \quad 8.5$$

In addition to preventing any amplification of rotational frequency noise, a low resonant frequency is desirable to reduce the transmissibility of any vibration having a frequency greater than the $\sqrt{2} f_n$. This can be seen from Equation 8-1. The larger the term $(f_d/f_n)^2$ becomes, the lower the transmitted force. The disturbing frequency, f_d , is that of the vibration being isolated; thus the only remaining variable is f_n . Reducing f_n by increasing the static deflection (Equation 8.2) reduces the vibration transmission. As Equation 8-3 indicates, the deflection may be increased by either decreasing the spring constant or increasing the weight W .

Application of the theory of vibration isolation to the interior of an induction motor presents several problems: (1) A minimum of space is available for the isolation material, (2) The low natural frequency required by Equation 8.5 requires both a low stiffness (high resiliency) and a relatively high compression force.

A survey of the isolation materials presently manufactured revealed that a waffle shaped pad (manufactured by Fabreka) designed for use under machinery came closest to meeting these requirements. Figure 8-2 shows samples of these pads and the modified stator core of a 5 HP, 2 Pole motor which was used for testing internal isolation. The material was cut into a strip and wound around the stator core O.D. A metal band was clamped around the pad to compress it and to supply a metal surface to permit pressing the assembly into the motor frame. The pad was compressed with a pressure of 50 lbs. per square inch and resulted in a natural frequency of approximately 20 cycles per second.



The natural frequency, f_n , of a resiliently mounted system is the frequency at which it will oscillate by itself if a force is exerted on the system and then released. A system may have up to six natural frequencies, but it will be found that in the practical selection of machine mountings, if the vertical natural frequency of the system is made low enough for a low transmissibility, the horizontal and rotational natural frequencies will generally be lower than the vertical and can be disregarded.

The curve in Figure 8-1 passes through unity transmissibility at $\sqrt{2} f_n$. Between zero cps and $\sqrt{2} f_n$ cps, the transmitted force is greater than the disturbing force. Although the amount of damping may affect the value of f_n , the transmissibility curve will always pass through f_n at $\sqrt{2} f_n$. An increase in the spring

FIGURE 8-2

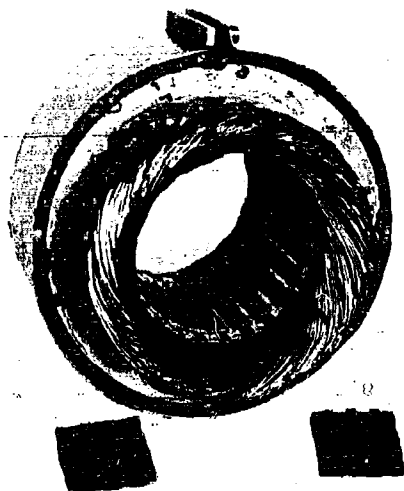


Table 8-7 lists the prominent 1/3 octave vibration acceleration levels for the original 2 Pole motor (not isolated) and the same unit modified to accommodate the isolated core. All frequency bands other than 315 cps indicate a lower vibration for the internally isolated unit. This reduction is greatest for the radial axes (Y and Z) in the 4000 cps band, which contains the double rotor slot frequencies described in Section 3. The next highest vibration reduction occurs in the 63 cps band indicating that appreciable amount of rotational frequency (60 cps) originates in the stator. The 315 cps band for the motor contains the preload band and its erratic variation is of no consequence. Internal isolation results in an appreciable decrease in vibration levels, not only of the magnetic noise but of the entire frequency spectrum.

TABLE 8-7 Internal Isolation
Vibration Acceleration Levels

Band	Axis	Not Isolated	Isolated
63	X	89	85
	Y	89	83
	Z	90	83
315	X	80	88
	Y	90	83
	Z	83	92
2000	X	93	90
	Y	95	92
	Z	100	98
4000	X	89	83
	Y	92	82
	Z	92	82
10,000	X	96	93
	Y	94	91
	Z	95	92
Overall	X	109	105
	Y	110	104
	Z	107	104

Values taken from Spectrograms 8-28 and 8-29.

Table 8-8 gives an indication of the attenuation of motor vibration between the stator core and frame of the isolated unit. Prominent one-third octave levels are shown for both the motor running at no load and for a half-voltage locked rotor condition. The latter test was conducted to eliminate all rotation-dependent noise and vibration.

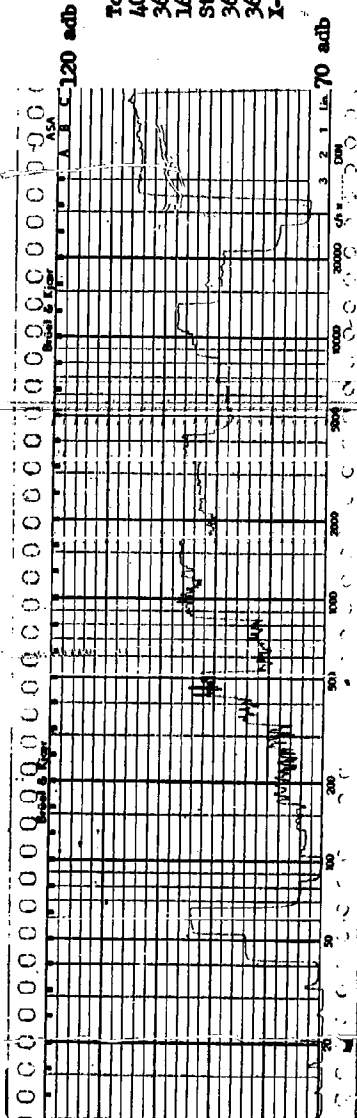
TABLE 8-8
Isolation Test
Vibration Acceleration Levels

Band	Running		Half Voltage	Locked Rotor
	Frame	Core	Frame	Core
63	84	90	*	*
125	73	95	105	111
250	84	91	115	122
315	87	88	107	103
2,000	87	100	99	106
4,000	82	89	91	96
10,000	88	77	*	*
Overall	102	107	122	124

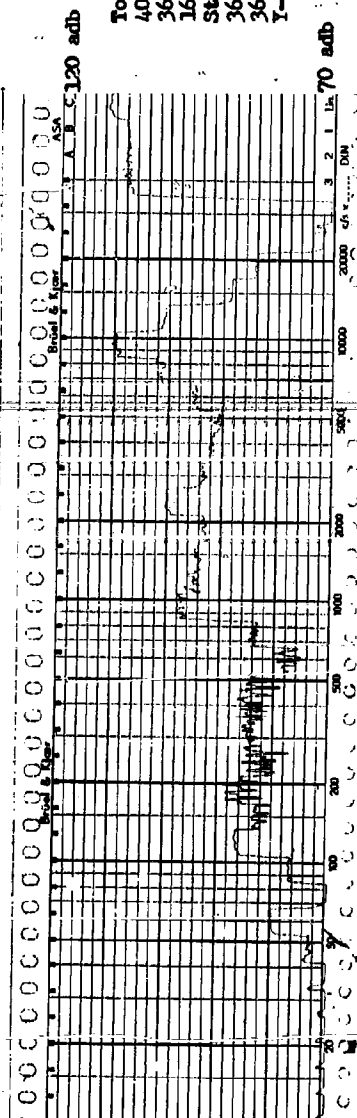
* Values less than 90 odb were below range of recording paper for the locked rotor condition.

Values taken from Spectrograms 8-30 and 8-31.

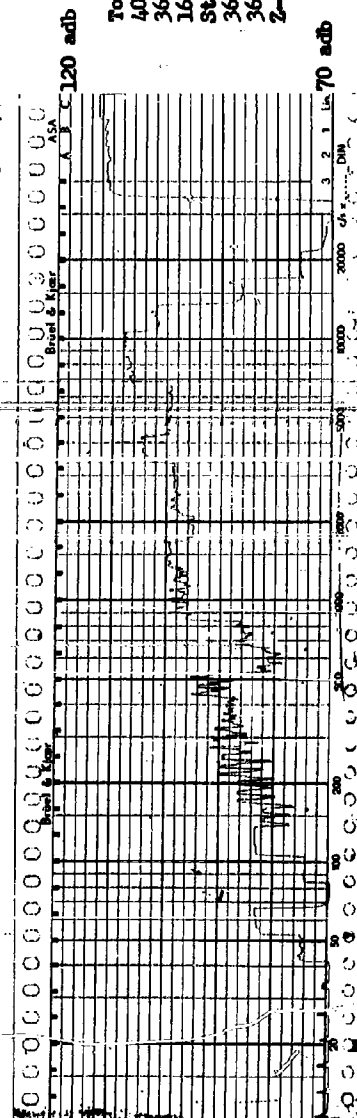
Although the effectiveness of internal isolation in reducing motor noise has been proven, several problems arise through their use. The isolation material is as efficient a thermal insulator as vibration isolator. The location of this material between the stator core and frame places it in the path of one of the main avenues of heat removal. In addition, the isolation material must be resistant to any contaminants in the atmosphere. Two isolation manufacturers have expressed the opinion that internal isolators can be made of materials resistant to both contaminants and the maximum hot spot temperature of Class B motors. Whether motors with such isolation can be cooled sufficiently is not apparent. It is recommended that this aspect receive further study.



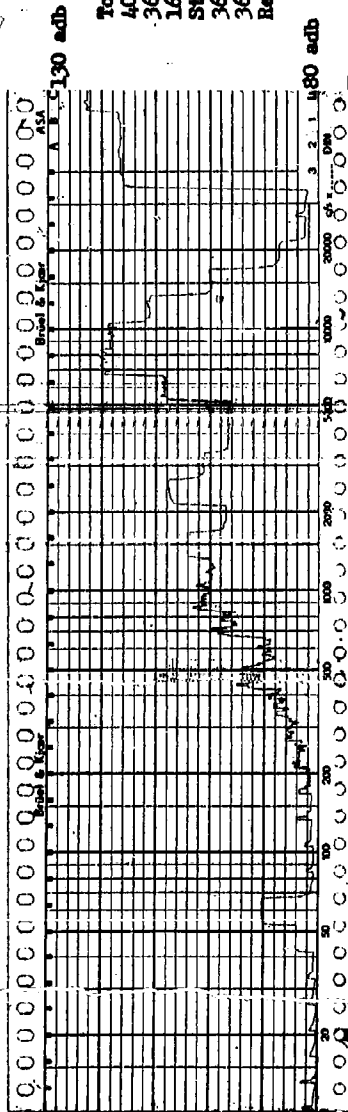
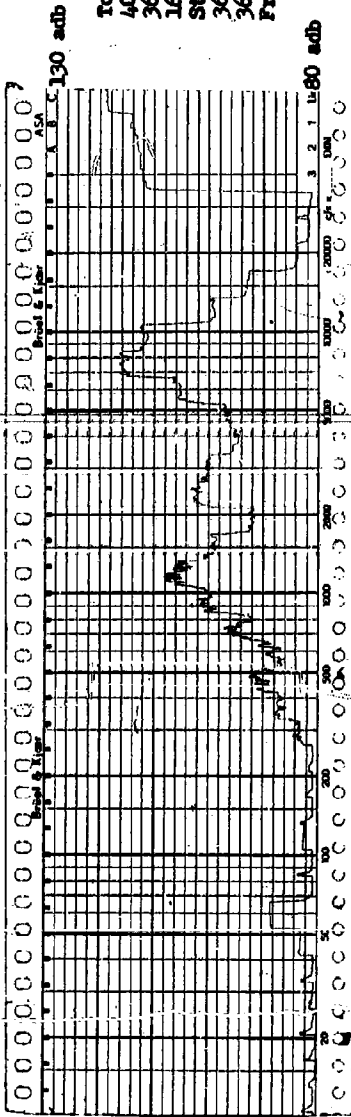
Tolerance Study
 40 HP 2 Pole
 364 Frame TEFC
 16 May 1960
 Structureborne
 36-36-36-36
 X-axis

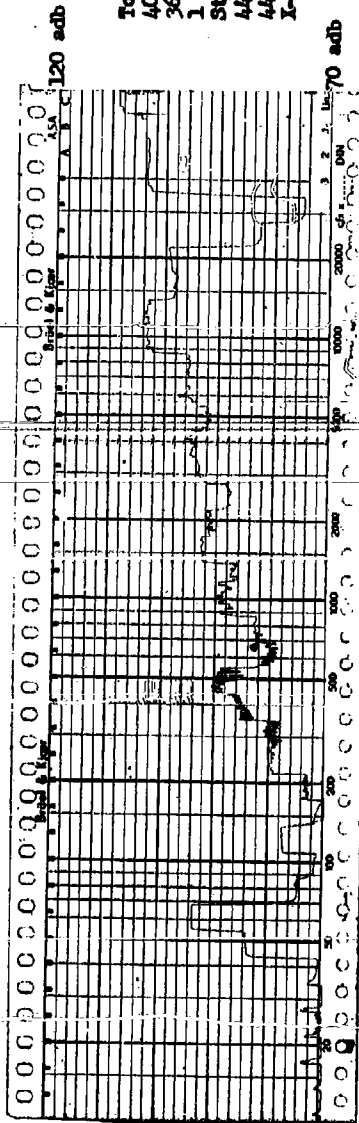


Tolerance Study
 40 HP 2 Pole
 364 Frame TEFC
 16 May 1960
 Structureborne
 36-36-36-36
 Y-axis

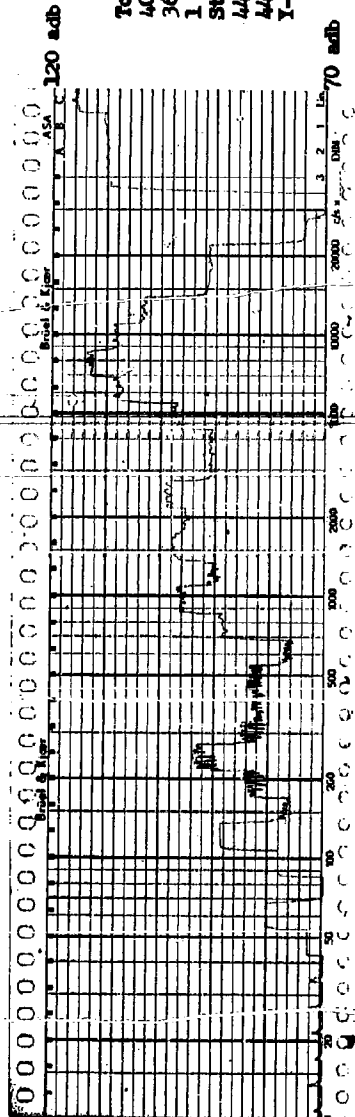


Tolerance Study
 40 HP 2 Pole
 364 Frame TEFC
 16 May 1960
 Structureborne
 36-36-36-36
 Z-axis

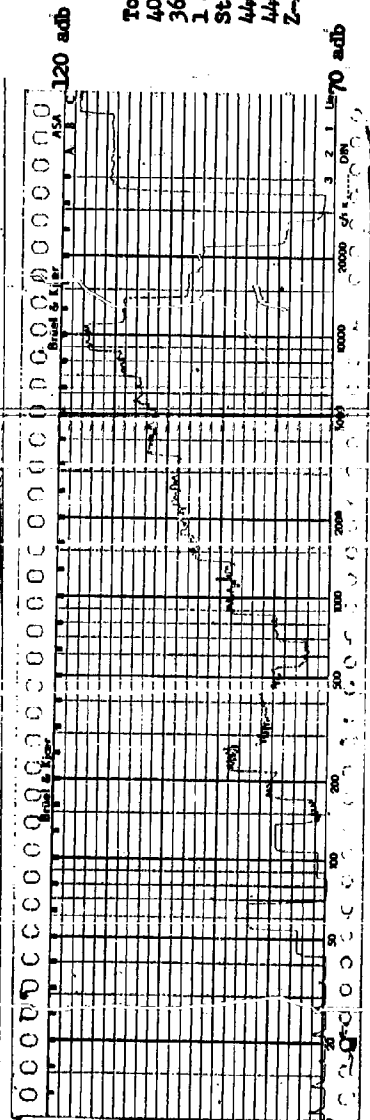




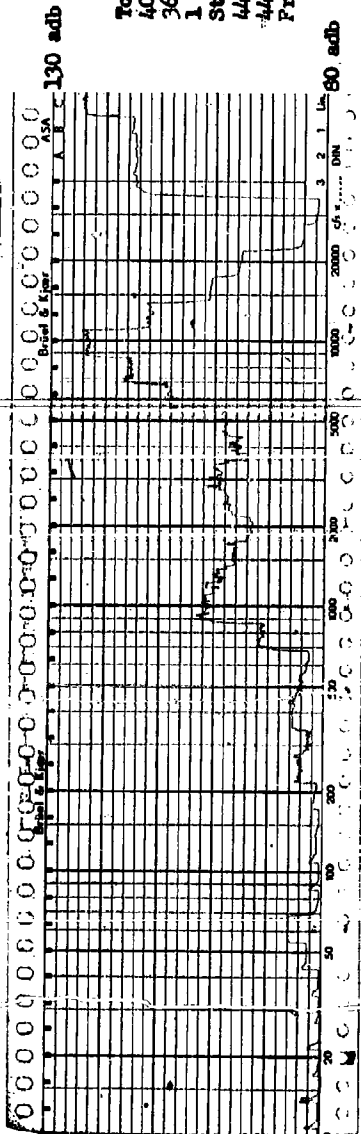
Tolerance Study
 40 HP 2 Pole
 364, Frame TEF3
 1 June 1960
 Structureborne
 44-36-26-36
 44-36-26-36
 I-Axis



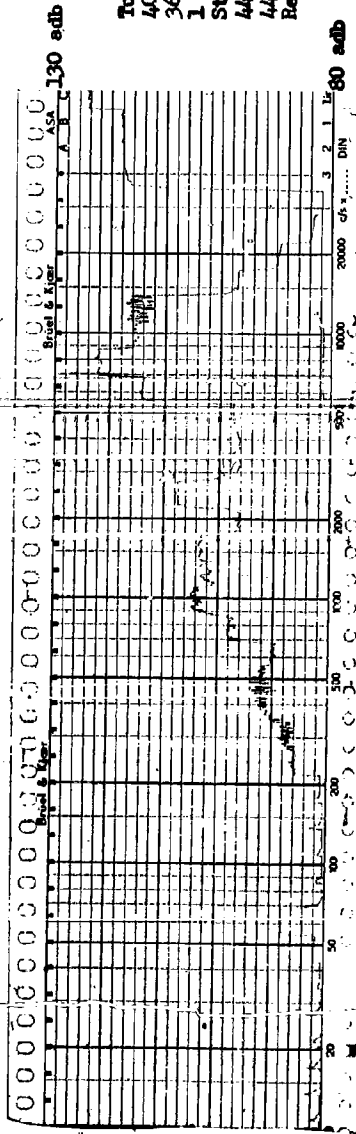
Tolerance Study
 40 HP 2 Pole
 364, Frame TEF3
 1 June 1960
 Structureborne
 44-36-26-36
 44-36-26-36
 Y-Axis



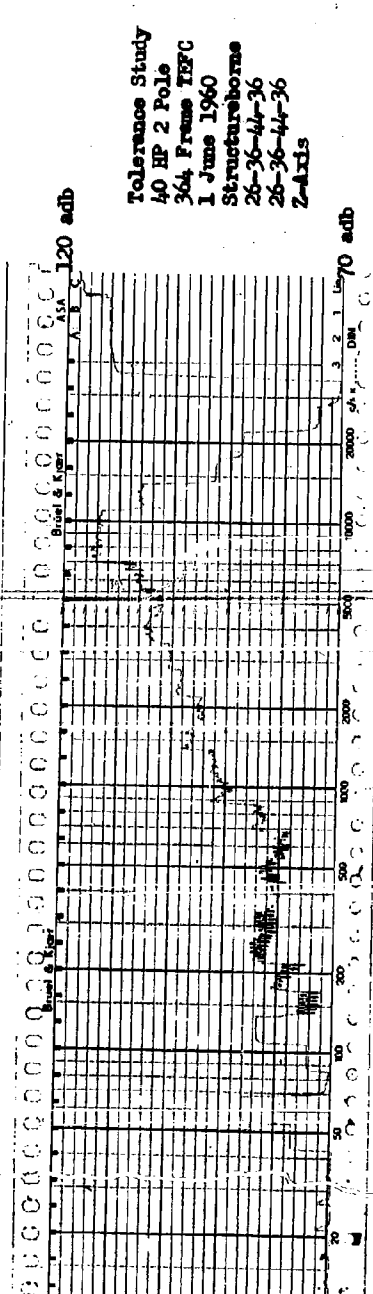
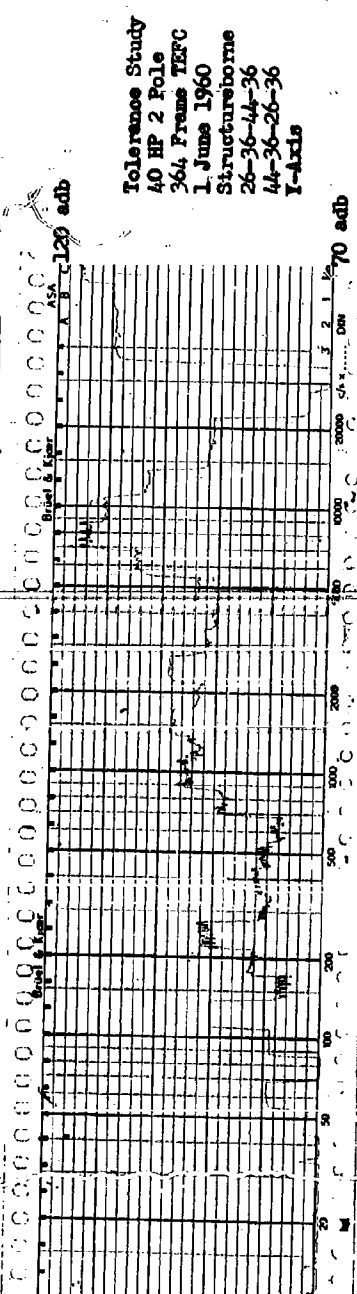
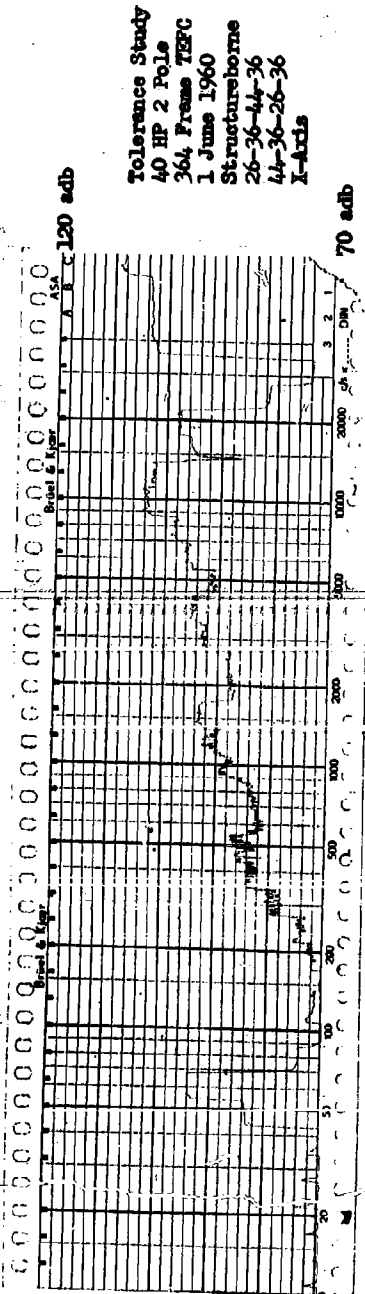
Tolerance Study
 40 HP 2 Pole
 364, Frame TEF3
 1 June 1960
 Structureborne
 44-36-26-36
 44-36-26-36
 Z-Axis

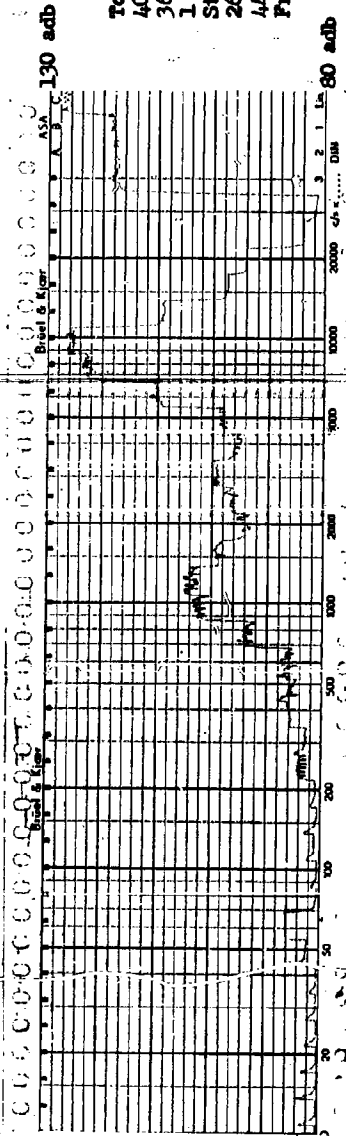


Tolerance Study
 40 HP 2 Pole
 364, Frame TERC
 1 June 1960
 Structureborne
 44-36-26-36
 44-36-26-36
 Front Hsg.

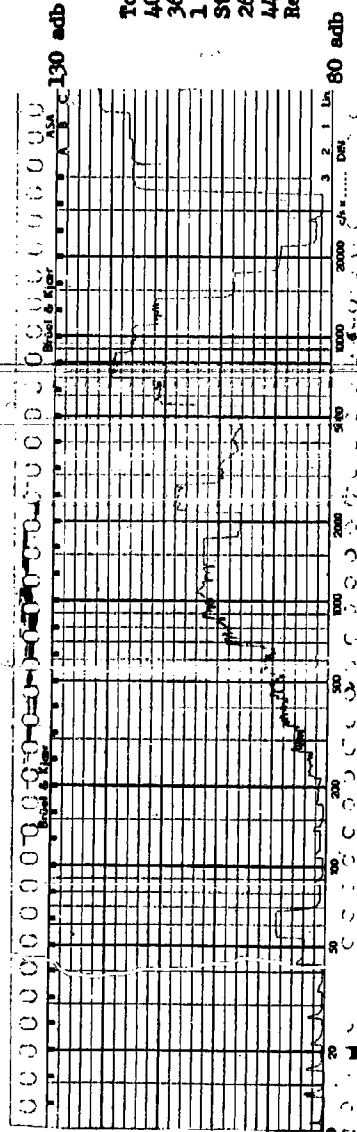


Tolerance Study
 40 HP 2 Pole
 364, Frame TERC
 1 June 1960
 Structureborne
 44-36-26-36
 44-36-26-36
 Rear Hsg.

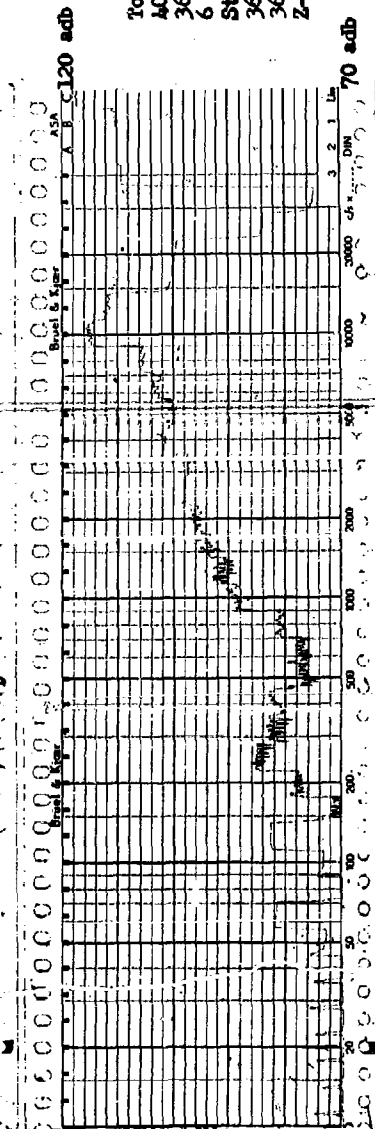
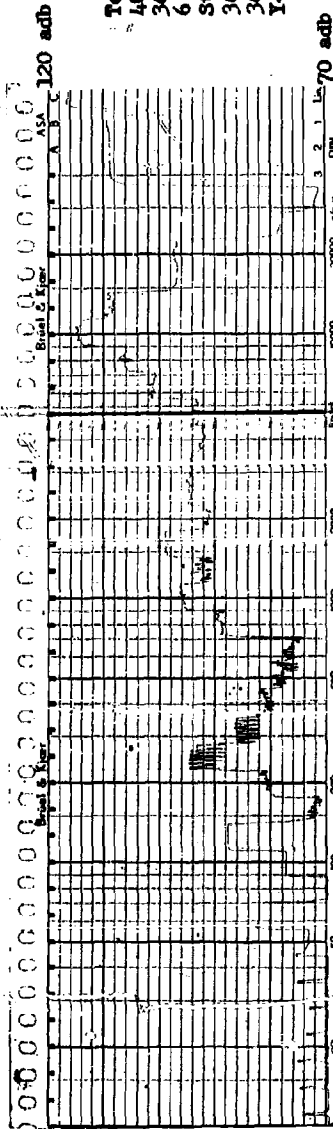
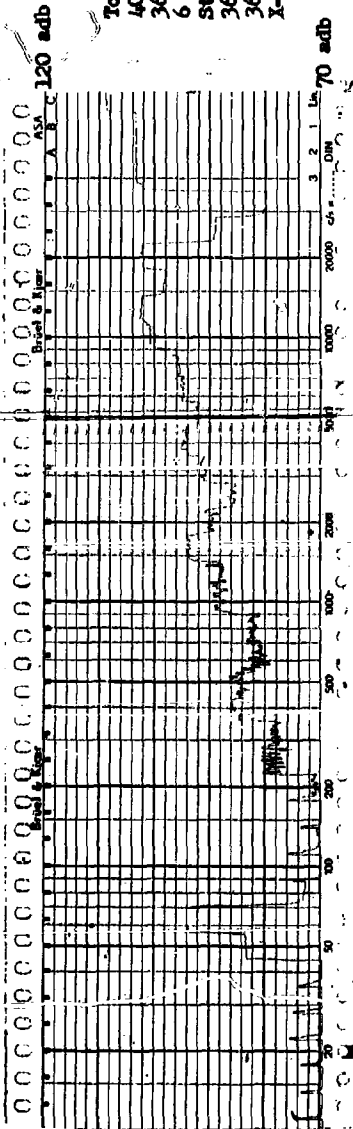


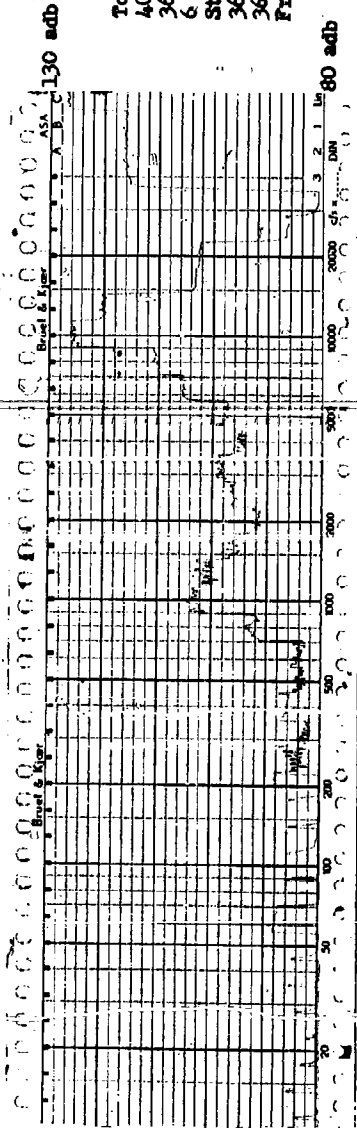


Tolerance Study
 40 HP 2 Poles
 364 Frame TEGC
 1 June 1960
 Structureborne
 26-36-44-36
 44-36-26-36
 Front Hsg.

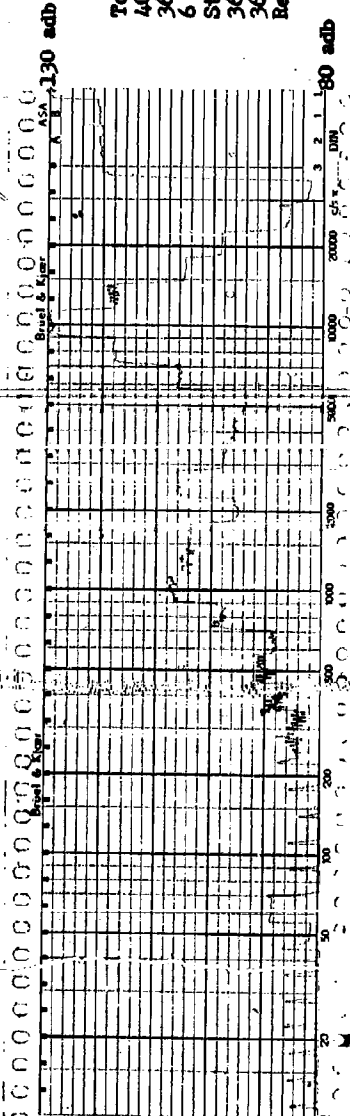


Tolerance Study
 40 HP 2 Poles
 364 Frame TEGC
 1 June 1960
 Structureborne
 26-36-44-36
 44-36-26-36
 Rear Hsg.

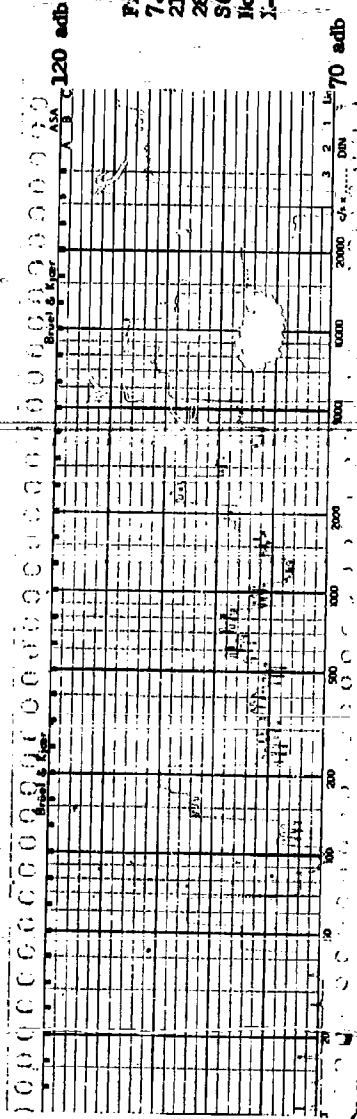




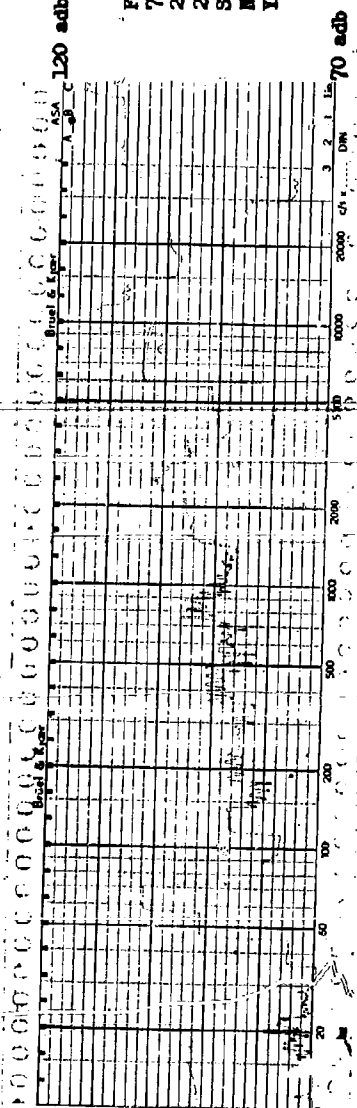
Tolerance Study
 40 HP 2 Pole
 364 Frame TEFC
 6 July 1960
 Structureborne
 36-36-36-36
 36-36-36-36
 Front Hsg.



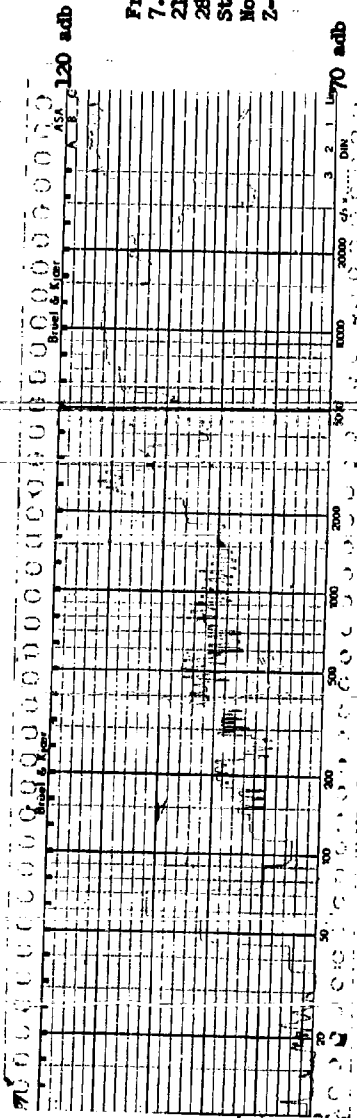
Tolerance Study
 40 HP 2 Pole
 364 Frame TEFC
 6 July 1960
 Structureborne
 36-36-36-36
 36-36-36-36
 Rear Hsg.



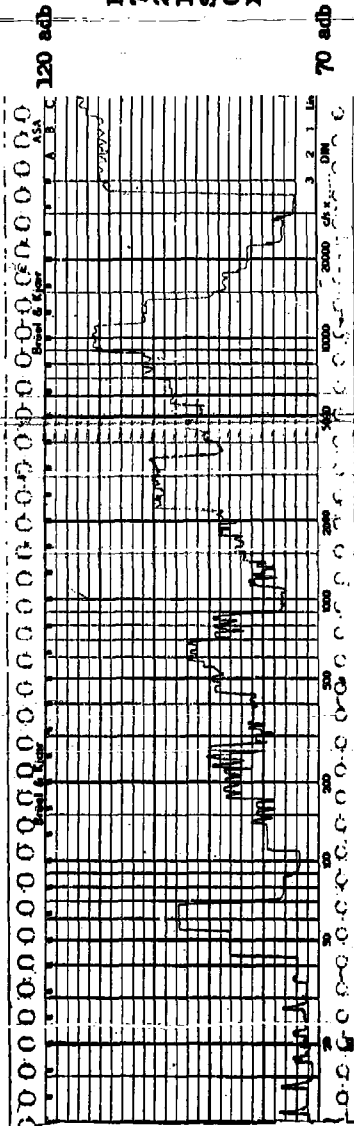
Frame Material
 7.5 HP 2 Pole
 213 Frame TEFC
 28 March 1960
 Structureborne
 Modular Iron
 Y-Axis



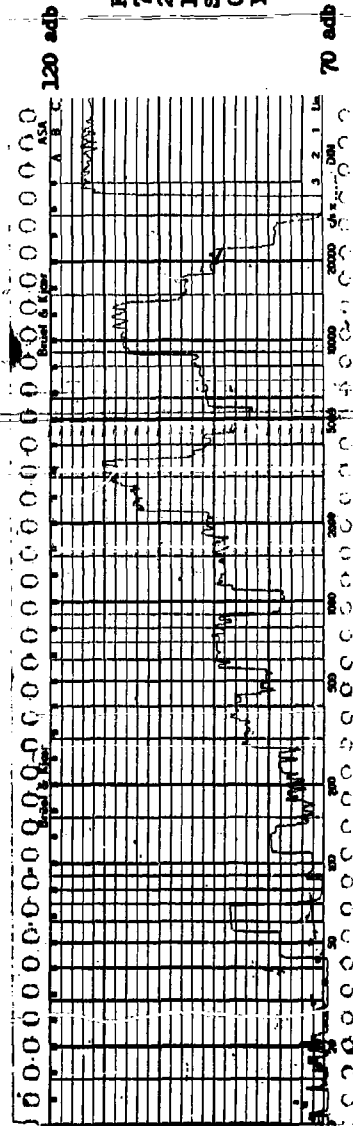
Frame Material
 7.5 HP 2 Pole
 213 Frame TEFC
 28 March 1960
 Structureborne
 Modular Iron
 Y-Axis



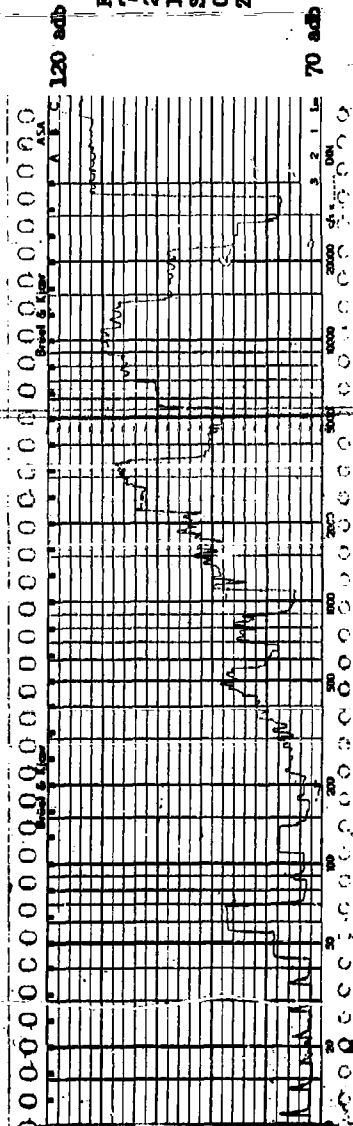
Frame Material
 7.5 HP 2 Pole
 213 Frame TEFC
 28 March 1960
 Structureborne
 Modular Iron
 Z-Axis



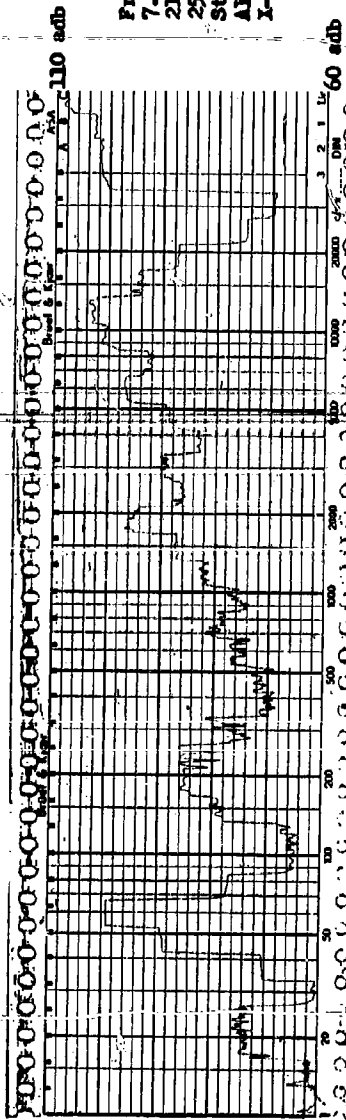
Frame Material
7.5 HP 2 Pole
213 Firms TERC
10 March 1960
Structureborne
Cast Steel
X - Axis



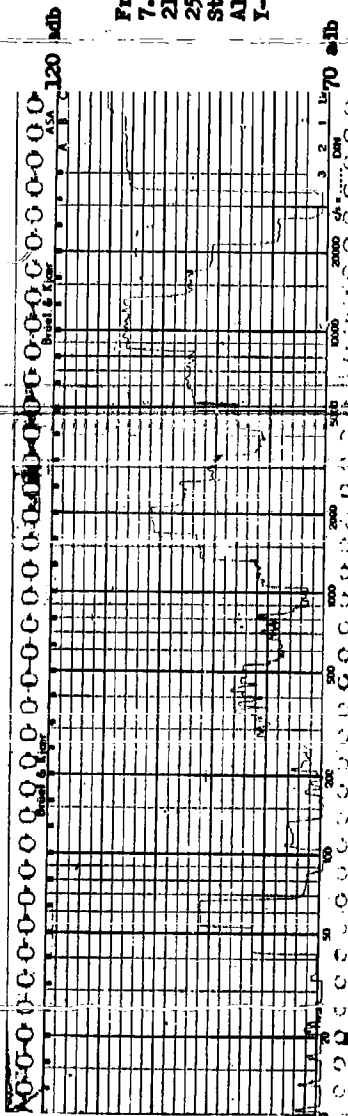
Frame Material
7.5 HP 2 Pole
213 Firms TERC
10 March 1960
Structureborne
Cast Steel
Y - Axis



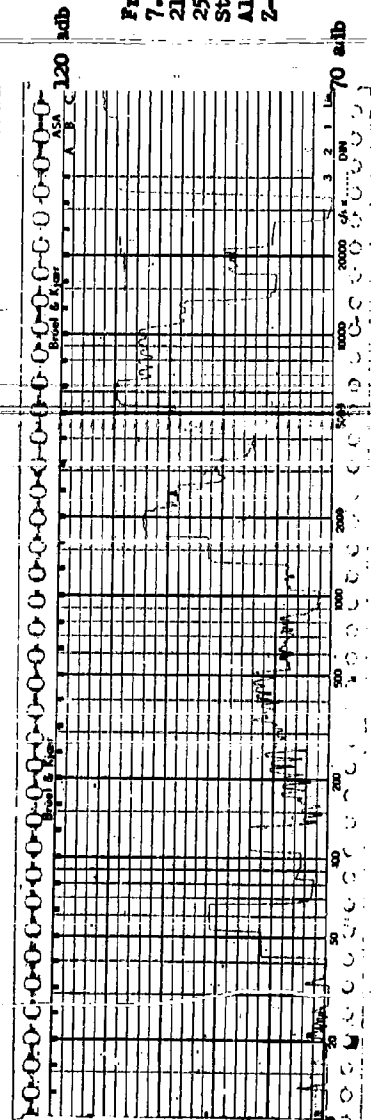
Frame Material
7.5 HP 2 Pole
213 Firms TERC
10 March 1960
Structureborne
Cast Steel
Z - Axis



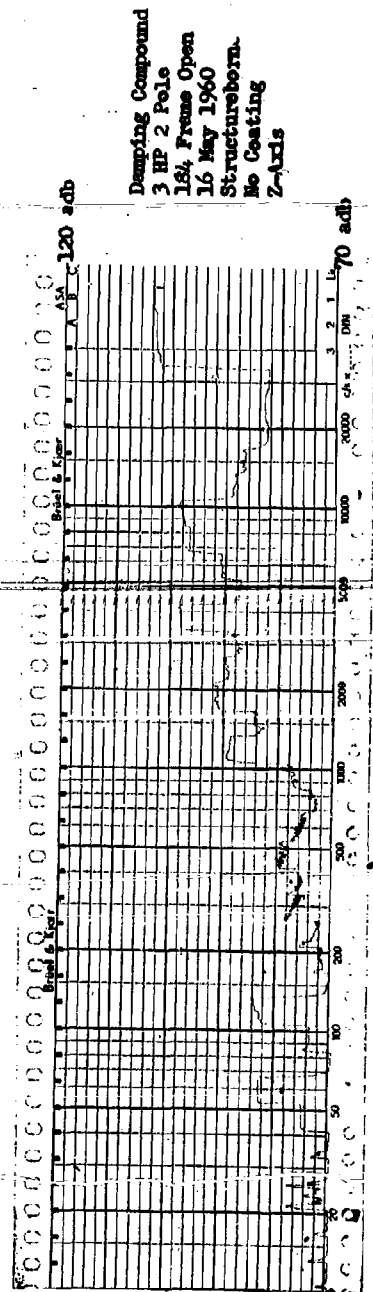
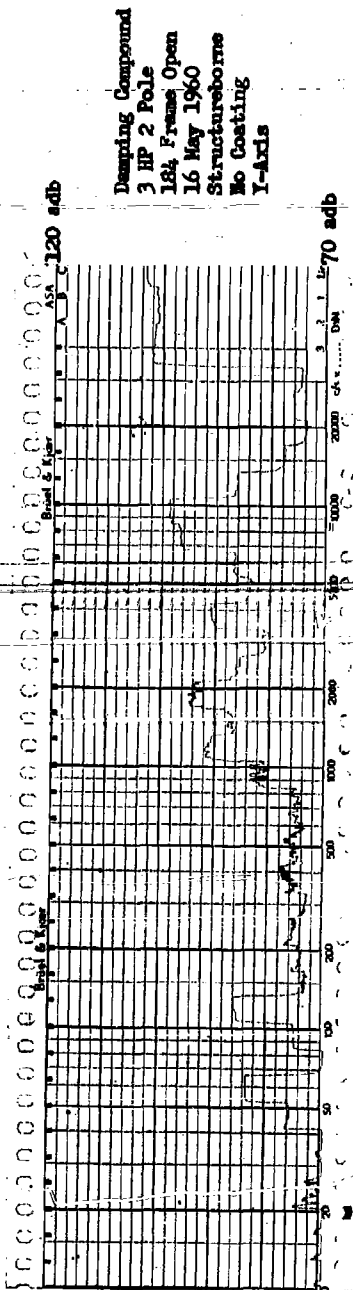
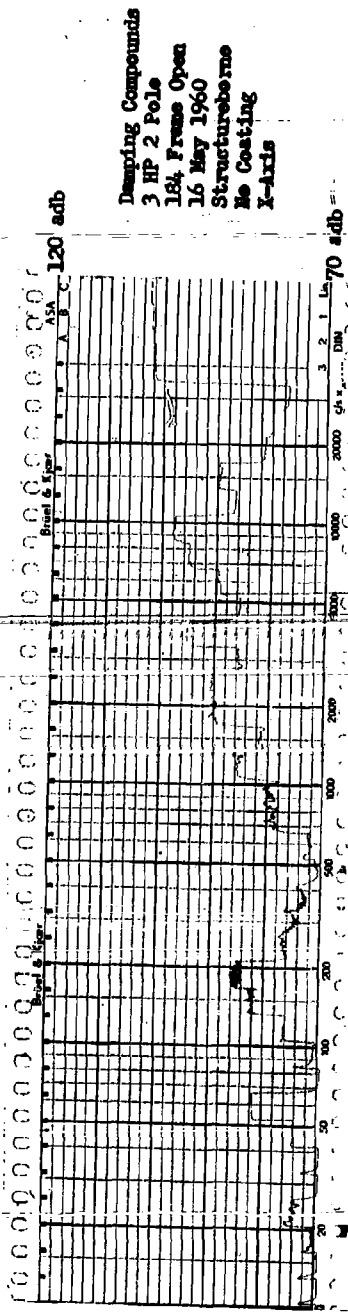
Frame Material
7.5 HP 2 Pole
213 Frame TEFC
25 March 1960
Structureborne
Aluminum
I-Axis

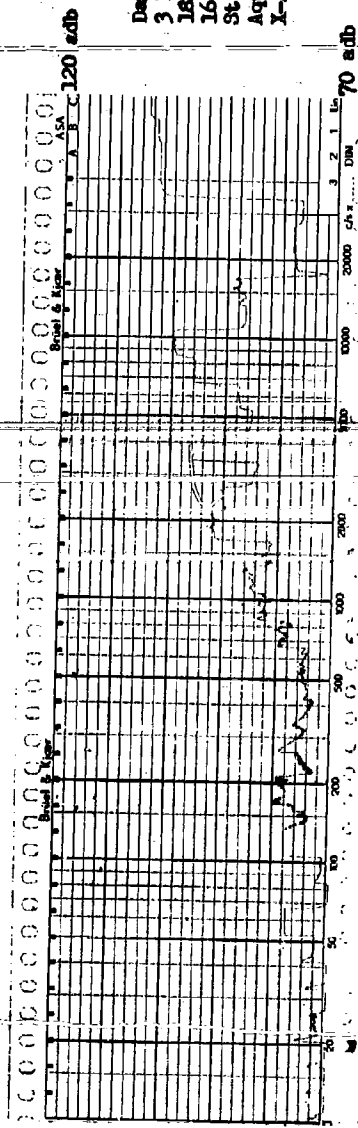


Frame Material
7.5 HP 2 Pole
213 Frame TEFC
25 March 1960
Structureborne
Aluminum
Y-Axis

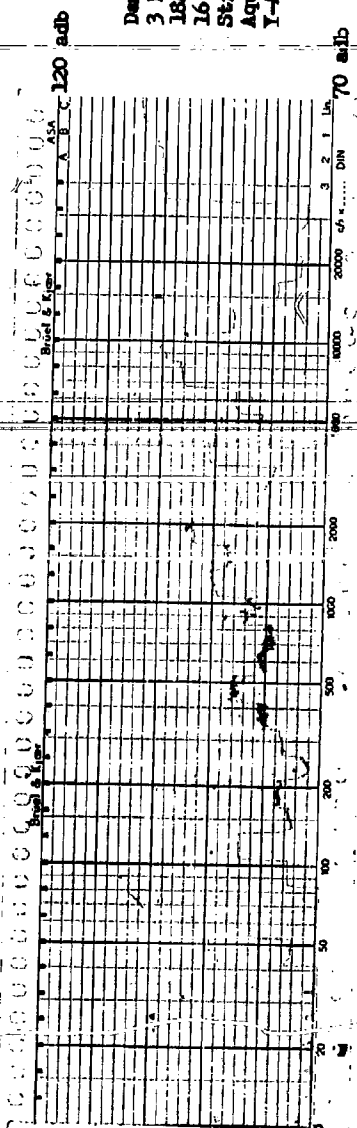


Frame Material
7.5 HP 2 Pole
213 Frame TEFC
25 March 1960
Structureborne
Aluminum
Z-Axis

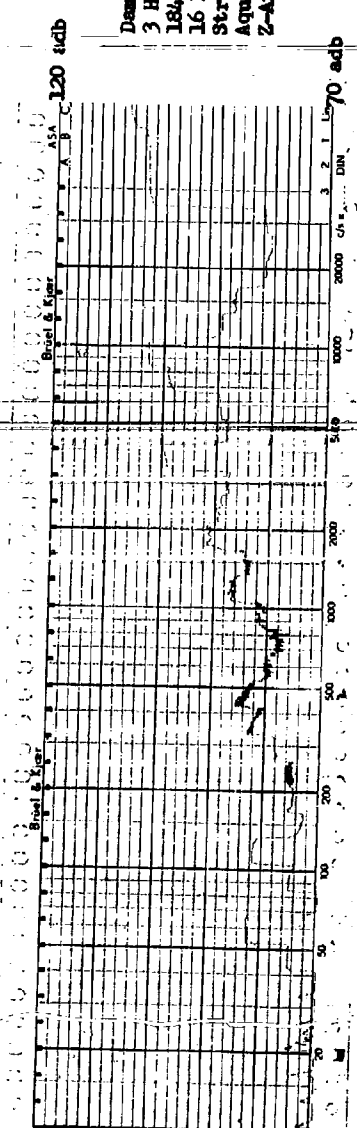




Damping Compound
 3 HP 2 Pole
 184, Frame Open
 16 May 1960
 Structureborne
 Aquaplas
 X-Axis

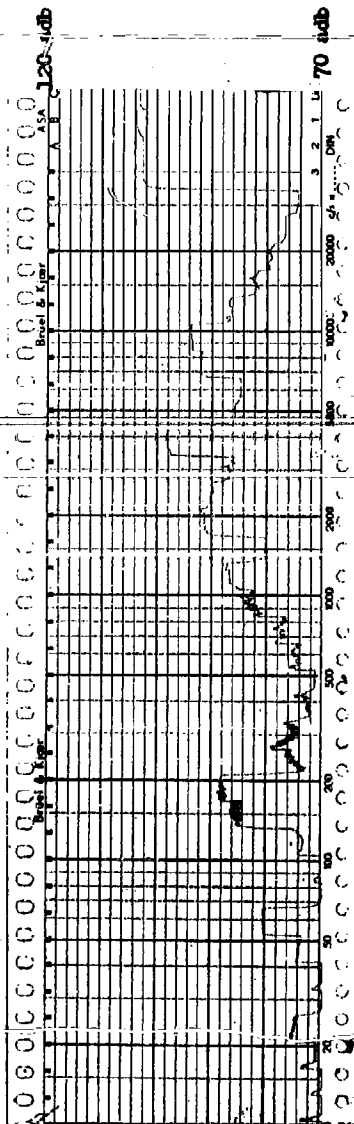


Damping Compound
 3 HP 2 Pole
 184, Frame Open
 16 May 1960
 Structureborne
 Aquaplas
 Y-Axis

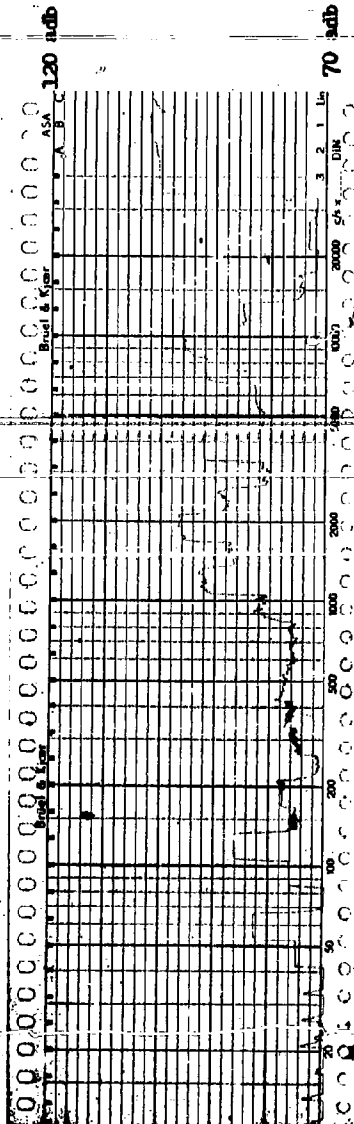


Damping Compound
 3 HP 2 Pole
 184, Frame Open
 16 May 1960
 Structureborne
 Aquaplas
 Z-Axis

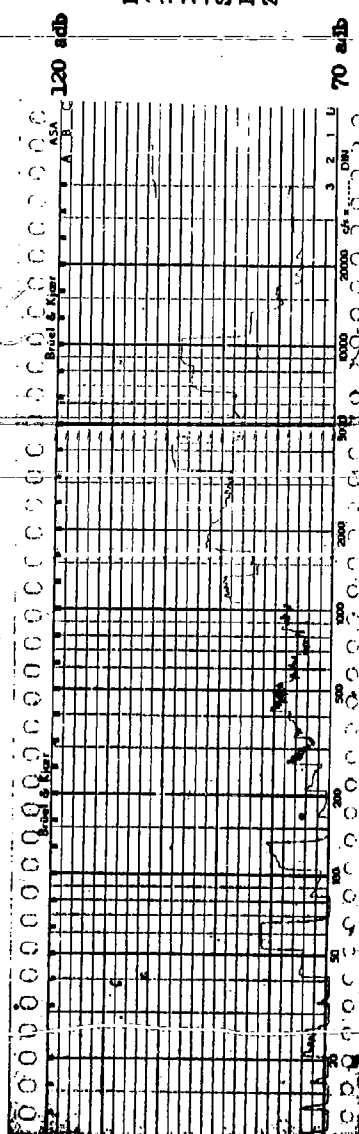
Damping Compounds
 3 HP 2 Pole
 184, Frame Open
 16 May 1960
 Structureborne
 EC-244
 Y - Axis



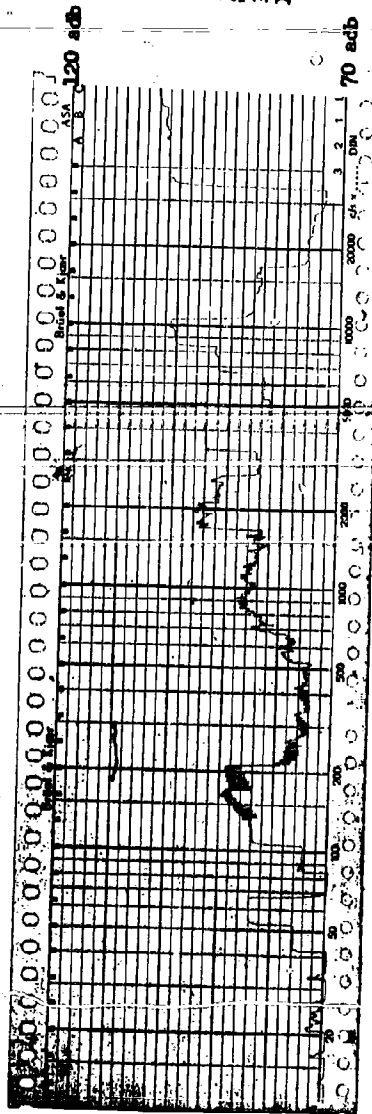
Damping Compounds
 3 HP 2 Pole
 184, Frame Open
 16 May 1960
 Structureborne
 EC-244
 Y - Axis



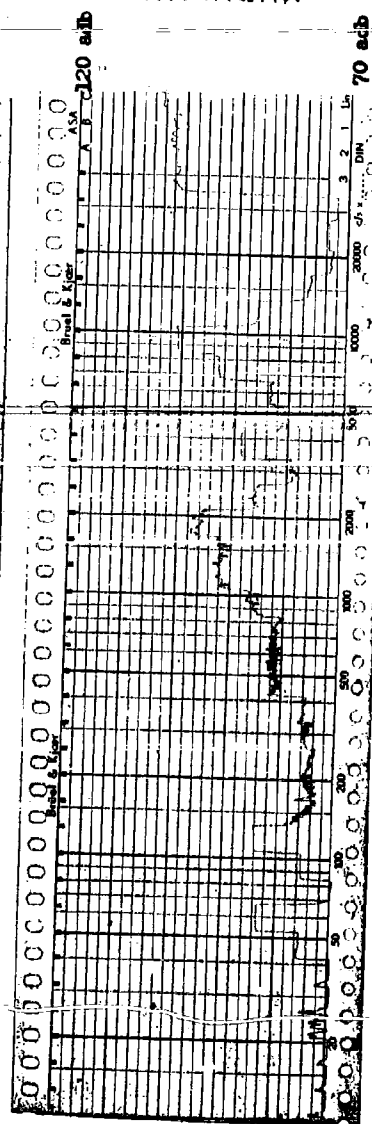
Damping Compounds
 3 HP 2 Pole
 184, Frame Open
 16 May 1960
 Structureborne
 EC-244
 Z - Axis



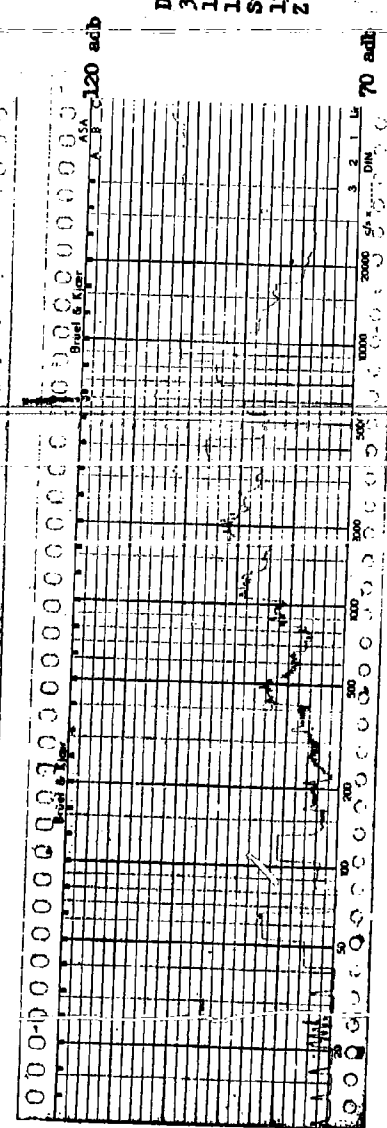
Damping Compounds
 3 HP 2 Pole
 184, Frame Open
 16 May 1960
 Structureborne
 1378
 X - Axis



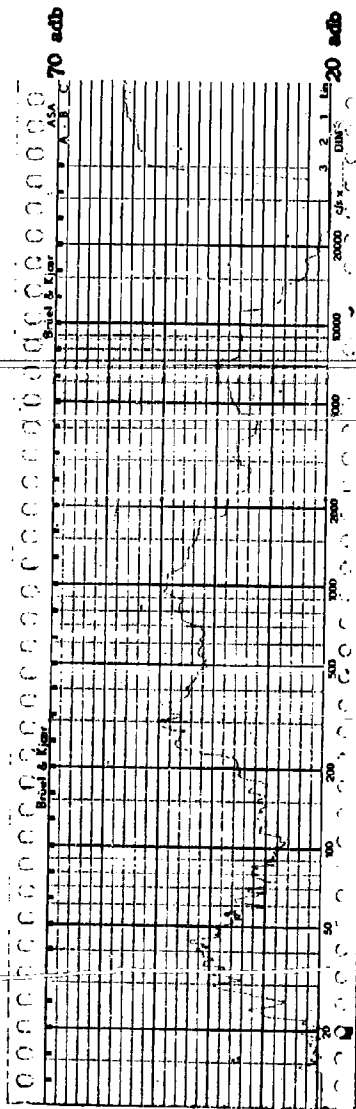
Damping Compounds
 3 HP 2 Pole
 184, Frame Open
 16 May 1960
 Structureborne
 1378
 Y - Axis



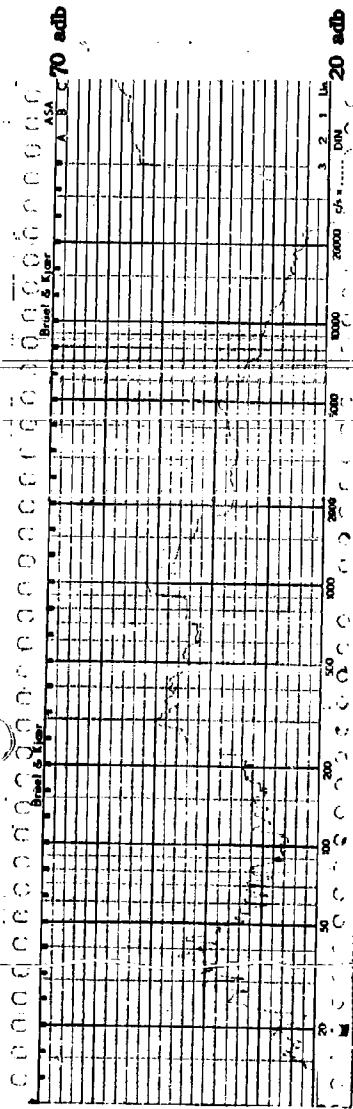
Damping Compounds
 3 HP 2 Pole
 184, Frame Open
 16 May 1960
 Structureborne
 1378
 Z - Axis



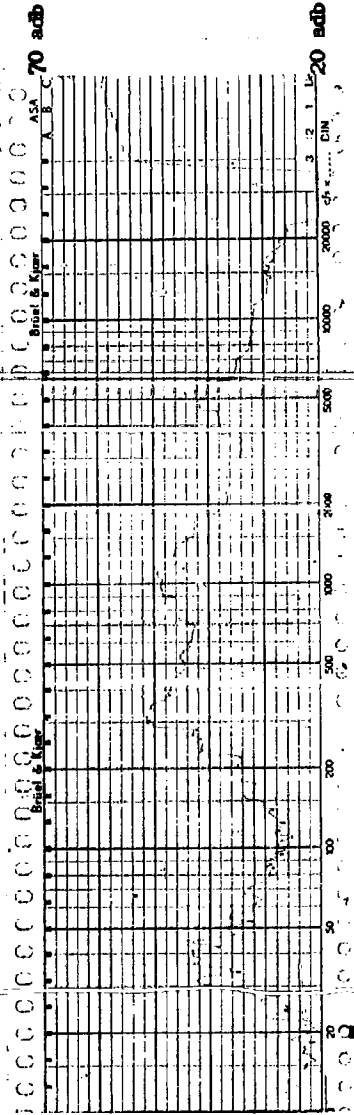
Damping Compounds
3 HP 2 Pole
184 Frames Open
27 April 1960
Airborne
3 Ft. Front End
No Coating



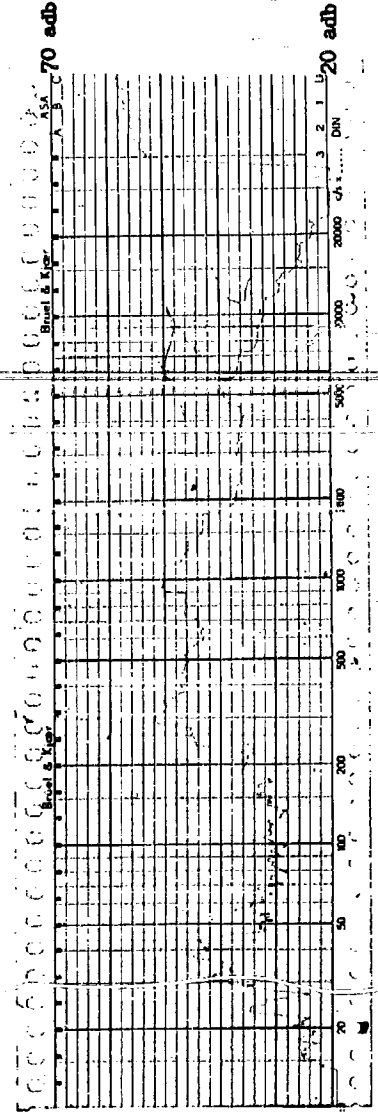
Damping Compounds
3 HP 2 Pole
184 Frames Open
27 April 1960
Airborne
3 Ft. Front End
Acquaplas



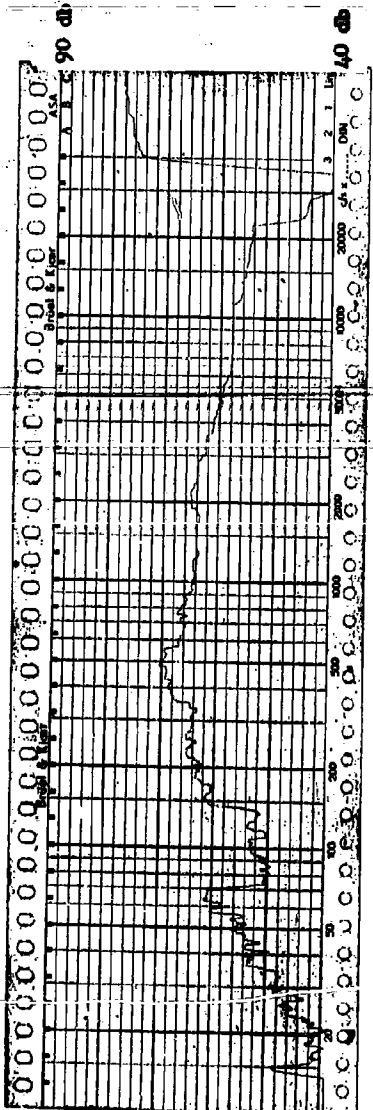
Damping Compounds
3 HP 2 Pole
184 Frame Open
27 April 1960
Airborne
3 Ft. Front End
EC-244



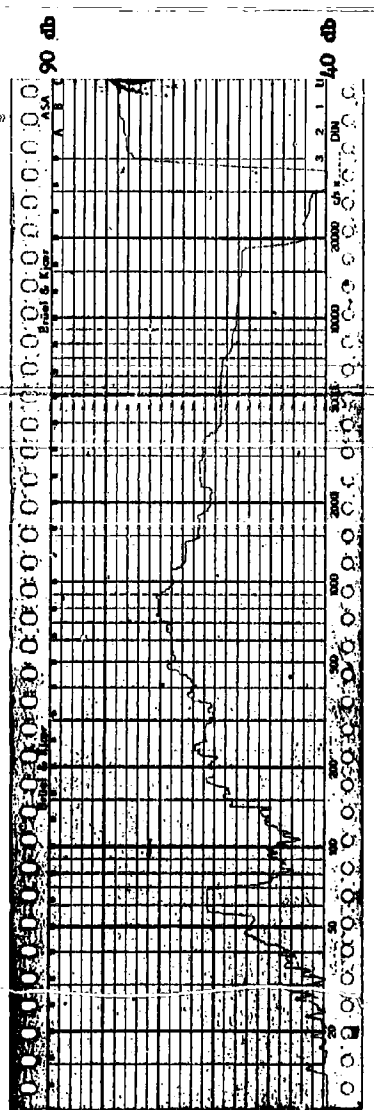
Damping Compounds
3 HP 2 Pole
184 Frame Open
27 April 1960
Airborne
3 Ft. Front End
1378



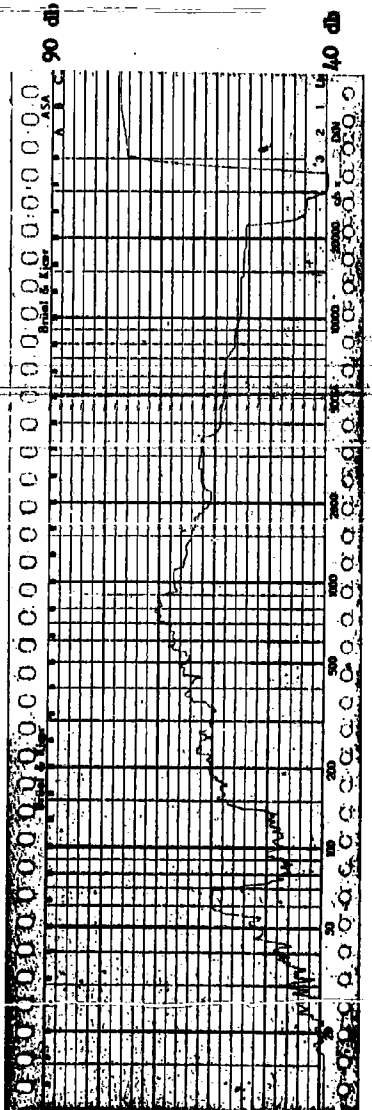
Damping Compounds
 5 Hp 2 Poles
 213 Frame TEFC
 20 April 1960
 Airborne
 3 Ft. Front End
 No Fan Bowl



Damping Compounds
 5 HP 2 Poles
 213 Frame TEFC
 20 April 1960
 Airborne
 3 Ft. Front End
 No Coating

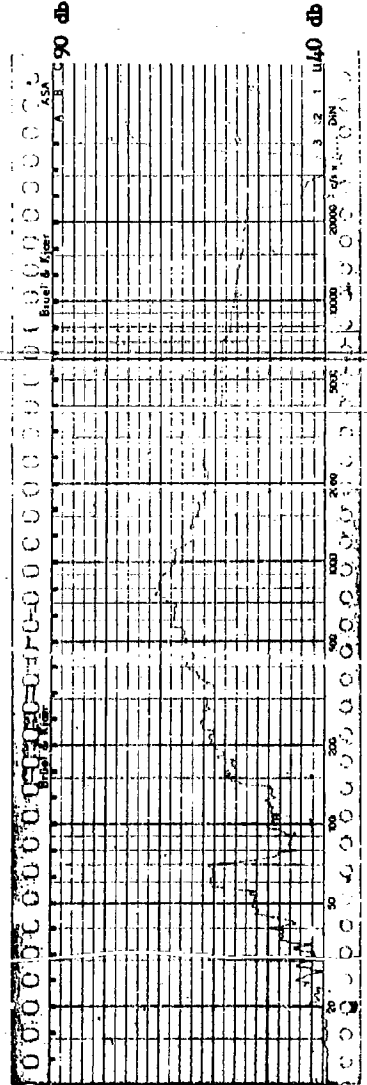
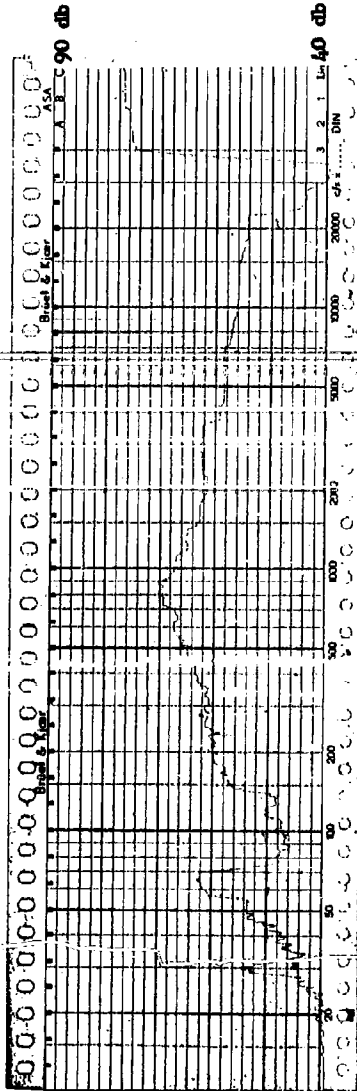


Damping Compounds
 5 HP 2 Poles
 213 Frame TEFC
 20 April 1960
 Airborne
 3 Ft. Front End
 Aquaplas

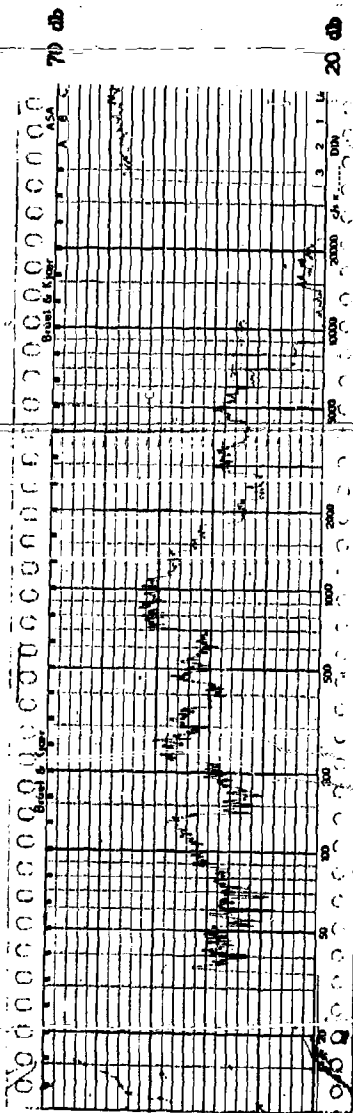


Damping Compounds
5 HP 2 Foils
213 Frames TEFC
20 April 1960
3 Ft. Front End
EC-244

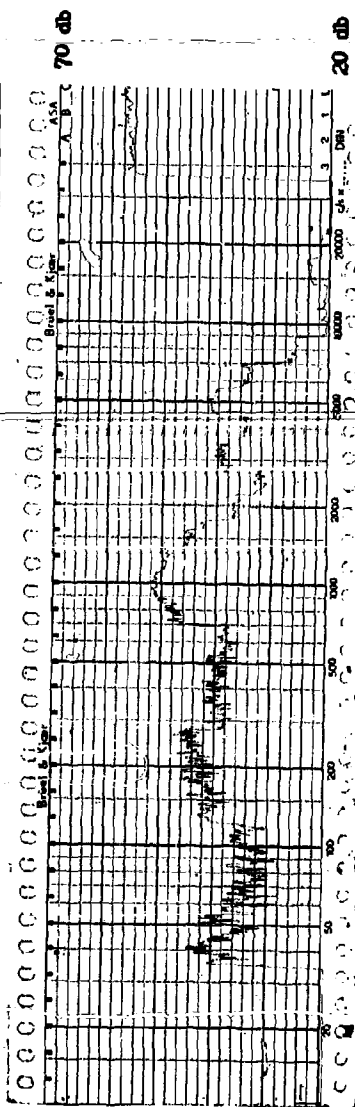
Damping Compounds
5 HP 2 Foils
213 Frames TEFC
20 April 1960
3 Ft. Front End
1378



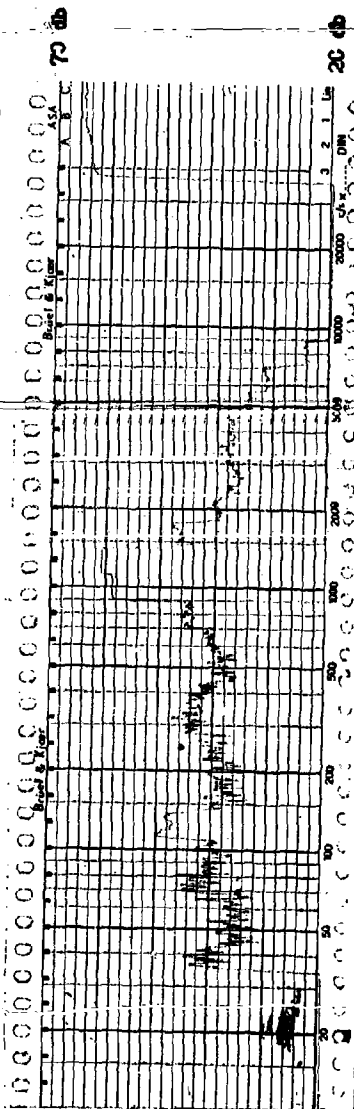
Encapsulation Test
3 HP 4 Pole
184 Frame Open
4 Sept. 1959
Airborne
3 Ft. Front End
Unencapsulated



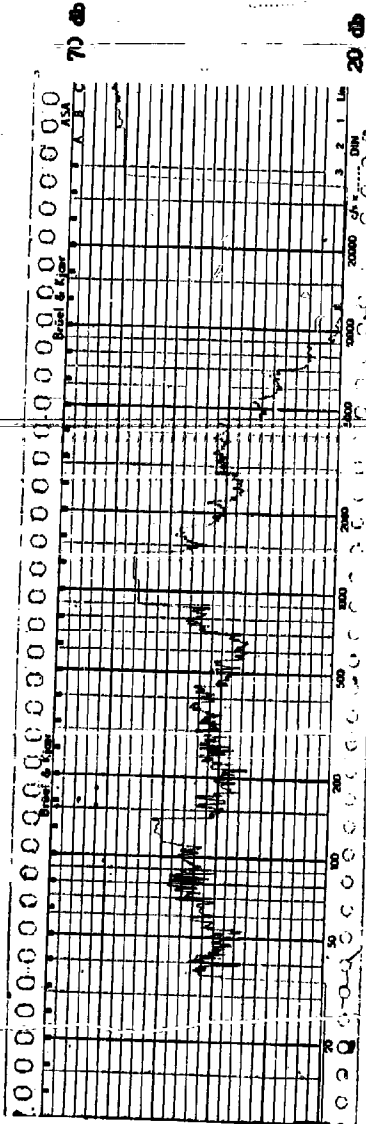
Encapsulation Test
3 HP 4 Pole
184 Frame Open
4 Sept. 1959
Airborne
2 Feet 12:00
Unencapsulated



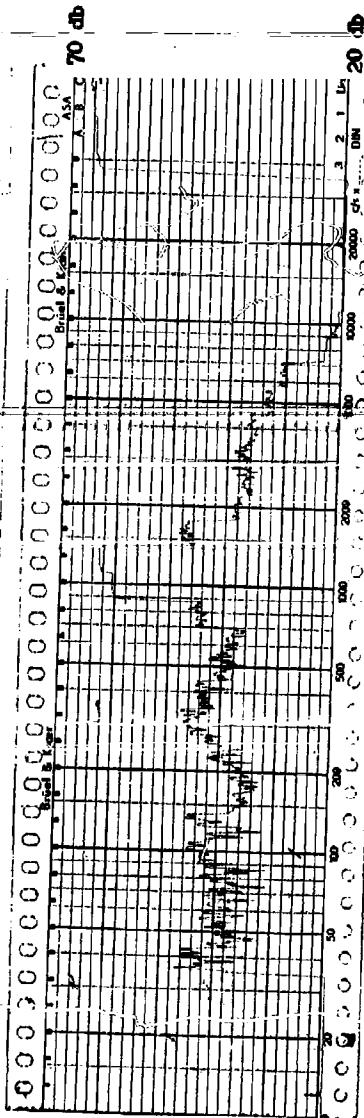
Encapsulation Test
3 HP 4 Pole
184 Frame Open
4 Sept. 1959
Airborne
2 Feet 1:30
Unencapsulated



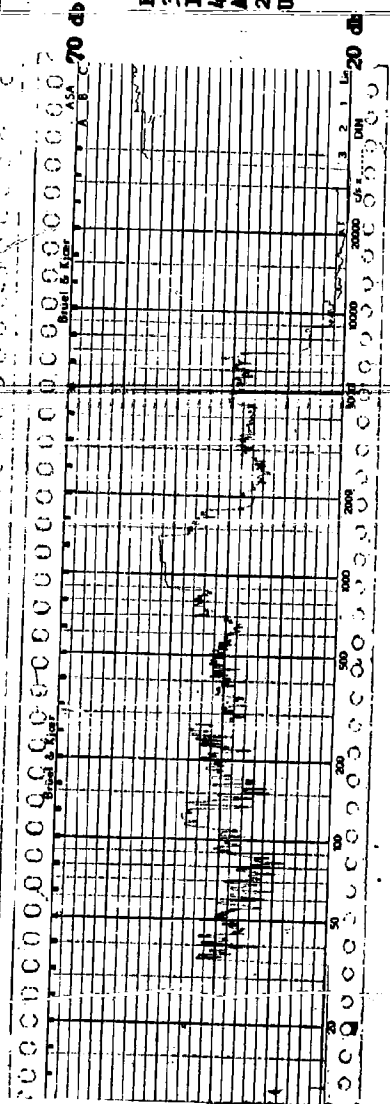
Encapsulation Test
3 HP 4 Poles
184 Frame Open
4 Sept. 1959
Airborne
2 Feet 3:00
Unencapsulated

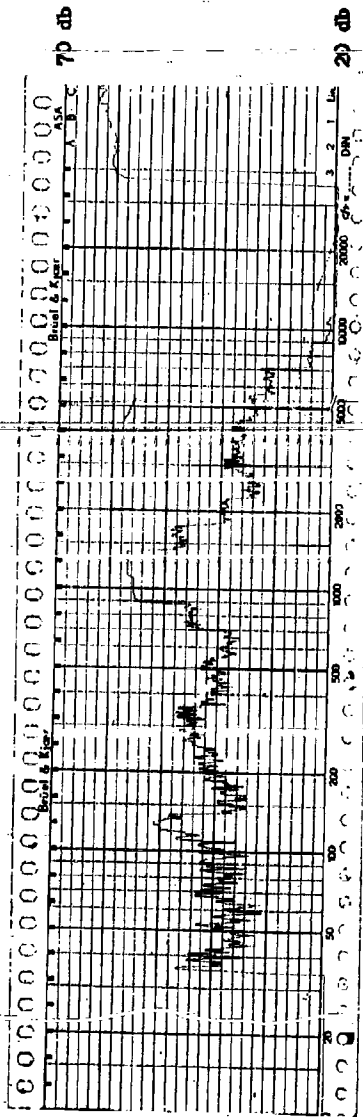


Encapsulation Test
3 HP 4 Poles
184 Frame Open
4 Sept. 1959
Airborne
2 Feet 4:30
Unencapsulated

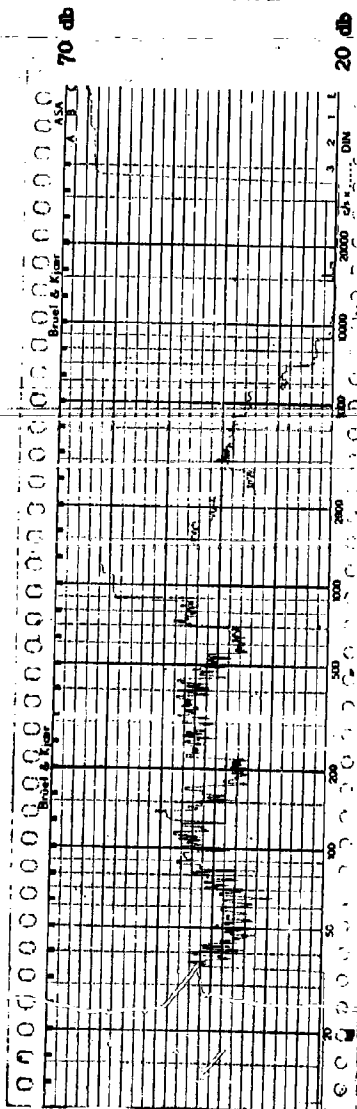


Encapsulation Test
3 HP 4 Poles
184 Frame Open
4 Sept. 1959
Airborne
2 Feet 6:00
Unencapsulated

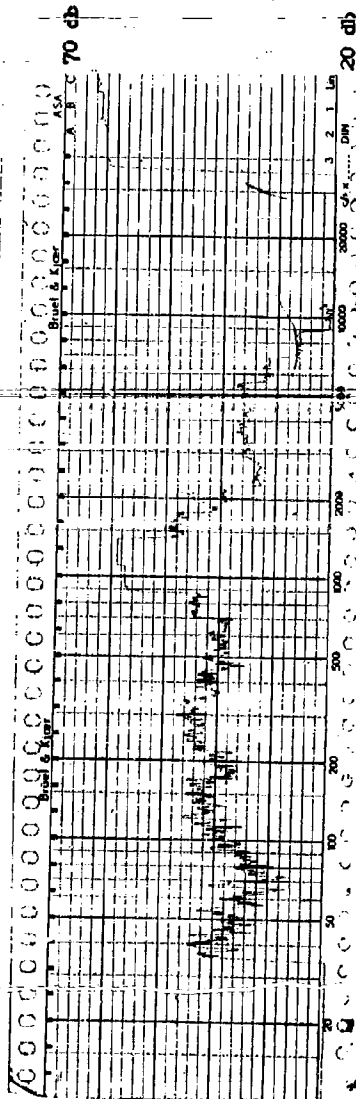




Encapsulation Test
 3 HP 4 Pole
 184 Frame Open
 4 Sept. 1959
 Airborne
 2 Feet 7:30
 Unencapsulated

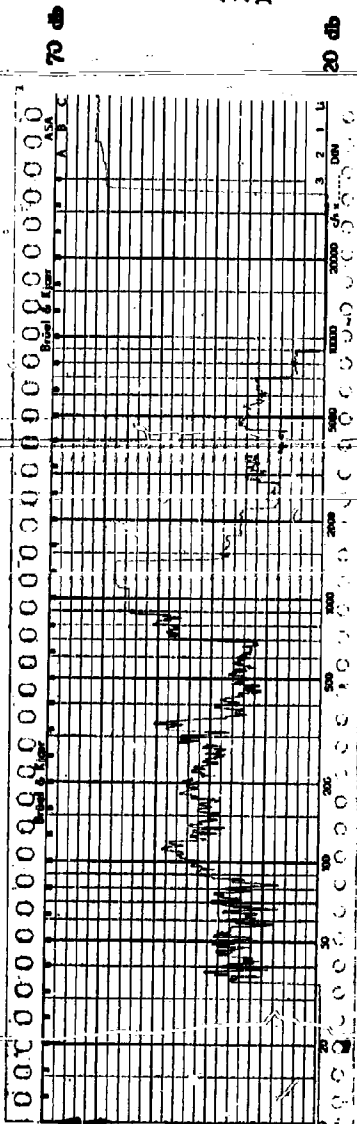


Encapsulation t
 3 HP 4 Pole
 184 Frame Open
 4 Sept. 1959
 Airborne
 2 Feet 9:00
 Unencapsulated

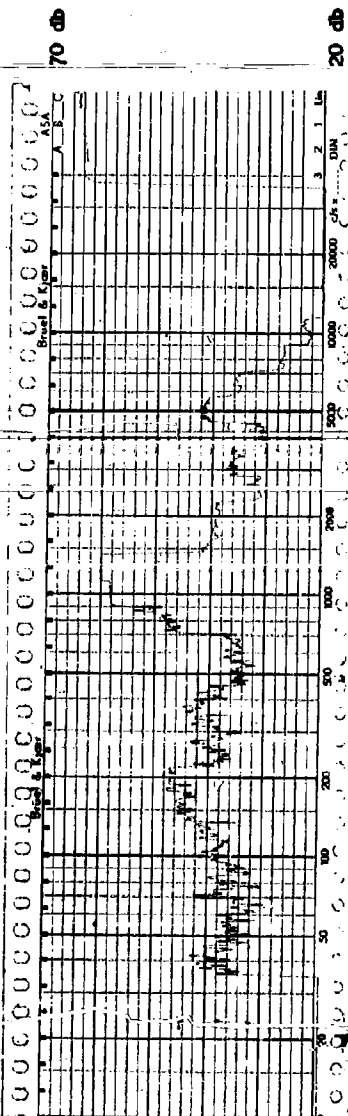


Encapsulation Test
 3 HP 4 Pole
 184 Frame Open
 4 Sept. 1959
 Airborne
 2 Feet 10:30
 Unencapsulated

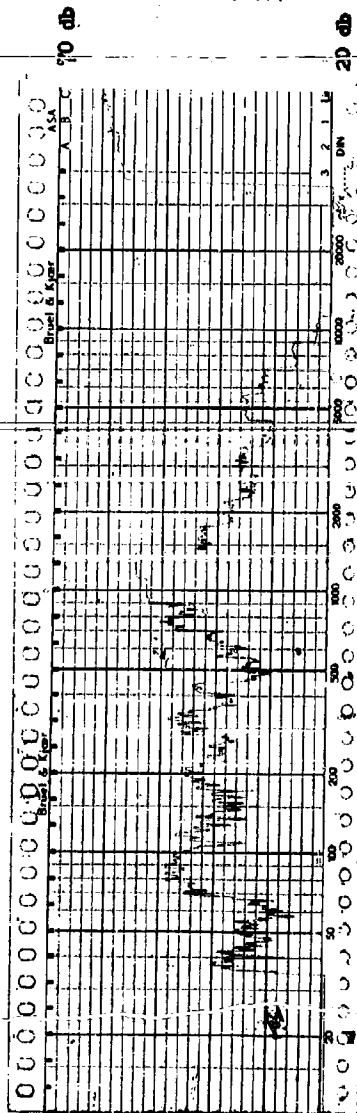
Encapsulation Test
3 HP, 4 Pole
184 Frame Open
28 Sept. 1959
Airborne
Front End
Encapsulated



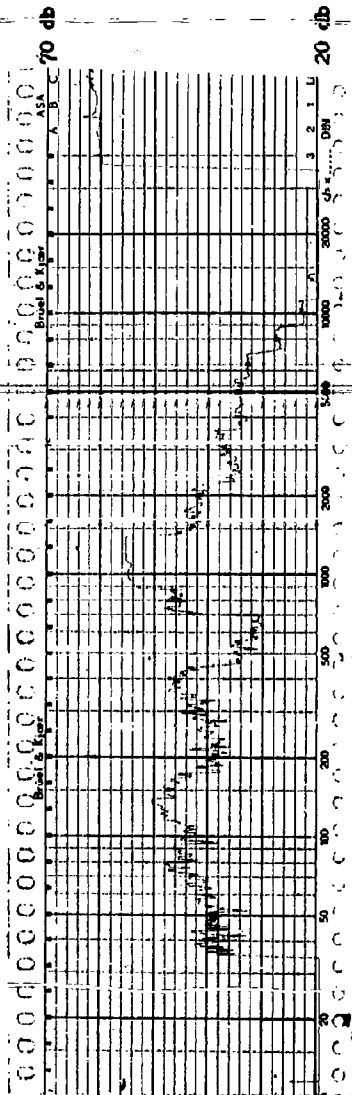
Encapsulation Test
3 HP, 4 Pole
184 Frame Open
28 Sept. 1959
Airborne
2 Feet 12:00
Encapsulated



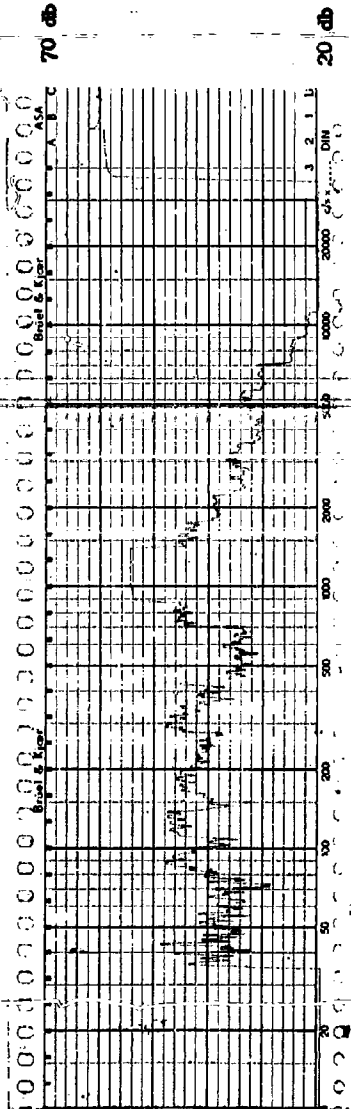
Encapsulation Test
3 HP, 4 Pole
184 Frame Open
28 Sept. 1959
Airborne
2 Feet 1:30
Encapsulated



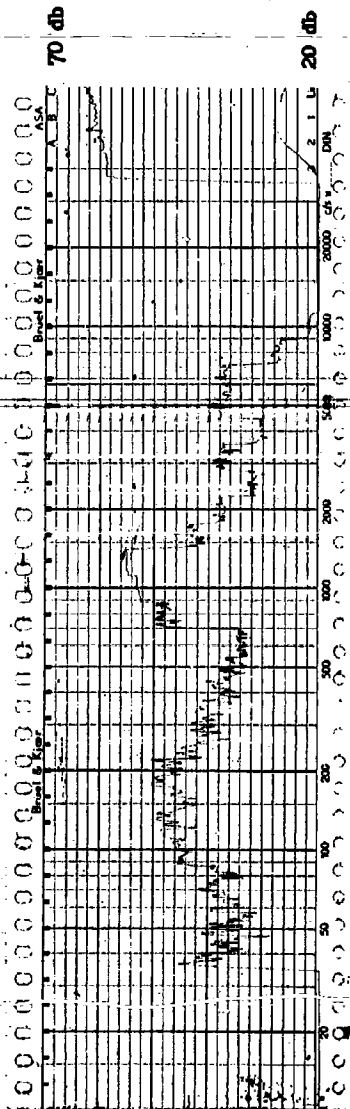
Encapsulation Test
 3 HP 4 Pole
 184, Frame Open
 28 Sept. 1959
 Airborne
 2 Feet 3:00
 Encapsulated



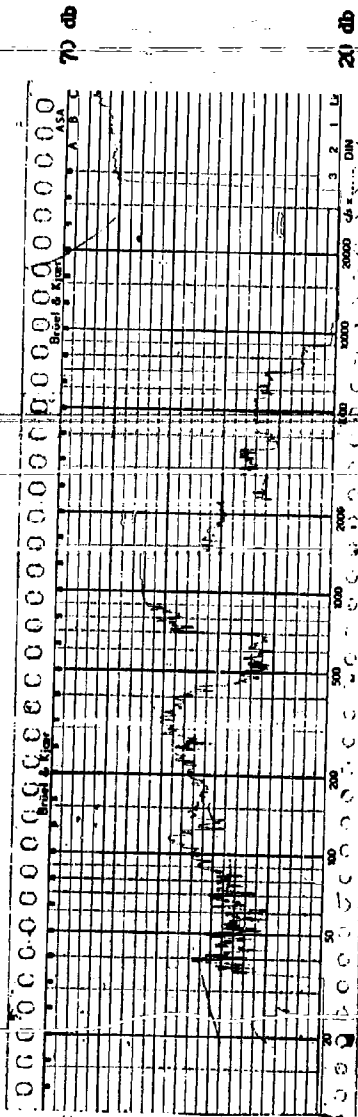
Encapsulation Test
 3 HP 4 Pole
 184, Frame Open
 28 Sept. 1959
 Airborne
 2 Feet 4:30
 Encapsulated



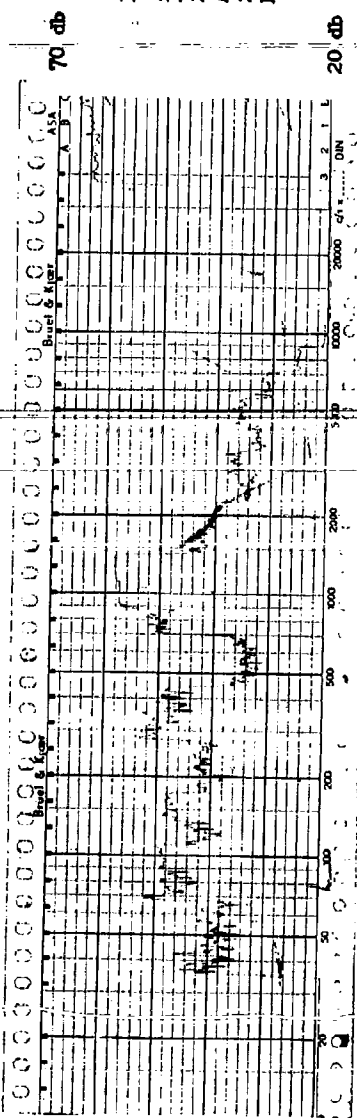
Encapsulation Test
 3 HP 4 Pole
 184, Frame Open
 28 Sept. 1959
 Airborne
 2 Feet 6:00
 Encapsulated



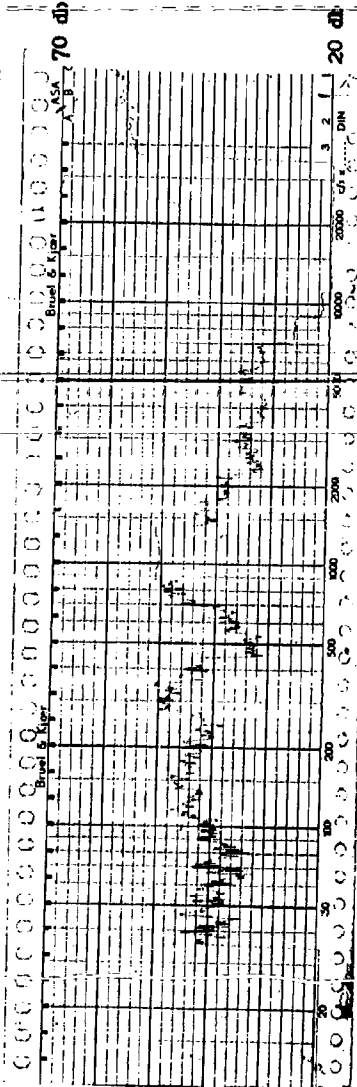
Encapsulation Test
3 HP 4 Pole
184 Frame Open
28 Sept. 1959
Airborne
2 Feet 7:30
Encapsulated

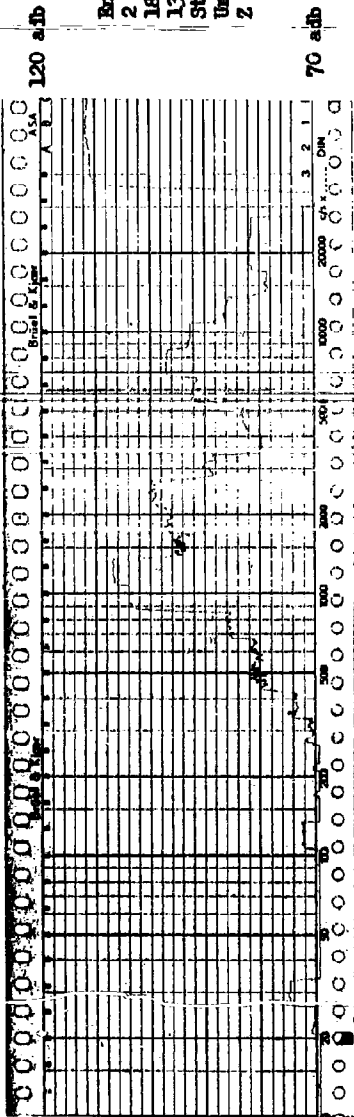


Encapsulation Test
3 HP 4 Pole
184 Frame Open
28 Sept. 1959
Airborne
2 Feet 9:00
Encapsulated

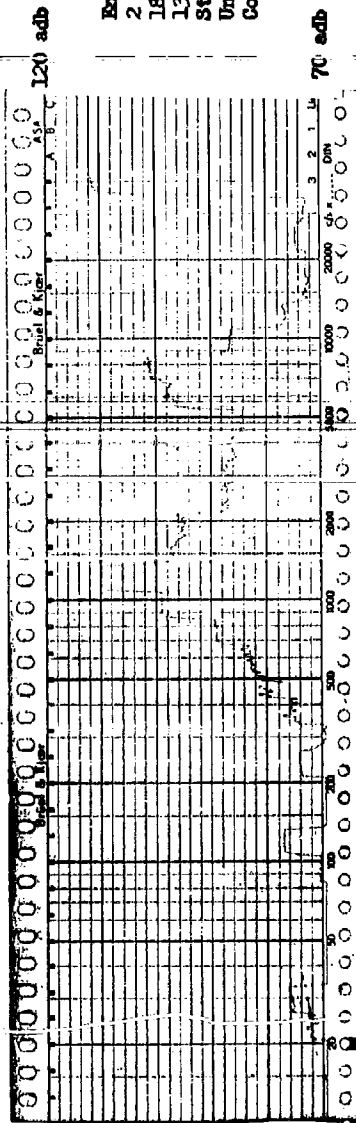


Encapsulation Test
3 HP 4 Pole
184 Frame Open
28 Sept. 1959
Airborne
2 Feet 10:30
Encapsulated



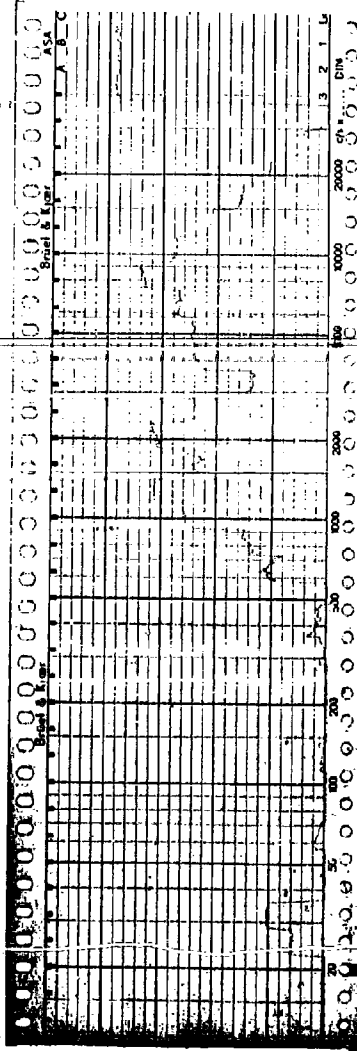


Encapsulation Test
 2 HP 4 Pole
 182 Frame Open
 13 October 1960
 Structureborne
 Unencapsulated
 2 - Axis



Encapsulation Test
 2 HP 4 Pole
 182 Frame Open
 13 October 1960
 Structureborne
 Unencapsulated
 Core

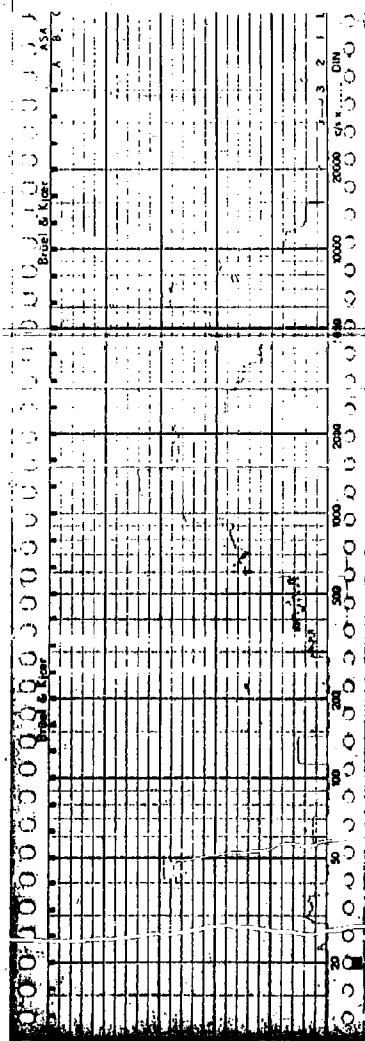
120 adB



Encapsulation Test
2 HP 4 Poles
182 Frame Open
26 October 1960
Structureborne
Encapsulated
Z - Axis

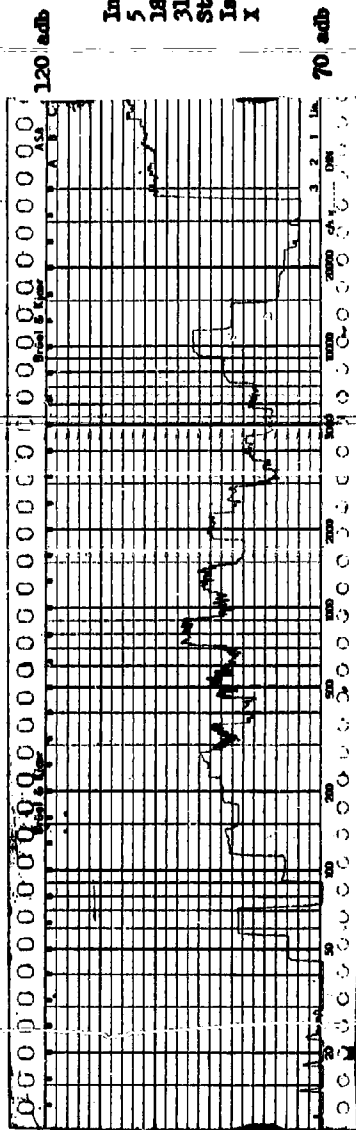
70 adB

120 adB

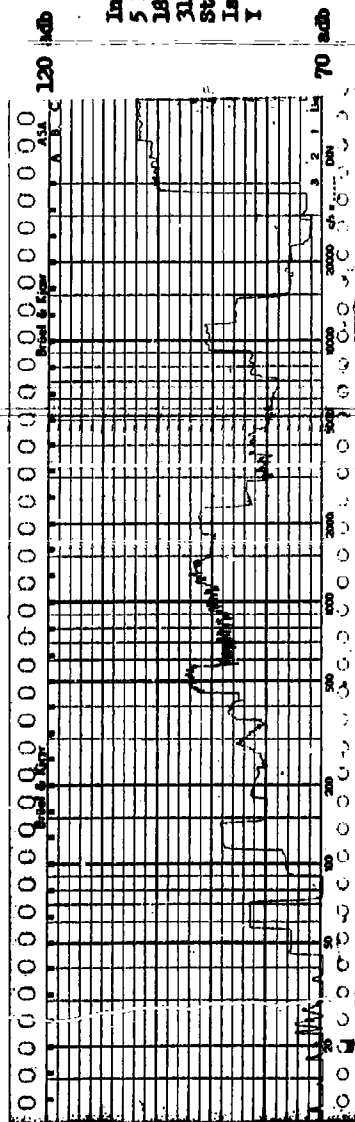


Encapsulation Test
2 HP 4 Poles
182 Frame Open
26 October 1960
Structureborne
Encapsulated
Core

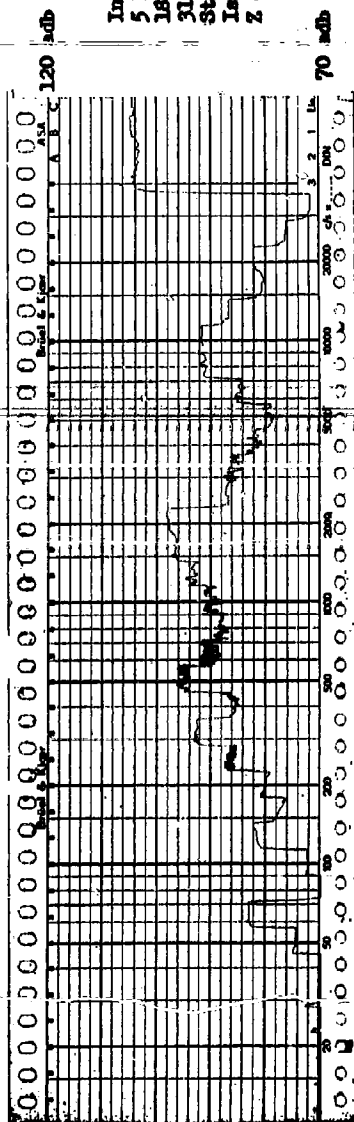
70 adB



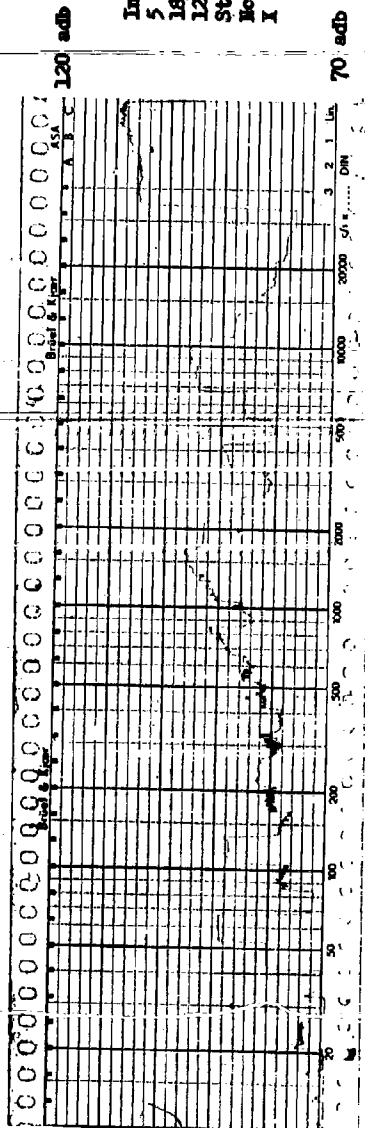
Internal Isolation
 5 HP 2 Pole
 184 Frames Open
 31 May 1960
 Structureborne
 Isolated
 X - Axis



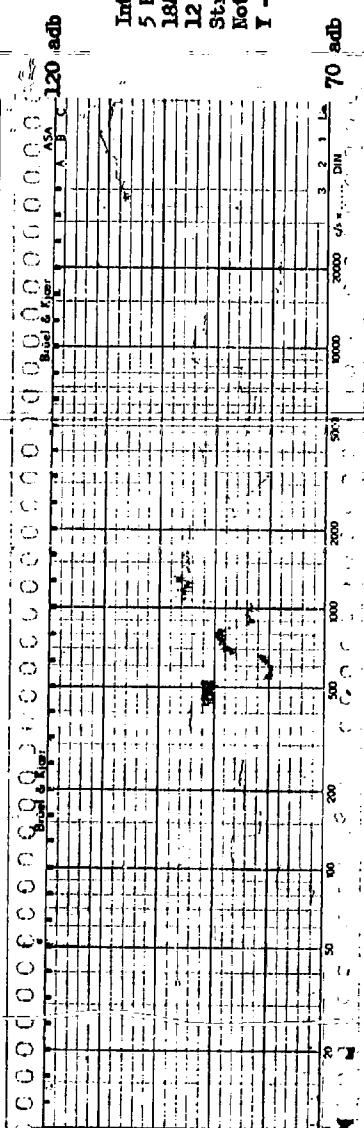
Internal Isolation
 5 HP 2 Pole
 184 Frames Open
 31 May 1960
 Structureborne
 Isolated
 Y - Axis



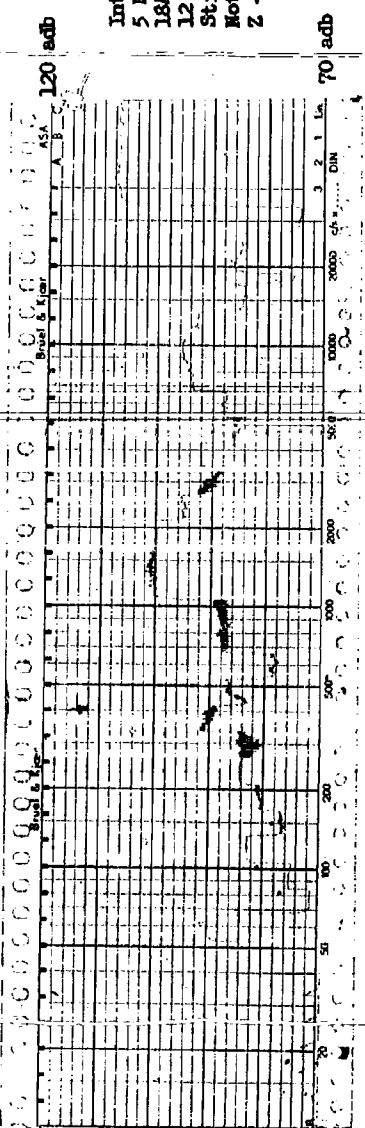
Internal Isolation
 5 HP 2 Pole
 184 Frames Open
 31 May 1960
 Structureborne
 Isolated
 Z - Axis



Internal Isolation
 5 HP 2 Pole
 184, Frame Open
 12 May 1960
 Structureborne
 Not Isolated
 X - Axis



Internal Isolation
 5 HP 2 Pole
 184, Frame Open
 12 May 1960
 Structureborne
 Not Isolated
 Y - Axis

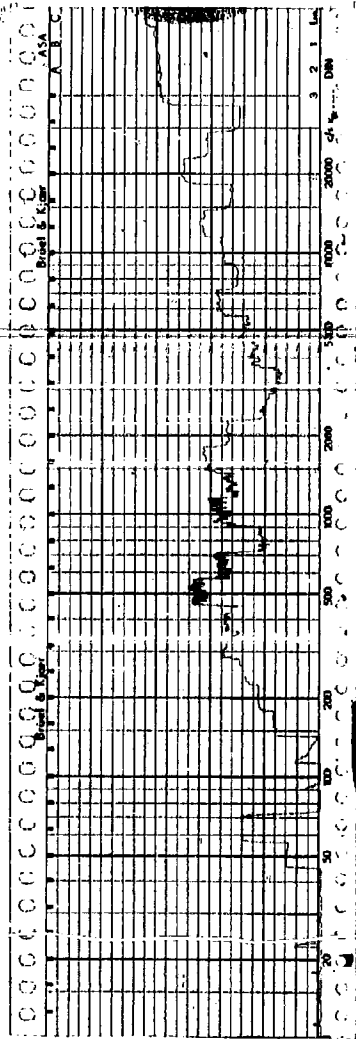


Internal Isolation
 5 HP 2 Pole
 184, Frame Open
 12 May 1960
 Structureborne
 Not Isolated
 Z - Axis

120 sdb

Isolation Test
5 HP 2 Pole
184 Firms Open
31 May 1960
Structureborne
No Load
Firms

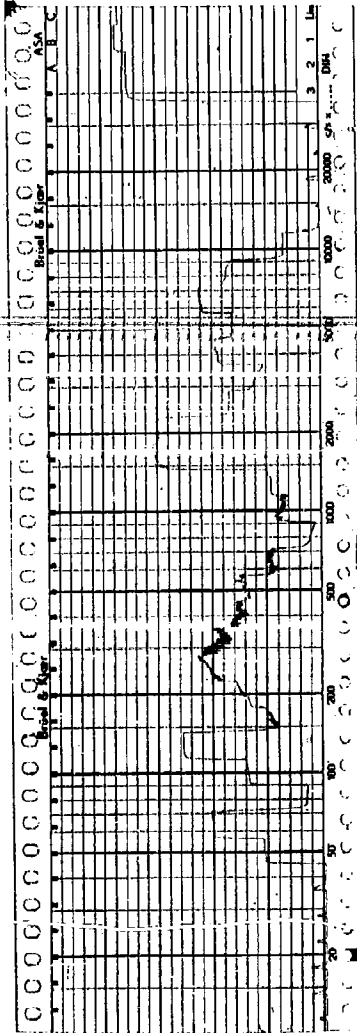
70 sdb

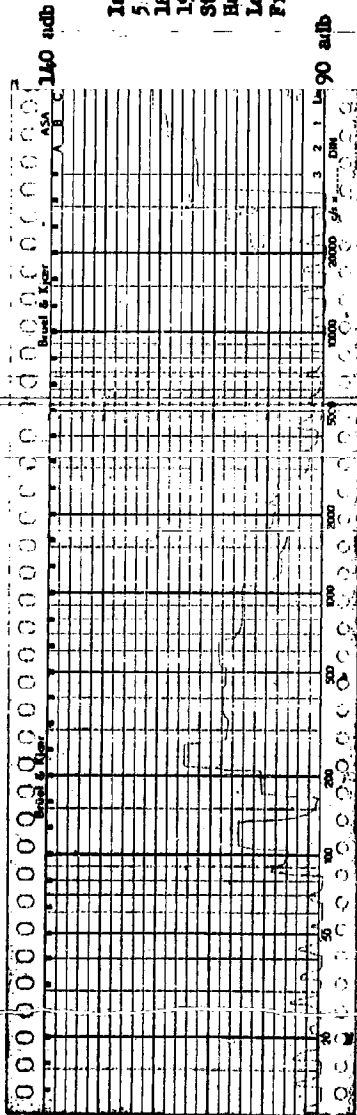


120 sdb

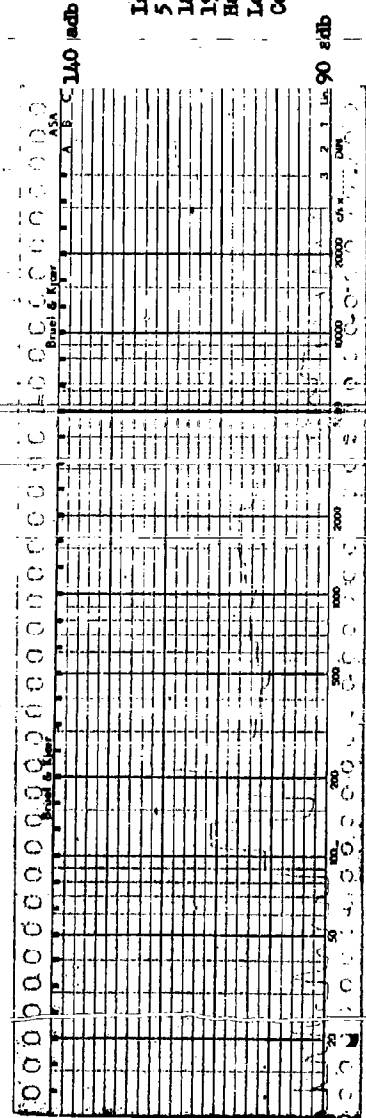
Isolation Test
5 HP 2 Pole
184 Firms Open
31 May 1960
Structureborne
No Load
Core

70 sdb





Isolation Test
 5 HP 2 Pole
 184, Frame Open
 19 May 1960
 Structureborne
 Half Voltage
 Locked Rotor
 Frame



Isolation Test
 5 HP 2 Pole
 184, Frame Open
 19 May 1960
 Half Voltage
 Locked Rotor
 Core

SECTION 9

PROTOTYPE MOTORS

9.1 RATINGS AND PURPOSE

Four prototype were built as part of this study. All were alternating current, 440 volt, 60 cycle, 3 phase, 2 Pole induction motors. One each of the following was furnished:

- 1) 5 HP, dripproof protected, 184 frame.
- 2) 5 HP, totally enclosed, fan cooled, 213 frame.
- 3) 40 HP, dripproof protected, 324 frame.
- 4) 40 HP, totally enclosed, fan cooled, 364 frame.

These motors were designed to meet the specifications of MIL-M-17060B to the maximum extent compatible with the low noise criteria developed in the preceding sections. The minimum acceptable performance values given in this Military Specification were considered to be design requirements.

The purpose of building and testing these motors was threefold:

- 1) To verify the conclusions of the individual studies. The different ratings, frame sizes, and enclosure types constitute a comprehensive check of the design criteria.
- 2) To determine the mutual compatibility of the design criteria. The motors were essentially a summation of the low noise condition of the individual studies.
- 3) To determine additional design criteria. Three principal aspects were planned for study in conjunction with the prototype motors: tolerances, use of external balance rings, and preload adjusters. Additional design criteria were developed as a result of the analyses of the prototype motors.

9.2 DESIGN DATA

The prototype motors incorporated all appropriate design criteria developed at the time of their design. The design criteria used for these motors are those in Section 10.1 that are marked with an asterisk. Those not marked were developed subsequent to the motor design. Specific data pertinent to these design criteria is furnished in Table 9-1. Masterplans of these motors are at the end of this chapter.

TABLE 9-1
Prototype Motors Design Data

Frame Size	184	213	324	364
Maximum Air Gap Flux Density	38,800	40,000	36,800	28,500
Number of Stator Slots	24	36	48	48
Number of Rotor Slots	32	28	38	56

Frame Size	184	213	324	364
Lowest Number Nodes/Slot Frequency	12	12	16	12
Stator Slot Neck Opening	.130	.130	.110	.130
Stew	1.33RS 1.00SS	1.00RS 1.29SS	1.00RS 1.26SS	1.17RS 1.00SS
Pitch Ratio	7/12	10/18	13/24	13/24
Interference Fit - Front Rear	.0002 .0003	.0003 .0003	.0002 .0003	.0001 .0002
No. Internal Fan Blades	7	6	6	10
No. External Fan Blades	-	4	-	4
Full Load Temp. Rise	62°C	58°C	66°C	67°C
Air Gap Length	.018"	.025"	.030"	.040"
Bearing Size	305	306 307	309	310
Motor Weight	93#	148#	445#	816#

Several comments are pertinent to the construction of these motors.

- 1) The desirability of short pitching the coils of the two pole motors to facilitate the winding of the motor made it impossible to reduce both the 5th and 7th stator harmonic. The pitch ratio selected for the prototype motors effectively attenuated only the 7th harmonic.
- 2) Open bearings were used because of the unavailability of shielded or sealed bearings meeting Amendment 2 of MIL-B-17931A.
- 3) The dripproof protected motors were built on the 184 and 324 frames specified by MIL-M-17060B. The NEMA frame sizes specified for 5 and 40 HP, 2 Pole DPP motors are the 213 and 326 respectively.
- 4) The motors were provided with external balance rings for fine balancing and in-place balancing. The totally-enclosed motors utilized a balance ring welded to the conical fan shroud. The other balance rings were machined from one piece of stock rather than fabricated. A discussion of the effect of balance rings on motor noise is presented in Section 9.3.2.
- 5) Preload adjusters similar to that shown in Figure 4-2 were incorporated in the motors' design. See discussion in Section 9.33. To facilitate the trial inclusion of this device,

the prototype motors have no provision for regreasing the bearings.

- 6) The space required by the preload adjuster and necessary clearance for adjustment occupied the space normally used for the stationary end cap bolts. Replacement of the stationary end caps with rotating end caps was made on an experimental basis. The rotating end caps fit on the shaft bearing seat and the bearing inner race presses against the end cap shoulder rather than the shaft shoulder. It was feared that obtaining a satisfactory face run-out of this shoulder might be difficult. The effect of this surface on bearing noise (not studied under this contract) is considered to be appreciable by some bearing experts. The face run-out of the shaft shoulder of all four motors was measured, as well as the face run-out of the rotating end cap held in place on the shaft by clamps which simulated the preload force. In all cases, the face run-out was less with the end caps in place. It appears that the preload force causes the rotating end cap to assume a position such that the surface irregularities are compensatory in nature. The use of rotating end caps is considered compatible with low noise design.

- 7) The use of preload adjusters and external balance rings affected both the overall length and weight of the machines. The preload adjusters were placed in the front bearing housings of all four units. This device extends beyond the bearing housing approximately one-half inch. This the balance rings of the dripproof protected motors and the fan-balance ring assemblies of the totally enclosed motors were located farther from the motor center. The components of the totally enclosed motors were designed so that standard fan housings could be used. Therefore, these motors were not lengthened at the front end. The dripproof protected units were lengthened approximately 1½ inches at this end and all the units were extended 1" for the rear balance ring. The 40 HP units are of a satisfactory weight, but the 5 HP motors with the balance rings slightly exceed the weight limit specified in MIL-M-17060B. Without the balance rings but with the totally enclosed fan-balance ring assembly, both motors meet the weight specification.

9.3 ADDITIONAL STUDIES

The third purpose of building these motors will be treated first because many of the steps necessary to conduct the additional studies affect the construction of the motors.

9.3.1 Tolerances

The attainability of reduced tolerances of three noise-affecting machine surfaces was studied in conjunction with building of the prototype motors:

- 1) Air gap eccentricity.
- 2) Out-of-roundness of bearing seat on shaft.
- 3) Shaft-bearing fit.

It was desired to hold the steel-to-steel air gap eccentricity to less than 2 mils. As mentioned in Section 8, ten motor tolerances plus internal and external bearing tolerances affect this eccentricity. However, it may be expected that many production variations will be of a compensating rather than an accumulative nature. The special precautions taken in the construction of these motors to reduce the air gap eccentricity were a 1 to 2 mil interference fit between bearing housing and frame and a 1 mil tolerance for the rotor turning. The measured eccentricity of the air gaps of all four motors was less than 1 mil.

The out-of-roundness of the bearing seats were held to less than 0.0001 inch by special grinding by skilled machinists. It was found that the eccentricity of the bearing seat with respect to the axis of rotation increased markedly after the rotor core was pressed on the shaft. Attempts to alleviate this condition by decreasing the core-shaft interference and grinding the bearing seats after the core was in place, met with little success. However, it is the out-of-roundness, not the eccentricity, that deforms the bearing inner raceway and creates bearing noise. The bearing seat eccentricity is but one cause of the air gap eccentricity described above which the four motors indicate may be adequately controlled.

The third tolerance investigated was the shaft-bearing fit. The study reported in Section 4 indicates the desirability of a light press fit (0.0001 inch to 0.0003 inch) between the shaft and bearing. The prototype motors use bearings with ABEC-7 external tolerances and the shaft bearing seat tolerances were those recommended for ABEC-7 bearings by the Anti-Friction Bearing Manufacturers Association. These tolerance limits permit sufficient variation that selective mating of parts is required but is not difficult. The measured shaft and bearing dimensions were such that over 90% of the bearings supplied could be used without exceeding the 0.0003 inch interference.

9.3.2 External Balance Rings

The rotor assemblies of the prototype motors were balanced as fine as possible using Gisholt machines. After assembly and without external balance rings, the motors' unbalance varied between .1 and .3 mils displacement of the bearing housing hub. After addition of the balance rings, which had also been dynamically balanced, the motors' unbalance increased to between .8 and 1.6 mils displacement. Unfortunately, the dynamic balancing equipment on hand at the time of this study (IRD Model 400) was

inadequate for balancing to less than .2 mils displacement. Lack of time prevented the acquisition of additional equipment; therefore, the motors were rebalanced to the maximum degree possible with the existing equipment. One-third octave analyses of the acceleration db levels produced by the motors with and without the balance-rings revealed that the balance rings not only increased rotational frequency (60 cps) vibration, but also the levels of the 125, 500, 800 and 2000 cps band. As the noise tests of the motors indicate, the 60 cycle levels are not as objectionable as the higher frequencies. Thus the prototype motors had a better frequency composition of vibration without the external balance rings.

Due to the inadequacy of the balancing equipment, no concrete conclusions as to the advisability of the use of external balance rings can be made. This work does indicate the need for a comprehensive study of motor balance and methods of correcting unbalance.

9.3.3 Preload Adjustor

It is shown in Section 4 that the bearing noise is highly dependent upon the axial preload force. This force is produced by the compression of a thrust washer, and in the normal operating range, is proportional to this compression. The normal variation in end play due to tolerance limits can be as great as 50 mils. For the spring characteristics of thrust washers normally used, this can cause an excessive variation in preload force. The use of a preload adjustor eliminates these problems concerning axial tolerances. The preload adjustor also permits the ready adjustment of the preload force that results in minimum motor noise. This adjustment may be made without motor disassembly but should be done with the motor at rest to prevent momentary overloading and subsequent bearing damage. The prototype motors were the first applications made of this device and no difficulties were encountered. Use of this preload adjustor is considered a great aid in minimizing bearing noise on a practical production basis.

9.4 NOISE ANALYSIS OF PROTOTYPE MOTORS

The analysis of the noise and vibration reduction achieved in the design of the prototype motors is necessary to satisfy the first two purposes of their construction. Both the verification of the individual studies and the mutual compatibility of the study results (design criteria) will be treated simultaneously with the analysis. The noise produced by all four motors will be analyzed for each noise source to facilitate reference to the individual studies. The noise produced by the four sources are treated in the following sub-sections:

9.4.1 Unbalance Noise

9.4.2 Magnetic Noise

9.4.3 Bearing Noise

9.4.4 Fan Noise

The one-third octave test data of the prototype motors is supplied in Spectrogram sheets 9-1 through 9-12. The structureborne noise recorded on the feet at the front and rear ends and the airborne noise recorded in the Allis-Chalmers reverberant sound room are furnished for the motors in order of increasing frame size. The sound spectrograms at various positions around the motor are essentially identical because of the reverberant room. Therefore, only a minimum number of sound pressure spectrograms are furnished. The sources of discrete frequencies and frequency bands of noise produced by these motors are furnished in tables 9-2 through 9-5. The primary and secondary rotor slot frequencies are those calculated using the formulas of Table 3-2 that have the least number of nodes. Spectrogram sheets 9-13 and 9-14 contain a narrow (6%) band analysis of the airborne noise produced by the 184 frame motor for illustrative and comparative purposes.

TABLE 9-2

Sources of Noise And Vibration
5 HP 2 Pole 184 Frame

1/3 Octave	Frequency	Source
63	60	Unbalance
125	120	Fundamental Radial Force Wave
200	Band	Preload Band
500	480	Bearing Noise
1600	1800	Primary Rotor Slot Frequency
2000		Radial Force Wave
4000	3720	Secondary Rotor Slot Frequency
		Radial Force Wave
6300	6300	Whistle
8000	Band	Bearing Friction & Surface Roughness

Frequencies taken from Spectrograms 9-1 through 9-3

TABLE 9-3

Sources of Noise And Vibration
5 HP 2 Pole 213 Frame

1/3 Octave	Frequency	Source
63	60	Unbalance
125	120	Fundamental Radial Force Wave
200	Band	Preload Band
1600	1800	Primary Rotor Slot Frequency
2000		Radial Force Wave
2500	Band centered at 2700	Bearing Noise
3150	3240	Secondary Rotor Slot Frequency
		Radial Force Wave
6300	Band	Bearing Wear-in (subsequently reduced)
8000	Band	Bearing Friction & Surface Roughness

Frequencies taken from Spectrograms 9-4 through 9-6.

TABLE 9-4

Sources of Noise And Vibration
40 HP 2 Pole 324 Frame

1/3 Octave	Frequency	Source
63	60	Unbalance
125	120	Fundamental Radial Force Wave
250	Band	Preload Band + 2nd Harmonic of 120 cps
1000	Band	Bearing Noise + 8th Harmonic of 120 cps
2500	2400	Primary Rotor Slot Frequency
4000	4440	Radial Force Wave
5000		Secondary Rotor Slot Frequency
10000		Radial Force Wave
12500	Band	Bearing Friction & Surface Roughness

Frequencies taken from Spectrograms 9-7 through 9-9

TABLE 9-5

Sources of Noise And Vibration
40 HP 2 Pole 364 Frame

1/3 Octave	Frequency	Source
63	60	Unbalance
125	120	Fundamental Radial Force Wave
250	240	Fan Blade Frequency
315	Band	Preload Band
500	480	Twice Fan Blade Frequency
3150	3240	Primary Rotor Slot Frequency
		Radial Force Wave
4000	Band	Rear Bearing Noise
10000	Band	Bearing Friction & Surface Roughness

Frequencies taken from Spectrograms 9-10 through 9-12

Determination of the noise reduction achieved in the design of the prototype motors requires comparison with the most nearly equivalent conventional (not low noise design) motors. Tests of such units reported in earlier sections will be used to minimize the amount of test data supplied. As outlined in Section 2, the test motors were modified in various manners to reduce noise generated by sources other than the one under study. Certain of the tests were conducted with conventional motors, however, and these include units similar to three of the prototype motors. The 5 HP, 2 Pole, 184 frame motor used in various tests was essentially identical to the 5 HP prototype motor and therefore cannot be used for comparative purposes. No tests of a motor similar to the 40 HP, 2 Pole, 324 frame DPP motor have been previously reported. Tests of a 40 HP, 2 Pole, 326 frame DPP motor meeting MIL-M-17060A are therefore supplied on Spectrograms 9-15 through 9-17. The following spectrograms are used for comparison with the prototype motors:

Prototype Motor	Structureborne Spectrogram Sheet	Airborne Spectrogram Sheet
184 Frame	3-4	Top Spectrogram on 5-1
213 Frame	7-4	Middle Spectrogram on 8-18
324 Frame	9-15 & 9-16	9-17
364 Frame	3-14	Top Spectrogram on 5-19

9.4.1 Unbalance Noise

The unbalance noise of these two pole prototype motors reflects in the 63 cps one-third octave of the structureborne spectrograms. The spectrograms of the 184 frame motor reveal that this band is one of the lowest levels recorded. The levels become progressively higher for the larger frames but only on the 364 frame motor is the unbalance noise level within 10 adB of the highest level produced. Thus, even considering the balancing difficulties previously described, it may be seen that unbalance is not the troublesome source of vibration in the prototype motors.

Comparing the prototype motors with their conventional counterparts reveals the prototype motors have approximately 10 adB less unbalance vibration along the axial (X) axis and 15 to 21 adB less along radial axes (Y and Z) for the 184, 213, and 324 frame motors. The 364 frame has essentially the same levels on the radial axes as its counterpart. With better dynamic balancing equipment, these levels could be further reduced.

9.4.2 Magnetic Noise

An investigation of the 120 cycle magnetic noise produced by the prototype motors reveals that the levels are almost identical to that of the conventional motors. This is consistent with the design features as the only criterion employed which would minimize this frequency vibration, was the limitation on the maximum air gap flux density. Both the prototype and conventional motors under discussion have air gap flux densities of less than 40,000 lines per square inch. The corresponding TEFC units have identical values, while the prototype DPP motors have slightly higher flux densities because of their somewhat cramped design. Thus, the 5 HP, 184 frame prototype has 4 adB more 120 cycle vibration than the conventional unit because its air gap flux density is higher than the 3 HP conventional motor. Note that the levels for the 5 HP totally enclosed motor are less than the DPP motor even though the flux density is higher. This is a result of the greater rigidity imparted to the stator core by the totally enclosed frame which

has continuous peripheral contact with the stator core. The 364 frame TEFC, 40 HP motor has lower values than the 324 DPP motor but also has less air gap flux density. The stiffening effect of the frame is less on the larger frame sizes.

Additional design criteria were employed to reduce the more objectionable slot frequency vibration. The test data indicates that the prototype motors have an average 13 db less primary rotor slot frequency vibration than the conventional motors. The secondary rotor slot noise of three smaller units is an average 8 db less than their counterparts. The secondary rotor slot frequency vibration is not evident on either 364 frame unit.

Even though the reduction of slot frequency vibration is greater than the 120 cycle magnetic noise, the level remains higher. However, the steps that should be taken to further reduce magnetic noise will be effective at both high and low frequencies. They are:

- 1) An increase in radial thickness of stator core. As shown in Section 3, this dimension has a pronounced effect on the deflection of the stator core due to the radial air gap force waves.
- 2) Frame modifications such as circumferential ribs to impart additional rigidity to stator core.
- 3) Rotation of successive stator core laminations to minimize permeance variation due to grain orientation.
- 4) The dripproof protected motors could have encapsulated windings to reduce stator core vibration.
- 5) Use of internal isolation material. If the above four steps are insufficient to reduce the high frequency vibration to acceptable limits, steps may be taken to attenuate this noise between the source and the motor frame. As shown in Section B, internal isolation of the stator core to reduce magnetic noise is feasible. However, additional work is necessary to evaluate the cooling of motors utilizing such isolation.

9.4.3 Bearing Noise

The principal design criteria employed to reduce bearing noise and vibration were the use of high quality, low vibration bearings, careful attention to mating parts, and setting the optimum preload force by means of the preload adjuster previously described. An investigation of the test data indicates that these steps have appreciably reduced bearing noise over a wide frequency range. The low frequency bearing noise has been essentially eliminated as a troublesome noise source. The preload band is pres-

ent due to the use of thrust washers but the level is minimized by the setting of the preload adjuster except where a greater or more important reduction of another frequency band was desired. The 184 frame motor reveals a slight preload band on the X-axis which was minimized by the setting of its preload adjuster. In the case of the 213 and 324 frame motors, the preload adjuster was locked at the setting that resulted in minimum high frequency bearing noise because of the appreciably higher levels at these frequencies. This high frequency bearing noise, reflected in bands from 8,000 cps to 20,000 cps, is caused by bearing friction and surface roughness of the bearing components. The prototype motors have an average of 7 to 24 db less vibration produced by this source. However, the levels in these bands remain the highest produced by the motors. Further reduction of this high frequency noise primarily requires use of ball bearings with lower values of high frequency vibration. If these bearings are not obtainable, the bearing noise may be attenuated by the use of isolation material between the bearings and the bearing housings.

The 213 frame motors are examples of a rather rare phenomena. These motors are some of the few tested where the magnetic noise in the middle frequency range of 1000 to 4000 cps was not more prominent than any other source. Narrow band analysis of the prototype motor revealed a band of bearing noise centered about 2700 cps which had higher levels. This is not a prominent bearing frequency and the even higher levels of this band on the conventional motor suggests a resonant condition.

9.4.4 Fan Noise

The prototype motors are no exception to the rule that fan noise is principally airborne in nature. Therefore, the analysis of this source of noise must concentrate on the sound pressure spectrograms. The airborne spectrograms of the four prototype motors and the specially tested 326 frame conventional motor were taken in the Allis-Chalmers reverberant sound room at Norwood, Ohio. This room, which has smooth concrete walls to provide high acoustic reflection, was designed to facilitate sound power conversion of the measured sound pressure levels. Table 9-6 furnishes the correction which must be added to sound pressure levels recorded in this room to obtain sound power levels. As an aid in comparing the airborne noise test results with MIL-E-22843, Table 9-7 furnishes the maximum sound power levels permitted for Grades B and C equipment and the corresponding sound pressure levels for the Allis-Chalmers Sound Room only. The levels for Grade A equipment are 20 db lower than the corresponding Grade B and C levels.

TABLE 9-6

**Sound Power Conversion
L_p to L_w**

To convert Sound Pressure Levels re 0.0002 dynes/sq. cm. recorded in the A-C Sound Room to Sound Power Levels re 10⁻¹³ watts, the following correction must be added.

1/3 Octave	Correction
10	
12.5	
16.	10.5
20	
25	
31.5	
40.	11.
50	
63	
80	
100	
125	11.5
160	
200	
250	12
315	
400	12.5
500	
630	13
800	
1000	13.5
1250	14
1600	14.5
2000	15
2500	15.5
3150	16
4000	16.5
5000	17.5
6300	18.
8000	19
10000	20

The reverberant room, in addition to facilitating sound power computation also permits more accurate determination of high frequency levels. Tests of many motors indicate higher sound power levels at high frequencies when measured in this room than when calculated from sound pressure levels measured under less reverberant conditions. It appears that the difference is due to absorption of high frequency noise under semi-anechoic conditions rather than amplification under reverberant conditions. The test conditions definitely affect the levels recorded and the above described tests were conducted under the more unfavorable condition.

The sound pressure levels at frequencies below 100 cps shown on the test data taken in the reverberant room are caused by the room ambient which fluctuates as shown in the third spectrogram of sheet 9-3. Repeated tests have verified that any levels on the

TABLE 9-7

**Sound Power Levels re 10⁻¹³ Watts
Permitted by MIL-E-22843
For Grade B & C**

1/3 Octave	Permitted Sound Power Level db re 10 ⁻¹³ Watts	Permitted Sound Pressure Level db re 0.0002 dynes/sq. cm. In A-C SOUND ROOM ONLY
40.	92	81
50	90	79
63	88.5	77.5
80	87	76
100	85	73.5
125	83.5	72
160	82	70.5
200	80	68
250	78.5	66.5
315	77	65
400	75	62.5
500	73.5	61
630	72	59
800	70	56.5
1000	68.5	55
1250	67	53
1600	65	50.5
2000	63.5	48.5
2500	62	46.5
3150	60	44
4000	58.5	42
5000	57	39.5
6300	55	37
8000	53.5	34.5
10000	52	32

motor spectrograms that are higher than the recorded ambient are due to the rapidly changing ambient rather than motor noise. This ambient condition was the result of the newness of the reverberant test facility which could not be corrected in time for these tests. However, as Table 9-7 indicates, the low frequency levels permitted by MIL-E-22843 are far higher than the ambient.

An investigation of the prototype spectrograms reveals that the prominent vibration frequencies are not transduced into airborne noise. This is due to two reasons; 1) the vibration levels have been reduced considerably and, 2) the prominent vibration is of high frequency which is readily attenuated in transmission and transduction. Thus, for the prototype motors, not only is fan noise not evident in structureborne tests, but unbalance, bearing, and magnetic noise are not evident in the airborne levels.

Comparison of sound pressure levels recorded under reverberant conditions with those taken under semi-anechoic conditions is difficult due to the approximately 10 db increase caused by the reverberant room. This variation is frequency dependent which compounds the difficulty. However, even under the more adverse test conditions, the prototype 184 frame motor can be seen to produce both lower levels and a better frequency distribution than its counterpart. The sound pressure level produced by this motor is

essentially constant (approximately 45 db) between 250 and 8000 cps. The only high frequency band that is more prominent than the rest is a 6300 cps band that reflects a slight whistle caused by air passing through and around the end turns. The overall levels of the 184 frame motors are the same but the reverberant ambient produces levels higher than those produced by the motor, thus the overall reading (designated on this spectrogram as Lin or C) is not indicative of the motor's noise output. Test of an earlier version of this motor in a semi-anechoic room revealed a 52 db overall reading. (See Spectrogram 3-16). The principal design feature that caused the reduction of fan noise was the shortening of the axial fan blade length until a temperature rise near the Class B limit resulted. The prototype 184 frame motor has 50% of the original length removed.

The comparison of the 324 frame prototype motor with its 326 frame conventional counterpart is considerably easier and more indicative of the reduction achieved because both motors were tested under identical reverberant conditions. The prototype motor has a 13 db lower peak and a 10 db lower overall reading. Again, the reduction is mainly a result of a reduced fan blade length. The 324 frame motor has a fan blade length only 25% of the original length (used in the 326 frame motor).

The 213 frame prototype motor has a peak level of 3 db less than the conventional motor and a 5 db lower overall level. This reduction is less than anticipated due to two modifications within the fan housing enclosure:

- 1) The inclusion of the preload adjustor in the fan end bearing housing required the placement of the fan nearer to the fan housing intake grid.
- 2) The incorporation of the balance ring and the unidirectional fan into one assembly prevented a reduction in the fan diameter over the customary bidirectional fan.

The factor which set the minimum diameter was the necessity of the balance ring occupying the space above the bearing housing hub. Thus the optimum design unidirectional fan could not be utilized. A reduction in fan diameter would have resulted in a large decrease in air velocity. The only modification that could be made was the reduction in axial length of the unidirectional blades which reduced the volume of cooling air.

The 364 frame totally enclosed prototype motor has a similar reduction in fan noise. The peak and overall levels of this motor are 4 and 6 db lower than those of the conventional motor recorded under semi-anechoic conditions. The balance ring and preload adjustor of this motor did not cause an oversize fan diameter but did cause the fan to be located nearer the intake grid. The fan noise of the totally enclosed motors could be further reduced by placing the pre-

load adjustor in the rear end bearing housing, thereby permitting optimum location of the fan. This design change would result in an increase in overall length of between $\frac{1}{2}$ and $\frac{3}{4}$ inch.

9.4.5 Narrow Band Analysis

Narrow band (6%) analyses were made of the vibration and airborne noise produced by the four prototype motors for two reasons:

- 1) to determine if differences in amplitude would be observed, and
- 2) to determine unknown discrete frequencies of noise.

No appreciable difference in amplitude was noted for any prominent frequency in any of the above tests. Also, whenever there was noise of an unknown frequency, narrow band analysis indicated the presence of a band of frequencies rather than a discrete frequency. Thus, the narrow band analyses of these motors furnished no additional information not supplied by the one-third octave analyses. Therefore, only one narrow band test is furnished for illustrative purposes. Spectrogram sheets 9-13 and 9-14 contain the narrow band analysis of the airborne noise recorded 3 feet from the rear end of the 184 frame motor.

9.4.6 Comparison With MIL-E-22843

Although Military specification MIL-E-22843 was not issued until just prior to the termination of this contract, a comparison of the noise produced by the prototype motors with this present BuShip specification may be of interest.

The airborne noise for any size equipment is the same and is specified in terms of sound power levels for one-third octave bands between 40 and 10,000 cps. Table 9-7 lists the permitted levels for grade B & C equipment and the corresponding sound levels as measured in the A-C sound room. The permitted levels at low frequencies are considerably higher than those produced by the prototype motors. The rapid decrease in permitted levels which approximates an ambient condition results in all the motors exceeding the specification at high frequencies. In the case of the 184 frame motor only the levels at frequencies greater than 4000 cps are above the specified limits. At the other extreme, the 364 frame totally enclosed motor exceeds the limits at all bands higher than 250 cps.

The structureborne noise produced by the prototype motors does not increase appreciably as a function of frame size. However, the adB levels permitted by MIL-E-22843 decrease as a function of motor weight. The weights of the four prototype motors are shown in Table 9-1. The corresponding adB levels permitted for Grade C equipment for all one-third octaves between 25 and 8,000 cps are 91, 88, 83, and 81 adB respectively in order of increasing frame size.

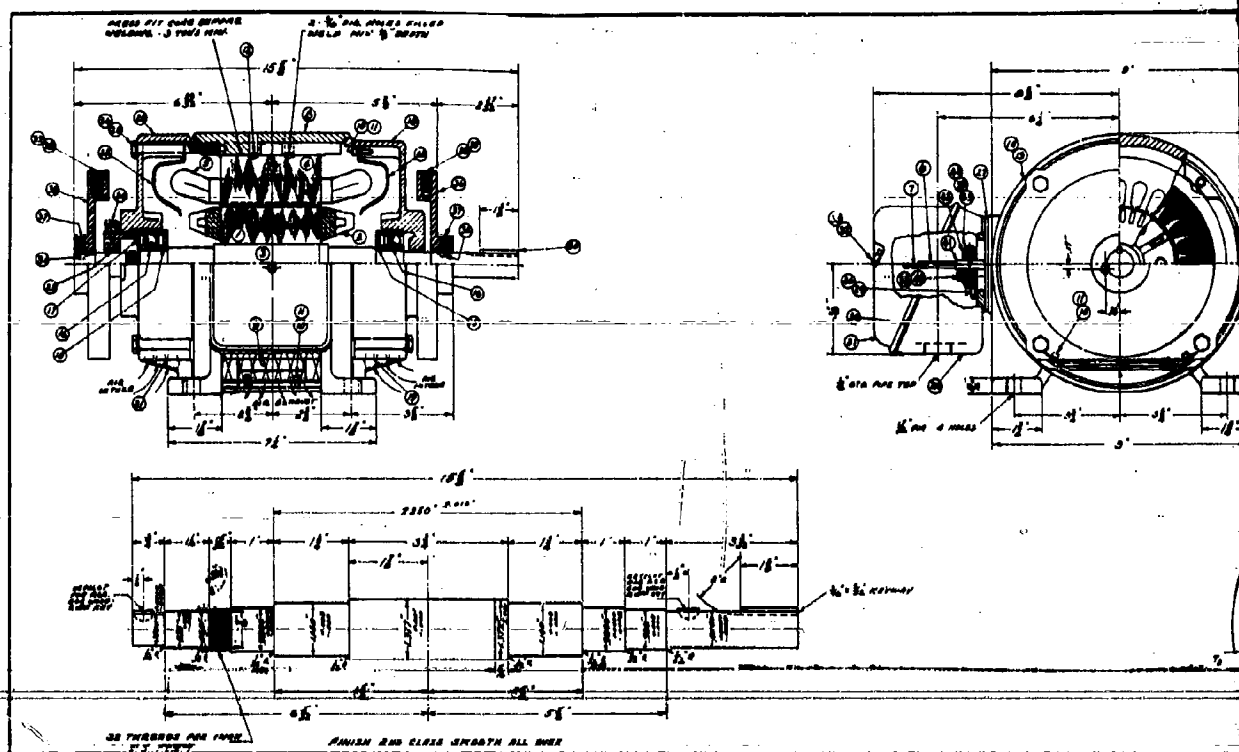
The 184 frame prototype barely exceeds the specified limit in the high frequency bands. The 213 motor exceeds the limit for units of its weight by a few db on some axes but the average band levels remain below the limit. The 324 frame motor has the highest structureborne levels and exceeds the specification for its weight by as much as 12 adb. The 364 frame motor has lower acceleration levels but again exceeds the specification.

In summary, the smaller two motors come very close to meeting the present structureborne specification and the 184 frame only exceeds the airborne specification at very high frequencies. The larger motors exceed both the airborne and structureborne limits by appreciable amounts.

9.5 GENERAL COMMENTS

A comparison of the prototype motors with each other indicate that the totally enclosed motors have lower vibration levels but higher airborne levels than the dripproof protected motors. The vibration is less due to the more rigid frame and continuous peripheral contact between the frame and stator core. The higher airborne levels are caused by the totally enclosed external fans. The vibration levels remain essentially constant as the motor size and rating increases. The airborne noise produced by the larger induction motor is greater because 1) the higher peripheral speed of larger fans and, 2) the larger frame is a more effective transducer of vibration into airborne noise.

2



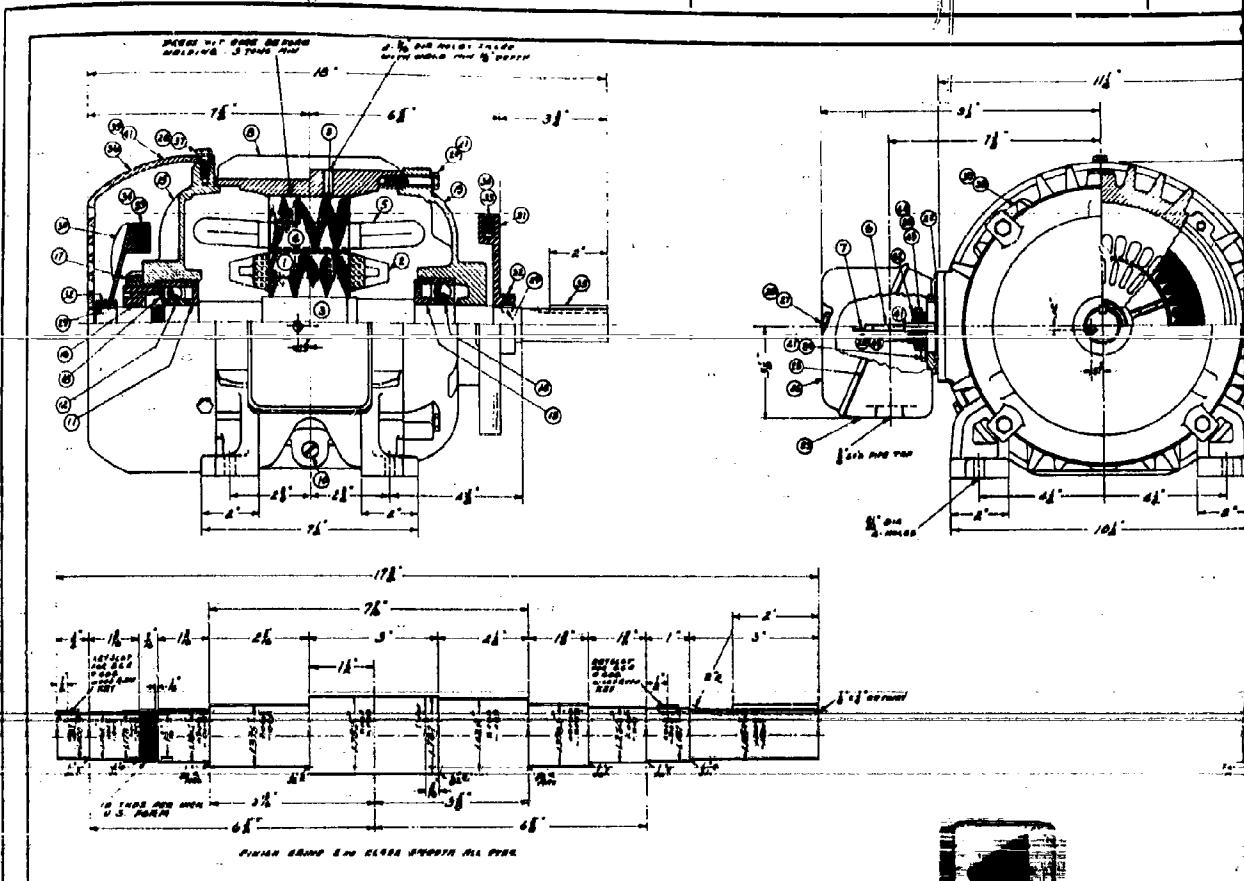
LIST OF MATERIAL QUANTITIES FOR ONE

NO.	NAME	QTY	MATERIAL	MAT'L SPEC.	ALLIS-CHALMERS	OR EQUIV	REMARKS
1	Drive Pulley	1	STEEL	SAE-A-232	17-11-102-001		SEE DRAW G
2	Drive Pulley Bolt	1	STEEL	SAE-A-232	17-11-102-001		SEE DRAW G
3	Drive Pulley Nut	1	STEEL	SAE-A-232	17-11-102-001		SEE DRAW G
4	Drive Pulley Washer	1	STEEL	SAE-A-232	17-11-102-001		SEE DRAW G
5	Spring Cone	1	STEEL	SAE-A-232	17-11-102-001		SEE DRAW G
6	Lock Cone (1-1/2\"/>						

5. SPRING SPECIFICATIONS -
 A - TYPE SPRING FOR Q1-Q2 SEE TYPE E CLASS I
 B - COIL SPRING FOR Q3-Q4 SEE TYPE E CLASS I
 6. HARD FINISHES TO PERM. SURF. AND ROTAR CASE - 4000
 FINISH, INTERIORS - .002" TO .005" FINISH
 7. NO AXIAL MOVEMENT OF SHAFT END PLY TAKEN UP BY
 FLESHED UP NOTER AND SPR FOR WISHER, SPRING
 WISHER CONSTANT - 250 LBS PER INCH
 8. NO APPLICABLE QVT. SPEC., BEST COMMERCIAL GRADE
 9. CRITICAL DIMENSIONS -
- | NO. | DESCRIPTION | TOLERANCE | REMARKS |
|-----|-------------------------|-----------|---------|
| 1 | SHAFT DIA. AT END SHIPT | .0005" ± | .0005" |
| 2 | SHAFT DIA. AT END SHIPT | .0005" ± | .0005" |
| 3 | SHAFT DIA. AT END SHIPT | .0005" ± | .0005" |
| 4 | SHAFT DIA. AT END SHIPT | .0005" ± | .0005" |
| 5 | SHAFT DIA. AT END SHIPT | .0005" ± | .0005" |
| 6 | SHAFT DIA. AT END SHIPT | .0005" ± | .0005" |
| 7 | SHAFT DIA. AT END SHIPT | .0005" ± | .0005" |
| 8 | SHAFT DIA. AT END SHIPT | .0005" ± | .0005" |
| 9 | SHAFT DIA. AT END SHIPT | .0005" ± | .0005" |
| 10 | SHAFT DIA. AT END SHIPT | .0005" ± | .0005" |
| 11 | SHAFT DIA. AT END SHIPT | .0005" ± | .0005" |
| 12 | SHAFT DIA. AT END SHIPT | .0005" ± | .0005" |
| 13 | SHAFT DIA. AT END SHIPT | .0005" ± | .0005" |
| 14 | SHAFT DIA. AT END SHIPT | .0005" ± | .0005" |
| 15 | SHAFT DIA. AT END SHIPT | .0005" ± | .0005" |
| 16 | SHAFT DIA. AT END SHIPT | .0005" ± | .0005" |
| 17 | SHAFT DIA. AT END SHIPT | .0005" ± | .0005" |
| 18 | SHAFT DIA. AT END SHIPT | .0005" ± | .0005" |
| 19 | SHAFT DIA. AT END SHIPT | .0005" ± | .0005" |
| 20 | SHAFT DIA. AT END SHIPT | .0005" ± | .0005" |
| 21 | SHAFT DIA. AT END SHIPT | .0005" ± | .0005" |
| 22 | SHAFT DIA. AT END SHIPT | .0005" ± | .0005" |
| 23 | SHAFT DIA. AT END SHIPT | .0005" ± | .0005" |
| 24 | SHAFT DIA. AT END SHIPT | .0005" ± | .0005" |
| 25 | SHAFT DIA. AT END SHIPT | .0005" ± | .0005" |
| 26 | SHAFT DIA. AT END SHIPT | .0005" ± | .0005" |
| 27 | SHAFT DIA. AT END SHIPT | .0005" ± | .0005" |
| 28 | SHAFT DIA. AT END SHIPT | .0005" ± | .0005" |
| 29 | SHAFT DIA. AT END SHIPT | .0005" ± | .0005" |
| 30 | SHAFT DIA. AT END SHIPT | .0005" ± | .0005" |
| 31 | SHAFT DIA. AT END SHIPT | .0005" ± | .0005" |
| 32 | SHAFT DIA. AT END SHIPT | .0005" ± | .0005" |
| 33 | SHAFT DIA. AT END SHIPT | .0005" ± | .0005" |
| 34 | SHAFT DIA. AT END SHIPT | .0005" ± | .0005" |
| 35 | SHAFT DIA. AT END SHIPT | .0005" ± | .0005" |
| 36 | SHAFT DIA. AT END SHIPT | .0005" ± | .0005" |
| 37 | SHAFT DIA. AT END SHIPT | .0005" ± | .0005" |
| 38 | SHAFT DIA. AT END SHIPT | .0005" ± | .0005" |
| 39 | SHAFT DIA. AT END SHIPT | .0005" ± | .0005" |
| 40 | SHAFT DIA. AT END SHIPT | .0005" ± | .0005" |
| 41 | SHAFT DIA. AT END SHIPT | .0005" ± | .0005" |
| 42 | SHAFT DIA. AT END SHIPT | .0005" ± | .0005" |
| 43 | SHAFT DIA. AT END SHIPT | .0005" ± | .0005" |
| 44 | SHAFT DIA. AT END SHIPT | .0005" ± | .0005" |
| 45 | SHAFT DIA. AT END SHIPT | .0005" ± | .0005" |
| 46 | SHAFT DIA. AT END SHIPT | .0005" ± | .0005" |

GENERAL NOTES





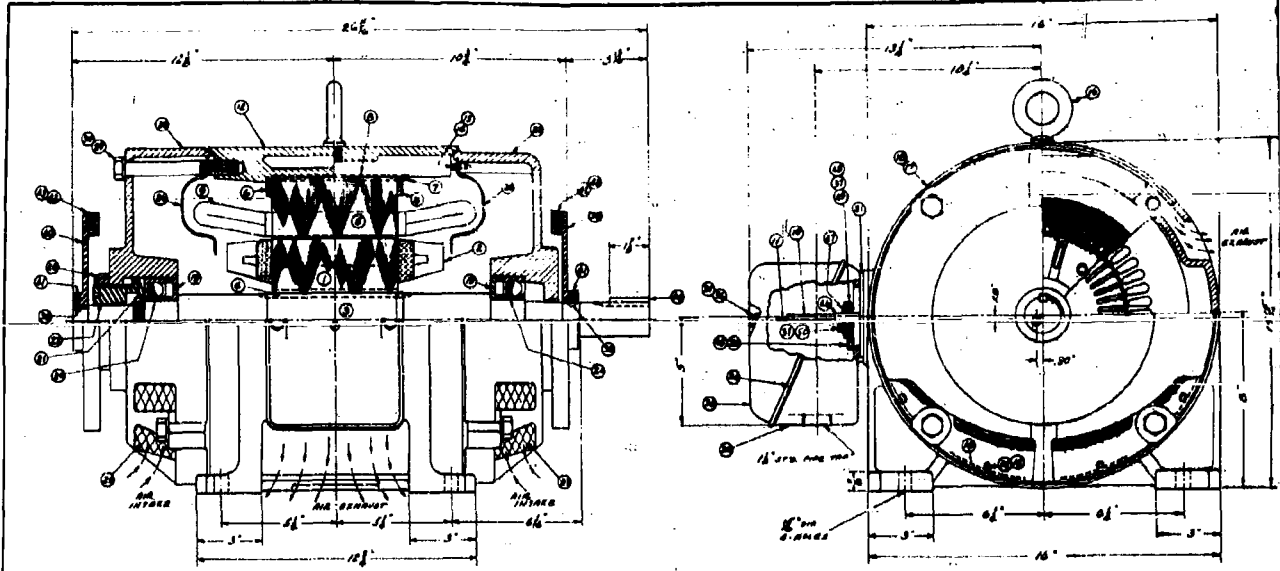
LIST OF MATERIAL QUANTITIES FOR ONE

PC NO.	NAME	NO.	MATERIAL	MAT'L APPX	ALLIS-CHALMERS	ALLIS-CHALMERS	ALLIS-CHALMERS	ALLIS-CHALMERS	ALLIS-CHALMERS	ALLIS-CHALMERS	REMARKS
1	ROTOR PUNCHING	100	STEEL	76" X 48" X 18"	76" X 48" X 18"	76" X 48" X 18"	76" X 48" X 18"	76" X 48" X 18"	76" X 48" X 18"	76" X 48" X 18"	SEE NOTE A
2	ROTOR ASSEMBLY	1	STEEL	76" X 48" X 18"	76" X 48" X 18"	76" X 48" X 18"	76" X 48" X 18"	76" X 48" X 18"	76" X 48" X 18"	76" X 48" X 18"	SEE NOTE B
3	STATOR PUNCHING	100	STEEL	76" X 48" X 18"	76" X 48" X 18"	76" X 48" X 18"	76" X 48" X 18"	76" X 48" X 18"	76" X 48" X 18"	76" X 48" X 18"	SEE NOTE C
4	STATOR ASSEMBLY	1	STEEL	76" X 48" X 18"	76" X 48" X 18"	76" X 48" X 18"	76" X 48" X 18"	76" X 48" X 18"	76" X 48" X 18"	76" X 48" X 18"	SEE NOTE D
5	ROTOR SHAFT	1	STEEL	4" X 18"	4" X 18"	4" X 18"	4" X 18"	4" X 18"	4" X 18"	4" X 18"	SEE NOTE E
6	ROTOR END BRACKET	2	STEEL	4" X 18"	4" X 18"	4" X 18"	4" X 18"	4" X 18"	4" X 18"	4" X 18"	SEE NOTE F
7	ROTOR END BRACKET	2	STEEL	4" X 18"	4" X 18"	4" X 18"	4" X 18"	4" X 18"	4" X 18"	4" X 18"	SEE NOTE G
8	ROTOR END BRACKET	2	STEEL	4" X 18"	4" X 18"	4" X 18"	4" X 18"	4" X 18"	4" X 18"	4" X 18"	SEE NOTE H
9	ROTOR END BRACKET	2	STEEL	4" X 18"	4" X 18"	4" X 18"	4" X 18"	4" X 18"	4" X 18"	4" X 18"	SEE NOTE I
10	ROTOR END BRACKET	2	STEEL	4" X 18"	4" X 18"	4" X 18"	4" X 18"	4" X 18"	4" X 18"	4" X 18"	SEE NOTE J
11	ROTOR END BRACKET	2	STEEL	4" X 18"	4" X 18"	4" X 18"	4" X 18"	4" X 18"	4" X 18"	4" X 18"	SEE NOTE K
12	ROTOR END BRACKET	2	STEEL	4" X 18"	4" X 18"	4" X 18"	4" X 18"	4" X 18"	4" X 18"	4" X 18"	SEE NOTE L
13	ROTOR END BRACKET	2	STEEL	4" X 18"	4" X 18"	4" X 18"	4" X 18"	4" X 18"	4" X 18"	4" X 18"	SEE NOTE M
14	ROTOR END BRACKET	2	STEEL	4" X 18"	4" X 18"	4" X 18"	4" X 18"	4" X 18"	4" X 18"	4" X 18"	SEE NOTE N
15	ROTOR END BRACKET	2	STEEL	4" X 18"	4" X 18"	4" X 18"	4" X 18"	4" X 18"	4" X 18"	4" X 18"	SEE NOTE O
16	ROTOR END BRACKET	2	STEEL	4" X 18"	4" X 18"	4" X 18"	4" X 18"	4" X 18"	4" X 18"	4" X 18"	SEE NOTE P
17	ROTOR END BRACKET	2	STEEL	4" X 18"	4" X 18"	4" X 18"	4" X 18"	4" X 18"	4" X 18"	4" X 18"	SEE NOTE Q
18	ROTOR END BRACKET	2	STEEL	4" X 18"	4" X 18"	4" X 18"	4" X 18"	4" X 18"	4" X 18"	4" X 18"	SEE NOTE R
19	ROTOR END BRACKET	2	STEEL	4" X 18"	4" X 18"	4" X 18"	4" X 18"	4" X 18"	4" X 18"	4" X 18"	SEE NOTE S
20	ROTOR END BRACKET	2	STEEL	4" X 18"	4" X 18"	4" X 18"	4" X 18"	4" X 18"	4" X 18"	4" X 18"	SEE NOTE T
21	ROTOR END BRACKET	2	STEEL	4" X 18"	4" X 18"	4" X 18"	4" X 18"	4" X 18"	4" X 18"	4" X 18"	SEE NOTE U
22	ROTOR END BRACKET	2	STEEL	4" X 18"	4" X 18"	4" X 18"	4" X 18"	4" X 18"	4" X 18"	4" X 18"	SEE NOTE V
23	ROTOR END BRACKET	2	STEEL	4" X 18"	4" X 18"	4" X 18"	4" X 18"	4" X 18"	4" X 18"	4" X 18"	SEE NOTE W
24	ROTOR END BRACKET	2	STEEL	4" X 18"	4" X 18"	4" X 18"	4" X 18"	4" X 18"	4" X 18"	4" X 18"	SEE NOTE X
25	ROTOR END BRACKET	2	STEEL	4" X 18"	4" X 18"	4" X 18"	4" X 18"	4" X 18"	4" X 18"	4" X 18"	SEE NOTE Y



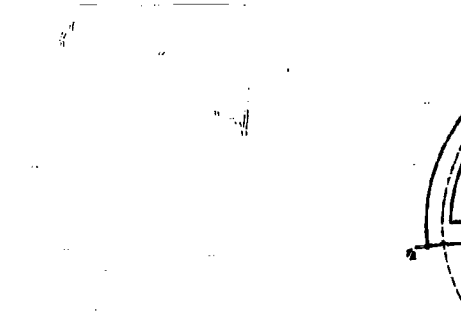
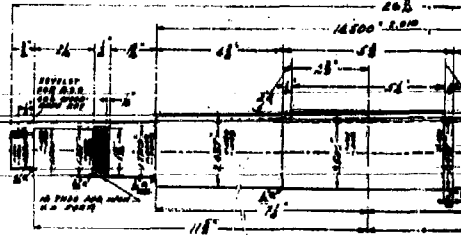
- ZINC PLATING PER QQ-S-385 TYPE II CLASS A
- FORCE REQUIRED TO PRESS SHAFT INTO ROTOR CORE MINIMUM, INTERFERENCE .002" TO .003" TIGHT
- NO AXIAL MOVEMENT OF SHAFT, AND PLAY TAKEN UP BY BELLOWS ADJUSTER AND SPRING WASHER, SPRING WASHER QUANTITY - 600 LBS PER INCH
- SEE NOTE A
- SEE NOTE B
- SEE NOTE C
- SEE NOTE D
- SEE NOTE E
- SEE NOTE F
- SEE NOTE G
- SEE NOTE H
- SEE NOTE I
- SEE NOTE J
- SEE NOTE K
- SEE NOTE L
- SEE NOTE M
- SEE NOTE N
- SEE NOTE O
- SEE NOTE P
- SEE NOTE Q
- SEE NOTE R
- SEE NOTE S
- SEE NOTE T
- SEE NOTE U
- SEE NOTE V
- SEE NOTE W
- SEE NOTE X
- SEE NOTE Y

GENERAL NOTES



LIST OF MATERIAL QUANTITIES FOR ONE

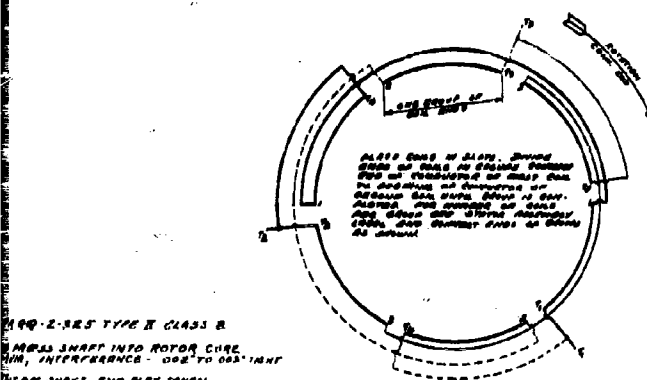
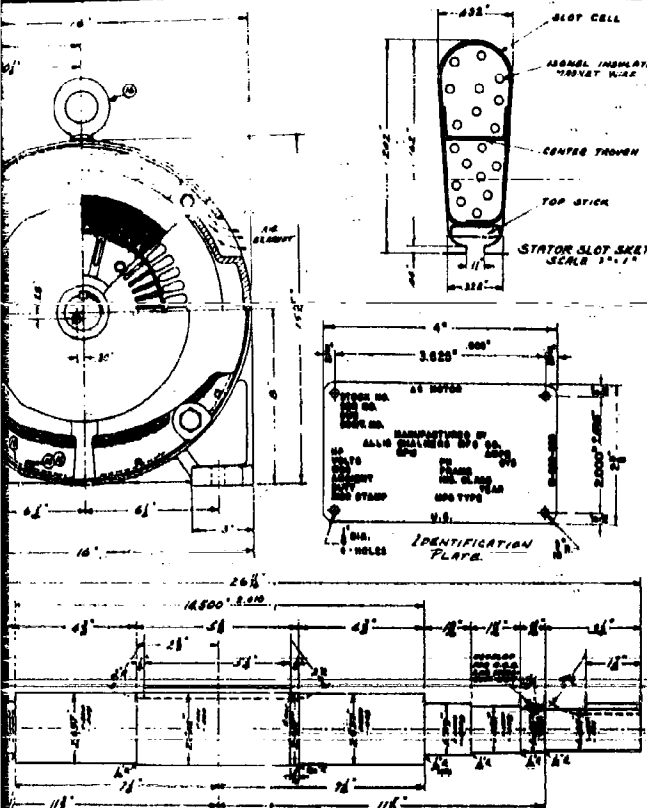
PC. NO.	NAME	NO. REQ.	MATERIAL	MAT. SPEC.	ALLIS-CHALMERS DWS NO.	BU SHIPS DWS NO.	GOVT. SPEC.	STD. NAVY STOCK NO.	REMARKS
1	ROTOR PUNCHING	1	STEEL	SAE 1045	SAE 1045-100				SEE NOTE B
2	ROTOR SHAFT	1	STEEL	SAE 1045	SAE 1045-100				SEE NOTE B
3	ROTOR PUNCHING	1	STEEL	SAE 1045	SAE 1045-100				SEE NOTE B
4	ROTOR PUNCHING	1	STEEL	SAE 1045	SAE 1045-100				SEE NOTE B
5	ROTOR PUNCHING	1	STEEL	SAE 1045	SAE 1045-100				SEE NOTE B
6	ROTOR PUNCHING	1	STEEL	SAE 1045	SAE 1045-100				SEE NOTE B
7	ROTOR PUNCHING	1	STEEL	SAE 1045	SAE 1045-100				SEE NOTE B
8	ROTOR PUNCHING	1	STEEL	SAE 1045	SAE 1045-100				SEE NOTE B
9	ROTOR PUNCHING	1	STEEL	SAE 1045	SAE 1045-100				SEE NOTE B
10	ROTOR PUNCHING	1	STEEL	SAE 1045	SAE 1045-100				SEE NOTE B
11	ROTOR PUNCHING	1	STEEL	SAE 1045	SAE 1045-100				SEE NOTE B
12	ROTOR PUNCHING	1	STEEL	SAE 1045	SAE 1045-100				SEE NOTE B
13	ROTOR PUNCHING	1	STEEL	SAE 1045	SAE 1045-100				SEE NOTE B
14	ROTOR PUNCHING	1	STEEL	SAE 1045	SAE 1045-100				SEE NOTE B
15	ROTOR PUNCHING	1	STEEL	SAE 1045	SAE 1045-100				SEE NOTE B
16	ROTOR PUNCHING	1	STEEL	SAE 1045	SAE 1045-100				SEE NOTE B
17	ROTOR PUNCHING	1	STEEL	SAE 1045	SAE 1045-100				SEE NOTE B
18	ROTOR PUNCHING	1	STEEL	SAE 1045	SAE 1045-100				SEE NOTE B
19	ROTOR PUNCHING	1	STEEL	SAE 1045	SAE 1045-100				SEE NOTE B
20	ROTOR PUNCHING	1	STEEL	SAE 1045	SAE 1045-100				SEE NOTE B
21	ROTOR PUNCHING	1	STEEL	SAE 1045	SAE 1045-100				SEE NOTE B
22	ROTOR PUNCHING	1	STEEL	SAE 1045	SAE 1045-100				SEE NOTE B
23	ROTOR PUNCHING	1	STEEL	SAE 1045	SAE 1045-100				SEE NOTE B
24	ROTOR PUNCHING	1	STEEL	SAE 1045	SAE 1045-100				SEE NOTE B
25	ROTOR PUNCHING	1	STEEL	SAE 1045	SAE 1045-100				SEE NOTE B
26	ROTOR PUNCHING	1	STEEL	SAE 1045	SAE 1045-100				SEE NOTE B
27	ROTOR PUNCHING	1	STEEL	SAE 1045	SAE 1045-100				SEE NOTE B
28	ROTOR PUNCHING	1	STEEL	SAE 1045	SAE 1045-100				SEE NOTE B
29	ROTOR PUNCHING	1	STEEL	SAE 1045	SAE 1045-100				SEE NOTE B
30	ROTOR PUNCHING	1	STEEL	SAE 1045	SAE 1045-100				SEE NOTE B
31	ROTOR PUNCHING	1	STEEL	SAE 1045	SAE 1045-100				SEE NOTE B
32	ROTOR PUNCHING	1	STEEL	SAE 1045	SAE 1045-100				SEE NOTE B
33	ROTOR PUNCHING	1	STEEL	SAE 1045	SAE 1045-100				SEE NOTE B
34	ROTOR PUNCHING	1	STEEL	SAE 1045	SAE 1045-100				SEE NOTE B
35	ROTOR PUNCHING	1	STEEL	SAE 1045	SAE 1045-100				SEE NOTE B
36	ROTOR PUNCHING	1	STEEL	SAE 1045	SAE 1045-100				SEE NOTE B
37	ROTOR PUNCHING	1	STEEL	SAE 1045	SAE 1045-100				SEE NOTE B
38	ROTOR PUNCHING	1	STEEL	SAE 1045	SAE 1045-100				SEE NOTE B
39	ROTOR PUNCHING	1	STEEL	SAE 1045	SAE 1045-100				SEE NOTE B
40	ROTOR PUNCHING	1	STEEL	SAE 1045	SAE 1045-100				SEE NOTE B
41	ROTOR PUNCHING	1	STEEL	SAE 1045	SAE 1045-100				SEE NOTE B
42	ROTOR PUNCHING	1	STEEL	SAE 1045	SAE 1045-100				SEE NOTE B
43	ROTOR PUNCHING	1	STEEL	SAE 1045	SAE 1045-100				SEE NOTE B
44	ROTOR PUNCHING	1	STEEL	SAE 1045	SAE 1045-100				SEE NOTE B
45	ROTOR PUNCHING	1	STEEL	SAE 1045	SAE 1045-100				SEE NOTE B
46	ROTOR PUNCHING	1	STEEL	SAE 1045	SAE 1045-100				SEE NOTE B
47	ROTOR PUNCHING	1	STEEL	SAE 1045	SAE 1045-100				SEE NOTE B
48	ROTOR PUNCHING	1	STEEL	SAE 1045	SAE 1045-100				SEE NOTE B
49	ROTOR PUNCHING	1	STEEL	SAE 1045	SAE 1045-100				SEE NOTE B
50	ROTOR PUNCHING	1	STEEL	SAE 1045	SAE 1045-100				SEE NOTE B



5. ZINC PLATING PER QQ-Z-385 TYPE B CLASS B
6. RINGS REQUIRED TO PRESS SHAFT INTO ROTOR CORE 30,000 LBS. MINIMUM, INTERFERENCE -.002 TO .005 INCH
7. NO AXIAL MOVEMENT OF SHAFT AND PLY TAKEN UP BY PRELOAD ROLLERS AND SPRING WARRER SPRING WARRER CONSTANT - 3000 LBS PER INCH
8. NO APPLICABLE GOVT. SPEC. - BEST COMMERCIAL GRADE
9. CRITICAL DIMENSIONS -
- | DESCRIPTION OF MEASUREMENT | DRAWING DIMENSION | PERMITTED DIMENSION |
|--|-------------------|---------------------|
| A. FRONT DIA. FIT ON SHAFT | 1.7715 ± .0005 | 1.7717 |
| B. FRONT DIA. FIT ON SHAFT | 1.7715 ± .0005 | 1.7718 |
| C. FRONT DIA. FIT ECCENTRICITY | — | .0005 |
| D. FRONT DIA. FIT ECCENTRICITY | — | .0006 |
| E. DIA. RUN OUT OF FRONT END CAP ATTACHED TO SHAFT | — | .0015 |
| F. FACE RUN OUT OF SHAFT | — | .0005 |
| G. FRONT DIA. RES. DIA. SECT | 3.8870 ± .0005 | 3.8875 |
| H. REAR DIA. RES. DIA. SECT | 3.8870 ± .0005 | 3.8875 |
| I. FRONT DIA. RES. DIA. SECT | 16.374 ± .001 | 16.375 |
| J. REAR DIA. RES. DIA. SECT | 16.374 ± .001 | 16.375 |
| K. FRONT DIA. RES. DIA. SECT | 16.374 ± .001 | 16.375 |
| L. REAR DIA. RES. DIA. SECT | 16.374 ± .001 | 16.375 |
| M. FRONT DIA. I.D. (R500) | 1.7715 ± .0005 | 1.7715 |
| N. REAR DIA. I.D. (R500) | 1.7715 ± .0005 | 1.7715 |
| O. FRONT DIA. O.D. (R500) | 3.8870 ± .0005 | 3.8875 |
| P. REAR DIA. O.D. (R500) | 3.8870 ± .0005 | 3.8875 |
| Q. AIR GAP ECCENTRICITY | — | LESS THAN .001 |

GENERAL NOTES

1



SPECIFICATIONS AND EXCEPTIONS

THE MOTOR DESIGNER'S REQUIREMENTS WILL conform STRICTLY WITH THE CONTRACT SPECIFICATION UNLESS OTHERWISE INDICATED BY THE SUPPLIER'S LIST OF EXCEPTIONS TO SAID SPECIFICATIONS. OVERALL LENGTH, IN ORDER OF ASSEMBLY.

DESIGN REQUIREMENTS

PERFORMANCE	DESIGN	EXCEPTION	POWER FACTOR
(1) LOCKED ROTOR (150.000%)	100.0	100.0	0.7
(2) GUARANTEED EFF	80.5	80.5	0.8
(3) GUARANTEED EFF	81.0	81.0	0.8
(4) GUARANTEED EFF	81.5	81.5	0.8
(5) NO LOAD (100.0%)	100.0	100.0	0.8
(6) STATOR TORQUE - NOT LESS THAN	100.0	100.0	% FL TORQUE
(7) PULLUP TORQUE - NOT LESS THAN	200.0	200.0	% FL TORQUE
(8) PULLUP TORQUE - NOT LESS THAN	200.0	200.0	% FL TORQUE

STATOR CORE

(1) BAR LENGTH **7.1** (2) CORE LENGTH **3.8** (3) BAR CAP **0.05**

ROTOR CORE

(1) BAR LENGTH **3.8** (2) CORE LENGTH **7.1** (3) BAR CAP **0.05**

WEIGHTS

(1) MOTOR COMPLETE **12.5** LBS. (2) ROTOR COMPLETE **4.5** LBS. (3) COP BATTERY **0.5** LBS.

BEARINGS

ANY OF THE FOLLOWING BARE BEARINGS MAY BE OBTAINABLE FOR REPLACEMENT:

TYPE	SIZE
ROTOR	3/8" BALL
STATOR	3/8" JOY'S
INDICATOR	NEW BATTERY

STATOR WINDING DATA

WINDING DATA	WINDING DATA	WINDING DATA
(1) COILS PER SLEEVE	2	
(2) COILS PER SLEEVE	2	
(3) COILS PER SLEEVE	2	
(4) COILS PER SLEEVE	2	
(5) COILS PER SLEEVE	2	
(6) COILS PER SLEEVE	2	
(7) COILS PER SLEEVE	2	

TREATMENT OF COMPLETE STATOR

THE COMPLETELY WOUND STATOR IS GIVEN:

1. POLYESTER ENAMEL 100% BY WEIGHT.
2. 3 DAYS AND BAKED IN VACUUM WITH THE FOLLOWING CURVE CYCLES RESPECTIVELY:
 - 3 HRS @ 250°C
 - 2 HRS @ 300°C
 - 1 HR @ 300°C

INSULATION	MATERIAL	GOVT. SPEC.
SLOT CELL	CLASSIC TROVET WIRE	NSG-100
INSULATION	CLASSIC TROVET WIRE	NSG-100
INSULATION	CLASSIC TROVET WIRE	NSG-100
INSULATION	CLASSIC TROVET WIRE	NSG-100
INSULATION	CLASSIC TROVET WIRE	NSG-100
INSULATION	CLASSIC TROVET WIRE	NSG-100

PERFORMANCE AT RATED VOLTAGE AND FREQUENCY

ACTUAL LOAD (%)	HIGH SPEED				LOW SPEED			
	EFF	AMP	WATT	HP	EFF	AMP	WATT	HP
25%	81.5	2.1	13.5	0.18	81.5	1.8	11.5	0.16
50%	81.5	2.2	14.0	0.18	81.5	1.8	11.5	0.16
75%	81.5	2.3	14.5	0.18	81.5	1.8	11.5	0.16
100%	81.5	2.4	15.0	0.18	81.5	1.8	11.5	0.16

SPEED TORQUE DATA

HIGH SPEED		LOW SPEED	
SPEED (RPM)	TORQUE (LBS)	SPEED (RPM)	TORQUE (LBS)
1800	1.5	900	3.0
1750	1.6	850	3.1
1700	1.7	800	3.2
1650	1.8	750	3.3
1600	1.9	700	3.4

LOCKED SATURABLE EXCITATION

HIGH SPEED		LOW SPEED	
EXCITATION (%)	EFF	EXCITATION (%)	EFF
100%	81.5	100%	81.5
90%	81.5	90%	81.5
80%	81.5	80%	81.5

HEATING-THERMISTERS IN DESIGN CERTIFICATION

HIGH SPEED		LOW SPEED	
TEMP (°C)	RESISTANCE (OHMS)	TEMP (°C)	RESISTANCE (OHMS)
100	100	100	100
150	150	150	150
200	200	200	200
250	250	250	250

HEATING-THERMISTERS IN DESIGN CERTIFICATION

HIGH SPEED		LOW SPEED	
TEMP (°C)	RESISTANCE (OHMS)	TEMP (°C)	RESISTANCE (OHMS)
100	100	100	100
150	150	150	150
200	200	200	200
250	250	250	250

SNOCK TEST REFERENCE:

SEE SNOCK TEST REPORT

ADAPTER MOUNTING:

SEE SNOCK TEST REPORT

REVISIONS

REV	DESCRIPTION
B	REVISION FOR S.S. 100 LBS. MOTOR TEST
A	CHANGED RESISTANCE TO 100 OHMS
A	ORIGINAL DESIGNATION

1. ALL DIMENSIONS SHALL BE IN INCHES UNLESS OTHERWISE INDICATED.

2. ALL DIMENSIONS SHALL BE TO UNLESS OTHERWISE INDICATED.

3. ALL DIMENSIONS SHALL BE TO UNLESS OTHERWISE INDICATED.

4. ALL DIMENSIONS SHALL BE TO UNLESS OTHERWISE INDICATED.

UNIT	CONVERSION	PERCENTAGE
1 INCH	25.4 MM	100%
1 FOOT	304.8 MM	100%
1 MILE	1609.34 M	100%
1 GALLON	3.785 L	100%
1 POUND	4.536 N	100%

3

MOTOR DATA

TYPE AND CLASS G

FRAME SIZE 56 DUTY CONTINUOUS

ENCLOSURE DIPLOMAT EXTENDED

COOLING NATURAL CONVECTION

SPEED CLASS GENERAL PURPOSE FL 1550

NR. OF VOLTS 230 CYCLE 60 PHASE 3

NAMEPLATE AMP. 1.8 TYPE OF ROTOR SCALAR

INSULATION CLASS F MOUNTING INDOOR

PERMISSIBLE AMBIENT TEMP 40 °C OR LESS

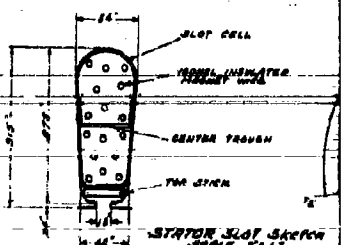
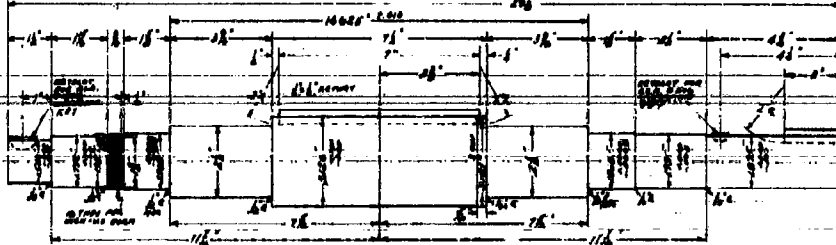
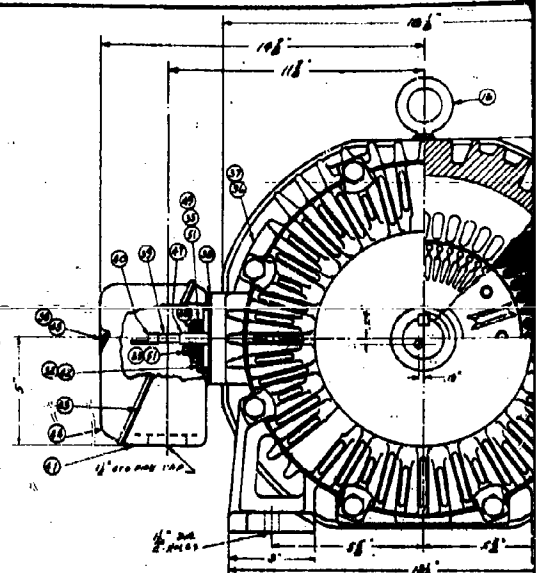
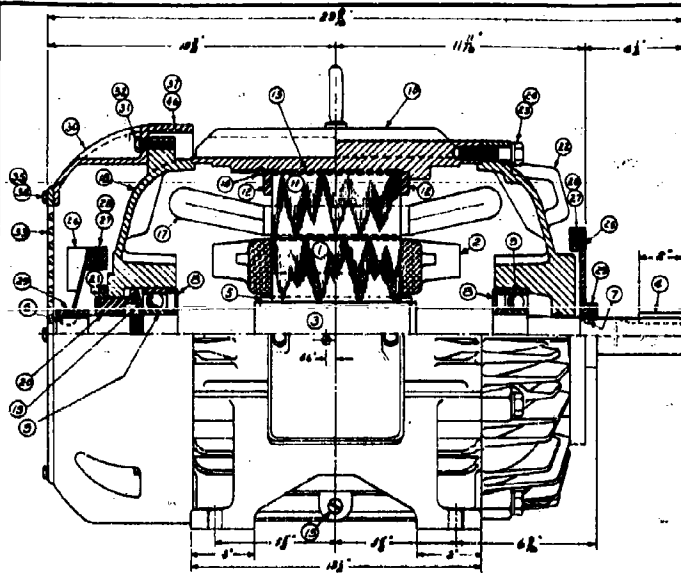
Navy SERVICE A

MASTER DRAWING

ALTERNATING CURRENT MOTOR

175.00V 575.00 Hz

ALLIS-CHALMERS MFG. CO.
NORWOOD, OHIO U.S.A.
57-003-288



LIST OF MATERIAL QUANTITIES FOR ONE

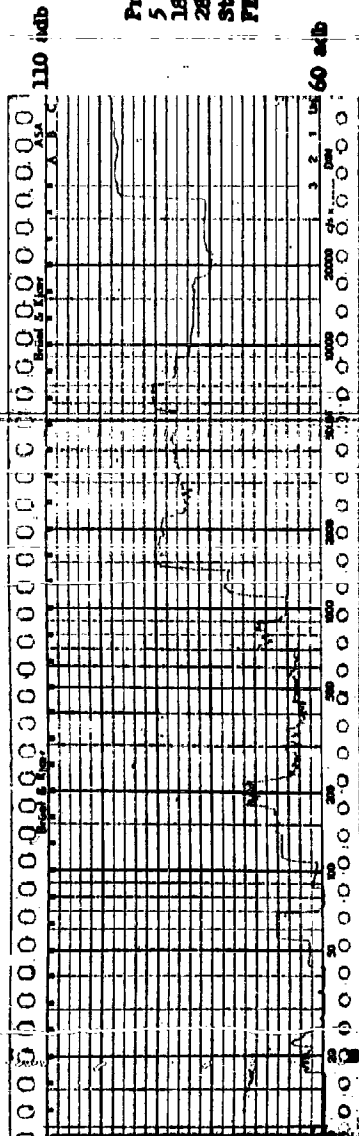
PO. NO.	NAME	NO. REQ.	MATERIAL	MAT'L. SPEC.	ALLIS-CHALMERS DWG NO.	ON SHIP DWG NO.	STO. NAVY STOCK NO.	REMARKS
1	Rotor Bushing	1	STEEL	SAE 5160	7-180-394-001			
2	Rotor Bush End Key	1	STEEL	SAE 5160	7-180-394-002			SEE NOTE 3
3	Rotor Bush	1	STEEL	SAE 5160	7-180-394-001			
4	Shaft Key	1	STEEL	SAE 5160	7-180-394-001			
5	Washer Key	1	STEEL	SAE 5160	7-180-394-001			
6	Washer Key	1	STEEL	SAE 5160	7-180-394-001			
7	Washer Key	1	STEEL	SAE 5160	7-180-394-001			
8	End Key	1	STEEL	SAE 5160	7-180-394-001			
9	End Key	1	STEEL	SAE 5160	7-180-394-001			
10	Spring Valve	1	STEEL	SAE 5160	7-180-394-001			
11	Spring Washer	1	STEEL	SAE 5160	7-180-394-001			
12	Spring Washer	1	STEEL	SAE 5160	7-180-394-001			
13	Key	1	STEEL	SAE 5160	7-180-394-001			
14	End Key	1	STEEL	SAE 5160	7-180-394-001			
15	End Key	1	STEEL	SAE 5160	7-180-394-001			
16	End Key	1	STEEL	SAE 5160	7-180-394-001			
17	End Key	1	STEEL	SAE 5160	7-180-394-001			
18	Spring Valve	1	STEEL	SAE 5160	7-180-394-001			
19	Spring Washer	1	STEEL	SAE 5160	7-180-394-001			
20	Spring Washer	1	STEEL	SAE 5160	7-180-394-001			
21	Spring Washer	1	STEEL	SAE 5160	7-180-394-001			
22	Spring Washer	1	STEEL	SAE 5160	7-180-394-001			
23	Spring Washer	1	STEEL	SAE 5160	7-180-394-001			
24	Spring Washer	1	STEEL	SAE 5160	7-180-394-001			
25	Spring Washer	1	STEEL	SAE 5160	7-180-394-001			
26	Spring Washer	1	STEEL	SAE 5160	7-180-394-001			
27	Spring Washer	1	STEEL	SAE 5160	7-180-394-001			
28	Spring Washer	1	STEEL	SAE 5160	7-180-394-001			
29	Spring Washer	1	STEEL	SAE 5160	7-180-394-001			
30	Spring Washer	1	STEEL	SAE 5160	7-180-394-001			
31	Spring Washer	1	STEEL	SAE 5160	7-180-394-001			
32	Spring Washer	1	STEEL	SAE 5160	7-180-394-001			
33	Spring Washer	1	STEEL	SAE 5160	7-180-394-001			
34	Spring Washer	1	STEEL	SAE 5160	7-180-394-001			
35	Spring Washer	1	STEEL	SAE 5160	7-180-394-001			
36	Spring Washer	1	STEEL	SAE 5160	7-180-394-001			
37	Spring Washer	1	STEEL	SAE 5160	7-180-394-001			
38	Spring Washer	1	STEEL	SAE 5160	7-180-394-001			
39	Spring Washer	1	STEEL	SAE 5160	7-180-394-001			
40	Spring Washer	1	STEEL	SAE 5160	7-180-394-001			

- 5. ZINC PLATING PER QQ-Z-385 TYPE X CLASS 2
 - 4. FORCE REQUIRED TO PRESS SHAFT INTO MOTOR CORE - 8000 MINIMUM, INTERFERENCE - .002" TO .003" TIENT
 - 3. NO AXIAL MOVEMENT OF SHAFT END KEY TAKEN UP BY AIRLOAD ADJUSTER AND SPRING WASHER, SPRING WASHER CONSTANT - 500 LBS PER INCH
 - 2. NO APPLICABLE GOVT. SPEC. BEST COMMERCIAL GRADE
1. CRITICAL DIMENSIONS -
- | | | |
|--|--------------------|-----------------------|
| SHAFT NAME AND POINT OF MEASUREMENT | ARRIVING DIMENSION | PERMISSIBLE VARIATION |
| 1. FRONT END FIT ON SHAFT | 1.842" ± .005 | ± .005" |
| 2. FRONT END FIT ON SHAFT | 1.842" ± .005 | ± .005" |
| 3. FRONT END FIT ECCENTRICITY | | ± .005" |
| 4. FRONT END FIT ECCENTRICITY | | ± .005" |
| 5. SHOT END OUT OF FRONT END CAP ATTACHED TO SHAFT | | ± .005" |
| 6. SHOT END OUT OF SHAFT END CAP ATTACHED TO SHAFT | | ± .005" |
| 7. FRONT END FIT ON FIT | 1.842" ± .005 | ± .005" |
| 8. FRONT END FIT ON FIT | 1.842" ± .005 | ± .005" |
| 9. FRONT END FIT ON FIT | 1.842" ± .005 | ± .005" |
| 10. FRONT END FIT ON FIT | 1.842" ± .005 | ± .005" |
| 11. FRONT END FIT ON FIT | 1.842" ± .005 | ± .005" |
| 12. FRONT END FIT ON FIT | 1.842" ± .005 | ± .005" |
| 13. FRONT END FIT ON FIT | 1.842" ± .005 | ± .005" |
| 14. FRONT END FIT ON FIT | 1.842" ± .005 | ± .005" |
| 15. FRONT END FIT ON FIT | 1.842" ± .005 | ± .005" |
| 16. FRONT END FIT ON FIT | 1.842" ± .005 | ± .005" |
| 17. FRONT END FIT ON FIT | 1.842" ± .005 | ± .005" |
| 18. FRONT END FIT ON FIT | 1.842" ± .005 | ± .005" |
| 19. FRONT END FIT ON FIT | 1.842" ± .005 | ± .005" |
| 20. FRONT END FIT ON FIT | 1.842" ± .005 | ± .005" |

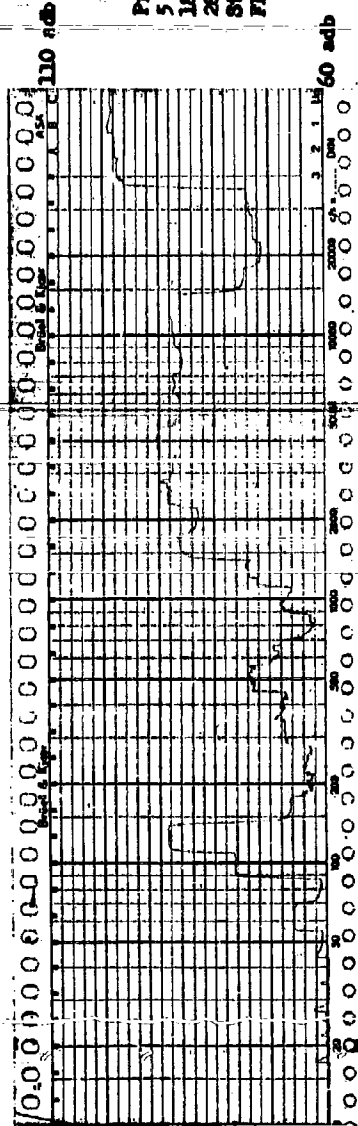
GENERAL NOTES

NO.	NAME	QTY	MATERIAL	STOCK NO.
47	SPRING VALVE	3	STEEL	SAE 5160 7-180-394-001
48	SPRING WASHER	1	STEEL	SAE 5160 7-180-394-001
49	SPRING WASHER	1	STEEL	SAE 5160 7-180-394-001
50	SPRING WASHER	1	STEEL	SAE 5160 7-180-394-001
51	SPRING WASHER	1	STEEL	SAE 5160 7-180-394-001

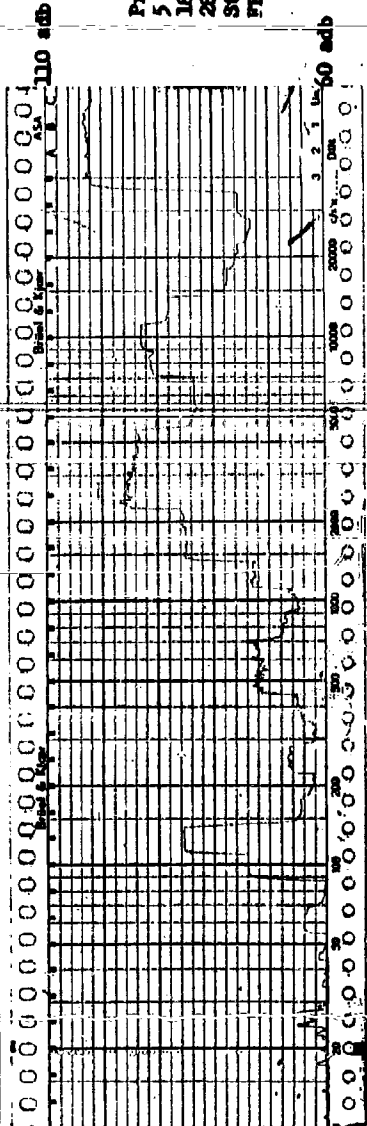
1



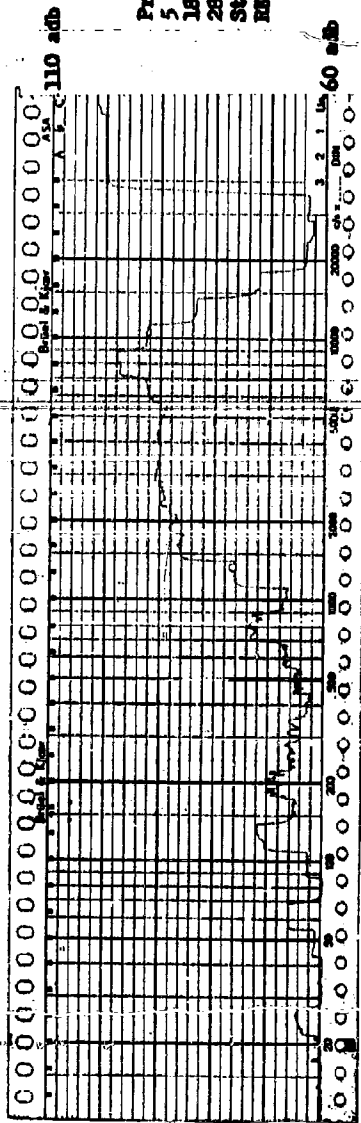
Prototype Motor
 5 HP 2 Pole
 184 Frame DFP
 28 March 1961
 Structureborne
 FE Y-Axis



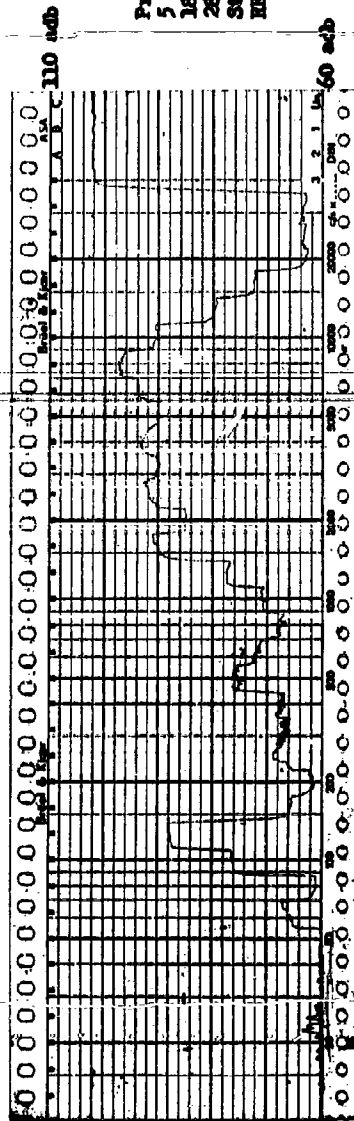
Prototype Motor
 5 HP 2 Pole
 184 Frame DFP
 28 March 1961
 Structureborne
 FE Y-Axis



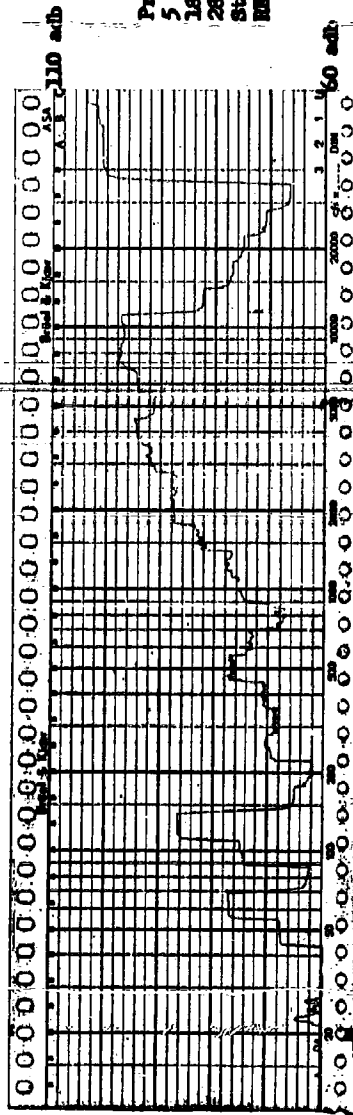
Prototype Motor
 5 HP 2 Pole
 184 Frame DFP
 28 March 1961
 Structureborne
 FE Z-Axis



Prototype Motor
5 HP 2 Pole
184 Frames IFF
28 March 1961
Structureborne
HE Z-Axis

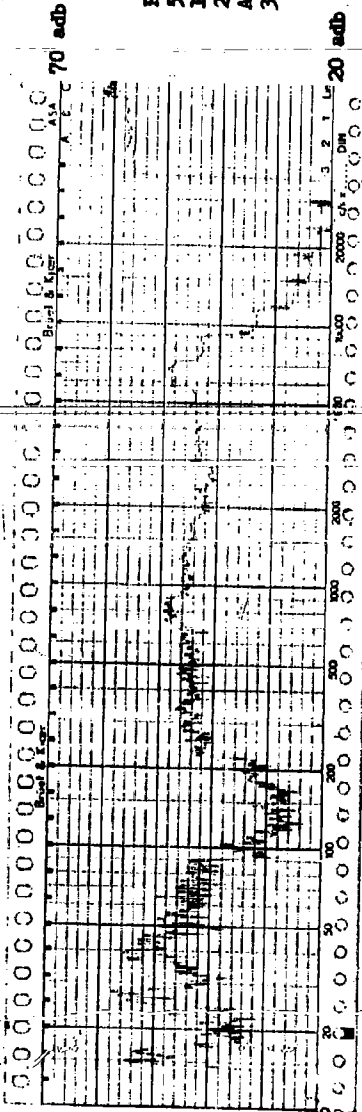


Prototype Motor
5 HP 2 Pole
184 Frames IFF
28 March 1961
Structureborne
HE Y-Axis

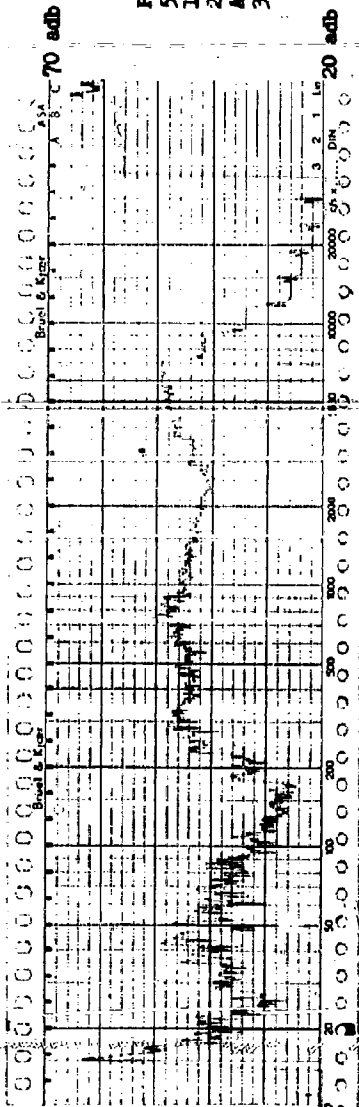


Prototype Motor
5 HP 2 Pole
184 Frames IFF
28 March 1961
Structureborne
HE Z-Axis

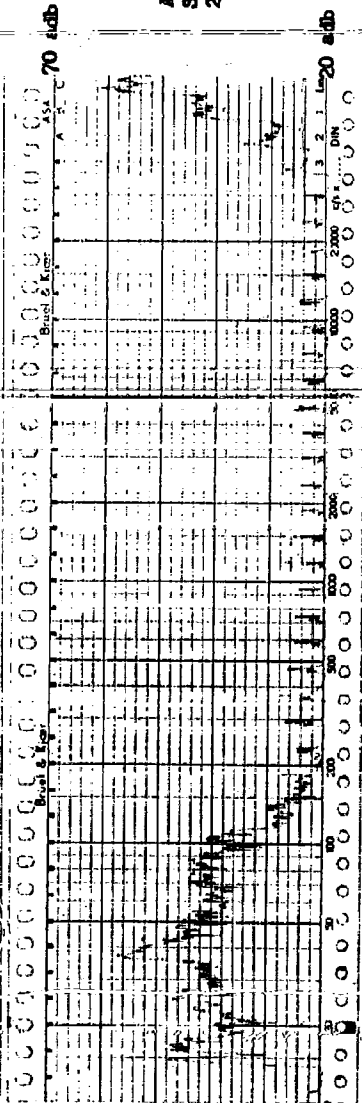
Prototype Motor
5 HP 2 Pole
184 Frames DPF
28 March 1961
Airborne
3 Ft. FE

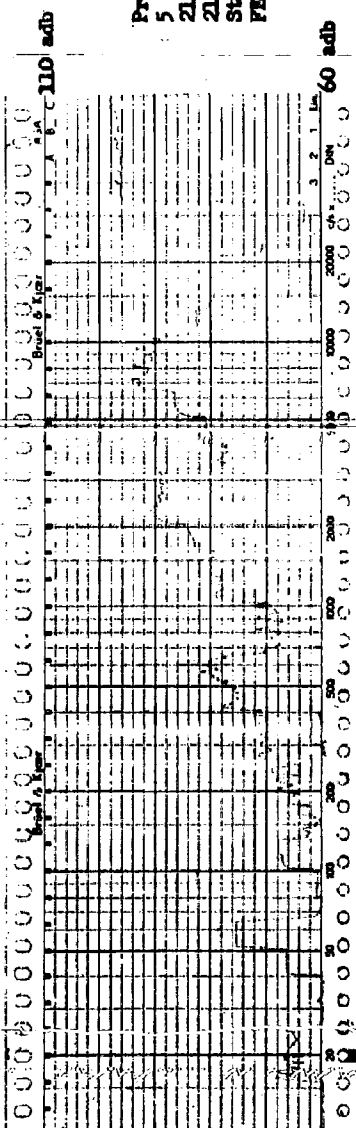
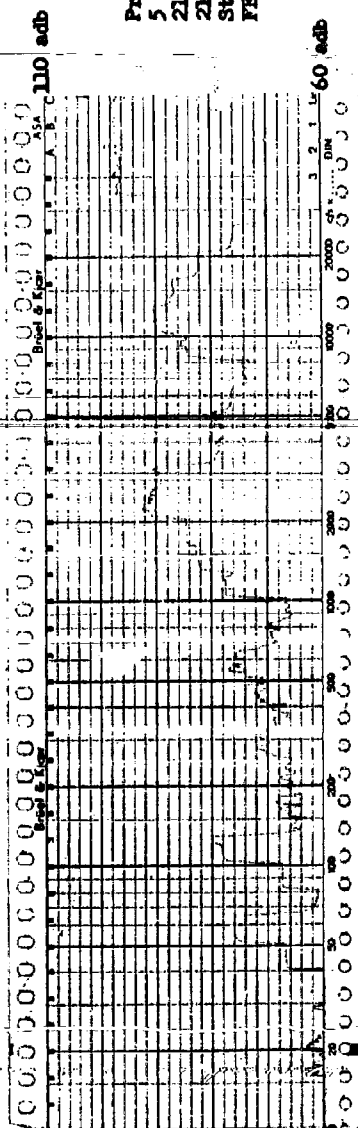
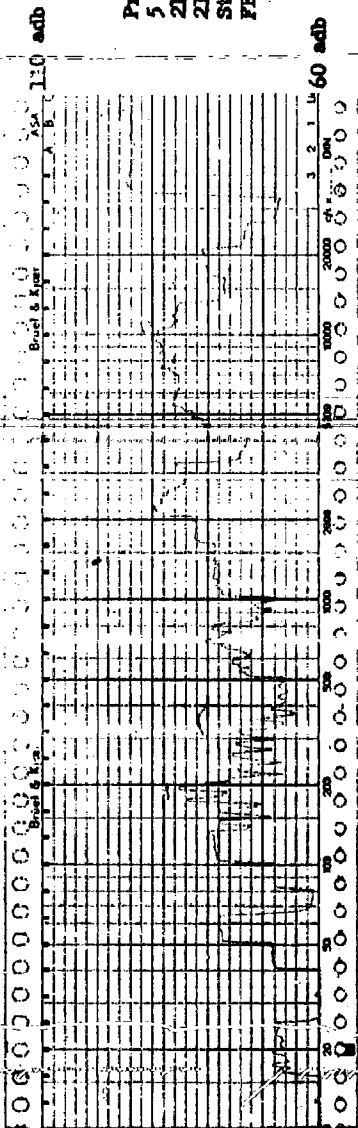


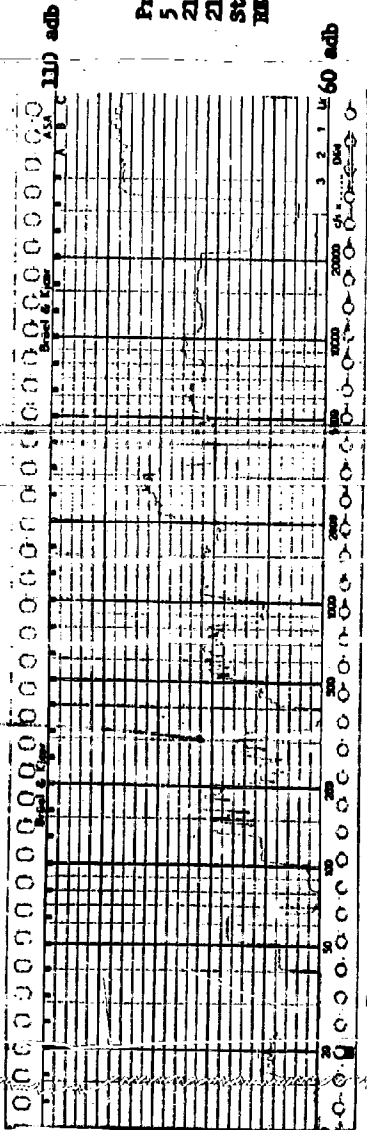
Prototype Motor
5 HP 2 Pole
184 Frames DPF
28 March 1961
Airborne
3 Ft. FE



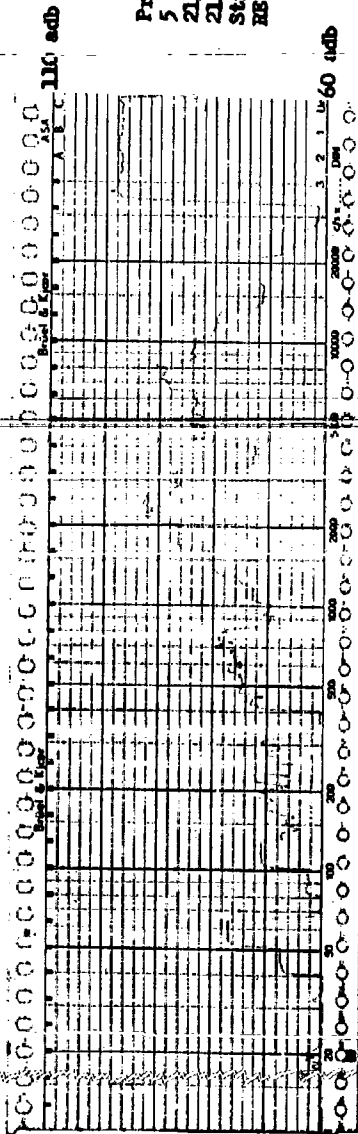
Ambient Level
Sound Room
28 March 1961



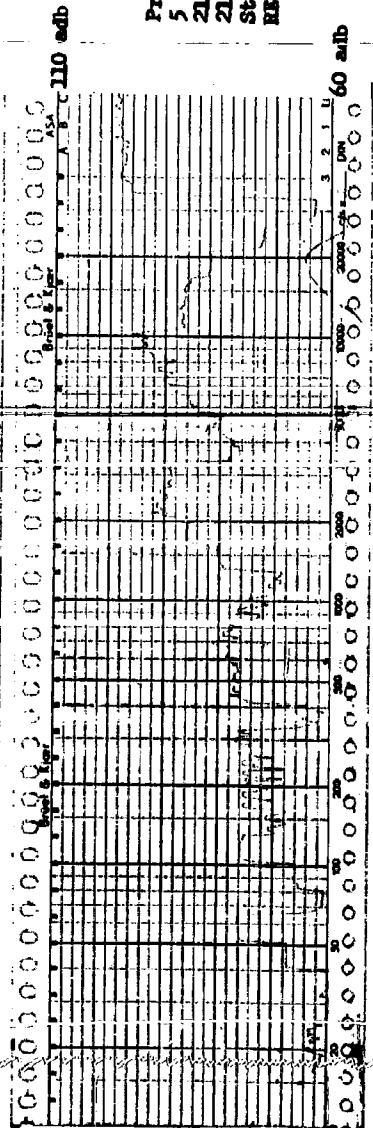




Prototype Motor
 5 HP 2 Pole
 213 Frame TEFC
 21 March 1961
 Structureborne
 RE X-Axis

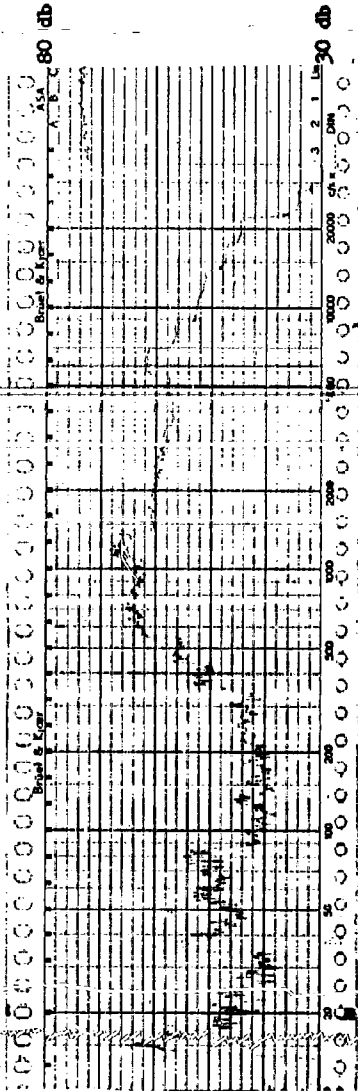


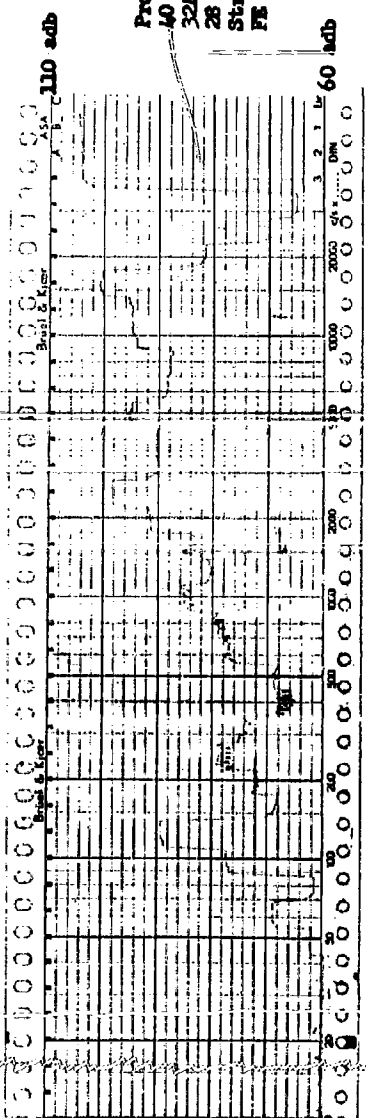
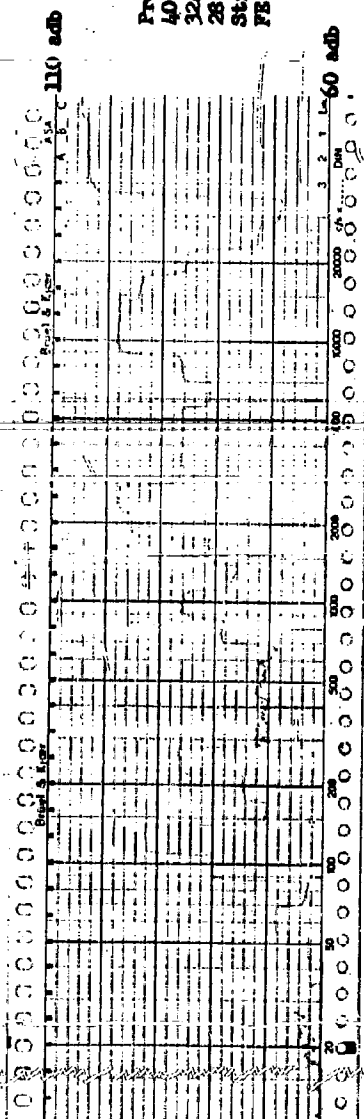
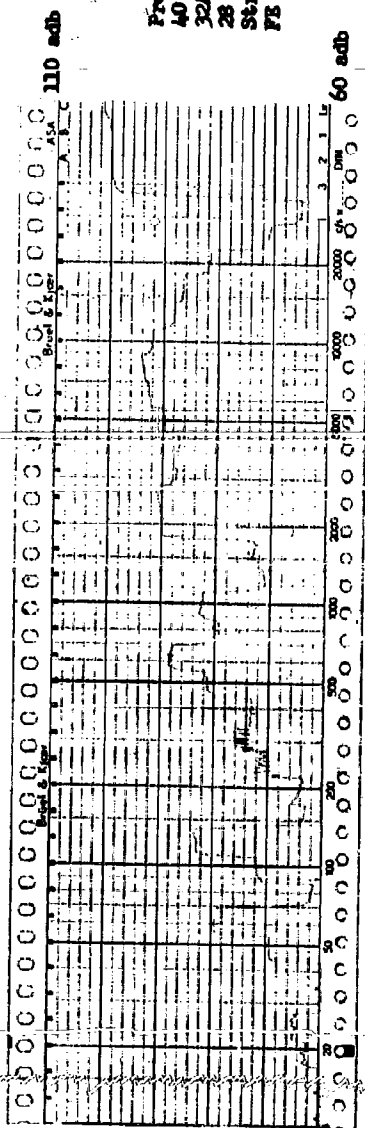
Prototype Motor
 5 HP 2 Pole
 213 Frame TEFC
 21 March 1961
 Structureborne
 RE Y-Axis

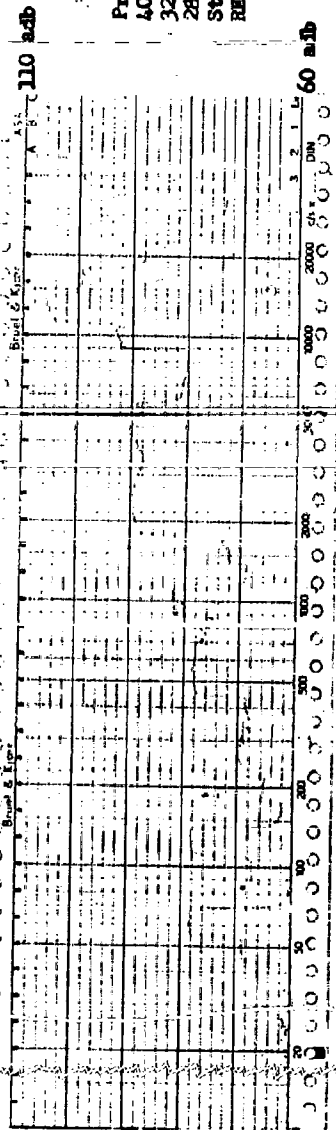


Prototype Motor
 5 HP 2 Pole
 213 Frame TEFC
 21 March 1961
 Structureborne
 RE Z-Axis

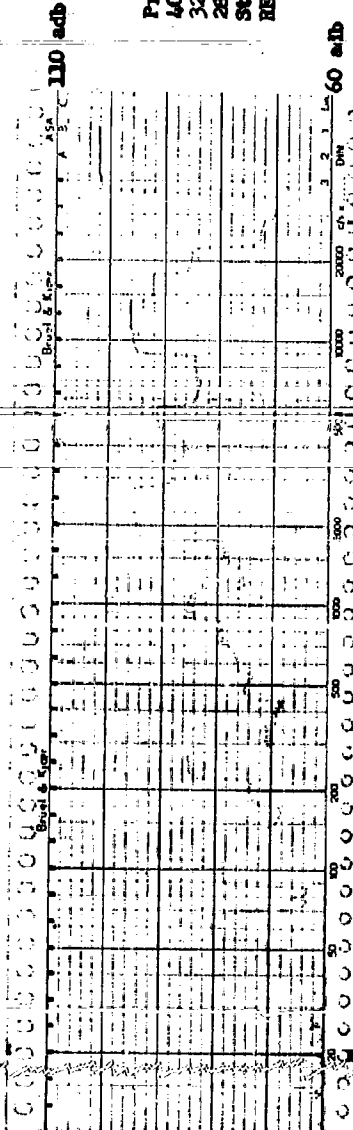
Prototype Motor
5 HP 2 Pole
213 Frame TEFC
14 March 1961
Airborne
3 Ft. FS



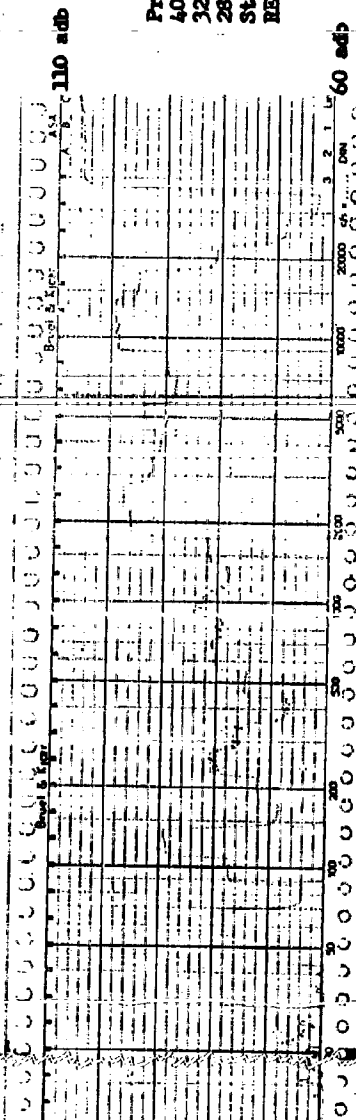




Prototype Motor
 40 HP 2 Pole
 324 Frame DPP
 28 March 1961
 Structureborne
 RE I-Axis

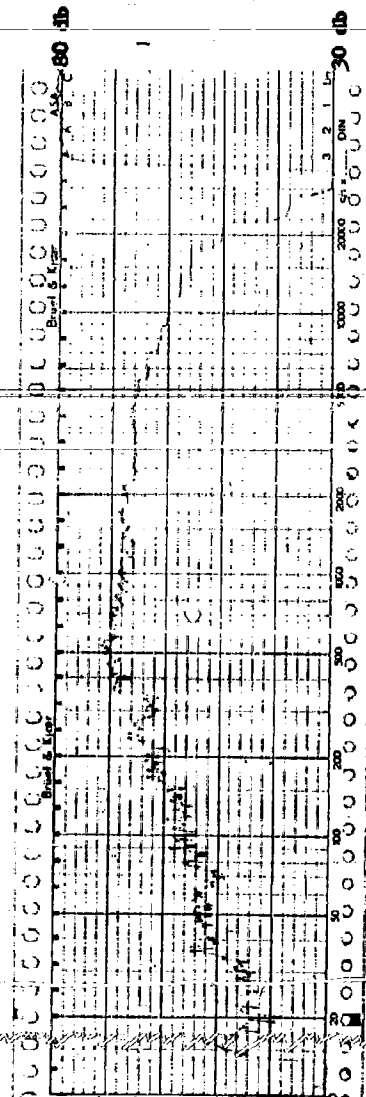


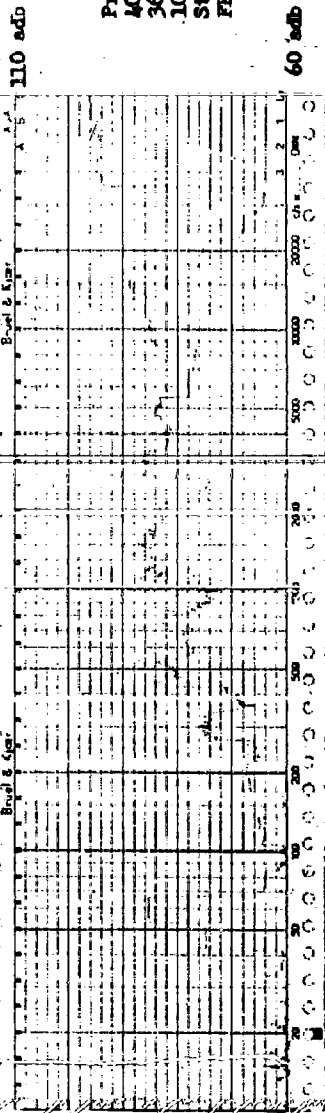
Prototype Motor
 40 HP 2 Pole
 324 Frame DPP
 28 March 1961
 Structureborne
 RE I-Axis



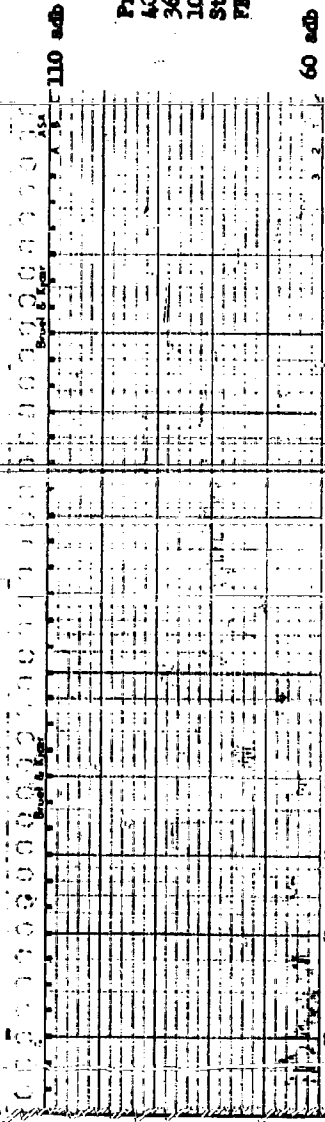
Prototype Motor
 40 HP 2 Pole
 324 Frame DPP
 28 March 1961
 Structureborne
 RE 2-Axis

Prototype Motor
 40 HP 2 Pole
 324 Frame DPP
 29 March 1961
 Airborne
 3 Ft. FE

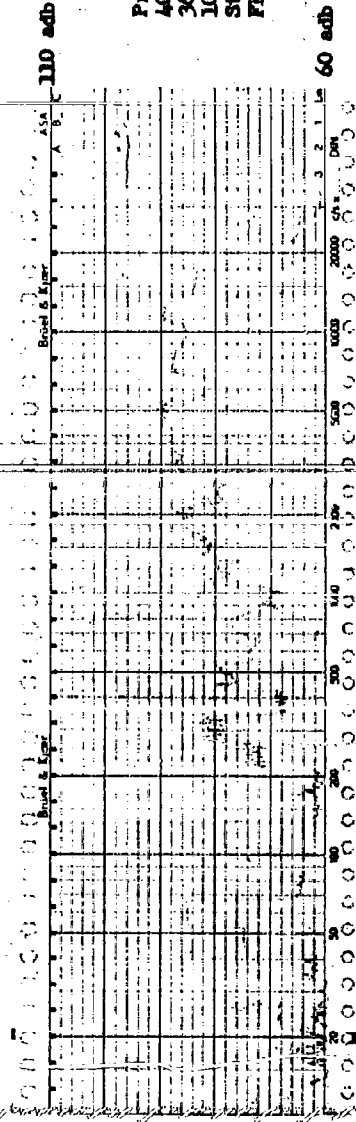




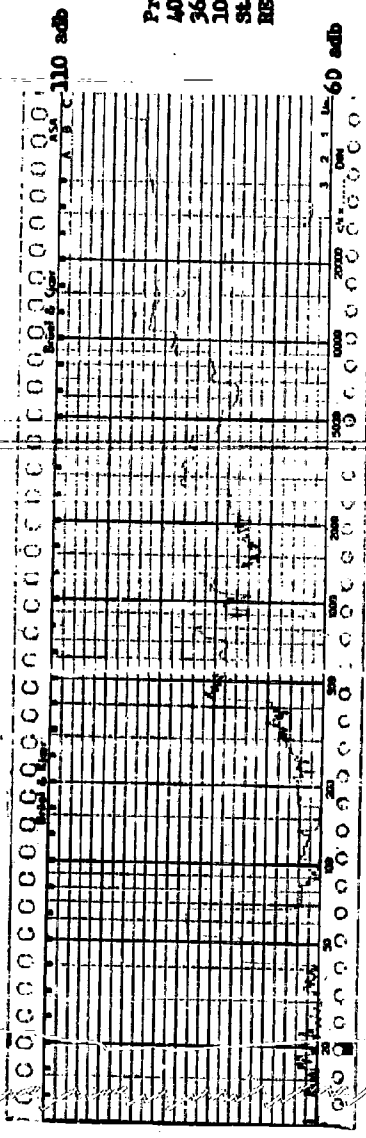
Prototype Motor
 40 HP 2 Pole
 364 Frame TEFC
 10 April 1961
 Structureborne
 FE Y-Axis



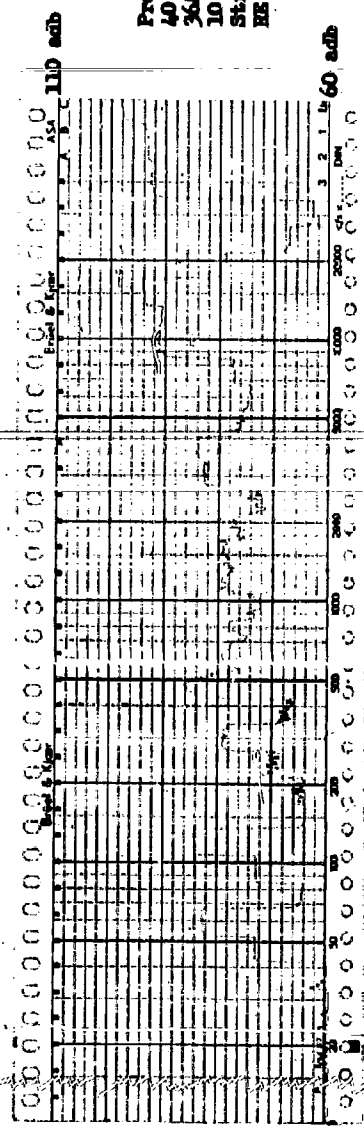
Prototype Motor
 40 HP 2 Pole
 364 Frame TEFC
 10 April 1961
 Structureborne
 FE Y-Axis



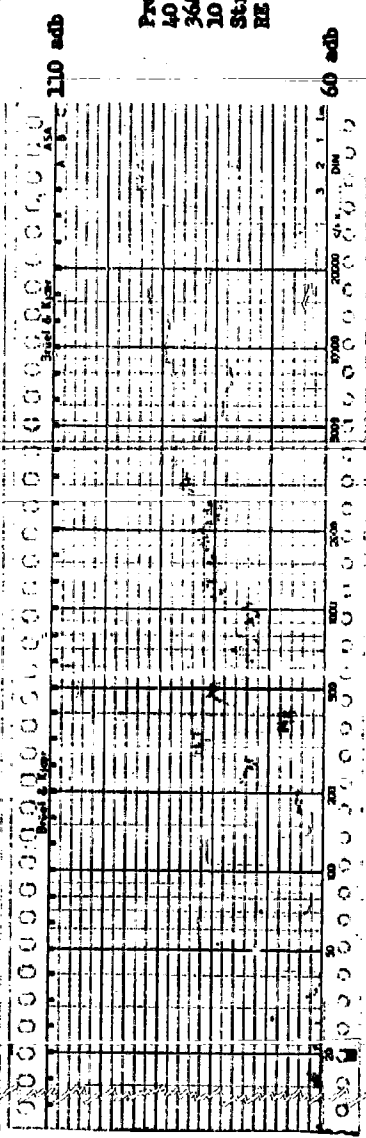
Prototype Motor
 40 HP 2 Pole
 364 Frame TEFC
 10 April 1961
 Structureborne
 FS Z-Axis



Prototype Motor
 40 HP 2 Pole
 364 Frames TEFC
 10 April 1961
 Structureborne
 RE X-Axis

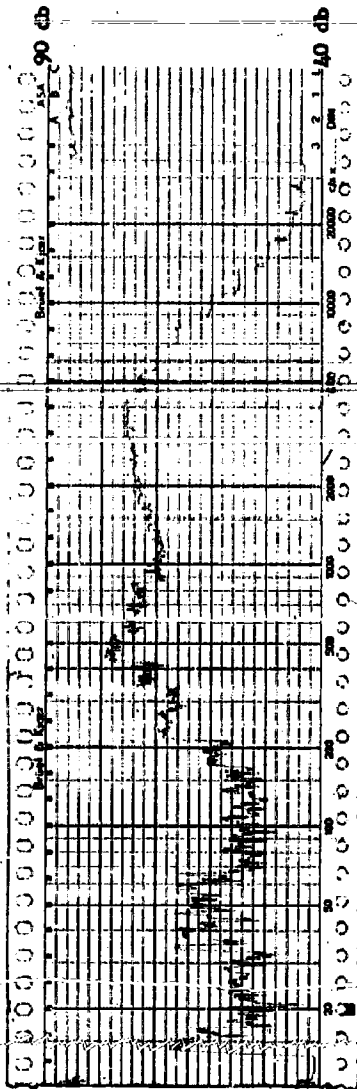


Prototype Motor
 40 HP 2 Pole
 364 Frames TEFC
 10 April 1961
 Structureborne
 RE Y-Axis

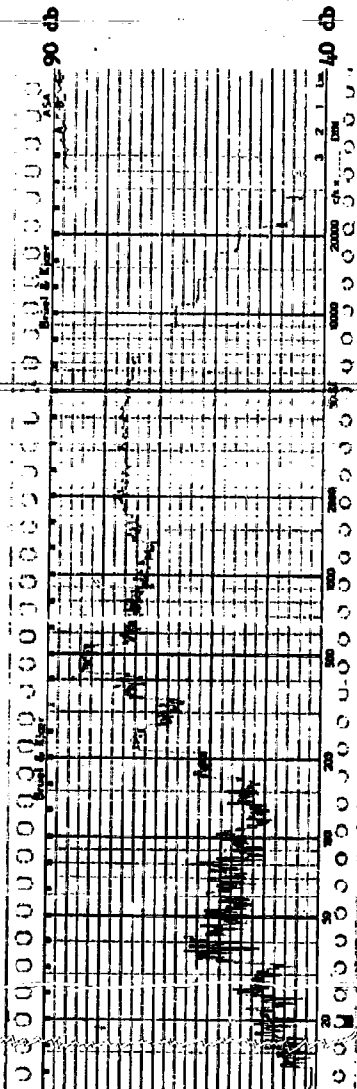


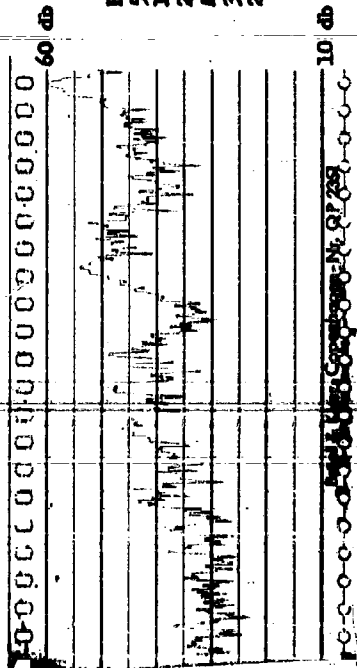
Prototype Motor
 40 HP 2 Pole
 364 Frames TEFC
 10 April 1961
 Structureborne
 RE Z-Axis

Prototype Motor
 40 HP 2 Poles
 364, Frame TREC
 10 April 1961
 Airborne
 3 Ft. HE

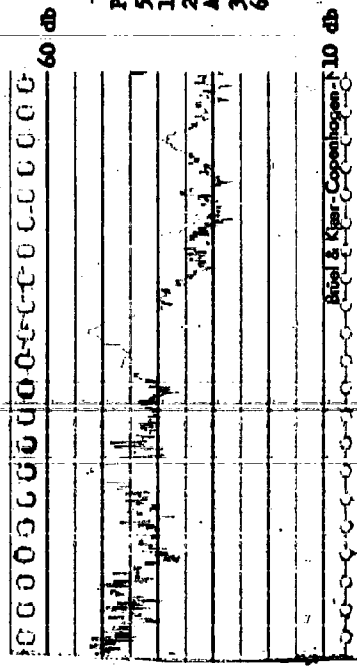


Prototype Motor
 40 HP 2 Poles
 364, Frame TREC
 10 April 1961
 Airborne
 3 Ft. FE

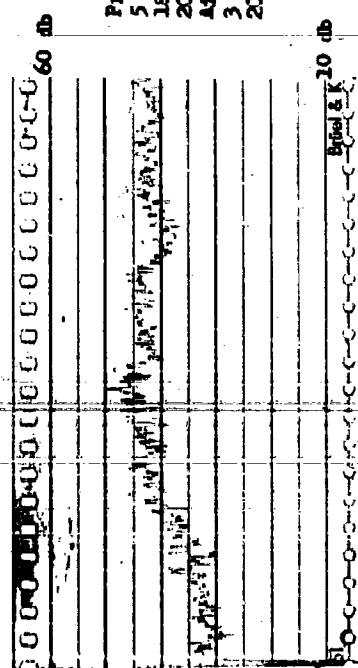




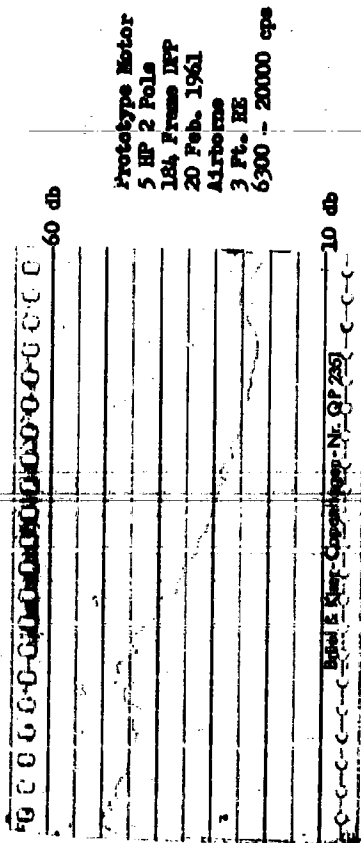
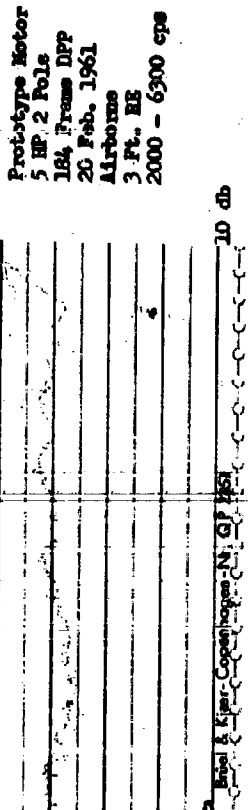
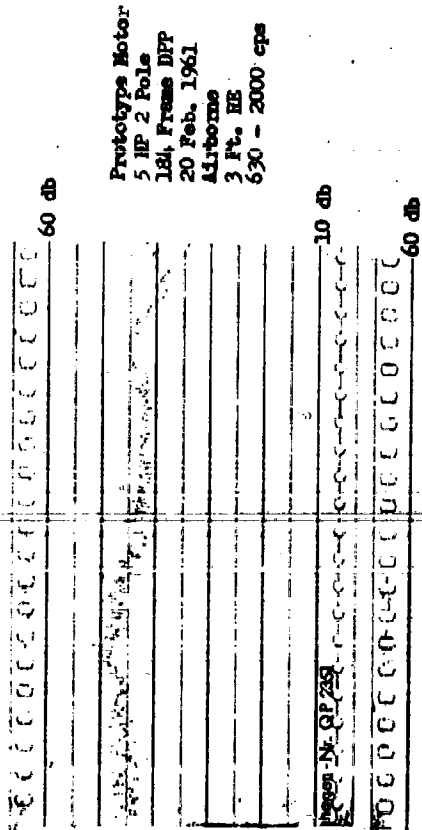
Prototype Motor
 5 HP 2 Pole
 184 Frames DPP
 20 Feb. 1961
 Airborne
 3 Ft. RE
 20 - 63 cps

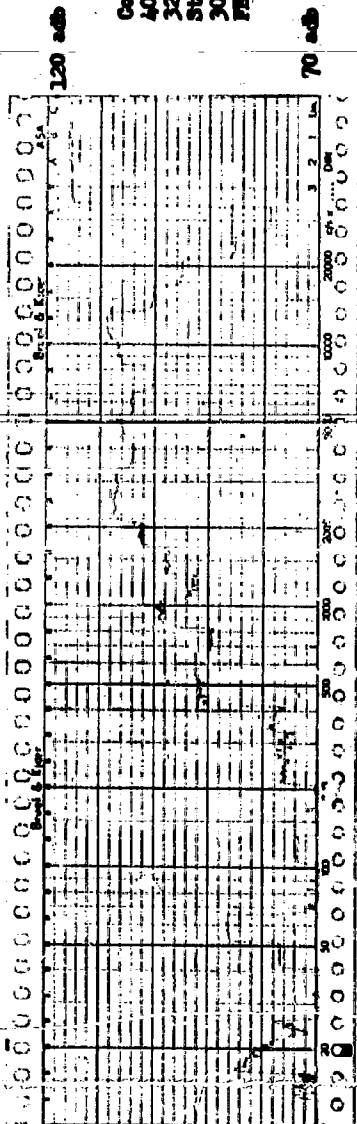


Prototype Motor
 5 HP 2 Pole
 184 Frames DPP
 20 Feb. 1961
 Airborne
 3 Ft. RE
 63 - 200 cps

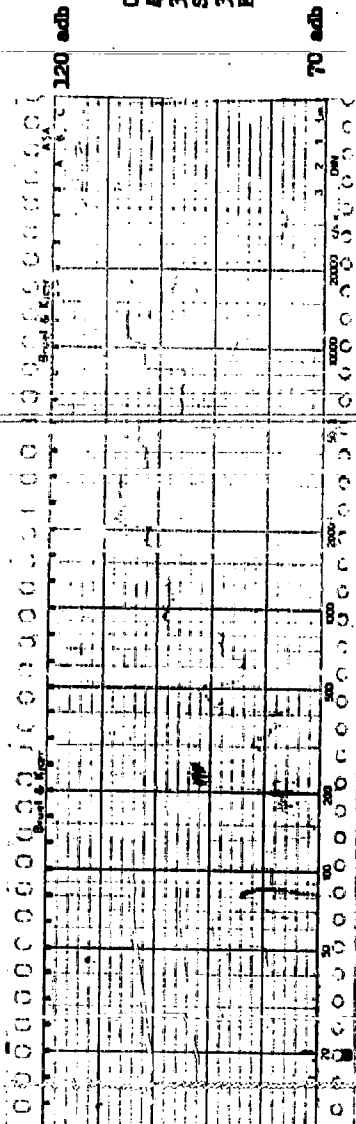


Prototype Motor
 5 HP 2 Pole
 184 Frames DPP
 20 Feb. 1961
 Airborne
 3 Ft. RE
 200 - 630 cps

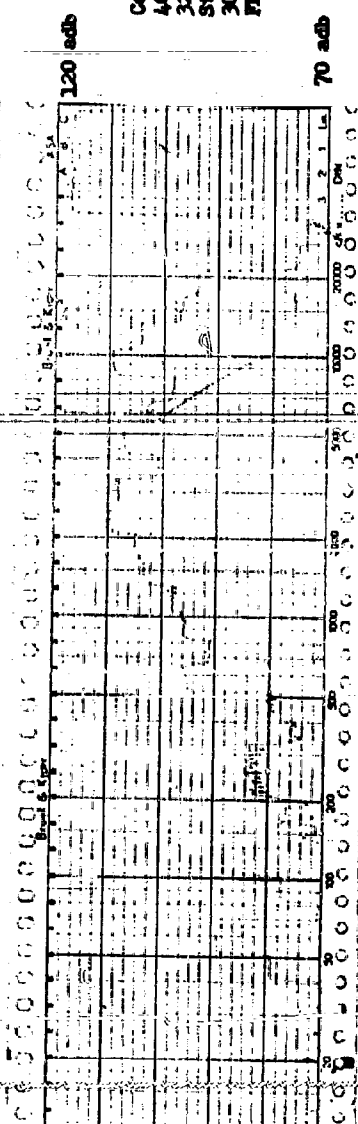




Conventional Motor
 40 HP 2 Pole
 326 Frames DFP
 Structureborne
 30 March 1961
 FE I-Axis



Conventional Motor
 40 HP 2 Pole
 326 Frames DFP
 Structureborne
 30 March 1961
 FE Z-Axis



Conventional Motor
 40 HP 2 Pole
 326 Frames DFP
 Structureborne
 30 March 1961
 FE Y-Axis

120 adb

Conventional Motor
40 HP 2 Pole
326 Frame DFP
Structureborne
30 March 1961
RE I-Axis

70 adb

130 adb

Conventional Motor
40 HP 2 Pole
326 Frame DFP
Structureborne
30 March 1961
RE Y-Axis

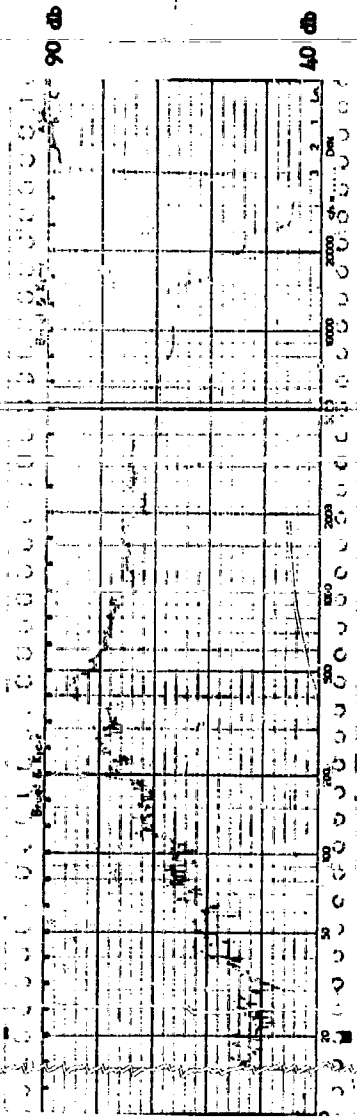
80 adb

130 adb

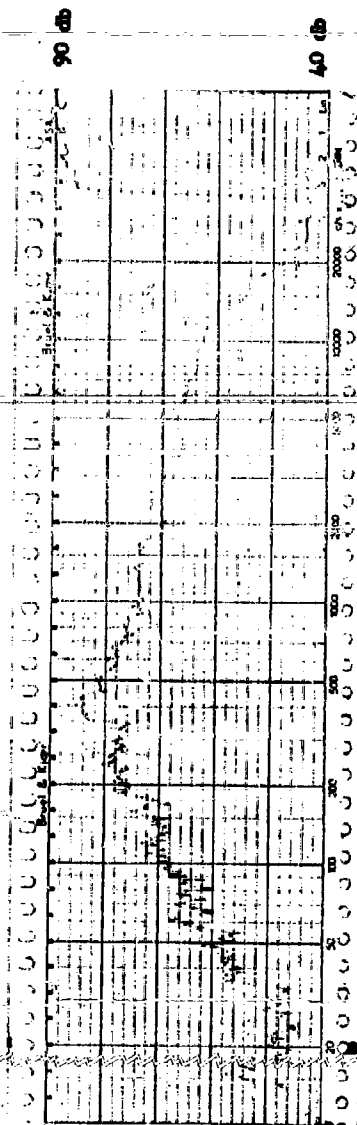
Conventional Motor
40 HP 2 Pole
326 Frame DFP
Structureborne
30 March 1961
RE Z-Axis

80 adb

Conventional Motor
40 HP 2 Pole
326 Frame DFP
Airborne
29 March 1961
3 ft. BE



Conventional Motor
40 HP 2 Pole
326 Frame DFP
Airborne
29 March 1961
3 ft. BE



SECTION 10 SUMMARY

The results and findings of this study fall into two categories: those which may be considered design criteria for low noise and vibration motors and facts concerning motor noise and vibration of a more general nature. These are treated in subsections 10.1 and 10.2 respectively.

10.1 DESIGN CRITERIA

The following design criteria for low noise and vibration induction motors are recommended. Numbers in parenthesis refer to the sections in which the criteria are developed. Those criteria available at the time of, and used in, the design of the prototype motors are indicated by an asterisk.

- *1) Use of low air gap magnetic flux densities. Maximum density of 40,000 lines per square inch is recommended. However, a low flux density is not consistent with compact motor design. (3)
- *2) Selection of proper rotor-stator slot combination to produce high node force waves. Acceptable combinations are listed in Table 3-7. Equations for calculating the number of nodes produced by all combinations are included in Table 3-2. This criterion is one of the most important in reducing the rotor slot frequency vibration and has no adverse effect on the motor performance. (3)
- *3) Skewing rotor bars, one rotor slot or one stator slot, whichever is the greater amount of skew. This amount is quite prevalent in industry and requires little or no design modification. (3)
- *4) Use of closed rotor slots to minimize permeance variation. Use of this and the following criterion will result in an increase of leakage flux and reactance. (3)
- *5) Use of narrow neck semi-closed stator slots. The minimum opening may be established as twice the thickness of the slot liner plus the diameter over insulation of the largest wire size plus 20 mils clearance. For frames larger than 286, the clearance should be increased to 30 mils. (3)
- 6) Increase in radial thickness of stator core. Only a minimum increase is possible without an increase in the frame dimensions. (3)
- 7) Frame modifications, such as circumferential ribs, to impart additional rigidity to stator core. Application of this criterion will result in a non-standard and possibly larger frame. (3)
- 8) Selection of stator core pitch to minimize 5th and 7th harmonic of air gap flux density. (3)
- 9) Rotation of successive stator core laminations to minimize permeance variation due to grain orientation. Punchings should be rotated preferably by 45° steps or if the number of stator slots prevents this, by 90° steps. (3)
- *10) Laminations should be annealed only if punchings are rotated as specified in criterion #9. (3)
- *11) Steel-to-steel eccentricity of air gap should be less than 2 mils. (3)
- *12) Use of low vibration ball bearings meeting Amendment 2 of MIL-B-17931A. (4)
- *13) Ball bearings should be preloaded by use of a thrust washer. (4)
- *14) The amount of preload force should be the minimum that takes up the internal clearance. If means for adjusting the preload are provided, the preload can be adjusted to give minimum motor noise. (4)
- *15) An interference fit of between 0.0001 and 0.0003 is recommended for the shaft-bearing fit. Use of ABEC-5 or higher bearings is an aid in obtaining the light press fit and is more compatible with the internal tolerances necessary to produce a low vibration bearing. (4)
- *16) The number of fan blades should be chosen to avoid producing the same frequency noise as produced by other sources. The important combinations to be avoided are:
 - a. Number of fan blades equal to number of poles (120 cps).
 - b. Number of fan blades equal to 1/2 number of rolling elements in the ball bearing.
 - c. Number of fan blades equal to $f_c P / 120$ where f_c equals the center frequency of any objectionable band.
 - d. Number of fan blades a multiple of the number of protruding ribs, lugs, etc.
 An odd number of fan blades will usually, but not always, meet the above requirements.
- *17) Clearance between fans and stationary parts should be sufficient to prevent a siren effect. The wide range of motor sizes, speeds, and constructions precludes the numerical determination of a permissible minimum clearance. (5)
- *18) Within the range of acceptable performance, cost, and the weight, the amount of cooling air necessary should be reduced by:
 - a. Use of low current and flux densities to minimize generated heat.
 - b. Use of sufficient iron and steel to convey generated heat to motor frame.
 - c. Full load operation at a temperature near the insulation class limit.
 - d. Use of higher temperature insulation systems.
 Items b, c, and d essentially cause an increase in the ratio of natural cooling (radiation and

- convection) to forced cooling on a given unit. (5)
- *19) The more efficient end-to-center cooling method should be used for dripproof protected motors. (5)
 - *20) The minimum axial length of fanblades of dripproof protected motors should be determined for each motor design for noise-sensitive applications. The principal reduction of the airborne noise of the dripproof protected prototype motors was realized by the use of this criterion. (5)
 - *21) Totally enclosed, fan cooled motors should use unidirectional rather than bi-directional external fans. (5)
 - *22) External fans should be aerodynamically designed. For example, backwardly inclined curved fan blades on a conical shroud as shown in Figure 5-3. (5)
 - *23) Sharp turns and constrictions in the airstream path should be eliminated. The areas that require special attention are:
 - a. The external fan housing opening and exhaust. The aerodynamic design of the fan housing must be performed in conjunction with the fan design, section 4.22.
 - b. The intake and exhaust ports of dripproof protected motors. Screening with a large percentage of open area should be used.
 - c. Area between air deflector and end turns. (5)
 - *24) Sharp edges in the airstream path should be eliminated. Parts in contact with high velocity air should be given prime considerations:
 - a. The fan should be smooth and free from burrs, blow holes, etc.
 - b. The fan bowl should present no sharp edges to the airstream. A cast fan bowl is preferable to a fabricated sheet steel one. If sheet steel is used, the edges should be rounded during the stamping process or coated with plastic or a similar material. (5)
 - *25) Rotor bars should be herringbone skewed to prevent an increase in bearing noise with load. (7)
 - 26) If herringbone skew cannot be used, the amount and manner of preload should be selected such that a change in preload force will not cause an increase in vibration. The vibration vs. preload characteristics must be determined for each size of bearing used and, until consistency is verified, for individual bearings. (7)
 - *27) As large an air gap as is consistent with meeting necessary starting current and power factor requirements should be used. (7)
 - *28) Machining operations should be performed with a minimum number of set-ups to maintain concentricity of turns and bores. (8)
 - *29) An ABEC-5 or higher tolerance is recommended for the bearing housing bores. (8)
 - *30) A light press fit (1 to 2 mills interference) is recommended between the bearing housings and frame. (8)
 - *31) The three casting materials evaluated in this study in the order of their preferred usage are:
 - a. Nodular iron
 - b. Cast steel
 - c. Aluminum (8)
 - 32) Ribbing of housings and yokes will increase their rigidity and reduce their vibration and the airborne noise generated by this vibration. Two important aspects about ribbing must be considered:
 - a. Use of circular rather than axial ribs will cause a greater reduction of deflections due to radial air gap forces.
 - b. Ribs should not interrupt a high velocity airstream. For example, the fan end bearing of TEFC motors should not be externally ribbed. (3, 5, & 8)
 - 33) For suitable applications, motor windings should be encapsulated to reduce stator core vibration. (8)

10.2 GENERAL CONCLUSIONS

The following facts concerning induction motor noise are of a more general nature than the design criteria. In many instances, they furnish the basis for the more specific design recommendations.

- 1) Specification of motor vibration must include the points of measurement and the axis along which the vibration is to be recorded. Vibrations recorded along mutually perpendicular axes at the same point are radically dissimilar.
- 2) The axis of measurement of motor vibration is often indicative of the direction of the generation of the vibration. Thus, vibrations caused by the radial air gap force waves will be reflected in the radial axes on the motor feet.
- 3) The effective source of 120 cycle magnetic noise is the air gap force wave created by the rotating fundamental (60 cps) magnetic field. The 120 magnetostrictive expansion is both smaller than and out of phase with the force wave deflection.
- 4) The principal effect of harmonics of the fundamental air gap flux wave is the production of stator core vibrations with frequencies approximately equal to $\frac{120R}{P}$ and $\frac{240R}{P}$ where R and P are the number of rotor slots and magnetic poles respectively.
- 5) A comparison of the noise producing aspects of solid lubricant sleeve bearings to ball bearings should be made when the numerous newly-developed sleeve materials have been evalu-

- ated and developed for application in the integral horsepower frame sizes.
- 6) Preloading of bearings other than those with low vibration characteristics causes an increase in recorded noise levels. The motor may sound quieter to the ear because of the removal of highly irritating rattling noise caused by the balls.
 - 7) Bearing locknuts should only be used where necessary to prevent slipping of the bearing on the shaft. Locknuts must not be overtightened.
 - 8) It is recommended that lower limits of permissible dirt count of lubrication used for low vibration bearings be established.
 - 9) Unidirectional fans or dripproof protected motors did not result in a reduction of motor noise because of the complicated airflow pattern.
 - 10) A comprehensive study of the effect of motor unbalance and means of correcting the unbalance is recommended.
 - 11) Conversion of the unbalance displacement values normally recorded to acceleration decibels (adb) levels may be highly inaccurate unless filtering networks are utilized.
 - 12) The bearing housings and frame have non-linear vibration transmission characteristics. Therefore, specification of motor vibration should only be made at points of prime interest, i.e., where this vibration is externally transmitted.
 - 13) The noise produced by various factors may either increase or decrease with motor load, but the overall effect will be an increased noise production.
 - 14) The measurement of motor noise under load presents the problem of isolating the noise produced by the loading device. The following method was employed in this study:
 - a. With motor isolated to highest degree obtainable, take noise measurements at load site, such as dynamometer, under no load condition (uncoupled).
 - b. Take noise measurements with motor connected to load with a flexible coupling (rubber, if possible) and driving a minimum load such as an unexcited dynamometer.
 - c. Take noise measurements with motor at full load (excited dynamometer).
- The corrected full load reading is:
 Reading "a" + (Reading "c" - Reading "b")
- This method relies on the isolation used (such as mounts, couplings, separate foundations, rooms, etc.) to minimize the noise change in the loading device due to load rather than the total noise produced by the loading device.
- 15) The use of damping compounds on cast or small fabricated motor components did not reduce motor noise. This observation may, or may not apply to large sheet metal enclosures mounted on the motor frame.
 - 16) Encapsulation of motor windings was found to affect the directivity of airborne noise radiation but not the sound power emitted.
 - 17) The effectiveness of internal isolation material in reducing motor noise has been established. The development of a functional system incorporating contaminant resistance and adequate cooling is strongly recommended.
 - 18) As the motor size and rating increase, the vibration levels produced will remain essentially constant.
 - 19) The airborne noise produced by larger induction motors will be greater because,
 - a. the higher peripheral speed of larger fans,
 - b. the larger frame is a more effective transducer of vibration into airborne noise.
 - 20) The degree of compactness of motor design is in an inverse relationship with the noise produced. The steps that must be taken to increase the horsepower rating in a given frame are the opposite of the steps to reduce motor noise.
 - 21) For the same motor speed and horsepower, the frame size specified by MIL-M-17060B is smaller for dripproof protected motors than for TEFC motors. This will result in dripproof protected motors having higher amplitudes of vibration but lower amplitudes of airborne noise than the TEFC motors of the same rating.

BIBLIOGRAPHY

- (1) Handbook of Noise Measurement, General Radio Co.
- (2) Test Code for Apparatus Noise Measurement, American Standard Z 24.7-1950.
- (3) Proposed Test Procedure for Noise Measurements on Rotating Electric Machinery AIEE No. 85, November 1960.
- (4) Noise Measurements of Shipboard Machinery & Equipment, MIL-STD-740 (Ships) 6 February 1961.
- (5) Sound Level Meters for Measurement of Noise and Other Sounds, American Standard Z 24.3-1944.
- (6) Octave Band Filter Set for the Analysis of Noise and Other Sounds, American Standard Z 24.10-1953.
- (7) Preferred Frequencies for Acoustical Measurements, American Standard S1.6-1960.
- (8) Electric Machinery (Book) Fitzgerald and Kingsley. McGraw Hill, 1952.
- (9) Principles of Electric and Magnetic Fields (Book) W.B. Boast, 2nd. Edition, 1956.
- (10) The Magnetic Noise of Polyphase Induction Motors, P.L. Alger, AIEE Trans., Vol. 73, 1954.
- (11) Mechanics of Materials (Book), E.P. Popov, Prentice-Hall, 1952.
- (12) Electric Machinery (Book), Vol. 11, Liwshitz-Garik and Whipple, Van Nostrand, 1956.
- (13) Induction Motor Slot Combination, G. Kron, AIEE Trans., Vol. 50, 1931.
- (14) Differential Leakage with Respect to the Fundamental Wave and to the Harmonics, M. Liwshitz-Garik, AIEE Trans., Vol. 63, 1944.
- (15) The Cause and Elimination of Noise in Small Motors, W.R. Appleman, AIEE Trans, Vol. 56, 1937.
- (16) Quiet Induction Motors, L.E. Hildebrand, AIEE Trans, Vol. 49, 1930.
- (17) Ball and Roller Bearing Engineering (Book), A. Palmgren, SKF Industries, 1959.
- (18) Handbook of Noise Control (Book), C.M. Harris, McGraw-Hill, 1957.
- (19) Calculation of Windage Noise Power Level in Large Induction Motors", M.E. Talent, AIEE Trans., Vol. 76, Pt. 3, 1957.
- (20) Vibration in Two-Pole Induction Motors Related to Slip Frequency, E.W. Summers, AIEE Trans., Vol. 74, Pt. 3, 1955.
- (21) Predetermination of Sound Pressure Levels of Magnetic Noise of Polyphase Induction Motors, E. Erdelyi, AIEE Trans., Vol. 74, Pt. 3, 1955.
- (22) The Use of Vibration and Shock Control in Reducing Noise Levels, D.H. Vance, Noise Control, March, 1956.

UNCLASSIFIED

UNCLASSIFIED